Cranfield University

Nattapol Niyomthai

PACKAGING AND CONFIGURATION DESIGN ASPECTS OF UCAV CONCEPT SYNTHESIS AND OPTIMIZATION

School of Engineering

Ph.D. Thesis

Cranfield University

School of Engineering

Aerospace Engineering Group

Ph.D. Thesis

2002

Nattapol Niyomthai

PACKAGING AND CONFIGURATION DESIGN ASPECTS OF UCAV CONCEPT SYNTHESIS AND OPTIMIZATION

Supervisor: Dr. Howard Smith

November 2002

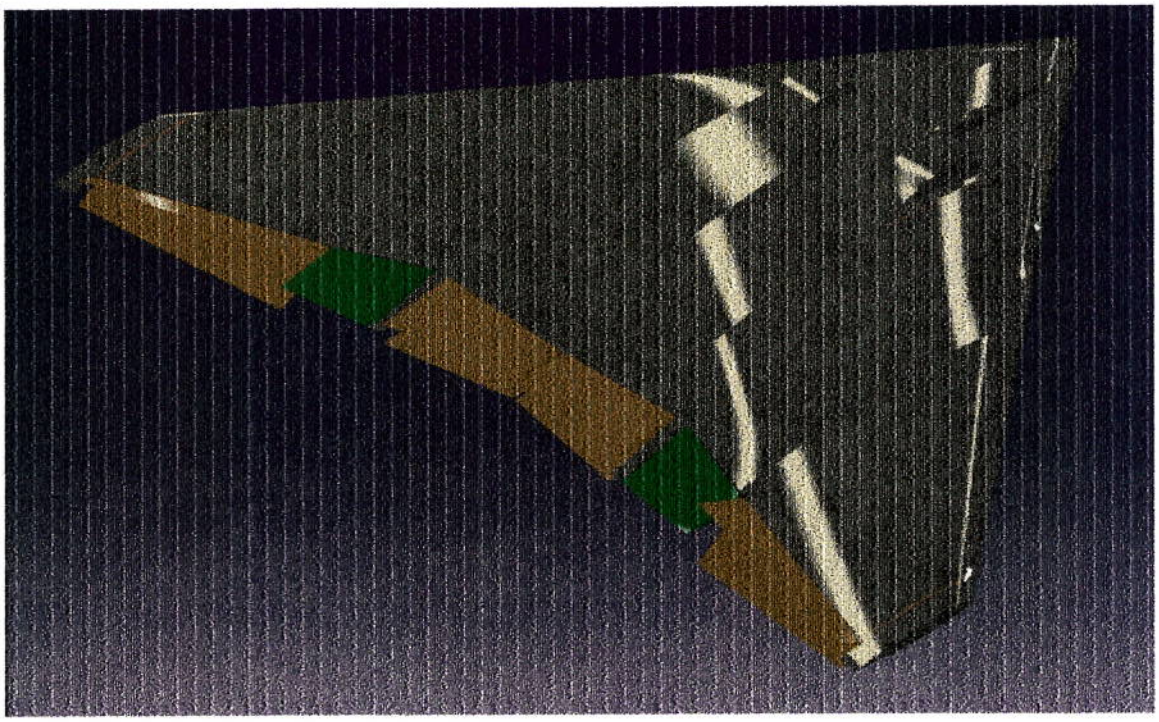

ABSTRACT

Uninhabited Combat Air Vehicle (UCAV) escapes the bounds of conventional ideas and opens a big window of new opportunities in combat aircraft design. A conceptual design methodology was produced to investigate the packaging and configuration design aspects of UCAV. To obtain first estimates of the major parameters that define the aircraft, an initial sizing program was developed to consider the primary design variables and constraints requirements. They are subsequently applied to a numerical design synthesis methodology for UCAVs.

The tailless UCAV was high on the list of interesting concepts because of the inherent benefits from the simple construction of a flying wing, its efficient low-drag aerodynamics, the ease of weapon and engine installation, and natural low observability of the design. A variety of packaging aspects was set up comprising of avionics bay, internal weapons carriage, propulsion system with the use of two-dimensional nozzle, undercarriage bay, and fuel tanks. The conceptual design possessed a flexible design layout for a wide range of configurations.

The aircraft synthesis models were described, and validation and comparison of results were presented where possible. The design methodology incorporated sufficiently accurate and realistic algorithms for the estimation of the packaging, geometry, layout, aircraft mass, and aircraft centre of gravity. A series of results was generated allowing a demonstration of several trade studies that could be accomplished. Results from a variety of particular designs were presented and discussed. Overall research conclusions were derived, and recommendations for further work prescribed. Appendices contained results of initial sizing program; publish data for avionics instruments, weapons, and UCAVs/UAVs; methodology implementation; and detailed aircraft parameters, packaging and configuration aspects of UCAV output data.

ACKNOWLEDGEMENTS

The Author would like to express my sincere appreciation to the following people:

My father for your love, your power, your encouragement throughout my study. You are my number-one hero forever.

My mother for your love, your kindness, your power that you have for me since my young age. Even now I grow up, but I still be a little son for you.

My lovely sisters for your love, your power, your encouragement. ***P'Vow***, you are my best doctor and sister. ***My little Wee***, you always be closed to me and encourage me that "I can do it".

Dr. Howard Smith for his supervision of the project, his encouragement, guidance, and support through the whole of this research program.

Professor John P. Fielding for his encouragement in processing an introduced letter to my sponsor for my research program.

Royal Thai Air Force for their support of sponsorship throughout my study.

George Dimitriadis for his support on the CATIA drawing to help me creating a very perfect picture of UCAV.

Flt. Lt. Otsin Nilubol for his kindness providing me the accommodation throughout the final year of my study.

Boonlom Family for their encouragement and their kindness for allowing me to be one member of the families.

Klinpayom Family and Chalermsanyakorn Family for their strongly support throughout my study.

All Thai Students in Cranfield for their great power encouraging me to fight with my study.

And finally, to the person who completed my heart. The most wonderful and loveliest person in the world. The person who always be the tremendous support for me when I needed it the most,

"N'bOw".

Table of Contents

List of Figures

List of Tables

List of Acronyms

AMRAAM	Advanced Medium-range Radar-guided Air-to-Air Missile
ATB	Advanced Technology Bomber
ATC	Air Traffic Control
ATD	Advanced Technology Demonstration
ATOL	Vertical Attitude Takeoff and Landing
ATR	Air Transport Racking, Automatic Target Recognition
AVE	Aeronef de Validation Experimental
BBW	Brake-By-Wire
BDA	Battle Damage Assessments
BLOS	Beyond-Line-of-Sight
C4ISR	Command, Control, Communications, Computers, Intelligence, Surveillance, and Reconnaissance
CAS	Closed Air Support
CEM	Combined Effects Munition
CG	Centre of Gravity
CIT	Combined Interrogator/Transponder
DARPA	Defense Advanced Research Projects Agency
DGPS	Differential Global Positioning System
DoD	Department of Defense
DS	Defense Suppression
EADS	European Aerospace and Defense Systems
ECM	Electronic Countermeasures
EMD	Engineering and Manufacturing Development
EO/IR	Electro-Optical and Infra-Red sensors
ESM	Electronic Support Measures
EUAV	Endurance Unmanned Aerial Vehicle
EWS	Electronic Warfare System
FBW	Fly-By-Wire
FLIR	Forward Looking Infra-Red
FMC	Foam Matrix Core
FMS	Flight Management System
FOAS	Future Offensive Aircraft System
GPS	Global Positioning System
HAE	High Altitude Endurance
HALE	High Altitude, Long Endurance
IFF	Identification – Friend or Foe
IFMU	In-Flight Management Unit
INS	Inertial Navigation System
IR	Infrared
ISR	Intelligence, Surveillance and Reconnaissance
JASSM	Joint Air-to-Surface Standoff Missile
JDAM	Joint Direct Attack Munitions
JSF	Joint Strike Fighter
JSOW	Joint Standoff Weapon
LO	Low Observable
LOE	Low Earth Orbit
LOS	Line-of-Sight
MLS	Microwave Landing System

MMS	Mission Management System
MoD	Ministry of Defense
MTI	Moving Target Indicator radar
MUAV	Micro Unmanned Aerial Vehicle
MVO	Multivariate Optimization
NACA	National Advisory Committee for Aeronautics
NASA	National Aeronautics and Space Administration
OCA	Offensive Counterair
O&S	Operations and Support
OTH	Over-the-Horizon
PTA	Pilotless Target Aircraft
RAM	Radar Absorbent Materials
RAS	Radar Absorbing Structure
RCS	Radar Cross Section
RPV	Remotely Piloted Vehicle
RS	Reconnaissance and Surveillance
RSTA	Reconnaissance, Surveillance and Target Acquisition
RTA	Reconnaissance and Target Acquisition
SAM	Surface-to-Air Missile
SAR	Synthetic Aperture Radar
SATCOM	Satellite Communications
SEAD	Suppression of Enemy Air Defenses
SEM	Standard Electronic Module
SFW	Sensor Fuzed Weapon
SHARC	Swedish Highly Advanced Research Configuration
SI	Surveillance and Intelligence
SMS	Store Management System
SSL	Standard Sea Level
STA	Surveillance and Target Acquisition
STOVL	Short Takeoff and Vertical Landing
SUAV	Small Unmanned Aerial Vehicle
TLAM	Tomahawk Land Attack Cruise Missile
TPSA	Technologies, Processes, and System Attributes
TUAV	Tactical Unmanned Aerial Vehicle
UAV	Unmanned/Uninhabited Aerial Vehicle
UCAV	Unmanned/Uninhabited Combat Air Vehicle
UDS	UCAV Demonstrator System
UHF	Ultra High Frequency
UOS	UCAV Operational System
VHF	Very High Frequency

List of Symbols

Basic Assessment of Aircraft Conceptual Design

AF		Airfoil factor
Alt_da	m	Dash altitude
Alt_ld	m	Landing altitude
Alt_to	m	Take-off altitude
AR		Wing aspect ratio
b_cal	m	Calculated wing span
BPR		Engine static bypass ratio
b_sp	m	Wing span requirement
CD		Drag coefficient
CD_cr		Cruise drag coefficient
CDf		Zero-lift drag coefficient
Cdflap		Flap drag coefficient
CDlv		Drag coefficient due to lift
CD_uc		Undercarriage drag coefficient
C_l		Fraction of chord of wing over which the flow is laminar
CL		Lift coefficient
CL_ap		Approach lift coefficient
CL_buffet		Buffeting life coefficient
CL_cr		Manoeuvre lift coefficient, Cruise lift coefficient
CL_us		Unstick lift coefficient
D	N	Drag
D_cr	N	Cruise drag
Den	kg/m^3	Density
E	sec	Endurance
E_loiter	sec	Loiter time
E_strafe	sec	Strafe time
F_f		Trailing edge flap factor
FF_es		Fuel mass fraction estimation
f(tap)		Taper ratio function
FTfac		Factor to allow for use of afterburning
g	m/s^2	Acceleration due to gravity
h	m	Cruise altitude
K		Induce drag factor
K_eng		Engine coefficient
K_INL		Inlet factor
K_PG		Engine installation factor
K_PIV		Wing variable sweep structural factor
KT		A constant data for a given engine in a defined Mach number range and operating condition
K_tail		Tail structural factor
L		Lift
L/D, L_D		Lift-to-drag ratio
L_H		Fuselage length over maximum fuselage height
M		Mach number, aircraft mass in various phases of flight
M_ac	kg	Air condition mass
Mach_cr_L		Cruise Mach number with stores
Mach_cr		Cruise Mach number with no stores
M_bomb	kg	Bomb mass
M_{crew}, *M_pilot*	kg	Crew mass
M_deice	kg	De-icing mass

$Mdrb_{exist}$	kg	Total existing aircraft mass at end of mission phase after bombs drop
M_elec	kg	Electric mass
M_{empty}	kg	Empty mass
M_eng	kg	Engine installation mass
M_fc	kg	Flight control mass
M_{ff}		Fuel fraction
M_fs	kg	Fuel system mass
M_{fuel}, *M_fuel*	kg	Total fuel mass
Mfuel_ava	kg	Maximum fuel capacity
Mfuel_re	kg	Total mission fuel mass required
Mfuel_res	kg	Reserve and trapped fuel
Mfuel_used	kg	Fuel used during the mission
M_furnish	kg	Furnishing mass
M_fuse	kg	Fuselage mass
M_gear	kg	Undercarriage mass
M_hydrau	kg	Hydraulics mass
M_i	kg	Total mass at end of each mission phase i
M_instru	kg	Instruments mass
Mld	kg	Design landing mass
Mld_Mto		Landing mass to take-off mass ratio
M_miscell	kg	Miscellaneous mass
$M_{payload}$	kg	Payload mass
$Mstf_{exist}$	kg	Total existing aircraft mass at end of mission phase after ammo fire
M_tail	kg	Empennage Mass
M_{TO}, *Mto*	kg	Design take-off mass
Mto_es	kg	Take-off mass estimation
Mu		Braking coefficient
Mu_gr		Ground friction coefficient
M_weap	kg	Armament mass
M_wing	kg	Wing mass
N_bomb		Number of bombs
N_eng		Number of engines
N_lim		Positive limit load factor
Nsus		Maximum sustainable load factor
Pilot		Number of crews
q	N/m^2	Maximum aerodynamic pressure
R	km	Range
$Ratio_{bomb}$		Bomb-drop ratio
$Ratio_{ammo}$		Ammo-firing ratio
Rcr_in	km	Cruise-in range
Rcr_out	km	Cruise-out range
Rdash_in	km	Dash-in range
Rdash_out	km	Dash-out range
RoC	m/s	Rate of climb
RoC_L_sp	m/s	Requirement of rate of climb with stores
RoC_sp	m/s	Requirement of rate of climb with no stores
R_S		Wetted area to wing area ratio
R_turn	m	Radius of turn
R_turn_L_sp	m	Requirement of radius of turn with stores
R_turn_sp	m	Requirement of radius of turn with no stores
s		Altitude factor
S	m^2	Wing area
sfc	mg/N/sec	Specific fuel consumption

sfcF		Fuel consumption factor
Sld_re	m	Landing distance
Sld_sp	m	Maximum landing distance
Sto_re	m	Take-off distance
Sto_sp	m	Maximum take-off distance
swe	deg	Wing quarter-chord sweep
swe_LE	deg	Wing leading edge sweep
T	N	Engine thrust in various phases of flight, Type factor
tap		Wing taper ratio
t_c		Wing thickness ratio
T_cr	N	Cruise thrust
Temp_ld	°C	Landing temperature
Temp_to	°C	Take-off temperature
Tfac		Engine thrust factor
Time_cl	sec	Time to climb
Time_cl_L_sp	sec	Requirement of time to climb with stores
Time_cl_sp	sec	Requirement of time to climb with no stores
T_rate	deg/sec	Sustained turn rate
T_rate_L_sp	deg/sec	Requirement of sustained turn rate with stores
T_rate_sp	deg/sec	Requirement of sustained turn rate with no stores
Tto_es	N	Engine thrust estimation
T_W		Thrust loading
V	m/s	Speed, velocity
Vapp	m/s	Landing approach speed
Vapp_sp	m/s	Maximum landing approach speed
V_cl	m/s	Climb velocity
V_cr	m/s	Cruise velocity
V_sl_L	m/s	Speed at sea level with stores
V_sl	m/s	Speed at sea level without stores
WLEH		Lift increment of wing with configuration increments at high speed
WLEL		Lift increment of wing with configuration increments at low speed
WLELD		Lift increment of wing leading edge at landing
WLETO		Lift increment of wing leading edge at take-off
W_S	N/m^2	Wing loading
WTELD		Lift increment of wing trailing edge at landing
WTETO		Lift increment of wing trailing edge at take-off
Δh	m	Altitude changes

Greek Symbols

σ	Air density ratio
τ	Correction factor for wing thickness

Notation and List of Variables

Packaging and Configuration Design Aspects of UCAV

Variable	Description	Unit	Type[1]
ABDS	Allowable bending stress	N/m^2	DV
AIDX	Aspect ratio of intake diffuser at a given x-position		DV
AII	Intake diffuser inlet aspect ratio		EV
AMEF	Effective Mach number		DV
AMOUNTAV	Amount of each avionics item		EV
AMVD	Aircraft Mach number		DV
ANZ	Aspect ratio of two-dimensional nozzle at a given x-position		DV
APTD	Aspect ratio of nozzle transition duct exit		DV
ATE	Total moment of aircraft with no weapons loaded and empty fuel tanks	kgm	DV
ATT	Total moment of aircraft with full load	kgm	DV
ATZF	Total moment of aircraft with empty fuel tanks	kgm	DV
AVCOUNT	Total number of avionics management systems		EV
AVSET	Total number of avionics items in each avionics suite		EV
AVSUITE	Total number of avionics suites		EV
AW	Gross wing aspect ratio		DV
AWSEK	Aspect ratio of each trailing edge control surface		DV
AWXTK	Aspect ratio of wing constructed panels		DV
BIDBX	Width of intake diffuser at a given x-position	m	DV
BII	Width of intake diffuser inlet	m	DV
BPTD	Width of nozzle transition duct exit	m	DV
BUMW	Main undercarriage wheel and tyre width	m	DV
BUMWK	Constant in correlation for main undercarriage wheel and tyre width		EV
BUNW	Nose undercarriage wheel and tyre width	m	EV
BW	Gross wing span	m	IV
BW2K	Spanwise stations at wing kinks	m	DV
BWB	Wing box gross span	m	DV
BWL	Total span of wing leading edge	m	DV
BWSE	All trailing edge control surfaces gross span	m	DV
BWSEK	Total span of each pair of trailing edge control surfaces	m	DV
BWTG	Total span of wing trailing edge	m	DV
CALGAM	Loading coefficient for additional lift distribution		DV
CBLGAM	Loading coefficient for basic lift distribution		DV
CCXALD	Coefficients for additional lift distribution		DV
CD	Total drag coefficient		DV
CD0	Parasite drag coefficient		DV
CDC	Component drag coefficient		DV
CDL	Induced drag coefficient		DV
CDLT	Induced drag coefficient due to trailing edge devices		DV
CDLW	Induced drag coefficient due to wing		DV
CDM	Miscellaneous drag coefficient		DV
CDP	Leakage and protuberance drag coefficient		DV

[1] This column was complied considering three types of variable: 1. EV (External Variables) are set as input data. 2. DV (Dependent Variables) are assigned a value as a result of a calculation within the synthesis code. 3. IV (Independent Variables) are set as input values, but may be modified by an optimizer linked to synthesis code.

CF	Flat-plate skin-friction drag coefficient		DV
CFG	Ground friction coefficient		EV
CLBCGTM	Rolling moment contribution		DV
CLBTA	Rolling increment effectiveness due to either trailing edge split elevons or inlaid control surfaces based on aileron characteristic		DV
CLBWG	Wing rolling moment with respect to sideslip about wing aerodynamic centre		DV
CLLSX	Section maximum lift coefficient increment with leading edge control surfaces		DV
CLMX	Total wing maximum lift coefficient		DV
CLSC	Airfoil section lift-curve slope in compressible flow		DV
CLSCI	Airfoil section lift-curve slope in incompressible flow		DV
CLSCXTK	Wing lift-curve slope of wing constructed panels		DV
CLTMX	Wing maximum lift coefficient increment with trailing edge control surfaces		DV
CLTSX	Section maximum lift coefficient increment with trailing edge control surfaces		DV
CLW	Lift coefficient appropriate to flight condition		DV
CLWG	Wing lift coefficient		DV
CLWLSC	Wing lift-curve slope		DV
CMCGTM	Pitching moment contribution		DV
CMFPCGL	Thrust effect upon pitching moment with inlet normal force due to turning of the air		DV
CMIWTTM	Wing pitching moment due to deflection of trailing edge control surfaces		DV
CMLWCGL	Wing pitching moment due to total wing lift through wing aerodynamic centre		DV
CMWCGL	Wing pitching moment about wing aerodynamic centre		DV
CNBCGTM	Yawing moment contribution		DV
CNBTA	Yawing increment effectiveness due to either trailing edge split elevons or inlaid control surfaces based on aileron characteristic		DV
CNBTR	Yawing increment effectiveness due to either trailing edge split elevons or inlaid control surfaces based on rudder characteristic		DV
CNBWCGA	Wing yawing moment with respect to sideslip about wing aerodynamic centre		DV
CWBC	Wing box centreline chord	m	DV
CWBK	Wing box chord at kink positions	m	DV
CWBT	Wing box tip chord	m	DV
CWC2	Wing chord at half semi-wingspan	m	DV
CWCC	Wing root centreline chord	m	IV
CWCN	Wing root chord of equivalent wing planform	m	DV
CWCP	Wing chord at engine bay position	m	DV
CWCT	Wing tip chord	m	IV
CWK	Wing chord at kink positions	m	IV
CWMA	Wing mean aerodynamic chord	m	DV
CWMG	Wing geometric mean chord	m	DV
CWPF	Relative wing chord at reference spanwise station corresponding to a number of equivalent points across span	m	DV
CWPFA	Average wing chord	m	DV
CWSE	Mean chord of trailing edge control surfaces	m	IV
CWSEK	Mean chord of each pair of trailing edge control surfaces	m	DV

CWSL	Mean chord of leading edge control surfaces	m	IV
CWSR	Mean chord of inlaid control surfaces	m	IV
CWWF	Wing chord at kink positions in area of wing fuel tank	m	DV
CWWIB1	Wing chord at weapon bay 1 position	m	DV
CWWIB2	Wing chord at weapon bay 2 position	m	DV
CWWSE	Wing chord at mid-span of trailing edge devices	m	DV
CWWSEK	Wing chord at mid-span of trailing edge devices	m	DV
CWX	Relative wing chord at reference spanwise station	m	DV
CWXTP	Wing root chord of constructed panel	m	DV
D	Air density at flight altitude	kg/m^3	DV
DII	Equivalent diameter of intake diffuser inlet	m	DV
DIE	Diameter of intake diffuser exit	m	DV
DPG	Diameter of engine	m	DV
DPGR	Maximum diameter of reference engine	m	EV
DRG	Aircraft drag at various phases of flight	N	DV
DT	Duration of time to perform mission segment	sec	DV
DTE	Average depth of rear spar	m	DV
DUMW	Main undercarriage wheel and tyre diameter	m	DV
DUMWK	Constant in correlation for main undercarriage wheel and tyre diameter		EV
DUNW	Nose undercarriage wheel and tyre diameter	m	DV
DUNWK	Constant in correlation for nose undercarriage wheel and tyre diameter		EV
DW	Maximum characteristic diameter of component	m	DV
EBP	Overall clearance on width of engine bay	m	DV
EBPH	Maximum engine bay width clearance	m	DV
EBPS	Minimum engine bay width clearance	m	DV
EHP	Overall clearance on height of engine bay	m	DV
EHPH	Maximum engine bay height clearance	m	DV
EHPS	Minimum engine bay height clearance	m	DV
ELUP	Distance between main undercarriage pintle and front of main undercarriage bay	m	EV
ETALSC	Ratio of section lift-curve slope		DV
EUSFOO	Fixed orifice oleopneumatic shock absorber efficiency		EV
EUST	Tire shock absorber efficiency		EV
FAMN	Function of Mach number to correct for compressibility effects		DV
FBPK	Constant factor for engine bay width clearance		EV
FBUMW	Factor for main wheel width clearance		EV
FBUMWK	Factor in correlation for main undercarriage wheel width		EV
FBUNW	Factor for nose wheel width clearance		EV
FBW2K	Spanwise stations to wing kinks as fraction of semi-wingspan		IV
FBWH	Function determining spanwise variation of cover and web thickness		DV
FC	Specific fuel consumption at various phases of flight	mg/Ns	DV
FC1UW	Taper ratio correction factor		DV
FCWD	Front spar position as a fraction of wing chord		IV
FCWFR	Axial factor in correlation for position of wing fuel tanks rear face		IV
FCWR	Rear spar position as a fraction of wing chord		IV
FCWSE	Ratio of trailing edge control surface's mean chord to its wing chord		DV
FCWSEL	Distance of leading edge of trailing edge control surface aft of rear spar as fraction of wing chord		DV

FDUMW	Factor for main wheel diameter clearance		EV
FDUMWK	Factor in correlation for main undercarriage wheel diameter		EV
FDUNW	Factor for nose wheel diameter clearance		EV
FDUNWK	Factor in correlation for nose undercarriage wheel diameter		EV
FF	Component form factor		DV
FFALD	Additional lift distribution		DV
FK	Induced drag factor		DV
FKE	Effective induced drag factor (ground effect)		DV
FKINK	Total number of kinks in area of wing tank		DV
FHPK	Constant factor for engine bay height clearance		EV
FLIDK	Factor on diffuser inlet diameter to define minimum diffuser length		EV
FLPK	Factor in correlation for length of engine		EV
FLSC	Plan-form parameter		DV
FM	Fuel mass fraction in each mission segment due to fuel burn and a discrete change in mass due to payload released		DV
FMDUM	Fuel mass fraction in each mission segment due to fuel burn		DV
FMPGK	Factor in estimation of mass of engine		EV
FMPIK	Factor in estimation of engine installation mass		EV
FMSA	Mass fraction of air systems for avionics bay		EV
FMSAK	Factor in correlation for mass of air systems		EV
FMSCK	Factor in correlation for mass of flying control systems		EV
FMSEK	Factor in correlation for mass of electrical systems		EV
FMSFK	Factor in correlation for mass of fuel system with fuel mass		EV
FMUHK	Factor in estimation of undercarriage hydraulics mass		EV
FMUMK	Factor in estimation of main undercarriage mass		EV
FMUNK	Factor in estimation of nose undercarriage mass		EV
FMW	Mass factor allowed for change in wing material		EV
FPWK	A series of trapezoidal panels for multi-kinks wing as fraction of wing semi-span	m	DV
FQ	Interference effects		EV
FTPG	Engine thrust factor		DV
FUGL	Gear load factor		EV
FUW	Function of taper ratio for torsional stiffness criterion		DV
FWIR	Inertia relief load factor		DV
FXLIB1	Axial factor in correlation for position of weapon bay 1		IV
FXLIB2	Axial factor in correlation for position of weapon bay 2		IV
FXLPG	Axial factor in correlation for position of engine bay		IV
FXXD	Front position of fuel tank as fraction of relative wing chord		DV
FXXR	Rear position of fuel tank as fraction of relative wing chord		DV
FY2BWP	Non-dimensional semi-wingspan		DV
FY2WFO	Spanwise factor in correlation for position of outer edge of wing tank		IV
FYIA	Coefficient A in calculation of Y-coordinate of diffuser centreline		DV
FYIB	Coefficient B in calculation of Y-coordinate of diffuser centreline		DV
FYPC	Factor on engine diameter in twin-engine installation		EV

FYSEI	Spanwise stations to inner edge of trailing edge control surfaces as fraction of semi-wingspan		IV
FYSEO	Spanwise stations to outer edge of trailing edge control surfaces as fraction of semi-wingspan		IV
FYSLI	Spanwise stations to inner edge of leading edge control surfaces as fraction of semi-wingspan		IV
FYSLO	Spanwise stations to outer edge of leading edge control surfaces as fraction of semi-wingspan		IV
FYSRI	Spanwise stations to inner edge of inlaid control surfaces as fraction of semi-wingspan		IV
FYSRO	Spanwise stations to outer edge of inlaid control surfaces as fraction of semi-wingspan		IV
FZIA	Coefficient A in calculation of Z-coordinate of diffuser centreline		DV
FZIB	Coefficient B in calculation of Z-coordinate of diffuser centreline		DV
GXYC	Material shear modulus	N/m^2	EV
H	Altitude to perform mission segment; Flight altitude for performance constraint comparison	m	EV
HAV	Height of each avionics item	m	EV
HBPTDI	Half-width of nozzle transition duct exit	m	DV
HBPTDO	Half-width of nozzle transition duct exit	m	DV
HHPTD	Half-height of nozzle transition duct exit	m	DV
HIB	Height overall of internal weapon bay	m	DV
HIDBX	Height of intake diffuser at a given x-position	m	DV
HII	Height of intake diffuser inlet	m	DV
HMAXAV	Maximum height of each avionics suite	m	DV
HNZ	Semi-major axis height of two-dimensional nozzle at a given x-position	m	DV
HOBST	Obstacle height	m	EV
HPG	Engine bay height	m	DV
HPTD	Height of nozzle transition duct exit	m	DV
HTIPB	Height due to tipback angle a trailing edge	m	DV
HTOTAV	Total height of each avionics suite	m	DV
HTTR	Transition height (Take-off performance)	m	DV
HUMB	Height of main undercarriage bay	m	DV
HUNB	Height of nose undercarriage bay	m	DV
HW	Wing height above ground	m	DV
HWIB	Height of weapon in internal weapon bay	m	EV
HWIBC	Clearance on height of weapons in weapon bay	m	EV
IWP	Input parameter in each mission segment to select options for weapon status and its relative mass		EV
K0LSC	Finite-span correction for wing lift-curve slope		DV
K1BLD	Finite-span correction for basic lift distribution		DV
KA	Aerodynamic terms for take-off and landing distance		DV
KAMS	Allowance for stringer mass		DV
KSKIN	Skin roughness value	m	EV
KT	Thrust terms for take-off and landing distance		DV
LAV	Length of each avionics item	m	EV
LCFL	Length of cockpit floor	m	DV
LD	Lift to drag ratio at various phases of flight		DV
LGC	Length of gun	m	EV
LIB	Length overall of internal weapon bay	m	DV
LIDG	Overall length of intake diffuser	m	DV
LIDS	Minimum length of intake diffuser	m	DV

LMAXAV	Maximum length of each avionics suite	m	DV
LPG	Overall length of engine	m	DV
LPGR	Length of reference engine	m	EV
LPTD	Overall length of nozzle transition duct	m	DV
LPTDS	Minimum length of nozzle transition duct	m	DV
LULG	Total length of all undercarriage leg elements	m	DV
LULG1K	Constant in correlation for undercarriage length		EV
LULG2K	Constant factor in correlation for undercarriage length		EV
LUMB	Length of main undercarriage bay	m	DV
LUMN	Length of each main undercarriage leg	m	DV
LUNB	Length of nose undercarriage bay	m	DV
LUNS	Length of nose undercarriage leg	m	DV
LW	Characteristic length of component	m	DV
LWF	Moment arm of centre of volume of wing fuel tank from aircraft nose	m	DV
LWIB	Length of weapon in internal weapon bay	m	EV
LWIBC	Clearance on length of weapons in weapon bay	m	EV
M	Mach number requirement to perform mission segment; Mach number for performance constraint comparison		EV
MAAV	Total mass of avionics instruments	kg	DV
MACM	Total mass of countermeasures suite	kg	DV
MACOMM	Total mass of communication suite	kg	DV
MAEW	Total mass of electronic warfare suite	kg	DV
MAFC	Total mass of flight control suite	kg	DV
MAIDEN	Total mass of identification suite	kg	DV
MANAV	Total mass of navigation suite	kg	DV
MARAD	Total mass of radar suite	kg	DV
MASEN	Total mass of sensor suite	kg	DV
MAV	Mass of each avionics item	kg	EV
MAWEPC	Total mass of weapon control and release suite	kg	DV
MAXLAV	Maximum length of each avionics items	m	DV
MCC	Mass of cockpit canopy	kg	DV
MCF	Mass of fuel in centre tank	kg	DV
MCI	Mass of cockpit instruments	kg	EV
MCP	Mass of crew	kg	EV
MCW	Mass of cockpit windscreen	kg	DV
MGA	Mass of ammunition	kg	EV
MGC	Mass of gun	kg	EV
MIBF	Mass of fuel in inboard tank	kg	DV
MIBXD	Mass of weapon bay doors	kg	DV
MIBXRF	Mass of weapon bay roof	kg	DV
MIBXSR	Mass of weapon bay structural surroundings	kg	DV
MIP	Mass of pylons in internal weapon bay	kg	EV
MITEM	Individual component mass	kg	DV
MMAXAV	Mass of each avionics suite	kg	DV
MOBF	Mass of fuel in outboard tank	kg	DV
MPB	Total mass of engine(s)	kg	DV
MPG	Total mass of propulsion system	kg	DV
MPGR	Mass of reference engine	kg	EV
MPI	Engine installation mass	kg	DV
MPTD	Total mass of two-dimensional nozzle(s)	kg	DV
MSA	Mass of air conditioning systems	kg	DV
MSAK	Constant in correlation for air systems mass		EV
MSC	Mass of flying control systems	kg	DV
MSCK	Constant in correlation for flying control systems mass		EV

MSDI	Mass of de-icing system	kg	DV
MSE	Mass of electrical systems	kg	DV
MSEK	Constant in correlation for electrical systems mass		EV
MSF	Mass of fuel system	kg	DV
MTE	Total empty mass	kg	DV
MTGF	Total mass of internal fuel	kg	DV
MTGM	Total aircraft mass at various phases of flight as a discrete change in mass due to payload released	kg	DV
MTIBXI	Additional mass effect of weapon bay	kg	DV
MTLR	Landing reference mass	kg	DV
MTOTAV	Total mass of each avionics suite	kg	DV
MTT	Total take-off mass	kg	DV
MTTM	Total existing aircraft mass at various phases of flight	kg	DV
MTTR	Take-off reference mass	kg	DV
MTZF	Total zero fuel mass	kg	DV
MUH	Mass of hydraulics associated with undercarriages	kg	DV
MUHK	Constant in correlation for mass of undercarriage hydraulics structure		EV
MUM	Structural mass of total main undercarriages	kg	DV
MUMG	Total mass of main undercarriages including hydraulics	kg	DV
MUMK	Constant in correlation for mass of main undercarriage structure		EV
MUMSLMX	Maximum static load of main undercarriage	kg	DV
MUN	Structural mass of nose undercarriage	kg	DV
MUNG	Total mass of nose undercarriage including hydraulics	kg	DV
MUNK	Constant in correlation for mass of nose undercarriage structure		EV
MUNSLMN	Minimum nose static load	kg	DV
MUNSLMX	Maximum nose static load	kg	DV
MWBCW	Total mass of wing structural box	kg	DV
MWC	Total mass of wing		DV
MWCFS	Mass of basic ribs in primary structural box	kg	DV
MWCX	Mass of miscellaneous attachments on wing	kg	DV
MWEP	Total mass of weapons	kg	DV
MWF	Mass of fuel in wing tank	kg	DV
MWIB	Total mass of weapons in weapon bay	kg	DV
MWIBF	Mass of fuel in optional weapon bay tank	kg	DV
MWIM	Relative weapon mass in internal weapon bay based on weapon status in each mission segment (Aircraft mass)	kg	DV
MWIR	Effective inertia relief load	kg	DV
MWIXR	Relative weapon mass in internal weapon bay based on weapon status in each mission segment (Aircraft centre of gravity)	kg	DV
MWL	Total mass of wing leading edge	kg	DV
MWLO	Mass of low observable treatments	kg	DV
MWLOR	Mass of low observable treatments	lb	EV
MWOB	Total mass of external stores	kg	DV
MWOM	Relative weapon mass of external stores based on weapon status in each mission segment (Aircraft mass)	kg	DV
MWOXR	Relative weapon mass of external stores based on weapon status in each mission segment (Aircraft centre of gravity)	kg	DV
MWSE	Total mass of trailing edge control surfaces	kg	DV
MWSEA	Total mass of trailing edge split elevons	kg	DV
MWSEF	Total mass of trailing edge flaps	kg	DV
MWSR	Total mass of inlaid control surfaces	kg	DV

MWT	Total mass of fixed wing trailing edge	kg	DV
MWXF	Total fuel mass in each tank	kg	DV
MWXP	Mass of external paint on wing	kg	DV
MXP	Total mass of external pylons	kg	EV
NENG	Number of engines		EV
NHWIB	Number of weapons in weapon bay in height		EV
NLWIB	Number of weapons in weapon bay in length		EV
NMISS	Reference number of current mission segment		DV
NTENG	Total engines installed on aircraft		DV
NTWIST	Twist Distribution		EV
NTY2BW	Number of equivalent points along semi-wingspan		DV
NW2SE	Number of trailing edge control surfaces on semi-span		EV
NW2SL	Number of leading edge control surfaces on semi-span		EV
NW2SR	Number of inlaid control surfaces on semi-span		EV
NWEPB	Number of internal weapon bays		EV
NWK	Number of kinks in wing		EV
NWWIB	Number of weapons in weapon bay in width		EV
OIE	Cross-sectional area of intake diffuser exit	m^2	DV
OII	Cross-sectional area of intake diffuser inlet	m^2	DV
OISX	Enclosing area from intake inlet to a given x-position	m^2	DV
OIX	Cross-sectional area of intake diffuser at a given x-position	m^2	DV
OPB	Cross-sectional area of engine bay	m^2	DV
OPN	Total nozzle exit area	m^2	DV
OWF	Cross-sectional area of separate wing tanks	m^2	DV
OWMX	Maximum cross-sectional area	m^2	DV
OWXA	Cross-sectional area at any fixed chordwise station	m^2	DV
OWXF	Cross-sectional are of fuel tanks corresponding to shape of airfoil	m^2	DV
PGC	Gap between engine bay and other bay	m	EV
PWFK	Span panels of separate wing tanks	m	DV
PWK	A series of trapezoidal panels for multi-kinks wing	m	DV
QALPHA	Aircraft angle of attack	deg	EV
QALPHAA	Average angle of attack	deg	DV
QBSSL	Local angle of sideslip	deg	EV
QCGUM	Angle off vertical from main undercarriage position to aircraft centre of gravity	deg	DV
QPTD	Reference slope angle of transition duct	deg	EV
QTALPHA	Total angle of attack	deg	DV
QTCL	Climb angle (Take-off performance)	deg	DV
QTWTC	Wing root-relative twist distribution across wingspan	deg	DV
QUSTD	Static tail-down angle	deg	DV
QUTIPB	Tipback angle	deg	DV
QW2	Wing mid-chord sweep of equivalent wing planform	deg	DV
QW2XTK	Wing mid-chord sweep of wing constructed panels	deg	DV
QW4	Wing quarter chord sweep of equivalent wing planform	deg	DV
QW4EF	Effective angle of sweepback in compressible flow	deg	DV
QWB	Wing box centreline sweep of equivalent wing planform	deg	DV
QWL	Wing leading edge sweep of equivalent wing planform	deg	DV
QWLR	Wing leading edge sweep	deg	IV
QWSA	Angle deflection for either trailing edge split elevons or inlaid control surfaces based on aileron characteristic	deg	EV
QWSE	Flap deflection angle at take-off and landing condition	deg	EV
QWSEH	Hinge-line sweep of trailing edge control surfaces	deg	DV
QWSEMX	Maximum angle deflection of flap	deg	EV

R	Distance travelled during mission segment	km	EV
RBCWN	Fractional of overall chord occupied by structural box		DV
RCWRTW	Value of fractional of overall chord occupied by structural box corrected for effect of thickness ratio variation across span		DV
RE	Non-dimensional Reynolds number		DV
RFUL	Fuel density	kg/m^3	EV
RGCW	Fraction of wing chord aft of leading edge to inertia axis		EV
RHCW	Fraction of wing chord aft of leading edge to flexural axis (70 percents semi-span)		DV
RHO	Box material property		EV
RLX	CG of centre of fuel volume		DV
RLUNM	Ratio of nose to main undercarriage lengths		EV
RLUPCW	Undercarriage CG position aft of mean ¼ chord point as fraction of MAC		EV
RLWAC	Wing aerodynamic centre location aft of wing quarter chord point as fraction of MAC		DV
RLWACK	Wing aerodynamic centre location of multi-kinks wing planform as fraction of wing root centreline chord		DV
RLWACTK	Wing aerodynamic centre location of wing constructed panel as fraction of wing root centreline chord		DV
RLWCC	Wing CG location aft of wing quarter chord point as fraction of MAC		DV
RLWCCTK	CG location of wing constructed panel as fraction of wing root centreline chord		DV
RLWCXTK	CG location of wing constructed panel as fraction of wing root chord at that panel		DV
ROIDX	Ratio of intake enclosing area to actual cross-sectional area		DV
ROIEI	Fixed area ratio for intake diffuser		EV
RPTD	Radius of nozzle transition duct entrance	m	DV
RSTIFF	Stiffness ratio		DV
RTP	Engine scale factor		IV
RTRN	Required load factor or turn rate for manoeuvre		EV
RTTRA	Circular arc (Take-off performance)	m	DV
RTW	Wing thickness ratio at inboard section	%	EV
RTWK	Thickness to chord ratio at wing kinks		DV
RTWLGI	Average wing thickness ratio in area of wing leading edge		DV
RTWM	Wing mean thickness to chord ratio		DV
RTWN	Equivalent thickness to chord ratio at centreline		DV
RTWSEMK	Average wing thickness ratio in area of trailing edge devices		DV
RTWT	Wing thickness ratio at outboard section	%	EV
RTWTGI	Average wing thickness ratio in area of wing trailing edge		DV
SEP	Required specific excess power for performance constraint comparison	m/s	EV
SEPCL	Specific excess power	m/s	DV
SLA	Landing approach distance	m	DV
SLD	Required landing distance	m	EV
SLF	Landing flare distance	m	DV
SLFR	Landing free roll distance	m	DV
SLGB	Landing braking distance	m	DV
SPTD	Planform projected area of two-dimensional nozzle	m^2	DV
SREF	Reference area of component	m^2	DV
STCL	Take-off climb distance	m	DV

STG	Take-off ground roll distance	m	DV
STGR	Rotation ground roll distance	m	DV
STLD	Total landing distance	m	DV
STO	Required take-off distance	m	EV
STTO	Total take-off distance	m	DV
STTR	Take-off transition distance	m	DV
SUMS	Shock absorber stroke	m	DV
SUMT	Main undercarriage tire stroke	m	DV
SW	Gross wing area	m^2	DV
SWET	Wetted area of component	m^2	DV
SWL	Total planform area of wing leading edge	m^2	DV
SWLF	Planform area of fixed wing leading edge forward of front spar	m^2	DV
SWSE	All trailing edge control surfaces planform area	m^2	DV
SWSEK	Planform area of each pair of trailing edge control surfaces	m^2	DV
SWSL	Total planform area of leading edge devices	m^2	DV
SWTF	Planform area of fixed section of wing trailing edge aft of rear spar	m^2	DV
SWTG	Gross area of wing trailing edge aft of rear spar	m^2	DV
SWWSE	Total wing planform area over trailing edge devices positions	m^2	DV
SWXTK	Total planform area of wing constructed panel	m^2	DV
T	Duration to perform mission segment	sec	EV
TAC	Type of aircraft		EV
TBD	Skin thickness required to meet bending and shear criterion (metal construction)	m	DV
TERMXF	Terms in mass estimation of wing trailing edge flaps	kg/m^2	DV
TERMXL	Terms in mass estimation of wing leading edge	kg/m^2	DV
TERMXT	Terms in mass estimation of fixed wing trailing edge	kg/m^2	DV
TIAF	Type of airfoils at wing inboard section		EV
TMAT	Type of materials		EV
TMISS	Type of missions (weapons and avionics selections)		EV
TOAF	Type of airfoils at wing outboard section		EV
TOTMAV	Total mass of avionics item	kg	DV
TPG	Engine thrust in various phases of flight	N	DV
TPGD	Total maximum sea-level static thrust of engines	N	DV
TPGDR	Maximum sea-level static thrust of reference engine	N	EV
TSEP	Required time to accelerate and climb	sec	EV
TSB	Effective thickness required to meet bending and shear criterion	m	DV
TTS	Skin thickness required to meet torsional stiffness	m	DV
TW	Thrust loading at various phases of flight		DV
TWB	Type of stores (weapons)		EV
ULNMS	Design load factor		EV
ULTN	Ultimate load factor for structural design (1.5.Proof factor)		DV
UW	Equivalent wing taper ratio		DV
UWBXF	Factor for utilisation of fuel in each tank		EV
UWF	Taper ratio of separate wing tanks		DV
UWK	Wing taper ratio in a series of trapezoidal panels		DV
UWRTW	Value of taper ratio corrected for thickness ratio variation across span		DV
V	Speed requirement to perform mission segment	m/s	EV
VD	Maximum design diving speed	m/s	EV

VF	Final speed at take-off and landing performance	m/s	DV
VFTG	Take-off speed	m/s	DV
VI	Initial speed at take-off and landing performance	m/s	DV
VIB	Volume of internal weapon bay	m^3	DV
VIDG	Volume of intake diffuser	m^3	DV
VMAXAV	Maximum volume of each avionics suite	m^3	DV
VPB	Total volume of engine bay	m^3	DV
VPTD	Volume of each nozzle transition duct	m^3	DV
VSTO	Take-off stall speed	m/s	DV
VUMB	Total volume of each main undercarriage bay	m^3	DV
VUNB	Total volume of nose undercarriage bay	m^3	DV
VVTD	Vertical speed at touchdown	m/s	EV
VWWF	Total fuel volume available for wing tanks	m^3	DV
WAV	Width of each avionics item	m	EV
WIB	Width overall of internal weapon bay	m	DV
WIB2C	Gap between weapon bay 2 and other bay	m	IV
WMAXAV	Maximum width of each avionics suite	m	DV
WNZI	Semi-major axis inner width of two-dimensional nozzle at a given x-position	m	DV
WNZO	Semi-major axis outer width of two-dimensional nozzle at a given x-position	m	DV
WPG	Engine bay width	m	DV
WS	Wing loading at various phases of flight	kg/m^2	DV
WTOTAV	Total width of each avionics suite	m	DV
WUMB	Width of main undercarriage bay	m	DV
WUMBC	Gap between main undercarriage bay and other bay	m	IV
WUNB	Width of nose undercarriage bay	m	DV
WWIB	Width of weapon in internal weapon bay	m	EV
WWIBC	Clearance on width of weapons in weapon bay	m	EV
XAR	Length overall of radar avionics suite	m	DV
XAWEPC	Length overall of weapon control avionics suite	m	DV
XAV	Total length of avionics compartments	m	DV
XAX1	Length overall of flight management avionics suite	m	DV
XCAUM	Distance from aircraft aft CG position to main undercarriage	m	DV
XCLUM	Distance from aircraft foerward CG position to main undercarriage	m	DV
XFR	Radome length	m	DV
XI	X-coordinate of diffuser centreline at front, centre and rear section from aircraft nose	m	DV
XIB1OD	Minimum distance of weapon bay 1 position from aircraft nose limit by wing box	m	DV
XIB1ODA	Minimum distance of weapon bay 1 position from aircraft nose limit by airfoil	m	DV
XIB1OR	Maximum distance of weapon bay 1 position from aircraft nose limit by wing box	m	DV
XIB1ORA	Maximum distance of weapon bay 1 position from aircraft nose limit by airfoil	m	DV
XIB2OD	Minimum distance of weapon bay 2 position from aircraft nose limit by wing box	m	DV
XIB2ODA	Minimum distance of weapon bay 2 position from aircraft nose limit by airfoil	m	DV
XIB2OR	Maximum distance of weapon bay 2 position from aircraft nose limit by wing box	m	DV

XIB2ORA	Maximum distance of weapon bay 2 position from aircraft nose limit by airfoil	m	DV
XID	X-coordinate of diffuser centreline from aircraft nose	m	DV
XIE	Distance of intake diffuser exit from aircraft nose	m	DV
XII	Distance of intake diffuser inlet from aircraft nose	m	DV
XP1O	Axial distance from aircraft nose to engine front face at outer edge	m	DV
XPEO	Maximum distance of engine position from aircraft nose limit by wing box	m	DV
XPEOA	Maximum distance of engine position from aircraft nose limit by airfoil	m	DV
XPIO	Minimum distance of engine position from aircraft nose limit by wing box	m	DV
XPIOA	Minimum distance of engine position from aircraft nose limit by airfoil	m	DV
XPTDR	Maximum distance of two-dimensional nozzle exit from aircraft nose limit by airfoil	m	DV
XTECG	Distance of aircraft centre of gravity from nose with empty mass	m	DV
XTTCG	Distance of aircraft centre of gravity from nose with full load	m	DV
XTZFCG	Distance of aircraft centre of gravity from nose with empty fuel tanks	m	DV
XUMBO	Axial distance from aircraft nose to outer edge of main undercarriage bay	m	DV
XUMBOD	Minimum distance of main undercarriage bay position from aircraft nose limit by wing box	m	DV
XUMBODA	Minimum distance of main undercarriage bay position from aircraft nose limit by airfoil	m	DV
XUMBOR	Maximum distance of main undercarriage bay position from aircraft nose limit by wing box	m	DV
XUMBORA	Maximum distance of main undercarriage bay position from aircraft nose limit by airfoil	m	DV
XUMT	Distance from main undercarriage to aircraft trailing edge	m	DV
XUNCA	Distance from nose undercarriage to aircraft aft CG position	m	DV
XUNM	Distance from nose undercarriage to main undercarriage	m	DV
XW2L	Distance of leading edge of half semi-wingspan from aircraft nose	m	DV
XWCL	Distance of leading edge of equivalent wing root chord from aircraft nose	m	DV
XWCQM	Distance of wing mean 1/4 chord point from aircraft nose	m	DV
XWFL	Distance of leading edge in area of wing fuel tank from aircraft nose	m	DV
XWIB1L	Distance of leading edge at weapon bay 1 from aircraft nose	m	DV
XWIB1O	Axial distance from aircraft nose to outer edge of weapon bay 1 front face	m	DV
XWIB2L	Distance of leading edge at weapon bay 2 from aircraft nose	m	DV
XWIB2O	Axial distance from aircraft nose to outer edge of weapon bay 2 front face	m	DV
XWKLK	Distance of leading edge of wing kinks from aircraft nose	m	DV
XWKLL	Distance of leading edge of wing tip chord from aircraft nose	m	DV

XWPGL	Distance of leading edge at engine bay from aircraft nose	m	DV
Y2IB1O	Spanwise station to outer edge of weapon bay 1	m	DV
Y2IB2O	Spanwise station to outer edge of weapon bay 2	m	DV
Y2P	Spanwise station of engine bay from aircraft centreline	m	DV
Y2PO	Spanwise station to outer edge of engine bay	m	DV
Y2SE1IS	Minimum spanwise station to inner edge of inboard trailing edge control surfaces	m	DV
Y2SEI	Spanwise stations to inner edge of trailing edge control surfaces	m	DV
Y2SEO	Spanwise stations to outer edge of trailing edge control surfaces	m	DV
Y2SL1IS	Minimum spanwise station to inner edge of inboard leading edge control surfaces	m	DV
Y2TGI	Spanwise station to inner edge of wing trailing edge	m	DV
Y2UMBO	Spanwise station to outer edge of main undercarriage bay	m	DV
Y2XTP	Extended panel	m	DV
YI	Y-coordinate of diffuser centreline at front, centre and rear section from centreline	m	DV
YIE	Spanwise distance of intake diffuser exit from aircraft centreline	m	DV
YII	Spanwise distance of intake diffuser inlet from aircraft centreline	m	DV
YIX	Y-coordinate of intake diffuser from aircraft centreline at station-x	m	DV
YMARM	Spanwise stations of individual components from aircraft centreline	m	DV
YPCH	Maximum distance between engine centrelines for twin-engine installation	m	DV
ZI	Z-coordinate of diffuser centreline at front, centre and rear section from centreline	m	DV
ZIX	Z-coordinate of intake diffuser from aircraft centreline at station-x	m	DV
ZTTCG	Reference vertical distance of aircraft centre of gravity from ground based on aircraft centreline	m	DV

CHAPTER 1

1 Introduction

This chapter gives an introduction to the research study, describing the definition of an unmanned aircraft, the advantages, and the need for Uninhabited Combat Aerial Vehicle (UCAV), enabling the research aims and objectives to be decided.

1.1 What are UAVs?

An Unmanned Aerial Vehicle, or UAV, is one of many similar types of aircraft, which do not carry a human operator onboard. UAV is defined as a powered, self-propelled aircraft that sustains flight through aerodynamic forces to provide vehicle lift, can fly autonomously or be remotely piloted, design to be returned and reused. This definition excludes lighter-than-air craft such as balloons, blimps, zeppelins, or airships; and it rules out ballistic missiles, which do not employ aerodynamic lift to achieve flight. Additionally it excludes cruise missiles and artillery projectiles. At the lower end of this scale are remotely controlled planes like those built and flown by modellers. Though a pilot is obviously not aboard the aircraft, a pilot throughout its flight controls the plane. UAV types currently fall into four broad categories.

Endurance – Endurance UAVs (EUAVs) are designed to operate at higher altitudes and longer ranges. EUAVs are operated over-the-horizon (OTH) and beyond-line-of-sight (BLOS), using satellite links for air vehicle control and sensor product downlink.

Tactical – Tactical UAVs (TUAVs) are designed to operate at lower altitudes and within line-of-sight (LOS) ranges of the controlling ground station. TUAVs are capable of missions of a few hours and use LOS links for air vehicle control and sensor downlink.

Small – Small UAVs (SUAVs) are designed to be man-portable and to operate within a few miles of the controlling station using LOS links. Small UAV missions may encompass a few minutes to a few hours.

Micro – Micro UAVs (MUAVs) are hand or smaller sized UAVs (six inches maximum). Their small size makes them less detectable and they are able to manoeuvre into spaces (i.e., open window of a building) where larger platforms could not go.

A similar type of aircraft is the remotely piloted vehicle (RPV), an unmanned vehicle capable of being controlled from a distance location through a communication link normally designed to be recoverable, which is essentially an enlarged version of the

remotely controlled plane. For many years, the military as target drones, test aircraft, and reconnaissance platforms have used RPVs.

In the Vietnam conflict, a thousand Lightning Bugs, remotely piloted vehicles (RPV) produced by the Ryan Aeronautical Co., flew more than 3000 reconnaissance sorties[70]. These missions, some of them up to 1400 nautical miles round trip, covered extremely hazardous territory. The Lightning Bugs saved the lives of countless manned-aircraft pilots and freed them for other missions.

UAV, on the other hand, differs from remotely piloted vehicle in that a pilot is not needed during most or all of the flight. Instead, computers control the plane. Most UAVs depend on pre-programmed flight paths guiding them to and from the area of interest, though human interaction is possible throughout the flight.

In the common terms "*drone*", defined as a land, sea, or air vehicle that is remotely or automatically controlled, RPV and UAV are used interchangeably; and these types of vehicles fall into three main categories.

- Pilotless target aircraft (PTA) are used to train personnel in air-to-air and surface-to-air target practise. They are also used for the testing of new weapons.

- Reconnaissance UAVs gather intelligence information over enemy territory, and the role of these vehicles in non-lethal.

- Strike UAVs or UCAVs are used as weapons delivery systems to take the offensive against an attacker with lethal military strikes.

Historically, UAVs have been primarily used for reconnaissance and observation but not for combat operations. Some of the better-known examples include the Navy's Pioneer, the Army's Hunter and the Air Force's Global Hawk, and Predator.

A new type of UAV is the Uninhabited Combat Aerial Vehicle (UCAV). As its name implies, the UCAV goes beyond observation and is designed to attack enemy targets. Though UCAVs are a subset of UAVs, they are differentiated by the fact that a UCAV is a lethal weapon system while a UAV is non-lethal. This is an important distinction.

1.2 Why UCAVs?

One of the greatest recent developments in military weaponry is the cruise missile, demonstrated by the Tomahawk. As represented repeatedly in Iraq and other world hot spots, the cruise missile can be used in identified attacks against heavily defended targets deep within enemy territory without risking a human pilot.

However, missiles can only be used once, and as their cost grows, the military must seek a more cost effective attack weapon. Although cruise missiles are closely related ancestors to UCAVs, they differ because they are one-way platforms, where UCAVs are two-way. Why UCAVs are more suitable than cruise missile: Colonel Michael

Leahy, the program manager of Defense Advanced Research Projects Agency (DARPA) Unmanned Combat Air Vehicle (UCAV) Advanced Technology Demonstration (ATD), replied that, "Every time you fire a cruise missile you lose all your high-cost targeting sensors. With UCAVs you keep the sensors on the vehicle and release the cheapest ordnance you can. Also, cruise missiles are fine if you know exactly where the target is, but they can't hunt down mobile, relocatable target[8]." Able to deliver a payload to a target and return to fight again, the UCAV combines the capability and relatively low cost of cruise missiles with the reusability of manned aircraft. This versatility would provide a battlefield commander with a wider range of options. Many visionaries see the role of UCAVs extending to operations such as SEAD and deep penetration strikes. In these roles UCAVs would complement manned strike packages.

The UCAV would launch from afar and fly to the target area, deliver precision weapons to attack the target, loiter in the area looking for better or additional targets to strike if necessary, and return to base after completing its mission, ready to fight another day.

Although keeping pilots out of harm's way is one advantage, it is not the main purpose of UCAV. The advantages of using UCAV are as followed:

- UCAV should have greater chances of survival than their manned complements. Survivability is based on how detectable the vehicle is to the opposition. Modern military aircraft are very large, heavy, complex, and expensive because of the human-related systems they must carry, for example, environmental systems, ejection seats, and instrumentation. By eliminating these needs, UCAV can be built much smaller, much lighter, and more aerodynamic than its manned counterpart. Being smaller, they would be harder to detect by radar. In addition, the absence of a cockpit means that the engine air intake can be buried in the upper surface, which is the most favourable position for maintaining low observability.

- The design of manned aircraft is strongly influenced by human safety factors, where UCAV can operate without regard for the physiological limitations of the human pilot in hazardous environments, including chemical, biological, and nuclear environments.

- The performance of the aircraft would no longer be limited by the tolerances of its human pilot, such as g tolerance, susceptibility to disorientation, or even physical endurance, but only by the strength of its airframe and the capabilities of its engine.

- The pilot in the cockpit doesn't always have the best idea of what is happening out on the battlefield. With UCAV, the operator is in the combat air operations centre, right where all the intelligence is gathered.

- Another major advantage of the UCAV is its cost. In today's environment of tight budgets, the military must find new ways to reduce its need for large numbers of expensive aircraft. Cockpit-less UCAV should be cheaper to build and operate than conventional strike aircraft. The solution accepted over

recent years has been to increase the survivability of manned aircraft through the use of advanced stealth treatments and avionics packages. The UCAV, on the other hand, could virtually eliminate the need for these expensive features. Because of its small size, UCAV offers greater "natural" stealth. In addition, the bulky, high radar reflective cockpit would not be needed so the aircraft could be given a very stealthy shape. Nor would extensive avionics be required because of the aircraft's expendability.

- Numerous weight penalties are associated with systems that are necessitated only or largely by the presence of a human pilot including displays, switches, g-seats, g-suits, oxygen, pressurization, and other environmental control systems. With the pilot onboard, the aircraft crew related features account for approximately 6 percent of the empty weight[92].

- Eliminating the requirement for a crew station gives the designer more freedom in configuring and packaging a new UCAV design. This reduces the layout of the vehicle in terms of structure, systems, and equipment location.

- Pilots need hundreds of hours each year in the air to maintain combat readiness, while UCAV operators can train in simulators.

UCAV should not be seen as an alternative, but as a system, which complements current manned aircraft and ground or sea-borne forces. For this to be possible to an overwhelming issue for the military, the UCAV must make to be affordable of future weapon systems.

1.3 Uninhabited or Unmanned

Being uninhabited is what differentiates UCAV from today's manned combat aircraft, but uninhabited does not necessarily mean unmanned. Under most UCAV concepts there is a "man in the loop." This means there is some level of human interface with the system to make decisions at various points in the mission. The man in the loop may operate from a ground station, another aircraft, or a ship; and the amount of interface varies between different concepts. There are some who envision UCAVs as fully autonomous systems where they seek and destroy the target without any human interaction at all. This type of UCAV is truly unmanned and would rely on its own onboard systems, such as automatic target recognition (ATR), to make decisions. The point is that all UCAV concepts call for an uninhabited aircraft, but there are different ideas as to the amount of man-in-the-loop participation.

1.4 The Need for Unmanned Combat Air Vehicle (UCAV)

In the 21st century, battle would be waged by fast, Unmanned Combat Air Vehicle (UCAV), would gain much of its ability from the absence of on-board humans.

The unmanned aircraft of the present have particular advantages such as cost or endurance, but they are either cruise missiles or reconnaissance vehicles. Air defence

systems are extremely tough to punch through without great risk to the pilots of the attacking aircraft. The Pentagon is interested in unmanned aircraft that can manoeuvre even more violently than manned fighters (which are limited to the pilot's tolerance of 9g) and that can take over some of the tough missions like the destruction of air defences and low altitude, high-speed reconnaissance[45]. The Pentagon is primarily interested in all-new UCAV concepts, particularly the tailless, stealth design. The following figure presents the evolution of unmanned aircraft from the period of Unmanned Aerial Vehicles to the revolutionary images of Uninhabited Combat Aerial Vehicle.

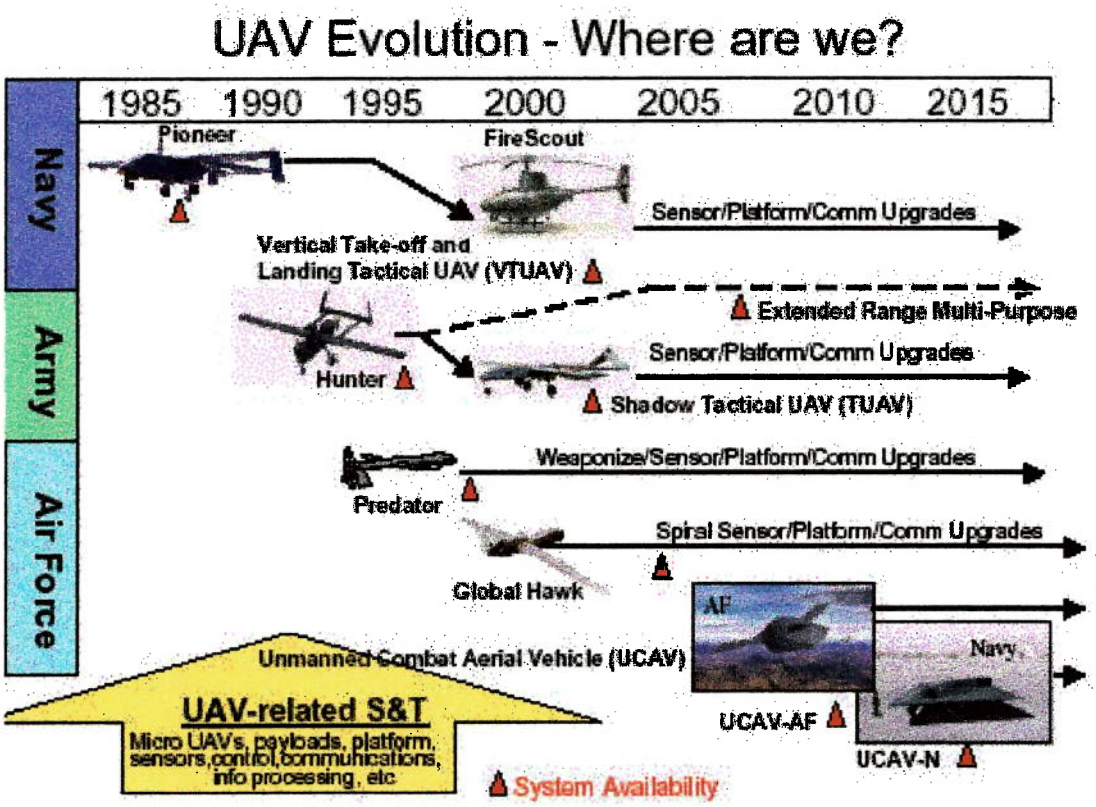

Figure 1-1: Evolution of Unmanned Aircraft[127]

The new UCAV could come in a range of sizes, depending on whether military planners want to use existing weapons or anticipate successful fielding of a new generation of small weapons. The UCAV is the common product of three converging trends:

- The need for pilots to concentrate on higher order tasks than simply flying an aircraft.
- The demand for more capable cruise missiles.
- The growing ability to build and operate very sophisticated unmanned aerial vehicles.

The UCAV is better suited for heavily defended high-risk targets than manned aircraft because it would keep pilots out of harm's way, and it would cost less to replace if shot down. This vehicle is best suited for those flight scenarios, which are determined to be dull, dirty, or dangerous by pilots. Dull scenarios require an extended length of time on station flying in a set pattern. Dirty missions include flight in environmentally hazardous conditions, exposure to chemical, or biological, agents. Dangerous missions require flight in a high threat environment where the probability of survival is low, for example the active Suppression of Enemy Air Defenses (SEAD) mission. Using UCAV for these three Ds would remove a huge burden from the manned combat aircraft.

With its small, low-observable design, the UCAV could penetrate at low altitude, get close to the target, take a synthetic aperture radar (SAR) imagery and transmit it back to a base station, have it interpreted, targets finalized and the strikes planned, allowing it to launch a weapon with great accuracy and be on the way home before enemy air defences could react.

However, the UCAV is a complement to manned aircraft, not a replacement. The UCAV will not completely replace the manned aircraft, but the presence, or absence, of a pilot is now a design trade that can be made in a logical way. Whereas manned aircraft is designed to be flown and maintained on an almost daily basis, the UCAV will be manufactured and then placed in extended storage until the time comes when it is ready to use. During peacetime and low-tension situations, the UCAV would probably not be flown, relying on the manned aircraft to project air power and control situations. During wartime, the UCAV would be deployed and conduct integrated tactical strike with the manned aircraft fleet.

The time for UCAV acceptance appears to be here for a number of reasons. First, declining force structure, people, and equipment necessitates innovative thinking about solutions that more cost-effectively accomplish missions. Secondly, technologies have emerged and matured as very significant enablers for unmanned missions. Finally, operations and support budgets are limited and there are opportunities for UCAV to provide lower operating cost and increased sorties rates.

With a potential service life of 40-plus years and a progressive migration to UCAV in all major roles, it is possible, even likely, that Rafale, Eurofighter Typhoon, F-22 and the Joint Strike Fighter are the last period combat aircraft that will be developed[99].

1.5 Objectives

The objective of this research program is to design an Uninhabited Combat Air Vehicle (UCAV), which leads to revolutionary design approaches by removing the constraints imposed by the pilots. The design is required to obtain a very compact and lightweight solution, thus reducing costs and vulnerability and increasing mission effectiveness.

In order to obtain first estimates of the major parameters that define the aircraft, a spreadsheet of initial sizing program for the military jet trainer aircraft has been set up

to consider the primary design variables and constraints requirements. They are then applied for a numerical design synthesis methodology for UCAV. The methodology incorporates advanced technology in the form of design for low observable (stealth) concept based on the "flying wing" design. This conceptual design will possess a flexible design layout for a wide range of configurations. The common thread behind all types of low observable technology is the desire to sharply reduce an aircraft's reflectivity and emissivity of optical, infrared, and acoustic or radar energy. A low observable aircraft will be more difficult for an opponent to detect and track.

The main objective of the project is concentrated on the packaging and configuration design aspects of the UCAV. Aircraft capable of being modelled with this methodology will have internal weapons carriage, internal engine bay providing one or two engines with two-dimensional nozzles, and air intake placed on the top of the aircraft in order to reduce the heat trial and hide the engine's compressor blades from radar detection. An option will additionally be set up for the external stores.

The design methodology will incorporate sufficiently accurate and realistic algorithms for the calculation of the geometry, packaging, layout, mass estimation, and aircraft centre of gravity. Additionally, the estimation of the aerodynamics, engine performance, stability and control, and performance properties of the aircraft will be developed, which are necessary for the investigation of the packaging and configuration design aspects of the UCAV. The aircraft geometry will be sized from the packaging layout and the requirements of the aircraft's missions. Finally, a numerical optimization routine will be linked to the synthesis, allowing the determination of optimum aircraft design variables for a given set of missions and performance requirements. A set of UCAV-optimized configurations will be made a comparison to find the perfect solution for the optimum design.

CHAPTER 2

2 Design Philosophy

The main purpose of this chapter is to describe the sufficient background and literature that are an essential part of a research program. In addition to the knowledge obtained from studying the earlier applicable information, the section aims to give an articulate explanation of the research and find out the 'state of the art'.

2.1 Background

The acquisition of literature relating to the UCAV technology has proven difficult in the past and will probably be difficult in the future, but the potential conclusion makes it a worthwhile quest.

2.1.1 Evolution of Unmanned Combat Aerial Vehicle (UCAV)

The history of unmanned flight began over two thousand years ago when a pioneering Chinese aviator flew "the recorded history's first remotely piloted vehicle (RPV) – a kite" with a piece of string as a downlink to the controller on the ground, over a breezy patch of Chinese landscape[56]. The first controlled flights, free from the restrictions of kite string, were subsequently achieved in the late nineteenth centuries. A pilotless aircraft, built by Samuel P. Langley, achieved the first heavier-than-air, powered, sustained, controlled flight. The steam-powered aircraft was named Aerodrome No. 5 and was launched over the Potomac River on 6th May 1896 for a flight lasting longer than one minute[84].

The kite sparked the imagination of inventors around the world for hundreds of years, and eventually led to the invention that would change aviation and the world forever, the airplane. Though unmanned aircraft held an inferior position to manned aircraft after the invention of airplane, accomplished by the Wright brothers in 1903, unmanned aircraft nevertheless continued to evolve. This fact became evident in World War I.

When the United States entered World War I in 1917, the Army and Navy were both concerned to develop their versions of the Flying Bombs. The Flying Bombs were among the first unmanned aircraft designed to deliver weapons; though very similar to cruise missiles, they were the earliest ancestors of the modern UCAVs. After great expense and effort were put into making these programs fly, very little success was achieved; but this did not prevent unmanned aviation from continuing to develop after World War I.

The advent of the radio control during the interwar years allowed the United States Armed Forces to experiment with the conversion of manned aircraft into unmanned strike weapons during World War II. Most of these efforts were unsuccessful, but this did not stop UCAV evolution. During the Cold War, the era of remotely piloted vehicles (RPV) was born under the code name "Red Wagon" in 1960, and a second program in 1961 code-named "Lucy Lee" followed it[29]. Unfortunately, both programs ran into higher than anticipated developmental costs and both were terminated. "Big Safari" was a quick-reaction management concept and would ultimately lead to success for unmanned reconnaissance aircraft. Through this program Ryan Aeronautical Co. was admitted a contract to modify four standard Q-2C Firebee target drones into reconnaissance UAVs designated as the 147A Firefly. It was not until the Vietnam War started in 1964, however, that UAVs got the opportunity to prove their operational worth. The 147s Firefly, later renamed the Lightning Bug for security reasons, were the workhorse UAVs during the war in Southeast Asia. They did battle damage assessments (BDA) after B-52 raids during Operation Linebacker, obtaining images of SA-2 sites in North Vietnam under a highly classified project called "Buffalo Hunter"[91],[134]. Their success led to the expanded role of UAVs, which led to the development of the UCAV. The first modern UCAVs were modified the 147s Lightning Bug; they were designated as the BGM-34A. Three variants of the BGM-34s were developed, but none ever achieved operational capability. Shortly after the official cease-fire in Vietnam, the BGM-34s were cancelled in the late 1970s.

The evolution of UCAVs was like the movements of the tide, constantly ebbing and flowing. Between World War I and the end of the Air Force's involvement with UAVs and UCAVs in 1979, there were numerous obstacles that caused the ebbs in the UCAV evolution. The obstacles included technological deficiencies, managerial impediments, political timidity, lack of service cooperation, competing weapon systems, and cost-effectiveness. These obstacles add to the UCAV's failure to achieve operational capability and stifled the Air Force's search of UAV technology in general. Throughout the 1980s, UAVs and UCAVs activities were essentially nonexistent.

UAVs and UCAVs had received and continued to receive significant attention in the 1990s. Two major operations in which the United States Armed Forces were involved were the Persian Gulf War in Southwest Asia and the peacekeeping operations in Bosnia. Though UCAVs were not used in either of these operations, UAVs were. The use of UAVs in these conflicts was significant in the advancement of unmanned aviation. The success of the UAVs in the Persian Gulf War and Bosnia led many planners and developers to consider roles other than reconnaissance and surveillance, that UAVs could accomplish in combat, and one of those roles is the Suppression of Enemy Air Defenses (SEAD) and lethal strike missions for UCAVs.

2.1.2 UCAV Review

"In the wee hours of the morning, a military conflict is about to escalate into war. A fleet of stealthy aircraft flies in low over enemy territory, several of them flip upside down and fire heat-seeking missiles into the enemy's radar system: mission accomplished. Suddenly fire is exchanged. The air vehicles retreat, except for one, which is shot down. The enemy searches the area and finds only the vehicle. No pilot will be found because there is no pilot[104]."

This type of scenario is what the US Air Force is envisioning as it designs a new breed of Unmanned Combat Air Vehicles. Where previous versions of unmanned aircraft have focused on surveillance and reconnaissance, the UCAV project combines advanced robotics, networking and communications technologies to make a smart system of fighting machines for combat.

There is still little information on how to design UCAV since this aircraft escapes from the bound of conventional ideas and thus opens a big window of new opportunities in combat aircraft design. Today, many university's researches, companies and organizations around the world are considering utilising this efficient concept.

2.1.2.1 University Challenges

The following two illustrations are presented.

In the United States, a group of seniors in the Department of Aeronautical and Astronautical Engineering at the University of Illinois had developed the Storm Shadow UCAV[32]. The design was completed in 1998 to satisfy a design project requirement. Upon completion, the Storm Shadow design was also presented to the American Institute of Aeronautics and Astronautics (AIAA) Undergraduate Design Competition.

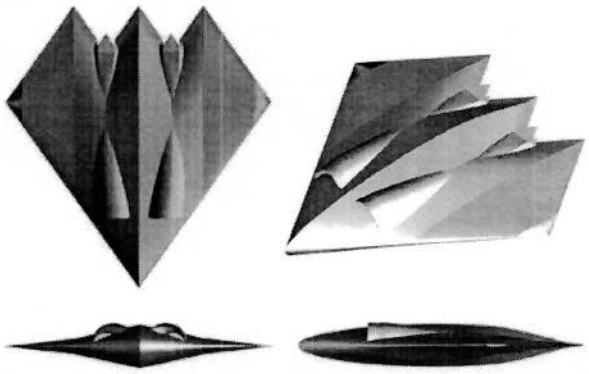

Figure 2-1: Storm Shadow UCAV

In the United Kingdom, the postgraduate students of the Aerospace Vehicle Design MSc course in the college of aeronautics; school of engineering, at Cranfield University had carried out the first phase preliminary design element of the U-99 Uninhabited Combat Air Vehicle (UCAV) or Uninhabited Tactical Aircraft (UTA) program[28]. The program of activities led to the completion of a detailed design study of a fully optimised configuration. The program committed 127,000 man-hours of staff and students in a capacity of Research Assistants. The cost value of this effort would be considerable in an industrial context. The first phase preliminary design of a baseline vehicle was completed in 1999, offered a first order indication of advantages and highlights many of the challenges still to be solved.

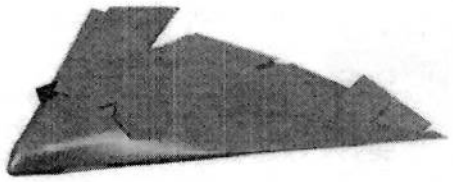

Figure 2-2: U-99 UCAV: Cranfield Aerospace Vehicle Design Group Project

2.1.2.2 Company Images

Britain is considering a UCAV for its future strike aircraft requirement. Senior military sources have revealed that seven companies, including British Aerospace and GEC Marconi, were contracted by the Ministry of Defense (MoD) to start work on the development of UCAV instead of a piloted bombers to meet its Future Offensive Aircraft System (FOAS) requirement to replace the RAF's Tornado[85,146].

Russia military experts are spurring various companies to begin working on a range of unmanned aircraft. Several contractors, the venerable Sukhoi design bureau among them, are devising concepts, although none have made it to flight-testing yet. Sukhoi will develop unmanned combat aircraft, capable of striking targets on the ground largely autonomously[49].

France's Dassault is already working on future UAV and UCAV technologies. A scale model UCAV demonstrator, the Aeronef de Validation Experimental (AVE) nicknamed "le Petit Duc," flew for the first time in July 2000. The tests were aimed at validating flight results with computer modelling. Dassault is developing its Rafale with the potential to act as a mother ship for UAVs and UCAVs. That means having the necessary equipment and systems on Rafale for data link communications with the UAVs and UCAVs[52,87].

Sweden's Saab has developed a UCAV demonstrator under its Swedish Highly Advanced Research Configuration (SHARC) program, a joint effort with the Swedish defense establishment. Wind tunnel tests of the UCAV design have been conducted, as well as extensive computer simulations. SHARC is expected to be a highly stealthy design, but it would not have high manoeuvrability or performance, in order to keep costs down[52,87].

Studies of advanced UCAVs are now being performed by the new European Aerospace and Defense Systems (EADS) conglomerate, which was established in the summer of 2000 through a merger of Matra-Aerospatiale of France, DaimlerChrysler of Gemany, and CASA of Spain. The company has produced conceptual designs for a UCAV that could be in service in the 2020 timeframe that features a flattened body with twin engine intakes, a tall twin tail, and a "zigzag" wing like that of the B-2 stealth bomber[52,87].

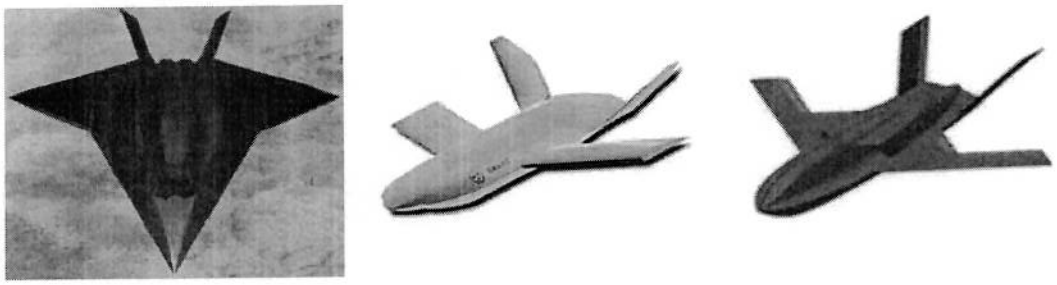

Figure 2-3: (Left) French's Dassault AVE UCAV, (Centre) Swedish's Saab SHARC UCAV, (Right) EADS UCAV

2.1.2.3 Organization Concepts

The U.S. Air Force is examining the potential for UCAV, using the Lockheed Martin F-16 as the basis of a demonstrator project, to explore technology requirements. These could either feed into all-new airframe designs, or are used as the basis for converting F-16 into UCAV for operational deployment[13].

The U.S. Navy is considering using the McDonnell Douglas F-18, as the basis of a proof-of-concept demonstrator, which could lead to a first-generation operational UCAV that, would follow the F-18E/F Super Hornet in 2020. The concept is likely to be the next lethal aircraft to fly from the decks of carriers – and probably from a large number of other naval vessels, including submarines[13, 18, 77].

2.1.2.3.1 Joint DARPA/Air Force

However, probably the Defense Advanced Research Projects Agency (DARPA) leads the biggest program that is presently being evolved in this field. DARPA involves with the U.S. Air Force to develop the UCAV program. The goal of the joint DARPA/Air Force UCAV Advanced Technology Demonstration (ATD) program is to demonstrate the technical feasibility for a UCAV system to effectively and affordably prosecute 21st century Suppression of Enemy Air Defenses (SEAD) and lethal strike missions within the emerging global command and control architecture. The UCAV ATD program's primary objective is to design, develop, integrate, and demonstrate the critical technologies pertaining to an operational UCAV system. The critical technology areas are command, control, and communications; human-systems interaction; targeting/weapons delivery; and air vehicle design. Life cycle cost models will be developed, which include verifiable estimates of acquisition and operation and support (O&S) costs. The critical affordability assumptions and technologies will be validated through concept and process demonstrations[130, 131].

DARPA and U.S. Air Force have selected four contractor teams for the first phase of the UCAV ATD program. The selected contractor team leads are Boeing, Lockheed Martin, Northrop Grumman, and Raytheon Systems. The Department of Defense (DoD) has provided specific mission objectives and guidance on overall system capability to the contractors, and each team will lead mission effectiveness and affordability trades to optimize a UCAV operational system (UOS) design. Based on

that UOS design, the industry teams determine the critical technologies, processes, and system attributes that a UCAV would have to possess to be effective. Each team lists those technologies, processes, and attributes that are immature and then develop maturation plan to reduce the number of items on that list. This plan is one of the major risk-reduction activities required by the ATD. They will then define a UCAV demonstrator system (UDS) to certify the critical technologies associated with their design[31, 90].

Boeing plans to use parts of its Joint Strike Fighter (JSF) to build a new-generation unmanned combat aircraft that could be used with F-22 and other manned aircraft handling the two toughest roles – striking deep behind enemy lines and suppressing air defenses[43, 44]. Boeing is also looking at a scaled-up version of the X-36 as a possible UCAV configuration. The company may call on the X-36 demonstrator for additional UCAV-related investigations to maintain their competitive position in DARPA's UCAV ATD program[43, 106].

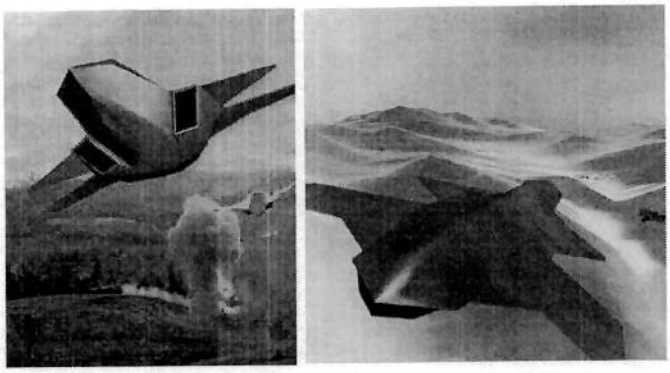

Figure 2-4: (Left) Boeing Concept Approach for UCAV, (Right) X-36 Larger Version Evolving into UCAV

Northrop Grumman is working on the design of a low-cost stealthy, reusable, double-delta planform/gull-winged UCAV of about half the size of a fighter aircraft to handle "dull, dirty and dangerous missions". One year later, the company has refined its gull-winged UCAV design to offer a smaller B-2-like aircraft for the DARPA's UCAV ATD program[76, 137].

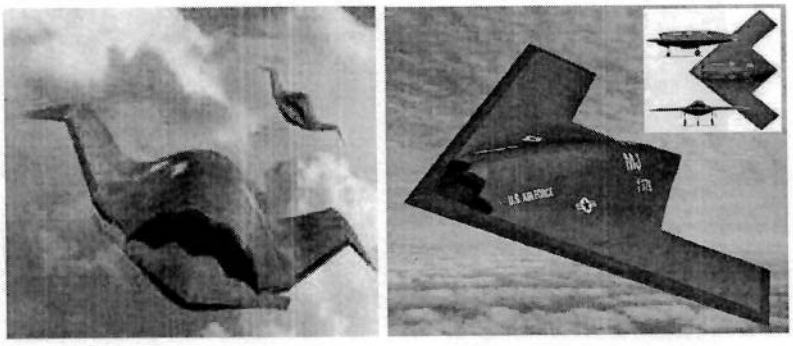

Figure 2-5: (Left) Northrop Gull-Winged UCAV, (Right) Northrop Latest Version of UCAV

Raytheon Systems approach for UCAV is looking at the entire system for ways to reduce life cycle costs while maintaining a very effective capability for the assigned missions. Aurora has participated as a member of the Raytheon team in the competition for the UCAV. Raytheon subsequently selects Aurora to perform the complete systems design for the actual full-scale Raytheon UCAV entry. The company will leverage substantial sensors, weapons, command, control, communication (C3) and vehicle technology-related investments that Raytheon Aircraft Company, team-mates, and the government are making, which have application to the DARPA's UCAV ATD program[110].

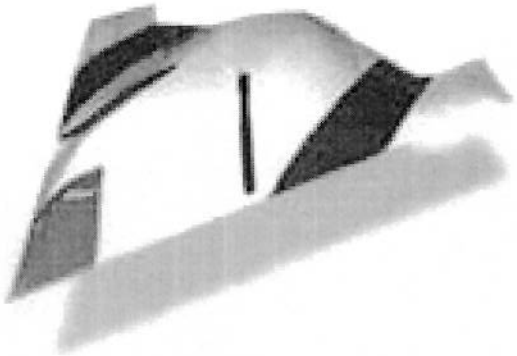

Figure 2-6: Raytheon-Aurora UCAV

However, Lockheed Martin already has contracted with the U.S. Navy to perform conceptual design studies of three UCAV types that include short takeoff and vertical landing (STOVL); vertical attitude takeoff and landing (ATOL); and one concept that's submarine launched[73].

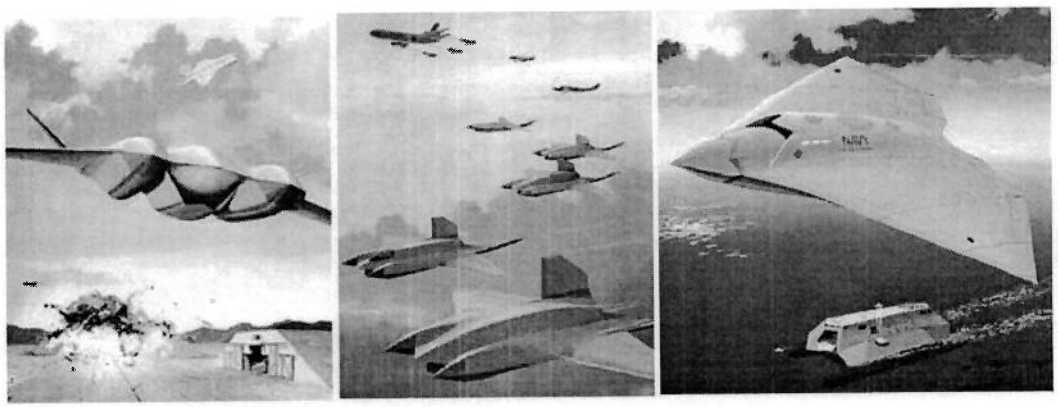

Figure 2-7: (Left) Lockheed Martin STOVL UCAV, (Centre) Lockheed Martin ATOL UCAV, (Right) Lockheed Martin Submarine Launched UCAV

Therefore, during the first phase of the program, only three industry teams have completed exhaustive mission effectiveness and affordability trades to optimize their

operational system design, identified critical technologies and issues, and planned their phase II demonstration program.

Finally, the DARPA and U.S. Air Force have selected Boeing to continue into the second phase of building UCAV to prove it is possible to have an operational UCAV by 2010 capable of destroying enemy air defenses in a high-threat environment as well as carrying out other strike missions. Phase two should be complete and UCAV should fly before the end of 2002[30],[136].

2.1.2.3.2 Joint DARPA/Navy

In addition to the joint DARPA/U.S. Air Force UCAV program, DARPA engages with the U.S. navy to develop the Navy Unmanned Combat Air Vehicle (UCAV-N) program. The goal of the joint DARPA/Navy UCAV-N ATD program is to demonstrate the technical feasibility for an unmanned system to effectively and affordably conduct sea-based surveillance, strike and suppression of enemy air defense (SEAD) missions within the emerging global command and control architecture. The primary objective of the UCAV-N ATD program is to design, develop, integrate, and demonstrate the critical and enabling technologies, processes, and system attributes (TPSA) pertaining to an operational UCAV-N system. The critical technology areas include, but are not limited to: shipboard integration, command-control-communications, human systems interface, targeting/weapons delivery, and air vehicle design and survivability[113],[116].

DARPA and U.S. Navy have selected two contractor teams for the first phase of the UCAV-N ATD program, Boeing and Northrop Grumman, while Lockheed Martin is working directly with the U.S. Navy on a classified program. The requirements for the UCAV-N ATD program are for a low-cost, carrier-based UCAV capable of up to 12 hours of autonomous flight. The platform also must demonstrate effective target identification and recognition, survivability, and lethal strike. The Navy desires to put UCAV-N into a low-cost Engineering and Manufacturing Development (EMD) phase in the 2007-2008 timeframe[48],[88].

Boeing's preliminary UCAV-N design calls for a 34-feet (10.36 metres) long vehicle with a wingspan of 44 feet (13.41 metres). The aircraft would stand 7 feet (2.13 metres) tall and would feature two large internal bays, allowing it to carry 4,000 pounds (1,814.37 kg) of munitions up to 650 nautical miles for Suppression of Enemy Air Defenses (SEAD) or strike missions[88]. Boeing has not yet released the details of its UCAV-N design.

As Northrop Grumman lost out to Boeing for a role in the first phase of efforts to develop an Air Force UCAV with DARPA, the company had already built a UCAV-N prototype, the Pegasus X-47A, just before winning one of two DARPA contracts for the Navy UCAV project in 2000[48],[88]. The X-47A is a scaled-down version of the eventual UCAV-N concept, sized specially for Pratt & Whitney's JT-15DC turbofan engine. The prototype is 28 feet by 28 feet (8.53 metres), and from a top view has a kite-like shape, as it is inherently stealthy. Payload would be 2,000-4,000 pounds (907.2-1,814.37 kg).

The full-scale X-47 UCAV-N will require more lift than is possible with the current kite configuration. The company officials have been looking at a "cranked kite" planform modification, adding rectangular wing extensions at the port and starboard points to provide additional lift to sustain 12 hours surveillance capability, required for the UCAV-N ATD program.

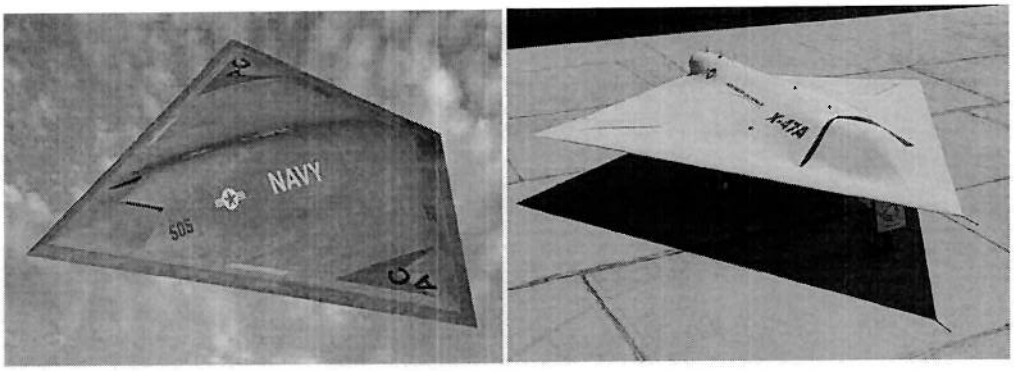

Figure 2-8: (Left) Northrop Grumman UCAV-N Concept, (Right) Northrop Pegasus X-47A Demonstration Aircraft

DARPA and U.S. Navy have recently awarded Northrop Grumman to continue its work on the UCAV-N prototype[113]. Under the $10 million contract modification, which runs until 2004, Northrop Grumman will conduct additional technology and risk-reduction studies, including modelling and simulation of autonomous flight operations from an aircraft carrier. Result of the Pegasus flight demonstrations later will be used in the UCAV-N program.

2.1.3 Encounters Renew Attraction of UAV

UCAVs became a bit less futuristic in October 2001 when they were used in combat for the first time over Afghanistan. The U.S. Air Force had been experimenting with a RQ-1 Predator armed with Hellfire anti-tank missiles earlier in the year. This was more of a technology demonstration effort than a scheme to actually arm the Predator. But when conflict broke out in the wake of the September 11th attack, the Predator was deployed to the Afghanistan theatre, including the armed version.

During at least one mission in October, it was used to track the convoy of a senior government official, and then to fire a missile near a bunker where the delegation took shelter. The mission was not successful, but accounts suggest the problem had to do with rules of engagement, not with the basic technology. As a result, further UCAV operations may take place. These first demonstrations of the UCAV in combat are reminiscent of the first use incidents of air-to-air combat in 1914 with pilots duelling with guns, bricks and other improvised weapons. They provide only a hint of their future potential[145].

The first use of the Predator as a UCAV raises an interesting question about future UCAVs. Considering that the U.S. Air Force and Navy have been studying unmanned air vehicles that perform like conventional strike aircraft. Their computer is briefed on a strike mission, and then the air vehicle flies out to the target and attacks it. The

Predator mission in Afghanistan suggests another alternative. The UAV serves as both a reconnaissance platform and a strike aircraft, searching out the target before attacking it. This raises some configuration questions as a relatively slow UAV like the Predator may be more versatile than a high-speed jet UAV for such missions.

Two UCAV demonstrators under development by the Air Force's Boeing and the Navy's Northrop Grumman, for future requirements, which are sleek, stealthy, and unmanned strike jets, should help to clarify the tactical potential of UCAVs.

2.1.4 UCAV Today

The Boeing Phantom Works advanced research and development unit and the Boeing Military Aircraft and Missile Systems Unmanned Systems organization are developing UCAV for the DARPA and the U.S. Air Force. Two X-45A air vehicles have been built, both having the same outer moldline with a stealthy, tailless design and aeropropulsion integration. The estimated 15,000 pound (6,800 kg) all-up mass X-45A vehicles are approximately 27 feet (8 metres) long, 3.7 feet (1.13 metres) high and 34 feet (10.5 metres) wide[135].

Foam technology originally designed for the manufacture of surfboards is finding application as the structural core material in the wings of the X-45A UCAV[101]. In X-45A wing production, the ribs, stringers, electrical conduit and other wing parts are machined into a single mold tool as part of the company's "Foam Matrix Core" (FMC) system. The FMC system from Foam Matrix is a patented process for producing net molded structures without the need for multi-piece assemblies. The system results in lofted composite parts that are lightweight and suited for structures like wings, control surfaces, doors and similar contoured parts. The X-45A entire wing, including all integral parts, is then molded to final shape as a single one-piece foam core. After curing, the foam core is wrapped in composite fibers and returned to the FMC mold tool for resin injection. After a final cure, the X-45A wing is removed from the tool and is ready for assembly. Benefits of the system include reduced parts count, seamless construction, reproducibility, shorter production-cycle time and lower cost. In addition, use of the foam eliminates hollow cavities in the structure. This improves damage resistance in handling and assembly and reduces the possibility of delamination or allowing water to enter the core.

The X-45A mission control console is incorporated into both the UCAV mission-control station trailer for local control at the test site and in the simulation laboratory for distributed control and operator workload experiments. It provides the operators with the decision aids and situation awareness necessary to control up to four air vehicles simultaneously[135].

On 22nd May 2002, the one of two Boeing X-45A UCAV technology demonstration aircraft made aerospace history by completing its first flight[10],[16]. This step marks the beginning of flight-testing of the first unmanned system designed from inception for combat. X-45A flew for 14 minutes at NASA's Dryden Flight Research Centre at Edwards Air Force Base in California, reaching airspeed of 195 knots and altitude of 7,500 feet (2,286 metres). Flight characteristics and basic aspects of aircraft operations, particularly the command and control link between the aircraft and the mission-control station, were successfully demonstrated.

Figure 2-9: Boeing X-45A UCAV Technology Demonstration Aircraft

Boeing designed the plane to have a 750-mile (1,200 km) range and fly at subsonic speeds. Officials expect each plane will cost $10 million to $15 million, or less than one-third the projected cost of the F-35 Joint Strike Fighter (JSF)[10].

A second X-45A will begin flying later this year, leading to the start of multi-aircraft flight-test demonstrations in 2003. Those coordinated flight tests are the technical heart of the program and the key to unlocking the transformational potential of this revolutionary weapon system.

Boeing envisions the X-45 taking part in strikes against high value targets, such as radar and surface-to-air missile (SAM) batteries. The next step on this path is the X-45B, which is currently being designed and will join the demonstration program in early 2005. It will be larger and more capable than its predecessors. The X-45B will include integrated avionics, two fully functional weapon bays, in corporation of low observable technologies, and provisions for the full sensor suite, and aerial refuelling. The X-45B will be a fieldable prototype aircraft that will lay the foundation for an initial operational system towards the end of this decade[10],[16].

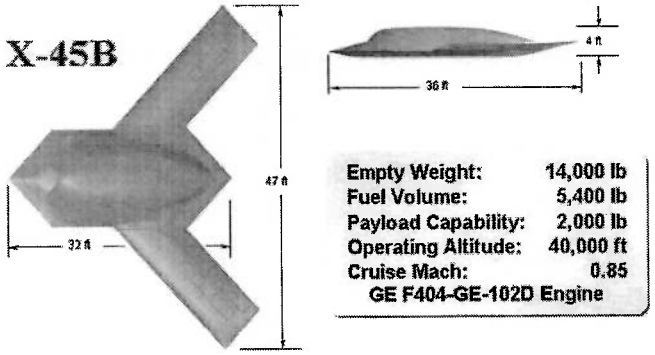

Figure 2-10: X-45B UCAV Fieldable Prototype Aircraft

2.2 Revolutionary Air Vehicle Potential

The UCAV concept was devised as a 'first-day' asset to be used primarily for the Suppression of Enemy Air Defenses (SEAD) role. The flying wing concept would lead a high potential for UCAV to accomplish this high-risk mission.

2.2.1 In Search of Flying Wing

At one time, designers regarded the flying wing as the ideal layout, promising large reductions in drag and structural weight, and so increased cruising speed and operating efficiency.

2.2.1.1 Where Flying Wing Came From

During the period around the Second World War, when it appeared that Nazi Germany might well conquer Great Britain and the Soviet Union, the Army Air Forces saw the need for a large bomber with intercontinental range. Such a plane, based in the U.S., must be able to cross the Atlantic and hit Germany with a large bomb load[37].

Jack Northrop saw this formidable requirement as made-to-order for his flying wing concept. Only a flying wing, freed of the weight and drag of a conventional fuselage and tail, could have the performance necessary to meet that need. Northrop began work on a full-scale version of his earlier designs, the N-1M since 1940. His marvellous XB-35 was succeeded in 1946 carried the entire concepts to the ultimate flying wing aircraft with a wing span of 172 feet (52.43 metres) and a length of 53 feet (16.15 metres). The XB-35 had a range of more than 7,500 miles (12,000 km) with a 10,000 pounds (4,500 kg) bomb load, powered by four reciprocating engines driving eight contra rotating propellers[37],[94],[133].

Plagued with engine and gearbox problems, the XB-35 design was adapted to be powered by eight turbojet engines and became the YB-49 all-metal flying wing bomber in 1947. Due to a barrier of technical and political problems, the YB-49 never reached production. Too advanced to be effectively manoeuvred by the control systems, of their day, the giant wings nevertheless went a long way toward validating Jack Northrop's faith in the basic design. Other planes were selected for operational use by the Air Force, however, and the flying wing concept was relegated to the future.

Jack Northrop never abandoned the hope that flying wings would one day find an application. In 1976, as stealth technology began to point toward the flying wing, this indicated to make an airplane hard for an enemy to detect, and even harder to attack. The new Advanced Technology Bomber (ATB) aircraft would have to cope with an exacting set of stealth requirements in order to survive in future combat scenarios. As a potential winner of the flying wing concept, Jack Northrop asked NASA to examine its aerodynamics and structural integrity. Their response was positive:

"...We re-examined considerable NACA XB-35/YB-49 wind tunnel data. Our analysis confirmed your much earlier conviction as to the load carrying and

efficiency advantages of this design approach, and studies performed for us by the major manufactures of large aircraft have further corroborated these findings.

We are continuing our related research and technology efforts, and have as yet found no reason to disagree with you as to the potential benefits of the tail-less span-loader approach.[94]"

Northrop was clear to move ahead with a stealthy Advance Tactical Bomber (ATB) concept based on the flying wing design. The flying wing configuration is kept alive today by the Air Force in the form of the Northrop B-2 stealth bomber. The Northrop B-2 was publicly unveiled for the first time on November 22nd, 1988. More than 15 years after the genesis of what was then called the Advanced Technology Bomber, the B-2 has emerged as a highly sophisticated weapon system capable of adapting to strategic or tactical roles, retaining for the U.S. Air Force an option to strike across hemispheric distances with an efficiency and probability of mission success more favourable than ever before. If it had not been for the wealth of aerodynamic data from the XB-35/YB-49 programme, approved as a concept by NASA in 1976, the Northrop Corporation would not have focused on the flying wing as the starting point for the world's most sophisticated aircraft.

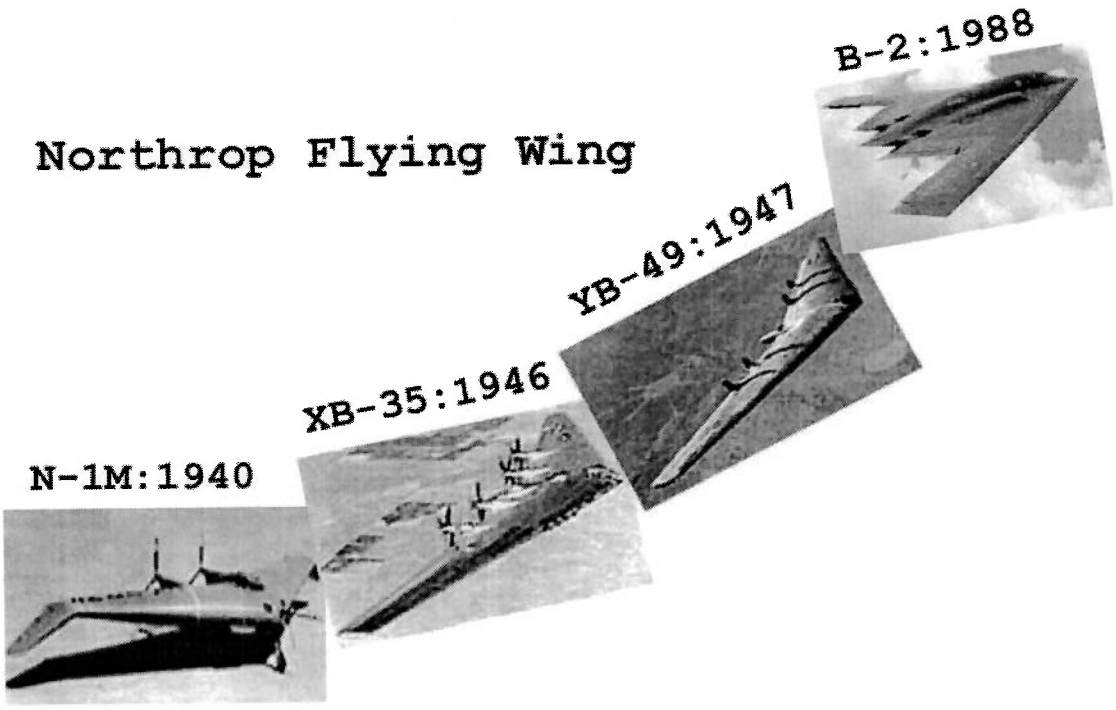

Figure 2-11: Northrop Flying Wing

2.2.1.2 Benefits Gain From Flying Wing

Rockwell studies of an advanced flying wing bomber showed that, its structure might account for only 13 percent of its take-off weight, compared with 20 percent for a conventional aircraft using the same technology. Boeing investigations of a giant

flying-wing freighter showed that it could carry half its maximum weight in payload, compared with less than 30 percent for a 747[117].

Since a pure flying wing possesses no fuselage and no horizontal tail surface, it may be possible to achieve a very low zero-lift drag coefficient. Alternatively, this gain may be taken in the form of a reduction in fuel consumption, engine power and take-off weight for a specified payload and range. The weight of the aircraft is distributed smoothly along the span of the wing, rather than being concentrated at its centre, so that the wing structure is less highly loaded, which reduces the bending moment at the root. Similarly, weapon bays no longer have to be confined to a narrow fuselage tube, but could be spread across the underside of the wing. An intrinsic aspect of this design is its stealth feature. Even the all-metal YB-49 was practically invisible to radar. On its first flight, the dumbfounded controllers had to come out of their building to find the plane above their heads.

The concept of the flying wing is, therefore, a better way to design aircraft, aerodynamically, structurally and because of its low-observable characteristics.

2.2.2 Tailless Scheme

Tailless UCAV is high on the list of interesting concepts because of the inherent benefits from the simple construction of a flying wing, its efficient low-drag aerodynamics, the ease of engine integration, and the natural low observability of the design.

In practice tailless aircraft is not easy to provide directional stability and control from a basically horizontal lifting surfaces. While tailless designs do exhibit relatively low drag, the theoretically achievable gains are not realised. Initially, the retention of a vertical fin is the most efficient way of providing directional stability and control. Additionally, longitudinal control is limited due to the short moment arm of the elevators. This means manoeuvre capability is limited and, as it may be difficult to use powerful high lift devices, the wing loading may be lower than on a comparable conventional design.

Recently, Boeing and the National Aeronautics and Space Administration (NASA) have developed a tailless research aircraft, the X-36, which could dramatically change the design of future stealthy fighters. The vehicle has no vertical or horizontal tails and uses new split ailerons (elevons) and a thrust-vectoring nozzle to provide yaw and only split ailerons to provide pitch directional control[35, 36, 122].

At the test altitude of 17,000 feet (5,181.60 metres), fighter-type manoeuvres such as 360-degree rolls and rolling pullouts were performed to demonstrate the agility of the X-36. A rolling pullout is a classic manoeuvre when dog-fighting. The aircraft is banked sharply in one direction, and then quickly rolled in the opposite direction while pulling Gs. Classified flight-test data show that the X-36 aircraft successfully demonstrated that a tailless aircraft can achieve levels of agility and manoeuvrability exceeding those of present-day fighters[115].

The tailless configuration has already been achieved in the Northrop B-2 stealth bomber. The split drag rudders on the outer wing provide yaw control and the outer

elevons afford primary pitch and roll control. The two inner sets of elevons are considered secondary control surfaces used only at low speed. The beaver-tail at centre controls pitch trimming and alleviate the gust loads.

Alternatively, Northrop Grumman has developed the new types of flight control surfaces providing for the Pegasus X-47A UCAV-N demonstrator. This tailless UCAV features two elevons at trailing edge to provide longitudinal control and four inlaids, small retractable control surfaces that take place of split drag rudders, to provide directional stability. The inlaids, two on the top of the wing structure and another two mirror-imaged on the bottom, are assumed to have a lower radar cross-section than split drag rudders on the wing's trailing edge[48].

Advantageously, a new tailless design with thrust vectoring and new types of control surfaces, would weigh less than a conventional aircraft and therefore probably cost less. Drag would decrease, so a given amount of fuel should take the aircraft farther. Stresses on the airframe would be reduced so that life-cycle maintenance costs would drop. Furthermore, the design would have less radar reflectivity, allowing it to get closer to a target without being seen.

2.2.3 Low Observable Features

To attain the necessary survivability in the projected battlefield of the 21st century, the UCAV would certainly require a significant amount of stealthiness to prevent the enemy forces from detecting its presence and thus compromise the execution of its mission.

Unlike some technologies, such as new materials or electronics, stealth directly affects the outside shape of the aircraft. Its influence on shape is important in the design of many subsystems. As the concept of the flying wing is a better way to design aircraft, aerodynamically and structurally, of all aerodynamic shapes and configurations on flying wing, tailless span-loader is intrinsically favourable to stealth technology required for UCAV design.

2.2.3.1 Definition of Stealth

Stealth is a word that comes from ancient roots, meaning, "to steal". Stealth is a design objective, not a single technical breakthrough, although some new technical features have been specially developed to attain it. It is also referred to as 'reduced observables', a slightly more accurate term. Like any design objective, stealth is compatible with some other objectives and conflicts with others, so the designers must arrive at a compromise, which is best for the specific mission.

The purpose of stealth is to improve the ability of weapon system to carry out its mission, by making it more difficult to detect. In the case of a true stealth aircraft, the goal is to achieve such a high level of stealth that the system will probably perform its mission without being detected at all. The important word here is probably. There is no such thing as an invisible aircraft. But neither is their certainty in a military operation. If the probability of detection is reduced, the chances that the vehicle will survive and complete its mission are accordingly increased. Stealth and its ability to

evade detection at range and in depth, is the only way for a single aircraft to penetrate modern air defences efficiently and at low cost.

Low-observables technology, or stealth, differs from other design qualities in a number of important ways. Its benefits are mainly apparent when it is given high priority, so that the aircraft is not just twice as difficult to detect as a conventional type, but ten or a hundred times more so. Since a variety of sensors would be required in the stealth concept, design of a stealthy UCAV requires careful trade-offs among different techniques. The great secrecy surrounding stealth programs is designed not simply to protect a particular stealth technology, as it is to protect the choice and mix of techniques that have been used in a specific system.

2.2.3.2 Designs for Stealth

To be stealthy, the aircraft must fulfil these accomplishments:

- Be hard to see with the eye
- The aircraft must absorb and scatter radar beams
- Heat from engines and moving parts must be minimal
- Contrails and other signs of aircraft should not be produced
- Make no sound (muffling the engines)

Stealth aircraft are, therefore, designed to minimize observable signatures in all areas including radar, infrared, aural, and visual, to achieve very low observable capability.

2.2.3.2.1 Radar Signature

In modern warfare, radar is the most reliable method for detecting aircraft. Radar is radio waves thrown out into air that bounce off of objects, return to the place of origin, and when calculated, can tell what something is, how far it is, and how fast it is moving. Reducing an aircraft's radar signature, or its vulnerability to being detected by radar, is thus a key element and perhaps the most important in the application of stealth technology.

The first and most important step in reducing an aircraft's radar signature is to reduce its Radar Cross Section (RCS). The RCS of aircraft is basically, how much echo the aircraft sends from radar. A successful stealth aircraft will have an RCS smaller than the radar wavelength it encounters, and thus will be for all practical purposes invisible to that radar. The two key methods of reducing RCS are to minimise the number of directions with high RCS returns and, to maximise the scattering of radar waves in all other directions. To accomplish these methods, the following aspects can reduce the radar cross section:

- Avoid surfaces at right angles to each other to limit the number of corner reflections. The shape of the aircraft is made to have an overall 'triangular' shape, making the overall shape reflect radio waves in such a manner that they

do not go back to the radar of the enemy or scatter radar waves in all other directions. The F-117 stealth fighter is a prime example of scattering. The entire aircraft is one, triangle. It has all flat surfaces, angled to deflect radar waves away from enemy base.

- Carry weapons and fuel internally, and shape a clean external geometry with no protuberances. The movement of the aircraft disrupting the air around it causes the turbulence. The shape of stealth aircraft is made so that is extremely aerodynamic, having the least amount of air resistance. This minimises turbulence, and the fuel costs, since the aircraft is not creating so much drag. The less turbulence, the less likely it is that the enemy's sensitive laser or radar detection equipments will pick up on the aircraft.

- The engine air intake design is also very critical for stealth, since it may allow radar waves to be reflected directly from the fan face. Good inlet design is virtually equivalent to poor stealth design. Therefore, it is necessary to achieve an acceptable compromise between the conflicting requirements of stealth and performance. The solution for this problem consists of the use of shielded intakes like the F-117 stealth fighter, and the use of long snaking (S-shaped) intake ducts that block completely the engine's fan face from the external view as on the F-22 tactical fighter.

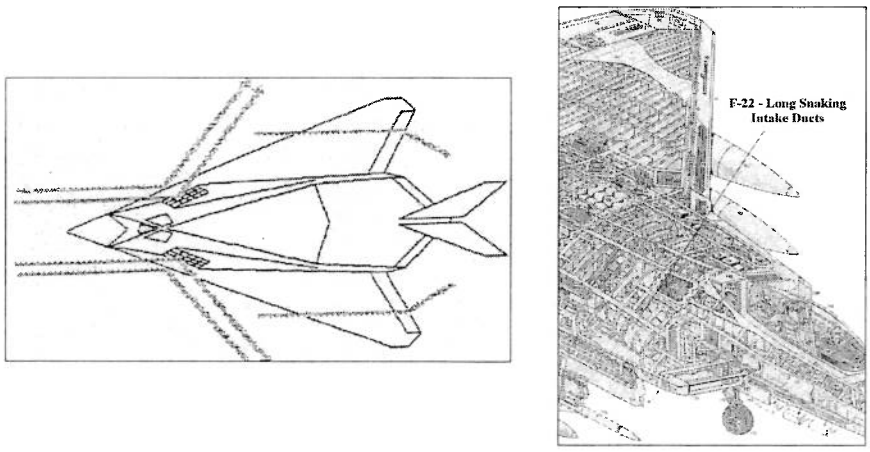

Figure 2-12: (Left) F-117 Shielded Intakes Reducing Radar Cross Section, (Right) F-22 Long Snaking Intake Ducts Reducing Radar Cross Section

- Reduction of radar cross section of nozzles is additionally very important, and is complicated by high material temperatures. The approach taken at Lockheed is to use ceramic materials, as assigned for the F-22. The ceramics may be either lightweight, parasitic sheets mounted on conventional nozzle structures or heavier structural materials forming saw-toothed edges[74].

- The wing leading edge is aimed to return in the same direction as the edge diffraction return from the trailing edge. This is done either by using identical sweep angles at the leading and trailing edges (thus, a wing with no taper, as

on the B-2), or by aligning the left wing leading edge at the same sweep angle as the right wing trailing edge (and vice versa).

- Once all wing returns are "aimed" in the same direction, the returns from doors, access panels, and other discontinuities can be "aimed" in the same direction by alignment of their edges. This is clearly seen on the B-2, where virtually every feature on the aircraft, including weapons bay doors, gear doors, inlets, nozzles, and access panels, is constructed using only lines, which are parallel to a wing leading edge.

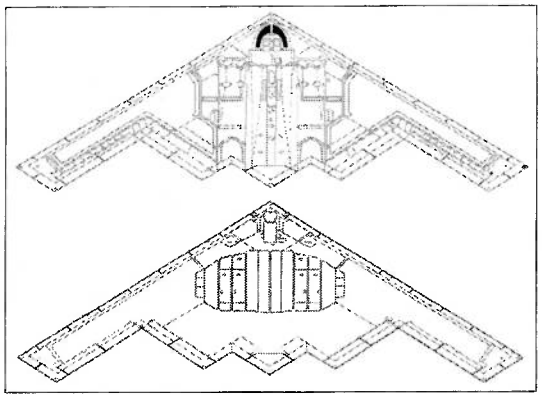

Figure 2-13: B-2 Alignment of Edges Reducing Radar Cross Section

- On-board antennas and radar systems are a major potential source of high radar visibility. The so-called in-band radar cross section is liable to be significant.

- In addition, the external skin aids in increasing the stealthiness of the aircraft. A common misunderstanding is that composite skin is used to make aircraft stealthy. In reality, many composites are partially transparent to radar, and expose the internal structure, wiring and components to the radar, which is the last thing a low observable designer wants. These components add up to an extremely large signature. In most low-observable aircraft, the outer surfaces of the aircraft are coated with a metallic paint, so that the radar cannot penetrate into the aircraft.

- Several special materials are used on the stealthy aircraft, including Radar Absorbing Materials (RAM), and Radar Absorbing Structure (RAS). RAM is used to absorb and kill ratio waves scattering from surface breaks instead of reflect them. RAS is used to minimise radar waves scattering from hard edges.

2.2.3.2.2 Infrared and Aural Signatures

Thermal, or infrared (IR), signatures are second in importance to RCS. To be stealthy, the aircraft must not give off too much heat. The heat not only makes it stand out on thermal imaging, but makes it a prime target of missile.

There are at least three aspects of the thermal signature:

- The heat of the engine components.
- The heat of the exhaust and other emissions from the aircraft.
- The heat of the aircraft itself.

The engine is the primary signature source. A useful technology here may be the use of high bypass engines buried internally behind a serpentine inlet duct; a technique referred to as line-of-sight blockage, to reduce the temperature of the gases, and the two-dimensional (2-D) nozzle to hide the hottest parts of the engine from as many angles as possible. One hundred percent line-of-sight blockage means that the front of the engine cannot be viewed from outside the aircraft. This feature is also beneficial to reduce the aural signature. On dry thrust, in the closed position, the 2-D nozzle restricts the rear view of the engines to a very narrow angle; thus, it would suppress both radar and thermal signatures. The 2-D nozzle is also effectively buried in a saw-toothed, again lowering the IR signature from every angle but directly behind the aircraft.

In addition, the airfoils play a role in increasing the stealthiness of the aircraft. Due to their behaviour at transonic speeds (about Mach 0.6 to 1.3), no shocks should form on the airfoils since the flow remains subsonic up to approximately Mach 0.95 (less than the maximum speed of the aircraft). This not only reduces the aural signature by eliminating the possibility of sonic booms, but also helps to reduce the IR signature since there is no temperature gradient across the shock.

Special material, Infrared (IR) Topcoat, is used on the aircraft to reduce the infrared signature, and ensure that the radar and infrared signatures are balanced.

2.2.3.2.3 Visual Signature

Visual detection is reduced primarily with camouflage paints, using colours and surface textures that cause the aircraft to reflect light at intensity and colour equal to that of the background.

2.2.3.2.4 Other Operational Aspects

Another operational aspect of stealth is its relationship to the electronic countermeasures (ECM) carried by the aircraft. ECM equipment installed on a low-RCS stealth aircraft can contribute a great deal to making the aircraft harder to detect. The lower the stealth aircraft's RCS, the less power will be needed by the ECM equipment to jam (burn through) and spoof (fool) the hostile radar. ECM is a last resort attempt to confuse the radar operator through jamming and ghost imaging.

To aid in keeping the aircraft stealthy, the UCAV would fly upside down except for takeoffs, landings, and when launching weapons. When inverted, the engine inlet, as well as landing gear doors, sensor access panels and weapons bay doors, are on top of the aircraft to avoid radar reflections that can be picked up by ground-based antennas. The extremely low observability of the UCAV will result in a reduction of the standoff distance at the weapon release point and will, in turn, reduce weapon sensor, guidance, and propulsion costs.

2.3 Aircraft Mission And Mission Control System

Survivability is a combination of susceptibility (the ability of a threat system to successfully engage an aircraft) and vulnerability (the probability that an aircraft will actually be damaged when a missile passes close enough to the aircraft to fuse). An aircraft can be made more survivable by reducing either its susceptibility to the threat system or its vulnerability to the exploded warhead, or a combination of both. The survival of UCAV on a particular mission is related to the type of mission being conducted, to the amount of support from friendly forces (susceptibility), and to the intensity and effectiveness of any hostile environment encountered during the execution of that mission (vulnerability). As signature reduction, or the reduction of the observables, makes the aircraft more difficult to detect and track, this approach would enhance the survivability of the UCAV.

Survivability of UCAV is a complex and critical issue. In the UCAV design, survivability features must be balanced carefully with objectives such as mission performance, cost, and maintainability. Further, increasing manoeuvrability beyond that which can be tolerated by a human pilot can increase UCAV survivability. Humans can tolerate +9g or +10g and –3g of acceleration, while UCAV might be designed to accelerate to ±20g. UCAV can be designed symmetrically to accelerate in any direction immediately. Anti-aircraft missiles are usually designed with a factor of three margins in lateral acceleration over that of the target aircraft, although a few missiles have acceleration capability as high as 80g. UCAV with a ±10g capability could outfly many missiles, and an acceleration capability of ±20g will make the UCAV superior to nearly all missiles[82],[83],[105]. Accordingly, in the future UCAV will be designed for very difficult threats at one end of the spectrum and relatively benign threat environments at the other end. The advantage of constancy will make the survivability tougher; use of multiple UCAVs in clusters will make it easier.

The advantages of unmanned strike operations are apparent. The UCAV will exploit various degrees of speed, stealth, manoeuvrability, and survivability and carry the necessary mission systems and weapons to make possible military actions deep within the heavily defended portions of enemy territory. Studies indicate that air-to-ground attack; especially suppression of enemy air defenses (SEAD), and deep penetration strikes will be the primary missions for UCAV.

2.3.1 Suppression of Enemy Air Defenses (SEAD) and Strike Mission

The effectiveness of combat operations depends to a great extent on the ability of aircraft to accomplish their assigned missions. Friendly aircraft are threatened by a variety of hostile enemy air defense systems. Action against enemy air defense systems, SEAD, may be carried out in either localised or campaign operations. Air, surface, or sub-surface forces of a joint force may be employed to suppress or destroy enemy air defenses. Surface and sub-surface organic firepower can concentrate on enemy defence systems within local areas of responsibility, allowing friendly aircraft to be employed against longer-range SEAD targets. SEAD activities may include the use of Electronic Warfare (EW) resources as well as lethal attack systems.

Suppression of Enemy Air Defenses (SEAD) is that activity that neutralizes, destroys, or temporarily degrades enemy air defense systems in a specific area by physical attack and/or EW. It is a critical mission area because its success or failure has a significant impact on all air operations and supported ground operations. Its activities complement both offensive and defensive operations. SEAD has two objectives:

- To minimise friendly aircraft attrition. Threat avoidance is the preferred doctrinal means for minimising aircraft attrition. This is usually accomplished by route planning, stealth, and standoff weapons.

- To maximise air power flexibility and effectiveness. In those instances when threat avoidance is not a viable option, for example, when threat locations are poorly known, or the demands of the military effort require the threat to be overcome to maximise air power flexibility, effectiveness, suppression or destruction of the threat is necessary.

SEAD is accomplished by destructive and disruptive action.

Destructive activity or physical attack offers more lasting and cumulative benefits through the attrition of enemy weapon systems and weapon control systems. It also provides the benefit effect of limiting the operation of enemy weapon control systems through the psychological effects on air defense operators of the threat of physical attack.

The objective of disruptive activity is to delay, disrupt confuse and/or deceive the effectiveness of the enemy air defense systems.

SEAD can, therefore, be accomplished with either fires or electronic means and by using either airborne or surface-based systems. For example, artillery can silence some defenses; airborne jammers can degrade acquisition systems; and escort aircraft may be tasked to defend aircraft conducting air-to-surface attacks, reconnaissance, air-mobile operations, search and rescue, and airborne command and control. Combining these assets increases the total effect of SEAD activities.

SEAD weapon systems also need increased stealth, range, and lethality. The fielding of stealth aircraft and longer-range standoff weapons allows the Air Force to strike targets with minimum exposure time in the lethal range of enemy air defence systems.

SEAD, as a result, is particularly appealing for UCAV because it is a 'dirty and dangerous' mission that pilots do not like to fly, but which is essential in combat air operations ranging from peacekeeping to full-integrated theatre warfare. Thus unmanned SEAD has the advantage of minimizing the inevitable resistance of pilots to expanding unmanned strike systems at the expense of manned platforms.

The interdiction mission will be more difficult since the UCAV must search for and find its targets based on cross signal from other theatre assets or information from its own sensors, transmit data back to the operator to choose aim points and responsibly give consent for weapons release that must be done in a very short time. This mission is particularly challenging because the targets are mobile, hard to kill, and defended by fixed and mobile surface-to-air missiles (SAM) and anti-aircraft artillery.

However, development of a revolutionary UCAV could improve efficiency in near future.

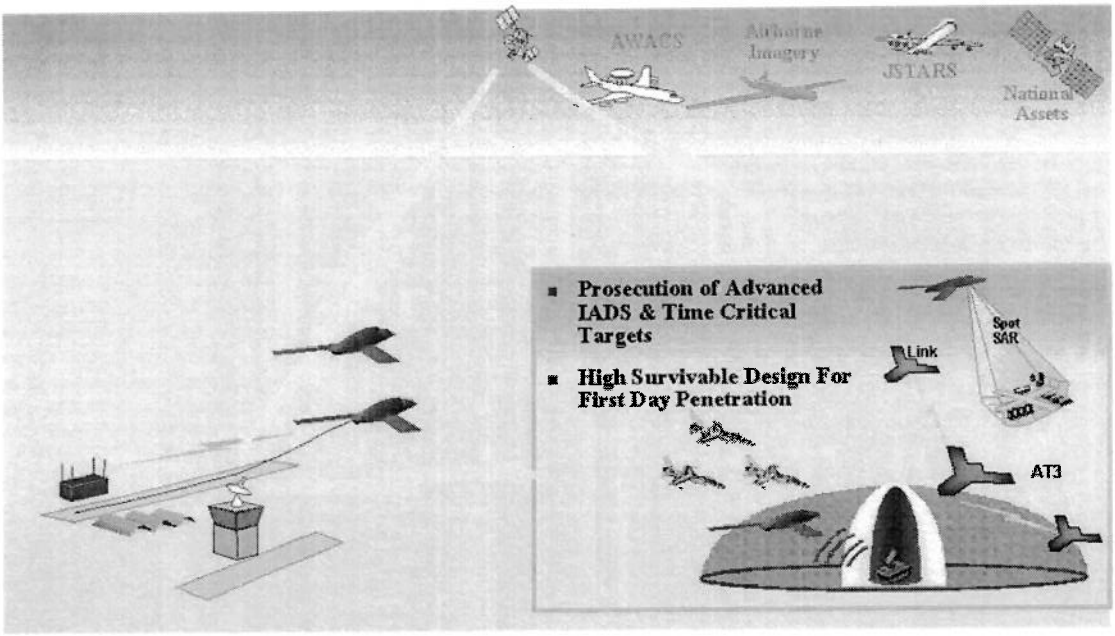

Figure 2-14: UCAV SEAD/Strike Concept[130]

The UCAV would perform these difficult and complex tasks, taking advantage of long-term presence in close proximity to the targets. Given the location, type of target, and desired weapons effects from Intelligence, Surveillance and Reconnaissance (ISR) and Command and Control (C^2) nodes, the UCAV performing a target attack mission would determine attack axes and tactics to optimize target acquisition, weapons effects, and indirect damage. The UCAV could operate as a low observable electronic support measures/electronic countermeasures (ESM/ECM) platform, by providing jamming against fire control tracking radar found around protected enemy targets, supporting multiple strike/bomber attack operations in stand off or close in orbits.

2.3.2 Alternative Roles for UCAV

During times of conflict, dominating the information spectrum has become as critical as occupying the land or controlling the air was in the past. Capturing rapid advances in computing power and capitalising on the corresponding speed of the information flow creates a tremendous advantage.

Information is collected; processed and distributed through an architecture that consists of command, control, communications, computers, intelligence, surveillance, and reconnaissance (C4ISR) assets. The strategic C4ISR assets are to provide capabilities that enable forces to generate, use, and share the information necessary to survive and succeed on every mission. These assets also include space platforms, such as satellites, which provide command and control of their battle.

Unmanned C4ISR is currently being done today with Unmanned Aerial Vehicles (UAVs). If UCAV, performing C4ISR missions, fly close to the enemy territory, the UCAV have the potential for significant contribution of providing the ability to supply responsive and sustained intelligence data from anywhere within enemy territory, day or night, regardless of weather, as the needs of the war fighter dictate.

Further in the future, UCAVs might be used for air-to-air combat. DARPA and U.S. Air Force are contemplating a role for UCAVs not only in the ground attack role, but even as fighter aircraft[47],[146].

2.3.3 UCAV Mission Effectiveness

The combat or mission effectiveness of UCAV on a specific mission is influenced by many factors:

- The availability of the weapon system for the mission
- The aircraft performance capabilities and handling qualities
- The target acquisition capability
- The type, effectiveness, and number of weapons carried
- The command, control, and communications and other supporting systems available
- The aircraft signatures and the countermeasures employed
- The tactics used and the terrain and weather conditions
- The ability of the aircraft to take a hit and survive.

The UCAV concept may contribute as an integrated part of the significant capabilities of these missions. This implies that the aircraft is a member of a tightly coupled system of systems and would work co-operatively with manned systems and exploit the emerging command, control, communications, computer, intelligence, surveillance and reconnaissance architecture to enable successful achievement of the proposed objectives.

2.3.4 UCAV Guidance

The basic component affecting UCAV capabilities is the control of UCAV. It is accomplished by three basic means, or combination of means:

- **Manual Control** wherein the operator(s) execute direct hands-on control inputs from a ground control station to establish air vehicle flight-path, speed, and altitude, and also pointing, and operation of the sensor package(s).

- **Pre-programmed Control** wherein the operator(s) pre-plan the UCAV mission profile and/or sensor package operation and upload or change mission requirements before and during the mission through the mission plan. Manual control override is available.

- **Fully Autonomous Control** wherein the UCAV mission profile and sensor package operation are totally planned from take-off to landing and uploaded prior to flight. Manual control override is available as an emergency procedure.

UCAV and sensor package control (manual) is provided through duplex uplink via line-of-sight, through communications relay, or via satellite. In the pre-programmed and fully autonomous modes of operation, mission monitoring and sensor package product download is provided via line-of-sight, communications relay, or satellite link.

UCAV mission planning always includes emergency profiles for lost link situations to provide the greatest possibility of reacquiring the link and safely recovering the air vehicle.

2.3.5 UCAV Operational Control and Communication

To facilitate operations in a combat environment, a flexible and agile control and communications architecture will be employed to ensure robust connectivity among large number of vehicles. The mission control station will be transportable and modular to the extent that all or portions of its functions can be land, sea, or air-based.

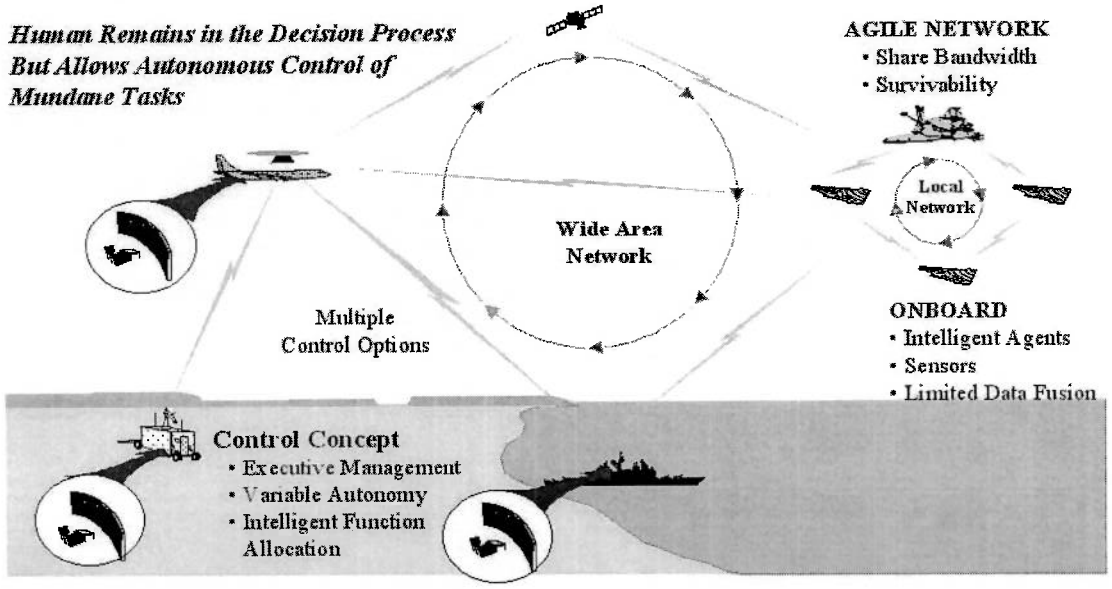

Figure 2-15: UCAV Control and Communication Concept[130]

A single control station using variable levels of autonomy will control multiple UCAVs. The controller will provide executive level mission management to remain in the decision process. Intelligent function allocation will allow autonomous control of

appropriate tasking. The controller may permit function changes such as from ground attack to air defense during a mission. Unplanned manoeuvres can be generated in real-time. Communications will be seamless with data passed through a variety of paths. Wide area and local airborne networks will allow redundancy among the force package and bandwidth sharing to ensure robust connectivity with the control station via line-of-sight, relay extension and/or satellite communications.

A variation of command, control and communication in combat environment is to use a manned mother ship and short-range communications for real-time control of UCAVs and increased battlefield flexibility. Lockheed Martin officials see an F-22 pilot controlling perhaps three unmanned aircraft armed with missiles flying in a fan tens-of-miles in front of him. The F-22 could remain electronically silent while receiving data from the UCAVs or from high-altitude reconnaissance aircraft or even satellites. With only two short pulses, the F-22 could have the UCAVs arm their weapons and fire[47]. This technology is now under study at Dassault Aviation to determine how the Rafale fighter could be used as a fighter leader to direct and co-ordinate an attack by UCAVs[62].

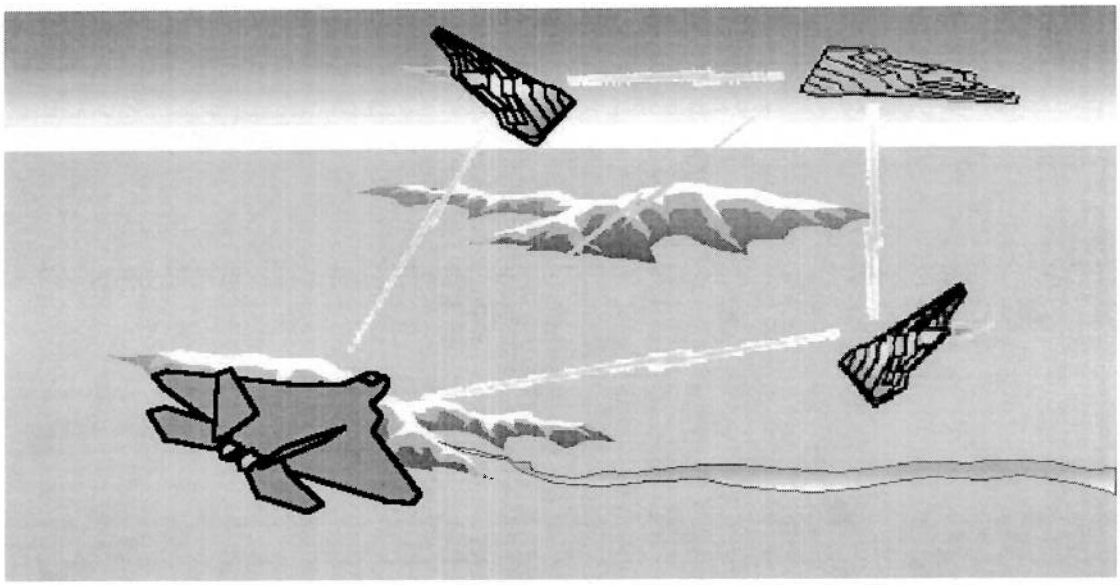

Figure 2-16: F-22 Could Control UCAVs to Perform Coordinated Missions

In future, the joint DARPA/Air Force UCAV ATD program will intend to develop the UCAV that has a high amount of intelligence on board, to make this aircraft looks, smells, and feels like a manned aircraft[68]. It should be able to detect targets; cooperate with other elements of a strike package; perform automatic rerouting during ingress (dash-out) and egress (dash-in); perform Synthetic Aperture Radar (SAR) imaging, decide which UCAV in a multiship flight should prosecute the attack; choose weapons and make decisions about bomb damage assessment; all without operator intervention. Moreover, if the UCAV is damaged or unable to operate within the rules of engagement, it should be able to automatically return to base and land without operator involvement. Those capabilities are distinctly different from other weapons that some may choose to portray as UCAVs.

2.4 Affordable Vehicle System

The UCAV weapon system will enable a new affordability paradigm by reducing operation and support (O&S) costs. UCAV, reflected in operations and support costs concepts such as the Uninhabited Combat Air Vehicle described in the study "New World Vistas"[82], or that proposed by DARPA[130,131,132], affords unique opportunities for affecting airpowers affordability. The potential for operations and support savings may be realized through a new paradigm in training, maintenance, and deployment. The key to this potential lies in two observations:

- Most non-combatant flying occurs as a result of the need to achieve and maintain pilot proficiency.

- Training to "operate" a UCAV can be made transparent to whether or not a vehicle is actually in flight.

The latter implies that training in the simulator and training in the aircraft are identical in principle and suggests an operational concept involving substantially less flying than today's manned systems demand. Typically, 80 percent of the life of a manned aircraft is spent flying training missions. Without the requirement to fly sorties to retain pilot proficiency, UCAVs will fly infrequently. The UCAV, on the other hand, would use simulation for training and its flight hours would be used primarily for combat or peacekeeping missions.

A pilot who interfaces with the aircraft through computerized interfaces and communication links will operate UCAV remotely. It will be possible to train pilots realistically without flying the aircraft a corresponding number of hours per month. It will only be necessary to fly the aircraft to check functionality and keep the aircraft in current flight status on a rotating basis – not to train the aircrews. This breaks the direct connection between realistic pilot training (which is required) and actual flight operations (which draw substantial recurring cost). Separating training from flight operations will allow O&S costs for the airframe to be reduced dramatically – perhaps up to 90% for this segment of cost[50,128].

UCAV pilots or operators are expected to maintain proficiency by practicing in a virtual environment. They would train using the same equipment that they would use in a real conflict. They would experience the same visual and aural cues that they would experience on an actual mission. Training this way avoids operating costs such as fuel, spare parts, and maintenance.

Designed for reduced maintenance, UCAVs can be maintained in flight ready storage. Storage of aircraft in a protective environment that permits rapid reconstitution of assets (minutes to hours) to meet wartime deployment or peacetime exercise requirements is a major and necessary part of the support concept. The study of a "hermetically-sealed storage bag" concept has been incorporated in recent combat UAV studies. Storage of aircraft in a dehumidified environment is a common practice by European air forces (Swedish, Danish, and British) as well as the U.S. Navy[128]. In addition, the Swedish, German, and Israeli armies employ dehumidification storage for a variety of mechanical and electronic systems, including ground vehicles, with excellent success.

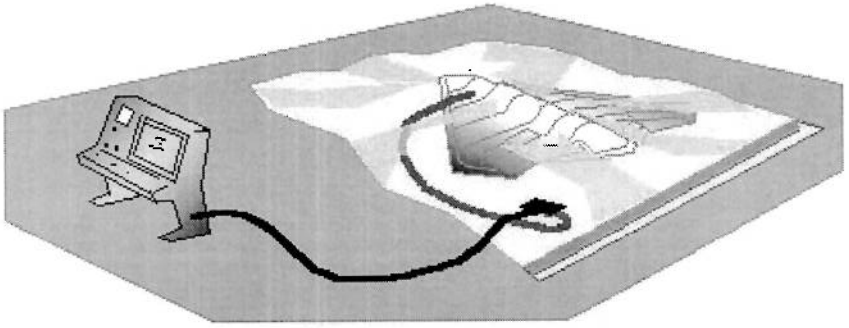

Figure 2-17: "Hermetically-Sealed Storage Bag" Concept for UCAV

The key to this result is the single requirement to maintain the relative humidity between 25% and 40%. Flight line bagging, "clam shell" shelters, hangars, and special storage containers have all been combined satisfactorily with dehumidification systems in both operational and support scenarios. Storage for ease of maintenance, rapid turnaround, and low cost appears to be readily available and will likely be used for unmanned aircraft in near future.

UCAV operational concepts from the joint DARPA/U.S. Air Force UCAV ATD program demand that the aircraft ultimately be stored for as long as 20 years, with periodic removals for exercises about every five years[67]. This has prompted Boeing to design a sealed humidity-controlled storage container about 15 feet (4.57 metres) wide, 6 feet (1.83 metres) high and more than 20 feet (6.10 metres) long, as shown in Figure 2-18.

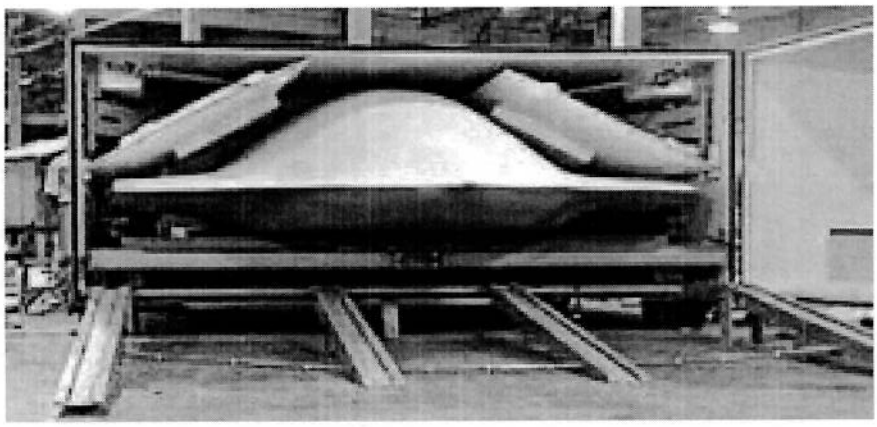

Figure 2-18: Boeing "Sealed Humidity-Controlled Storage Container" Concept for UCAV

This container, which is fabricated from glass-fibre materials surrounding a honeycomb core, is fitted with several interface ports so system health-checks can be run on stored vehicles. Wings are removed during storage and kept with the vehicles. The ports also will permit maintainers to monitor conditions inside the closed container and to download updated operational flight plans into stored vehicles as necessary. Conceptually, Boeing engineers envision as many as 50-100 vehicles being

stored at one site, with their containers hooked into a central maintenance computing system that will monitor the state of each of those stowed vehicles.

Cost of ownership for UCAV weapon system will be fundamentally different than those of the manned aircraft fleet. These systems will break the linkage between total force size and cost of ownership of the force. A reduced maintenance design with condition based maintenance, minimized on-board sensors, reduced fluid systems, and a modular avionics architecture will reduce touch manpower.

Over half of the O&S cost is direct manpower and indirect manpower support. Most of the direct manpower is assigned to service and maintain the aircraft (ground support). Anything that can be done in the design to reduce the manpower for unscheduled maintenance (adjustments and repairing failed items) or servicing the aircraft (moving the aircraft around the base, weapons loading, refuelling, inspection, and scheduled maintenance) will have a big impact on O&S costs.

Vehicle equipment should be made more reliable, so that it would operate for extended periods without maintenance. Aircraft should be designed with build-in test features and easy access to troublesome equipment. Since the UCAV does not have to be flown during peacetime to maintain operator proficiency, there is a large reduction in peacetime O&S costs by not having the maintenance and support manpower. A summary of the concepts is shown in Figure 2-19.

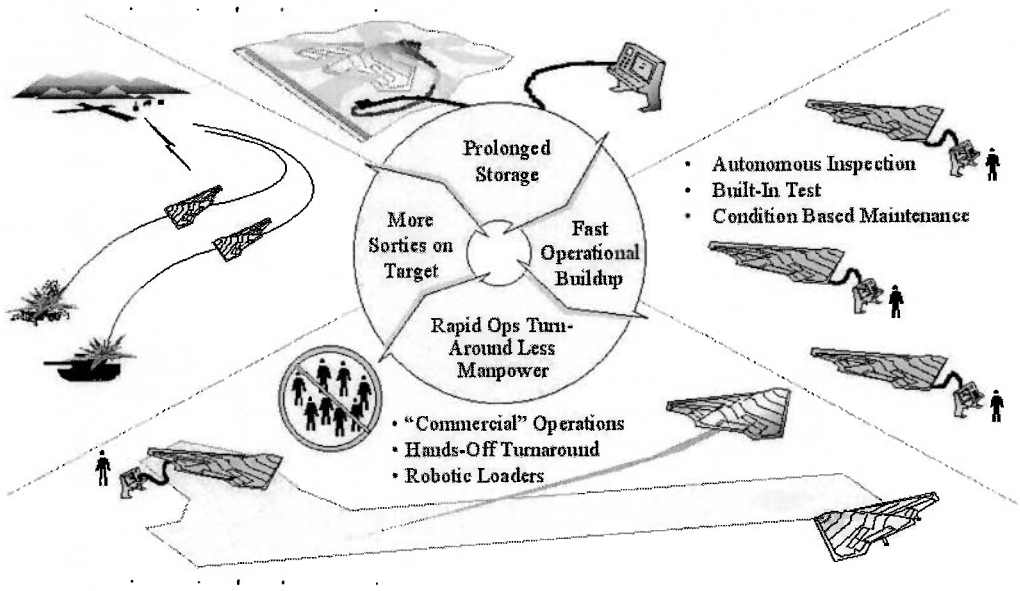

Figure 2-19: Storage and Deployment Concept of UCAV[130]

Primarily because UCAV "operators" conduct routine training in simulators, DARPA and other aerospace companies have suggested UCAVs will save 50% to 80% in daily flight operations and support costs compared to manned system, for example, F-16 wing, as shown in Figure 2-20[130].

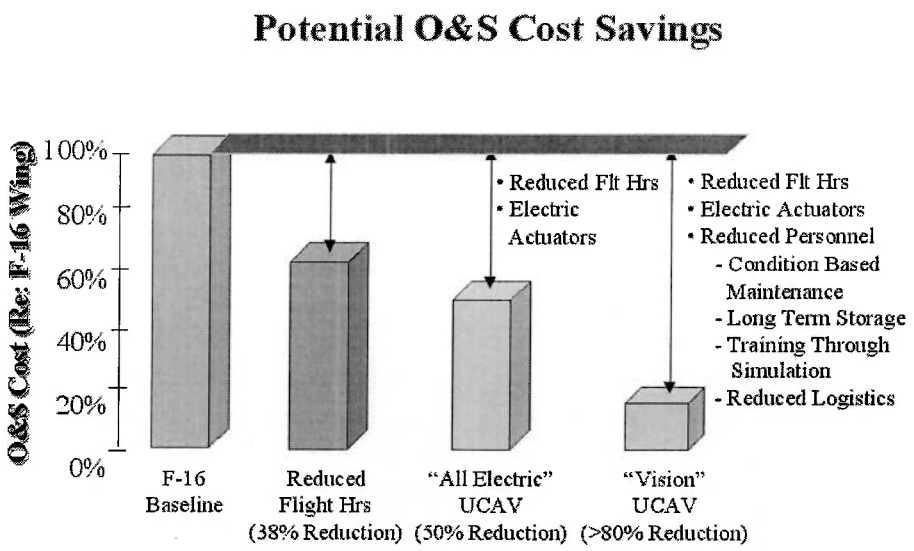

Figure 2-20: Estimated Cost Savings of UCAV Fleet[130]

In addition, O&S costs would be reduced by a change in crew ratios. The U.S. Air Force maintains a pilot-to-fighter ratio of about 1.3 to 1[26]. With UCAVs the ratio will be reversed. One operator will manage several UCAVs at once. The operator to UCAV ratio will be between one to four and six and will be possible because of the high degree of onboard autonomy that UCAVs are expected to possess. The UCAVs are anticipated to take-off, fly to the target, and return to base on their own[68]. The operator, under normal circumstances, would only be involved in authorizing weapons delivery. With the UCAV accomplishing some of the basic flying tasks on its own, the operator is free to concentrate on the cognitive aspects of the mission such as planning the mission execution.

In term of system costs, DARPA estimates that, UCAV will be approximately one-third the cost of a JSF, and the JSF itself is intended to be inexpensive compared to the cost of earlier fighters. This estimate would put the cost of UCAV at about $10 million to $15 million[10]. UCAVs are inexpensive because they do not need the life support systems, instruments, or escape systems required by manned aircraft. They will be smaller and will require fewer materials, which will also add to the savings[101].

With an emphasis on "affordable vehicle integration," system cost containment and innovative solutions to the architecture software development for Boeing X-45A UCAV demonstrators have been a hallmark of the effort[67]. Boeing's target is to limit new software for the system to 40% of the total. In other words, 60% of the software in the vehicles is reused from other programs and weapons such as the Joint Direct Attack Munitions (JDAM), the Apache helicopter, and the E-3 AWACS. Software reuse targets will become even more aggressive as the UCAV effort evolves and importantly saving costs.

Lower maintenance, training, operation and support costs, and system costs are only some of the advantages of UCAVs over traditional manned aircraft. As a result, the UCAV system will prove to be the affordable vehicle system in near future.

2.5 Flight Control System

The UCAV can be operated by an electrical flight control system utilising high speeds computers to control various systems functions emerged in parallel with fly-by-wire (FBW). FBW allows UCAVs to be very unstable, which makes them inherently much more manoeuvrable, because they are easier to flip around in one direction or the other. FBW enables the aircraft to handle this because the on-board computers make corrections to the flight controls and the flight path. FBW also makes the aircraft much safer because of the extensive redundancies available. A comprehensive build-in-test capability is also included, to ensure that the system is 'safe to fly' prior to each flight and to identify and locate failures.

All high performance aircraft since the mid-1970s have employed a fly-by-wire control system[11]. The use of a full-time FBW system reduces lags and overshoots – characteristic of a mechanical system with better kinematics, providing great improvements in flying qualities and major improvements in response time from the pilot-airframe marriage.

Control surfaces are operated by the computer in a complex pattern of integrated motions to reduce wear and tear on the wings and to decrease aerodynamic loads and buffeting. This reduces stress on structural materials and increases aerodynamic efficiency.

The control surfaces themselves could also be revised to some extent. Thrust vectoring has shown the potential to provide both longitudinal and lateral control. The utilization of nonaxisymmetric (or two-dimensional) nozzles facilitates thrust vectoring and thrust reversing capabilities, which improve the overall aircraft manoeuvrability and agility. Furthermore, they improve the reduction take-off and landing distances[14, 21, 22, 39, 81].

The nonaxisymmetric nozzles have been successfully accommodated for pitch vectoring and thrust reversing, which direct the exhaust flow away from the axial direction[15, 23, 81, 97, 98]. Furthermore, the cross-sectional shape of nonaxisymmetric nozzles (rectangular instead of circular) could be easily modified for thrust vectoring in the lateral direction, that is, yaw vectoring. Yaw vectoring controls at high angles of attack may increase jet aircraft agility and effectiveness. Additionally, yaw-vectoring capability at low speeds could complement aircraft control during short take-off and landing operations. Accurate integration of yaw vectoring concepts with nonaxisymmetric nozzles, which already possess a pitch thrust vectoring capability may provide a simultaneous pitch and yaw vectoring capability.

The X-36 has proved the feasibility of controlling actively a vertical tailless vehicle by the use of thrust vectoring for flight control[36]. The thrust vectoring enhances agility and makes the aircraft more efficient in cruise. The use of this approach has already been tested in tailless scale models with great success. The tailless X-45A UCAV design shares some features with the X-36. The wing shape is similar, as are the trailing-edge control surfaces and the yaw-axis-vectoring exhaust nozzle. The low-observable nozzle has no external moving parts and is still nominally classified. The X-45A is considerably larger than the X-36 and is autonomous, rather than being

remotely piloted, but there are enough similarities to reduce some of the basic design risks.

The Pegasus X-47 UCAV-N demonstrator has a fixed, circular nozzle, but the definitive design has a V-shaped exhaust, which does not appear to feature thrust vectoring. Instead the Pegasus has a simple flight control system, comprising a pair of one-piece elevons at wing trailing edge, and two sets of upper- and lower-surface 'inlays' flaps on the top and bottom of the wing structure. The elevons are used for pitch and roll control and the inlays flaps work like the split rudders on the B-2, providing yaw control and added drag to decelerate and increase descent angles. One of the issues the Northrop Grumman examined closely was the airflow effect the inlays flaps have on the elevons that are positioned directly behind them. The Pegasus demonstrator's principal task is to show that this configuration can be made to land safely on a carrier, which requires very reliable and accurate control of the landing flight path[121].

As part of the overall design, the flight control system design, qualification, and certification processes have to cover many UCAV configurations including the carriage of a wide range of aircraft stores. The potential variation in aircraft mass, inertia and centre of gravity, due to the carriage and release of a range of different stores is obvious. The aircraft and its flight control system have to be designed for carriage of a large number of such stores, including a very large number of possible symmetric and asymmetric combinations. Other significant factors that need to be taken into account in the designs are: fuel state, performance schedules, powerplant interface, and undercarriage operation and ground handling. All of these can have a significant effect on the design in term of stability, handling and airframe loading. For all combinations of stores, the flight control system can offer protection against over-stressing of the airframe and provide automatic stall and spin prevention[41].

In term of undercarriage operation and ground handling, the brake control system is required to be cooperated with the flight control system. Without the operator to sense ground contact, direction, deceleration, and runway conditions, the roll of UCAV brake control system safety and predictability become key characteristics with brake-by-wire (BBW) concept[27]. The brake control system must work reliably, safety modes must yield acceptable fault mitigation, the system must maintain predictable deceleration, prevent tire damage, and not introduce unacceptable direction changes.

In addition to the vehicle returning with potentially explosive fuel, the UCAV may be returning with armed munitions. The potential for a disaster just became much worse. Having a safe, reliable, always available, high performance brake control to ensure vehicle recovery and parking is critical to the safety of the mission and air base personnel.

In a combat situation, base choices may be severely restricted, and the safety and reliability of the brake control system may be the deciding factor in the deploy ability of the UCAV system. If the UCAV cannot be recovered, rearmed, replenished, and refuelled safely under any operational condition, its military value becomes severely diminished. The brake control system is a critical element in the achievement of these objectives.

2.6 Flight Safety

The safety areas that are corresponding to those of manned aircraft, such as flight system integrity and the safe carriage of explosives, are of course still essential to UCAV operations. Once the operating regime has been established, the impact of safety statistics on the system design must be investigated. Figure 2-21 offers an outline graphical means for identifying the most probable factors in accessing the safe operation of UCAVs. These elements are likely to be the most significant in the certification process.

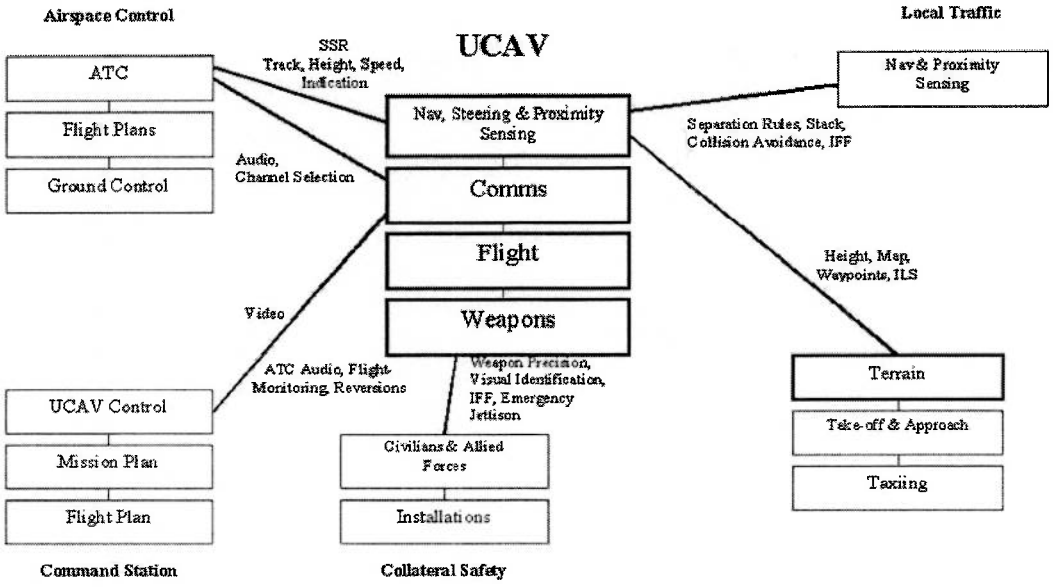

Figure 2-21: Safety Relationship within UCAV Environment[139]

The additional points in Figure 2-21 associate the safe operation of the UCAV with:

- The flight integrity of the air vehicle itself.
- Continuous monitoring by a high integrity command link to the control station.
- Communication with Air Traffic Control (ATC) while in controlled airspace.
- Clear adherence to separation rules.
- Safe terrain-clearance, steering and recovery to base.

These points are attached to the various operational phases of a mission that impact safety in the following tables, which lists the comparison between UCAVs and manned aircraft safety. This must be regarded as a preliminary list but it covers the types of issues being considered at present for inclusion in a safety case for the most capable UCAVs. Certain aspects such as the integrity of communications and those

comprising 'an interrogation mark' in the table pose special problems for the designer and will probably demand the most extensive consideration in the certification process.

Operational Requirement	Common Risk Issues	Uninhabited Combat Aerial Vehicles	Manned Aircraft
Effect of Forced Diversion	Emergency Landing Clearance	Emergency Hand-off to Local Operator for Approach, Landing & Taxi	
Effect of Terrain Impact	Risk to Persons and Property on Ground	Planned Safe-Cut-Down Zones?	Risk to Own Crew; Crew may steer to open space
Effect of Mid-Air Collision	Risk to Passengers and Aircrews; Risk to Persons and Property on Ground	Traffic Alert & Collision Avoidance System (TCAS)?	Risk to Own Crew; 'See (& Be Seen)'

Operational Profile	Common Risk Issues	Uninhabited Combat Aerial Vehicles	Manned Aircraft
Delivery & Hangarage	Electrical, Powered Equipment Tests, Equipping, Towing/Parking	Unpacking & Rigging; Release Testing	
Ground/Deck Handling	Day/Night Fuelling; Stores Loading & Checkout, EMI	Launchers; Remote Safe-Arm	Pilot Responsibility for Safe-Arm
Start-Up	Ground Crew Proximity; Hold-Downs & Chocks	Remote Commands to Ground Crew & Engine Start; Limited 'Pilot' Visibility	Pilot Direct Commands to Ground Crew
Taxiing and Holding	Speed Control & Separation; Response to Ground Control; Taxiway Steering	Limited 'Pilot' Visibility; Definition of Responsibilities; Fault-Case Ground Procedure; High Integrity Video Comms; High Integrity Ground Control	Pilot Accountability
Take-off and Climb	System Checkout & Abort Decision; Noise Abatement; Icing; Change-Over to Outbound Controller	Launch-Area Clearance; High Integrity Video Comms; Definition of Accountability	Pilot Accountability; High Integrity Cockpit Display & Controls (Redundancy Management)

Table 2-1: Comparison of Some Safety Issues – Uninhabited Combat Aerial Vehicles and Manned Aircraft[139]

Operational Profile	Common Risk Issues	Uninhabited Combat Aerial Vehicles	Manned Aircraft
Out-Bound	Height Separation; Way-Point Selection and Steering; High Integrity Flight Control & Terrain Avoidance; Emergency Jettison; Fuel-Tank Jettison	Small UCAVs Only: - Simplex Flight & Steering System? High Integrity Navigation and High above Terrain; High Integrity Video Comms & Comms Relay; Ground Controller to Flight Commander Change-Over; Intra-Flight Comms?	Life-Support Systems; Navigation Monitoring & Recovery by Pilot; Terrain-Following Radar
Controlled Airspace Operations	Unambiguous, Fault-Tolerant Communication with Multiple ATC Officers on Multiple Frequencies	RadioNav Integrity; ATC Comms Integrity; Unambiguous Voice Comms; TCAS? Multi-Source Comms Monitoring	Pilot Interprets & Executes ATC Commands
Uncontrolled Airspace Operations	See & Be Seen; Emergency Landing/Diversion; Terrain & Obstacle Collision Avoidance	Digital Map Display; Visual Sensor Integrity and Resolution; Cut-Down Integrity & Estimated Hit Location; High Integrity Low-Alt Comms Link	Pilot Operates Eyes-out Collision Avoidance; Navigation by Visual Terrain Features
Approach to Target	Mission Planning & Rehearsal; Rendezvous Timing	Dual-Monitored Target Area-Sensing; Dispensed CMs? Response to Flight Commander	Pilot-Monitored Target-Area Sensing; Essential Pilot-Protection Systems
Weapon Release	High Integrity Stores Management; Precision Targeting	Continuous Ground Control Visual Monitor/Command; Video Data Relay	Pilot Determines Target Identification; Responsible for Weapon Arm & Release
In-Bound	Changeover to Inbound ATC Officer	Changeover to new UCAV Controller	
Stack	Joining Procedures; Separation		

Table 2-2: (Continued) Comparison of Some Safety Issues – Uninhabited Combat Aerial Vehicles and Manned Aircraft[139]

Operational Profile	Common Risk Issues	Uninhabited Combat Aerial Vehicles	Manned Aircraft
Approach and Landing	Approach Procedures; Undercarriage, Flap & Brake Monitoring and Reversion; Landing-Aid Integrity	High Integrity Autoland, Autobraking & Autosteering	Visual/Procedural Approach

Table 2-3: (Continued) Comparison of Some Safety Issues – Uninhabited Combat Aerial Vehicles and Manned Aircraft[139]

It is certain that UCAVs must follow the same rule in the way that all aircraft operated with the most fundamental principle of safe operation, from the earliest years of aviation, that the general public must be protected from any form of flying machine. In point of fact, the first international treaty on flight in 1899 banned the release of weapons for this reason[140].

UCAVs are defined to be air vehicles that are designed to return to an operating base after each mission. It is reasonable to predict that UCAV certification will thus follow at least the current aircraft release procedures for an equivalent role, although some of the missile certification issues may also be included in the early stages of the debate. The air-vehicle certification processes that are an intimate relation between all aircraft and UCAVs are:

- The background in which the vehicle was to be used.
- The roles of the operators of the vehicle and its supporting ground systems, such as ATC and Navigation Aids.
- The ability of the vehicle to continue in its safe operation in all its specified operational conditions.

UCAVs will involve additional safety considerations related to the carriage of explosive ordnance since the weapons must be armed or released.

The ability to maintain safe flight is basically associated with a range of redundant and reversionary features in the design. A logical process of proofs emerges that combine structural and reliability testing with the analysis of failure modes and reversions in order to prove that each design has low probability of unsafe air-vehicle failure. The UCAV systems will require these processes of verification and validation. The responsibility of the UCAV designer is to interpret all the rules listed in the tables above in terms of the implementation features of the air-vehicle and its supporting infrastructure. Predictions of safe UCAV operation should be offered similar to those of existing air operations, including further safety designs on weapons carriage.

The interest in using UCAVs for many different operations, as well as tasks currently out by manned aircraft, has provoked a valuable and necessary debate on the on-going safety of these systems.

2.7 Weapons Systems Challenge

Throughout the history of unmanned aviation, UAVs and UCAVs have had to compete with manned aircraft and cruise missiles for funding, operational use, and consideration in the aviation world. Today, UCAVs face additional competition from newly emerging space-based systems. The comparison and contrast of UCAVs against the three types of challenging systems will be described.

2.7.1 Manned Aircraft

Under most concepts UCAVs do not replace manned aircraft, but they do complement manned aircraft by flying those missions most appropriately suited for unmanned platforms – dull, dirty, and dangerous. As previously discussed, some advantages that UCAVs have over manned aircraft are as followed:

- UCAVs offer a tremendous cost saving over equivalent manned systems. Without the cockpit, UCAVs should be cheaper to build and operate than conventional strike aircraft.

- By eliminating the cockpit and pilot-related systems, UCAV can be built much smaller and lighter that will have greater chances of survival than manned aircraft.

- The pilot is strongly influenced by human safety factors in hazardous environments, including chemical, biological, and nuclear environments, where UCAV can operate without regard for the physiological limitations of human pilot in these factors.

- The limitations of human capabilities to put human beings in fighter aircraft are referred to high gravitational force, susceptibility to disorientation, or even physical endurance. The development of UCAV will permit up to double-digit G turns that will able to outperform enemy fighters both on the ground and in the air.

- Without the cockpit, the UCAV designer has more freedom in configuring and packaging a new configuration that reduces the layout of the vehicle in terms of structure, systems, and equipment location. In addition, a new UCAV design will reduce numerous weight penalties associated with systems that are necessitated by the presence of the human pilot.

- UCAV technology promises to be as effective as manned aircraft, particularly in the SEAD role. The first mission that UCAVs fly will most likely be SEAD, which is one of the most dangerous combat missions flown. Without a human on board, UCAVs will be able to take some risks that otherwise would not be prudent. This point leads to what is probably the most obvious benefit that no friendly lives will be risked to accomplish the mission.

Although the UCAV is potentially a high payoff system, it is also a higher risk solution than manned aircraft. The disadvantages of operating UCAV are to be realized.

- A UCAV is a higher risk solution to the requirements of the combat air forces because it is a new technology, and leaders and planners have little or no experience with UCAVs. They do have confidence, however, in manned systems such as JSF and F-22. The Air Force has a long story of developing, procuring, and modifying manned aircraft; and there is more corporate knowledge in dealing with the more mature technology.

- The other risk in employing UCAVs is integrating them into the force structure. They may have to operate with manned aircraft, and this integration presents problems to the planners by planning UCAVs to complement with manned aircraft in completing the missions.

- A final advantage that manned aircraft have over unmanned aircraft is greater flexibility. It is unlikely that technology will give rise to a computer that duplicates the human brain, all five human senses, judgement, and human intuition in the near future. Having a man in the loop can make up for some of this lost of human qualities and flexibility, but it will not be the same as having a man on the scene.

2.7.2 Cruise Missiles

The cruise missiles, one of UCAV early ancestors, are another type of weapon systems that UCAV will have to challenge with. The benefits that UCAVs have over the cruise missiles are consequently described:

- UCAVs and cruise missiles are very similar in many ways, but the main technical difference is that cruise missiles do not come back when the mission is complete. The fact that UCAVs are reusable gives them an advantage in term of cost-effectiveness. With UCAVs employing small, inexpensive, smart weapons, they could destroy targets at a fraction of the cost of weapon systems such as the $1 million Tomahawk land attack cruise missile (TLAM). Each time a TLAM destroys a target, that weapon system, including its engine, airframe and sensor suite, is disappeared. With UCAV, the only part of the system that does not return for subsequent use is the munitions.

- Additionally, UCAVs promise to be more flexible than cruise missiles. UCAVs have the capability to accept mission changes, abort missions without self-destructing, and strike relocatable targets. Having a man in the loop affords UCAVs a great deal of flexibility. Colonel Leahy, the program manager of DARPA UCAV ATD program, points out that, "Cruise missiles are launched from a long way out. UCAVs operate from much closer because of their reduced signature. This will allow for better target acquisition, and it will compress the time between the moment the decision is made to destroy the target and the moment the target is actually destroyed[8]." The UCAVs are launched from afar and fly to the target area, deliver precision weapons to

attack the target, loiter in the area looking for better or additional targets to strike if necessary, and return to base after completing its mission.

- There is a class of standoff weapons that includes the joint standoff weapon (JSOW) and the joint air-to-surface standoff missile (JASSM), which can be launched from manned platforms[112]. These weapons are very capable and are competitive with UCAVs; but because these systems must be launched from manned platforms, all of the advantages that UCAVs will potentially have over manned aircraft will also be advantages over these systems. These advantages include cost-effectiveness and minimal risk to pilots; and if the aircraft stands off to minimise the risk to the aircrew, the cruise missiles lose their flexibility and perform similarly to other long-range missile systems like TLAM.

There are, however, some advantages that cruise missiles have over UCAVs.

- The major advantage is that the armed forces are familiar with cruise missiles. The technology has been around for a long time, and the risk in investing in further cruise missile technology is low compared to UCAVs.

- The cruise missiles have been successfully employed in combat, and they have been integrated with manned assets successfully. Cruise missiles do not have the airspace concerns that UCAVs have because planners have learned how to deconflict airspace for cruise missile use.

- Command and control is not nearly the issue with cruise missiles as it is with UCAVs. Cruise missiles are fully autonomous, and their command and control and bandwidth requirements are minimal.

2.7.3 Space-Based Systems

A third potential competitor for UCAVs is the space-based system. There are many concepts within the DoD's research and development circles that employ space-based weapons systems capable of delivering precision force against ground-based targets. These systems will have the potential to project power to any point on the earth with minimal sensor to shooter delay, and they will provide decision makers a near continuous coverage of all global hot spots.

The greatest advantage that the space-based systems will have over UCAVs is that it will take time to mobilize and deploy UCAVs to the theatre of operations. Space-based systems will be in place continuously and will strike at a moment's notice. This potential advantage grows as the system's orbital altitude is increased, reaching its peak with systems placed at geosynchronous orbit, which effectively provides access to almost half the earth's surface from a single platform. Alternatively, if the space-based platform can be placed in low earth orbit (LOE), the range to the target can be minimised at the cost of reduced ground and time coverage for each platform. Given the immense volume of near-earth space, a space-based system can consist of many platforms, providing reliability through redundancy. A weapon system with enough space-based platforms at the proper orbital altitude(s) can potentially ensure global,

full-time coverage and provide the ability to conduct prompt and sustained operations anywhere on the planet.

However, there are numerous disadvantages that space-based systems have over UCAVs. They are mostly associated with costs and socio-political concerns, as discuss below:

- Research and development on space-based systems are expensive and so are procurement and operating costs. The costs associated with transporting the space vehicle from the earth's surface to an earth orbit, and then afterwards transporting it back to the surface will be significant. Once in the orbit, each platform is automatically difficult to service and maintain.

- Another significant space-based limitation is the criticality of the vehicles position or orbit. Space-based systems cannot currently loiter over a target since orbital mechanics require constant movement around the earth. Therefore, a space-based system needs multiple vehicles to provide constant coverage as well as the ability to position a vehicle when and where needed, as previously discussed. This would add significantly to the overall system costs. While one UCAV can loiter in the area searching for better aims and deliver precision weapons to attack the target, thus reducing system costs.

- One must also consider the social and political implications of militarising space. Establishing space dominance will be costly and threatening to an increasingly interdependent international community. Placing an offensive-capable platform in space that continuously holds any nation or group of individuals at risk will undoubtedly be recognized as a direct threat to friendly or enemy nations. Additionally, a truly effective constellation of space-based platforms could easily become a high-value target in plain sight for a determined enemy[3].

Conclusion: As space-based weapons systems can immediately cover a large theatre of operations, therefore, they can support the armed forces for military plans dealing, for example, with missile defense systems. One key mission is an early warning against missile attack to enhance timeliness and usefulness to guarantee high system performance. In term of the first two systems, UCAVs are a cross between cruise missiles and manned aircraft in many ways. The key is to find a way to allow UCAVs to capitalize on the advantages of both types of systems and minimize the disadvantages.

2.8 Summary

The literature search and the sufficient background were an invaluable principal step in the development of the design aspects of Uninhabited Combat Aerial Vehicle concept synthesis. Since this aircraft breaks away from conventional concepts, therefore, the design will be challenged and open a big window of new opportunities in combat aircraft design.

CHAPTER 3

3 Basic Assessment of Aircraft Conceptual Design

The aim of this chapter is to determine the aircraft conceptual design to understand the process in advance of activating the Uninhabited Combat Aerial Vehicle (UCAV) design. An initial sizing study for the military jet trainer was performed on a Microsoft Excel spreadsheet to consider the primary design variables and constraints requirements. An optimization process was then used to determine the optimum aircraft design. Many textbooks and theses have given an outstanding explanation of the optimization process; therefore, a brief description will only be described in this chapter. The main purpose of this chapter is to gather all information on the major parameters needed for the conceptual design process for UCAV and to understand the use of the optimization technique to find out the solution.

3.1 Explanation of Optimization

According to various sources, an optimization is briefly defined as a process that deals with problems of minimising or maximising a function of several variables, usually subject to equality and/or inequality constraints. In the other word, the function of optimization is a comparison of different design concepts and configuration variations within a given concept to determine the one which best meet the specification. The optimization of the configuration of the aircraft within the constraints established by the specification is an essential feature of the design process. Most commonly the optimization criterion is the minimization of mass or some aspect of cost.

In practice, the size and mass of a given class of aircraft are very closely related. As a general rule the lightest aircraft, which can be designed to fulfil a given task, is the most efficient and has the greatest potential for development providing this has been built in to the concept from the outset. On the contrary, the accurate prediction of costs is difficult because of their major dependence upon the organisational characteristics of particular manufacturers and operators, although comparisons on relative basis are valuable. It has also been stated that both the direct operating and life cycle costs are fairly closely related to mass for a given type of aircraft and technology standard[58]. For initial design purposes, mass is a much more convenient criterion to use for optimization since fundamentally it is a function only of the specification. For these reasons the minimization of mass as an optimization criterion is always worthy of consideration. Nevertheless, a potential manufacturer or operator will always wish to evaluate the potential of the aircraft in terms of costs derived from its own organisational procedures.

The methods and process of optimization have experienced expeditious improvement in recent years, and many new names have been created to characterise the procedures

that the mathematical techniques resemble. Mathematical techniques are powerful optimization tools, which can deal with the variation of a large number of parameters at one time. One such technique is multivariate optimization (MVO), which makes use of penalty functions and gradient-projection-restoration procedures to minimise the chosen optimization criterion – the objective function (take-off mass is selected). Care is necessary in the definition of the parameters to reduce the possibility of sudden changes to the optimising path arising from discontinuities in the formulation.

The MVO is a powerful tool. However, some involvement is advantageous for its use for the type of work involved in the optimization of conceptual design, appropriately described as follow:

- Optimization process may require a very large number of iterations to reach a solution.

- It is possible that the optimizer may be unable to find a solution within the limits of the input data and the constraints imposed. This can be investigated by diminishing the constraints in the first instance or setting new bounds for design variables.

- Optimization process is sometimes unsuccessful in achieving a solution. If the limits of the input design variables or the constraints have been modified, an error may have been found. The explanation of this is that in seeking to find a solution, the optimizer has moved to a situation where one or more of the parameters in the problem, such as wing structural mass, has taken a negative value and the impossibility of calculating the value of a power of such a term is the source of the apparent, but not real, error. Again the problem may be considered by reduction of the constraints or requirements, until a solution can be achieved.

3.2 Initial Sizing Study

In order to obtain first estimates of the major parameters that define the UCAV design, an initial sizing study was performed. It is in initial sizing study that the basic questions of configuration arrangement, size and mass, and performance are answered. Aircraft must normally meet very inflexible range, endurance, and velocity objectives while carrying a given payload. It is important, to be able to predict the minimum aircraft mass and fuel mass needed to accomplish a given mission.

A spreadsheet for the initial sizing of the military jet trainer aircraft has been set up to consider the primary design variables and constraints requirements. The variables and constraints are set by the prospective optimizer (customer or a company-generated guess as to that future customers may need) to incorporate the calculation of the estimation of mass, aerodynamics, engine performance, fuel capacity through the mission, and performance properties of the aircraft.

The primary design variables include parameters such as wing aspect ratio, wing area, wing taper ratio, wing thickness to chord ratio, quarter chord sweep; altitude, cruise Mach number and speed; estimated take-off mass, estimated engine thrust, and

estimated fuel mass fraction. Typical parameters, which are numerically defined in the constraints or design requirements, are such as payload and type of payload, take-off and landing field length, cruise range and/or loiter requirements, climb requirements, and manoeuvring requirements.

These primary design variables are used to make the first estimate of the required total mass and fuel mass to determine if it really will perform the design mission. Actual mass, aerodynamics, and installed propulsion characteristics are analysed and subsequently used to do a detailed sizing calculation. Furthermore, the performance capabilities of the design are calculated and compared to the design requirements mentioned above.

Optimization techniques are then used to find the lightest aircraft that will both perform the design mission and meet all performance requirements. With the aid of Microsoft Excel Solver as a multivariate (mathematical) optimization technique allows the determination of optimum aircraft design variables for a given set of data. The results of this optimization include a better estimate of the required total mass and fuel mass to meet the mission. The results also include required revisions to the engine and wing sizes. After some number of iterations requiring a new or revised design layout, results are then obtained showing the parameters requirements for setting up the aircraft configuration.

Figure 3-1 outlines the initial sizing program for the military jet trainer aircraft in greater detail. The interdiction or low-level strike mission was the selection of mission profiles for initial sizing study. This sizing arrangement will be briefly presented in this chapter. The final results and comparison of data with the specifications of similar aircraft will subsequently be shown in the appendix of the thesis.

3.2.1 Aircraft Characterization Variables

A list and brief description of the aircraft design variables, available in the initial sizing program for the military jet trainer aircraft, is described in the following text.

Design Variable	Unit	Description
Mto_es	kg	Estimated take-off mass
Tto_es	N	Estimated engine thrust at SSL
FF_es		Estimated fuel mass fraction
AR		Wing aspect ratio
t_c		Wing thickness ratio
tap		Wing taper ratio
S	m^2	Gross wing area
swe	degree	Wing quarter-chord sweep
swe_LE	degree	Wing leading edge sweep
h	m	Cruise altitude
Mach_cr_L		Cruise Mach number (stores)
Mach_cr		Cruise Mach number (clean)
V_sl_L	m/s	Level speed at SSL (stores)
V_sl	m/s	Level speed at SSL (clean)

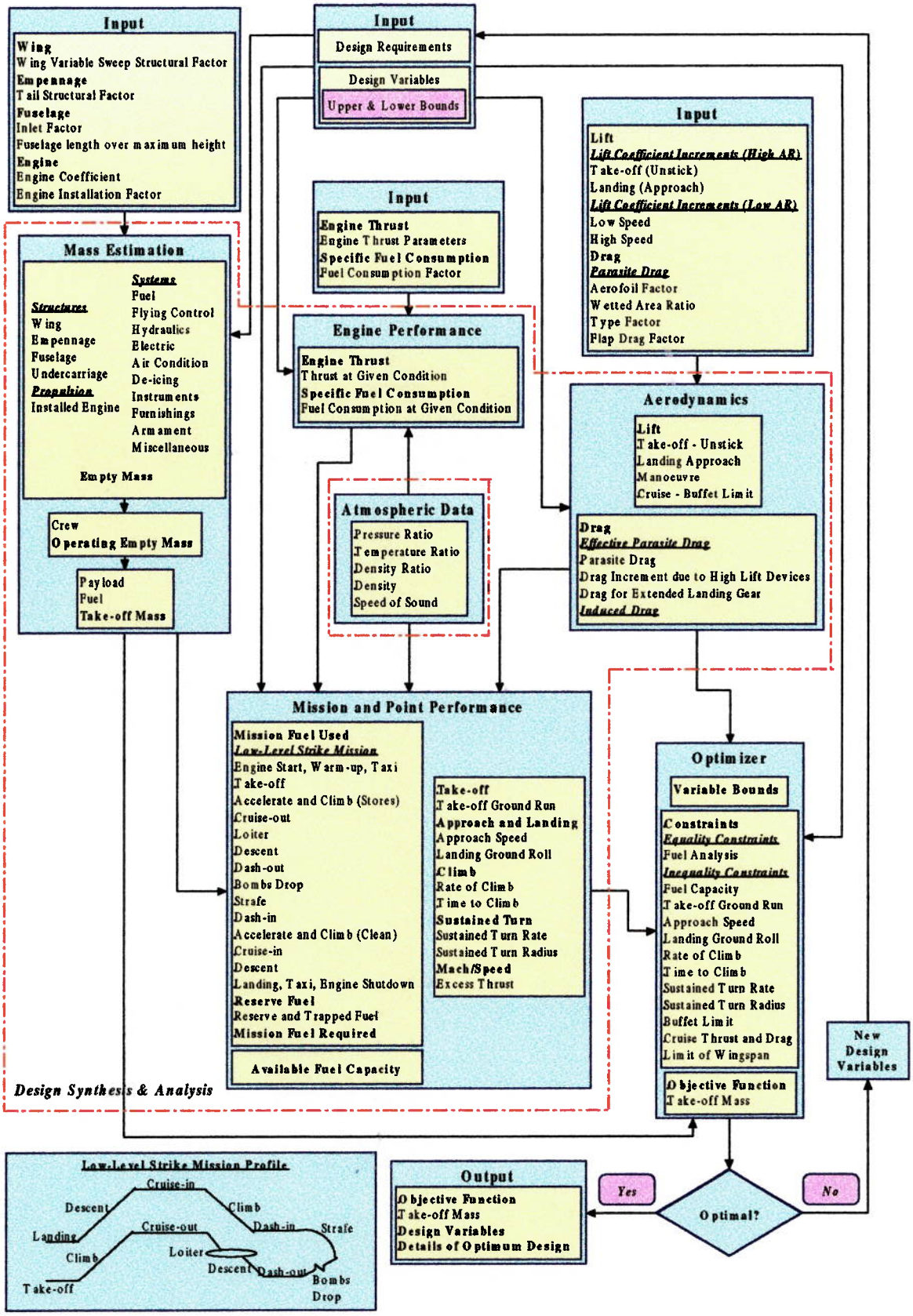

Figure 3-1: Initial Sizing Program for Military Jet Trainer Aircraft

Additionally, the text below details a list and brief description of the data that determines the overall design requirements of the aircraft.

Variable	Unit	Description
Pilot		Number of pilots
Sto_sp	m	Maximum take-off distance
Temp_to	°C	Temperature at take-off
Alt_to	m	Altitude at take-off
Sld_sp	m	Maximum landing distance
Temp_ld	°C	Temperature at landing
Alt_ld	m	Altitude at landing
Vapp_sp	m/s	Maximum landing approach speed
Rcr_out	km	Cruise-out range
Rcr_in	km	Cruise-in range
Rdash_out	km	Dash-out range
Rdash_in	km	Dash-in range
Alt_da	m	Altitude at dash
E_loiter	sec	Loiter time
E_strafe	sec	Strafe time
b_sp	m	Maximum wing span
N_lim		Positive limit load factor
RoC_L_sp	m/s	Rate of climb (stores)
RoC_sp	m/s	Rate of climb (clean)
time_cl_L_sp	sec	Time to climb (stores)
time_cl_sp	sec	Time to climb (clean)
T_rate_L_sp	deg/sec	Turn rate (stores)
T_rate_sp	deg/sec	Turn rate (clean)
R_turn_L_sp	m	Radius of turn (stores)
R_turn_sp	m	Radius of turn (clean)
BPR		Engine bypass ratio
N_eng		Number of engines
N_bomb		Number of bombs

These characterization variables are dealing with the computation of the actual mass, aerodynamics, installed propulsion characteristics, mission fuel mass analysis, and performance capabilities, which are explained in the following sections.

3.2.2 Design Take-off Mass Build-up

Design take-off mass is the total mass of the aircraft as it begins the mission for which it was designed. It can be broken into crew mass, payload mass, fuel mass, and empty mass. The empty mass includes the structures, engines, landing gear, fixed equipment, and anything else not considered a part of crew, payload, or fuel. Equation (3.1) outlines the take-off mass build-up.

$$M_{TO} = M_{crew} + M_{payload} + M_{fuel} + M_{empty} \tag{3.1}$$

The crew and payload mass are both known since they are given in the design requirements. The only unknowns are the fuel mass and empty mass. However, they are both dependent on the total aircraft mass. The empty mass is estimated using a

statistical correlation, which requires an estimation of the take-off mass. The fuel mass is assumed using fuel fraction accumulating with take-off mass estimation and is kept as a sizing variable, subjected to variation with the fuel mass obtained from mission fuel calculation, during the optimization process.

The estimation of the aircraft's design take-off mass is, therefore, the critical part of the conceptual design, since it will deeply affect the whole sizing of the vehicle. Additionally, it should be noted that the take-off mass estimation is linked to other modules such as the performance and mission fuel calculations. Due to this fact, an initial guess of take-off mass has to be performed and an iterative (optimization) process follows on until the values converge. An initial estimation of the value of take-off mass is usually obtained by comparing the design requirements of the aircraft with the mission capabilities of similar aircraft.

3.2.2.1 Empty Mass Estimation

To accomplish a more detailed mass estimation, it is necessary to perform a breakdown of the aircraft into several of its major components and estimate the individual mass of each of them. This is usually performed using statistical correlation built up from previous aircraft. The representation of the empty mass consists of: a variable mass, which is primarily dependent upon the take-off wing loading and the thrust loading, and an absolute mass, which is fixed in items of the total aircraft mass.

The equations are the use of empirical formulae, obtained from several references[4, 5, 93, 102, 125]. These formulae are usually simple and require only a relatively small amount of initial information. They are particularly suitable for an initial sizing study when it is desired to carry out wide ranging parametric analyses. Where it isn't mentioned all units are SI.

It is convenient to deal with mass estimation data in three groups: structure, propulsion, and systems and equipment.

3.2.2.1.1 Structure Group

Airframe structure typically accounts for half, or rather more, of the empty mass. The structural mass prediction is based on a detailed assessment of the contributions of all structural components. It is denoted by the wing, empennage, fuselage, and undercarriage contributions. The engine-related structure is not included as the penalty for buried engine installation is small, usually less than 0.5% of the total aircraft mass. The structural mass of these components is consequently described in details.

3.2.2.1.1.1 Wing

The wing structure is taken to include the primary structure of the wing box, fixed wing leading and trailing edges, high lift devices and control surfaces, but not the control operating systems. The basic formula for wing structural mass is completely empirical but does include allowance for the effect of all the main geometric factors together with the primary structural design considerations. However, it does not

specifically include details of such items as inertial relief, types of high lift devices or any special features. The wing structural mass is represented as *M_wing*.

$$M\_wing(lb) = \left[3.08 \times \left(\frac{K\_PIV \times N\_\lim \times Mto\_es}{t\_c} \times \left\{ \left[\tan(swe\_LE) - \frac{2 \times (1 - tap)}{AR \times (1 + tap)} \right]^2 + 1.0 \right\} \times 10^{-6} \right)^{0.593} \times [(1 + tap) \times AR]^{0.89} \times (S)^{0.741} \right] \quad (3.2)$$

Where *K_PIV* is the wing variable sweep structural factor, which is 1.00 for fixed wings and 1.175 for variable swept wings. *Mto_es* is take-off mass estimation, *(lb)*.

3.2.2.1.1.2 Empennage

The total mass of the empennage is often less than 3% of the take-off mass of the aircraft. In practice, there can be wide variations in the masses of both the horizontal and vertical tail surfaces due to, among other things, differing fuselage layouts and hence tail arms. For convenience of initial sizing study, the empennage mass is integrated with that of the wing, but the contribution of the empennage can be separated by tail structural factor. The empennage mass is represented as *M_tail*.

$$M\_tail(lb) = \left[5.4 \times \left(\frac{K\_PIV \times N\_\lim \times Mto\_es}{t\_c} \times \left\{ \left[\tan(swe\_LE) - \frac{2 \times (1 - tap)}{AR \times (1 + tap)} \right]^2 + 1.0 \right\} \times 10^{-6} \right)^{0.455} \times [(1 + tap) \times AR]^{0.611} \times (S \times K\_tail)^{0.534} \right] \quad (3.3)$$

Where *K_tail* is the tail structural factor, which is 0.4 for fixed wings and 0.53 for variable swept wings.

3.2.2.1.1.3 Fuselage

The fuselage makes a large contribution to the structural mass, but it is much more difficult to predict by a generalized method than the wing mass. The most important parameter is the surface area of the fuselage structure and it is necessary to estimate this as accurately as possible. The following formula provides a basis for more accurate estimation of fuselage mass for the military jet trainer aircraft. The fuselage mass is described as *M_fuse*.

$$M\_fuse(lb) = \left[10.43 \times (K\_INL)^{1.42} (q \times 10^{-2})^{0.283} \times (Mto\_es \times 10^{-3})^{0.95} \times (L\_H)^{0.71} \right] \quad (3.4)$$

Where *K_INL* is the inlet factor, which is 1.25 for inlets on fuselage and 1.00 for inlets in wing root or elsewhere. The parameter, *q*, is indicated as maximum aerodynamic pressure, *(lb/ft²)*. *L_H* refers to the fuselage length over maximum fuselage height, which is ranged between 8.0 to 12.0 for the air force, and 6.0 to 11.0 for the navy.

3.2.2.1.1.4 Undercarriage

The basic mass prediction effectively assumes the mass of undercarriage, combining the main gear and the nose gear, of 4% of the aircraft mass. The undercarriage controls are also the most important consideration. The following formula gives a basic estimation of undercarriage mass, including the undercarriage controls. The undercarriage mass is defined by *M_gear*.

$$M\_gear(lb) = 62.21 \times \left(Mto\_es \times 10^{-3}\right)^{0.84} \tag{3.5}$$

Providing a completely detailed mass estimate is performed, undercarriage mass estimation requires more accurate availability of details of the undercarriage geometry, dimensions, tyre and brake details and basic loading.

3.2.2.1.2 Propulsion Group

Propulsion is defined as the installed engine component. It usually contributes about one-fifth of the empty mass. Where possible, engine mass should be derived from data supplied by engine manufacturers whether this be for a design study or existing engine. Because of the many small items involved with the bare engine, it is best to base the mass prediction of the installation on the basic mass of engine multiplied by an appropriate factor. The following formula for the propulsion mass is divided into two conditions mainly based on the static engine thrust. The propulsion mass is represented by *M_eng*.

$$M\_eng = \left[\frac{Tto\_es}{K\_eng \times \left(5 + \frac{BPR}{10} - \left[1 - \frac{Tto\_es}{45000}\right]\right)}\right] \times K\_PG \times N\_eng \tag{3.6a}$$

Where the engine thrust, *Tto_es*, is less than 45,000 N.

$$M\_eng = \left[\frac{Tto\_es}{K\_eng \times \left(5 + \frac{BPR}{10}\right)}\right] \times K\_PG \times N\_eng \tag{3.6b}$$

Where the engine thrust, *Tto_es*, is greater than or equal to 45,000 N.

The parameter, *K_eng*, is the engine coefficient, which is between 9 to 11 for propulsion engines having bypass ratios up to about 8, and 8 for engines having bypass ratios of 10 or more. *K_PG* refers to the engine installation factor, which is 1.2 for turbojet engines buried in fuselage, and 1.25 for those buried in wing.

3.2.2.1.3 Systems and Equipment Group

Systems and equipment are the group of all the items not included in the structures group and the propulsion group, which go to make the basic empty mass of the aircraft. In total, they can contribute a large part of the overall mass of the aircraft, possibly in excess of 20% and only rarely less than 10%. The group consists of several basic systems and equipment, which contain of many small components and which interact with one another. They are characterized subsequently in details.

3.2.2.1.3.1 Fuel System

In general, the fuel system is considered as part of the engine installation. But for initial sizing study, it is included in the total system mass. The residual fuel, which is some fuel in the tanks that cannot be used, is usually quoted as part of the basic mass of an aircraft separately from the fuel system mass. But for initial sizing study, it is convenient to include the residual fuel with the fuel system. Military combat aircraft tend to have a high fuel system mass because the system is complex, uses separate flexible tanks and makes provision for reduced vulnerability. The fuel system mass provided for an initial sizing study is:

$$M\_fs = 0.022 \times Mto\_es \tag{3.7}$$

Where M_fs is the fuel system mass that for military combat aircraft with integral fuel tanks, the mass is likely to be between 1.7% and 2.2% of take-off mass, or values in excess of 4% for complex system.

3.2.2.1.3.2 Flying Control System

The actuators of the control surfaces may be included either as part of the control item or part of the power supplies, often hydraulic. For convenient, the formula carried out for the mass of flying control system is quoted as the sum of the flying control and the hydraulics systems, which may be more useful. Additionally, the aircraft is a two seat jet trainer with dual control, the flying control system mass is thus:

$$M\_fc = 0.19 \times Mto\_es^{0.75} \tag{3.8}$$

Where M_fc represents mass of the flying control system.

3.2.2.1.3.3 Power Supply Systems

The power required to operate services on an aircraft is usually provided hydraulically and electrically and if any, pneumatically. Correlation of information of these systems is very difficult as they vary widely between different roles of the aircraft and in most instances it is possible only to give general trends.

It has long been recognized that there are advantages in using only one power supply source, which, because of avionics, has to be electric. Thus electric actuating systems are used on general aviation aircraft and military trainer types. However, the advantages of high-pressure hydraulic systems have meant that in the past, they have been preferred for situations where large power and rapid response is required. An initial sizing study is, therefore, employed both the hydraulic/pneumatic and electrical systems.

3.2.2.1.3.3.1 ***Hydraulic and Pneumatic systems***

Hydraulic and pneumatic systems typically contribute about 1% of the total mass, or rather less. They are associated together in that in the great majority of cases, they provide the power for most of the major actuation requirements. The equation for the mass of hydraulic/pneumatic systems with the use of powered controls is given by:

$$M\_hydrau = 3.2 \times Mto\_es^{0.5} \tag{3.9}$$

Where *M_hydrau* refers to mass of the hydraulic and pneumatic systems.

3.2.2.1.3.3.2 ***Electrical systems***

The electrical systems are relatively heavy when electrical power is used for primary actuation. The following formula is a good guide for interpreting the mass of the electrical systems for the military jet trainer aircraft.

$$M\_elec = 0.17 \times Mto\_es^{0.84} \tag{3.10}$$

Where *M_elec* is the mass of the electrical systems.

3.2.2.1.3.4 Environmental Control Systems

Air conditioning and pressurisation, where fitted, are effectively part of one system. At one time they were considered as being in the equipment, rather than systems category. However, because of air conditioning can be very closely integrated with both engine compressor off-takes and aircraft de-icing systems, it is, therefore, convenient to manage both air conditioning and de-icing systems as one system under the general description of environmental control. The environmental control systems may not be required for the military jet trainer aircraft, but from the starting point, it is valuable to involve these systems for an initial sizing study.

3.2.2.1.3.4.1 ***Air Conditioning, Pressurisation and Oxygen***

The air conditioning system is to be expected that in practice it is more directly a function of the number of human beings carried by the aircraft. For military jet trainer aircraft, the mass of the air conditioning system assumes 30 kg for each crew or 0.9% of the total take-off mass. The mass of air conditioning system is defined as *M_ac*.

$$M\_ac = 0.009 \times Mto\_es \tag{3.11}$$

3.2.2.1.3.4.2 ***De-icing***

The minimum coverage of the de-icing system is usually the engine air intake. It is important to be noted that hot air de-icing is common for aircraft powered by gas turbines, but there are exceptions in the case of military jet aircraft with engines buried in the fuselage, the penalty of long hot air ducts is greater than alternative de-icing techniques. The mass of the de-icing system should, therefore, be reduced to about half of the value obtained from a typical allowance. *M_deice* represents mass of the de-icing system.

$$M\_deice = 0.08 \times Mto\_es^{0.7} \tag{3.12}$$

3.2.2.1.3.5 Instruments

In certain cases the instrument mass, being relatively small, is combined with avionics. In addition to the cockpit panel instruments and the supporting devices, the instruments item often includes radio, radar, automatic controls, navigation, safety protection such as fire precautions and special handling equipment. They are subjected to rapid change with new technology. Due to this reason, it is most desirable to use the actual masses of these instruments. However, for an initial sizing study the mass of the instruments is assumed approximately:

$$M\_instru = 54.4 + 9.1 \times N\_eng + 0.006 \times Mto\_es \quad (3.13)$$

Where *M_instru* is mass of the instruments and *N_eng* represents number of engines specified as the design requirements.

3.2.2.1.3.6 Furnishings

The mass of furnishings for either the military combat or military trainer aircraft is considered on the ejection seats, which is likely to be in the range of 60 kg to 90 kg per crew member. For military jet trainer aircraft, the mass of furnishings is:

$$M\_furnish = 60 \times Pilot \quad (3.14)$$

Where *M_furnish* is the mass of furnishings and *Pilot* refers to number of crews designated as the design requirements.

3.2.2.1.3.7 Military Armament

Military jet trainer aircraft may carry some level of fixed armament, such as guns. Few remarks on general trends are useful to present a formula for the prediction of military aircraft armament mass, since this must be specified as a basic requirement for a given role. The total mass of the military armament including guns and ammunition is approximately 6.5% of the total take-off mass.

$$M\_weap = 0.065 \times Mto\_es \quad (3.15)$$

Where *M_weap* represents the total mass of the armament.

3.2.2.1.3.8 Miscellaneous Items

The external paint is in association with a number of items, which do not clearly fall in any one of the categories so far discussed. The majority of aircraft have an external coat of paint for decorative, camouflage and protective purposes. An approximate allowance for the external paint is:

$$M\_miscell = 0.5 \times S \quad (3.16)$$

Where *M_miscell* is the mass of external paint and *S* represents gross wing area designated as the design variables.

Conclusion: Basically the total empty mass of the aircraft is the sum of all those components described above in structure, propulsion, and systems and equipment groups. Figure 3-2 demonstrates a linear relationship between empty mass and total

aircraft take-off mass of the existing military jet trainer aircraft (data obtained from Jane's All the World Aircraft[64] 1998-99). The trend line is established to be an adequate representation as the minimum allowable value of empty mass at the current state-of-the-art of aircraft conceptual design.

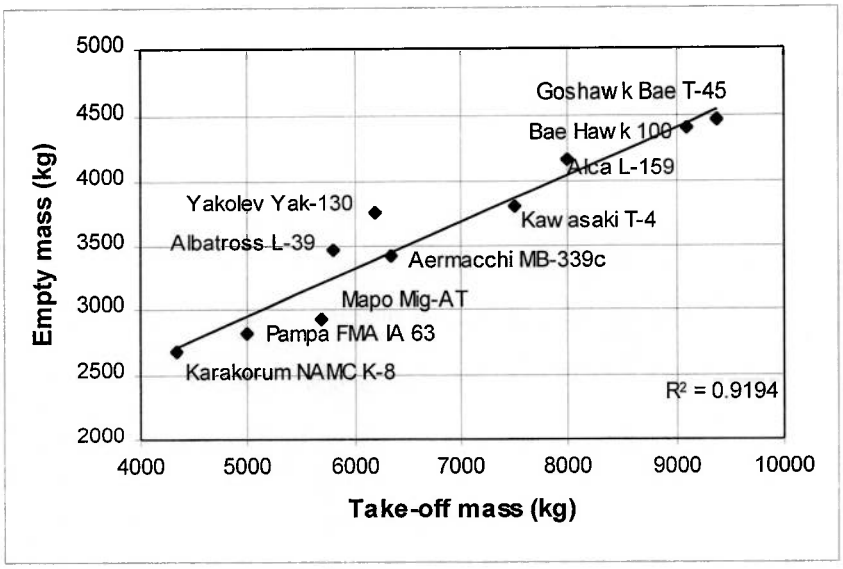

Figure 3-2: Mass Trends for Military Jet Trainer Aircraft

3.2.2.2 Operating Empty Mass

The operating empty mass is defined as the basic empty mass plus those items necessary for the aircraft to be operational. For the military combat or military jet trainer aircraft, the only items of interest are the crew provisions and the residual fuel. However, in this initial sizing study, at present the residual fuel has included in the mass of fuel systems in systems and equipment group mentioned above. Thus, in this section, the additional operational items correspond only to the crew provisions. Typical allowances for military crewmember provide a mass of 200 lb or 90 kg of flight equipments per crewmember to be carried. The mass of crew provisions is represented as *M_pilot*.

$$M\_pilot = 90 \times Pilot \tag{3.17}$$

The mass of these additional items is then added to the empty mass to accomplish the operating empty mass.

3.2.2.3 Disposable Mass

The disposable mass is the sum of the payload and fuel appropriate to a given mission. A 200 kg-bomb is considered as a payload for military jet trainer aircraft carrying externally to perform a mission. For the fuel mass, at the starting point, it is estimated by assuming fuel fraction accumulating with the design take-off mass estimation and is kept as a sizing variable, subjected to variation with the fuel mass obtained from mission fuel calculation, during the optimization process. The following formulae represent the mass of payload and fuel.

$$M\_bomb = 200 \times N\_bomb \tag{3.18}$$

$$M\_fuel = FF\_es \times Mto\_es \tag{3.19}$$

Where *M_bomb* is the mass of payload and *N_bomb* refers to number of bombs designating as the design requirements. *M_fuel* represents the mass of fuel and *FF_es* is the fuel mass fraction estimation specified as the design variables.

Conclusion: The sum of the operating empty mass and the disposable mass contributes the design take-off mass. Once the total take-off mass is performed, it is kept as a sizing variable, after linking to other modules, subjected to variation with the initial take-off mass estimation during the iterative process until the values converge.

3.2.3 Aerodynamic Modelling

The representations of aerodynamic characteristics are of fundamental importance to the design synthesis process. For an initial sizing study, an accurate evaluation of them requires knowledge of many details of a design. It is, therefore, intended to enable an expeditious estimation of aircraft aerodynamic characteristics to be undertaken. Open literatures proposed by Howe[58],[59] provide the application of clear and effective formulae to be obtained. Certain significant characteristics are linked to performance and mission fuel analyses, and are retained as parameters to be optimized during the process. The aerodynamic module consists of the estimation of lift and drag coefficients, which are briefly described in details.

3.2.3.1 Lift Estimation

The estimation of lift characteristics requires wing geometry parameters and aircraft configuration such as wing quarter-chord sweep, wing aspect ratio, flight Mach number, and type of high lift system. For the purposes of preliminary design, the lift estimation is limited to the take-off, landing approach, manoeuvre, and cruise (buffet limit) phases of the flight. It is applicable to all moderate to high-aspect ratio (AR≥5) and low-aspect ratio (AR<4.5) configurations.

3.2.3.1.1 Take-off Condition – Unstick Lift Coefficient

The unstick lift coefficient is assumed to be independent of the angle of nose-up rotation. For moderate to high-aspect ratio configurations, the unstick speed is assuming lift off at 1.1 times the relevant stall speed with the high lift devices setting in the take-off configuration.

$$CL\_us = 0.8 \times (1.5 + WLETO + WTETO) \times \cos(swe) \tag{3.20a}$$

Where *WLETO* is the lift coefficient increment of leading edge devices, which can be taken as 0.4 when they are fitted and set at their take-off position, but zero when they are not employed. *WTETO* is the lift coefficient increment of trailing edge flaps at take-off setting, which the typical values are given in Table 3-1.

For low-aspect ratio configurations, the unstick speed is accepted lift off at 1.15 times the relevant stall speed.

$$CL\_us = 0.75 \times \left[\left(AR/2 \right)^{0.5} \times \cos(swe) + WLEL \right] \quad (3.20b)$$

Where *WLEL* is the lift coefficient increment at low speed flight appropriate to a given aircraft-configuration, which is provided in Table 3-2.

Trailing Edge Flap Configurations	Lift Coefficient Increments for Typical Part Span Effects	
	Take-off (Unstick): *WTETO*	Landing (Approach): *WTELD*
Plain flap	0.3	0.6
Single-slotted flap	0.5	1.0
Double-slotted and Fowler flaps	0.7	1.35
Triple-slotted flap	0.8	1.55

Table 3-1: Trailing Edge Flap Configurations and Typical Lift Coefficient Increments due to Moderate to High-Aspect Ratio Wings

Configuration Increments	Lift Coefficient Increments	
	Low Speed: *WLEL*	High Speed: *WLEH*
Leading edge extension (LEX)	0.3	0.6
Variable geometry leading edge	0.4	0.8
Close coupled canard	0.5	0.8
Variable geometry leading edge and close coupled canard	0.6	1.0

Table 3-2: Configuration Increments and Lift Coefficient Increments due to Low-Aspect Ratio Wings

3.2.3.1.2 Landing Approach Condition

The landing approach lift coefficient is calculated similarly to the lift at take-off condition. The approach is made at a speed, which is 1.3 times the stalling speed with the high lift devices in the landing configuration. For moderate to high-aspect ratio aircraft, the approach lift coefficient is:

$$CL\_ap = 0.6 \times (1.5 + WLELD + WTELD) \times \cos(swe) \quad (3.21a)$$

Where *WLELD* is the lift coefficient increment due to the deployment of leading edge devices in the landing setting, which can be approximately taken as 0.65, but zero when leading edge devices are not used. *WTELD* is the lift coefficient increments due to the deployment of the trailing edge flaps to the landing setting. The typical values for different flap configurations are provided in Table 3-1 above.

If the approach is lower, made at 1.2 times the stalling speed, the higher approach lift coefficient is possible by increasing the factor of 0.6 in equation (3.21a) to nearly 0.7. This may be acceptable in some circumstances.

For low-aspect ratio configurations, the approach speed is at 1.2 times the relevant stall speed, and the approach lift coefficient is:

$$CL\_ap = 0.7 \times \left[\left(AR/2 \right)^{0.5} \times \cos(swe) + WLEL \right] \quad (3.21b)$$

3.2.3.1.3 Manoeuvre Condition

In manoeuvres, the high lift devices are assumed not deployed. For moderate to high-aspect ratio and low-aspect ratio configurations, the maximum lift coefficient for manoeuvre case can be obtained respectively as:

$$CL\_cr = 1.35 \times \cos(swe) \quad (3.22a)$$

$$CL\_cr = \left[\left(AR/2 \right)^{0.5} \times \cos(swe) + WLEH \right] \times (1 - 0.25 \times Mach\_cr) \quad (3.22b)$$

Where *WLEH* represents the lift coefficient increment at high-speed flight appropriate to a given configuration as presented in Table 3-2 above.

3.2.3.1.4 Cruise Condition – Buffet Limit

The maximum lift coefficient, which may be assumed for cruise is limited by buffet considerations. Buffet boundary is caused by the airflow hitting the horizontal stabilizers producing the violently turbulent separated air behind a normal shock wave. Allowing a typical buffet margin and assuming high lift devices are not extended, the maximum lift coefficient at cruise condition may be specified as:

$$CL\_buffet = 0.65 \times \cos(swe) \quad (3.23a)$$

The above equation is based on moderate to high-aspect ratio wings. For low-aspect ratio configurations, it is suggested that performance analysis should be based on a limiting lift coefficient at cruise of:

$$CL\_buffet = 0.4 \times CL\_cr \quad (3.23b)$$

Where *CL_cr* is the lift coefficient in manoeuvres, obtained from equation (3.22b).

3.2.3.2 Drag Estimation

The initial lift estimation from previous section is helpful to reduce to a minimum the number of parameters required to estimate drag. Significant drag characteristics are needed by the performance analyses in its cruise configuration over much of the speed range, and for take-off and landing settings to evaluate the required distance. For an initial sizing study, the estimation of drag characteristics are considered only for the subsonic region, and are applicable for either moderate to high-aspect ratio or low-aspect ratio configurations.

In subsonic speeds, there are two kinds of drag: parasite or zero-lift drag and drag due to lift or induced drag. The parasite drag is made up of two components, which are drag due to the shape and surface friction of the aircraft in incompressible flow conditions and compressibility wave drag due to the volume of the aircraft. Additionally, the induced drag is the combination of vortex drag or lift induced drag in incompressible flow and wave drag due to lift. The following formula represents the total drag expressed in coefficient form:

$$CD = CDf + CDlv \quad (3.24a)$$

In practice, it is found that the induced drag is approximately a function of the square of the lift with a proportionality factor called the induced drag factor. Furthermore, the zero-lift drag is effectively combined with the total drag increment due to deployment of the high lift devices, and drag for an extended landing gear, appeared as the effective zero-lift drag. The total drag coefficient can, therefore, be written as:

$$CD = CDf + Cdflap + CD\_uc + K \times CL^2 \tag{3.24b}$$

Where K refers to the induced drag or drag-due-to-lift factor.

3.2.3.2.1 Parasite (Zero-Lift) Drag

The parasite or zero-lift drag coefficient is mainly based on the wing reference area (S), wing quarter-chord sweep (swe), thickness ratio (t_c), and flight Mach number (M). The zero-lift drag coefficient can be represented below:

$$CDf = \left[\begin{array}{l} 0.005 \times \left(1 - \dfrac{2 \times c_l}{R\_S}\right) \times \tau \times \left[1 - 0.2 \times M + 0.12 \times \left\{\dfrac{M \times \cos(swe)^{0.5}}{(AF - t\_c)}\right\}^{20}\right] \\ \times R\_S \times T \times S^{-0.1} \end{array} \right] \tag{3.25a}$$

Where AF is an aerofoil factor, which depends upon the airfoil design. It may be as high as 0.93 for a specially designed advanced aerofoil, but can be as low as 0.75 for earlier aerofoil intended primarily for use in incompressible flow conditions. c_l is the function of chord of wing over which the flow is laminar, which is zero for fully turbulent flow. τ is a correction factor for wing thickness as shown:

$$\tau = \left[(R\_S - 2)/R\_S + 1.9/R\_S \times \left\{1 + 0.526 \times \left(t\_c/0.25\right)^3\right\} \right] \tag{3.25b}$$

However, the value of this factor is usually close to unity. R_S is a factor, which is effectively the ratio of overall wetted area to the reference area, and T is a type factor, which effectively allows for variation of the shape from the streamlined ideal. These factors are given for different classes of aircraft prescribed in Tables 3-3 and 3-4 respectively.

Type of Aircraft	Wetted Area Ratio: R_S
Tailless types (delta)	2.5-3.0
Single-engine propeller type (normal)	3.75-4.0
Small twin-engine propeller type (low and high wing loading)	4.0, 5.0
Bombers, jets	4.25
Jet trainers	4.5
Interceptors, strike aircraft, clean[1]	4.0-5.0
Strike aircraft with external stores, up to	6.0
Airliners, executive jets, freighters, turboprop airliners	5.5

Table 3-3: Wetted Area Ratio for Different Classes of Aircraft

[1] The higher value is when the weapons are carried internally, although an integrated wing-fuselage configuration tends to have a lower value.

Typical Aircraft	Type Factor: *T*
Very streamlined aircraft with negligible slipstream effects	1.0
Jet airliners, executive jets	1.1-1.2
Turboprop airliners	1.4
Combat aircraft, jet trainers, clean	1.2
Strike aircraft, trainers with external stores up to	1.85
Large freighters	1.2-1.3
General aviation aircraft with retractable landing gear	1.5
General aviation aircraft with fixed landing gear	2.0-2.5
Agricultural types	2.5

Table 3-4: Aircraft Type Factor for Different Classes of Aircraft

The total drag coefficient increment due to deployment of the high lift devices are considered in three configurations. For cruise configuration, where the high lift devices retracted, the drag is kept zero. At climb-out configuration, the high lift devices is at take-off setting and is applied as:

$$Cdflap = \frac{(0.03 \times F\_f - 0.004)}{AR^{0.33}} \tag{3.26a}$$

For aborted landing configuration, a typical drag for high lift devices at landing setting is:

$$Cdflap = \frac{0.15 \times F\_f}{AR^{0.33}} \tag{3.26b}$$

Where F_f is a flap drag factor, which is provided for different flap types as shown in Table 3-5. For the drag produced by leading edge devices, it is assumed to be negligible for an initial sizing study.

Trailing Edge Flap Types	Flap Drag Factor: F_f
Single slotted	1.0
Double slotted and Fowler	1.2
Triple slotted	1.5
No flaps provided	0.133

Table 3-5: Flap Drag Factor for Different Trailing Edge Flap Types

A typical drag coefficient for an extended landing gear, CD_uc, is considered only for an aborted landing configuration, specified value as 0.03.

3.2.3.2.2 Drag Due to Lift (Induced Drag)

As previously mentioned, the induced drag coefficient is proportional to the square of the lift coefficient with a compatibility 'drag-due-to-lift' factor.

$$CDlv = K \times CL^2 \tag{3.27a}$$

Where *CL* is the lift coefficient appropriate to the given flight-condition. The induced drag factor *K* is mainly based on wing aspect ratio, wing quarter-chord sweep, wing thickness ratio and flight Mach number given as:

$$K = \frac{\left(1 + 0.12 \times M^6\right)}{\pi \times AR} \times \left\{ 1 + \frac{\left(0.142 + f(tap) \times AR \times \left(10 \times t\_c\right)^{0.33}\right)}{\cos(swe)^2} + \frac{0.1 \times \left(3 \times N\_eng + 1\right)}{\left(4 + AR\right)^{0.8}} \right\} \quad (3.27b)$$

Where *N_eng* is the number of engines designated as the design requirements. The taper ratio function *f(tap)*, for most purposes, may be applied a value of 0.0062, or may be given as:

$$f(tap) = 0.005 \times \left\{1 + 1.5 \times (tap - 0.6)^2 \right. \quad (3.27c)$$

Conclusion: The aerodynamics module explains the operation and theory behind the available lift and drag estimation, together with all the relevant equations and factors appropriate to an initial sizing study.

3.2.4 Engine Performance Modelling

The design synthesis process requires the information of certain basic engine characteristics. It is important to use the most accurate possible representation of the variation of thrust and specific fuel consumption with flight conditions. The characteristics of a known engine are always highly desirable to be obtained. Sometimes the detailed characteristics are not available, but even when they are, it should be noted that there are likely to be some flight conditions where the engine has to operate at settings other than the optimal design values and consequently the specific fuel consumption becomes greater than would otherwise be the case. Therefore, it may be useful to have generalised representations of their variation with flight conditions.

The applicable descriptions of engine performance presented by Howe[58] provide sufficient details for an initial sizing study. Furthermore, the engine performance estimation requires the atmospheric data for the variation with flight conditions, which can be obtained from ESDU datasheet[38]. The engine performance module consists of the estimation of engine thrust and the specific fuel consumption characteristics, which are explained in details.

3.2.4.1 Thrust Estimation

For an initial sizing study, the estimation of engine thrust for turbofan engine are considered as it is applied to the military jet trainer aircraft. The maximum thrust available is primarily dependent upon three main parameters: flight speed or Mach number, flight altitude, and engine operating conditions. It is convenient to relate operating thrust values to a datum, sea level static dry condition, and so the thrust at any given condition can be defined as:

$$T = Tfac \times Tto\_es \times N\_eng \quad (3.28a)$$

Where *Tto_es* is the datum sea level static dry thrust designated as the design variables for an initial sizing. *Tfac* is the engine thrust factor, which is dependent upon flight conditions mentioned above and the engine bypass ratio (*BPR*). In subsonic speed, according to the purposes of the preliminary design, the engine thrust factor can be written as:

$$Tfac = FTfac \times \left[KT1 + KT2 \times BPR + \left(KT3 + KT4 \times BPR\right) \times M\right] \times \sigma^{s} \qquad (3.28b)$$

Where *FTfac* is a factor to allow for the use of afterburning. At this stage, it is assumed to be unity that is without the use of afterburner under basic, dry operating condition.

KT1, KT2, KT3 and *KT4* are assumed to be constant for a given engine in a defined flight speed and engine operating condition. Typical values are prescribed simultaneously in Table 3-6.

Bypass Ratio: *BPR*	Mach Number Range	Engine Operating Condition	KT1	KT2	KT3	KT4	Altitude Factor: *s*
1 or lower	0-0.4	Dry	1.0	0	-0.2	0.07	0.8
		Wet	1.32	0.062	-0.13	-0.27	0.8
	0.4-0.9	Dry	0.856	0.062	0.16	-0.23	0.8
		Wet	1.17	-0.12	0.25	-0.17	0.8
	0.9-2.2	Dry	1.0	-0.145	0.5	-0.05	0.8
		Wet	1.4	0.03	0.8	0.4	0.8
3 to 6	0-0.4	Dry	1.0	0	-0.6	-0.04	0.7
	0.4-0.9	Dry	0.88	-0.016	-0.3	0	0.7
8	0-0.4	Dry	1	0	-0.595	-0.03	0.7
	0.4-0.9	Dry	0.89	-0.014	-0.3	0.005	0.7

Table 3-6: Engine Thrust Parameters

σ is the relative air density at flight altitude and *s* is the altitude factor which being a power of air density, is varied proportionally to the thrust. Up to 11 km altitude, this power varies in range of around 0.6 for a high bypass ratio engine, up to about 0.85 for an engine of nominally zero bypass ratios. Above 11 km altitude the thrust variation is more or less directly proportional to the relative density, thus the altitude factor can be conveniently assumed to be unity based on the 11-km altitude condition as a datum. Typical values of the altitude factor are prescribed simultaneously in Table 3-6 above.

3.2.4.2 Fuel Consumption Estimation

The specific fuel consumption is defined as the rate of fuel consumption per resulting thrust, which is an indication of the efficiency of an engine. The determination of the variation of specific fuel consumption for turbofan engine is based on flight speed, air density at flight altitude, and engine bypass ratio. Up to 11 km altitude, the specific fuel consumption can be defined as:

$$sfc = sfcF \times \left(1 - 0.15 \times BPR^{0.65}\right) \times \left[1 + 0.28 \times \left(1 + 0.063 \times BPR^{2}\right) \times M\right] \times \sigma^{0.08} \qquad (3.29a)$$

Where *sfcF* is a fuel consumption factor, which is 20 mg/N/s for large subsonic turbofan engines; 24 mg/N/s for low-bypass-ratio subsonic engines, and 27 mg/N/s for subsonic engine with bypass ratio less than or equal to 1.

Above 11 km altitude, the specific fuel consumption should be assumed to be constant with altitude, which can be unity based on the 11-km altitude condition as a datum, corresponding to the engine thrust. Thus, the specific fuel consumption at altitudes above 11 km can be defined as:

$$sfc = sfcF \times \left(1 - 0.15 \times BPR^{0.65}\right) \times \left[1 + 0.28 \times \left(1 + 0.063 \times BPR^{2}\right) \times M\right] \times 0.907 \qquad (3.29b)$$

Where 0.907 is $\sigma^{0.08}$ at 11 km altitude.

Conclusion: The engine performance module provides the effective estimation of engine thrust and the specific fuel consumption in details appropriate for an initial sizing study.

3.2.5 Mission Fuel Mass Analysis

The design take-off mass *Mto* obtained from Section 3.2.2 is used to perform the estimation of mission fuel mass. The required amount of mission fuel depends upon the mission to be flown, the aerodynamics of the aircraft, and the engine's fuel consumption. The deep strike mission, as shown in Figure 3-1, is considered as a design mission to determine the mission fuel mass for an initial sizing study. Mission fuel mass can be written as:

$$Mfuel\_re = Mfuel\_used + Mfuel\_res \qquad (3.30)$$

Where *Mfuel_re* is the total mission fuel mass required, that is subjected to variation with the fuel mass obtained from the calculation of take-off mass estimation above, during the optimization process. *Mfuel_used* is the fuel actually used during the mission and *Mfuel_res* is the reserve fuel required by design specifications, and also "trapped fuel", which is the fuel that cannot be pumped out of the tanks.

To determine the fuel mass actually used during the mission, the fuel-fraction method will be used. The equations obtained for the method are described in the literatures proposed by Roskam[102] and Raymer[96]. In this method the aircraft mission is broken down into a number of mission phases. The fuel fraction for each phase is defined as the ratio of end mass to begin mass. The product of all these fuel fractions will provide the final fuel fraction. The fuel mass used during the mission is then found from unity minus the final fuel fraction, accumulating with the design take-off mass. The value for mission fuel mass can finally be determined. Each of the mission phases is presently discussed in more detailed.

3.2.5.1 Engine Start, Warm-up, Taxi and Take-off

For an initial sizing study, the take-off aspect is assumed to be included with the phase of a ground run. Begin mass is the design take-off mass *Mto*. For this segment a fuel fraction is estimated from statistical databases historically, which is reasonably defined as:

$$M1/Mto = 0.99 \qquad (3.31)$$

3.2.5.2 Accelerate and Climb

Following the mission profile of the low-level strike in Figure 3-1, the aircraft climbs and accelerates to cruise altitude in two phases, after taking-off with stores loaded and dashing-in from attacking the enemy. The fuel fraction for an aircraft in these two stages can be obtained from either the historically statistical databases or the empirical formula represented as:

$$M_i / M_{i-1} = 1.0065 - 0.0325 \times M \tag{3.32}$$

This formula determines the fuel fraction for an aircraft climbing and accelerating to a cruise altitude and to a cruise Mach number (M) in the subsonic region.

3.2.5.3 Cruise

A fuel fraction in this phase is calculated during sustained straight-and-level flight at near-constant conditions. As this mission phase usually results in the large amount of fuel burn, it can, therefore, be broken down into a number of segments and summed the values of fuel to give the totals. By employing the Breguet's range equation, the expression can be obtained, which represents the fuel fraction as a function of cruise range (R), lift-to-drag ratio (L/D), specific fuel consumption (sfc), and cruise speed (V). Once the atmospheric data and mass value have been initialised, the lift and drag are determined, and the first guess of the cruise leg fuel burn is made. After the first run, the average mass is re-calculated at the mid-point of the cruise range to determine the aerodynamic parameters, and then obtained the typical fuel burn at cruise.

$$M_i / M_{i-1} = \exp\left(\frac{-R \times sfc}{V \times (L/D)}\right) \tag{3.33}$$

A fuel fraction for cruise stage of this mission profile is calculated in two phases after the first and second climbs. The cruise ranges are specified in the design requirements, and the specific fuel consumption at flight conditions are obtained from the engine performance modules.

3.2.5.4 Loiter

This phase allows the optimizer to indicate the duration that the aircraft should hold at one particular altitude and Mach number, normally before the attacking phase or at the end of the mission before landing. The fuel fraction for this phase follows from manipulating the Breguet's endurance equation, which is based on loiter duration (E), lift-to-drag-ratio (L/D), and the specific fuel consumption (sfc). The procedure is similar to that for the cruise phase, except that the iteration on final mass is only performed once for the entire loiter duration.

$$M_i / M_{i-1} = \exp\left(\frac{-E \times sfc}{L/D}\right) \tag{3.34a}$$

Where loiter duration (E) is designated in the design requirements and the specific fuel consumption is obtained from the engine performance modules.

To maximise cruise or loiter efficiency, the aircraft should fly at approximately the velocity for maximum lift-to-drag-ratio. The most efficient cruise for a jet aircraft occurs at a slightly higher velocity yielding an *L/D* of 86.6% of the maximum *L/D*, and the most efficient loiter arises exactly at the velocity for maximum *L/D*. As the cruise lift-to-drag ratio has previously obtained from the cruise phase, it is, therefore, convenient to determine an *L/*D for the most efficient loiter by using this relation defined as:

$$\left(L/D\right)_{ltr} = \left(L/D\right)_{MAX} = \frac{(L/D)_{cr}}{0.866} \tag{3.34b}$$

3.2.5.5 Dash-out

This mission phase takes place either at high or low altitude according to the mission profile selected, when before the aircraft aggression. The fuel fraction in this phase is similar to the calculation during cruise stage. The dash range and speed are required in the design requirements and so the fuel fraction can be determined from the Breguet's range equation as presented in equation (3.33).

3.2.5.6 Bombs Drop

The bombs drop mission phase specifies the dropping of the total payload mass. It is assumed that no fuel penalty is assessed and no range credit is taken, so the fuel mass fraction for this phase is defined as:

$$M_i / M_{i-1} = 1.00 \tag{3.35a}$$

The total fuel fraction up to this point in the mission is required to find the total existing aircraft mass, as needed to be subtracted from the bomb or payload mass, to perform the bomb-drop ratio for the correction of the fuel fraction for the next phase.

$$Mdrb_{exist} = M_i - M\_bomb \tag{3.35b}$$

$$Ratio_{bomb} = Mdrb_{exist} / M_i \tag{3.35c}$$

Where $Mdrb_{exist}$ is the total existing aircraft mass at end of mission phase after bombs drop, and $Ratio_{bomb}$ defines the bomb-drop ratio.

3.2.5.7 Strafe

The strafe mission phase specifies the firing of a fraction of the total armament mass. The fuel fraction in this phase is similar to that of the loiter stage performing for the entire strafe duration. The ammo firing duration is required in the design requirements and employs the Breguet's endurance equation, as presented in equation (3.34a), to determine the fuel fraction for this phase. This ratio then needs to be corrected for the mass change, which has occurred during the bombs-drop. The corrected ratio is thus found as:

$$\left(M_i / M_{i-1}\right)_{correction} = \left\{1 - \left(1 - \frac{M_i}{M_{i-1}}\right) \times Ratio_{bomb}\right\} \tag{3.36a}$$

The total fuel fraction up to this point in the mission is required to find the total existing aircraft mass, as needed to be subtracted from the armament mass, to perform the ammo-firing ratio for the correction of the fuel fraction for the next phase.

$$Mstf_{exist} = M_i - M\_weap \tag{3.36b}$$

$$Ratio_{ammo} = {Mstf_{exist}}/{M_i} \tag{3.36c}$$

Where $Mstf_{exist}$ is the total existing aircraft mass at end of mission phase after ammo firing, and $Ratio_{ammo}$ defines the ammo-firing ratio.

3.2.5.8 Dash-in

This mission phase resembles to the dash-out stage, carried out when after the aircraft aggression. The fuel fraction in this phase follows Breguet's range equation as presented in equation (3.33), performing the calculation similar to that during the cruise stage. The unique exception for the fuel fraction ratio in this stage is that it requires the correction for the mass change, which has occurred during the ammo firing. Thus the corrected fuel fraction ratio for the dash-in mission phase is represented as:

$$\left({M_i}/{M_{i-1}}\right)_{correction} = \left\{1-\left(1-\frac{M_i}{M_{i-1}}\right)\times Ratio_{ammo}\right\} \tag{3.37}$$

3.2.5.9 Descent

A fuel fraction for descent stage of this mission profile is considered in two phases: at the end of cruise-out range and cruise-in range. A very small amount of fuel penalty is assessed during this mission phase. For an initial sizing study, the fuel fraction for an aircraft is, therefore, estimated from the historically statistical databases, which is reasonably defined as:

$${M_i}/{M_{i-1}} = 0.99 \tag{3.38}$$

3.2.5.10 Landing, Taxi and Engine Shutdown

During the landing phase, the value of the mass of fuel burned is difficult to estimate, as each aircraft will have a different landing procession. As the results do not change dramatically from one aircraft to the next, a fuel mass fraction has been applied to reduce aircraft mass by 0.5% during the landing phase, reasonably defined as:

$${M_i}/{M_{i-1}} = 0.995 \tag{3.39}$$

3.2.5.11 Total Mission Fuel Mass

To the end of mission calculations, the total fuel fraction is obtained from the product of these fuel fractions and, therefore, the fuel used during the mission (*Mfuel_used*) can be achieved.

$$M_{ff} = \left(\frac{M1}{Mto}\right)\prod_{i=1}^{i=n}\left(\frac{M_{i+1}}{M_i}\right) \quad (3.40a)$$

$$Mfuel\_used = \left(1 - M_{ff}\right) \times Mto \quad (3.40b)$$

The reserve and trapped fuel (*Mfuel_res*) typically 6% is generally specified as a requirement for either an additional range or an additional loiter duration to achieve the mission. Finally, the value for mission fuel mass (*Mfuel_re*) can be determined from equation (3.30), which is subjected to variation with the fuel mass obtained from using fuel fraction accumulating with take-off mass estimation (*M_fuel*) presented in equation (3.19), during the optimization process.

3.2.5.12 Maximum Fuel Capacity

It is necessary to check the aircraft's available fuel capacity in order to carry sufficient fuel mass required. In this initial sizing program, the available fuel capacity is assumed to obtain from wing fuel tank independently. The available fuel capacity will be made liable to alteration with the mission fuel during the optimization process. From open literature proposed by Torenbeek[125], the available fuel capacity can be determined from:

$$Mfuel\_ava = 420 \times b\_cal \times S \times t\_c \times \frac{\left(1 - 0.89 \times tap + 0.49 \times (t\_c)^2\right)}{AR} \quad (3.41)$$

Conclusion: The mission fuel mass module provides the total fuel mass required for the mission, obtained from the product of the fuel used during the mission and a supplement reserve fuel, which is subjected to variation with the initial fuel mass estimation during the optimization process. The available fuel capacity is required to capacitate the total mission fuel alteration.

3.2.6 Point Performance Analysis

The size and mass of an aircraft are critically dependent upon the point performance capabilities. In order to estimate the point performance and relate it to that required, the aircraft mass in various phases of the flight, and the aerodynamic and engine performance characteristics, computing in the previous sections, are needed. The performance requirements that are considered in this analysis consist of climb performance, level turning flight, and take-off and landing field length. They are compared to the design requirements during the optimization process. Several textbooks have presented the efficient information for the estimations of the point performance capabilities[6,7,9,96,102].

To enable the point performance to meet the design requirements, it is intended to establish the combinations of the two fundamental parameters: the wing loading and the thrust loading, in various phases of the flight. They are represented as:

$$W\_S = {(M \times g)}/{S} \quad (3.42a)$$

$$T\_W = {T}/{(M \times g)} \quad (3.42b)$$

Where W_S is the aircraft wing loading and T_W is the thrust to weight ratio respectively. The acceptable combinations of these two parameters will in general be different for each of the various performance requirements as well as being dependent upon other aircraft characteristics such as the engines and wing configuration. The following sub-sections explain the point performance capabilities in details.

3.2.6.1 Take-off Performance

The military take-off requirements are frequently specified in terms of maximum allowable ground run, which the aircraft accelerates from zero velocity to gain a flight speed at which it can lift off and climbs to clear a specified 50-feet (15.24 metres) obstacle height. For an initial sizing study, an existing empirical formula is updated with new data obtained from previous sections, to perform the estimation of take-off ground run. The method makes the use of the unstick or take-off lift coefficient (CL_us) and the parasite drag coefficient (CDf) generated by the aerodynamic modules, the aircraft wing loading and the uninstalled thrust to weight ratio. Take-off parameters such as altitude, temperature and percentages of fuel and payload on board are all taken into account in the calculation of the equation parameters. After simplifying, the estimation of take-off ground run can be defined as:

$$Sto\_re = \frac{0.0447 \times (W\_S)_{TO}}{(Den)_{TO} \times \left[\begin{array}{l} CL\_us \times \left\{ \begin{array}{l} 0.75 \times \dfrac{(5+BPR)}{(4+BPR)} \times (T\_W)_{TO} - \\ Mu\_gr \end{array} \right\} \\ -0.72 \times CDf \end{array} \right]} \tag{3.43}$$

Where BPR is the engine by pass ratio specified in the design requirements and $(Den)_{TO}$ is the air density at take-off altitude obtained from the atmospheric module. Mu_gr is the ground friction coefficient for different surfaces of runway that a concrete surface type has been selected with a typical value of 0.03.

3.2.6.2 Approach and Landing Performance

In general, approach and landing performance is much like taking off, only in the reverse direction. One difficulty is the determination of the ratio of the design landing mass to the take-off mass. For simplicity in the absence of more precise information, an analysis of existing aircraft has been undertaken that for military jet trainer aircraft the ratio varies between 0.85 and 0.95. The stalling characteristics of the aircraft in the landing configuration are then established, such that the required approach speed can be determined, which is usually 1.3 times the stalling speed represented as:

$$Vapp = 1.3 \times \sqrt{\frac{2 \times Mld \times g}{(Den)_{LD} \times S \times CL\_ap}} \tag{3.44a}$$

$$Mld = Mto \times Mld\_Mto \tag{3.44b}$$

Where Mld_Mto is the ratio of the design landing mass to the take-off mass and Mld is the design landing mass. CL_ap is the approach drag coefficient generated by the aerodynamic modules. $(Den)_{LD}$ is the air density at landing altitude obtained from the atmospheric module. The approach speed $Vapp$ is one of the required constraints compared to that in the design requirements during the optimization process.

The estimation of the landing ground roll distance needs the assumption of an average constant value of deceleration forces, which are equal to their instantaneous value evaluated at 70% of approach speed. Landing parameters such as altitude, temperature and percentages of fuel and payload on board are all taken into account in the calculation of the equation parameters. After simplifying, the estimation of landing ground roll distance can be defined as:

$$Sld\_re = \frac{1.69 \times (Mld \times g)^2}{g \times (Den)_{LD} \times S \times CL\_ap \times \left[\frac{(D)_{LD} + Mu \times}{(Mld \times g - (L)_{LD})} \right]_{0.7Vapp}} \quad (3.44c)$$

Where *Mu* is the braking coefficient for different surfaces of runway, which has a much higher value than the ground friction coefficient because the brakes are applied. A typical value of 0.4 for concrete surface type has been selected for this analysis. Drag and lift are the deceleration forces evaluated at $0.7Vapp$.

3.2.6.3 Climb Performance

Two significant aspects of climb performance have been considered for an initial sizing study: the rate of climb and the time to climb. Rate of climb is a vertical velocity, which takes the aircraft to an operating altitude, and time to climb to a given altitude is the change in altitude over a vertical velocity. To meet the best climb requirements, the aircraft must be able to climb from sea level to an operating altitude with best rate of climb or in as short a time as possible. To determine the climb requirements, the methods make the use of air density, altitude, aircraft mass in climb phase of flight, drag, thrust, and the climb velocity.

$$RoC = (V\_cl \times (T\_W)_{CL}) - \left(\frac{(Den)_{CL} \times (V\_cl)^3 \times CDf}{2 \times (W\_S)_{CL}} \right) - \left(\frac{2 \times K \times (W\_S)_{CL}}{(Den)_{CL} \times V\_cl} \right) \quad (3.45a)$$

$$Time\_cl = {}^{\Delta h}/_{RoC} \quad (3.45b)$$

Where *RoC* is the rate of climb, *Time_cl* is the time to climb, and Δh is an altitude changes. The estimation of climb requirements is assumed to be based on a steady climb, at a given mass, constant-thrust setting and constant climb velocity.

3.2.6.4 Sustained Turn Performance

Manoeuvre requirements are a major factor in the design of combat aircraft. One of manoeuvre capabilities may be defined in terms of turn rate. For an initial sizing study, the estimation of sustained turn rate has been considered. Sustained turn rate is a measure of the ability of an aircraft to manoeuvre without losing either speed or altitude. In a sustained turn the thrust must equal the drag and the lift must equal load factor times aircraft mass as the horizontal component of the lift exerts the centripetal force required to turn. Thus the maximum load factor for sustained turn can be expressed as the product of the thrust loading and lift-to-drag ratio defined as:

$$Nsus = (T\_W)_{CR} \times (L\_D)_{CR} \quad (3.46a)$$

The sustained manoeuvring capability of the aircraft depends strongly on its maximum lift coefficient and its thrust. From equation (3.46a) the lift-to-drag ratio can be determined in terms of the basic aerodynamics coefficients:

$$(L\_D)_{CR} = {CL\_cr}/{CD\_cr} \tag{3.46b}$$

Where CL_cr is the maximum lift coefficient in manoeuvre condition obtained from equation (3.22), and CD_cr is the total drag coefficient at cruise stage obtained from the simplified methods in equation (3.24). After computing the maximum sustained load factor, the estimation of sustained turn rate can be determined.

$$T\_rate = \frac{g \times \sqrt{(Nsus)^2 - 1}}{V\_cr} \tag{3.46c}$$

The sustained turn rate is usually expressed in degrees per second. Equation (3.46c) generates radians per second, which must be multiplied by 57.3 to get degrees per second. The sustained turn rate is one of the required constraints compared to that in the design requirements during the optimization process.

On the other hand, the estimation of sustained turn can be determined in term of turn radius. In level turning flight, turn rate is based on the maximum load factor and speed as defined in equation (3.46c), and is also corresponding to speed over turn radius. With these relations, the estimation of sustained turn radius can be determined.

$$R\_turn = \frac{V\_cr}{T\_rate} = \frac{(V\_cr)^2}{g \times \sqrt{(Nsus)^2 - 1}} \tag{3.46d}$$

3.2.6.5 Mach/Speed Performance

It is difficult to calculate the maximum level flight speed of an aircraft at a given altitude and mass, because the thrust and drag models will be changing non-linearly with speed. This can lead to problems with the constraint calculations of the optimization process. In order to achieve an efficient and robust constraint, the actual constraint has been altered, so that it is not maximum speed, but rather excess thrust.

Conclusion: The point performance module provides an overview of the methods of calculation and detail of the equations used to estimate the aircraft point performance. In fact, additional calculations are also needed such as specific excess power, attained (instantaneous) turn, to provide more effective sizing process. The point performance analyses are the entirely required constraints compared to those in the design requirements during the optimization process.

3.2.7 Constraint Evaluation

A brief description of the objective function and all of the constraints calculated in the sizing and performance analysis for military jet trainer aircraft is listed in detail.

The objective function is the design take-off mass, *Mto*. It is applied as a target converging to meet the required take-off mass, which is setting as the design variable. Constraint 1 requires the fuel mass analysis throughout the mission to meet the total

fuel mass estimated by fuel fraction in the form of equality constraint. Constraint 2 ensures that the available fuel capacity of the aircraft can capacitate the total fuel throughout the mission performing an inequality constraint.

$$Constr(1) = Mfuel\_re - M\_fuel = 0 \quad (3.47)$$

$$Constr(2) = Mfuel\_ava - Mfuel\_re \geq 0 \quad (3.48)$$

Constraints 3 through 17 are the inequality constraints for the point performance analysis calculations as specified in section 3.2.6. Constraint 3 is the required take-off ground run distance.

$$Constr(3) = Sto\_re - Sto\_sp \leq 0 \quad (3.49)$$

Constraints 4 and 5 are the requirements for rate of climb and time to climb during first-climb phase that fully equipped with payload. These requirements are similar for constraints 10 and 11 at second-climb stage except no stores loaded.

$$Constr(4,10) = RoC - RoC\_sp \geq 0 \quad (3.50)$$

$$Constr(5,11) = Time\_cl - Time\_cl\_sp \leq 0 \quad (3.51)$$

Constraint 6 ensures that the maximum lift coefficient during cruise-out phase is in the limit of buffet considerations, which is also required for constraint 12 at cruise-in stage with no stores loaded. Constraint 7 requires the difference between thrust and drag at cruise-out stage, similar to that of constraint 13 at cruise-in stage.

$$Constr(6,12) = CL\_cr - CL\_buffet \leq 0 \quad (3.52)$$

$$Constr(7,13) = D\_cr - T\_cr \leq 0 \quad (3.53)$$

Where CL_cr in equation (3.52) refers to the lift coefficient calculated during cruise phases not the maximum lift coefficient for manoeuvre condition represented in equation (3.22).

Constraints 8 and 9 are the requirements for sustained turn rate and sustained turn radius during cruise-out phase, similar to constraints 14 and 15 at cruise-in stage.

$$Constr(8,14) = T\_rate - T\_rate\_sp \geq 0 \quad (3.54)$$

$$Constr(9,15) = R\_turn - R\_turn\_sp \leq 0 \quad (3.55)$$

Constraint 16 is the required landing ground roll distance. Constraint 17 ensures that the approach speed is in the limit that specified by the design requirements.

$$Constr(16) = Sld\_re - Sld\_sp \leq 0 \quad (3.56)$$

$$Constr(17) = Vapp - Vapp\_sp \leq 0 \quad (3.57)$$

Finally, constraint 18 checks the limit of wingspan.

$$Constr(18) = b\_cal - b\_sp \leq 0 \quad (3.58)$$

Conclusion: This section provides all of the constraints required for an initial sizing study. Most of these constraints cope with the aircraft performance.

After completing overall calculations including constraints evaluation, the optimization tool is then used to perform an iterative process to find the lightest aircraft that will both perform the design mission and meet all constraints requirements. After some number of iterations requiring a new or revised design

layout, results are then obtained showing the parameters requirements for setting up the aircraft configuration. The final results and comparison of data with the specifications of existing similar aircraft will subsequently be shown in the appendix of the thesis.

3.3 Summary

The conceptual design for the military jet trainer aircraft, presented in this chapter, was a valuable step to understand the process in advance of activating the Uninhabited Combat Aerial Vehicle design. Moreover, it is worthy to gain all information on the major parameters needed for the conceptual design process for UCAV and to understand the use of optimization technique to find out the solution.

CHAPTER 4

4 Concept of Configuration and Design Aspect

This chapter describes the overall structure of the synthesis and optimization process for an Uninhabited Combat Aerial Vehicle (UCAV) design. A brief description of the procedure used throughout this thesis to describe the model structure is explained. This chapter also explains the concept of packaging and configuration design aspects, which is the primary objective of this project. An initial sizing program determined in previous chapter provides an invaluable step to perform the synthesis and analysis process for UCAV design presented in this chapter and the rest of entire thesis.

4.1 Overall Arrangement

The overall structure of the synthesis and optimization process for the UCAV design is carried out via a large *FORTRAN* code containing various isolated modules. Figure 4-1 presents a diagrammatic representation of the operations of the whole program.

In fact, the overall arrangement used is not entirely new; alternatively it is described as an application of an existing analytical technique to the solution of a problem. The primary process for the analysis is possibly similar to the existing procedures; on the other hand, the analytical techniques utilized at each stage in various modules of the process are different from or are the combination of existing techniques based on validation against a few existing design aspects.

From the overall arrangement, it can be seen that the optimizer has ultimate control of the program, and is responsible for converting the aircraft design parameters such that all constraints are met, and a minimum objective function is achieved. The individual models of the overall arrangement are subsequently explained in details.

4.1.1 Input Data

The input data required for the synthesis of UCAV design consists of six data files: the packaging specification, the design variables, the external variables, the airfoil coordinates, the weapon selections and dimensions, and the avionics instruments and dimensions. All these input data are mainly applied for setting the packaging and configuration design aspects of UCAV to perform the calculations throughout the procedure.

The *packaging specification* provides the optimizer to select the options required for the conceptual sketch of aircraft. The *design variables* contain all of the main design parameters and the optimizer control values.

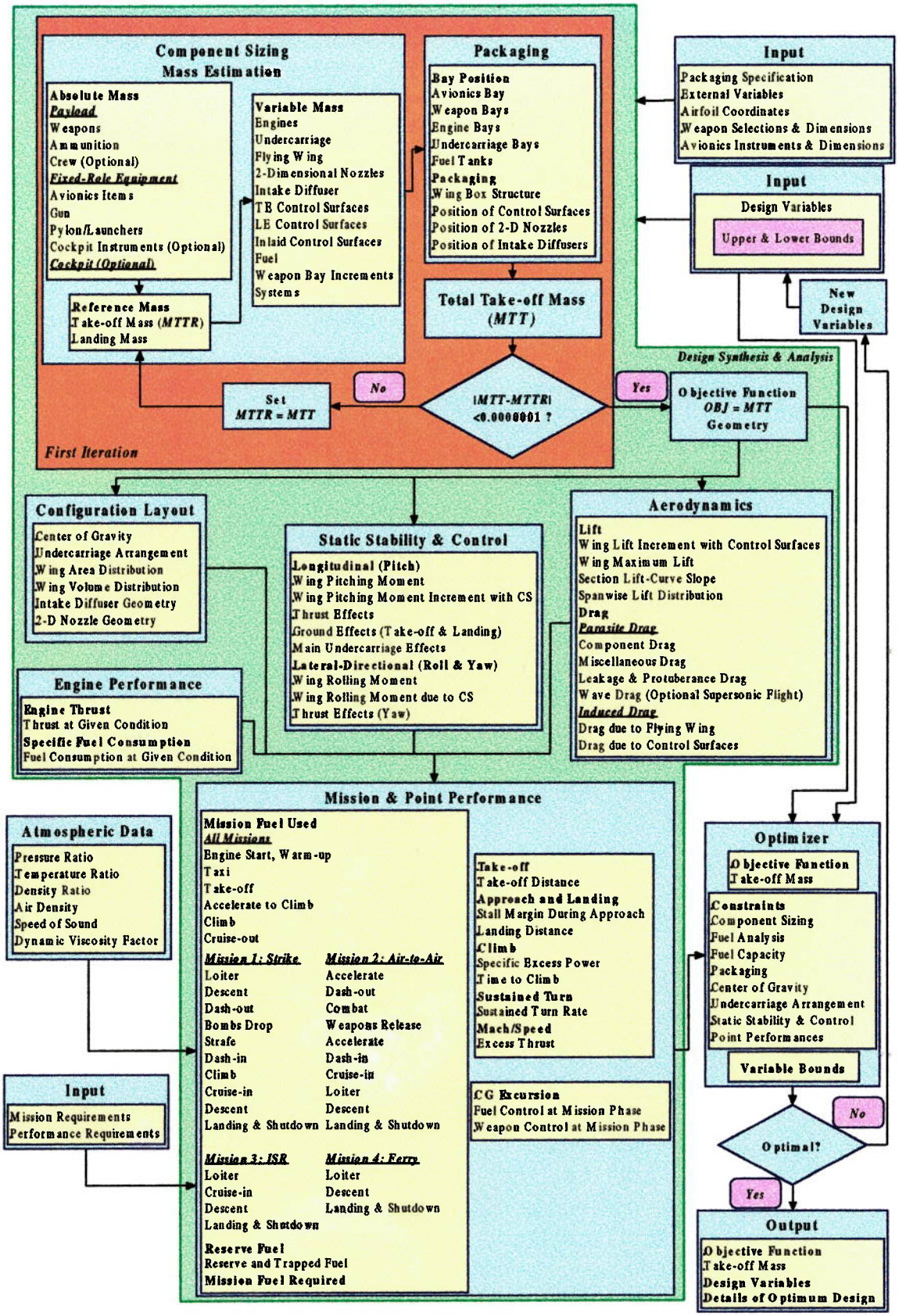

Figure 4-1: UCAV Overall Program Flowchart

The design parameters, corresponding with the options of the packaging specification, are required for producing an initial model of the baseline design and controlled by the optimizer within the margin of control values during the iterative process in order to produce the final design aspect of the aircraft. The *external variables* contain all of the mandatory data required for implementing the overall calculations throughout the entire process. Overall lists and brief descriptions of the packaging specification are given in section 4.2 and the design variables are presented in Chapter 5.

The *airfoil coordinates* provides the data for setting the configuration design aspects of the aircraft that control the extrusion of all the packaging during the optimization process. The *weapon selections and dimensions* give all details of weapons to be loaded on the aircraft either internally or externally, and provide weapon dimensions to size for the internal weapon bays. Finally, the *avionics instruments and dimensions* provide all details of the avionics items required by the aircraft and the dimensions of all items to size for the avionics bays. Both the weapons selected and the avionics instruments are based on the mission of the aircraft, which is set by the user in the packaging specification. Lists of weapons and avionics instruments selected for UCAV are given in the appendix of the thesis.

The input data, except the aircraft design variables, are only performed on the very first call (i.e. file open and read) to the synthesis module. All of the following procedures are performed every time the synthesis is called.

4.1.2 Component Sizing and Packaging

The next stage in the design process is to size all the components of the aircraft and set up the packaging so that an overall configuration can be analysed. As mentioned in the literature search of Chapter 2, the UCAV configuration is based on the flying wing concept, thus the primary methods of calculations have been developed specifically for this design. The components that are predicted in this section of the program are divided into two main groups based on the mass representation: an absolute mass and a variable mass.

The components representing an absolute or a fixed mass are composed of payload (i.e. weapon(s), ammunition and crew (optional manned aircraft)), and fixed-role equipment (i.e. avionics items, gun, pylon/launcher(s), and cockpit instruments (optional)). The manufacturer basically sizes all the fixed mass components, thus they are available for packaging. For variable mass contribution, the components include wing, engine(s), intake diffuser(s), two-dimensional nozzle(s), undercarriage, control surfaces, fuel tanks, and systems. Once the components sizing has performed, the packaging can be set up and followed by the calculations in the next stage. Details of component sizing and packaging calculations are given in Chapter 5.

4.1.3 Mass and Volume Estimation

The mass estimation of the aircraft is of fundamental importance in the design as it has a major effect upon other calculations throughout the entire procedure. Hence it is essential to predict the aircraft mass as accurately as possible. The mass estimation methods used for the UCAV design synthesis have been gathered from various sources[4,5,78,79], and make some modifications and improvements to the basic

algorithms, which are particularly suited to the estimation of aircraft component and system masses at the conceptual design stage. The methods are either empirical or theoretical derivations based on historical data.

In order to produce a realistic aircraft design, the volume available for fuel storage must be estimated, so that necessary provision for all of the required design mission fuel can be made. Once the packaging has set up, the volume available for fuel storage in integral tanks in the wings can be achieved, and by allowing the available volume enclosing the packaging to be filled with fuel. The volume of overall fuel tanks is estimated using simple geometric shapes. A full description of mass and volume estimation is given in Chapter 5.

4.1.4 Configuration Layout

The configuration layout is considered separately in four tasks: the aircraft centre of gravity, the undercarriage arrangement, the wing area and volume distribution, and the geometries of intake and two-dimensional nozzle ducts.

Once the configuration design aspect has achieved, it is unavoidable to consider the centre of gravity of the aircraft. The position of the centre of gravity is determined by taking the moments about the aircraft nose of all the components. The centre of gravity of aircraft is calculated in three cases: with no weapons loaded and fuel tanks empty (empty mass), weapons loaded and fuel tanks empty (zero fuel mass), and full loaded (total mass). It is assumed that payload and fuel proportioning is available to maintain the centre of gravity between the range of forward and aft limitations.

The centre of gravity has a major effect upon the packaging particularly the undercarriage arrangement. The main landing gear must be located behind the centre of gravity in order to prevent the aircraft from tail touching the ground during the aircraft nose-up attitude. This is measured from the angle off the vertical from the main landing gear to the centre of gravity compared to the tipback angle. Details of aircraft centre of gravity and the undercarriage arrangements are given in Chapter 6.

The next stage of the configuration layout is to determine wing area and volume distribution. The term 'wing' is applied in this calculation instead of 'aircraft' as the main configuration of UCAV is based on the flying wing concept. The method used in this stage was developed by Lovell[78], with some modifications by the author to be acceptable to several aspects of UCAV design. This module is required for the wave drag analysis on condition that the aircraft flies in supersonic region.

In addition, the geometries of intake and two-dimensional nozzle ducts play an important role for the packaging. The geometry of intake serpentine-duct makes the use of a cubic curve fits according to the internal component arrangement. The geometry of nozzle duct needs providing a good transition from circular to rectangular cross-section that the nozzle area must be constant without causing excessive losses, and it must also be fitted to the wing trailing edge area with minimum extrusion. A detailed description for the geometries of intake serpentine-duct and nozzle circular-to-rectangular duct follows the synthesis equations proposed by Seigers[108] and Burley[19] respectively, with some modifications to accommodate the flying wing configuration, as presented in Chapter 6.

4.1.5 Aerodynamic Modelling

The flying wing concept provides itself for a relatively simple aerodynamic analysis, since it does not have a fuselage or tails. The aerodynamic module consists of two sections that predict available lift coefficient, and aircraft drag respectively. These two models are based on empirical correlations making the use of relatively simple empirical algorithms for their aerodynamic prediction. The methods break the overall lift and drag values down into smaller parts, and relies on the interpolation of many sets of empirical tables and figures for the estimation of each part. The characteristics of lift and drag were chosen and considered for their ability to predict the relevant aerodynamic properties in subsonic speed regimes, and their applicability to low-aspect ratio wing configurations.

This aerodynamic module provides an uncomplicated method for the design synthesis process in order to accomplish the investigation of various packaging and configuration design aspects for UCAV. The more complex and accurate methods for the prediction of aerodynamic performance may be required to provide the correct balance of accuracy and efficiency. Details of aerodynamic module are given in Chapter 7.

4.1.6 Static Stability and Control Modelling

The simple method of static stability and control is required for the design synthesis process to determine the sizes and to consider the positions of control surfaces in which they affect directly to the packaging and configuration design aspects, and the mass estimation of the UCAV flying wing. The sizes and positions are also based on the number of control surfaces set by the packaging specification as they may perform different functions (e.g. flaps, ailerons, elevators, or split elevons) during the flight. A brief description of static stability and control module applied for the design synthesis process is given in Chapter 7.

4.1.7 Engine Performance Modelling

The engine performance analysis applied for the design synthesis process of UCAV is similar to that applied for an initial sizing study of the military jet trainer aircraft presented in section 3.2.4 of Chapter 3. The most possible representation of the variation of thrust and specific fuel consumption with flight conditions are required for the point performance, and the mission performance to determine the mission fuel mass.

The operating thrust values at any given condition are related to a datum, sea-level static dry thrust of the known engine. However, the size of the engine designed for UCAV is controlled by the engine scale factor (set as the design variables), to be fitted into the aircraft. As the static dry thrust is parametrically independent upon the engine size, therefore, for engines with similar characteristics but different sizes, it is also decided to scale the static dry thrust data before proceeding to perform the operating thrust values at any flight conditions. Detail of reasonable static dry thrust is represented with the engine sizing in Chapter 5, and additional explanation for engine performance module is given in Chapter 7.

4.1.8 Mission and Point Performance Analysis

The mission performance analysis for UCAV design is considered with four typical mission profiles: the low-level strike mission, the counterair mission, the surveillance and reconnaissance mission, and the ferry mission. The aim of this calculation is to accumulate the avionics instruments and the weapons required for that particular mission, to size the avionics bays and the weapon bays in order to achieve the investigation of various packaging and configuration design aspects of UCAV. Furthermore, the integral fuel tanks and the available volume enclosing the packaging can capacitate the total mission fuel alteration.

The methods used to determine the mission fuel mass are almost similar to those represented in section 3.2.5 of Chapter 3, with some modifications and improvements to achieve more accurate methods applied for UCAV. Historically, the bombs drop mission phase defines that no fuel penalty was assessed, so the fuel fraction is assumed to be unity. For the UCAV design with an internal weapon bay, this mission phase starts from bay-doors open, release weapons, and ends after doors closed. As a result, range credit has been taken and so fuel penalty is occurred. Therefore, the accurate method of fuel-fraction estimation will be required for this mission phase.

Additionally, the methods used to determine the point performance are almost similar to those represented in section 3.2.6 of Chapter 3, with some modifications and improvements to accomplish more accurate methods applied for UCAV. Details of mission and point performance analysis are given in Chapter 7.

4.1.9 Centre of Gravity Excursion

The CG excursion module is required to examine the range of the aircraft centre of gravity to remain within the acceptable limits throughout the mission, which is affected by fuel and payload fractions during each mission phase. For each of these phases, the user can set the payload requirements either to release the weapons or to contain full stores back to base. The CG excursion module will be called at the end of each of the mission phases to determine the aircraft mass and centre of gravity and will be set as constraints subjected to remain within the acceptable CG limits. All details of the CG excursion module including input data for weapon control module are given in Chapter 7.

4.1.10 Aircraft Synthesis and Output Routines

Once overall calculations including constraints evaluation have been completed throughout the synthesis process, the optimization tool is then used to perform an iterative process. The output routines are initiated, and results of the design study are written to the respective files. These are written to allow the accurate comparison of competing designs, and contain enough data for a sketch of the aircraft to be produced.

Chapter 8 will make the comparison and discussion of the results and discuss the problems specifically associated with attempting to program the overall arrangement of the procedures.

4.2 Packaging and Configuration Design Aspects

The packaging aspects have been set up comprising of avionics and sensor bays, internal weapon bays, engine bays, undercarriage bays, intake diffusers, two-dimensional nozzles, and fuel tanks. The wing centreline and the wingspan of the aircraft are probably two of the most critical variables as far as packaging aspects are concerned. This is because it is necessary to fit all the above components internally to perform configuration design aspect, thus requiring sufficient volume. One of the design objectives is to avoid at all cost the use of any fairing on the shape of aircraft, thus reducing its radar observability. The following sections describe the packaging and configuration design aspects of UCAV in greater details. Additionally, Figure 4-2 (see following page) presents a diagrammatic representation of the operations of these packaging and configuration design aspects, which all details are given in Chapter 5 and Chapter 6.

4.2.1 Avionics Bay

The avionics instruments required for UCAV have been gathered to form the avionics bay and sensor bay. The data file containing the avionics instruments and dimensions specifically, '*datavi.dat*', is only performed on the first call to the synthesis module, based on the typical mission of the aircraft set by the user in the *packaging specification.* They are needed to estimate the dimensions, volume, and mass of the avionics and sensor bays applicable for the packaging design. The lists of all avionics items will subsequently be presented in the appendix of the thesis.

The avionics bay consists of vehicle and flight control suite, navigation suite, communication suite, and identification suite, appearing as the Flight Management System (FMS). The sensor bay consists of all radar and sensor equipments available as the Mission Management System (MMS). The UCAV would require the FMS to enable the variable control consistent with the UCAV mission description, concept of operations and the combination on-board/off-board targeting. The aircraft would require the MMS capable of detecting inbound enemy missiles and identifying ground targets, automatic target recognition with some on-board reasoning or decision making capability from the FMS, and a data link that require a variable bandwidth and the ability to break up a message and send it via several frequencies.

Because the UCAV is designed to operate independently of human control for the majority of its mission, a flight control computer is the primary avionics item arranged for the aircraft. Able to access the onboard integrated avionics system, the centre of gravity control, and fly-by-wire control system, the computer is able to maintain control of the aircraft at all times. Several air data transducers supply the flight computer with necessary airspeeds and altitudes. The unit has a built in an identification – friend or foe (IFF) system to assist in attitude and heading references. The UCAV utilizes a Differential Global Positioning System (DGPS) for its pre-programmed aircraft navigation as well as general aircraft position data to ensure reliable autonomous control. The VHF data link and adaptive DGPS antenna were designed for military use in areas filled with hostile electronic environments. The antenna is the primary system used to feed data to the FMS.

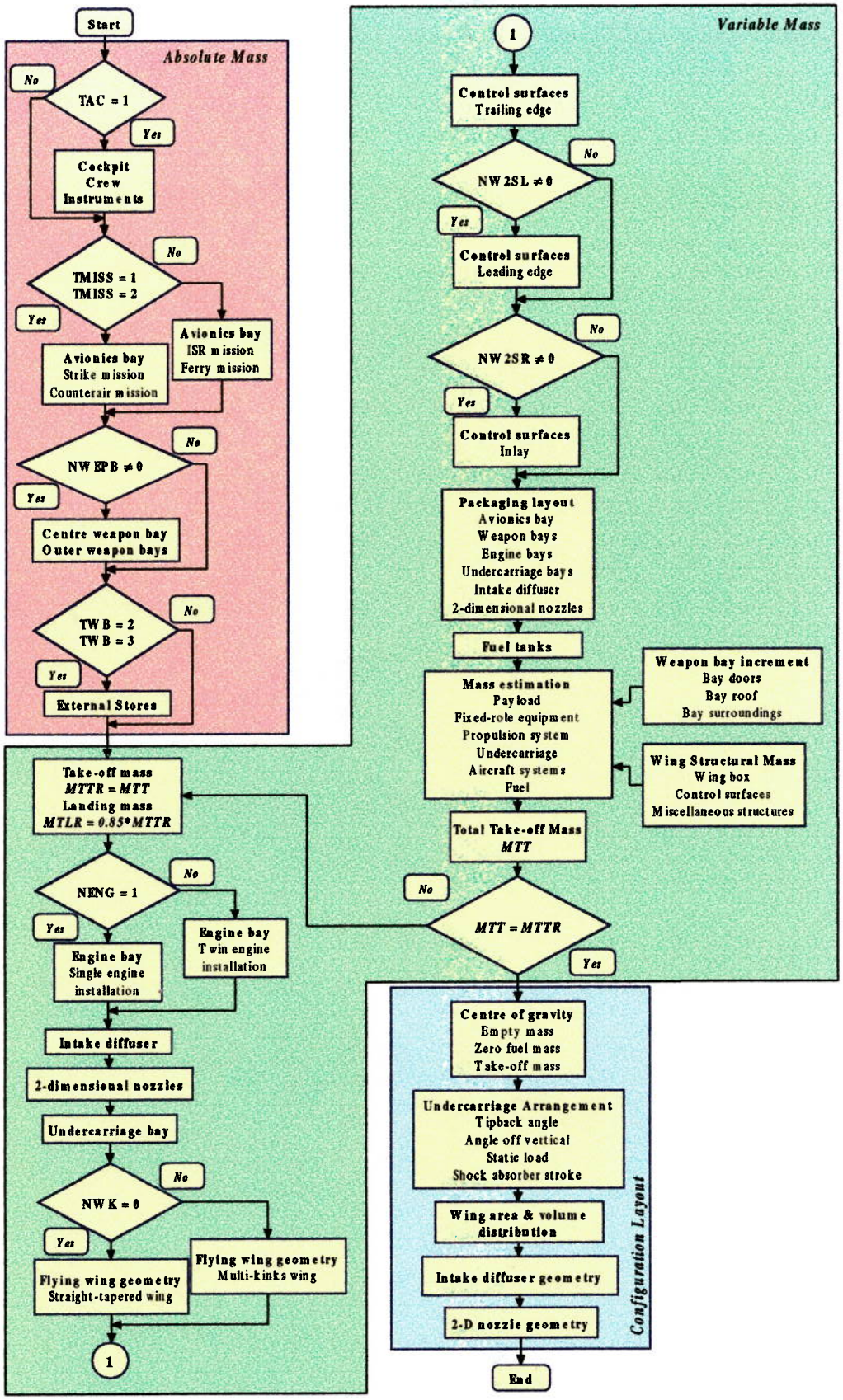

Figure 4-2: UCAV Packaging and Configuration Design Aspects Flowchart

The Forward Looking Infra-Red (FLIR) provides final targeting, imaging, and man-in-loop flight control. The system is capable of detecting thermal differences and can penetrate darkness and fog to identify people and targets. The FLIR is located in the sensor bay at the nose of the aircraft giving it the ability to see below and in front of the aircraft.

Furthermore, weapon control and release equipments are needed for UCAV to provide appropriate interfaces to the weapons. The electronic warfare system may also be required to confuse the radar operator through jamming, as mentioned in the literature search of Chapter 2.

All of these systems should be tested, replaced and/or changed while in operational status or dormancy without impact to the systems. To provide a favourable environment and excellent access to the avionics, most units should be contained in a single air-conditioned bay, located so that access is comfortable for all maintenance personnel from the ground without support equipment and additionally lower program costs. Due to rapid advances in the capability of avionics, allowance for avionics growth should be made in terms of volume. If such an allowance were not made, increasing the capability of the avionics suite would degrade reliability and maintainability, and be more expensive.

4.2.2 Internal Weapon Bay

Carriage of weapons is the purpose of most military aircraft. The weapons are substantial portion of the aircraft's total mass. This requires that the weapons be located near the aircraft's centre of gravity. Otherwise the aircraft would pitch up or down when the weapons are released.

External carriage is the lightest and simplest, and offers the most flexibility for carrying alternate weapon stores. Once an aircraft has dropped its external load, it has become relatively clean aerodynamically and is better suited for rapid exit from the combat area, aided by the fact that no excessive structural mass penalty is paid when compared with the essentially useless mass of an empty internal weapon bay.

On the contrary, external weapons possess extremely high drag, significantly degrading the aircraft range and performance. They also provide additional radar and visual reflection points, essentially degrading the low observable characteristics of the configuration. To avoid these problems, the lowest-drag option for weapons carriage is internal. Although this is partly due to the mass penalty imposed by an internal weapon bay and its required doors, but is also due to the prevalent desire to maximize dogfighting performance at the expense of alternate mission performance. However, only an internal weapon bay can completely eliminate the weapons' contribution to radar cross section.

The weapons selected for UCAV have been obtained from typical types used with the modern combat aircraft to form weapon bay. The data file containing the weapon selections and dimensions namely, '*datweap.dat*', is only performed on the first call to the synthesis module, based on the typical mission of the aircraft set by the user in the *packaging specification*. They are needed to estimate the dimensions, volume, and mass of the internal weapon bays, or obtain only the mass of weapons for an optional

external load, applicable for the packaging design. The list of weapons and their dimensions will subsequently be shown in the appendix of the thesis.

To carry a combat fighter-sized weapons payload, the size of UCAV could be reduced 10-15%[45]. Maximum flexibility for internal weapon bay should also be considered in order to permit the integration of current and future weapons. This is especially important when setting the dimensions of the weapon bay. With the use of new small weapons now under development could allow them to cut aircraft weight from 15,875 kg, about the size of an F-16, to less than 6,800 kg[45]. The development of small, highly accurate bombs and missiles are expected to greatly multiply the payload and striking power of the relatively small UCAV[46].

Clearance around the weapons is also important for safety. If the weapons are mounted near each other, there should be a clearance on the order of 0.075m[96]. The structural integrity of the airframe and suspension equipment should permit carriage and delivery of a wide range of weapons as well internal fuel tanks, practice munitions, and defensive countermeasures. The concept of suspension equipment designed for UCAV may employ the vertical eject launcher as designed on F-22, which can be supported a wide range of weapons used for all air-to-air and air-to-ground missions[75].

The system will be installed in the weapon bays. To fire a missile or release the weapon, the weapon bay door of the referring missile will open, the mechanism will carry the missile outside the aircraft, the missile can lock and it is fired. When the missile is away, the ejection system will retract into the weapon bay again and the bay door closes to preserve the fighters stealthiness. Figure 4-3 shows an AIM-120 AMRAAM being launched from the vertical eject launcher of F-22. It should be noted that the motor of the missile is not ignited until it has been ejected well clear of the aircraft.

Figure 4-3: An AIM-120 AMRAAM Launched from Vertical Eject Launcher of F-22 Raptor

During the optimization process, the size and initial mass of the weapons and weapon bay remains constant. Only the position may be varied by changing the value of two independent coordinates describing the positioning of the bays in the longitudinal and lateral directions. Internally, specifying the number of store points in the vertical, longitudinal and lateral directions may vary the arrangement of the weapons. Furthermore, an option of none, one, two or three weapon bays is possible, and the options of no stores, external stores, and combined internal and external stores are also attainable. The dimensions of the weapon bays are one of the main sizing drivers for the wing configuration, significantly influencing its geometry, layout and mass.

4.2.3 Engine Bay

Modern engine technology is needed for UCAV that will permit the construction of propulsion systems able to survive long-term storage and maintainability requirements. The engine shall have performance and affordability features consistent with mission requirements and support concepts. Technology developments will be needed to produce an engine, which is sufficiently robust to enable the manoeuvrability of UCAV to reach maximum potential. If UCAV could be designed to use a variant of a commercial engine with good specific performance, its affordability would be assured. However, engine size will strongly affect the dimensions of the aircraft.

To determine the engine bay for UCAV, the synthesis follows some approach given by Lovell[78]. The dimensions for the engine are obtained by scaling from some nominal engine size by whatever scale factor is required to provide the desired thrust. The scale factor is the ratio between the required thrust and the actual thrust of the nominal engine. One of the fundamental decisions to be taken during, or perhaps before, the formative stage of a design concerns the number of engines. To a large extent, this is a policy decision influenced by considerations of safety, cost-effectiveness and availability. The number of engines has a profound influence on aircraft packaging, dictating the disposition of intake ducts, weapon bay, undercarriage bay and fuel tanks. A twin-engine installation should have enough separation between engines to prevent damage to the engine. If twin engines are together, this requires at least 0.3 m of clearance between engines[96].

4.2.4 Intake Diffuser

Principal aspects of intake are the intake position, its shape and components including the inlet cross-section and the length and variation of the duct cross-section leading to the engine. The geometry is slightly different for twin- or single-engine aircraft. The three-dimensional curvature of the intake is necessary in order to hide the engine face from the intake as much as possible. This will reduce the infrared, acoustic and radar emissions from the aircraft when viewed head-on.

4.2.5 Two-Dimensional Nozzle

The UCAV requires nonaxisymmetric or two-dimensional nozzles to hide the hottest parts of the engine from as many angles as possible. The potential benefits of two-dimensional nozzles are the reduced and directionalized infrared and radar signatures. The change from circular to rectangular cross-section is achieved by means of the transition section. The transition section or duct connects the axisymmetric engine to the nonaxisymmetric nozzle through a smooth progression of geometrically similar cross-sections. The duct must be as short as possible to minimize the mass of the propulsion system installation. Additionally, It must be long enough to prevent any flow separation, which could adversely affect performance and create severe wall cooling problems. To prevent the flow separation, Burley[19] suggests that the maximum angles to change from circular to rectangular cross-section should not be greater than 45 degree.

4.2.6 Packaging Specification

Before beginning with the detailed coding of the aircraft design synthesis process, it is necessary to set up the *packaging specification* to define the conceptual sketch for UCAV. At this stage, no calculations have been made concerning the design, apart from those required for initial sizing. This represents a variety of particular designs, which is capable of being modelled using this design synthesis process. Table 4-1 lists the major packaging specifications and summarize the options, which are included in the design synthesis along with the principal geometry details.

Variable	Packaging Specification		Code	Detailed Options
Flying Wing				
TAC	Type of aircraft		0	Unmanned aircraft
			1	Manned aircraft
TMAT	Type of materials		1	Aluminium alloy construction
			2	Carbon-fibre composite construction
NWK	Total number of kinks in wing		0	Straight tapered wing
			1 ...	Multi-kinks wings
Control Surfaces				
NW2SE	Number of trailing edge control surfaces on semi-span		1	Split elevons
			2 ...	Flaps and Split elevons
NW2SL	Number of leading edge control surfaces on semi-span		0	No LE control surfaces
			1 ...	Applied LE control surfaces
NW2SR	Number of inlaid control surfaces on semi-span		0	No split drag rudders
			1	A pair of split drag rudders
Packaging Aspects				
TWB	Type of stores		0	No stores
			1	Internal stores
			2	External stores
			3	Combined internal and external stores
NWEPB	Number of weapon bays		0	No weapon bay
			1	Single weapon bay on centreline
			2	Two weapon bays outboard of engines
			3	One inner bay and two outer bays
TMISS	Type of missions		1	Low-level strike
			2	Counterair
			3	Surveillance and Reconnaissance
			4	Ferry
NENG	Number of engines		1	Single-engine installation
			2	Twin-engine installation
Airfoil and Twist				
TIAF	Inboard	Type of airfoils	1	Symmetrical airfoil
TOAF	Outboard		2	Asymmetrical airfoil
RTW	Inboard	Wing thickness ratio	9	9% thickness ratio
			12	12% thickness ratio
RTWT	Outboard		15	15% thickness ratio
			18	18% thickness ratio
NTWIST	Twist distribution		0	Untwisted wing
			1	Twisted wing

Table 4-1: UCAV Packaging Specifications

From Table 4-1, the ***packaging aspects*** *section* provides additional explanation for the user to select the precise options to perform the packaging aspects, as shown below:

Code	TWB	NWEPB	TMISS	NENG
OPT1	0	0	3	All
OPT2	1	1	All	1
OPT3	1	2	All	All
OPT4	1	3	All	1
OPT5	2	0	1 to 3	All
OPT6	3	1	All	1
OPT7	3	2	All	All
OPT8	3	3	All	1

Table 4-2: Additional Explanation for Packaging Aspects

To clearly understand the arrangements of UCAV packaging aspects, Figure 4-4 provides these arrangements based on options 1 to 4 in details. It should be noted that the arrangements in options 5 to 8 are similar to those shown in the figure. The only difference is that the packages provide the optional external stores.

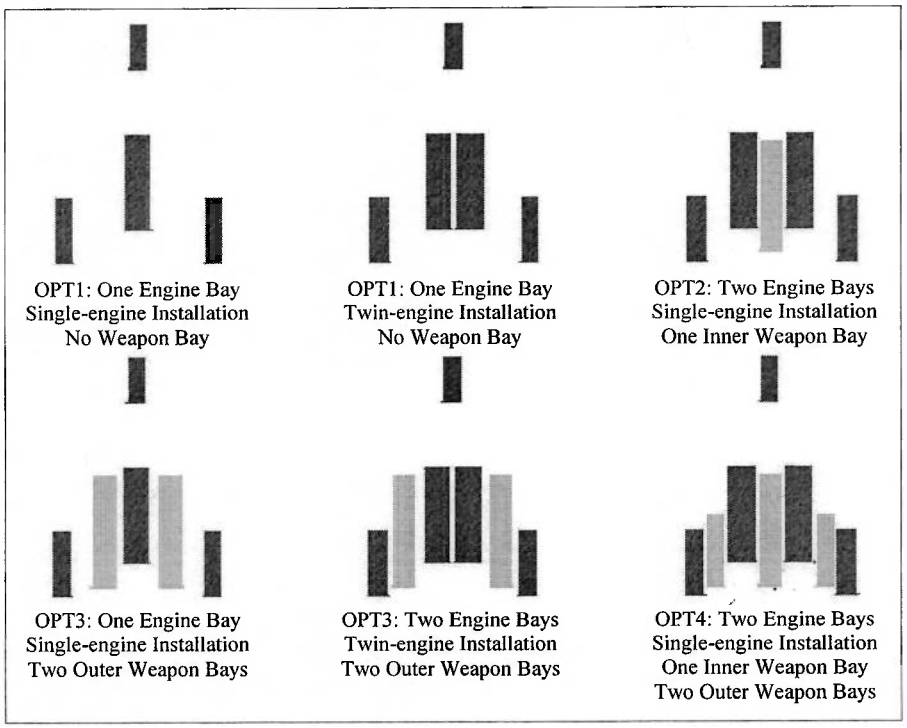

Figure 4-4: Arrangements of UCAV Packaging Aspects

4.2.7 Airfoils

The concept of airfoils selected for UCAV configuration is an attempt to choose all types of either symmetrical or asymmetrical airfoils to fit all the components internally without the use of any fairing on the shape of aircraft. This would be

helpful if, in future, the new type of airfoils is required to fit these components. The airfoil coordinates are one of the main sizing drivers for all the components, significantly affecting the arrangement of their positions in the vertical, longitudinal and lateral directions.

The data file containing the airfoil coordinates namely, '*dataf.dat*', is only performed on the first call to the synthesis module, based on the type of the airfoils (symmetrical or asymmetrical) selected and the wing thickness ratio, set by the user in the *packaging specification*. The airfoils selected for UCAV have been obtained from typical NACA series to set the configuration design aspects of the UCAV. They are selected for the inboard and outboard sections of the wing. There is an intermediate region where there is a transition from one airfoil shape to the other. Figure 4-5 shows this division graphically.

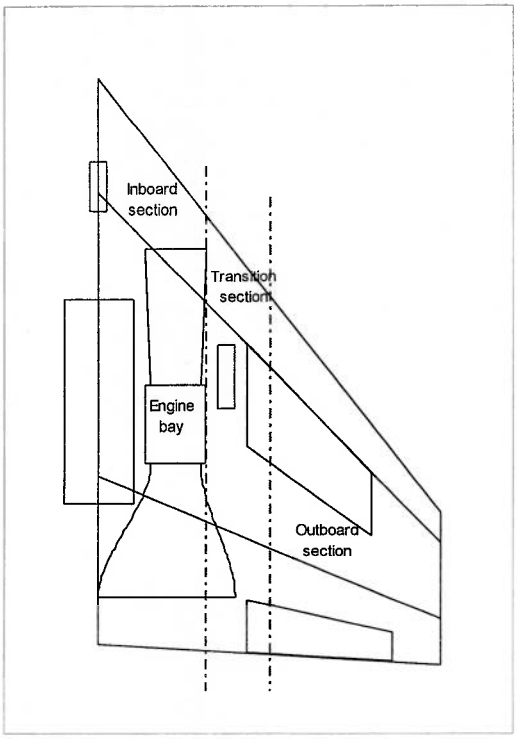

Figure 4-5: Spanwise Distribution of Airfoils

The inboard section extends between the spanwise stations of the outer edge of engine bay. The transition area between both airfoil shapes starts at the outer edge of engine bay station and extends to the half of the semi-wingspan. From this location outboard, the airfoil used corresponds to the outboard section one.

4.2.8 Flying Wing Configuration Layout

The concept of flying wing configurations has been considered with several designs based on two main categories: the straight-tapered wing and multi-kinks wing. One of these configurations was a near-delta planform, similar to the U-99 UCAV as shown in Chapter 2. The wing planform is not a pure delta, since its trailing edge has a sweep angle of 6-degree, providing a low reflection from incoming radar wave. The concept of a near-delta planform configuration is also similar to the kite- or diamond-shape

planform concept of the X-47 Pegasus UCAV, whereas, the trailing edge of the X-47 applies 30-degree sweep angle.

The use of serrated trailing edge, therefore aligning the edges to the same directions as on the leading edges was also considered, as on the stealth bomber B-2. The use of this type of trailing edges is known to produce non-linear aerodynamic effects[2] that will increase the complexity of the flight control system. With the options of number of kinks in wing (NWK) set by the user in the *packaging specification*, Figure 4-6 presents some concepts of the several designs of flying wing configurations considering for UCAV design.

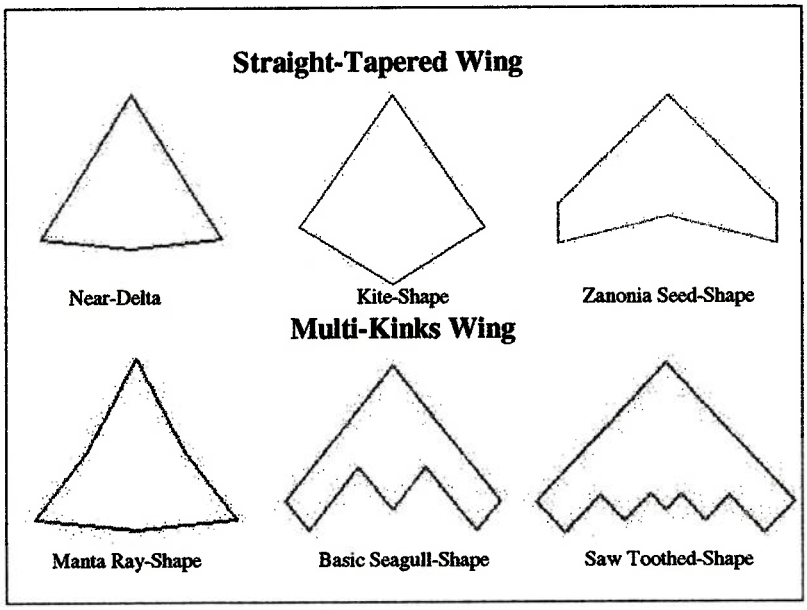

Figure 4-6: UCAV Flying Wing Configuration Layouts

4.2.9 Configuration Sketch

Details of the aircraft design synthesis for the UCAV will be discussed in the next three chapters. Figure 4-7 shows how the options listed in the packaging specification are incorporated into some configuration design aspects of UCAV.

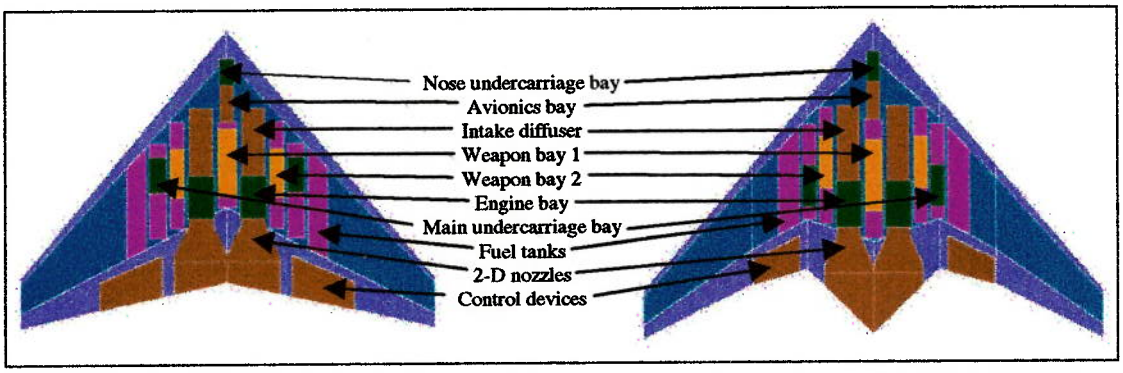

Figure 4-7: UCAV Configuration Design Aspects

4.3 Summary

This chapter has outlined the operation of the overall structure of the design synthesis and optimization process for UCAV design. Furthermore, the detailed descriptions of the packaging and configuration design aspects have presented. The following chapters provide additional details for the methods of calculation based on these descriptions and discuss the results and problems associated with attempting to program the overall arrangement of the procedures.

CHAPTER 5

5 Airframe Estimation

The previous chapter has presented the overall structure of the synthesis and optimization process for UCAV design. Details of packaging and configuration design aspects have also displayed. This chapter describes in details the methods and calculations required to determine the aircraft components and packaging layout, estimate the mass, and predict the internal volume available for fuel storage. Separate sub-sections explain the aircraft design variables established to produce a realistic design. All variable names shown are the same as contained in the synthesis code.

5.1 Component Sizing and Packaging

According to the literature search written in Chapter 2, the flying wing concept would lead a high potential to accomplish the high-risk mission, therefore, it was selected for the UCAV design. Although, the design synthesis process has covered a wide range of military aircraft types, no work has been published concerning a design synthesis process of the flying wing configuration.

The aircraft design synthesis process described in this thesis, has been developed for the UCAV flying wing design maintaining intentionally simple, acceptable to the number of variables to be kept at minimum, and powerfully develop the code. The requirements for the variables and constraints were built from the outset to be able to allow variation of the geometrical parameters of the aircraft, thus providing some margin to perform an optimization. Therefore, it was necessary to determine relationships between the various geometrical parameters of the aircraft to certify consistency across the design.

The following sections provide detailed descriptions of the entire components sizing and packaging for the UCAV. All the equations are almost obtained from Lovell[78] and Seigers[108], with some modifications and developments by the author to accommodate the flying wing configuration.

5.1.1 Aircraft Characterization Variables

Before beginning with the detailed coding of the component sizing and packaging, a list and brief description of the aircraft *design variables*, available in the design synthesis process for UCAV, is described in the following text. It should be noted that a large number of design variables could cause the optimizer to become trapped in local minima, and reduce the chances of true convergence, due to the increased number of solution paths.

Design Variable	Unit	Description
Flying Wing		
BW	m	Gross wing span
CWCC	m	Wing root centreline chord
CWCT	m	Wing tip chord
FCWD		Front spar position as a fraction of wing chord
FCWR		Rear spar position as a fraction of wing chord
QWLR (X)	deg	Wing leading edge sweep
CWK (X)	m	Wing chord at kink positions
FBW2K (X)		Spanwise stations to wing kink as fraction of wing semi-span
Control Surfaces		
CWSE	m	Mean chord of trailing edge control surfaces
FYSEI (X)		Spanwise stations to inner edge of trailing edge control surfaces as fraction of wing semi-span
FYSEO (X)		Spanwise stations to outer edge of trailing edge control surfaces as fraction of wing semi-span
CWSL	m	Mean chord of leading edge control surfaces
FYSLI (X)		Spanwise stations to inner edge of leading edge control surfaces as fraction of wing semi-span
FYSLO (X)		Spanwise stations to outer edge of leading edge control surfaces as fraction of wing semi-span
CWSR	m	Mean chord of inlaid control surfaces
FYSRI		Spanwise station to inner edge of inlaid control surfaces as fraction of wing semi-span
FYSRO		Spanwise station to outer edge of inlaid control surfaces as fraction of wing semi-span
Packaging Aspects		
FY2WFO		Spanwise factor in correlation for position of outer edge of wing tank
FCWFR		Axial factor in correlation for position of wing fuel tanks rear face
FXLIB1		Axial factor in correlation for position of weapon bay 1
FXLIB2		Axial factor in correlation for position of weapon bay 2
FXLPG		Axial factor in correlation for position of engine bay
RTP		Engine scale factor

Table 5-1: UCAV Design Variables

The design variables for UCAV design are placed in the same data files with the packaging specification presented in previous chapter, namely, '*datinput.dat*'. All the variable names shown are the same as contained in the aircraft design synthesis code. The design parameters, corresponding with the options of the packaging specification, are required for producing an initial model with the packaging aspect of the baseline design and controlled by the optimizer within the margin of control values during the iterative process in order to produce the final design aspect of the aircraft.

5.1.2 Absolute Component Mass Contribution

An absolute mass can be defined as the mass of the components, which is fixed in items of the total aircraft mass. The groups of components representing an absolute or

a fixed mass are composed of payload and fixed-role equipments. The payload group consists of weapons, ammunition, and crew (optional manned aircraft). A group of fixed-role equipments are composed of avionics instruments, gun, pylon/launchers, and cockpit instruments (optional manned aircraft). Basically, the sizes and masses of these components can be obtained from the manufacturers, thus they are available for packaging and total mass calculation. However, the weapons and avionics are required to accomplish the detail sizing of the bays before being fitted into the aircraft, thus providing an easy access for maintenances and services. The following sub-sections provide the sizing methods for the avionics and weapon bays in details.

5.1.2.1 Avionics Bay

Gathering the avionics equipment desired for combat aircraft or UAVs, to estimate the dimensions, volume, and mass for the packaging, carries out the avionics bay. Figure 5-1 clearly explains the schematic representation of the method of calculations for the avionics bay.

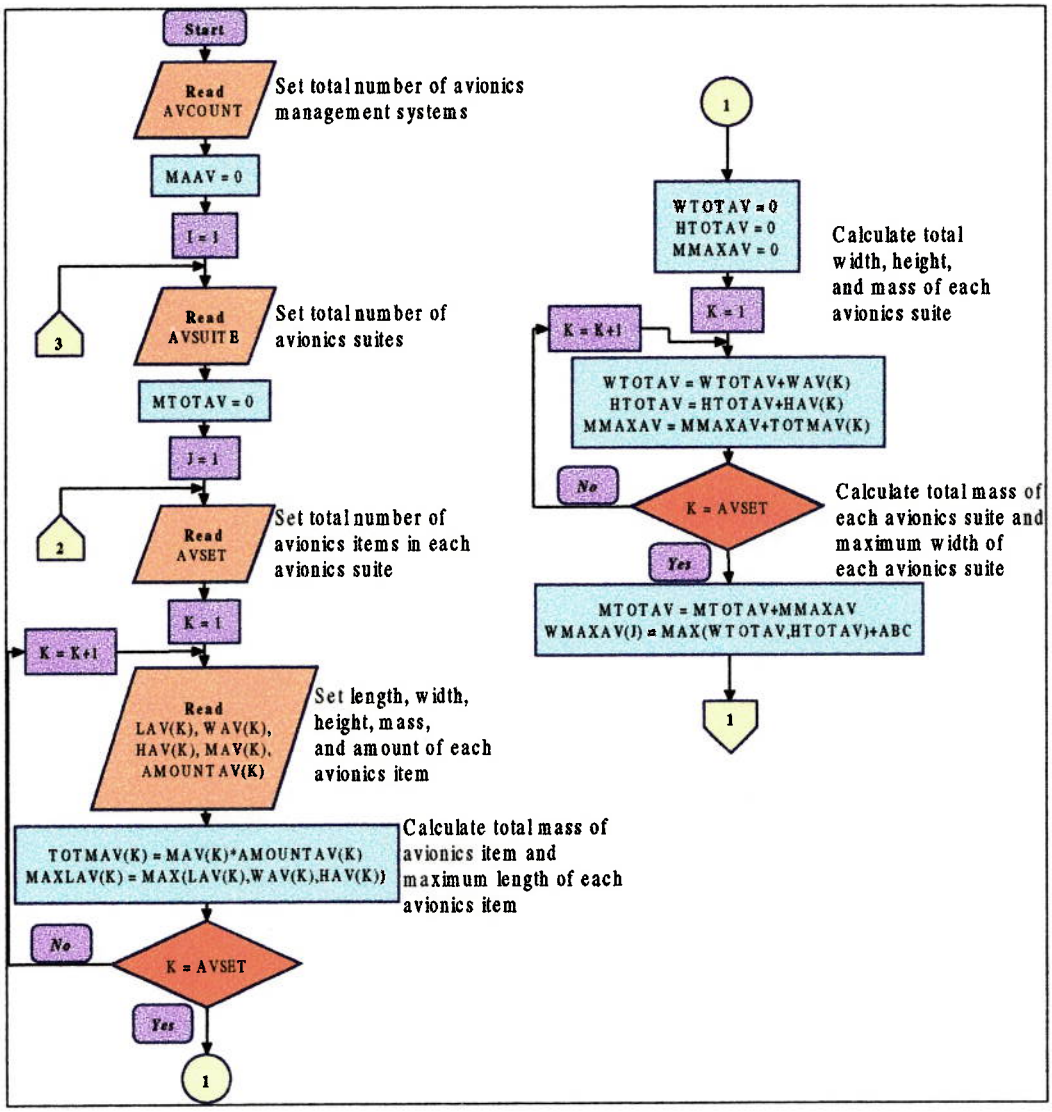

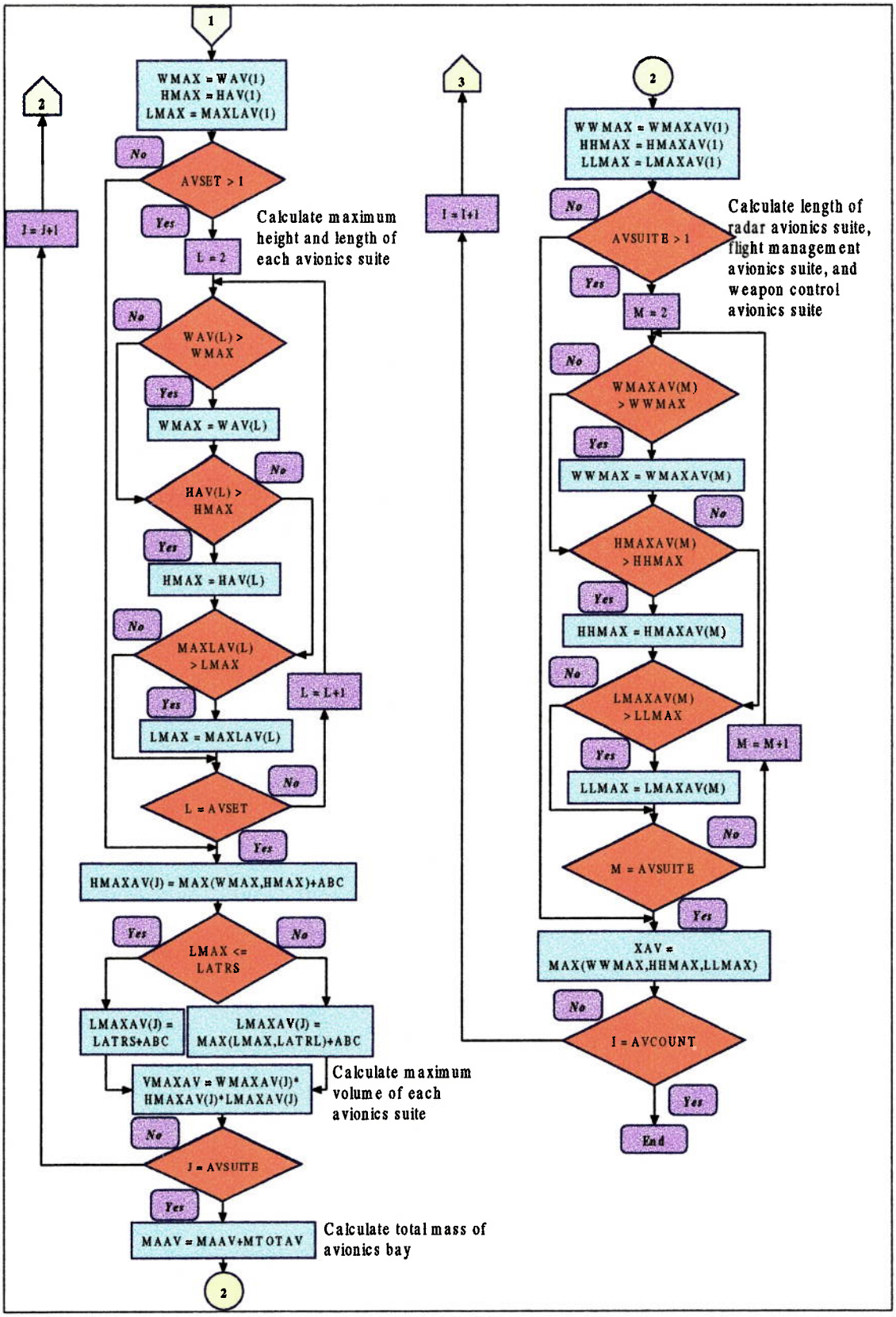

Figure 5-1: Flowchart Representing Method of Calculations for Avionics Bay

The avionics bays are divided into four main compartments: Mission Management System (MMS) containing radar suite and sensor suite; Flight Management System (FMS) containing flight control suite, navigation suite, communication suite, and identification suite; Store Management System (SMS) containing weapon control and release suite; and Electronic Warfare System (EWS) containing electronic warfare suite and countermeasures suite. An option from the packaging specification, TMISS, is required to choose the type of missions for selecting the equipments in each suite to be synthesized.

From the flowchart in Figure 5-1, a group of external variables, maximum length, width, and height of the equipments in each suite are compared with the dimensions of Air Transport Racking (ATR) (LATRS for short size and LATRL for long size), adding up with some clearances (ABC), to achieve the maximum dimensions lengthwise (LMAXAV), in width (WMAXAV), and in height (HMAXAV) for each suite, and then accomplish the total length of avionics compartments (XAV) required to synthesize the geometry of packaging from nose to tail of the aircraft. The total length of avionics compartments represent the length of radar avionics suite (XAR), the length of flight management avionics suite (XAX1), and the length of weapon control avionics suite (XAWEPC). Additionally, the total mass (MTOTAV) and volume (VMAXAV) accounting are obtained. The total avionics mass is the sum of all avionics items, given by:

$$MAAV = \begin{bmatrix} (MARAD + MASEN)_{MMS} + \\ (MAFC + MANAV + MACOMM + MAIDEN)_{FMS} + \\ (MAWEPC)_{SMS} + (MAEW + MACM)_{EWS} \end{bmatrix} \quad (5.1)$$

Where the subscripts represent the four main avionics compartments. The avionics mass will be used in the calculations of the total mass and centre of gravity of the aircraft.

5.1.2.2 *Internal Weapon Bay*

The synthesis methodology of the weapon bay is designed to allow a great deal of flexibility for the specification of the weapons loaded while maintaining an overall simple algorithmic structure. The options of packaging aspects presented in Table 4-2 of Chapter 4 play an important role for the sizing and packaging of the weapon bays. An external variable, TMISS, is required to choose the type of missions for selecting the maximum dimensions of weapons required for that mission to be synthesized.

An external variable, NWEPB, chooses the number of weapon bay to be synthesized. Thus, if NWEPB = 1, a single bay located on the centreline is chosen representing 'weapon bay 1'. If NWEPB = 2, two bays outboard of the engine bay are selected standing for 'weapon bay 1' and 'weapon bay 2' respectively. Finally, if NWEPB = 3, then both an inner and two outer bays are implemented. The inner bay represents 'weapon bay 1' and the one of the outer bays serve as 'weapon bay 2'. Alternatively, NWEPB = 0 allows the implementation of no weapon bay.

Additionally, an option of external stores is available from an external variable, TWB. If TWB = 1, the internal weapon bays are chosen. If TWB = 2, the external stores are

selected. Finally, if TWB = 3, then both internal and external stores are implemented. Alternatively, TWB = 0 allows the implementation of no any stores.

A group of external variables, NLWIB, NWWIB, NHWIB, control the number of store stations lengthwise, in width, and in height, respectively. Adding up with some clearances, LWIBC, WWIBC and HWIBC, the weapon bay dimensions are found as:

$$LIBx = NLWIBx \times LWIBx + LWIBxC \quad (5.2a)$$

$$WIBx = NWWIBx \times WWIBx + WWIBxC \quad (5.2b)$$

$$HIBx = NHWIBx \times HWIBx + HWIBxC \quad (5.2c)$$

Where the lowercase x represents the counting number of the weapon bays, corresponding to NWEPB mentioned above. These dimensions are used in the calculations of weapon bay volume, weapon bay increments and the packaging sizing. The volume of the weapon bays is then given by:

$$VIBx = LIBx \times WIBx \times HIBx \quad (5.2d)$$

The overall mass of weapons are the sum of weapons in the weapon bays including an optional external stores, if selected, which is given by:

$$MWEP = MWIB + MWOB \quad (5.2e)$$

The weapon mass is used in the calculations of total mass, centre of gravity of aircraft, and weapon control during the mission for aircraft CG excursion. Associated with the weapons are the fixed masses of the pylon/launchers, MIP for the internal weapons, and MXP for the external stores.

5.1.2.3 Cockpit (Optional Manned Aircraft)

The cockpit sizing is considered being in a group of an absolute mass, as the value of cockpit dimensions can be obtained from the data of typical fighter cockpit. It is an option of this design synthesis on condition that manned combat aircraft is defined. An external variable, TAC, selects the options of UCAV or manned aircraft to be synthesized. The method used to determine the cockpit layout is available from the open literature proposed by Lovell[78], which will not be mentioned here. Only the cockpit mass is shown:

$$MCW = WCWSC \times \left(0.0011475 \times VD^2 \times \sin^2(QCWSC) + 5.83\right) \quad (5.3a)$$

$$MCC = WCCAN \times \left(0.00011818 \times VD^2 + 10.74\right) \quad (5.3b)$$

Where MCW is the mass of cockpit windscreen and MCC is the mass of cockpit canopy. Associated with the cockpit is the fixed mass, MCI for the instruments, oxygen system, pyrotechnics, furnishings, and armour, represented in a group of fixed-role equipment, and MCP for the crew mass, represented in a group of payload.

5.1.3 Variable Component Mass Contribution

The components that are considered in this section consist of engine and its bay, intake diffuser, two-dimensional nozzle, undercarriages and their bays, wing, and control surfaces. They are varied directly with the design parameters throughout the synthesis process. The following sub-sections provide the sizing methods for these components in details.

5.1.3.1 Engine Bay

The methods applied for the development of the engine and its bay was obtained from the design synthesis proposed by Lovell[78], with some adjustments for the flying wing configuration. An external variable, NENG, is required to choose the number of engines to be synthesized corresponding to the options of packaging aspects presented in Table 4-2 of Chapter 4. Thus, if NENG = 1, a single-engine installation is chosen in which it represents either a single engine located on the centreline or two engines outboard of the centre weapon bay. If NENG = 2, twin-engine installation located on the centreline is selected. Hence, the number of total engines installed on the aircraft can be defined as:

$$NTENG = 2 \times NENG \quad \text{, If NWEPB = 1 or 3} \tag{5.4a}$$

$$NTENG = NENG \quad \text{, If NWEPB = 0 or 2} \tag{5.4b}$$

A set of external variables defines a reference engine in terms of the lengths, diameters and masses. According to the engine sizing methods presented by Lovell, the engine sizing is determined in four sections comprising of the gas generator, reheat section including refuelling, nozzle, and thrust reverser, if fitted. However, the methods used in this synthesis process require that the entire original engine be retained for sizing, with modifications where appropriate to accommodate the two-dimensional nozzles. Using an engine scale factor (RTP), which is the design variable, the reference engine is scaled to match the aircraft thrust requirements according to a set of correlations given below, and acceptable for its bay to fit inside the shape of the aircraft. In terms of the overall length and diameter of the engine, the following scaling is used:

$$LPG = LPGR \times RTP^{FLPK} \tag{5.4c}$$

$$DPG = DPGR \times RTP^{0.5} \tag{5.4d}$$

The total nozzle exit area is required for calculating the exit area of two-dimensional nozzle in order to provide a smooth progression of geometrically similar cross-sections from the axisymmetric engine to the nonaxisymmetric nozzle through the transition section or duct. Thus, it can be specified as:

$$OPN = NENG \times 0.25 \times PI \times RTP \times DPGR^2 \tag{5.4e}$$

The geometry of engine bay is defined by applying a set of vertical and horizontal clearances to the scaled value of the engine diameter. The clearances are defined as the sum of all gaps between the engine bay and the engine; include the gap between the engines in twin-engine installation. However, they are limited to a range between specified maximum and minimum values, which are set as constraints during the optimization process. The overall clearances on height and width for the engine bay are found as:

$$EHP = FHPK \times DPG \quad \text{, Where EHPS} \leq \text{EHP} \leq \text{EHPH} \tag{5.5a}$$

$$EBP = FBPK \times DPG \quad \text{, Where EBPS} \leq \text{EBP} \leq \text{EBPH} \tag{5.5b}$$

Thus, the height and width of engine bay is given by:

$$HPG = DPG + EHP \tag{5.5c}$$

$$WPG = DPG + EBP \tag{5.5d}$$

For the twin-engine installation, the maximum distance between the centreline of the engines can be defined as:

$$YPCH = \max(FYPC \times DPG, WPG) \text{ , If NENG} = 2 \quad (5.5e)$$

Where $FYPC$ represents the engine diameter factor for twin-engine installation. The minimum value is defined by FYPC = 1.122.

For the single-engine installation, the cross-sectional area of the engine bay is assumed to be ellipses with the lengths of the major and minor axes fixed by the sum of the engine diameter and clearance. For the twin-engine installation, the modified expression for the cross-sectional area defined by Mothersill[89] is obtained. Thus, the cross-sectional areas of the engine bay are given by:

$$OPB = NENG \times 0.25 \times PI \times HPG \times WPG \text{ , If NENG} = 1 \quad (5.6a)$$

$$OPB = \begin{bmatrix} (0.25 \times PI \times HPG \times WPG) + \\ (HPG \times \max(WPG, FYPC \times DPG)) \end{bmatrix} \text{ , If NENG} = 2 \quad (5.6b)$$

The cross-sectional area and the overall length of engine are used in the calculation of engine bay volume. Thus the total volume of the engine bay is defined as:

$$VPB = OPB \times LPG \quad (5.6c)$$

The mass of propulsion system is considered in two parts: the total mass of engines and the engine installation mass. The mass of engine can also be determined by using an engine scale factor to scale a mass of reference engine to match the aircraft thrust requirements according to the correlation factor applied. The engine installation mass is taken as a linear function of the mass of uninstalled engine(s). The number of total engines (NTENG) is used in the calculation, as it requires the total mass of engines installed on the aircraft. Thus, the total mass of engines and the engine installation mass are found as:

$$MPB = NTENG \times MPGR \times RTP^{FMPGK} \quad (5.7a)$$

$$MPI = FMPIK \times MPB \quad (5.7b)$$

Hence, the total mass of the propulsion system is given by:

$$MPG = MPB + MPI \quad (5.7c)$$

The static dry thrust of the engine is parametrically independent upon the engine size. Therefore, the engine thrust can also be determined by using an engine scale factor to scale the reference engine static dry thrust to match the requirements for engines with similar characteristics but different sizes. The number of total engines (NTENG) is again used in the calculation, as it requires the total static dry thrust of the engines. Hence, the total static dry thrust can be determined by:

$$TPGD = NTENG \times TPGDR \times RTP \quad (5.8)$$

The total static dry thrust of the engines is used in the calculations of the variation of thrust with flight conditions required for the point and mission performance analysis.

5.1.3.2 Intake Diffuser

The geometry of intake diffuser is relatively complex that it is necessary to hide the engine face from the intake as much as possible, in order to reduce the infrared,

acoustic and radar emissions from the aircraft. A detailed description follows the synthesis equations proposed by Lovell[78] and Seigers[108], with some modifications to accommodate the flying wing configuration. The principal aspects of the intake diffuser are described in this sub-section comprising of the inlet cross-section, its shape and components, and the intake position and its length. The geometry of the intake duct is subsequently described in the part of configuration layout in Chapter 6.

The total cross-sectional area of the intake diffuser exit (OIE) is assumed to be corresponding to the total nozzle exit area of the engine (OPN), described in the equation (5.4e) above. Assuming a fixed area ratio (ROIEI), which is an external variable, the cross-sectional area of the intake inlet can be found as:

$$OII = {}^{OIE}/_{ROIEI} \tag{5.9a}$$

From this inlet area, an equivalent inlet diameter for each intake diffuser is defined:

$$DII = 2 \times \left(\frac{OII}{NENG \times PI} \right)^{0.5} \tag{5.9b}$$

The diameter of intake diffuser exit (DIE) is corresponding to that of the engine (DPG), presented in equation (5.4d). The equation of equivalent inlet diameter (DII) is checked for a sizing correlation in order to establish how good the anticipation will be, by using the method of related coefficient of determination (R^2) obtained from Microsoft Excel. The results of the correlation for the engines for which the data was available are shown in Figure 5-2, together with the gradient of the trend line and R^2. A value of 0.9713 is good enough not to cause significant errors.

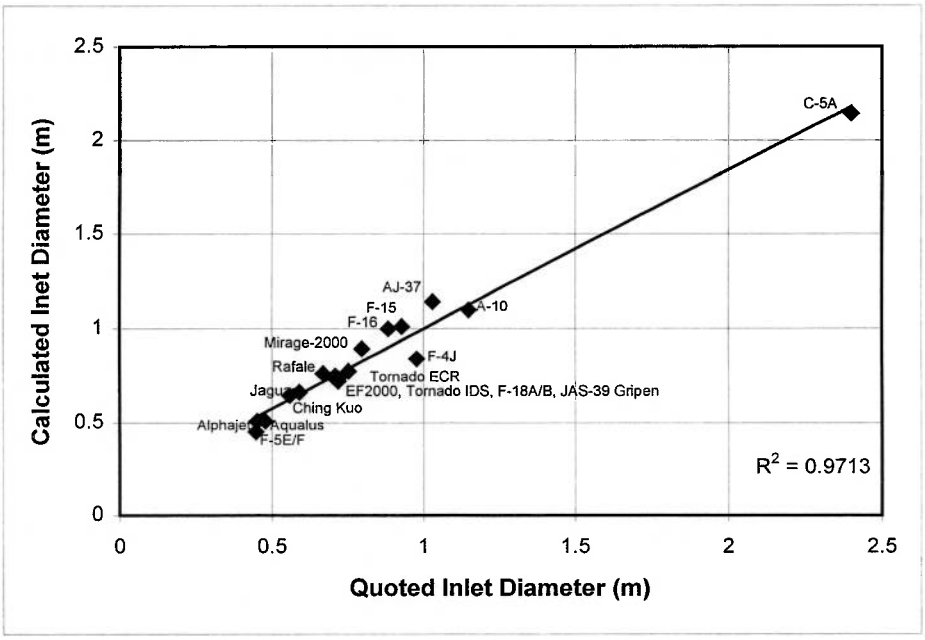

Figure 5-2: Correlation Results of Engine Equivalent Inlet Diameter

The intake inlet is assumed to be rectangular in cross-section and mounted smoothly on the surface of the aircraft. An aspect ratio for the intake (AII), which is specified as a design constant, where the width and height of the intake inlet can be obtained:

$$BII = \left(\frac{AII \times OII}{NENG} \right)^{0.5} \tag{5.10a}$$

$$HII = \frac{OII}{NENG \times BII} \tag{5.10b}$$

In order to ensure a satisfactory entry flow at the engine compressor, a minimum length of intake diffuser is required. It is determined by applying a correlation factor for minimum requirement of diffuser length to the equivalent inlet diameter:

$$LIDS = FLIDK \times DII \tag{5.11a}$$

Assume the intake inlet is positioned aft of the nose undercarriage bay. The position of intake diffuser exit from aircraft nose is determined by using a correlation factor for the position of engine front face (FXLPG), which is the design variable, to the aircraft length at engine station. Thus, the positions of intake inlet and exit from aircraft nose are found as:

$$XII = XFR + LUNB + 0.5 \times XAX1 \tag{5.11b}$$

$$XIE = \left[\begin{array}{l} XFR + LUNB + XAX1 + \\ (CWCP - XFR - LUNB - XAX1 + XWPGL) \times FXLPG \end{array} \right] \tag{5.11c}$$

Once the intake positions have been performed, the overall length of intake diffuser is available. It requires meeting a minimum value to ensure an acceptable flow at the engine compressor, which is set as a constraint during the optimization process. Thus, the overall length of intake diffuser is given by:

$$LIDG = XIE - XII \text{ , Where LIDG} \geq \text{LIDS} \tag{5.11d}$$

The volume of the intake diffuser is then given by:

$$VIDG = 0.5 \times LIDG \times (OII + OIE) \tag{5.12}$$

The mass of the intake diffuser is usually included in the prediction of the propulsion system installation. The intake position and the overall length obtained above are subsequently used in the calculations of the geometry of intake duct, and the packaging aspects for the internal component arrangements.

5.1.3.3 Two-Dimensional Nozzle

The requirement for the nonaxisymmetric or two-dimensional nozzle(s) is to hide the hottest part of the engine from as many angles as possible in order to reduce the infrared and radar signatures. Furthermore, it can be easily fitted to the wing trailing edge area of the flying wing design. Thus, the geometry of the nozzle duct needs providing a good transition from circular to rectangular section that the nozzle area should be constant without causing excessive losses.

Assume the width of each two-dimensional nozzle exit extends between the inboard sections of the wing trailing edge area slightly symmetrical in relation to the centreline of engine, and accessible for the remaining area to be equipped with the

trailing edge control surfaces. Then the total nozzle exit area of the engine (OPN) is used for the constant transition to estimate the exit height. Thus, the width and the height of each nozzle exit are given by:

$$BPTD = Y2P + 0.5 \times YPCH + WPG \tag{5.13a}$$

$$HPTD = OPN / (NENG \times BPTD) \tag{5.13b}$$

The aspect ratio of each two-dimensional nozzle exit is found as:

$$APTD = BPTD / HPTD \tag{5.13c}$$

To define the overall length and the volume of the nozzle transition duct, the half scales of the width and the height of the two-dimensional nozzle are needed. Thus, at the entrance, the half scale is the radius of the engine diameter (DPG) given by:

$$RPTD = 0.5 \times DPG \tag{5.14a}$$

The half scales of the width of nozzle exit are determined in two parts: inboard and outboard, that the width is slightly different between single- and twin-engine installations. The half-width and half-height of the nozzle exit are given as follows:

$$HBPTDO = BPTD - Y2P - 0.5 \times YPCH \tag{5.14b}$$

$$HBPTDI = BPTD - HBPTDO \tag{5.14c}$$

$$HHPTD = 0.5 \times HPTD \tag{5.14d}$$

In order to ensure a satisfactory flow to prevent the flow separation, the maximum angles to change from circular to rectangular cross-section should not be greater than 45 degree. From this data, the equation to determine the minimum length of the nozzle duct has been developed by using an external variable, QPTD, to set the required slope angle to meet the requirements that the duct must be as short as possible to minimize the mass of the propulsion system installation and it should be long enough to prevent any flow separation. Thus, the minimum length of the nozzle transition duct can be found as:

$$LPTDS = \frac{(RPTD - 0.5 \times (RPTD - HBPTDO)) - (RPTD - 0.42525 \times (RPTD - HBPTDO))}{0.05 \times \tan(QPTD)} \tag{5.15a}$$

The overall length of the nozzle transition duct is determined by considering the maximum distance from aircraft nose to the position where the height of the nozzle exit is corresponding to the relative thickness of airfoil at aircraft trailing edge in area of engine position (XPTDR). The XPTDR is then subtracted from the sum of distance to intake inlet from aircraft nose (XII), the length of intake duct (LIDG), and the length of engine (LPG), performing the overall length of the nozzle duct (LPTD). It requires meeting a minimum value to ensure a satisfactory flow to prevent the flow separation at the nozzle exit, which is set as a constraint during the optimization process. Hence, the overall length of the nozzle transition is given by:

$$LPTD = XPTDR - (XII + LIDG + LPG) \text{ , Where LPTD} \geq \text{LPTDS} \tag{5.15b}$$

The XPTDR is required in order to prevent the extrusion of the nozzle duct geometry from the aircraft trailing edge or at least performing minimum extrusion. Moreover,

the area between the nozzle exit and the aircraft trailing edge can be provided for the thrust vectoring structure, if fitted.

The volume of each two-dimensional nozzle is then given by:

$$VPTD = \begin{bmatrix} \left[0.5 \times \left\{\frac{PI}{4} \times HPG \times WPG + 4 \times HBPTDO \times HHPTD\right\} \times LPTD\right] + \\ \left[0.5 \times \left\{HPG \times \max(WPG, YPCH) + 4 \times HBPTDI \times HHPTD\right\} \times LPTD\right] \end{bmatrix} \quad (5.16)$$

The mass of the nozzle is usually included in the prediction of the propulsion system installation. However, the mass of the two-dimensional nozzle is certainly not being accounted on that general prediction. Thus, it is necessary to perform separate mass estimation for it. The mass estimation method of the two-dimensional nozzle proposed by Teixeira da Costa[123] has been obtained, which is based on the planform-projected area of the nozzle. The projected area is approximated as the average width between the nozzle's ends multiplied by the overall length, given by:

$$SPTD = 0.5 \times (DPG + HBPTDO + HBPTDI) \times LPTD \quad (5.17a)$$

The total mass of the two-dimensional nozzles is, therefore, found as:

$$MPTD = NTENG \times 22 \times SPTD \quad (5.17b)$$

The principal dimensions of the two-dimensional nozzle are used in the calculation of the geometry of nozzle duct, which is subsequently described in Chapter 6.

5.1.3.4 Undercarriage Bay

The geometry of the main and nose undercarriages are derived from a number of correlations with a reference landing mass. One difficulty is the determination of the ratio of the design landing mass to the take-off mass. For simplicity in the absence of more precise information, the ratio summarized by Howe[58] for the military combat aircraft has been obtained to determine the reference landing mass for this design synthesis process. Thus, the landing mass is given by:

$$MTLR = 0.85 \times MTTR \quad (5.18)$$

By examining the variation of the sum of the total undercarriage lengths with the reference landing mass, the following correlation was found:

$$LULG = \left(\frac{MTLR}{LULG1K}\right)^{LULG2K} \quad (5.19a)$$

The ratio of the length of the nose leg to the length of one main undercarriage leg (RLUNM) enables the length of the nose undercarriage leg to be found, and thus the length of each main leg.

$$LUNS = \frac{(LULG \times RLUNM)}{(RLUNM + 2)} \quad (5.19b)$$

$$LUMN = 0.5 \times (LULG - LUNS) \quad (5.19c)$$

The wheel dimensions with the reference landing mass are assuming a fixed requirement for ground hardness. Thus, the wheel diameter and width of the main undercarriage are given by:

$$DUMW = FDUMWK \times MTLR + DUMWK \quad (5.20a)$$

$$BUMW = FBUMWK \times MTLR + BUMWK \quad (5.20b)$$

The width of the nose undercarriage wheel (BUNW) is assumed to be constant setting as an external variable. For the diameter of the nose undercarriage wheel, the following equation is specified:

$$DUNW = FDUNWK \times MTLR + DUNWK \quad (5.20c)$$

The structural mass for the main and nose undercarriages and the mass of the associated hydraulics are derived from a number of correlations with a reference landing mass to obtain the linear relations given by:

$$MUM = FMUMK \times MTLR + MUMK \quad (5.21a)$$

$$MUN = FMUNK \times MTLR + MUNK \quad (5.21b)$$

$$MUH = FMUHK \times MTLR + MUHK \quad (5.21c)$$

The total mass of the main and nose undercarriages are obtained by including a proportion of the undercarriage hydraulics to the structural mass. Thus, the gross mass of the main and nose undercarriages are found as:

$$MUMG = MUM + MUN + MUH - MUNG \quad (5.22a)$$

$$MUNG = MUN \times \left(1 + \frac{MUH}{(MUN + MUM)}\right) \quad (5.22b)$$

The length of the undercarriage bays is assumed to be the sum of the wheel radius and the leg length. Thus, the undercarriage bay length for each main undercarriage and nose undercarriage are found as:

$$LUMB = 0.5 \times DUMW + LUMN \quad (5.23a)$$

$$LUNB = 0.5 \times DUNW + LUNS \quad (5.23b)$$

Assuming that the wheels are placed vertically in the undercarriage bays when retracted. For the bay height and width, a set of external variables, FDUMW, FBUMW, FDUNW, and FBUNW, are used in the calculations to allow clearances for the retracted undercarriages. Thus the undercarriage bay height and width for each main and nose undercarriage can be found as:

$$HUMB = FDUMW \times DUMW \quad (5.24a)$$

$$WUMB = FBUMW \times BUMW \quad (5.24b)$$

$$HUNB = FDUNW \times DUNW \quad (5.25a)$$

$$WUNB = FBUNW \times BUNW \quad (5.25b)$$

The bay volume required for the each main and nose undercarriage is then given by:

$$VUMB = HUMB \times WUMB \times LUMB \quad (5.26a)$$

$$VUNB = HUNB \times WUNB \times LUNB \quad (5.26b)$$

The geometries of undercarriage bays are subsequently used in the calculations of the packaging layout, and the undercarriage arrangements described in the part of configuration layout in Chapter 6.

5.1.3.5 Flying Wing

The wing planform is the most relatively complex, as it is required to pack all the components internally. The concept of flying wing configurations has been considered with several designs based on two main categories: the straight tapered wing and multi-kinks (-cranks) wing. An option from the packaging specification, NWK, selects the types of these configurations to be synthesized.

For the multi-kinks wing configuration, generally there can be any number of kinks in the wing leading edge and a different number, occurring at different spanwise stations, in the trailing edge. For the purposes of calculation, wherever there is kink in one edge, a kink is also assumed to exist in the other edge at the same spanwise station, so that the wing planform becomes divided into a series of trapezoidal panels. Figure 5-3 presents the planform of multi-kinks wing, where the lowercase *m* represents the number of kinks in wing (NWK).

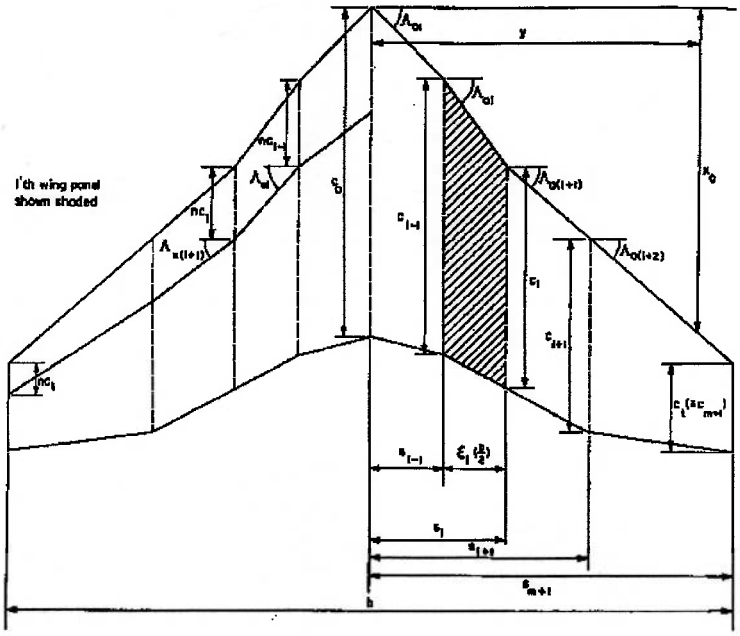

Figure 5-3: Multi-Kinks Wing Configuration[51]

Assuming there are kinks at NWK apparent spanwise stations on a semi-wing, excluding the wing centreline, the semi-wingspan is divided into NWK+1 trapezoidal panels. When NWK = 0, the semi-wingspan has straight leading and trailing edges.

The optimizer determines the size of the flying wing, and the outstanding dimensions are calculated by the optimizer-provided values of gross wingspan (BW), wing root centreline chord (CWCC), wing tip chord (CWCT), front spar fraction (FCWD), rear spar fraction (FCWR), wing leading edge sweep (QWLR (X)), wing chord at kink positions (CWK (X)), and fractional spanwise stations at wing kinks (FBW2K (X)). The multi-kinks wing configurations are based on the last three variables. The wing

leading edge sweep (QWLR (X)) of the straight tapered wing configuration is referred to QWL. The unit of all sweeps is given in degree for ease of use, but is immediately converted to radians in the calculation paths. In this sub-section, the detailed descriptions of wing sizing are shown only the main parameters required.

If there are kinks at NWK, the spanwise stations at wing kinks are found as:

$$\sum_{X=1}^{NWK} BW2K(X) = FBW2K(X) \times 0.5 \times BW \tag{5.27}$$

Where BW2K (NWK+1) is the semi-wingspan. As mentioned in section 4.2.7 of Chapter 4, the wing thickness ratio set by the user in the packaging specification, has been selected for inboard (RTW) and outboard (RTWT) sections of the wing, corresponding to the NACA airfoils. There is an intermediate region where there is a transition from one airfoil shape to the other. On condition that the positions of wing kinks are in the area of transition section, the wing thickness ratios (RTWK (X)) are assumed determining by interpolating data between two parameters.

One of the most important parameters required for the calculations throughout the procedure is the gross wing area. For the straight tapered wing configuration, the gross wing area is given by:

$$SW = \frac{CWCC}{2} \times (BW + UW \times BW) \tag{5.28a}$$

Where UW is the wing taper ratio, defined as the ratio between the tip chord and the centreline root chord. The wing gross area for the multi-kinks wing types is the sum of the areas between the trapezoidal panels, given by:

$$SW = \sum_{X=1}^{NWK+1} (CWK(X-1) + CWK(X)) \times PWK(X) \tag{5.28b}$$

Where PWK (X) represents a series of trapezoidal panels for multi-kinks wing planform, defined as:

$$\sum_{X=1}^{NWK+1} PWK(X) = BW2K(X) - BW2K(X-1) \tag{5.28c}$$

Once the gross wing area has been obtained, the wing aspect ratio is performed:

$$AW = \frac{BW^2}{SW} \tag{5.29}$$

In order to determine the overall aerodynamic characteristics of multi-kinks wing configurations, it is a useful device to define an equivalent straight-tapered wing planform, which is suitably representative of the true wing planform. However, it would be expected to be a reasonable representation of the true wing aerodynamically only for wings where the leading edge sweepback is constant, or has only minor changes over the greater part of the span. The equivalent wing planform can be accomplished by defining the tip and root chords relative to the planform geometry of the true wing configuration. Assume the wing tip chord (CWCT) of the equivalent wing is fixed relative to the true wing and the planforms of the equivalent and true

wings have equal areas. Thus, the wing root chord of equivalent wing planform is found as:

$$CWCN = \left(\frac{SW}{0.5 \times BW}\right) - CWCT \tag{5.30}$$

The wing leading edge sweep of the equivalent wing planform is then determined by:

$$QWL = \tan^{-1}\left(\frac{XWKLL - XWCL}{0.5 \times BW}\right) \tag{5.31a}$$

Where XWCL is the distance of leading edge of equivalent wing root chord (CWCN) from aircraft nose, and XWKLL is the distance of leading edge of wing tip chord (CWCT) from aircraft nose, defined as:

$$XWCL = \sum_{X=1}^{NWK} \frac{[\tan(QWLR(X)) - \tan(QWLR(X+1))] \times BW2K(X) \times (0.5 \times BW - BW2K(X))}{0.5 \times BW} \tag{5.31b}$$

$$XWKLL = \sum_{X=1}^{NWK+1} PWK(X) \times \tan(QWLR(X)) \tag{5.31c}$$

The wing leading edge sweep of equivalent wing planform is used in the calculations of wing quarter-chord sweep and wing mid-chord sweep as follows:

$$QW4 = \tan^{-1}\left(\tan(QWL) - \frac{CWCN}{2 \times BW} \times (1 - UW)\right) \tag{5.31d}$$

$$QW2 = \tan^{-1}\left(\tan(QW4) - \frac{CWCN}{2 \times BW} \times (1 - UW)\right) \tag{5.31e}$$

The mean aerodynamic chord is also one of the most important parameters required for the calculations throughout the procedure. It is used in the calculations of aircraft centre of gravity, aerodynamics, and static stability and control. For the straight tapered wing planform, the mean aerodynamic chord is given by:

$$CWMA = \tfrac{2}{3} \times CWCC \times \left(UW + \frac{1}{(1+UW)}\right) \tag{5.32a}$$

The method proposed by ESDU series 76003[51] provides the good estimation for determining the mean aerodynamic chord for the multi-kinks wing planform. The mean aerodynamic chord is based on a series of trapezoidal panels, the wing chord at kink stations, and the taper ratio between those wing chords. A series of trapezoidal panels used in this method is represented as a fraction of semi-wingspan, given by:

$$\sum_{X=1}^{NWK+1} FPWK(X) = \frac{PWK(X)}{0.5 \times BW} \tag{5.32b}$$

Thus, the mean aerodynamic chord for the multi-kinks wing planform is found as:

$$CWMA = \tfrac{2}{3} \times \left[\frac{\sum_{X=1}^{NWK+1} CWK(X-1)^2 \times \left(1 + UWK(X) + UWK(X)^2\right) \times FPWK(X)}{\sum_{X=1}^{NWK+1} CWK(X-1) \times (1 + UWK(X)) \times FPWK(X)}\right] \tag{5.32c}$$

The position of the mean aerodynamic chord (parallel to wing centreline) is defined by establishing the chordwise position of its quarter-chord point relative to the aircraft nose. The following equations represent the position of wing quarter-chord point from aircraft nose applicable for the straight tapered wing and multi-kinks wing planforms respectively.

$$XWCQM = CWCC \times \frac{(1+2\times UW)}{12} \times AW \times \tan(QWL) + 0.25 \times CWMA \tag{5.33a}$$

$$XWCQM = AW/_{12} \times \left\{ \sum_{X=1}^{NWK+1} \left[\begin{array}{l} FPWK(X) \times CWK(X-1) \times \\ 3 \times (1+UWK(X)) \times \\ \sum_{\substack{I=1 \\ (X>1)}}^{X-1} FPWK(I) \times \tan(QWLR(I)) + \\ (1+2\times UWK(X)) \times FPWK(X) \times \\ \tan(QWLR(X)) \end{array} \right] \right\} + \frac{CWMA}{4} \tag{5.33b}$$

The geometric or standard mean chord of the wing is also used as a reference length to non-dimensionalise pitching moment coefficients. Generally, the geometric mean chord is positioned on the wing centreline so that its quarter-chord point is concurring with the quarter-chord point of the mean aerodynamic chord, as shown in Figure 5.4.

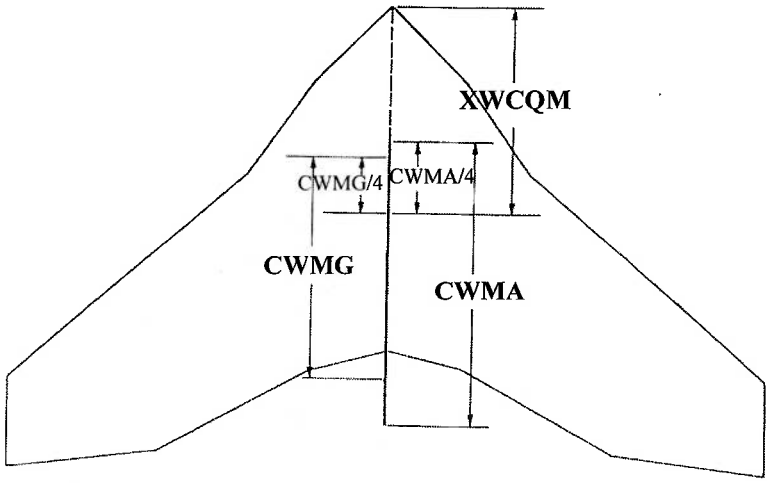

Figure 5-4: Position of Mean Aerodynamic Chord and Geometric Mean Chord

The equations representing the geometric mean chord for the straight tapered wing and the multi-kinks wing planforms are given by:

$$CWMG = \frac{CWCC \times (1+UW)}{2} \tag{5.34a}$$

$$CWMG = \sum_{X=1}^{NWK+1} \frac{CWK(X-1) \times (1+UWK(X)) \times FPWK(X)}{2} \tag{5.34b}$$

The structural box of the wing is defined by front and rear spars at fixed fractions of the chord. The methods of calculations applied for the wing box parameters are

almost similar to those used for the wing parameters described above. These parameters are based on chords and span of wing structural box. Assume the wing box gross span (BWB) is equal to the wing gross span (BW). Chords of wing box at root, tip and kink positions are given by:

$$CWBC = CWCC \times (FCWR - FCWD) \tag{5.35a}$$

$$CWBT = CWCT \times (FCWR - FCWD) \tag{5.35b}$$

$$\sum_{X=1}^{NWK} CWBK(X) = CWK(X) \times (FCWR - FCWD) \tag{5.35c}$$

Once the chords and span of wing box have been obtained, they are used in the calculations of wing box gross area (SWB), taper ratio (UWB), aspect ratio (AWB), and chord of wing box of equivalent wing planform (CWBCN), following the methods applied for the wing parameters. The wing box centreline sweep of equivalent wing planform is then given by:

$$QWB = \tan^{-1}\left(\tan(QWL) - \frac{CWCN}{BWB} \times (FCWR - FCWD) \times (1 - UW) \right) \tag{5.36}$$

The principal dimensions of wing and wing box structures described above are subsequently used in the calculations of packaging layout, wing fuel volume and wing structural mass, and involved with all modules throughout the entire process.

5.1.3.6 Control Surfaces

The control surfaces and/or high-lift devices designed for UCAV consist of trailing edge, leading edge and inlaid control surfaces. The options set by the user in the packaging specification, NW2SE, NW2SL, and NW2SR select the number of these control surfaces respectively to be synthesized. NW2SL and NW2SR can be set as zero providing no leading edge and/or inlaid control surfaces have been selected.

NW2SE selects the trailing edge control surfaces in various types based on their functions. If NW2SE = 1, the TE control surfaces represent the split elevons performing all duties of flaps, elevators, rudders, and ailerons. If NW2SE = 2, the inboard control surfaces act for flaps and the outboard control surfaces serve as split elevons performing all duties of elevators, rudders, and ailerons. Assuming that maximum two pairs of trailing edge control surfaces would be sufficient to control the UCAV.

However, if inlaid control surfaces are selected, they are directly responsible for the duties of rudders and ailerons. Thus, the trailing edge control surfaces are only acting for the functions of flaps and elevators. This option can provide a big change for the dimensions of control surfaces, the size of the aircraft and the total mass involved, as discussed afterwards in Chapter 8.

The principal dimensions of the control surfaces are calculated by the optimizer-provided values of mean chords (CWSE, CWSL, CWSR), and spanwise stations at inner and outer edge of control surfaces as fractions of semi-wingspan (FYSEI (X), FYSEO (X), FYSLI (X), FYSLO (X), FYSRI (X), FYSRO (X)). The trailing edge control surfaces are placed next to the two-dimensional nozzles in the available trailing edge area. Similarly, the leading edge control surfaces are located next to the

intake in the available leading edge area. The inlays are placed on the wing surfaces behind the area of wing fuel tanks. The main parameters required are only determined in this sub-section.

The minimum spanwise stations of the trailing edge and leading edge inboard control surfaces are based on the position of the propulsion system, given by:

$$Y2SE1IS = Y2SL1IS = Y2P + 0.5 \times YPCH + WPG + PGC \tag{5.37}$$

For the inlaid control surfaces, the variable control values are bounded at half of semi-wingspan. The spanwise stations at inner and outer edge of all control surfaces are derived with similar methods, thus only the stations of trailing edge control surfaces are shown:

$$\sum_{X=1}^{NW2SE} Y2SEI(X) = FYSEI(X) \times 0.5 \times BW \text{ , Where Y2SEI (1)} \geq \text{Y2SE1IS} \tag{5.38a}$$

$$\sum_{X=1}^{NW2SE} Y2SEO(X) = FYSEO(X) \times 0.5 \times BW \tag{5.38b}$$

The spanwise stations of the trailing edge and leading edge inboard control surfaces require meeting minimum spanwise values to ensure an enough space available for the two-dimensional nozzles, which are set as constraints during the optimization process.

The total span and the planform area of each pair of control surfaces (presented by trailing edge types) are given by:

$$\sum_{X=1}^{NW2SE} BWSEK(X) = 2 \times [Y2SEO(X) - Y2SEI(X)] \tag{5.39}$$

$$\sum_{X=1}^{NW2SE} SWSEK(X) = CWSEK(X) \times BWSEK(X) \tag{5.40}$$

Where CWSEK (X) is the mean chord of each pair of trailing edge control surfaces. The aspect ratio of each trailing edge control surface (method also applied for leading edge and inlaid control surface) is then found as:

$$\sum_{X=1}^{NW2SE} AWSEK(X) = \frac{BWSEK(X)}{2 \times CWSEK(X)} \tag{5.41}$$

The gross area and fixed section of trailing edge and leading edge are used in the wing structural mass estimation procedure, and are calculated as follows (equations applied for trailing edge are shown):

$$SWTG = \left(SW - \frac{SW \times Y2TGI}{0.5 \times BW} \right) \times (FCWSEL + FCWSE) \tag{5.42a}$$

$$SWTF = SWTG - SWSE \tag{5.42b}$$

Where Y2TGI is the spanwise stations at inner edge of wing trailing edge located next to the two-dimensional nozzle. FCWSEL is an external variable representing distance of leading edge of trailing edge control surface aft of rear spar as a fraction of wing chord. FCWSE is the ratio of trailing edge control surface's mean chord to its wing chord.

The principal dimensions of the control surfaces described above are subsequently used in the calculation of wing structural mass, aerodynamic, and the static stability and control.

5.1.4 General Packaging Layout

The next stage in the design synthesis of UCAV is to define an arrangement for the positions of the major components within the aircraft. The wing centreline and the wingspan are probably two of the most critical variables as far as packaging aspects are concerned. This is because they are necessary to fit all the components internally to perform configuration design aspect. An arrangement starts with performing the spanwise station of the bays and then follows by sizing the chordwise positions.

The options of packaging aspects presented in Table 4-2 of Chapter 4 play an important role for the packaging layout. With these options, the sum of bays width determined in the previous sections, plus some allowable clearances between each bay achieve the spanwise positions of the bays. The option of NWEPB = 3 (one inner and two outer weapon bays) is selected as an example to determine the spanwise position of all the bays. The following equations present this packaging layout (specifying the outer edge of the bays) starting from centre weapon bay, starboard engine bay, outer weapon bay, and at last main undercarriage bay.

$$Y2IB1O = 0.5 \times WIB1 \quad (5.43a)$$

$$Y2PO = Y2IB1O + PGC + WPG \quad (5.43b)$$

$$Y2IB2O = Y2PO + WIB2C + WIB2 \quad (5.43c)$$

$$Y2UMBO = Y2IB2O + WUMBC + WUMB \quad (5.43d)$$

The outer edge of the bays are considered to define a layout for their chordwise positions within the aircraft, as their relative wing chord at this section is smaller than that at the inner edge or the centre section. The chordwise position of the engine bay from the aircraft nose is obtained from the position of intake diffuser exit, given by:

$$XP1O = XII + LIDG \quad (5.44a)$$

The chordwise position of weapon bays from the aircraft nose is calculated by applying the optimizer-provided values of axial factors (FXLIB1, FXLIB2) to the wing chords at their existing stations, added with the distance of leading edge of their wing chords from aircraft nose.

$$XWIB1O = CWWIB1 \times FXLIB1 + XWIB1L \quad (5.44b)$$

$$XWIB2O = CWWIB2 \times FXLIB2 + XWIB2L \quad (5.44c)$$

The chordwise position of main undercarriage bay is based on the mean aerodynamic chord (CWMA) and the position of wing quarter-chord point (XWCQM). Thus, it affects directly to the packaging and configuration aspects of the aircraft. An external variable, RLUPCW, sets the CG position of main undercarriage bay aft of the wing quarter-chord point and ELUP gives the distance between main undercarriage pintle and front of main undercarriage bay. Hence, the chordwise position of main undercarriage bay is found as:

$$XUMBO = XWCQM + RLUPCW \times CWMA - ELUP \quad (5.44d)$$

The chordwise position of the bays requires the forward and aft constraints to control their bays within the aircraft, during the optimization routine. These constraints are based on the relative wing chord at their spanwise stations. The following equations determine the methods for calculating the relative wing chord at reference spanwise station along the semi-wingspan for the straight taper wing and multi-kinks wing planform respectively.

$$CWX = CWCC - \frac{CWCC \times (1 - UW) \times Y2W}{0.5 \times BW} \tag{5.45a}$$

$$CWX = \sum_{X=1}^{NWK+1} CWK(X-1) - \frac{\left[CWK(X-1) \times (1 - UWK(X)) \times (Y2W - BW2K(X-1)) \right]}{PWK(X)} \tag{5.45b}$$

The constraints for controlling the chordwise position of bays are determined from two conditions: the constraint sized by the thickness of airfoil along chordwise station, and the limitation between front and rear spars.

The thickness of airfoil along chordwise station is determined by applying the airfoil coordinates (Y-upper/C and Y-lower/C) to the relative wing chord of bays simultaneously with the distance from nose to its pair of coordinates (X/C). The bays height is then required to compare with the relative thickness and thus, obtain the forward and aft limit positions, as illustrated in Figure 5-5.

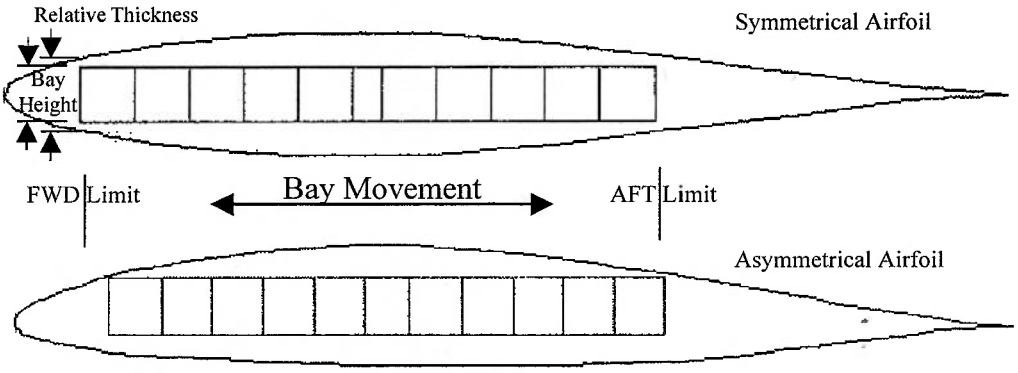

Figure 5-5: Bay Height Compared with Relative Thickness of Airfoil Obtain Forward and Aft Constraints

The airfoils coordinates applied for determining the constraints of each bay can be varied along the semi-wingspan based on the location of that bay (inboard, transition or outboard region), referred to section 4.2.7 and Figure 4-5 of Chapter 4.

The constraints obtained from the wing box structures to control the chordwise position of bays are calculated by applying the front (FCWD) and rear (FCWR) spar fractions to their relative wing chords, added with the distance of leading edge of their wing chords from aircraft nose.

Once the forward and aft constraints of two conditions have been performed, their absolute values are required to control the chordwise position of their bays. These constraints ensure that the chordwise position of the bays can be controlled within the aircraft, performing inequality functions.

$$\max(XPIO, XPIOA) \le XP1O, \qquad \text{(Engine Bay)} \quad (5.46a)$$
$$XP1O + LPG \le \min(XPEO, XPEOA)$$

$$\max(XIB1OD, XIB1ODA) \le XWIB1O, \qquad \text{(Weapon Bay 1)} \quad (5.46b)$$
$$XWIB1O + LIB1 \le \min(XIB1OR, XIB1ORA)$$

$$\max(XIB2OD, XIB2ODA) \le XWIB2O, \qquad \text{(Weapon Bay 2)} \quad (5.46c)$$
$$XWIB2O + LIB2 \le \min(XIB2OR, XIB2ORA)$$

$$\max(XUMBOD, XUMBODA) \le XUMBO, \qquad \text{(Main UC Bay)} \quad (5.46d)$$
$$XUMBO + LUMB \le \min(XUMBOR, XUMBORA)$$

5.2 Mass and Volume Estimation

The mass estimation of the aircraft is of fundamental importance in the design as it has a major effect upon other calculations throughout the entire procedure. Hence, it is necessary to predict the aircraft mass as accurately as possible. The aircraft mass is calculated from the sum of the individual component mass. From previous section, the component mass of avionics instruments, weapon(s), propulsion system, two-dimensional nozzle(s), and undercarriages have been obtained. Moreover, many of the components, which are fixed in items of the total aircraft mass, have been obtained their mass straightaway from the manufacturers. In this section, the remaining component mass of wing structural mass, weapon bay increments, aircraft systems, and also fuel mass are determined, and finally complete the aircraft mass.

Generally, some of the components particularly the aircraft systems are themselves power functions of the aircraft mass. Thus, it is necessary to employ an iterative process to first converge the absolute value of aircraft mass, as shown in the overall program flowchart (Figure4-1 of Chapter 4). The method of doing this is to first assume an initial value for the aircraft mass (MTTR), and then to calculate the design total mass (MTT), which results from the sum of the component mass, mentioned above. In general, the design total mass is different to the assumed value. Repeat the process by replacing the assumed value with the calculated value performing the loop calculations until the value being achieved where the two are equal.

In order to produce a realistic aircraft design, the volume available for fuel storage must be estimated, so that necessary provision for all of the required design mission fuel can be made. The following sections provide detail descriptions of the mass and volume estimation for the UCAV.

5.2.1 Wing Structural Mass Estimation

The UCAV concept is primarily based on the flying wing configuration. Thus, the prediction of wing structural mass is one of the most important part in this design synthesis. The wing lends itself to mass analysis because of its well-defined structural role. The theoretical-based methods[5],[79] have been obtained for the wing structural

mass prediction, with some appropriate changes where required to develop the more accurate methods applicable for all flying wing configuration. Structural components making a significant contribution towards the structural mass of wing include the primary structure of wing box, wing control surfaces and enclosed structure, and wing miscellaneous structure.

The most important parameters having a major impact on the wing structural mass are the wing's geometry and thickness, the design aircraft mass (MTTR), the design load factor (ULNMS), and the design diving speed (VD). The former two parameters have been discussed previously, and the latter two parameters are external variable input by the user. In the synthesis process, the ultimate load factor (ULTN) is required, which is calculated by multiplying the correct design load factor by the safety factor of 1.33 for the unmanned aircraft and by that of 1.5 for the manned aircraft. The options from the packaging specification, TAC, is needed to select the type of aircraft for selecting the safety factor, and TMISS is required to select the type of missions for choosing the correct design load factor to be synthesized. The typical design load factors applicable for various missions (aircraft) are shown in Table 5-2.

Mission	Low-level Strike	Counterair	ISR	Ferry
Design (Limit) Load Factor	7.33	8.67	6.00	4.00

Table 5-2: Typical Design (Limit) Load Factors[93],[96]

Additionally, the materials selected for the aircraft have an influence to the wing structural mass estimation. Generally, the method of wing structural mass calculation is based upon a database of existing aircraft. However, use of an advance material (i.e. carbon-fibre composite) may result in an insufficient prediction. To allow for this, the mass factor and the material factors are needed for changes in the structural material. These factors are selected corresponding to an option set by the user in the packaging specification, TMAT, specifying the type of materials.

For the mass factor (FMW), a value of 1.0 corresponds to conventional aluminium alloys, but this may be reduced to 0.85 approximately for a carbon-fibre composite structure[78],[96]. The complete structural mass is determined by multiplying the calculated mass by this factor. The mass factor is applied for calculating the structural mass of the control surfaces and auxiliary attachment structure. The material factors are used in the calculations of the wing structural box. These factors consist of the material shear modulus (GXYC) and the box material property (RHO). The typical values of these material factors are given in Table 5-3.

	Material Shear Modulus GXYC (N/m^2)	Box Material Property RHO
Aluminium Alloys	2.90×10^{10}	2,800
Carbon-Fibre Composite	3.20×10^{10}	2,000

Table 5-3: Typical Values of Material Factors[5]

5.2.1.1 Wing Structural Box

The wing structural box is designed to satisfy either adequate torsional stiffness to meet the flutter requirement, which is a function of design diving speed (VD), or bending and shear constraints under the worse loading case (maximum bending). In general, bending rather than torsional considerations influence design of the root regions of the wing surface. However, the torsional stiffness requirements are of greater relative importance particularly in the outboard region of the wing, the importance of torsional stiffness becomes apparent as wing aspect ratio increases[79]. The torsional stiffness and bending considerations are determined in the form of the thickness of the covers and vertical webs. The mass of wing structural box is determined from the possible conditions of these thickness values.

The torsional stiffness is frequently based on the inner 70 percent of the semi-wingspan. Hence the mass estimation of wing structural box on this function may be based on the assumption of a constant skin thickness from the centreline to 70 percent semi-span. This value of the skin thickness required is given by:

$$TTS = \left\{ \left[\frac{0.0067 \times VD^2 \times (1+UW)^4 \times CWCN \times AW^2 \times (RCWRTW \times \cos(QWB) + RTWN) \times (0.91 + 0.49 \times UWRTW)}{\cos^3(QWB) \times (RBCWN \times RTWN)^2 \times (1 - 0.7 \times (1 - UWRTW))^2 \times \sec^3(QWL - 11) \times GXYC} \right] \times \left[\frac{0.9 \times (RGCW - 0.1) \times (1.3 - RHCW)}{(0.9 - 0.33 \times UW) \times (1 - 0.1 \times RSTIFF) \times FAMN} \right]^2 \right\} \quad (5.47)$$

Where:

RTWN	=	Equivalent thickness to chord ratio at centreline
RBCWN	=	Fractional of overall chord occupied by structural box
UWRTW	=	Value of taper ratio corrected for thickness ratio variation across span
RCWRTW	=	Value of fractional of overall chord occupied by structural box corrected for effect of thickness ratio variation across span
RHCW	=	Fraction of wing chord aft of leading edge to flexural axis (70% semi-span)
RSTIFF	=	Stiffness ratio
FAMN	=	Function of Mach number to correct for compressibility effects

The steps necessary to perform the calculations of these parameters are described in DAeT notes[5], and they are not mentioned here.

The affect of airload is alleviated by inertia forces, which should be considered while calculating the bending and shear criterion for the wing structural box. The effective inertia relief load is determined by the sum of individual component mass (including fuel) and its relative spanwise positions divided by 44 percent of the semi-span.

$$MWIR = \sum_{I=1}^{N} \frac{MITEM(I) \times YMARM(I)}{(0.22 \times BW)} \quad (5.48a)$$

Where N represents the total number of components on aircraft (including fuel in all tanks). To determine the bending and shear criterion, the inertia relief load factor is required, which is found as:

$$FWIR = 1 - \left(0.1 + \frac{MWIR}{MTTR} \right) \tag{5.48b}$$

The effective thickness of the bending and shear criterion required in the wing structural box covers the root region of the wing surface, as mentioned above. This value of the thickness required is given by:

$$TSB = \left[\frac{0.59 \times ULTN \times MTTR \times FWIR \times}{AW \times (1 + UW) \times \sec(QW4) \times \sec(QWB)} \right] \tag{5.48c}$$
$$RBCWN \times CWCN \times RTWN \times ABDS$$

Where:
ABDS = Allowable bending stress

The steps to determine the equivalent cover thickness (ABDS) are again available in DAeT notes[5], which is not included here.

This effective thickness of the bending and shear criterion consists of the actual cover skin and the equivalent thickness due to spreading the stringer area across the chord of the box. The ratio of skin to stringer area can vary, thus, the skin thickness required for bending and shear consideration can be assumed as about 67 percent of TSB for a conventional skin-stringer construction[5]. This effective thickness calculation is applicable for both types of material selection.

However, if TMAT = 1, the skin thickness of bending and shear criterion required for only metal construction is also considered. This skin thickness covers the inner 70 percent of semi-wingspan to meet the bending and shear condition. This value of skin thickness required is found as:

$$TBD = \frac{0.327}{(0.3 + 0.7 \times UW)} \times TSB \tag{5.48d}$$

Once all these values of effective thickness have been accomplished, the mass of wing structural box can be obtained. As mentioned above, the mass of wing structural box is calculated from the possible conditions of these thickness values. On condition that TBD ≥ TTS the torsional stiffness requirement is automatically covered and thus, the bending and shear criterion is critical (metal construction). Therefore, the mass of wing structural box based on the bending and shear criterion is determined, which is found as:

$$MWBCW = \left[\frac{6.3 \times ULTN \times MTTR \times FWIR \times BW \times}{\sec(QWB) \times RHO \times FBWH} \right] \tag{5.49a}$$
$$ABDS$$

Where, FBWH is the function determining the spanwise variation of cover and web thickness[5].

If TTS ≥ 0.67TSB the torsional stiffness is critical across the whole span of the box, thus, the mass estimation of wing structural box based on this condition is obtained, which is given by:

$$MWBCW = \left[\begin{array}{l} 0.022 \times \left(\dfrac{RHO \times BW^3}{GXYC} \right) \times \\ \left(KAMS + \dfrac{0.9 \times RTWN}{RBCWN} \right) \times \\ \left(\dfrac{RCWRTW}{RBCWN} + \dfrac{RTWN}{RBCWN \times \cos(QWB)} \right) \times FUW \times \\ \left(\dfrac{VD \times \cos^{1.5}(QWL - 11) \times (RGCW - 0.1) \times (1.3 - RHCW)}{\left(1 - \dfrac{0.51}{AW^2}\right) \times FAMN \times RTWN \times \cos(QWB)} \right)^2 \end{array} \right] \quad (5.49b)$$

Where KAMS is the allowance for stringer mass and FUW is function of taper ratio for torsional stiffness criterion[5]. RGCW is an external variable defined as fraction of wing chord aft of leading edge to inertia axis.

Finally, if there is a further possible intermediate condition that TBD<TTS<0.67TSB the mass of wing structural box is given by the greater of those two values.

5.2.1.2 Control Surfaces and Enclosed Structure

The mass estimation for control surfaces and enclosed structure are considered in four main segments comprising of the wing leading edge including both fixed and moving parts (leading edge devices if available), the fixed wing trailing edge, the trailing edge devices, and the inlaid control surfaces. The principal methods proposed by Lovell[78] have been obtained with some modifications to develop the more accurate methods available for all flying wing configuration.

The mass estimation for the wing leading edge is considered by the mass per unit area, which is split into four terms. This method includes both the fixed area of wing leading edge and the moving parts of leading edge devices (if available) to be synthesized. The following equations detail the mass estimation for the leading edge.

$$TERM1L = 0.522 \times \frac{ULTN}{SW} \times MTTR \times FWIR \times \left(\frac{SWL \times RTWLGI}{BWL} \right)^2 \quad (5.50a)$$

$$TERM2L = 0.00007285 \times \left(\frac{ULTN \times MTTR \times FWIR}{SW \times RTWLGI} \right) \times \left(\frac{SWL}{BWL} \right)^{0.125} \quad (5.50b)$$

$$TERM3L = 0.000056 \times VD^2 \quad (5.50c)$$

$$TERM4L = 1.536 \times BWL^{0.75} \quad (5.50d)$$

Where:

SWL = Gross area of wing leading edge
BWL = Total span of wing leading edge

RTWLGI = Average wing thickness ratio in area of wing leading edge

Once the mass per unit area of wing leading edge has been performed, the total mass is obtained. The mass factor (FMW) is used in the calculation to determine the accurate mass of the wing leading edge corresponding to the material selected. Thus, the total mass of wing leading edge is found as:

$$MWL = \left[\begin{array}{l} FMW \times (SWSL + SWLF) \times \\ (TERM1L + TERM2L + TERM3L + TERM4L) \end{array}\right] \quad (5.50e)$$

Where:
SWLF = Planform area of fixed wing leading edge forward of front spar
SWSL = Total planform area of leading edge devices

The mass estimation for the fixed section of wing trailing edge is also considered by the mass per unit area, which is split into three terms. The methods require the average depth of rear spar to determine the mass per unit area. The following equations show the complete methods in details.

$$DTE = \frac{1.54 \times SWTG \times RTWTGI}{BWTG} \quad (5.51a)$$

$$TERM1T = 1.482 \times \left(\frac{ULTN \times MTTR \times FWIR}{SW}\right)^{0.25} \times \left(\frac{SWTG}{BWTG}\right)^{0.5} \quad (5.51b)$$

$$TERM2T = \left[\begin{array}{l} \dfrac{0.0030223 \times ULTN \times MTTR \times FWIR \times SWTG}{SW \times BWTG \times DTE^{0.5}} \times \\ \left(\dfrac{SWTG}{BWTG} - \dfrac{SWSE}{BWSE}\right)^2 \end{array}\right] \quad (5.51c)$$

$$TERM3T = 0.646 \times \left(\frac{SWTG}{SWTF}\right)^2 \times DTE^{0.5} \quad (5.51d)$$

Where:
BWTG = Total span of wing trailing edge
RTWTGI = Average wing thickness ratio in area of wing trailing edge
SWSE = Total planform area of trailing edge devices
BWSE = Total span of trailing edge devices

The mass factor (FMW) is also used in the mass estimation of fixed wing trailing edge and thus, the total mass is given by:

$$MWT = FMW \times SWTF \times (TERM1T + TERM2T + TERM3T) \quad (5.51e)$$

The mass estimation for trailing edge devices is based on the option of NW2SE from the packaging specification to select the total number of control surfaces to be synthesized. On condition that NW2SE = 1, the total mass of trailing edge devices is given by the greater of flap mass or split-elevon mass. If NW2SE > 1, the sum of flap mass and elevon mass are obtained. The mass factor (FMW) is used in the calculation to determine the accurate mass of the trailing edge devices corresponding to the material selected.

The mass per unit area of the trailing edge flaps is split into three terms. The total mass is obtained from the sum of each pair of flaps. The following equations detail all the calculations:

$$TERM1F = \left[\sum_{X=1}^{NW2SE-1} \begin{array}{l} 0.151 \times \left(\frac{MTTR \times FWIR}{SW} \right) \times \sin^2(QWSEMX) \times \\ (1.54 \times RTWSEMK(X) \times CWSEK(X))^{0.5} \times \\ (SWSEK(X))^{0.125} \end{array} \right] \quad (5.52a)$$

$$TERM2F = \sum_{X=1}^{NW2SE-1} \frac{0.384 \times CWSEK(X) \times (SWSEK(X))^{0.5}}{1.54 \times RTWSEMK(X) \times CWSEK(X)} \quad (5.52b)$$

$$TERM3F = \sum_{X=1}^{NW2SE-1} FMW \times SWSEK(X) \quad (5.52c)$$

$$MWSEF = (TERM1F + TERM2F) \times TERM3F \quad (5.52d)$$

Where:
QWSEMX = Maximum angle deflection of flap
RTWSEMK = Average wing thickness ratio in area of trailing edge devices

Assuming that the split-elevon mass is determined by using the available methods applied for the aileron, thus the total mass is given by:

$$MWSEA = FMW \times SWSEK \times \left[\begin{array}{l} \left(\frac{0.00009795 \times VD^2}{AWSEK^{0.125}} \right) + \\ \left(\frac{14.14 \times CWSEK \times \cos^2(QWSEH)}{CWWSEK^{0.5}} \right) \end{array} \right] \quad (5.53)$$

Where:
CWWSEK = Wing chord at mid-span of trailing edge devices

Hence, the total mass of trailing edge devices (MWSE) can now be obtained corresponding to the options described above.

The mass estimation for inlaid control surfaces is based on the option of NW2SR from the packaging specification to select the total number of control surfaces to be synthesized. If inlaid control surfaces are used (NW2SR = 1), the mass estimation follows the similar methods of split-elevon mass in equation (5.53) above. The total mass of the inlaid control surfaces is represented by MWSR.

5.2.1.3 Miscellaneous Structure

There are a number of items that need to be added to the wing structural mass. Among of these is the miscellaneous attachment on wing such as the actuators of the overall control surfaces. The external paint is also associated within this group. Moreover, an allowance of 500 lb was assumed to be made for the use of Low Observable treatments (RCS and IR) on the aircraft, as required by the AIAA Request for Proposal (RFP) for an unmanned strike fighter[32]. Additionally, the miscellaneous structure should add the mass of basic ribs in the primary structural box to complete the total wing structural mass. The following equations summarise all the miscellaneous items required for the flying wing.

$$MWCX = 0.0235 \times \begin{pmatrix} MWBCW + MWL + MWT + \\ MWSE + MWSR \end{pmatrix} + 18.14 \quad (5.54a)$$

$$MWXP = 0.341 \times SW \quad (5.54b)$$

$$MWLO = 0.45359237 \times MWLOR \quad (5.54c)$$

$$MWCFS = \left[\left(\frac{3.1 \times SW \times RBCWN \times (CWCN \times RTWN)^{0.5}}{(1+UW)} \right) \times \left(\begin{matrix} (1+UW+UW^2) + 1.1 \times CWCN \times RTWN \times \\ (1+UW+UW^2+UW^3) \end{matrix} \right) \right] \quad (5.54d)$$

Where:

MWCX = Mass of miscellaneous attachment on wing

MWXP = Mass of external paint on wing

MWLO = Mass of LO treatments. MWLOR is an external variable represented the mass of 500 lb allowable LO treatments and the number 0.45359237 is the conversion factor from English to SI units.

MWCFS = Mass of basic ribs in primary structural box

5.2.1.4 Complete Wing

Once all the wing structural components have been obtained, the total mass of wing structure can be defined.

$$MWC = \left[\begin{matrix} (MWBCW)_{WingBox} + \\ (MWL + MWT + MWSE + MWSR)_{Devices} + \\ (MWCX + MWXP + MWLO + MWFCS)_{Miscellaneous} \end{matrix} \right] \quad (5.55)$$

This method of wing structural mass estimation applied for different flying wing configurations is proved to be more accurate than the other methods, as shown in Figure 5-6.

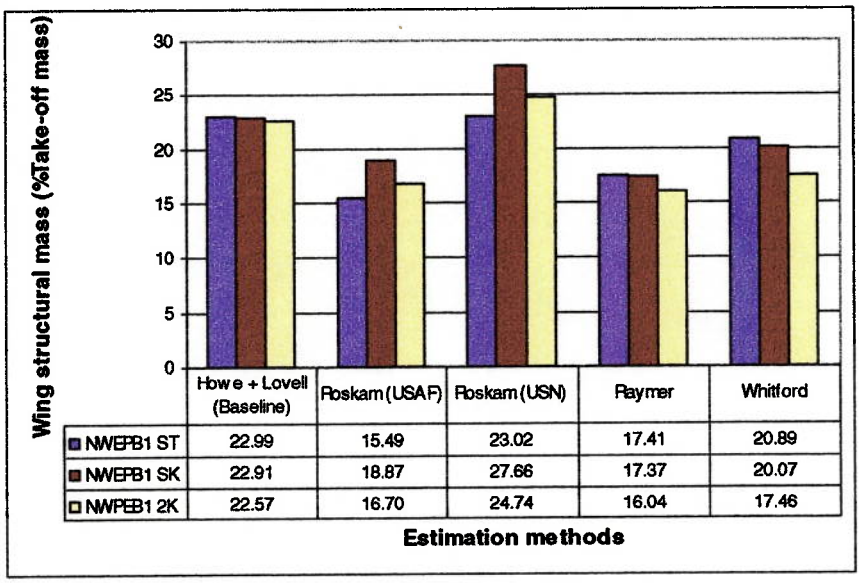

Figure 5-6: Comparison of Wing Structural Mass Estimation Methods

Three example models of the straight-tapered wing and the multi-kinks wing configurations with single weapon bay at centreline have been selected showing that the above theoretical-based method provides more accurate results as compared to these empirical methods obtained from Raymer[96], Roskam[103], and Whitford[17]. It should be stated however, that the multi-kinks flying wing configurations are substantially different from the straight-tapered flying wing configurations; therefore great caution should be taken in analysing the results. Unfortunately, since there were no available data concerning the method of wing structural mass estimation for the multi-kinks flying wing configurations, it was unavoidable to straightforwardly assume that the theoretical-based correlation described above would be valid achievable to provide the acceptable results.

5.2.2 Weapon Bay Increments

The weapon bay sizing and the weapon mass required have been determined in previous section. However, as the weapons are loaded internally, the weapon bay itself provides an additional effect of mass increments on the aircraft. The weapon bay increments can be broken down into contributions from the doors, the surroundings including the door mechanisms, the weapon bay roof, and the weapon support structure. The methods of mass estimation for the weapon bay increments proposed by Seigers[108] provide the useful information for this design synthesis of UCAV. The most important parameter having a major impact on the weapon bay increments is the design diving speed (VD). This parameter affects directly to the weapon bay doors when they are opened to release the weapons. The detailed information about the mass estimation for the weapon bay increments may be found in Seigers note[108]. However, there are some changes on the calculation of weapon bay surroundings determined on the flying wing configuration, as the presented method is based on the conventional configuration.

The mass of the surroundings is given by an equation relating the weapon bay unit area to the average mass per unit area. For the flying wing configuration, this average mass per unit area refers to the wing structural mass (MWC) per square meter of wing-wetted area[96]. For simplicity to determine the weapon bay unit area, the bay is assumed to have a rectangular cutout. The equation represented the weapon bay unit area is also obtained from Seigers note[108], which will not be mentioned here. In summary, the additional mass effect of the weapon bay is given by:

$$MTIBxI = MIBxD + MIBxSR + MIBxRF + 0.03 \times (MWIBx + MIPx) \qquad (5.56)$$

Where:

MIBxD	=	Mass of weapon bay doors
MIBxSR	=	Mass of weapon bay structural surroundings
MIBxRF	=	Mass of weapon bay roof
MWIBx	=	Total mass of weapons in weapon bay
MIPx	=	Mass of internal pylon/launchers

The lowercase *x* represents the counting number of the weapon bays, as described in sub-section 5.1.2.2 above.

5.2.3 Systems Mass Estimation

Having considered the geometry of the major components for the packaging Layout, there are a number of other items that the precise geometry is unimportant but account must be taken of the associated mass and volume. The aircraft systems are in association with these items. The systems components necessarily applicable for UCAV consist of the environmental control systems including the avionics cooling system and the de-icing system, the electrical systems, the flying control systems, and the fuel systems. They are themselves power functions of the aircraft total mass, which are defined as follows:

$$MSA = (MSAK + FMSAK \times MTTR) \times FMSA \quad \text{(Air-condition)} \quad (5.57a)$$

$$MSDI = 0.08 \times MTTR^{0.7} \quad \text{(De-icing)} \quad (5.57b)$$

$$MSE = MSEK + FMSEK \times MTTR \quad \text{(Electric)} \quad (5.57c)$$

$$MSC = MSCK + FMSCK \times MTTR \quad \text{(Flying control)} \quad (5.57d)$$

The fuel systems are based on the mass of the total internal fuel, which is given by:

$$MSF = FMSFK \times MTGF \quad \text{(Fuel)} \quad (5.57e)$$

MTTR is the design take-off mass and *MTGF* is the mass of total internal fuel subjected to variation with the design mission fuel during the optimization process. The other parameters are the external variables, which are the constant values correlated with these aircraft systems.

The aircraft systems are mainly located closed to the avionics bay behind the nose undercarriage bay on the wing centreline. Thus, due to the flying wing configuration, the aircraft provide sufficient volume to contain all these systems and the avionics bay. The location of the aircraft systems is also suitable to manage the whole aircraft.

5.2.4 Volume Estimation

The volume available for fuel storage must be estimated in order to produce a realistic aircraft design, so that necessary provision for all of the required design mission fuel can be made. Once the packaging has been set up, the volume available for fuel storage in integral tanks in the wings can be achieved, and by allowing the available volume enclosing the packaging to be filled with fuel. As the UCAV concept is based on flying wing configuration, there is sufficient volume available to contain the fuel throughout the mission.

The total volume available for the fuel storage in the wing is determined in the area of wing box between the front and rear main wing spars, outboard of the main undercarriage bay to about 80 percent of the semi-wing span, where the remaining volume at the tip is kept available for the electronic warfare and countermeasures suite. The volume and shape of the wing tank varies along the wing kinks (if selected) and the transition area between the inner and outer airfoil shapes. The geometry of wing tank is calculated by the optimizer-provided values of spanwise factor of wing tank's outer edge (FY2WFO) and the axial factor of wing tank rear face (FCWFR). The final shape of wing tank must also provide enough space for the inlaid control surfaces, if applied. On condition that, the wing kinks are in the area of wing tank,

they are broken down into separate tanks and determine the available volume in each tank and sum up for the total wing fuel tank.

To determine the volume of wing fuel tank, it is necessary to first obtain the cross-sectional area of tanks corresponding to the shape of airfoil, which is relatively complex. The methods proposed by Lovell[78] is obtained, which require the front and rear positions of the tank as fraction of relative wing chord and integrate the thickness of airfoil between these positions, thus providing the cross-sectional area.

$$OWXF = \left[\begin{array}{l} 0.34641 \times HWXF \times CWXF \times \\ \left\{ 5 \times \left(FXXR^{3/2} - FXXD^{3/2} \right) - 3 \times \left(FXXR^{5/2} - FXXD^{5/2} \right) \right\} \end{array} \right] \tag{5.58}$$

A factor of 80 percent is applied to the maximum available volume to account for the capacity lost due to the present of structural items. Thus, total tapered volume available for the fuel storage in the wing is found as:

$$VWWF = \sum_{X=1}^{FKINK+1} \left[\begin{array}{l} 0.8 \times \left(\frac{2 \times PWFK(X)}{3} \right) \times \\ \left(1 + UWF(X) + UWF(X)^2 \right) \times OWF(X-1) \end{array} \right] \tag{5.59}$$

Where *FKINK* is the total number of wing kinks in area of wing tank. *PWFK, UWF,* and *OWF* are the span panels, taper ratio and cross-sectional area of separate tanks, respectively.

The available volume enclosing the packaging to be filled with fuel is considered the remaining volume at front, rear and top of the weapon bays and at front and rear of the main undercarriage bay. The method to determine the volume of these fuel tanks also requires the cross-sectional area of tanks coinciding to the shape of airfoil. The volume is then determined by multiplying the cross-sectional area to the width of the bays. The top tank is assumed to occupy only 50 percent of the total volume above the weapon bay, in order to provide the weapon support and deployment mechanisms. The volume of the top tank is obtained by performing the total volume in area of weapon bay and then deducts the volume of weapon bay from this volume. The remaining volume is then split into two, so the volume of top tank is available. A factor of 80 percent is also applied to these tanks to allow for structure and the small volume lost.

For the ferry cruise mission, it is assumed that the weapon bays could be fitted with auxiliary fuel tanks. It is also assumed that 80 percent of the gross volume of each weapon bay could be used to carry fuel. As the mass of the fuel tanks would certainly be greater than of any payload, it is assumed that the support structure can cope with the increased mass. An option from the packaging specification, TMISS, selects the ferry mission to allow for the determination of weapon bay tanks to be synthesized.

Once the volume available for fuel storage in each tank has been obtained, it is necessary to determine the fuel mass in order to perform the total aircraft mass and confirm the mission fuel mass. The fuel mass is accomplished by applying the fuel density (RFUL) to the available fuel volume. In this design synthesis, the JP-4 fuel is selected having the density of 776.50 kg/m^3. Another parameter required to determine

the actual fuel mass for the available volume in the tank is a fuel factor allowing for utilization of fuel in that tank. If this factor is unity, the total fuel capacity is contained in the overall available fuel volume. With the fuel density and the fuel factor, the fuel mass in each tank is found as:

$$MWXF = UWBXF \times VWXF \times RFUL \tag{5.60}$$

Hence, the total fuel mass of the aircraft is obtained from the sum of the fuel mass in each tank. This total fuel mass (MTGF) is subjected to variation with the mission fuel mass during the optimization process in the form of an equality constraint. The MTGF is used in the calculations of the mass of fuel systems mentioned above in equation (5.61e), the total aircraft mass, and the mission fuel control examining the range of the aircraft centre of gravity to remain within the acceptable limits.

5.2.5 Complete Aircraft

The empty mass of the aircraft (MTE) is the sum of the separate aircraft structures and systems defined above and some additional mass that are external variables.

$$MTE = \begin{bmatrix} (MAAV + MXP + MIP1 + MIP2 + MGC + MCI)_{Fixed-equipment} + \\ (MPG + MPTD)_{\text{Pr opulsion}} + (MWC)_{Wing} + \\ (MUM + MUN + MUH)_{Undercarriage} + \\ (MTIB1I + MTIB2I)_{Weapon-bay-increments} + (MCW + MCC)_{Cockpit} + \\ (MSA + MSDI + MSE + MSC + MSF)_{Systems} \end{bmatrix} \tag{5.61a}$$

The total mass of the aircraft at take-off (MTT) is thus obtain by the sum of the empty mass, the payload and the total fuel mass:

$$MTT = MTE + (MGA + MWEP + MCP)_{Payload} + MTGF \tag{5.61b}$$

The mass estimation is iterative, as stated above; an iteration procedure is necessary to determine MTT. An iterative loop within the design synthesis is used so that the total aircraft mass always matches the sum of the component masses. The final converged value of MTT is saved using as the starting value for the corresponding calculation at the next stage into the design synthesis routines.

5.3 Summary

This chapter has presented the methods of aircraft geometry and packaging descriptions for the UCAV, and give relevant algorithms as used in the synthesis code. Moreover, the mass estimation equations and procedures have been detailed and the aircraft volume available for fuel storage has also predicted. The total aircraft mass is then obtained from the converged value of the first iterative process and saved applying as the starting value for the corresponding calculation at the next entry into the design synthesis process.

CHAPTER 6

6 Configuration Layout

This chapter describes the methods and algorithms used to determine the configuration layout of the UCAV. Four main parts have been considered comprising of the aircraft centre of gravity, the undercarriage arrangement, the wing area and volume distribution, and the geometries of intake and two-dimensional nozzle ducts. The previous chapter has explained the methods of detailed component sizing and packaging, estimation of mass, and prediction of volume available for fuel storage. Once the configuration design aspect has achieved, it is necessary to consider all these arrangements of the configuration layout mention above, as they have a major effect upon the packaging particularly for the flying wing configuration. This chapter explains these arrangements in details.

6.1 Aircraft Centre of Gravity

Once the aircraft is sized and the required mass of the fuel is known, a more detailed arrangement of internal components can be worked out. The final procedure in sizing ensured that sufficient internal volume existed so that all items required to be carried internally would fit, but the specific locations of each component also are important. This is because the position of the centre of gravity of aircraft must be controlled so that, at all times throughout the mission, as fuel is burned and payload offloaded or expended, the static margin of aircraft will remain at acceptable values.

6.1.1 Centre of Gravity of Components

The centre of gravity of a component composed of a single element is located at the centre of its volume, which may be determined by integration, by published closed-form solutions (for standard shapes), or by various graphical methods. For the components of constant cross-section down their length, their centres of gravity are at their mid-spans.

The aircraft systems are assumed to have no net moment about the centre of gravity. However, their CG location can be most closely estimated by referring to the system layout in the aircraft. Generally, the methods estimating the CG location of the aircraft systems are based on the selected parameters determined by engineering judgement and experience from the result of averaging actual balance data for a broad spectrum of types of conventional aircraft. Alterations to these guidelines are required for the flying wing aircraft configurations. For simplicity, the CG position of aircraft systems used in this design synthesis are mainly located closed to the avionics bay behind the nose undercarriage bay on the wing centreline, where the aircraft could

provide sufficient volume to contain these systems, and their location is suitable for controlling the entire aircraft.

To determine the position of the centre of gravity of the engine, it was recommended by all sources to obtain the data from the manufacturer. However, in this design synthesis the size of the actual engine can be varied from the baseline based on the optimizer-provided value of engine scale factor. Due to this reason, the CG location of the engine is assumed to locate at the mid-span down its length, following the method proposed by Lovell[78]. Similarly, this assumption is also applied to the two-dimensional nozzle.

The location of the centre of gravity of the main undercarriage is at the pintle of its leg, which is assumed to be at a fixed distance, ELUP, aft of the front or forward of the rear of the main undercarriage bay. The pintle is also positioned at a fixed fraction, RLUPCW, of the wing mean aerodynamic chord, aft of the wing mean quarter chord point, XWCQM. For the nose undercarriage, the location of the centre of gravity is assumed to act at the mid-point of the length of the undercarriage bay.

6.1.2 CG of Centre of Wing Volume

The mass of the structure of the wing is assumed to act at the centre of volume of the wing. The method of estimation for the CG location of the wing proposed by Cranfield DAeT notes[5] stated that for the fixed-swept wings without body carried through structure, the total wing mass acted at 35 percents of the wing semi-span measured outboard from the side of the body and on the 45 percent wing chord line. Additionally, the method proposed by Roskam[103] specified that the CG location of wing for the swept wing planform acted at 70 percent of the distance between the front and rear spar behind the front spar at 35 percent of the wing semi-span measured outboard from the side of the body. These two methods, however, were based on the conventional net wing planform, which might not provide the accurate result for the flying wing configuration.

The empirical method developed by Lovell[78] was selected, which determined the CG location of the wing based on the gross wing planform. The centre of volume is defined by the distance aft of the mean quarter chord point of the wing, XWCQM, as a fraction of the mean aerodynamic chord, which is found as:

$$RLWCC = \left[\frac{1}{56} \times \left\{ 13 - \frac{\left(27 \times UW^2 + 1.75 \times AW \times \left(1 - UW^2\right) \times \right)}{\left(1 + 4 \times UW + UW^2\right) \times \tan(QWL)} \right\} \right] \qquad (6.1)$$

Where UW, AW, and QWL are the wing taper ratio, gross wing aspect ratio, and wing leading edge sweep, respectively. This method, however, is suitable only for the straight tapered wing configuration. No any methods have acknowledged for the estimation of CG location based on multi-kinks wing planform. One of the alternative approaches is that, an equivalent straight-tapered wing planform may be needed, which is suitably representative of the true wing planform. With this method, it is only useful to determine the overall aerodynamic characteristics of the aircraft.

Another method developed and modified by the author has followed the method of DATCOM[57] applied for predicting the location of the wing aerodynamic centre for the non-straight-tapered wing planforms. The multi-kinks wing is divided into a series of trapezoidal panels with each panel having conventional, straight-tapered geometry. There is a difference between the construction geometry used to determine the inboard and the remaining outer panels, as shown in Figure 6-1.

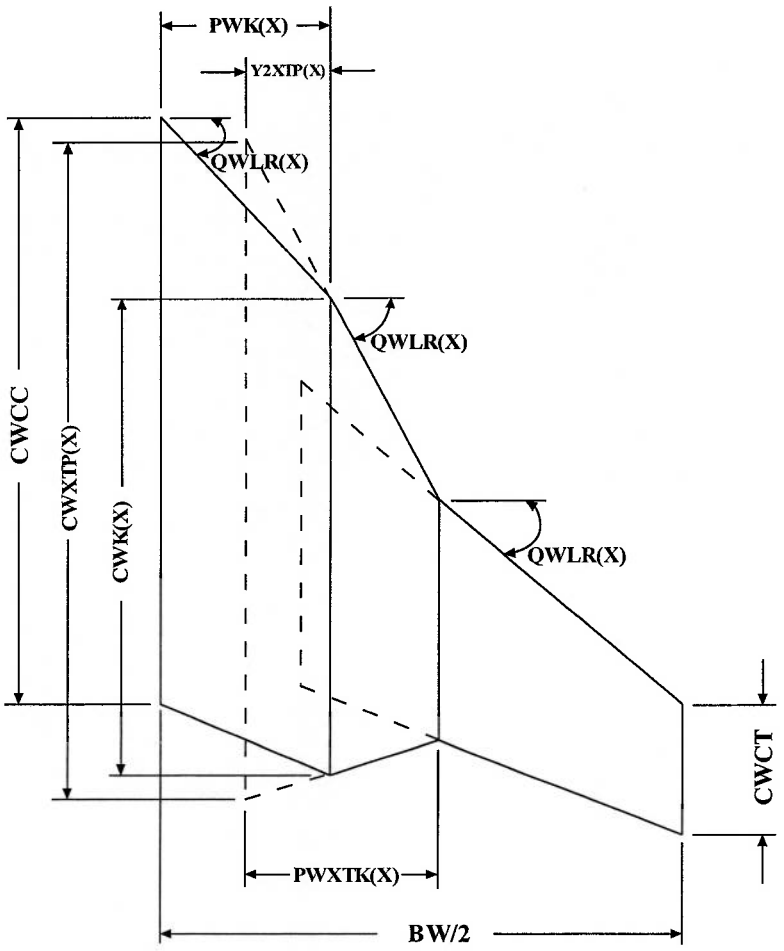

Figure 6-1: Constructed Panels of Multi-Kinks Wing Planform Used to Determine Wing CG Location

The geometry of the inboard panel defines that the leading and trailing edges extends to the wing centreline. The tip-chord span station is fixed at the break formed by the discontinuity in the sweep of the leading edge of the combined wing. For the geometry of the remaining outer panels, the leading and trailing edges extends to the mid-point between the wing centreline and the breaks formed by the discontinuity of the sweeps of the leading edge of the combined wings.

Then, for each of the constructed panels, the individual CG location is estimated by treating each constructed panel as a complete wing and applying the equation 6.1 presented above. These CG locations are fractions of the mean aerodynamic chord of the constructed panels, which are required to convert to fractions of the wing root

chord of those panels. Then all the CG locations of the outer panels are required to convert to fractions of the wing root centreline chord, given by:

$$\sum_{X=1}^{NWK} RLWCCTK(X) = \left[\begin{array}{l} \left(\dfrac{RLWCXTK(X) \times CWXTP(X)}{CWXTP(0)} \right) - \\ \left(\dfrac{Y2XTP(X) \times \tan(QWLR(X+1))}{CWXTP(0)} \right) + \\ \left(\dfrac{XWKLK(X)}{CWXTP(0)} \right) \end{array} \right] \tag{6.2}$$

Where:

RLWCCTK = CG location of wing constructed panel as fraction of wing root centreline chord (At root chord RLWCCTK (0) = RLWCXTK (0))

RLWCXTK = CG location of wing constructed panel as fraction of wing root chord of that panel

CWXTP = Wing root chord of constructed panel (CWXTP (0) = CWCC)

Y2XTP = Extended panel

XWKLK = Distance of leading edge of wing kinks from aircraft nose

The individual CG location (RLWCCTK) derived for each constructed panel is then combined in accordance with the weighted-area relationship to establish the predicted CG location for the multi-kinks wing planform.

$$RLWCCK = \sum_{X=1}^{NWK+1} \frac{SWXTK(X) \times RLWCCTK(X-1)}{SWXTK(X)} \tag{6.3}$$

Where:

SWXTK = Total planform area of wing constructed panel

This CG location for the multi-kinks wing configuration is a fraction of the wing root centreline chord. Converting this CG location to a fraction of the mean aerodynamic chord, hence it is found as:

$$RLWCC = \frac{(RLWCCK \times CWCC) - XWCQM}{CWMA} \tag{6.4}$$

Figure 6-2 shows the results of the method of weighted-area relationship applied for predicting the CG location of the true multi-kinks wing planforms compared to the method determined by an equivalent wing planform. Three example models of different multi-kinks wing planforms with various packaging aspects have been selected showing that the massed-area relationship method based on the true wing planform provides more accurate results as compared to the method using an equivalent wing. To approve these results, three models of straight tapered wing configuration with various packaging aspects have also determined performing as the guidelines to check for the accurate results between these two methods applied for the multi-kinks wing planforms.

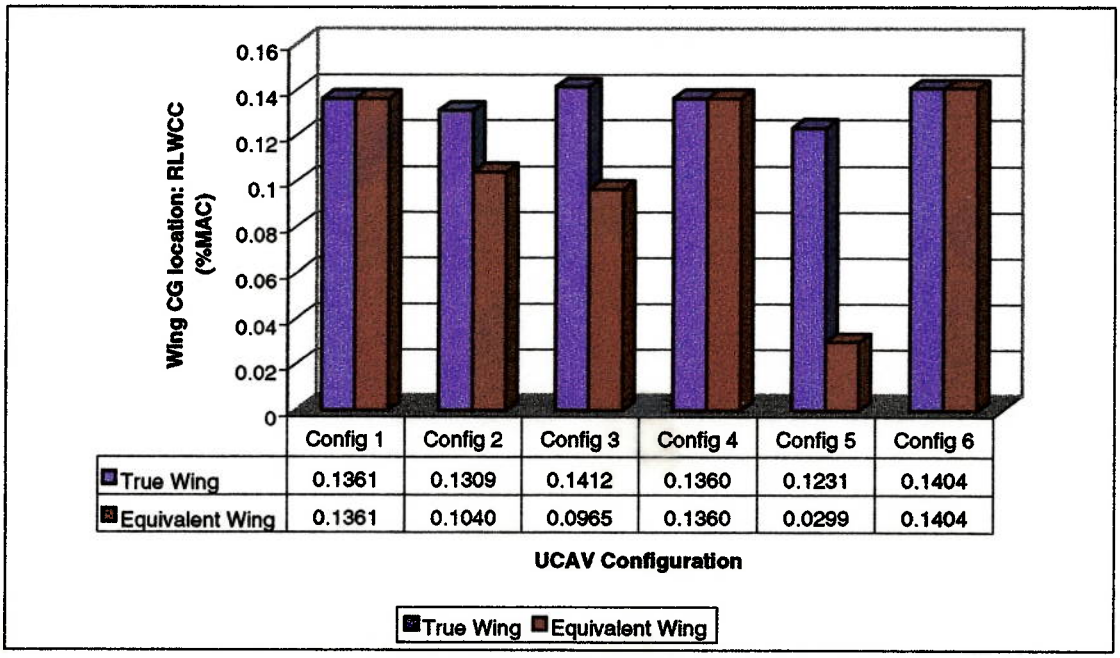

UCAV	Description of Configuration
Config 1	Straight tapered wing with one weapon bay at centre
Config 2	Single-kink wing with one weapon bay at centre
Config 3	Two-kinks wing with one weapon bay at centre
Config 4	Straight tapered wing with two weapon bays outboard of twin engines
Config 5	Two-kinks wing with two weapon bays outboard of twin engines
Config 6	Straight tapered wing with one centre weapon bay and two outboard bays

Figure 6-2: Comparison of Wing CG Locations as Fraction of MAC

6.1.3 CG of Centre of Fuel Volume

According to the detailed description of fuel volume estimation explained in section 5.2.4 of Chapter 5, the volume available for fuel storage in the aircraft are in the integral wing tanks and the available volume enclosing the packaging. The former provides tapered planform tank and the latter accommodates the rectangular planform tanks. The centre of gravity of the fuel is located at the centre of volume. The method proposed by Lovell[78] is obtained, with some modifications to determine the centre of volume of the rectangular planform tank. The method requires the front and rear positions of the tank as fraction of relative wing chord and integrate the moment of the thickness distribution of airfoil between these positions.

$$RLX = \frac{3}{7} \times \left[\frac{7 \times \left(FXXR^{2.5} - FXXD^{2.5} \right) - 5 \times \left(FXXR^{3.5} - FXXD^{3.5} \right)}{5 \times \left(FXXR^{1.5} - FXXD^{1.5} \right) - 3 \times \left(FXXR^{2.5} - FXXD^{2.5} \right)} \right] \tag{6.5}$$

The moment arm of the centre of volume of rectangular planform tanks from aircraft nose are determined by applying the centre of volume (RLX) to the relative wing chord at their existing stations, added with the distance of leading edge of their wing chords from the aircraft nose. Additionally, similar method is required to determine the moment arm of the centre of volume of wing tank from aircraft nose, with some changes applicable for the tapered planform tank.

$$\sum_{X=1}^{FKINK+1} LWF(X) = \frac{\left[\begin{array}{l}\left(\begin{array}{l}3\times CWWF(X-1)\times RLWF\times\\(1+UWF(X))\times(1+UWF(X)^2)\end{array}\right)+\\\left(\begin{array}{l}(XWFL(X)-XWFL(X-1))\times\\(1+2\times UWF(X)+3\times UWF(X)^2)\end{array}\right)\end{array}\right]}{4\times(1+UWF(X)+UWF(X)^2)} + XWFL(X-1) \qquad (6.6)$$

This method can be applied for either straight-tapered or multi-kinks wing planforms. For the multi-kinks wing configuration, the wing tank is broken down into separate tanks corresponding to the number of wing kinks in area of the wing tank and determines the moment arm of centre of volume in each tank.

6.1.4 Complete Aircraft

The position of the aircraft centre of gravity is determined by summing the mass of components and their moments about the aircraft nose to their CG locations, then dividing the total moment by the total mass. This calculation must be completed for each possible aircraft mass and loading configuration. In this design synthesis, the centre of gravity of the possible aircraft mass is calculated in three cases: with no weapons loaded and fuel tanks empty (empty mass), weapons loaded and fuel tank empty (zero fuel mass), and full loaded (total aircraft mass). For the loading conditions, it is assumed that payload and fuel proportioning throughout the mission is available to maintain the actual variation of the centre of gravity between the range of forward and aft limitations, corresponding to those of the above three cases of possible aircraft mass. The actual variation of centre of gravity throughout the mission is fully described following the mission performance analysis in Chapter 7.

The total aircraft pitching moment from aircraft nose with empty mass is found as:

$$ATE = \left[\begin{array}{l}\left\{\begin{array}{l}(MARAD+MASEN)\times(XFR-0.5\times XAR)+\\\left(\begin{array}{l}MAFC+MANAV+\\MACOMM+MAIDEN\end{array}\right)\times(XIID+0.5\times XAX1)+\\MAWEPC\times(XIID+0.5\times XAX1)+\\(MAEW+MACM)\times 0.425\times BW\times\tan(QWL)\end{array}\right\}+\\\left\{\begin{array}{l}MXP\times(XW2L+0.25\times CWC2)+\\MIP1\times(XWIB1O+0.5\times LIB1)+\\MIP2\times(XWIB2O+0.5\times LIB2)+MGC\times(XFR+0.5\times LGC)\end{array}\right\}+\\\{MPG\times(XP1O+0.5\times LPG)+MPTD\times(XP2O+0.5\times LPTD)\}+\\\left\{\begin{array}{l}MWC\times(XWCQM+RLWCC\times CWMA)+\\MUMG\times(XWCQM+RLUPCW\times CWMA)+\\MUNG\times(XFR+0.5\times LUNB)\end{array}\right\}+\\\left\{\begin{array}{l}MTIB1I\times(XWIB1O+0.5\times LIB1)+\\MTIB2I\times(XWIB2O+0.5\times LIB2)\end{array}\right\}+\left\{\begin{array}{l}(MCW+MCC+MCI)\times\\(XFR+0.5\times LCFL)\end{array}\right\}\\\{(MSA+MSDI+MSE+MSC+MSF)\times(XIID+0.25\times XAX1)\}\end{array}\right] \qquad (6.7a)$$

The distance of the aircraft centre of gravity from the aircraft nose with empty mass is then given by:

$$XTECG = \frac{ATE}{MTE} \tag{6.7b}$$

The total aircraft pitching moment from aircraft nose with zero fuel mass is determined by adding the contributions of the total pitching moment of the payload (weapons and ammunition, if selected) to the aircraft pitching moment with empty mass (ATE).

$$ATZF = ATE + \begin{bmatrix} MWIB1 \times (XWIB1O + 0.5 \times LIB1) + \\ MWIB2 \times (XWIB2O + 0.5 \times LIB2) + \\ MWOB \times (XW2L + 0.25 \times CWC2) + \\ MGA \times (XIID + 0.25 \times XAX1) + \\ MCP \times (XFR + 0.5 \times LCFL) \end{bmatrix} \tag{6.8a}$$

The distance of the aircraft centre of gravity from the aircraft nose with zero fuel mass is then given by:

$$XTZFCG = \frac{ATZF}{(MTE + MWEP + MGA + MCP)} = \frac{ATZF}{MTZF} \tag{6.8b}$$

To determine the centre of gravity of aircraft when the entire fuel tanks are full, the contributions to the total pitching moment of the fuel in the tanks enclosing the weapon bays and the main undercarriage bay, the wing tanks, and the auxiliary fuel tanks inside the weapon bays (if provided) are calculated and added to the total aircraft pitching moment with zero fuel mass (ATZF). Hence, the total aircraft pitching moment from aircraft nose with total mass (take-off mass) is found as:

$$ATT = ATZF + \begin{bmatrix} \begin{Bmatrix} MCF1 \times LWCF1 + \\ MCF2 \times LWCF2 + \\ MCF3 \times LWCF3 \end{Bmatrix} + \begin{Bmatrix} MIBF1 \times LWIBF1 + \\ MIBF2 \times LWIBF2 + \\ MIBF3 \times LWIBF3 \end{Bmatrix} + \\ \begin{Bmatrix} MOBF1 \times LWOBF1 + \\ MOBF2 \times LWOBF2 \end{Bmatrix} + MWF \times LWF + \\ \begin{Bmatrix} MWIB1F \times (XWIB1O + 0.5 \times LIB1) + \\ MWIB2F \times (XWIB2O + 0.5 \times LIB2) \end{Bmatrix} \end{bmatrix} \tag{6.9a}$$

The distance of the aircraft centre of gravity from the aircraft nose with total aircraft mass is then given by:

$$XTTCG = \frac{ATT}{(MTE + MWEP + MGA + MCP + MTGF)} = \frac{ATT}{MTT} \tag{6.9b}$$

The results of centre of gravity from these possible aircraft masses are then specified the minimum value being the forward CG (XTCGL) and the maximum value being

the aft CG (XTCGA). They have a major effect upon the packaging particularly the undercarriage arrangement, which are described in the following section.

6.2 Undercarriage Arrangement

Some aspects of the general sizing and layout of the undercarriage are described in section 5.1.3.4 of Chapter 5. This section summarises the undercarriage arrangements, which are one of the most important parts of the design synthesis for the UCAV. Generally, there are several common options for the undercarriage arrangement. For the UCAV, it was decided to use the tricycle layout for the landing gear design, with two main wheels aft of the centre of gravity and the nose wheel forward of the CG. With the tricycle layout, the centre of gravity is ahead of the main wheels so the aircraft is stable on the ground. Moreover, this type of arrangement naturally provides a good ground clearance for the tail of the aircraft particularly the trailing edge of the flying wing, as its configuration has no any tail surfaces with a high moment arm from the centre of gravity of the aircraft, which is also useful in terms of loading the weapons into the bays.

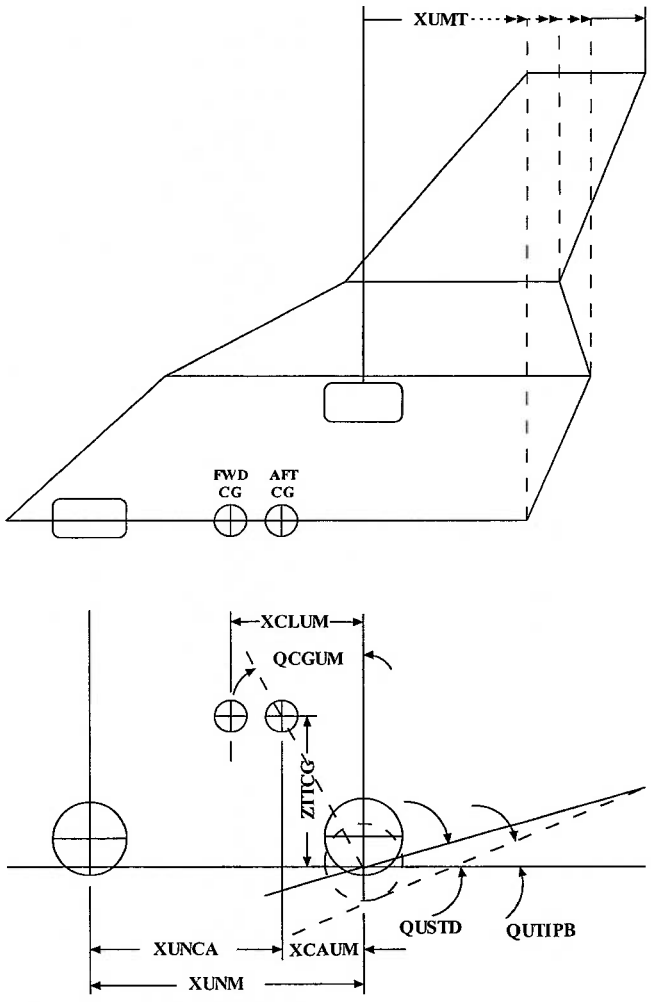

Figure 6-3: Undercarriage Arrangement of UCAV

However, to meet this requirement of ground clearance, it is found that the sizing constraint for the length of the main undercarriage must be applied so that the trailing edge of the aircraft does not touch the ground during the aircraft nose-up attitude. This is determined by performing the angle off the vertical from the main undercarriage position to the aircraft centre of gravity (QCGUM) and compared to the greater value between the tipback angle (QUTIPB) and minimum required angle of 15 degree[96], as shown in Figure 6-3 above. The tipback angle is defined as the maximum aircraft nose-up attitude with the tail touching the ground and the strut fully extended. It should be noted that, in some conditions the flying wing might provide higher value of sweepback angle that the tail at wing tip or at wing kink positions (for multi-kinks wing) extends further than that at the wing centreline, thus to determine the ground clearance, the distance from the main undercarriage to the trailing edge of the aircraft (XUMT) is selected from the maximum value between the distance to the tail at wing centreline, at wing kink positions, and that at wing tip. Hence, for a good ground clearance, the relation is found as:

$$QUTIPB = \tan^{-1}\left(\frac{HTIPB}{XUMT}\right) \tag{6.10a}$$

$$QCGUM = \tan^{-1}\left(\frac{XCAUM}{ZTTCG}\right), \text{ Where QCGUM} \geq \max(\text{QUTIPB},15) \tag{6.10b}$$

Where *HTIPB* is the height due to tipback angle at trailing edge. *ZTTCG* is the reference vertical distance of aircraft CG from ground measured to wing centreline.

The estimation of the wheel and tire size, determined in section 5.1.3.4 of Chapter 5, is usually based upon the smallest tire rated to carry the calculated static loads. The actual tires to be used for a final design layout must be selected from the manufacturers. The following equations, proposed by Raymer[96], define the calculation of the static loads on the tires, corresponding to the illustration shown in Figure 6-3 above.

$$MUMSLMX = MTT \times \frac{XUNCA}{XUNM} \text{ (Maximum static load)} \tag{6.11a}$$

$$MUNSLMX = MTT \times \frac{XCLUM}{XUNM} \text{ (Maximum nose static load)} \tag{6.11b}$$

$$MUNSLMN = MTT \times \frac{XCAUM}{XUNM} \text{ (Minimum nose static load)} \tag{6.11c}$$

To assure that the static loads carried by the nose undercarriage are satisfied within the limit, a fraction of the minimum nose static load to the total load should be greater than 5 percent and that of the maximum nose static load to the total load should be less than 20 percent[96]. The results from the specified nose static loads provide the final sizes of the tires in order to select the actual tires for the aircraft.

Additionally, the undercarriage must absorb the shock of a severe landing. The tires themselves provide some shock-absorbing ability by deflecting when a bump is encountered. For the shock-absorbing gears, the oleopneumatic shock strut or 'oleo', which is the most common type, is selected for the UCAV. The required deflection of the shock-absorbing system or the 'stroke' is based upon the vertical speed at

touchdown, the shock-absorbing material, and the amount of wing lift still available after touchdown. The following equation, proposed by Raymer[96], determines the stroke of the shock absorber, which is derived from the energy considerations.

$$SUMS = \frac{VVTD^2}{(2 \times GR \times EUSFOO \times FUGL)} - \frac{EUST \times SUMT}{EUSFOO} \qquad (6.12)$$

The vertical speed at touchdown (VVTD) is established in various specifications for different types of aircraft. For the UCAV, the vertical speed of 10 ft/s (3.05 m/s) is selected, which is the valued required by most Air Force aircraft. The vertical energy of the aircraft, which must be absorbed during the landing, requires the efficiencies of the shock absorber and tires. The actual shock absorber efficiencies of the fixed orifice oleopneumatic (EUSFOO) and tire (EUST) types are selected for this analysis with the efficiency of 0.65 and 0.47, respectively[96].

The shock absorber and tires act together to decelerate the aircraft from the landing vertical speed to zero vertical speed. This vertical deceleration rate is called the gear load factor (FUGL). Typical value of 3 is chosen for this analysis, which is permitted for Air Force fighter[96]. For tires it is assumed that the tire deflects only to its rolling radius, so the tire stroke (SUMT) is estimated to be equal to half the diameter minus the rolling radius. The rolling radius is the radius when under load being approximately equal to two-thirds of tire radius.

To insure that the shock absorber stroke is clearly satisfied, a minimum value of 8 inches (0.2 metres) for the stroke is recommended performing an inequality constraint during the optimization process.

6.3 Wing Area and Volume Distribution

The next stage of the configuration layout is to determine the wing area and volume distribution. The term 'wing' is applied in this calculation instead of 'aircraft' as the primary configuration of the UCAV determined in this design synthesis is based on the flying wing concept. Basically, the aircraft internal volume is used as a measure of the reasonableness of a new design, by comparing the volume to existing aircraft of similar mass and type. Another use of the area and volume distribution is to predict and minimise the supersonic wave drag and the transonic drag rise. An accurate estimation of the internal volume can be obtained by a graphical integration process using a number of flying wing cross-sections. The cross-sectional areas of a number of cross-sections are determined and plotted against the chordwise location, and then the integrated area under the resulting curves gives the internal volume.

The method used in this stage was developed by Lovell[78], with some changes by the author to be acceptable to several aspects of UCAV design. On condition that the multi-kinks wing planforms are selected, to obtain reasonable accuracy, the flying wing cross-sections should be plotted and measured anywhere that the discontinuity of the sweeps of the leading edge of the combined wings occurs. This can be performed by determining the cross-sectional areas at the distance aft of apex (aircraft nose) in each trapezoidal panel, and then sum the overall results obtaining the total cross-sectional area at that section. For simplicity, the method of estimation of the

wing area and volume distribution applicable for all flying wing planforms is illustrated in the following flowchart.

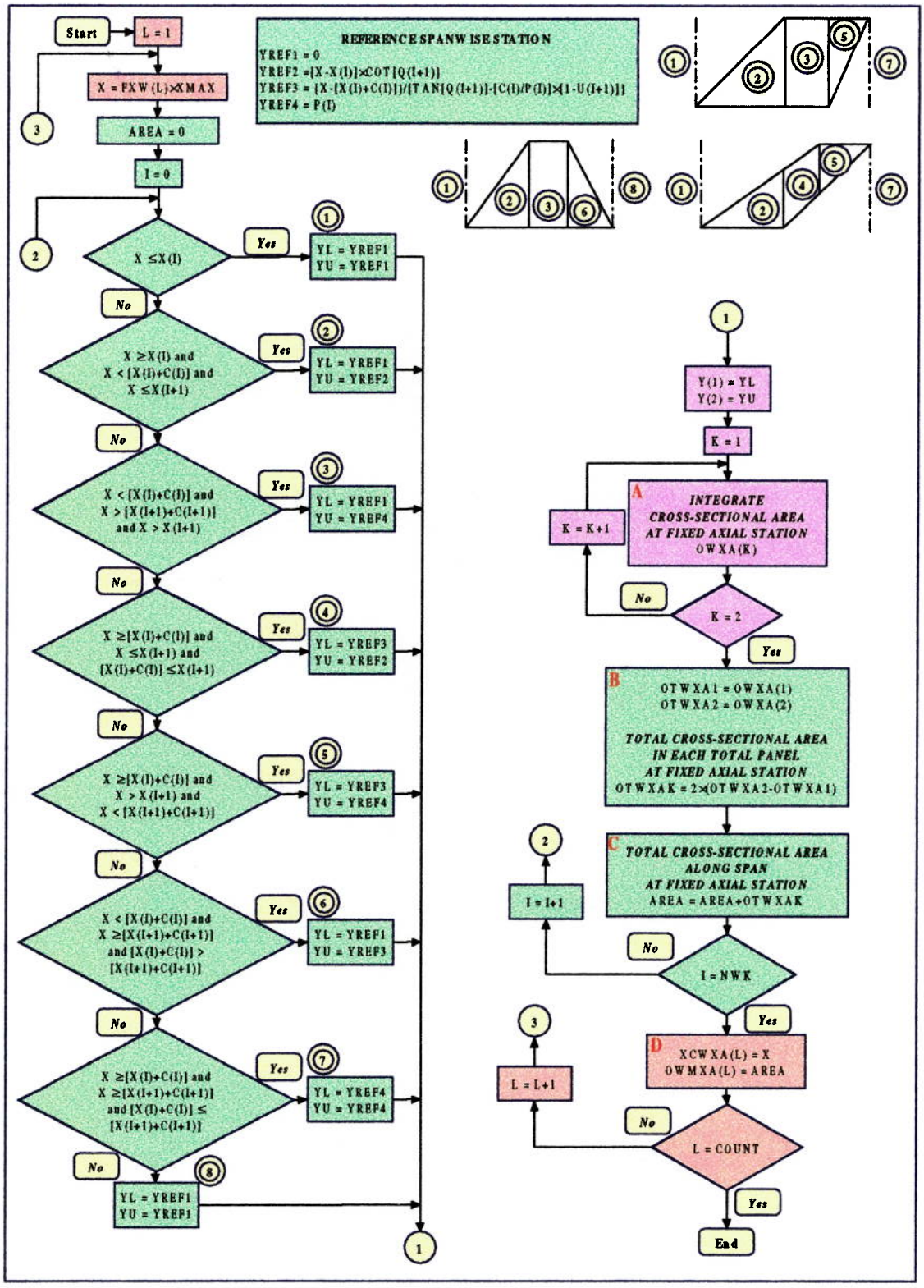

Figure 6-4: Wing Area and Volume Distribution Flowchart

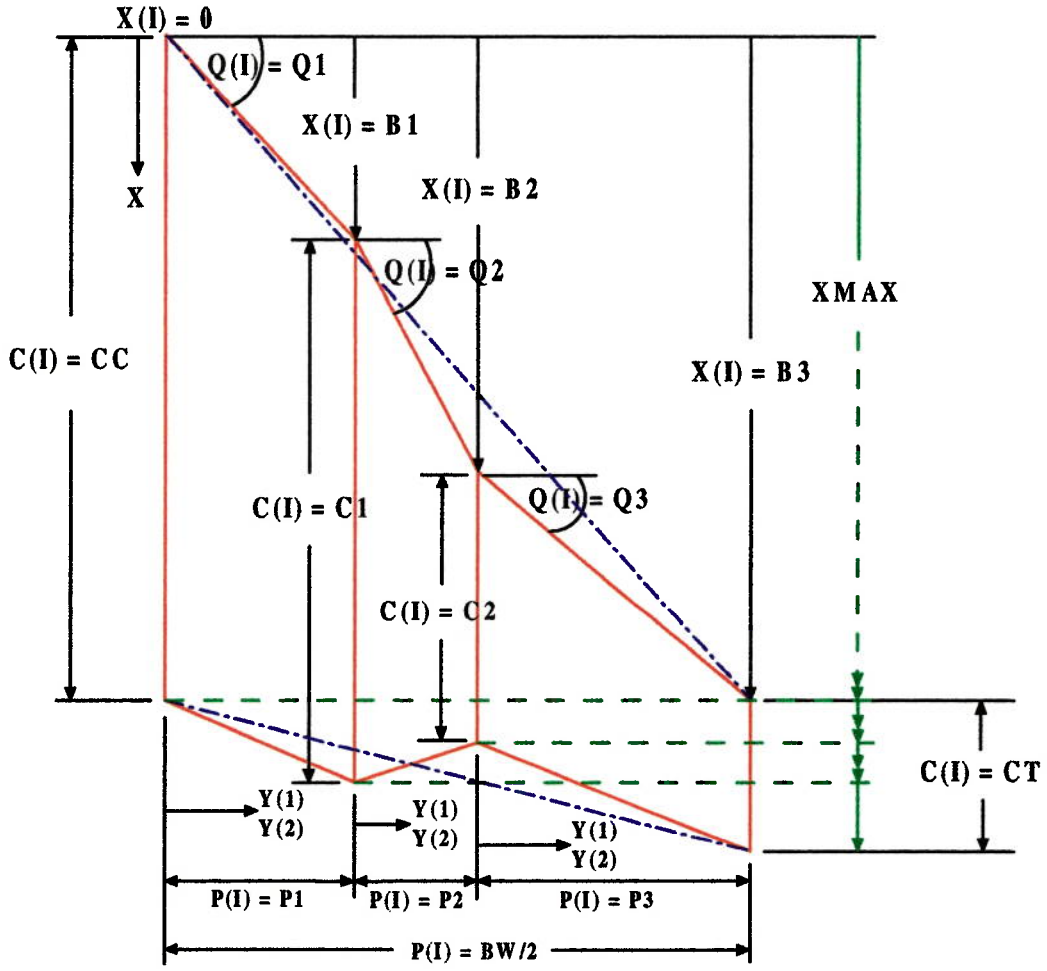

Figure 6-5: Constructed Panels of Flying Wing Planform Used to Determine Wing Area and Volume Distribution

Figure 6-5 presents the illustration of some features of the flying wing planforms corresponding to the method of calculation from the flowchart to determine the wing area and volume distribution. *XMAX* defines the maximum length of the aircraft from wing apex (aircraft nose) to any point on the trailing edge. The distance aft of apex (X) to determine the cross-sectional area at fixed chordwise station is set by applying the non-dimensional factors (FXW) to the maximum length (XMAX). A series of trapezoidal panels is then considered from the number of kinks (NWK) to accomplish the calculations of the cross-sectional area in each panel (I = 0 to NWK).

At any fixed chordwise station, the thickness distribution is integrated across the panel (semi-wingspan for straight tapered wing planform, NWK = 0) providing the cross-sectional area at that section. Depending on the value of the distance aft of apex (X), the lower-limit spanwise value (YL) may occur at the wing root centreline chord (or wing chord at kinks for the outer panels of multi-kinks wing planform, if selected), YL = YREF1, or the trailing edge, YL = YREF3, as shown in Figure 6-4 above. Similarly, the upper-limit spanwise value (YU) may occur on the leading edge, YU = YREF2, the tip chord (or wing chord at kinks), YU = YREF4, or on the trailing edge if it is swept forward, YU = YREF3.

According to frame A in the flowchart of Figure 6-4, after obtaining the lower- and upper-limit spanwise value at any fixed chordwise station, the method used to determine the wing cross-sectional area can be performed (K = YL to YU). They are divided into eight terms, defined as follows:

$$OW2XA1 = \cos^{-1}\left(\frac{QWXA1}{QWXA2}\right) \tag{6.13}$$

Where:

$$QWXA1 = P(I) - [(X - X(I)) \times (1 - U(I+1)) \times \cot(Q(I+1))] \tag{6.13a}$$

$$QWXA2 = \begin{bmatrix} \{(X - X(I)) \times (1 - U(I+1)) \times \cot(Q(I+1))\} + \\ P(I) - \{2 \times Y(K) \times (1 - U(I+1))\} \end{bmatrix} \tag{6.13b}$$

$$OW2XA2 = \frac{3\sqrt{3} \times TC(K) \times P(I)}{2 \times C(I) \times (1 - U(I+1))} \tag{6.14}$$

$$OW2XA3 = 0.5 \times \left[\frac{C(I)}{P(I)} \times (1 - U(I+1)) \times \tan(Q(I+1))\right]^{0.5} \tag{6.15}$$

$$OW2XA4 = \left[\frac{(X - X(I)) \times (1 - U(I+1)) - P(I) \times \tan(Q(I+1))}{2 \times (1 - U(I+1)) \times \tan(Q(I+1))}\right]^{2} \tag{6.16}$$

$$OW2XA5 = \frac{C(I)}{P(I)} \times (1 - U(I+1)) + 3 \times \tan(Q(I+1)) \tag{6.17}$$

$$OW2XA6 = \begin{bmatrix} \log\left|\sec(OW2XA1) + \tan(OW2XA1)\right| - \\ \tan(OW2XA1) \times \sec(OW2XA1) \end{bmatrix} \tag{6.18}$$

$$OW2XA7 = 2 \times \left[C(I) \times \left\{1 - (1 - U(I+1)) \times \frac{Y(K)}{P(I)}\right\}\right]^{0.5} \tag{6.19}$$

$$OW2XA8 = [(X - X(I)) - Y(K) \times \tan(Q(I+1))]^{1.5} \tag{6.20}$$

Where:

X	=	Distance aft of apex (aircraft nose) to any fixed chordwise station
X (I)	=	Distance of leading edge of wing kinks from aircraft nose
C (I)	=	Wing chord at kink positions (including wing root centreline chord)
P (I)	=	Semi-span of straight tapered wing planform (Span of a series of panels of multi-kinks wing planform)
U (I)	=	Taper ratio over semi-span of straight tapered wing planform (Taper ratio of a series of panels of multi-kinks wing planform)
Q (I)	=	Wing leading edge sweep
Y (K)	=	Spanwise values at any fixed chordwise station
TC (K)	=	Thickness to chord ratio at spanwise values

All the terms described above are then combined producing the integrated equation for the cross-sectional area at any fixed chordwise station.

$$OWXA(K)=\left[OW2XA2\times\left(\begin{matrix}OW2XA3\times OW2XA4\times OW2XA5\times\\ OW2XA6+OW2XA7\times OW2XA8\end{matrix}\right)\right]_{K=YL}^{K=YU} \quad (6.21)$$

The result obtained from the above calculations is based on the semi-wingspan (or each panel on the semi-wingspan), thus it must be summed up to complete the overall cross-sectional area of that total panel (OTWXAK) at any fixed axial station, as illustrated in frame B in the flowchart of Figure 6-4. Carrying on to frame C, on condition that the straight tapered wing planform is chosen, the overall cross-sectional area (OTWXAK) is already obtained over the total span at that fixed chordwise station performing AREA. On the other hand, if the multi-kinks wing planform is selected, the overall cross-sectional area over the total span (AREA) is the sum of the entire OTWXAK in each total panel, thus an iterative routine is needed to complete the cross-sectional area of the remaining outer panels at that fixed chordwise station.

At this stage (frame D), the overall cross-sectional area over the total span (OWMXA) at the actual-fixed chordwise station (XCWXA) is achieved. The second iterative routine is then required to determine the OWMXA of the remaining sections along the maximum length (XMAX). Once the cross-sectional areas of a number of cross-sections are accomplished, the area under the resulting curves is integrated to determine the internal volume. Additionally, the maximum cross-sectional area (OWMX) is obtained applicable to predict the transition drag rise and the wave drag on the aircraft on condition that the aircraft further operates in supersonic region.

The following figures show some cases of the wing area and volume distribution plot. Three wing planforms have been determined comprising of straight tapered wing, single-kink wing, and two-kinks wing planforms respectively.

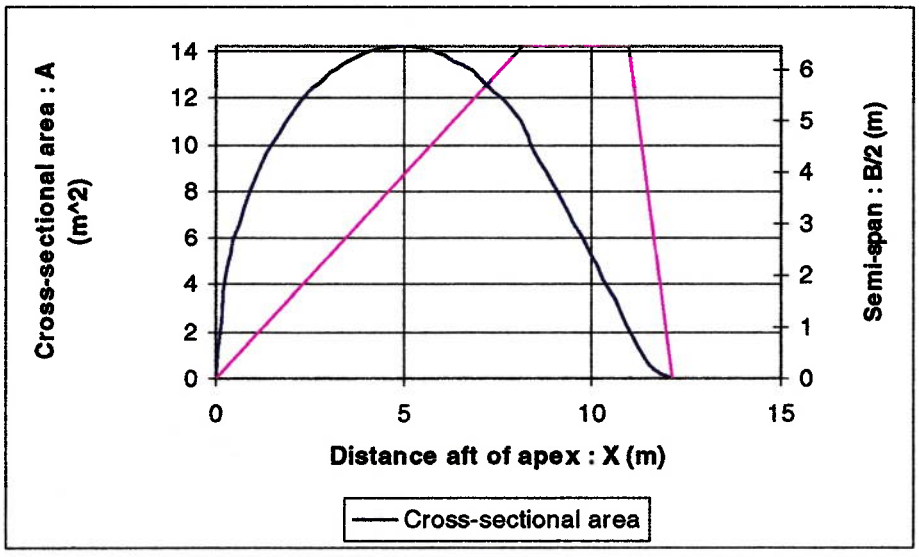

Figure 6-6: Wing Area and Volume Distribution Plot: Straight Tapered Wing Planform

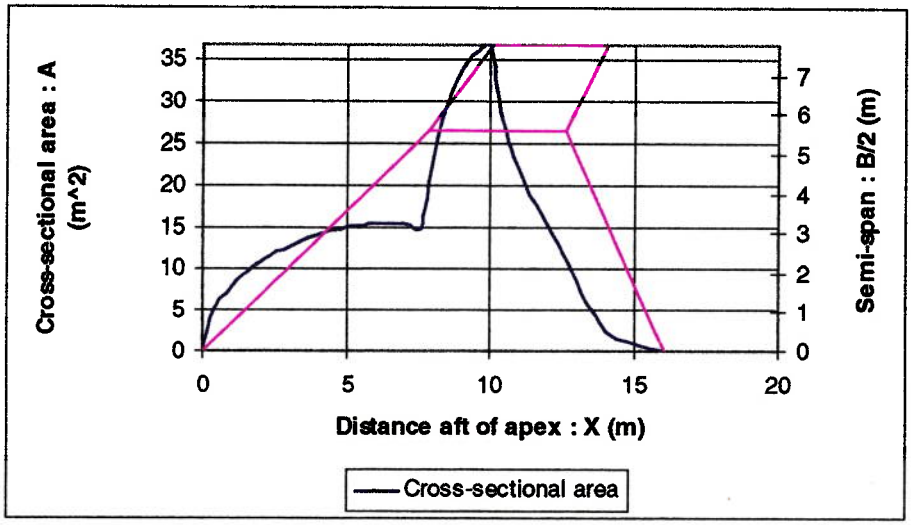

Figure 6-7: Wing Area and Volume Distribution Plot: Single-Kink Wing Planform

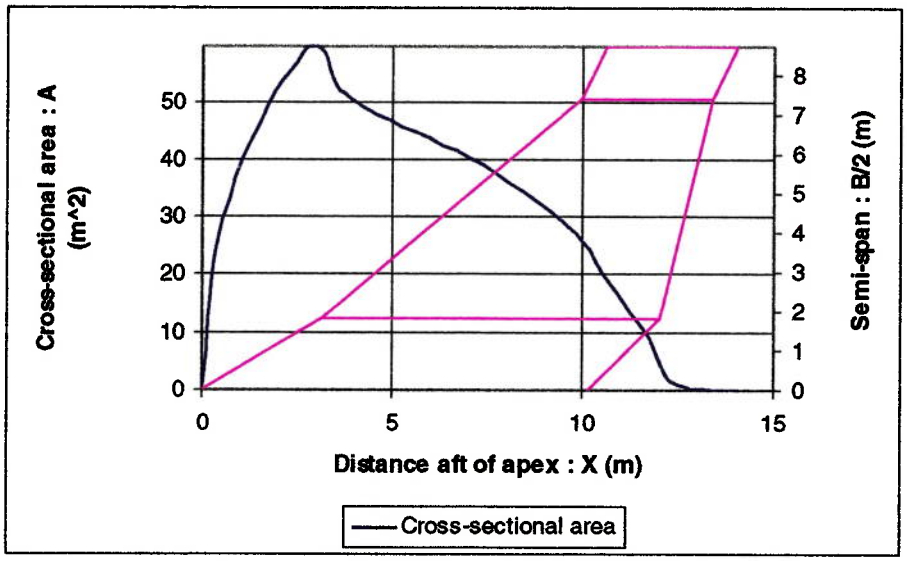

Figure 6-8: Wing Area and Volume Distribution Plot: Two-Kinks Wing Planform

6.4 Geometry of Intake Diffuser and Two-Dimensional Nozzle

The principal aspects of the intake diffuser and the two-dimensional nozzle have described previously in Chapter 5. In this section, the layout of their geometries is concerned. The geometries of intake and two-dimensional nozzle ducts play an important role for the packaging. As mentioned earlier, the geometry of the intake serpentine-duct makes the use of cubic curve fits according to the internal component arrangement particularly the weapon bays. The geometry of the nozzle duct needs providing a good transition from circular to rectangular cross-section that it must be fitted to the wing trailing edge area with minimum extrusion. The conic lofting methods, proposed by Seigers[108] and Burley[19], used to determine the geometries of

intake diffuser and two-dimensional nozzle ducts respectively have been considered with some changes to accommodate the flying wing configuration.

6.4.1 Intake Diffuser

The geometry of the intake diffuser duct requires the coordinates in three axes located at front, centre, and rear sections (XI, YI, ZI) to set the curve fits consistent with the weapon bays arrangement. The distance from the intake inlet to any fixed station along the intake duct (XID) is determined by applying the non-dimensional factors (FXW) to the overall length of intake diffuser (LIDG). For a given station, the ratio of the enclosing area to the actual cross-sectional area is given by ROIDX. This value is assumed to vary linearly from the intake inlet to the rear diffuser station, which is located one engine diameter ahead of the engine front face, defined as:

$$ROIDX = 1 + \left(\frac{4}{PI} - 1\right) \times \frac{XID}{LIDG} \tag{6.22}$$

Similarly, the cross-sectional area as well as the aspect ratio is assumed to vary linearly from the intake inlet to the engine front face. At the engine face, the aspect ratio is equal to 1. Hence, the cross-sectional area and the aspect ratio at any axial station of intake diffuser duct is defined as:

$$OIX = \left(\frac{OII}{NENG}\right) + \left(\frac{OIE - OII}{NENG \times LIDG} \times XID\right) \tag{6.23}$$

$$AIDX = AII + \left(\frac{1 - AII}{LIDG} \times XID\right) \tag{6.24}$$

Using the values defined above, it is possible to determine the dimensions of a given diffuser station, by applying the ratio ROIDX to the cross-sectional area obtaining the enclosing area up to that actual station and thus the width and the height can be achieved.

$$OISX = OIX \times ROIDX \tag{6.25}$$

$$BIDBX = \sqrt{AIDX \times OISX} \tag{6.26a}$$

$$HIDBX = {}^{OISX}\!/_{BIDBX} \tag{6.26b}$$

The Z- and Y- coordinates of the centre of any given station (XID) are given by:

$$ZIX = ZI + FZIA \times X^3 + FZIB \times X^2 \tag{6.27a}$$

$$YIX = YI + FYIA \times X^3 + FYIB \times X^2 \tag{6.27b}$$

For the front section of the intake diffuser, the distance X is measured rearwards from the intake inlet (XII). The coordinate A and B in calculation of the Z- and Y-coordinates for the front section are given by:

$$FZIA = \frac{-2 \times (ZI1 - ZII)}{(XI1 - XII)^3} \tag{6.28a}$$

$$FZIB = \frac{3 \times (ZI1 - ZII)}{(XI1 - XII)^2} \tag{6.28b}$$

$$FYIA = \frac{-2\times(YI1-YII)}{(XI1-XII)^3} \tag{6.29a}$$

$$FYIB = \frac{3\times(YI1-YII)}{(XI1-XII)^2} \tag{6.29b}$$

In order to find the centreline coordinates in the area of the centre and the rear sections, the distance X is measured from XI1 and XI2 respectively. Similarly, the coordinate A and B in calculation of the Z- and Y- coordinates can be obtained from the same relationships as determined in equations (6.28) and (6.29). The terms (ZI1-ZII) and (YI1-YII) are replaced by (ZI2-ZI1) and (YI2-YI1) for the centre section and (ZI3-ZI2) and (YI3-YI2) for the rear section of the intake diffuser, respectively. Figure 6-9 illustrates some cases of the geometry of the intake diffuser applied for the twin- and single-engine installation located on the wing centreline.

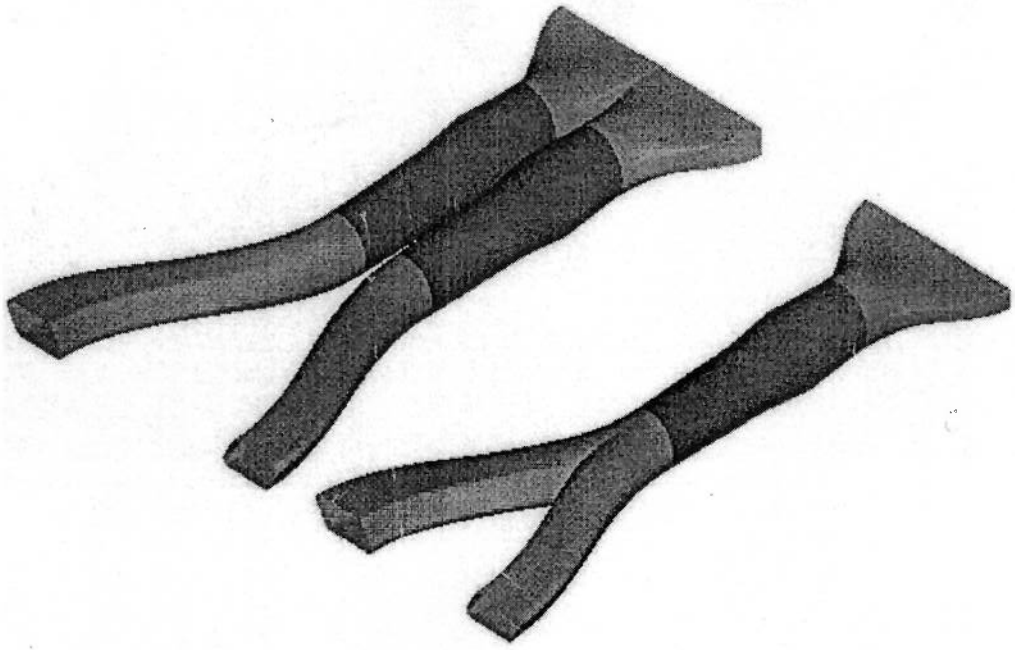

Figure 6-9: Geometry of Intake Diffuser

6.4.2 Two-Dimensional Nozzle

The geometry of the two-dimensional nozzle duct is based on the half scales of width (HBPTDI, HBPTDO) and height (HHPTD) of the nozzle exit and the half scale of the radius at entrance (RPTD). The distance from the nozzle entrance to any fixed station along the nozzle duct (XNZ) is determined by applying the non-dimensional factors (FXW) to the overall length of nozzle (LPTD). The following equations determine the semi-major axis width (inner and outer) and height of the nozzle duct at a given station:

$$WNZI = RPTD - \left[(RPTD - HBPTDI)\times FXW^2 \times (3 - 2\times FXW)\right] \tag{6.30a}$$

$$WNZO = RPTD - \left[(RPTD - HBPTDO)\times FXW^2 \times (3 - 2\times FXW)\right] \tag{6.30b}$$

$$HNZ = RPTD - \left[(RPTD - HHPTD) \times FXW^2 \times (3 - 2 \times FXW)\right] \quad (6.31)$$

At nozzle entrance the aspect ratio is equal to 1 and it is assumed to vary linearly to the nozzle exit, which is found as:

$$ANZ = \frac{WNZI + WNZO}{2 \times HNZ} \quad (6.32)$$

Figure 6-10 shows the geometry of the two-dimensional nozzle assuming that it is symmetrical in relation to the centreline of engine.

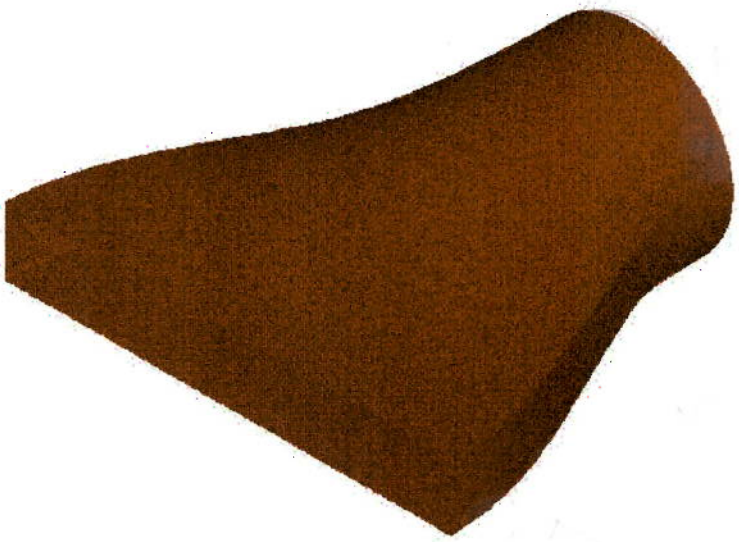

Figure 6-10: Geometry of Two-Dimensional Nozzle

6.5 Summary

This chapter has presented the methods of configuration layout descriptions for the UCAV. The centre of gravity of aircraft components have been located and determined the position of aircraft centre of gravity of the possible aircraft mass in three cases. Moreover, the arrangement of the undercarriage was also achieved. The synthesis code of the wing area and volume distribution plot was developed, which could be applied for all flying wing planforms. Finally, the sizing of the geometry of intake diffuser and the two-dimensional nozzle was accomplished. All these arrangements are necessary to be considered as they affect directly to the aircraft packaging and some cases have also affected the aircraft characteristics described in the following chapter.

CHAPTER 7

7 Characteristic Analyses

This chapter is divided into five main parts describing the respective modules: aerodynamic, static stability and control, engine performance, mission and point performance, and centre of gravity excursion. These characteristic modules are necessary for the analysis of the UCAV packaging and configuration design aspects. The aerodynamic module consists of two sections that predict available lift coefficient, and aircraft drag respectively. The method of static stability and control estimation is briefly explained, which is required to determine the sizes and to consider the positions of control surfaces consistent with the internal component arrangement. The additional explanation of engine performance analysis is given in this chapter, where the principal method is similar to that applied for an initial sizing study presented in chapter 3. The performance calculations are split into two parts – those that are used in the estimation of mission performance and fuel burn, and those that deal with the specific performance requirements and help to size the aircraft. The centre of gravity excursion module is required to examine the range of the aircraft CG to remain within the acceptable limits throughout the mission. The final section gives the description of the entire constraint functions used in the UCAV synthesis codes.

7.1 Aerodynamic Modelling

As mentioned previously, the aerodynamic module consists of two sections. The first section estimates the available lift coefficient based on wing configuration and geometry, and the presence of control surfaces. The second section predicts the aircraft drag based on wing geometry, lift coefficient, the external stores and cockpit (an option, if selected), and the presence of retractable components such as the control surfaces and the undercarriage. These two models are based on empirical and semi-empirical correlations making the use of relatively simple empirical algorithms for their aerodynamic prediction. This aerodynamic module provides an uncomplicated method for the design synthesis process in order to accomplish the investigation of various packaging and configuration design aspects for UCAV.

7.1.1 Lift Estimation

The lift model is composed of four parts: the lift-curve slope, the spanwise lift distribution, the wing maximum lift coefficient, the wing lift increment due to control surfaces. The spanwise lift distribution also includes the effect of wing twist distribution and angle of attack from the lift-curve slope taken into account. The estimation of lift characteristics requires wing geometry parameters and aircraft configuration such as wing sweep, wing aspect ratio, flight Mach number, and type of control surface and high lift system. The lift characteristics are considered for their

ability to predict the relevant aerodynamic properties in subsonic regions, and their applicability to low-aspect ratio wing configurations. This model is based on the methods obtained from several open literatures[25],[57],[58],[86], which seems to present the procedures with the required precision to achieve the proposed analysis. Most of the methods rely on the interpolation of many sets of empirical tables and graphical figures for the estimation of each part. The following sub-sections give a brief description of these models in details.

7.1.1.1 Lift-Curve Slope

The method presented in DATCOM[57] was applied. This method is basically the semi-empirical method estimating the airfoil section lift-curve slope at subsonic speeds up to the critical Mach number. The method accounts for the development of the boundary layer towards the airfoil trailing edge for the airfoils with maximum thickness less than approximately 20 percent. Thus, the input data is based on the geometric properties of the wing planform consisting of wing thickness ratio, the Prandtl-Glauert compressibility parameter ($\beta = \sqrt{1-M^2}$), and the trailing edge angle between straight lines passing through points at 90 and 99 percent of the chord on the upper and lower airfoil surfaces. To understand clearly, the latter is illustrated in the following figure.

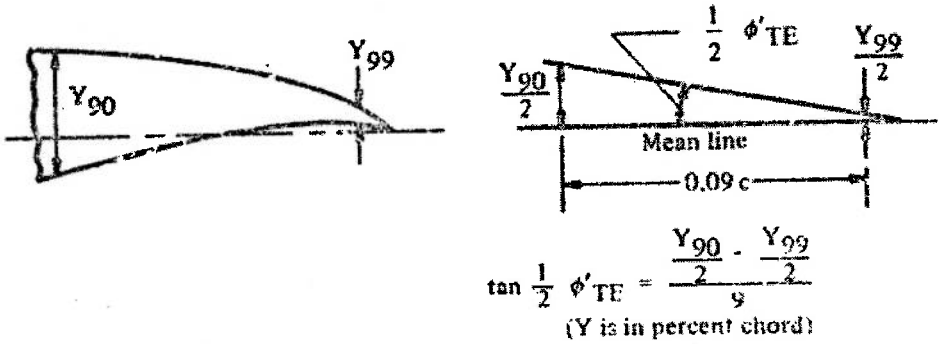

Figure 7-1: Trailing Edge Angle Between Straight Lines Passing Through Points 90 and 99 Percent of Chord

Based on this data, the airfoil section lift-curve slope in incompressible flow (CLSCI) is read off the graphs in DATCOM. This methodology presents the advantage of accounting for the effects of compressibility, thus modelling the usual rearwards shift of the aerodynamic centre as the Mach number increases. The airfoil section lift-curve slope is used in the calculations of the section lift-curve slope in compressible flow, the wing lift-curve slope, performing the spanwise lift distribution, subsequently presented in the following sub-section, and the static stability and control performance.

7.1.1.2 Spanwise Lift Distribution

The spanwise lift distribution for any typical wing consists of two parts: the calculation of the *basic* lift distribution, which is the local lift distribution that depends principally on the twist of the wing and no change with the angle of attack,

and the *additional* lift distribution, which is the local lift distribution produced completely due to the change of wing angle of attack. The methods representing the estimation of the spanwise loading of the wing are obtained from the procedures proposed by ESDU 83040[86] and Chudoba[25], which provide an assumption in subsonic flight. These methods are beneficial for the conceptual design purpose as at this step of this design synthesis only some aerodynamic input data are necessary and are generally those available.

To determine the spanwise lift distribution, the semi-span is divided into a number of equivalent points (NTY2BW). At first step of the calculations, it is necessary to obtain the wing lift-curve slope along these spanwise stations, which is defined as:

$$CLWLSC = CLSC \times \cos(QW4) \times K0LSC \tag{7.1}$$

Where *CLSC* is the section lift-curve slope in compressible flow and *K0LSC* is the finite-span correction for wing lift-curve slope. The former is determined by applying the airfoil section lift-curve slope (CLSCI) obtained from above sub-section to the ratio for section lift-curve slope correction (RLCAPH)[25]. This ratio is determined from the average of the theoretical data for the airfoils of NACA series as a function of the effective Mach number [M cos(Λ)] for several airfoil thickness ratios perpendicular to the wing quarter-chord line. The airfoil thickness ratios selected are corresponding to the options from the packaging specification (RTW, RTWT), and thus the ratios for section lift-curve slope correction are shown in the following figure.

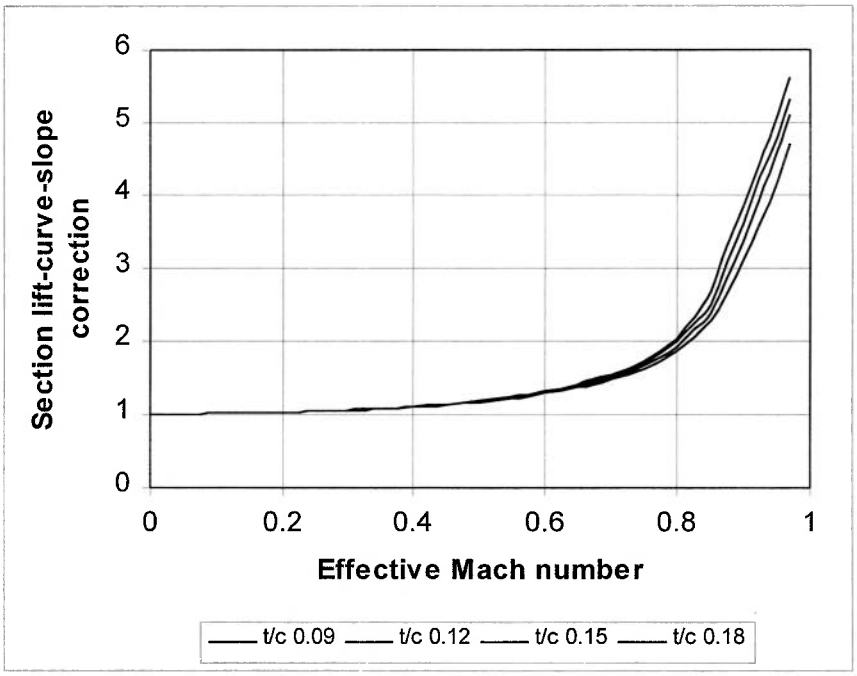

Figure 7-2: Section Lift-Curve Slope Correction[25]

The value of the finite-span correction for wing lift-curve slope (K0LSC) is given in terms of the plan-form parameter, defined as:

$$K0LSC = \frac{FLSC}{FLSC \times \sqrt{1 + 4/FLSC^2} + 2} \tag{7.2a}$$

The plan-form parameter is given by:

$$FLSC = \frac{AW}{ETALSC \times \cos(QW4)} \text{ , and} \tag{7.2b}$$

$$ETALSC = \frac{CLSC}{2 \times PI} \tag{7.2c}$$

ETALSC is the ratio of the section lift-curve slope. The plan-form parameter (FLSC) is determined in order to take the wing sweep and the compressibility effects into account.

The spanwise lift distribution for any variation of angle of attack or twist is determined from the semi-empirical method, namely Diederich method, proposed by Chudoba[25], which is defined as:

$$CRLGAM = (CLWLSC \times QALPHAA \times CALGAM) + CBLGAM \tag{7.3}$$

Where:

CLWLSC	=	Wing lift-curve slope
QALPHAA	=	Average angle of attack
CALGAM	=	Loading coefficient for additional lift distribution
CBLGAM	=	Loading coefficient for basic lift distribution

The wing lift-curve slope was already mentioned above. For this design synthesis, the spanwise loading can be determined due to the incidence either for untwisted and uncambered wings or taken account of camber and twist, based on the options from the packaging specification. For the latter, the spanwise camber and twist distributions are modelled as local changes in the incidence of airfoils. Therefore, it is necessary to determine the spanwise distribution of the local zero-lift angles of a camber wing section and add the results to the incremental local twist angles, performing the local total twist angles. Basically, a curve of the local effective incidence angle as a function of span is obtained. This curve is derived from the two straight segments representation, which are then brought into the calculation as shown in Figure 7-3.

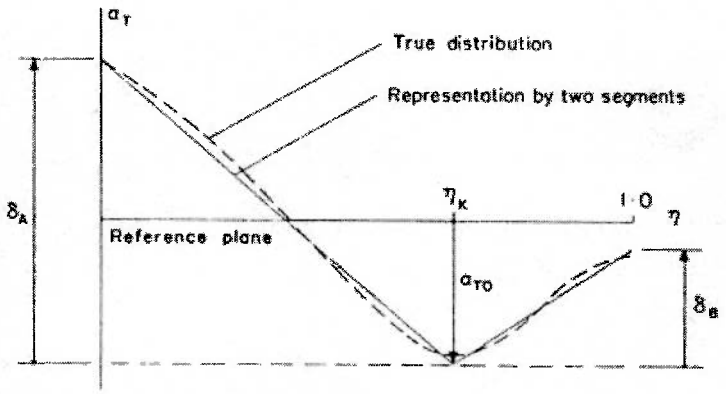

Figure 7-3: Approximation of Effective Twist Distribution by Straight Segments[86]

On condition that the twist wing is selected, the two constraints are established concerning the twist of the wing. On the inboard and the airfoil transition sections, the twist is zero. This results in a constant value for the local incidence (local zero-lift angles) from the wing centreline up to the outer edge of engine bay spanwise station (for symmetrical airfoil, this local incidence is zero). From this position until the end of transition section at the half of semi-wingspan, it is assumed that the effective local incidence would decrease linearly to zero. On the outboard section, a linear twist can be applied. This is implemented on the synthesis code by setting a twist rate for this region of the wing.

The steps necessary to perform the calculations of the twist distribution are fully described in ESDU 83040[86], which is not mentioned here. For this design synthesis, it is assumed that the effective twist distribution is determined on the clean wing planform without any deflections of aerodynamic control surfaces. The results of twist distribution applied for some cases based on the straight tapered wing planform with one weapon bay at centreline are illustrated in Figure 7-4.

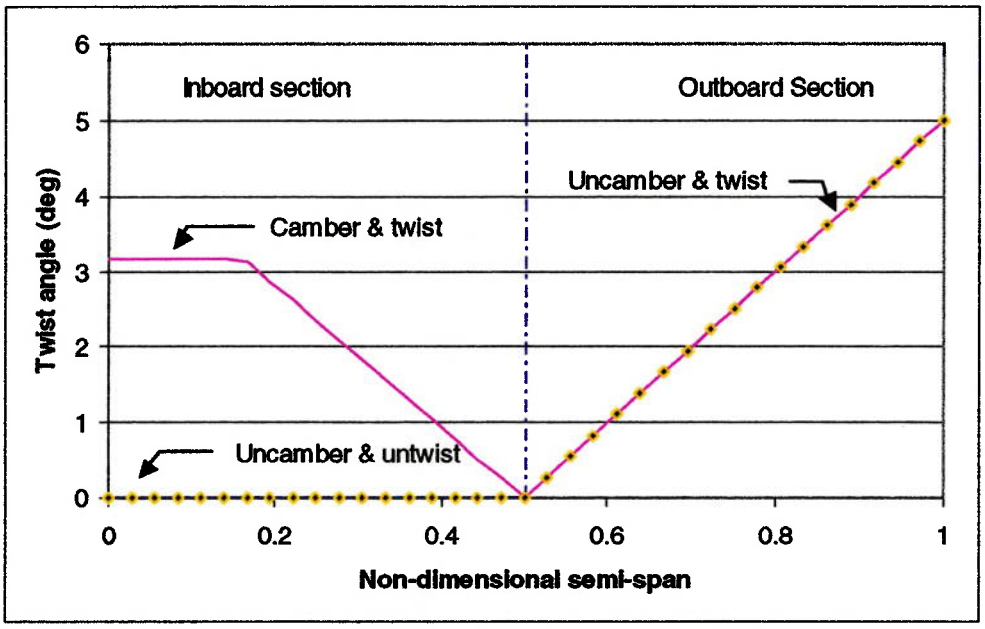

Figure 7-4: Effective Twist Distribution: Straight Tapered Wing Planform

The twist at the wing root centreline is set to zero and the results of the root-relative twist distribution across the span are summed with the angle of attack at root (QALPHA), which is an input data, performing the total angle of attack condition during flight (QTALPHA).

$$\sum_{X=0}^{NTY2BW} QTWTC(X) = QTWT(X) - QTWT(0) \tag{7.4a}$$

$$\sum_{X=0}^{NTY2BW} QTALPHA(X) = QALPHA + QTWTC(X) \tag{7.4b}$$

The average angle of attack (QALPHAA) in then determined with the method of chordal-trapezium-formula, as shown in the following figure and equation.

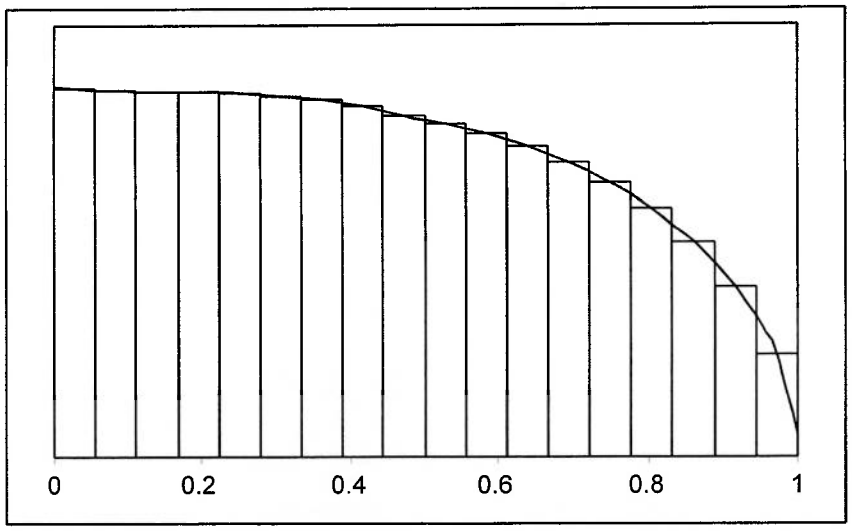

Figure 7-5: Method of Chordal-Trapezium-Formula

$$QALPHAA = \sum_{X=1}^{NTY2BW} \left[0.5 \times \left\{ \begin{matrix} (QTALPHA(X-1) \times CALGAM(X-1)) + \\ (QTALPHA(X) - CALGAM(X)) \end{matrix} \right\} \times \{FY2BWP(X) - FY2BWP(X-1)\} \right] \quad (7.5)$$

Where *FY2BWP* is the non-dimensional semi-wingspan.

The method used to determine the *additional* lift distribution across the span is applicable for the entire range of the aspect ratios, involving with the wing chord, the ellipse and the function varied with wing sweep; the extent to which each of these three functions enters the lift distribution varies with aspect ratio[25].

$$CALGAM = \left[\begin{matrix} \left(CC1ALD \times CWPF/CWPFA\right) + \\ \left(CC2ALD \times 4/PI \times \sqrt{1 - FY2BWP^2}\right) + \\ \left(CC3ALD \times FFALD\right) \end{matrix} \right] \quad (7.6)$$

Where:

CWPF = Relative wing chord at reference spanwise station corresponding to a number of equivalent points across the span

CWPFA = Average wing chord $(\bar{c})$

The three coefficients for additional lift distribution, *CC1ALD, CC2ALD,* and *CC3ALD* are based on the plan-form parameter (FLSC) obtained above, which is involved with the aspect ratio. These coefficients vary with the aspect ratio in such a way that CC1ALD is unity for infinite aspect ratio, CC2ALD is unity for zero aspect ratio, and the sum of all three coefficients is always unity. The three coefficients are read off the charts obtained the data from Chudoba[25], as illustrated in the following figure.

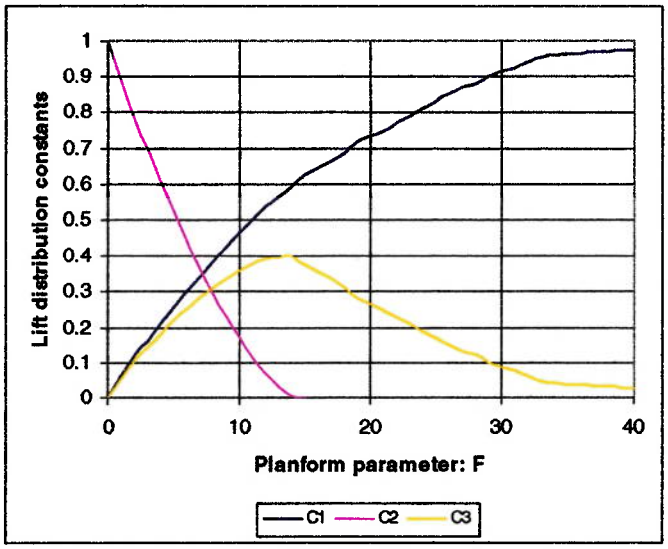

Figure 7-6: Coefficients for Additional Lift Distribution

The function *FFALD* is the additional lift distribution component due to sweep, which is based on the effective angle of sweepback in compressible flow defined by:

$$QW4EF = \tan^{-1}\left[\frac{\tan(QW4)}{\sqrt{1-AMVD^2}}\right] \tag{7.7}$$

Where *AMVD* is aircraft Mach number. Additionally, the function *FFALD* is read off the graphs obtained the data from Chudoba. On condition that the effective angle of sweepback is equal to zero, the value of FFALD performs an elliptical distribution.

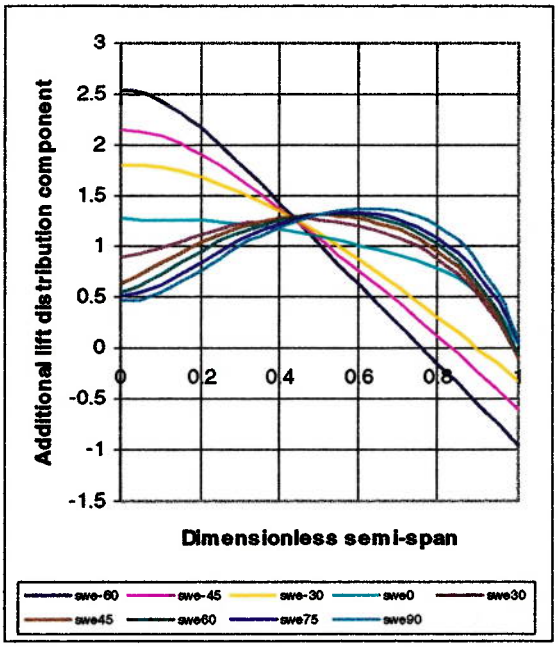

Figure 7-7: Additional Lift Distribution Component Due to Sweep

The method used to determine the *basic* lift distribution is based on the lift-curve slope and the additional lift distribution. The Diederich method stated that the wing lift-curve slope (CLWLSC) provides the better results in the equation for the basic load distribution than the section lift-curve slope (CLSC)[33]. Thus, the basic load distribution is defined as:

$$CBLGAM = K1BLD \times CLWLSC \times (QTALPHA - QALPHAA) \times CALGAM \qquad (7.8a)$$

Where *K1BLD* is the finite-span correction for basic lift distribution, which is the constant value, based on the plan-form parameter (FLSC).

$$K1BLD = \frac{FLSC \times \sqrt{1 + 4/FLSC^2} + 2}{FLSC \times \sqrt{1 + 36/FLSC^2} + 6} \qquad (7.8b)$$

Once the spanwise lift distribution is achieved, it is applied for the calculations of the local section lift coefficient distribution, the bending moment distribution, and the shear force distribution. The results of these calculations applied for some cases based on the straight-tapered wing planform with one weapon bay at centreline are illustrated in the following figures.

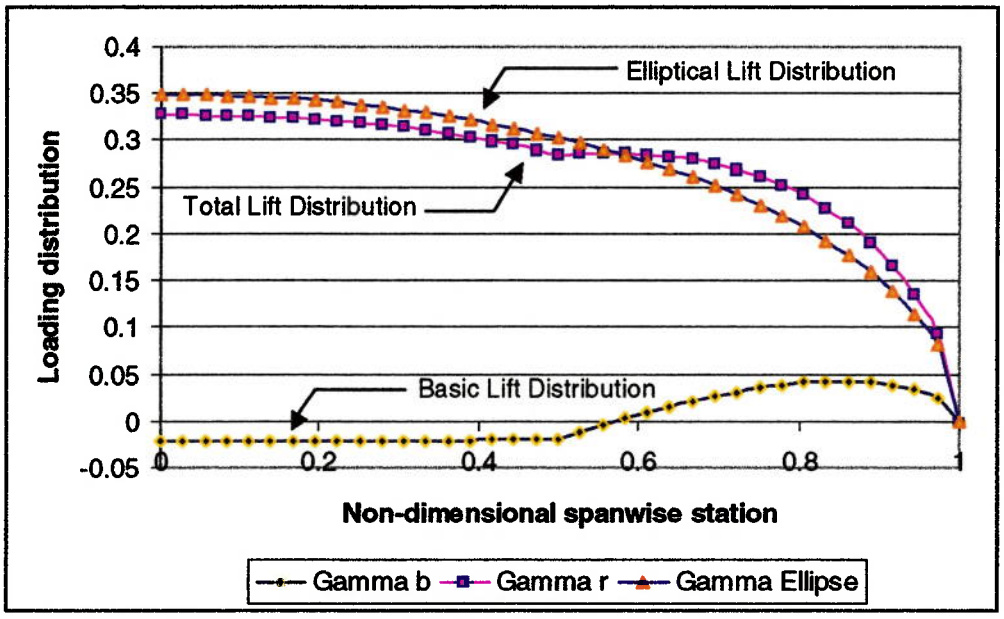

Figure 7-8: Spanwise Lift Distribution

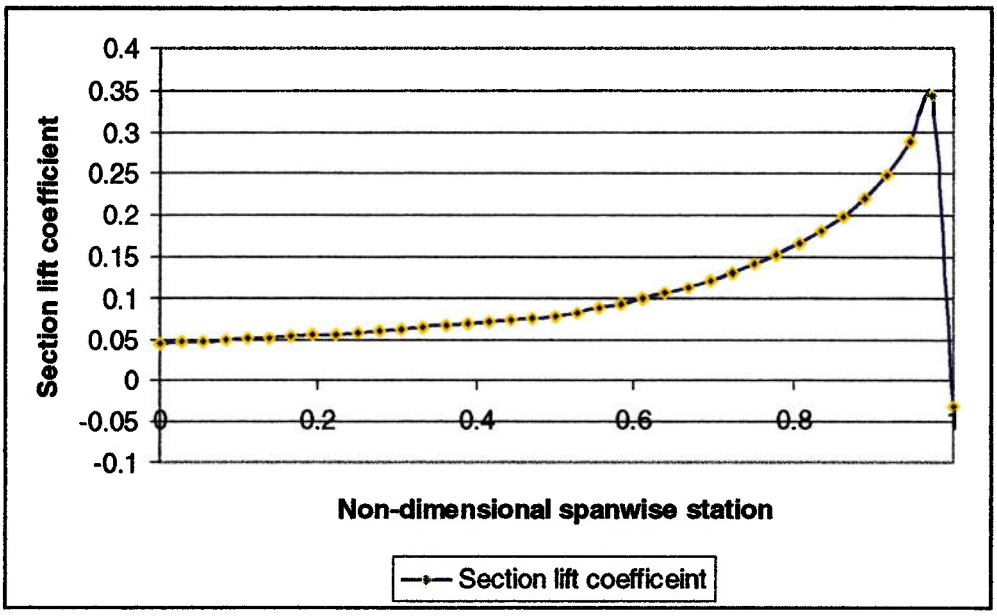

Figure 7-9: Local Section Lift Coefficient Distribution

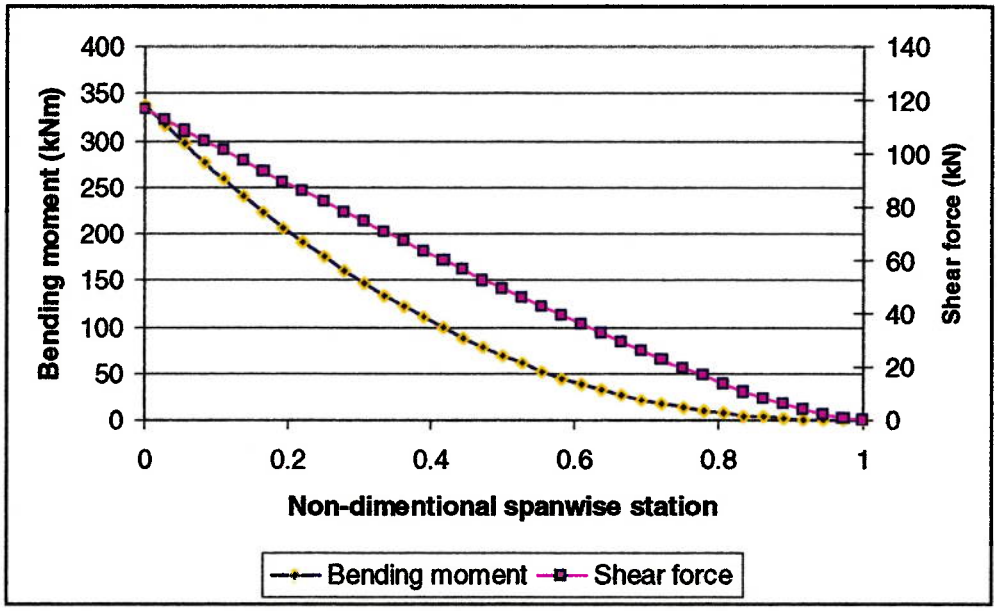

Figure 7-10: Bending Moment and Shear Force Distribution

The local lift curve of this example shown in Figure 7-9 provides a rather uncommon behaviour at the wingtip. As the wing chord at tip is very closed to zero and thus, a result of the mathematical modelling of the load distribution is incapable of simulating accurately the wingtip effects on near-zero taper and zero taper wings. Figure 7-11 illustrates a potential flow modelling of a delta wing, which provides the unrealistic result of an infinite suction at wingtips. In fact, this does not arise, as the flow cannot maintain itself attached and thus, separates, generating the shown spanwise pressure distribution.

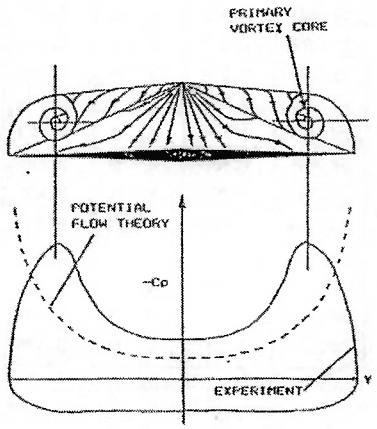

Figure 7-11: Spanwise Pressure Distribution Over Delta Wing[61]

According to equation (7.3) above, the product of the first two parameters: the wing lift-curve slope (CLWLSC) and the average angle of attack (QALPHAA) provide the wing lift coefficient (CLWG), which is subsequently used in the calculations of the static stability and control performance.

7.1.1.3 Wing Maximum Lift

The wing maximum lift coefficient strongly affects the aircraft take-off mass to perform the design mission. In theory, the estimation of maximum lift is probably the least reliable of all of the calculations used in the aircraft conceptual design. Even refined wind tunnel tests cannot predict the maximum lift with great accuracy. Frequently the aircraft must be modified during the flight test to accomplish the predicted maximum lift.

For simplicity, the calculation of the maximum lift coefficient used in this design synthesis is obtained from the semi-empirical method described in DATCOM[57]. A precise estimate of the maximum lift coefficient from this method is not critical for the determination of the aircraft mission. The method is based on a statistical analysis of different studies. Basically, it is arranged for use on plain wings with symmetrical airfoils. On condition that, the option of asymmetrical airfoils is selected (TIAF or TOAF = 2), it is, however, still applied with this method subjected to the consequent assumptions.

The UCAV can be designed to fly upside-down or to 'reverse' its roll altitude according to the typical flight segment in a manoeuvre situation. With the reverse flight attitude, the angle of attack is being negative. Thus, the maximum accessible lift will be slightly reduced due to the negative camber (compared to a symmetrical airfoil configuration), which will induce the boundary layer separation at an earlier stage. By delaying the boundary layer separation, the flow at the trailing edge from the two-dimensional high-aspect ratio nozzles performs as an ejection pump, sucking the boundary layer, and also develops the lift on the central region of the wing. The assumptions of these two effects would correspondingly compensate for obtaining the maximum lift coefficient approximately equivalent to a symmetrical wing.

As previously mentioned, the lift characteristics applied for this design synthesis are considered in subsonic regions applicable to low-aspect ratio wing configurations. Thus the maximum lift coefficient applied for a low aspect ratio wing is determined from the charts in DATCOM, which is based on the following condition:

$$AW \leq \frac{3}{(FC1UW+1)\times\cos(QWL)} \tag{7.9}$$

Where $FC1UW$ is the taper-ratio correction factors, which is also obtained from chart in DATCOM. This condition above is set as an inequality constraint during the optimization routine.

The total maximum lift coefficient for the clean wing is the sum of the maximum lift due to wing and the maximum lift increment due to vortex flow. The latter is a function of the Mach number. Of the several curves available on the chart of the maximum lift due to wing, it is only necessary to digitise the one corresponding to the highest leading edge radius, due to the fact that the both airfoils used at the inboard and outboard sections of the wing have a very high value for this parameter. This parameter is called 'the leading-edge sharpness parameter', which represents as a function of thickness ratio based on typical airfoil types, as provided in Table 7-1.

Airfoil Type	**Leading-Edge Sharpness Parameter: *DELTAY***
NACA 4 digit	26 t/c
NACA 5 digit	26 t/c
NACA 64 series	21.3 t/c
NACA 65 series	19.3 t/c

Table 7-1: Leading-Edge Sharpness Parameter for Common Airfoils

The wing maximum lift coefficient is subsequently used in the calculation of performance analysis. The method used to determine the angle of attack for maximum lift is also available from DATCOM. It is applied for the calculation of ground clearance for the wing trailing edge not touching the ground during the aircraft nose-up attitude. However, the calculation of the angle off the vertical compared to the tipback angle, described in section 6.2 of Chapter 6, provides plenty good ground clearance, thus this does not provide any concern.

7.1.1.4 Wing Lift Increment with Control Surfaces

According to sub-section 5.1.3.6 of Chapter 5, the control surfaces and/or high-lift devices designed for UCAV consist of trailing edge, leading edge and inlaid control surfaces. The last two devices may not be provided as maintained by the options set by the user in the packaging specification.

The trailing edge control surfaces are performed in various types based on their functions in accordance with the number of these devices to be selected. The methods used to determine the lift increment due to the trailing edge control surfaces are based on the plain flap type, which are suitable for the flying wing configuration. Moreover,

it should be noted that the ailerons, elevators and rudders are also a form of the plain flap, thus applicable to these methods. Additionally, they are applied for the calculations of the lift increment due to the inlaid control surfaces, if fitted. The plain flap is simply a hinged portion of the airfoil, typically with a flap chord of approximately 30 percent of the airfoil chord. The plain flap increases lift by increasing camber. For a typical airfoil, the maximum lift arises with a flap deflection of about 40-45 degree[96]. Thus, the lift increment due to the trailing edge and inlaid control surfaces acting as a plain flap is based on the ratio of flap chord to wing chord, the wing thickness ratio in area of flap, and the flap deflection angle.

On condition that the leading edge control surfaces are equipped, the methods applied for the lift increment are based on the leading-edge flap type. The leading edge flaps change the lift of an airfoil by changing the effective angle of attack similar to the trailing edge flaps. However, a positive leading-edge flap deflection (nose down) is unlike the trailing edge flaps, as it causes a loss in lift instead of an increase in lift. In general, the change in lift per degree of flap deflection is smaller for leading edge flaps than for the trailing edge flaps. The leading edge flaps alone produce a very small amount of lift for take-off and landing, because they are effective only a fairly high angles of attack. However, they are very useful when used in combination with the trailing edge flaps, as they prevent the premature airflow separation caused by the flaps[96]. The lift increment due to the leading edge control surfaces acting as the leading-edge flap is based on the ratio of flap chord to wing chord, the wing thickness ratio in area of flap, the wing leading edge radius in area of flap, the wing aspect ratio, and the flap deflection angle.

The calculations of the wing lift coefficient increment due to the control surfaces used in this design synthesis are obtained from the semi-empirical methods described in DATCOM[57]. It consists of four parameters: the section lift coefficient increment, wing lift coefficient increment, section maximum lift coefficient increment, and wing maximum lift coefficient increment. The estimation of these parameters from the DATCOM methods provides good results applicable for the determination of the aircraft mission. The results obtained from the calculations of section maximum lift coefficient increment for some cases of UCAV are compared with the approximated values from test data, as shown in the following table.

UCAV Configuration (Straight Tapered Wing Planform)	**Section Maximum Lift Coefficient Increment: $\Delta C_{l_{max}}$**		
	Trailing Edge Plain Flap		**Leading Edge Flap: *CLLSX***
	Take-off: *CLTSXTO*	**Landing: *CLTSXLD***	
Baseline value from test data[96]	**0.54-0.72**	**0.90**	**0.30**
NWEPB=3: NW2SE=1: One pair of TE flaps	0.5931	0.8018	-
NWEPB=1: NW2SE=1: One pair of TE flaps	0.6690	0.9045	-
NWEPB=1: NW2SE=2: One pair of inboard TE flaps & NW2SL=1: One pair of LE flaps	0.5712	0.7722	0.3010

Table 7-2: Comparisons of Section Maximum Lift Coefficient Increment

7.1.2 Drag Estimation

In subsonic speeds, the aircraft drag is dependent of two major factors: parasite or zero-lift drag and drag due to lift or induced drag. This provides the total aircraft drag expressed in coefficient form:

$$CD = CD0 + CDL \tag{7.10}$$

The estimation of drag characteristics is based on wing geometry parameters, the lift coefficient, the presence of the retractable components such as the control surfaces, the weapon bay doors and the undercarriage, and the presence of external stores and cockpit (an option, if selected). Significant drag characteristics are required by the performance analyses in its cruise configuration over much of the speed range, and for take-off and landing settings to evaluate the required distance. This model is based on the methods proposed by Howe[58] and Raymer[96], which provides application of clear and effective formulae for the design synthesis. The methods used to estimate both the zero lift and the induced drags are briefly described in details.

7.1.2.1 Parasite (Zero-Lift) Drag

The parasite or zero-lift drag coefficient determined in the subsonic regions consists of three parts: the component drag, the miscellaneous drag, and the leakage and protuberance drag. The total parasite drag is the sum of these three parts given by:

$$CD0 = CDC + CDM + CDP \tag{7.11}$$

They are described individually in the following sub-sections.

7.1.2.1.1 Component Drag

The method used to determine the component drag is called the component build-up method, which estimates the parasite drag of each component of the aircraft using a calculated flat-plate skin-friction drag coefficient (CF), a component 'form factor' (FF), and the interference effects (FQ). The component drag is also based on the wetted area (SWET) and the reference area (SREF) of those components. The component build-up equation is given by:

$$CDC = \sum\left[\frac{CF \times FF \times FQ \times SWET}{SREF}\right] \tag{7.12}$$

Where the summation sign refers to the several components of the aircraft. For the UCAV design, which is built on the flying wing configuration, this method applies for four components: the wing, the cockpit (optional manned aircraft), the external stores (optional external loads), and the weapon bay doors. The latter is affected by the parasite drag during the typical flight segment in the manoeuvre situation.

The estimation of the flat-plate skin-friction coefficient provides for a surface of components with both laminar flow and turbulent flow. It is based upon the Reynolds number, the Mach number, and the skin roughness. The turbulent flow flat-plate skin-friction coefficient is considered for determining the components mentioned above, thus providing a conservative approach to the drag estimation. However, for the wing planform, it may have turbulent flow over effectually the entire wetted area, and

possibly 10-20 percent of laminar flow may be seen towards the front of the wing. Thus, an average flat-plate skin-friction coefficient can be calculated performing the weighted average of the two (say, 10% laminar and 90% turbulent). The flat-plate skink-friction coefficient applied for the laminar and turbulent flows is given by the following equations, respectively:

$$CF = \frac{1.328}{\sqrt{RE}}, \text{ Laminar flow} \tag{7.13a}$$

$$CF = \frac{0.455}{(\log_{10}(RE))^{2.58} \times (1 + 0.144 \times M^2)^{0.65}}, \text{ Turbulent flow} \tag{7.13b}$$

Where *RE* refers to the non-dimensional (actual) Reynolds number, which is base on the air-density at present altitude, the aircraft speed, the dynamic viscosity factor (μ), and the characteristic length. The latter refers to the mean aerodynamic chord of wing and the total length of those components. On condition that the surface of the wing is relatively rough, the use of a 'cut-off' Reynolds number may be established, depending on the skin roughness value of typical surface applied on wing. Two values of skin roughness are considered, based on the option of TMAT in the packaging specification selecting the type of materials to be synthesized. Table 7-3 provides these values of skin roughness corresponding to the surface of wing:

Surface	Skin Roughness Value: *KSKIN* (m)
Camouflage paint on aluminium	0.116×10^{-5}
Smooth moulded composite	0.006×10^{-5}

Table 7-3: Skin Roughness Value[96]

The cut-off Reynolds number is determined by the following equation, and the lower of the actual Reynolds number and the cut-off Reynolds number are considered to estimate the turbulent flow flat-plate skin-friction coefficient for the wing.

$$RE = 38.21 \times \left[\frac{CWMA}{KSKIN}\right]^{1.053}, \text{ Cut-off Reynolds Number (Subsonic)} \tag{7.14}$$

Where *CWMA* is the mean aerodynamic chord of the wing.

The estimations of the component form factor applied for the wing, the cockpit (optional manned aircraft), the external stores (optional external loads), and the weapon bay doors are presented in the following equations, respectively:

$$FF = \left[\begin{array}{l}\left[1 + \frac{0.6 \times RTWM}{0.5} + 100 \times RTWM^4\right] \times \\ \left[1.34 \times M^{0.18} \times (\cos(QW2))^{0.28}\right]\end{array}\right], \text{ Wing} \tag{7.15a}$$

$$FF = \left[1 + 60 \times \left(\frac{DW}{LW}\right)^3 + \frac{LW}{400 \times DW}\right], \text{ Cockpit canopy (Option)} \tag{7.15b}$$

$$FF = 1 + \left(\frac{0.35 \times DW}{LW}\right), \text{ External stores (Option)} \tag{7.15c}$$

$$FF = 1 + \frac{DW}{LW}\text{ , Weapon bay doors} \qquad (7.15d)$$

Where:

DW = Maximum characteristic diameter of component
LW = Characteristic length of component
RTWM = Wing mean thickness to chord ratio

It is decided to use the average value for the wing thickness to chord ratio performing the component form factor of the wing, as the actual thickness ratio varies with the wingspan. Thus the mean thickness to chord ratio (RTWM) is determined, based on the wing area.

The estimations of the component interference factor are determined from the increment of the parasite drag due to the correlative interference between components. As there are no other components to interfere with the wing, the interference factor is equal to 1. This value of the interference factor is also applied for the weapon bay doors and the cockpit canopy (if manned aircraft is selected). For the external stores mounted directly on the wing, the interference factor is approximately 1.5.

7.1.2.1.2 Miscellaneous Drag

There are two miscellaneous components on the UCAV flying wing to be considered for determining the parasite drag in the subsonic regions: the trailing edge flaps, and the undercarriage. These components are affected by the drag during take-off and landing condition. The flap contribution to parasite drag is caused by the separated flow above the flap. The estimation method proposed by Raymer[96] provides an uncomplicated equation for determining the parasite drag on the flaps.

$$CDM = 0.0144 \times \left(\frac{CWSE}{CWWSE}\right) \times \left(\frac{SWWSE}{SW}\right) \times (QWSE - 10) \qquad (7.16)$$

Where:

QWSE = Flap deflection angle at take-off and landing condition
SWWSE = Total wing planform area over trailing edge device positions
CWWSE = Wing chord at mid-span of trailing edge devices

The landing-gear drag is estimated by applying the typical 'drag area' values to the frontal area of the wheels and struts. The value of drag area for the regular wheel and tire is approximately 0.25, and that for the round strut is about 0.30[96]. The sum of the landing gear drags divided by the wing reference area (SW) then obtains the parasite-drag coefficients. The total landing gear drag should be increased by 7 percent due to the gear wells left open when the gears are down, and also multiplied by a factor of 1.2 to account for the correlative interference.

7.1.2.1.3 Leakage and Protuberance Drag

It is difficult to predict the drag caused by leaks and protuberances. Typically, these drag increments are estimated as a percent of the total parasite drag. It is assumed that leakage and protuberances cause an increase of 10 percent, which are permitted for the fighter aircraft[96].

7.1.2.2 Drag Due to Lift (Induced Drag)

The estimation of induce drag coefficient determined for the UCAV consists of two parts: the drag due to wing and the drag due to trailing edge devices. The total induced drag coefficient is the sum of these two parts given by:

$$CDL = CDLW + CDLT \tag{7.17}$$

The induced-drag coefficient due to the wing is proportional to the square of the lift coefficient with a proportionality factor called the 'drag-due-to-lift' factor.

$$CDLW = FK \times CLW^2 \tag{7.18}$$

Where CLW is the lift coefficient appropriate to the given flight-condition. The method used to determine the induced drag factor is obtained from an uncomplicated method proposed by Howe[58], which has been previously described in section 3.2.3 of Chapter 3. However, when a wing is near the ground less than the half span away, the induced drag factor can be substantially reduced due to the ground effect. This can be explained as a trapping of a cushion of air under the wing[34]. The reduction in induced drag coefficient is based on a function of the wing height above the ground to the wingspan, which can be estimated by applying the induce drag factor to the approximated ground effect factor[96], defined as:

$$FKE = FK \times \left[\frac{33 \times \left(HW/BW \right)^{1.5}}{1 + 33 \times \left(HW/BW \right)^{1.5}} \right] \tag{7.19}$$

Where HW refers to the wing height above the ground. The effective induced drag factor (FKE) is used in the calculation of the induced drag coefficients during the take-off and landing conditions. Figure 7-12 estimates the percent reduction in induced drag coefficient compared to the ratio of the wing height above ground to the wingspan, with constant lift coefficient.

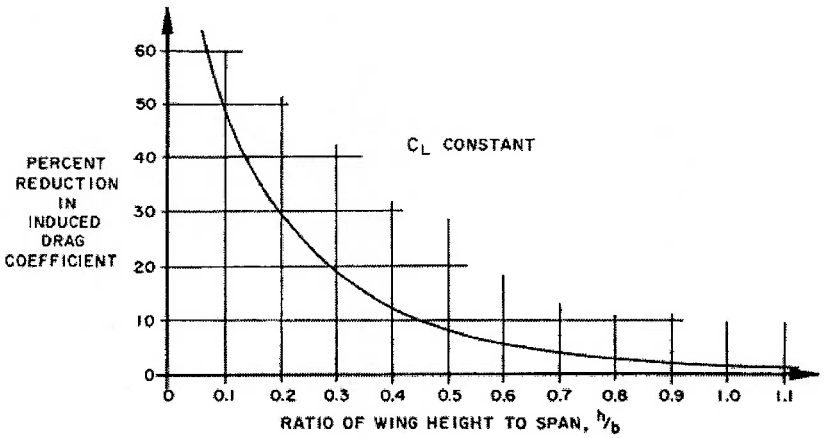

Figure 7-12: Percent Reduction in Induced Drag Coefficient[34]

The induced drag coefficient due to the trailing edge flaps is occurred when the flap is deflected. This is because the aircraft would gain an increase in lift and thus, this

additional lift in the area of the flaps affects the induced drag. The following equation proposed by Raymer[96] can be applied for the estimation of the induced drag coefficient due to the trailing edge flaps:

$$CDLT = 0.14^2 \times CLTMX^2 \times \cos(QWSEH) \tag{7.20}$$

The induced drag due to the trailing edge flaps is added to the drag due to lift for the total lift using the clean wing drag due to lift factor during the take-off and landing conditions.

7.2 Static Stability and Control Modelling

In this design synthesis process, the simple method used to determine the static stability and control is required in order to find out the sizes and to consider the positions of control devices, as they affect directly to the packaging and configuration design aspects, and the mass of the UCAV. Additionally, the option of the number of control devices set by the user in the packaging specification is influenced to the estimation of sizes and positions of these devices due to their different performing functions (e.g. flaps, ailerons, elevators, split elevons, or split drag rudders) during the flight. The location of the wing aerodynamic centre is considered to begin with, as it is a critical term for the flying wing configuration to achieve the estimation of this module. The static longitudinal and lateral-directional stabilities and controls are subsequently determined to accomplish the requirements. This model is based on the methods obtained from DATCOM[57], with some modifications to accommodate the flying wing configuration. Most of the methods again depend on the interpolation of many sets of empirical tables and graphical figures for the prediction of each part.

As mentioned above, this static stability and control module provides an uncomplicated method for the design synthesis process in order to accomplish the investigation of the sizes and positions of the control devices on the aircraft consistent with the internal component arrangement. The more complex and accurate methods may be required to provide the correct balance of accuracy and efficiency for the static stability and control of the flying wing tailless aircraft.

7.2.1 Wing Aerodynamic Centre

According to ESDU 70011[72], the estimations of the wing aerodynamic centre compared with a wide range of test data indicate that the aerodynamic centre position is predicted generally to within 3 percent of the mean aerodynamic chord. It is thus decided to apply a value of 3 percent of the mean aerodynamic chord for the location of the wing aerodynamic centre of the UCAV flying wing. This must be measured from the aircraft nose by adding the above value to the distance of wing quarter-chord point (XWCQM). This location is, however, suitable only for the straight tapered wing planform. To determine the wing aerodynamic centre for the multi-kinks wing configuration, the method proposed by DATCOM[57] is obtained. This method has been applied with some modifications for determining the CG location of wing, presented in section 6.1.2 of Chapter 6. The additional calculations are required to accomplish the location of wing aerodynamic centre for multi-kinks wing planform. Figure 6-1 also illustrates the wing geometry parameters applied for this estimation.

The multi-kinks wing is divided into a series of trapezoidal panels with each panel having conventional, straight-tapered geometry. For each of the constructed panels, the individual wing aerodynamic centre location can be estimated by treating each constructed panel as a complete wing and applying a value of 3 percent of the MAC for these panels. These wing aerodynamic centre locations are fractions of the MAC of the constructed panels. They are required to convert to fractions of the wing root chord of those panels. All the wing aerodynamic centre locations of the outer panels are then needed to convert to fractions of the wing root centreline chord, which can be determined following the method presented in equation 6.2 of Chapter 6.

The additional calculations require the determination of individual wing lift-curve slope for each of the constructed panels based on its particular area, given by:

$$CLSCXTK = \frac{AWXTK \times 2 \times PI}{\left[2 + \sqrt{\left\{\left(\frac{AWXTK^2 \times \left(\sqrt{1-AMEF^2}\right)^2}{\left(CLSCI/2 \times PI\right)^2}\right) \times \left\{\left(1 + \frac{\tan^2(QW2XTK)}{\left(\sqrt{1-AMEF^2}\right)^2}\right) + 4\right\}\right\}}\right]} \quad (7.21)$$

Where:

CLSCXTK	=	Wing lift-curve slope of wing constructed panels
AWXTK	=	Aspect ratio of wing constructed panels
QW2XTK	=	Wing mid-chord sweep of wing constructed panels
AMEF	=	Effective Mach number

The individual lift and wing aerodynamic centre location derived for each constructed panel are then combined in accordance with the weighted-area relationship to establish the predicted wing aerodynamic centre location for the multi-kinks wing configuration.

$$RLWACK = \sum_{X=1}^{NWK+1} \frac{CLSCXTK(X) \times SWXTK(X) \times RLWACTK(X-1)}{CLSCXTK(X) \times SWXTK(X)} \quad (7.22)$$

This wing aerodynamic centre location for the multi-kinks wing planform is a fraction of the wing root centreline chord. Converting this wing aerodynamic centre location to a fraction of the mean aerodynamic chord, it is found as:

$$RLWAC = \frac{(RLWACK \times CWCC) - XWCQM}{CWMA} \quad (7.23)$$

The RLWAC for the multi-kinks wing configuration may vary more than 3 percent, due to the stability of the aircraft with this wing planform. This may be useful to consider the role of the UCAV flying at supersonic speeds, as at these speeds the wing aerodynamic centre typically moves to about 45 percent of MAC[96]. On condition that the straight tapered wing is selected, the parameter RLWAC refers to the value of 0.03 (3 percent of MAC).

7.2.2 Longitudinal Stability Estimation (Pitch)

Generally, the major contributors to the aircraft pitching moment about the centre of gravity consist of the wing, tail, fuselage, and engine contributions. However, as the concept of the UCAV design is based on the flying wing configuration, thus the pitching moment on this type of aircraft is primarily effected by wing. Based on the flying wing configuration, the wing or aircraft pitching moment contribution includes the lift through the wing aerodynamic centre, the wing moment about the aerodynamic centre, the pitching moment increment due to the deflection of the control devices, and the engine contributions. The latter refers to the vertical force produced at the inlet front face due to the turning of the freestream airflow. The engine thrust may not affect the aircraft pitching moment, as the engine is located inside the aircraft on the centreline providing its vertical distance from the centre of gravity be equal to zero. The following equation presents the pitching moment contribution of the UCAV in coefficient form as fraction of mean aerodynamic chord:

$$CMCGTM = CMLWCGL + CMWCGL + CMIWTTM + CMFPCGL \quad (7.24)$$

Where:

CMLWCGL = Wing pitching moment due to total wing lift through wing aerodynamic centre

CMWCGL = Wing pitching moment about wing aerodynamic centre

CMIWTTM = Wing pitching moment due to deflection of trailing edge control devices

CMFPCGL = Thrust effect upon pitching moment with inlet normal force due to turning of the air

The steps necessary to perform the calculations of the individual aircraft pitching moment contribution are entirely described in DATCOM[57] and they are not included here. The concept of the UCAV design is based on sweepback flying wing planform. According to this type of aircraft, the lift through the wing aerodynamic centre and the wing moment about the aerodynamic centre consistently produce the negative values of pitching moment. This is because the wing aerodynamic centre position is located behind the aircraft centre of gravity, and thus rotates the aircraft nose down. The vertical force at the inlet front face produces the positive pitching moment, so the pitching moments from wing and that from vertical force partially cancel each other out. This vertical force is based on the engine mass flow rate into inlet, thus this stabilized pitching moment directly affects the sizes of the engines and the dimensions of the intake diffuser. Assuming that the thrust vectoring is not fitted, the operation of the wing control devices is unavoidable to accomplish the additional positive or negative pitching moment to trim and control the aircraft.

Based on the flying wing planform, the wing trailing edge control devices must be used for trim and control. Because of the short moment arm of such a control, therefore, the sizes and positions of these devices on the aircraft must be concerned. On condition that the control devices are positioned outboard to the wing tip, they gain the largest available distance to the centre of gravity location. So a small deflection of control devices produces an additional pitching moment to trim and control the aircraft. This moment varies linearly with the sweep angle, which can be defined that for the wing with large sweep angle, only small deflections of the control devices are needed. In accordance with the outboard position the sizes of the control

devices are reduced corresponding to the wing sweep angle, which provide sufficient volume of wing box for the internal component arrangement, thus performing lighter aircraft.

On the other hand, if the position of the wing trailing edge control devices moves towards the inboard location, their distance to the centre of gravity location becomes shorter. This results that either the sweep angle must be increased or the control devices enlarge the sizes to produce the additional pitching moment to trim and control the aircraft. This affects directly to the packaging of the aircraft that the additional volume of wing box must be needed to support the internal component arrangement, and thus providing an increment on the mass of aircraft.

Table 7-4 shows some examples of the flying wing geometries based on the straight tapered wing planform with single weapon bay at wing centreline, applying the different positions of the trailing edge control devices to trim and control the aircraft.

Parameter	Unit	Trailing Edge Control Devices (TECS)	
		Inboard	Outboard
TECS total span	m	6.9715	3.9356
TECS mean chord	m	1.8967	0.6168
TECS total planform area	m^2	13.22	2.43
TECS total mass	kg	173.77	24.91
Wing gross span	m	20.1232	13.1186
Wing root centreline chord	m	14.1126	9.5367
Wing leading edge sweep	deg	52.7040	48.4783
Wing aspect ratio		2.4056	2.4620
Wing taper ratio		0.1855	0.1175
Wing gross area	m^2	168.34	69.90
Engine diameter	m	1.0866	0.7336
Engine length	m	2.3082	1.5584
Intake diffuser length	m	3.2098	1.4672
Total aircraft mass	kg	10207.66	5058.14

Table 7-4: Examples of Flying Wing Geometries Determined by Applying Different Positions of Trailing Edge Control Devices for Longitudinal Static Stability and Control Estimation

7.2.3 Lateral-Directional Stability Estimation (Roll and Yaw)

The lateral-directional analysis is similar to the longitudinal analysis in many ways. However, it really encircles two closely coupled analyses: the yaw (directional) and the roll (lateral). Both yaw and roll analyses are actuated by the yaw angle, and that the roll angle actually has no direct effect upon any of the moment terms. Generally, the deflection of either rudder or aileron will produce moments in both yaw and roll. Based on the flying wing configuration, these moments are produced by the control devices called the split drag rudders as seen on the B-2 stealth bomber, and the use of thrust vectoring at the two-dimensional nozzle exit, if fitted. The split drag rudders are directly responsible for the duties of rudder and aileron. It must be noted that, in this

design synthesis the split drag rudders may refer to the split elevons, as they also perform the function of the elevator to trim and control the aircraft.

Additionally, the lateral-directional analysis for the UCAV flying wing provides an option of the inlaid control surfaces located as two mirror-imaged on the top and bottom of the wing structure, as seen on the Pegasus X-47 Naval UCAV. In term of stealth design, the inlays are assumed to have a lower radar cross-section than the split drag rudders on the wing's trailing edge[48]. In terms of stability and control, the inlays reduce the load of the trailing edge control devices, as they are directly responsible for the duties of rudder and aileron, thus providing the effective elevons acting as a function of elevator to trim and control the aircraft.

The main contributors to the aircraft yawing and rolling moments based on flying wing configuration include the wing moment with respect to sideslip about wing aerodynamic centre, the wing moment due to deflection of either trailing edge split elevons or the inlaid control surfaces (if selected), and the engine contributions. The latter refers to the thrust effects upon yawing and rolling moments. Assuming that all engines are running, the direct-thrust moments cancel each other. On condition that, single-engine installation is selected locating at aircraft centreline, the engine thrust does not affect the moments, thus equal to zero. The following equations present the yawing and rolling moment contributions of UCAV in coefficient form as fraction of mean aerodynamic chord:

$$CNBCGTM = CNBWCGA \times QBSSL + CNBTA \times QWSA + CNBTR \times QBSSL \quad (7.25)$$

$$CLBCGTM = CLBWG \times QBSSL + CLBTA \times QWSA \quad (7.26)$$

Where:

CNBWCGA	=	Wing yawing moment with respect to sideslip about wing aerodynamic centre
CNBTA	=	Yawing increment effectiveness due to either trailing edge split elevons or inlaid control surfaces based on aileron characteristic
CNBTR	=	Yawing increment effectiveness due to either trailing edge split elevons or inlaid control surfaces based on rudder characteristic
CLBWG	=	Wing rolling moment with respect to sideslip about wing aerodynamic centre
CLBTA	=	Rolling increment effectiveness due to either trailing edge split elevons or inlaid control surfaces based on aileron characteristic
QBSSL	=	Local angle of sideslip (β)
QWSA	=	Angle deflection for either trailing edge split elevons or inlaid control surfaces based on aileron characteristic

The steps necessary to perform the calculations of the individual aircraft yawing and rolling moment contributions are entirely described in DATCOM[57] and they are not included here. As mentioned above, both yaw and roll analyses are actuated by the yaw or sideslip angle (β), for a sweepback wing planform the stabilized wing yawing moment produces a positive value as an increase in drag on the side of the wing. However, a negative value of the wing rolling moment with respect to a sideslip angle is stabilized due to dihedral effect. This rolling moment tends to keep the aircraft level because it sideslips downward whenever a roll is established. The dihedral effect rolls the aircraft away from the sideslip direction.

The wing yawing and rolling moments due to deflection of control devices are determined and developed from the methods applied for aileron, proposed by DATCOM[57], as no work has been published concerning an analysis of the split drag rudders, the split elevons or the inlaid control surfaces. The function of these devices provide the upper and lower parts either moving in unison as an ordinary control surface, or moving independently. The wing with different lift increments on either side due to deflection of split elevons or inlaid control surfaces provide the yawing moment in the opposite direction from the rolling moment. This can be defined by, deflecting the port control in unison to produce lift increment and opening the starboard control to the different degree to produce the lift and drag increment. The difference in lift increment creates the positive rolling moment, to perform the same function as an aileron. However, the drag produced by an increased lift creates a negative yawing moment. On the contrary, the asymmetric drag increment from the opening starboard control produces positive yawing moment to perform the same function as a rudder.

The main consideration of this code is to determine the sizes of the split elevons and/or the inlaid control surfaces and to examine their positions consistent with the internal component arrangement based on the estimation for zero yaw stability, and thus comparing the aircraft mass. The results of this comparison are discussed in Chapter 8.

7.3 Engine Performance Modelling

The engine performance module provides the information of certain basic engine characteristics for the design synthesis of UCAV. The most possible representation of variation of thrust and specific fuel consumption with flight conditions are the two primary characteristics, which are necessary for the estimations of the mission performance to determine the available fuel required to complete the aircraft mission. Moreover, they are needed for the point performance analysis to compare the delivered performance of the designed aircraft with the required performance figures. The characteristics of a known engine are always highly to be obtained. On condition that the detailed characteristics are unavailable, and no existing engines come closed enough to provide these desired characteristics to be rubberised, therefore, it may be useful to have generalised representations of their variation with flight conditions.

The method proposed by Raymer[96] provides the estimation of the possible representation of engine thrust and specific fuel consumption varied only at cruise condition. Moreover, they are applicable for commercial transports, and limit the value of engine bypass-ratio range from zero to 6, which seems not to provide all the required information to achieve the proposed analysis. The method proposed by Lovell[78] provides the acceptable estimation of these engine characteristics varied with flight conditions. However, the method is relatively complex and requires particular program, which is not available at this stage to accomplish the analysis.

The method proposed by Howe[58] seems to present the procedures with the required precision to achieve the proposed estimation. This method determines the variable thrust with flight conditions in the form of the engine thrust factor, which is dependent upon the flight speed or Mach number, flight altitude, engine operating

conditions, and the engine bypass ratio. The variation of specific fuel consumption with flight conditions is dependent upon the flight speed or Mach number, the flight altitude, the engine bypass ratio, and the fuel consumption factor. The latter parameter is determined by reference to the actual specific fuel consumption of a given engine at a critical datum condition. In this design synthesis, the fuel consumption factor of the subsonic turbofans is selected, which gives a typical value of 20 mg/N/s[58]. The method used to determine the engine characteristics has previously described in section 3.2.4 of Chapter 3. Equation (3.28a) needs some changes to accommodate the synthesis code of UCAV, which is given by:

$$TPG = FTPG \times TPGD \tag{7.27}$$

Where:

TPG = Engine thrust in various phases of flight
FTPG = Engine thrust factor
TPGD = Total maximum sea-level static thrust of engines

The total maximum static thrust of engines (TPGD) is obtained from sub-section 5.1.3.1 of Chapter 5. It is parametrically independent upon the engine size, which is determined by applying an engine scale factor (RTP) to scale the reference engine static dry thrust (TPGDR) corresponding to the total number of engines (NTENG) installed in the aircraft.

7.4 Mission and Point Performance Analysis

The performance analysis module represents the conclusion of all the previous calculations, since it accommodates the data obtained from the component sizing, aerodynamic, engine performance, and the mass estimation. The performance calculations consists of two parts: those that are used in the estimation of mission performance and fuel burn, and those that deal with the specific performance requirements and help to size the aircraft. They are described separately in details.

7.4.1 Mission Performance Estimation

As previously mentioned, the mission performance module carries out four typical mission profiles: the low-level strike mission, the counterair mission, the intelligence, surveillance and reconnaissance (ISR) mission, and the ferry mission. The former is the primary mission for UCAV. The counterair and the ISR missions are considered for the alternative roles for UCAV, as described in the literature search of Chapter 2. The ferry mission is determined considering the use of auxiliary fuel tanks carried inside the internal weapon bays for a ferry range.

The purpose of this calculation is to accumulate the avionics instruments and the weapons required for that particular mission, to size the avionics bays and the weapon bays in order to achieve the investigation of various packaging and configuration design aspects of UCAV. Moreover, it is important to estimate the available volume enclosing the packaging and the volume of the integral tanks in the wing accessible to capacitate the total mission fuel alteration. This mission fuel is then subjected to variation with the total fuel mass of the aircraft (MTGF) during the optimization process.

The mission performance analysis of each mission profile is developed in separate codes as a subroutine. The option from the packaging specification, TMISS, is required to select the typical mission for calling the relative code of that mission to be synthesized. Each code requires the mission requirement variables, which are set as the input data files. Mission codes and explanations are given in Table 7-5 and Table 7-6, respectively.

Mission Segment	UCAV Mission Profile			
	Low-level Strike	Counterair	ISR	Ferry
Cruise-out	R, M, H	R, M, H	R, M, H	R, M, H
Cruise-in	R, M, H	R, M, H	R, M, H	-
Dash-out	R, M, H	R, M, H	-	-
Dash-in	R, M, H	R, M, H	-	-
Loiter	T, H	T, H	T, H	T, H
Strafe/Combat	T, M, H	T, M, H	-	-
Weapon Release	T, V, H	T, V, H	-	-

Table 7-5: UCAV Mission Performance Codes

Variable	Description
R	Distance travelled during mission segment
T	Duration to perform mission segment
M	Mach number requirement to perform mission segment
V	Speed requirement to perform mission segment
H	Altitude to perform mission segment

Table 7-6: UCAV Mission Variable Descriptions

The methods used to determine the mission fuel mass are almost similar to those represented in section 3.2.5 of Chapter 3, with some changes and improvements to accomplish more accurate methods applied for UCAV. The fuel used is determined by breaking the mission into mission segments, as detailed in Figure 4-1 of Chapter 4. For each mission segment, the change in aircraft mass is calculated as either a mission-segment mass fraction due to fuel burned, or as a separate change in mass due to payload released. The product of all these fuel fractions will provide the final fuel fraction. The fuel mass used during the mission is then determined from unity minus the final fuel fraction, accumulating with the design take-off mass. A 6 percent allowance is added to the mission fuel to account for reserve and trap fuel, which is generally specified as a requirement for either an additional range or an additional loiter duration to achieve the mission. The value of mission fuel mass can finally be determined.

Basically, the mission segments during ground run (take-off, and landing), and also climb segment and descent segment, the estimation of a fuel mass fraction of these segments is estimated from historically statistical databases. The more accurate

method is provided to determine these fuel mass fractions in this design synthesis. According to this method, the fuel mass fraction is based on the duration of time to perform the mission segment, and the variation of given thrust and specific fuel consumption at each mission segment, which is given by:

$$FMDUM = 1 - (DT \times FC \times TW) \tag{7.28}$$

The duration of time (DT) to perform the individual mission segment is obtained from the point performance analysis described in the following sub-section. The variation of engine thrust (TPG) and specific fuel consumption (FC) at each mission segment are obtained from the engine performance module mentioned above. The thrust determined in this equation is represented in term of thrust loading (TW), which is varied at individual mission segment.

The remaining mission segments varied with flight conditions, the fuel mass fraction (FMDUM) is obtained from the Breguet 's range and endurance equations, as given in equation (3.33) and (3.34a) of Chapter 3, and are again represented as follows:

$$FMDUM = \exp\left(\frac{-R \times FC}{V \times LD}\right), \text{ Breguet's range equation} \tag{7.29a}$$

$$FMDUM = \exp\left(\frac{-T \times FC}{LD}\right), \text{ Breguet's endurance equation} \tag{7.29b}$$

Generally, the method used to determine the fuel mass fraction at each mission segment is performed as a mission-segment mass fraction due to fuel burned. However, during the mission segment due to payload released, the fuel mass fraction must be corrected by the payload-released ratio for the next phase. For simplicity, the method used to determine the fuel mass fraction for all mission segments in this design synthesis is calculated as a discrete change in mass due to payload released and fuel burned. Based on this method, an input parameter in each mission segment is set up to select the options for the weapon status and its relative mass required for that segment. Table 7-7 gives the detailed description of these options.

Option of input parameter in each mission segment: **IWP (X)**	Description of weapon status required for each mission segment	Relative weapon mass based on weapon status in each mission segment	
		Internal weapon bay: **MWIM**	External stores: **MWOM**
1	Weapon loaded on aircraft	MWIM = 0	MWOM = 0
2	Weapon released	MWIM = MWIB	MWOM = MWOB
3	No weapon loaded on aircraft	MWIM = 0	MWOM = 0

Table 7-7: Option of Input Parameter in Accordance with Weapon and Weapon Mass Required for Individual Mission Segment (Aircraft Mass)

Before starting the estimation of the mission performance analysis, it is necessary to assume two reference take-off masses given by:

$$MTTM(X) = MTT \text{ , Where X = NMISS = 0} \tag{7.30a}$$

$$MTGM(X) = MTT \text{ , Where X = NMISS = 0} \tag{7.30b}$$

Where *NMISS* represents reference number of current mission segment. Starting the estimation of the fuel mass fraction in each mission segment (NMISS = NMISS+1), the fuel mass fraction (as a discrete change in mass due to payload released and fuel burned) is found as:

$$FM(X) = 1 - \left[(1 - FMDUM) \times \left(\frac{MTGM(X-1)}{MTTM(X-1)} \right) \right], \text{ Where X = NMISS} \qquad (7.31)$$

The total existing aircraft mass at this point in each mission segment due to fuel burned is then given by:

$$MTTM(X) = FM(X) \times MTGM(X-1) \text{ , Where X = NMISS} \qquad (7.32)$$

The total existing aircraft mass (MTTM) requires to be subtracted from the mass of weapon corresponding to weapon status in each mission segment, in order to perform the payload-released ratio for the correction of the fuel mass fraction for the next segment. Therefore, the existing aircraft mass at the end of each mission segment, as a discrete change in mass due to payload released, is found as:

$$MTGM(X) = MTTM(X) - MWIM - MWOM \qquad (7.33)$$

On condition that IWP (X) = 1, it is assumed that the aircraft carries the weapon to perform that mission segment. According to this weapon status, the relative weapon mass is zero (MWIM = 0, MWOM = 0). Thus, the payload- or weapon-released ratio is equal to unity. If IWP (X) = 2, it represents the weapon released or bomb dropped segment. At this stage it is assumed that all weapons either the internal weapons or the external stores are released. The existing aircraft mass at the end of this mission segment (MTGM) is immediately less than the total existing aircraft mass (MTTM), thus providing the weapon-released ratio less than unity. If IWP (X) = 3, it is assumed that no weapon is loaded on the aircraft to perform that mission segment, thus providing the relative weapon mass due to this weapon status equal to zero. The weapon-released ratio is again unity. The method used to determine the fuel mass fraction is developed in separate code as a subroutine and is called into each mission segment to complete the estimation of fuel mass fraction.

Historically, the weapon released or bomb dropped segment defines that no fuel penalty was assessed, so the fuel mass fraction is assumed to be unity. For the UCAV design with an internal weapon bay, this mission segment starts from bay-doors open, release weapon(s), and ends after doors closed. As a result, range credit has been taken and so fuel penalty is occurred. Therefore, the estimation of the fuel mass fraction due to weapon releasing is unavoidable to be determined to provide the accurate fuel burned during this mission segment. The fuel mass fraction is based on the duration to perform weapon-released segment at required altitude and speed set in the mission performance codes. The estimation is obtained from manipulating the Breguet's endurance equation and then determined the final fuel mass fraction following equation (7.31) above.

7.4.2 Point Performance Estimation

The point performance analyses are used to predict the aircraft capabilities by comparing the distributed performance of the designed aircraft with the specific performance requirements. They critically affect the size and mass of the aircraft. The

size of the aircraft has a major impact on the UCAV packaging, and therefore the point performance analyses must be accurate. The point performance calculations considered in this designed synthesis consist of take-off and landing field length, climb performance, and level turning flight. They are applied to the entire missions selected for UCAV. The point performance calculations are compared to the design requirements setting as constraints during the optimization process, using a system of codes for maximum flexibility. The point performance constraint codes and their explanations are given in Table 7-8 and Table 7-9, respectively.

Constraint	Altitude	Mach Number	Data
Take-off	H	-	STO
Landing	H	-	SLD
Sustained Turn	H	M	RTRN
Excess Power	H	M	SEP
Accelerate/Climb	H	M	TSEP
Mach Number	H	M	-

Table 7-8: UCAV Point Performance Constraint Codes

Variable	Description
H	Flight altitude for performance constraint comparison
M	Mach number for performance constraint comparison
STO, SLD	Required take-off and landing distance
RTRN	Load factor or turn rate for manoeuvre
SEP	Specific excess power for performance constraint comparison
TSEP	Required time to accelerate and climb

Table 7-9: UCAV Point Performance Constraint Variable Descriptions

The methods used to determine the point performance are almost similar to those described in section 3.2.6 of Chapter 3, with some changes and improvements to achieve more accurate methods applied for UCAV. The take-off and landing distances are broken down into phases for more accurate analysis[96]. The duration to perform the take-off and landing segments are required to determine the accurate fuel mass fraction, as previously described in the mission performance module.

Considering take-off analysis, the various phases consist of the take-off ground roll, the transition to climb, and the climb phase. The take-off ground roll includes two parts: the level ground-roll and the ground roll during rotation to the angle of attack for lift-off. The following equation presents the total take-off distance:

$$STTO = STG + STGR + STTR + STCL \tag{7.34}$$

The level ground-roll is determined by integrating the ground roll from initial speed to its instantaneous value of finial speed evaluated at 70 percent of take-off speed, which assumes as an average constant value of acceleration forces:

$$STG = \left(\frac{1}{2 \times GR \times KA}\right) \times \ln\left(\frac{KT + KA \times VF^2}{KT + KA \times VI^2}\right) \tag{7.35a}$$

Where:

$$KT = TW - CFG \text{ , Thrust terms} \tag{7.35b}$$

$$KA = \left(\frac{D}{2 \times WS}\right) \times (CFG \times CLMX - CD0 - CDL) \text{ , Aerodynamic terms} \tag{7.35c}$$

D	=	Air density at flight altitude
WS	=	Wing loading at various phases of flight
TW	=	Thrust loading at various phases of flight
VI	=	Initial speed (zero at take-off)
VF	=	Final speed (70% take-off speed)
GR	=	Gravitational acceleration (9.80665 m/s^2)
CLMX	=	Maximum lift coefficient
CFG	=	Ground friction coefficient

The ground friction coefficient for take-off condition is represented as the ground rolling friction coefficient, which depends mainly on the conditions of the runway surface. The dry concrete surface type is selected for the take-off analysis with a typical value of 0.03. The drag terms (CD0 and CDL) may include the additional drag of landing gear down, flaps at take-off position, and the aircraft in ground effect, as described in the aerodynamic module.

The take-off speed is assumed to be 1.1 times the stall speed, which is found by setting the total maximum lift (with take-off flaps) at stall speed equal to weight and solving for stall speed. The rotation ground-roll distance is assumed from the time to rotate the aircraft to lift-off attitude. A typical assumption for small aircraft is that rotation takes one second, thus the rotation ground-roll distance is equal to the take-off speed.

$$STGR = VFTG = 1.1 \times VSTO \tag{7.36}$$

During the transition to climb, the aircraft accelerates from take-off speed to climb speed, which is 1.2 times the stall speed (military aircraft). Thus, the average speed during transition is assumed to be 1.15 times the stall speed. The transition distance can be determined by two conditions based on the clearance of aircraft from the specified 50-feet (15.24 metres) obstacle height (military aircraft). On condition that the obstacle height is cleared before the end of the transition segment, the transition distance is given by:

$$STTR = \sqrt{RTTRA^2 - (RTTRA - HTTR)^2} \text{ , Where HTTR} \geq \text{HOBST} \tag{7.37a}$$

On the other hand, if the aircraft follows an approximately circular arc until it reaches the climb angle, the transition distance is then given by:

$$STTR = RTTRA \times \sin(QTCL) \text{ , Where HOBST} \geq \text{HTTR} \tag{7.37b}$$

Where:

HOBST	=	Obstacle height (50 feet for military aircraft)
HTTR	=	Transition height
RTTRA	=	Circular arc
QTCL	=	Climb angle

The steps necessary to perform the calculations of the transition height, the circular arc and the climb angle are fully described by Raymer[96], and they are not included here. Finally, the horizontal distance travelled during the climb to clear the obstacle height is found as:

$$STCL = \frac{HOBST - HTTR}{\tan(QTCL)} \text{ , Where HOBST} \geq \text{HTTR} \tag{7.38}$$

On condition that the obstacle height was cleared during transition, then the climb distance (STCL) is equal to zero.

The duration to perform the individual take-off segment can now be determined, and the sum of the total duration to accomplish the take-off mission phase is then used in the calculation of the fuel mass fraction, described previously in the mission performance module.

Considering the landing analysis, the landing is much like take-off, only backward. The landing distance is split into the approach distance, the flare distance, and the ground roll. The landing ground roll includes the free roll distance and the braking distance. The following equation presents the total landing distance:

$$STLD = SLGB + SLFR + SLF + SLA \tag{7.39}$$

The methods used to determine the individual landing distance are determined from the above calculations as applied for the take-off analysis. The aircraft speed is now referred to the landing speed or touch down speed. The landing speed is assumed to be 1.1 times the stall speed (military aircraft), which is found by setting the total maximum lift (with landing flaps) at stall speed equal to the landing weight and solving for stall speed.

The approach begins with obstacle clearance over 50-feet object with the approach speed equal to 1.2 times the stall speed. The aircraft decelerates from the approach speed to the landing speed during the flare. After touchdown, the aircraft rolls free for one second before applying the brakes. For the braking distance (SLGB), the initial speed is now equal to 70 percent of the landing speed and the final speed being zero. The ground friction coefficient for landing condition is represented as the ground braking friction coefficient, which a typical value of 0.3 is applied for the dry concrete surface type. The drag terms (CD0 and CDL) include the additional drag of landing gear down, flaps at landing position, and the aircraft in ground effect.

Once the estimation for landing distance is accomplished, the duration to perform the landing segment is determined, and is used in the calculation of the fuel mass fraction during the landing mission segment.

The specific excess power is also considered for the point performance analysis of UCAV. It represents the ability of an aircraft to accelerate and/or climb. The method used to determine the specific excess power is available in the entire open literatures of aircraft conceptual design, given by:

$$SEPCL = \frac{V \times (TPG - DRG)}{WS \times SW \times GR} \tag{7.40}$$

This constraint provides the user to define that the aircraft should have a level of performance over and above that required achieving a certain performance constraint.

7.5 Centre of Gravity Excursion

The centre of gravity excursion module is required to examine the range of the aircraft centre of gravity to remain within the acceptable limits throughout the mission. The range of the aircraft centre of gravity is affected by fuel burned and/or payload released during each mission segment. In this design synthesis, the fuel burned throughout the mission is assumed to vary linearly in all tanks. This module also requires the input parameter (IWP) in each mission segment to select the options for the weapon status and its relative mass required for that segment. Table 7-10 gives the detailed description of these options.

Option of input parameter in each mission segment: **IWP (X)**	Description of weapon status required for each mission segment	Relative weapon mass based on weapon status in each mission segment	
		Internal weapon bay: **MWIXR**	External stores: **MWOXR**
1	Weapon loaded on aircraft	MWIXR = MWIB	MWOXR = MWOB
2	Weapon released	MWIXR = 0	MWOXR = 0
3	No weapon loaded on aircraft	MWIXR = 0	MWOXR = 0

Table 7-10: Option of Input Parameter in Accordance with Weapon and Weapon Mass Required for Individual Mission Segment (Aircraft Centre of Gravity)

On condition that IWP (X) = 1, it is assumed that the aircraft carries the weapon to perform that mission segment. According to this weapon status, the aircraft centre of gravity is changed due to only fuel burned, thus the relative weapon mass is still occupied the weapon onboard to determine the aircraft centre of gravity at that segment (MWIXR = MWIB, MWOXR = MWOB). If IWP (X) = 2, it represents the weapon released or bomb dropped segment. At this stage it is assumed that all weapons either the internal weapons or the external stores are released. With no weapon loaded onboard at the end of mission segment, thus the relative weapon mass is equal to zero. The aircraft centre of gravity at this stage is affected by both fuel burned and the weapon released. If IWP (X) = 3, it is assumed that no weapon is loaded on the aircraft to perform that mission segment, thus providing the relative weapon mass due to this weapon status equal to zero. The aircraft centre of gravity at this stage is changed due to only fuel burned.

For each of these segments, the user can set the payload requirements either to release the weapon during weapon-released segment or to contain full stores back to base. The CG excursion module is developed in separate code and is called at the end of each of the mission segments to determine the aircraft centre of gravity at that segment, using the methods described in equation (6.8) and (6.9) of Chapter 6. The entire centre of gravity is then set as constraints subjected to remain within the acceptable limits.

Figure 7-13 illustrates the centre of gravity excursion diagram of some cases of the UCAV based on single-kink wing planform with one weapon bay at centreline. The low-level strike mission is considered in this estimation.

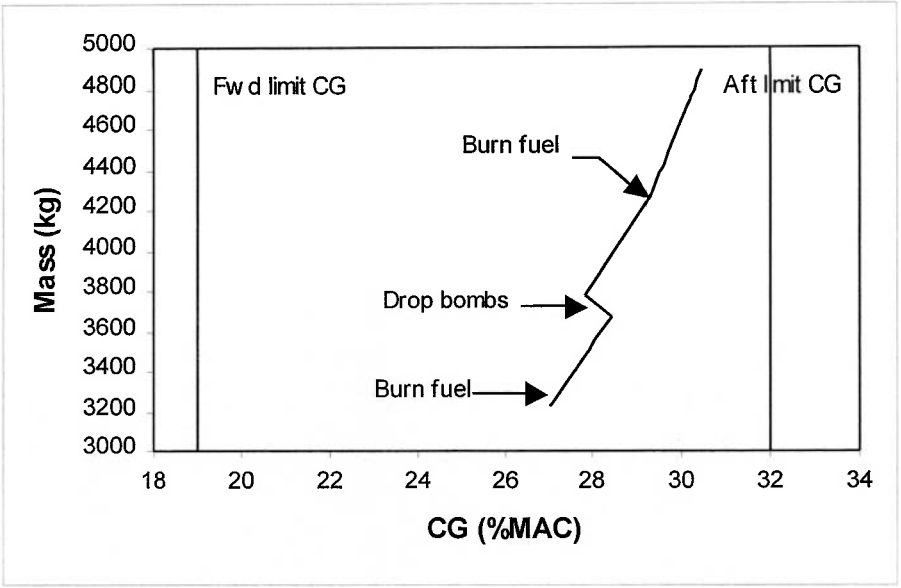

Figure 7-13: Centre of Gravity Excursion

7.6 Constraint Estimation

A brief description of the objective function and all of the constraints estimated in the design synthesis of UCAV is listed in details. It must be noted that, the number representing the constraints may not be in accordance with that shown in the output data of UCAV. This is because some constraints perform a loop routine during the optimization process.

The objective function is the design take-off mass, MTT. It is applied as a target converging value to meet the required take-off mass. Constraint 1 requires the fuel mass analysis throughout the mission to meet the total fuel mass of the aircraft obtained from the sum of fuel storage in integral wing tanks, the available tanks enclosing the packaging, and the auxiliary tanks carried inside the internal weapon bays (if selected). This is calculated in the form of equality constraint. On condition that the weapon bay is located at aircraft centreline, Constraint 2 checks the available volume at front and rear of the weapon bay to carry the same amount of fuel performing an equality constraint. This constraint is needed to allow sizing of the wing root centreline chord to easily fit the weapon bay at this span location.

Constraints 3 and 4 ensure that the available volume aft of the rear spar and forward of the front spar can be fitted with the actuators for controlling the control devices of the aircraft. They are estimated in the form of equality constraint.

Constraint 5 ensures that the aircraft weight and lift distribution are equivalent during flight conditions. Constraint 6 is required for lateral trim analysis to determine the sizes of the split elevons and/or the inlaid control surfaces and to examine their positions consistent with the internal component arrangement based on the estimation for zero yaw stability.

The remaining constraints described below are estimated in the form of inequality constraints during the optimization process.

Constraint 7 through 11 ensures that the overall clearances on height and width for the engine bay are limited to a range between specified maximum and minimum values, as described in Chapter 5.

Constraints 12 through 14 check the requirements of the UCAV based on multi-kinks wing planform. Constraint 12 ensures that the spanwise stations of all wing kinks are in the appropriate positions through the wingspan providing the positive trapezoidal panels. Constraint 13 checks that the taper ratios of individual panel of multi-kinks wing configuration are not greater than unity. Constraint 14 ensures that the wing leading edge sweeps of individual panel are constant or have only minor changes over the grater part of the span due to the overall aerodynamics characteristics, as described in Chapter 5.

Constraint 15 ensures that the aircraft does not suffer from excessive pitch-up characteristics near stall. This constraint has been taken from Lovell[78], given by:

$$CUC(15) = 3.2 - \left(AW \times \left[\tan(QW4)\right]^{0.8}\right) \tag{7.41}$$

Constraint 16 ensures that the volume at tip area is available for installing the electronic warfare equipments in both port and starboard wings. Constraint 17 checks that the volume at nose area of the aircraft is available for the radar suite of UCAV.

Constraints 18 through 25 ensure that the chordwise position of the bays can be controlled within the aircraft at their relative span locations, as described in Chapter 5. Constraint 26 checks that the half of the semi-wingspan covers the main package available for the integral wing tanks to be fitted at outboard section.

Constraint 27 checks that the overall length of intake diffuser is not less than a minimum value in order to ensure an acceptable entry flow at the engine compressor. Constraint 28 requires that the overall length of the two-dimensional nozzle is not less than a minimum value in order to ensure a satisfactory flow to prevent the flow separation. Both constraints have been described in Chapter 5.

Constraint 29 through 42 ensures that the trailing edge control surfaces, the leading edge control surfaces, and the inlaid control surfaces are located in their appropriate positions and achieve the design requirements. The minimum spanwise location required for the inboard trailing edge and leading edge devices must not affect the position of the propulsion system. The span of each device ensures the minimum value required and the devices do not interfere with each other.

Constraint 43 ensures that the available fuel capacity of the aircraft can capacitate the total fuel throughout the mission. Constraints 44 and 45 check the limitation of

forward and aft positions available for aircraft centre of gravity. Constraints 46 through 50 ensure that the undercarriage are located in their appropriate locations achieving the design requirements as described in Chapter 6.

Constraint 51 ensures that the sizes and the positions of trailing edge split elevons are accessible to trim and control the aircraft on the estimation of longitudinal stability, as described in section 7.2 above.

Constraint 52 ensures that the thrust-to-weight ratio is adequate to achieve the performance of the aircraft. Constraint 53 ensures that the requirement for the maximum lift coefficient applied for a low aspect ratio wing is achieved, as described in section 7.1 above.

Constraints 54 through 60 are the constraints for the point performance calculations as described in section 7.4 above. Constraints 61 and 62 ensure that the aircraft centre of gravity at the end of each mission segment is subjected to remain within the acceptable limits of the aircraft forward and aft CG, as described in section 7.5.

7.7 Summary

This chapter has presented the methods of characteristic analyses for the UCAV, and give relevant algorithms as applied in the synthesis code. Moreover, the option of input parameter in each mission segment to select the options for the weapon status and its relative mass required for that segment are explained. They are needed to perform the accurate estimations of the fuel mass fraction and the aircraft centre of gravity at the end of each mission segment throughout the entire mission. The last part gives the description of the entire constraint functions applied for the UCAV design synthesis process.

CHAPTER 8

8 Generation of Results

The aim of this chapter is to demonstrate the capabilities of the software tool described in the previous chapters and its operation with the optimization tool capable of performing the studies identified. The option of packaging specification, role, capability and mission specification will have a significant effect on the size, shape, and mass of a proposed aircraft.

The first section presents a demonstration of optimizer convergence, validates the accuracy of the aircraft sizing methodology against real data for the Pegasus X-47 UCAV-N, and makes the comparison of aircraft masses with the existing UCAVs and some configuration aspects of the UAVs. The remainder of the chapter is structured to simulate the selection process that would take place in the early design stages of an air combat aircraft. By using the UCAV conceptual design and optimization synthesis, the advantages of alternative configurations can be compared in a consistent and through manner, with visibility of configuration, mass, and performance data. The results from all of the above studies are presented, and discussed with appropriate.

8.1 Development of Design Synthesis Model

The previous chapters have detailed the UCAV design synthesis model and its operation with the optimization tool is presented in the following sub-sections. The optimizer convergence is presented and discussed. The selected mission and point performance data with brief description are all detailed. The UCAV design synthesis code is validated using model configuration for the Pegasus X-47 UCAV-N. Finally, some possible masses produced by this code with several configurations are compared to those of the existing UCAVs and some configuration aspects of the UAVs.

8.1.1 Optimization Convergence Plot

Before any results of the optimization process are presented, the convergence of the UCAV conceptual design and optimization synthesis needs to be established. According to the explanation of optimization described in section 3.1 of Chapter 3, care is necessary in the definition of the parameters to reduce the possibility of the sudden changes to the optimising path arising from discontinuities in the formulation. Furthermore, inaccurate definition of internal iteration loop for the take-off mass described in Chapter 5 may lead to variations in the objective function. The overall program must be satisfactory to ensure that the design variables follow a logical sequence, and the continuity of the objective and constraint functions obtain no region within the validity of the optimization variables, which is undefined. This confirms

that the optimization function is operating correctly, increasing confidence in the validity of the results presented in the following sections.

The optimization tool applied for the design synthesis is called 'LSGRG2', which applies an implementation of the Generalized Reduced Gradient (GRG) algorithm able to solve large, sparse non-linear optimization problems. The process is described in greater details in the 'LSGRG2 User's Guide'[69].

Figure 8-1 presents the variation in some major parameters including the objective function, the take-off mass, with increasing numbers of iterations called by the optimization tool LSGRG2 to the aircraft synthesis routines. It can be seen on the plot that the objective function varies abruptly from the starting evaluation loop to about 25 iterations. This is because the inaccurate definition of internal iteration loop for the take-off mass may lead to these variations as discussed above. From this loop the optimizer converges the parameters smoothly and continuously, and that a solution close to a feasible design is reached after about 200 iterations. However, this design probably does not meet all of the constraints either for the packaging aspects or the performance requirements that still have been too large at that point. The optimizer can be seen to continue to investigate the gradients at the current trial point, but may make sudden changes to different points in the design space as mentioned above on successive iterations, until a solution can be achieved.

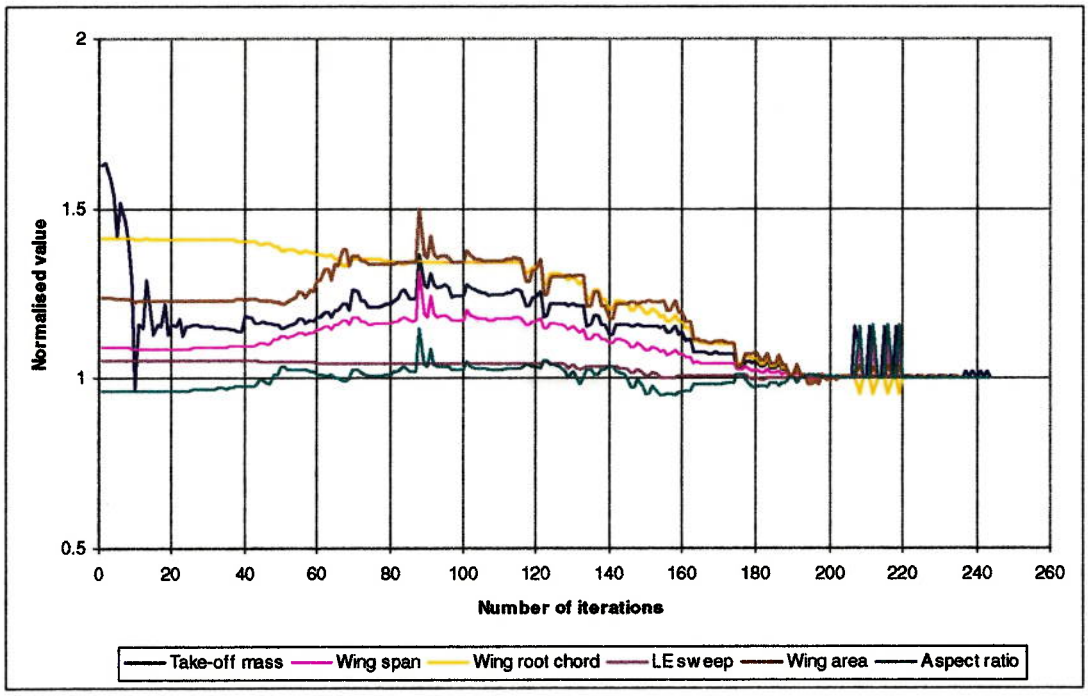

Figure 8-1: UCAV Design Synthesis Model – Example of Optimization Convergence Plot

Figure 8-2 illustrates an example of one final configuration design aspect of the UCAV developed by this design synthesis model. The configuration is based on straight-tapered wing planform with single weapon bay located at the centreline of the aircraft. The 1,000-lb (460-kg) GBU-32 Joint Direct Attack Munition (JDAM) is

loaded in the weapon bay. The radar and sensor bays are located at the aircraft nose providing sufficient volume adjacent to the bays in the leading edge area forward of the intake diffuser to install the antenna. The avionics bay is forward of the weapon bay providing sufficient volume on each side for the intake diffuser. Two engines, one on each side of the weapon bay provides the volume usage efficiency. The two-dimensional nozzles are integrated within the trailing edge providing the remaining space at the end to install the thrust vectoring. Two pairs of trailing edge control devices are fitted next to the nozzles in the available trailing edge area. The fuel tanks are located outboard of the engines and on the top of the weapon bay. The remaining volume outboard of the wing tanks on both sides of the wing box is available for the electronic warfare equipments. The output data from the UCAV design synthesis code for this configuration is included in Appendix D.

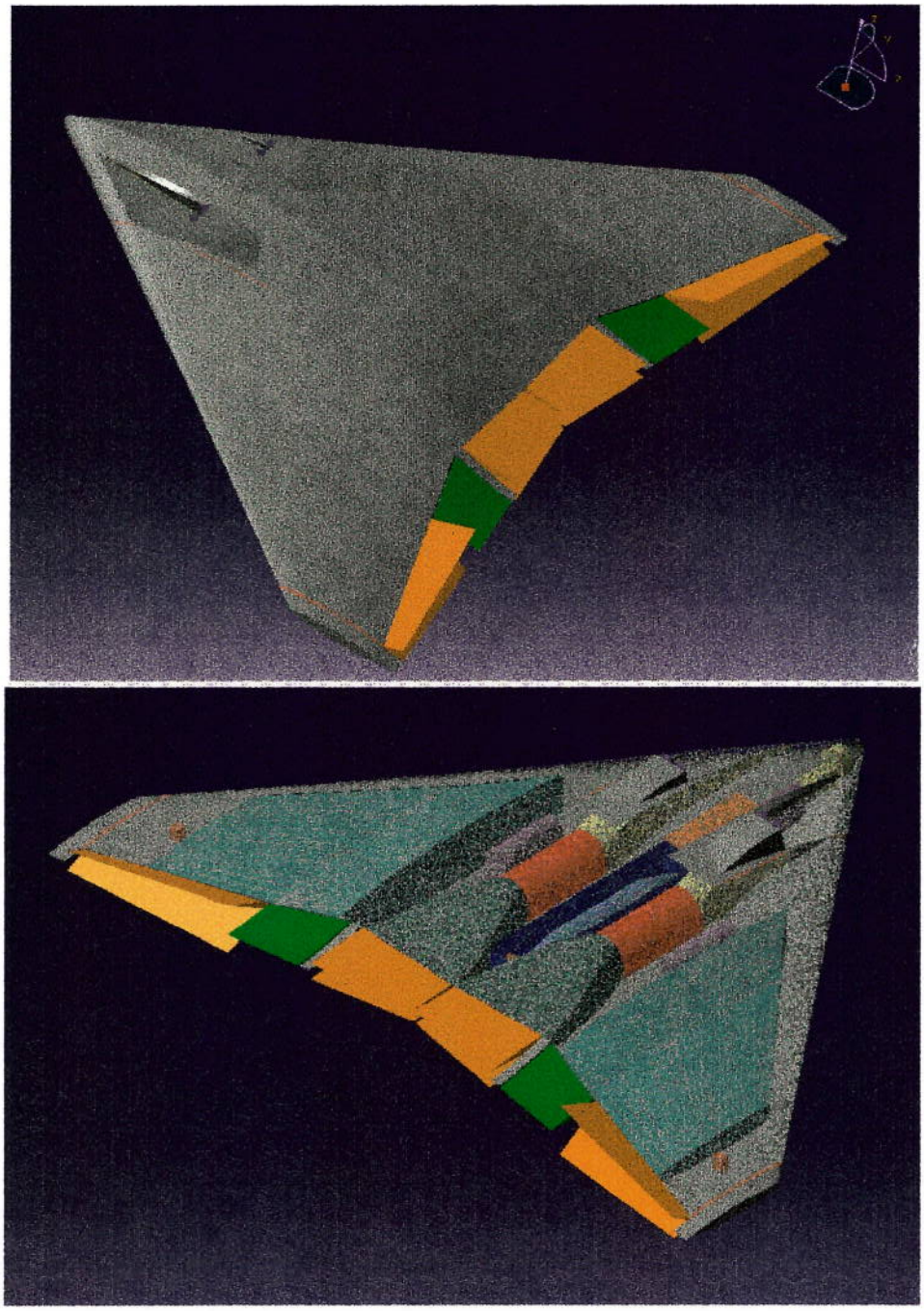

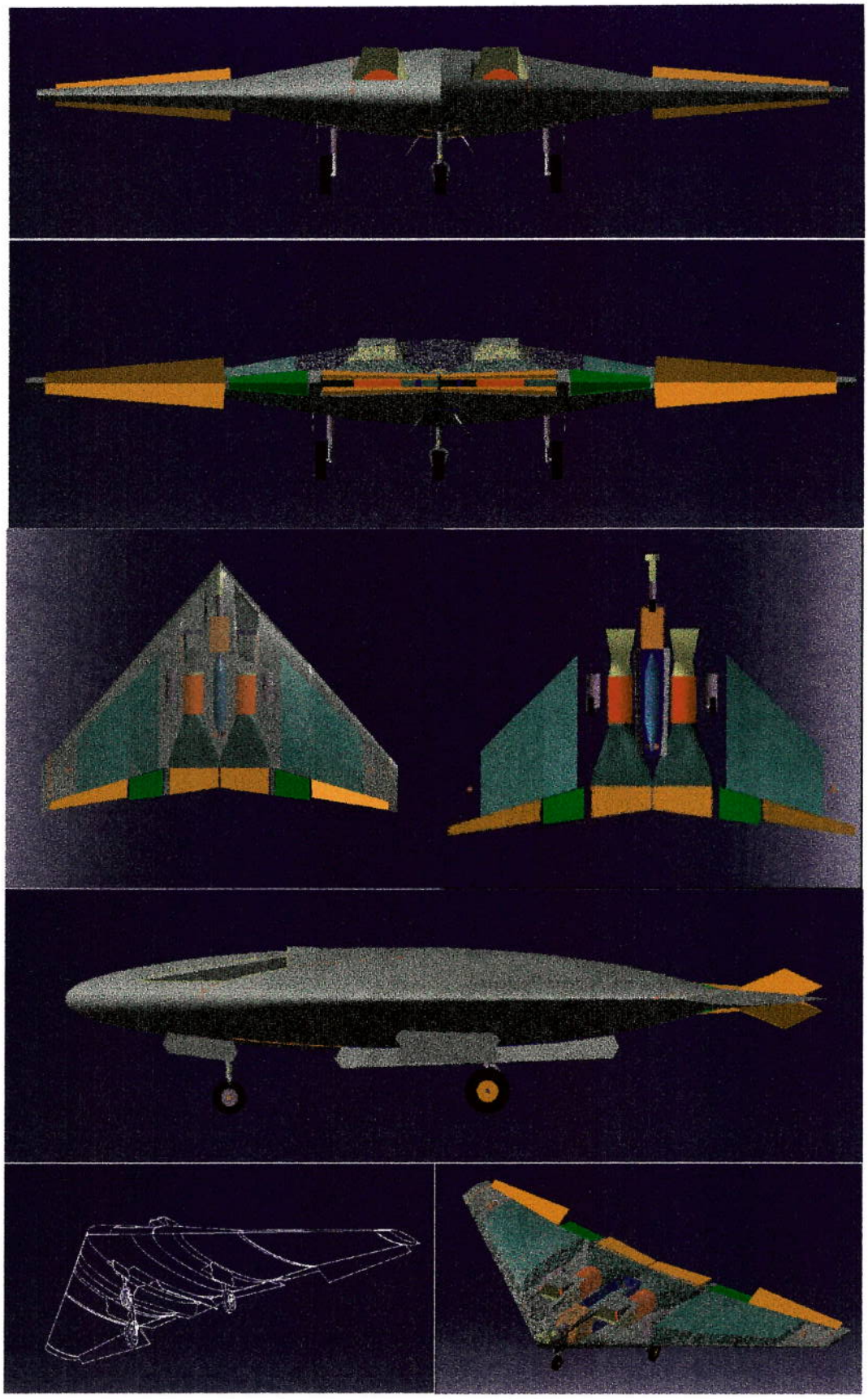

Figure 8-2: Example UCAV Configuration

8.1.2 Definition of Performance Parameters

To produce realistic results, a conceivable set of point and mission performance parameters is required. In order to prevent the investigations from becoming too large and perhaps detracting from emphasis on model capability, only a single mission has been considered. The mission chosen is a low-level strike mission, specifying as the primary role required for the UCAV. The performance requirements are determined by the author in order to be the representative of the UCAV mission, and are not meant to represent the specifications for any particular aircraft. Mission and point performance data are all detailed.

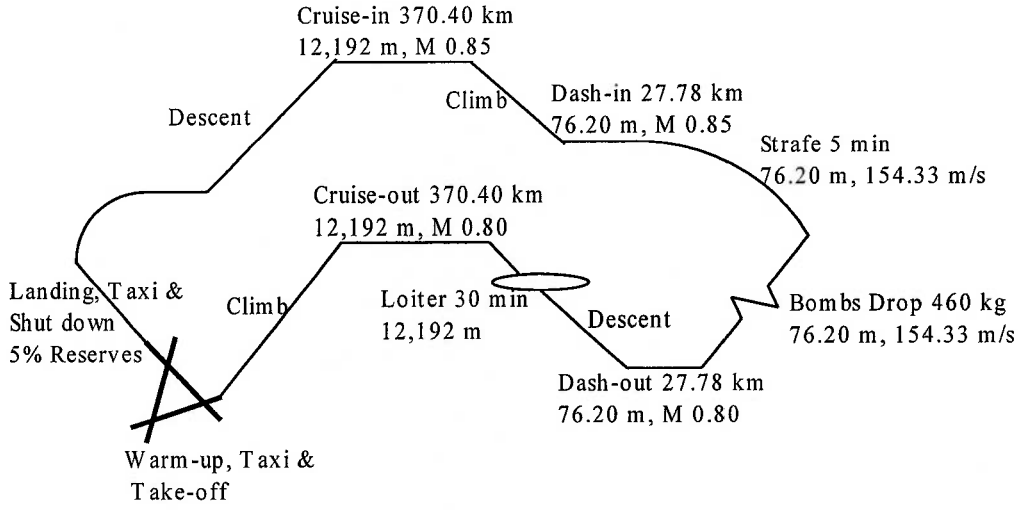

Figure 8-3: UCAV Mission Performance Requirements

The UCAV is required to perform the following 15-segment mission, with an internal weapons load based on the 1,000-lb (460-kg) GBU-32 Joint Direct Attack Munition (JDAM). The JDAM is a low-cost guidance kit produced by Boeing that converts existing unguided free-fall bombs into accurately guided "smart" weapons. The JDAM equipment consists of a new tail section that contains an Internal Navigation System (INS)/Global Positioning System (GPS). Currently equipments are being produced for usage with the 1,000-lb MK-83 bomb, and 2,000-lb MK-84 bomb. The tests performed to assess this weapon have proved it to be highly accurate and can be delivered in any "flyable" weather. The JDAM can be launched from more than 15 miles from the target with updates from GPS satellites to help guide the weapon to the target location. Figure 8-4 illustrates the aspect of the JDAM and the further detail and dimension are presented in the list of weapons in Appendix B.

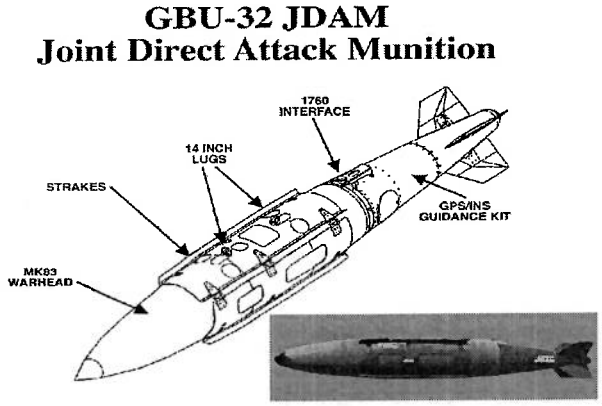

Figure 8-4: GBU-32 Joint Direct Attack Munition (JDAM)[71]

The descriptions of the mission performance for the aircraft are as follows:

Mission Segment	Description
Engine start, warm-up	Fuel fraction is estimated from statistical databases historically of 0.99.
Taxi	Fuel fraction is estimated from statistical databases historically of 0.99.
Take-off	At sea-level with temperature of 95-degree Fahrenheit (35-degree Celsius)
Accelerate and climb	To 40,000 feet (12,192 metres) and Mach number 0.80
Cruise-out	200 nautical miles (370.40 kilometres) at 40,000 feet (12,192 metres) and Mach number 0.80 to the target area
Loiter	30 minutes (1,800 seconds) at 40,000 feet (12,192 metres) over target area
Descent	To 250 feet (76.20 metres) and Mach number 0.80
Dash-out	15 nautical miles (27.78 kilometres) at 250 feet (76.20 metres) and Mach number 0.80
Bombs drop	5 minutes (300 seconds) starts from bay-doors open, release bomb(s), and ends after doors closed at 250 feet (76.20 metres) and speed 300 knots (154.33 m/s)
Strafe	5 minutes (300 seconds) at 250 feet (76.20 metres) and speed 300 knots (154.33 m/s), and fire ammunition with mass of 80 kg (if manned aircraft is selected)
Dash-in	15 nautical miles (27.78 kilometres) at 250 feet (76.20 metres) and Mach number 0.85
Climb	To 40,000 feet (12,192 metres) and Mach number 0.85
Cruise-in	200 nautical miles (370.40 kilometres) at 40,000 feet (12,192 metres) and Mach number 0.85 back to base
Descent	To altitude at sea-level prepared for landing
Landing, Taxi, Shut down	At sea-level with temperature of 86-degree Fahrenheit (30-degree Celsius)

Table 8-1: Definition of Mission Performance Parameters

After taxiing and ground movements, the mission is completed with 6 percent reserve fuel remaining. The mission fuel mass is assumed to variation only with the fuel in the integral tanks during the optimization process.

The point performance requirements for the aircraft are as follows:

Constraint	Description
Take-off	At sea-level with 100 percent weapons load and total distance of 5,000 feet (1,524 metres)
Landing	At sea-level with no weapons load and total distance of 5,000 feet (1,524 metres)
	At sea-level with maximum approach speed of 130 knots (66.88 m/s)
Sustained turn	At 250 feet (76.20 metres) and speed 350 knots (180 m/s) with turn rate of 20 degree per second to fire ammunition (if manned aircraft is selected)
Excess power	From sea-level to 40,000 feet (12,192 metres) with specific excess power of 80 ft/s (24.38 m/s) and 100 percent weapons load
Accelerate and climb	From Mach number ≈ 0.20 at sea-level to Mach number 0.80 at 40,000 feet (12,192 metres) in 6 minutes (360 seconds) with 100 percent weapons load
Mach number	Maximum level flight speed of Mach number 0.80 at 40,000 feet (12,192 metres) with 100 percent weapons load

Table 8-2: Definition of Point Performance Parameters

According to section 5.2.1 of Chapter 5, the maximum design load factor applied for the low-level strike mission is set at 7.33g. The ultimate load factor is calculated according to the aircraft configuration, by multiplying the above design load factor by the safety factor of 1.33 for the unmanned aircraft and by that of 1.5 for the manned aircraft.

8.1.3 Validation and Comparison with Existing Aircraft

In order to prove the accuracy of the methodology of the UCAV design and optimization synthesis, the existing UCAV would be modelled. According to the flying wing configuration, the only aircraft that could validate with this methodology is the Northrop Grumman Pegasus X-47 UCAV-N (see section 2.1.2.3 of Chapter 2), with the Pratt and Whitney JT15D-5C high-bypass turbofan engine. The major parameters of the Pegasus X-47 were obtained from the Internet[48,88], as no references have been published the details of this new UCAV. The engine specification was taken from Jane's Aero Engines[53]. The aircraft was generated using the UCAV conceptual design synthesis and optimization model, although the optimization process was not allowed to alter the major parameters. In this way, the complete aircraft could be modelled and the empty masses calculated by internal iterations to

reach the final values. The remaining calculated values are then compared to demonstrate the accuracy of the model.

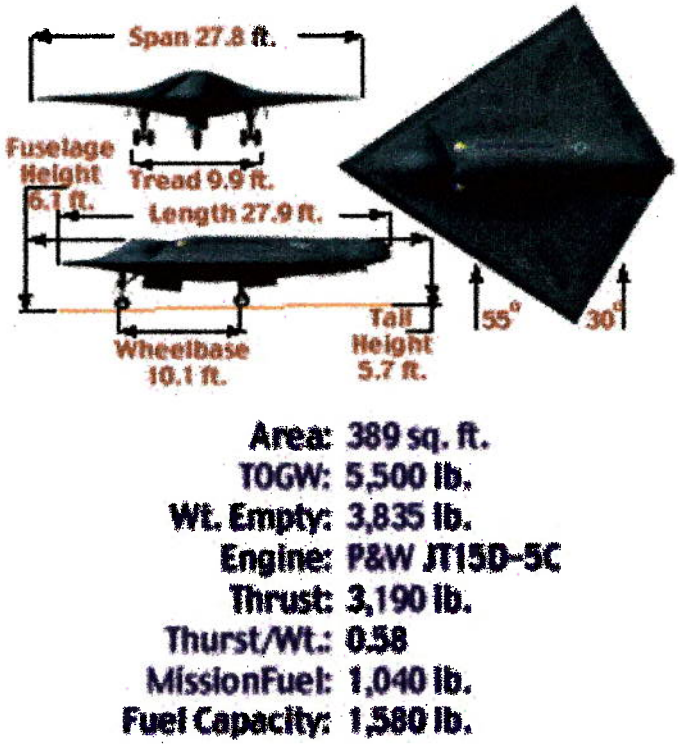

Figure 8-5: Configuration and Geometry of Pegasus X-47 UCAV-N

Due to the lack of data for the aircraft design missions of the Pegasus X-47, the aircraft was generated using the design synthesis code with the low-level strike mission described above to determine the mission fuel required. The cruise ranges have been reduced until the mission fuel mass was correlated to the real data. The thickness ratios at inboard and outboard sections are assumed 18 percent and 9 percent, respectively. The weapon bay of the Pegasus X-47 has been designed to carry the 500-lb (226.80-kg) bomb[48]. For this analysis, the 241-kg MK-82 bomb seemed to be the correlated data suitable for its weapon bay and thus was selected obtaining its dimensions to size the weapon bay and assumed the weapon mass of 226.80-kg bomb to be loaded.

The packaging aspect of the Pegasus X-47 is similar to one option defined by the *packaging specification* applicable for the UCAV design synthesis code, as presented in Table 4-2 and Figure 4-4 of Chapter 4. The single engine is located at the aircraft centreline with two weapon bays, one on each side. The fuel tanks are located outboard of the weapon bays. Furthermore, the configuration layout is a kite-shape planform, which is one of the flying wing configurations considering for the UCAV design, as illustrated in Figure 4-6 of Chapter 4.

The relevant data are presented in Table 8-3. Figures in bold are those input to the models to ensure that the overall configuration layouts are unchanged from the

existent aircraft. All other values are calculated from those parameters and the output data from the UCAV design synthesis code for the Pegasus X-47 is included in Appendix D.

Aircraft	**Pegasus X-47 UCAV-N**			
Parameter	**Unit**	**Quoted**	**Calculation**	**%**
Wingspan	**m**	**8.47**	**8.47**	
Wing centreline chord	**m**	**8.50**	**8.50**	
Leading edge sweep	**deg**	**55.00**	**55.00**	
Wing area	**m^2**	**36.04**	**36.04**	
Wing taper ratio		**0.00**	**0.00**	
Thrust to weight ratio		**0.58**	**0.58**	
Weapon mass	**kg**	**226.80**	**226.80**	
Engine maximum thrust	N	14,190.00	14,167.09	-0.16%
Engine maximum diameter	m	0.686	0.688	0.28%
Engine length	m	1.531	1.461	-4.56%
Engine mass	kg	302.00	240.24	-20.45%
Aircraft empty mass	kg	1,739.53	1,792.46	3.04%
Mission fuel mass	kg	471.74	471.50	-0.05%
Aircraft take-off mass	kg	2,438.07	2,490.76	2.16%
Undercarriage wheelbase	m	3.08	2.48	-19.62%
Undercarriage tread	m	3.02	2.88	-4.80%

Table 8-3: Quoted and Calculated Aircraft Parameters: Invariable Major Parameters

The UCAV design synthesis code gives the accurate results, with only the engine mass and the undercarriage wheelbase providing significant errors for the aircraft parameters. For the engine mass, the baseline data was obtained from the manufacturer of an existing engine. On the contrary, the calculated value was based on an engine scale factor being sized from a reference engine optimized as a rubber engine for this application, thus the inaccurate result may be performed. The positions of nose and main undercarriage from the aircraft nose used for the Pegasus X-47 were not available, although wheelbase was known. Additionally, its CG and approach angle were unknown. These uncertainties lead to the inaccuracy of the undercarriage wheelbase and the tread gained from the calculation. The engine maximum thrust is seen to be excellent, varying by only 0.16 percent. The mission fuel mass is obtained from the reduction of cruise ranges to 60 nautical miles (111.12 kilometres) performing the close correlation varying by only 0.05 percent. Although the avionics instruments and their mass applied for the Pegasus X-47 are not available, the calculated aircraft empty mass varies only 3.04%, which is precisely closed to the baseline. The quoted take-off mass shown is the sum of the aircraft empty mass, the 500-lb payload, and the mission fuel mass required, which is slightly less than the given gross value of 5,500 lb (2,494.76 kg), as shown in Figure 8-5. The data shown may result for the maximum take-off mass of the aircraft. However, the calculated aircraft take-off mass varies by only 2.16%, which is seen to be excellent compared to the baseline. Overall, the results are very good and allow high confidence in the utility of the models to validate the additional results.

Alternatively, to further ascertain that the methodology of the UCAV design and optimization synthesis provides the accurate results, the model was used to regenerate the aircraft, allowing the major parameters of the overall configuration layouts to be sized by the optimizer to alter the overall values. Only the taper ratio remained constant and the weapon mass of 226.80-kg bomb was loaded in the weapon bay. The results of the relevant data are presented in Table 8-4.

Aircraft	**Pegasus X-47 UCAV-N**			
Parameter	**Unit**	**Quoted**	**Calculation**	**%**
Weapon mass	**kg**	**226.80**	**226.80**	
Wing taper ratio		**0.00**	**0.00**	
Wingspan	m	8.47	8.76	3.46%
Wing centreline chord	m	8.50	8.01	-5.76%
Leading edge sweep	deg	55.00	55.96	1.75%
Wing area	m^2	36.04	35.09	-2.64%
Engine maximum thrust	N	14,190.00	13,142.61	-7.38%
Engine maximum diameter	m	0.686	0.663	-3.43%
Engine length	m	1.531	1.407	-8.07%
Engine mass	kg	302.00	221.20	-26.75%
Thrust to weight ratio		0.58	0.55	-5.17%
Aircraft empty mass	kg	1,739.53	1,751.92	0.71%
Mission fuel mass	kg	471.74	457.96	-2.92%
Aircraft take-off mass	kg	2,438.07	2,436.68	-0.06%
Undercarriage wheelbase	m	3.08	2.51	-18.56%
Undercarriage tread	m	3.02	2.84	-5.85%

Table 8-4: Quoted and Calculated Aircraft Parameters: Variable Major Parameters

As can be seen, the UCAV design synthesis code again presents the accurate results, with only the same parameters of the engine mass and the undercarriage wheelbase providing significant errors. As compared to the calculated value in Table 8-3, by allowing the optimizer to alter the overall parameters would accomplish the optimum aircraft design for a given configuration. The empty mass moves closer to the baseline value varying by only 0.71 percent. The aircraft take-off mass gives the more accurate result, varying by only 0.06 percent. Lack of data for the aircraft design missions prevents direct comparison of those results. Overall, the results are once more very good and show the high accuracy of all of the aircraft sizing modules, which will produce aircraft of the correct overall size.

To prove other accuracy of the methodology of the UCAV design and optimization synthesis, the four UCAV configurations produced by this code were compared with the correlated data of major aircraft design parameters available from Jane's Unmanned Aerial Vehicles and Targets[90] to check the validity of the design synthesis relationships. As there were only small numbers of existing UCAVs, thus it was also decided to gather some correlated data obtained from some aspects of the existing

UAVs. The full description of the existing UCAVs and UAVs selected is presented in Appendix B.

Because of the lack of design data available in the literature, the correlated data that can make the comparison are the empty mass and the available fuel mass of the aircraft. However, to compare these quoted data with the take-off mass of individual aircraft seem to perform the big gap between the differences in mass. This is because some aspects of UCAVs and/or UAVs are very small and light, while some aspects are larger and heavier depending on the purpose of the designs in order to perform the typical mission. Moreover, most of the UAVs are operated with the piston-propeller engines, and they are only designed to perform the primary role of intelligence, reconnaissance, surveillance and target acquisition. As the UCAV is designed for the aim of performing the combat mission with the use of the jet engine(s), thus the correlated data of the UCAV configurations produced by the UCAV design synthesis model will be only related to those existing aircraft with the similar designs and missions.

The four UCAV configurations used to compare the correlated data with the existing UCAVs and UAVs consist of two straight-tapered wing and two single-kink wing planforms. Two different packaging aspects were selected for both configurations (see Figure 4-4 of Chapter 4). One option is the single weapon bay located at the aircraft centreline with two-engine installations outboard of the weapon bay. They are represented as 'NWEPB1 ST' applied for the straight-tapered wing planform, and 'NWEPB1 SK' for the single-kink wing planform. Another aspect selected is composed of one weapon bay at the aircraft centreline and two weapon bays located outboard of the engines. They are expressed as 'NWEPB3 ST' and 'NWEPB3 SK' applied for the straight-tapered wing and the single-kink wing planforms, respectively.

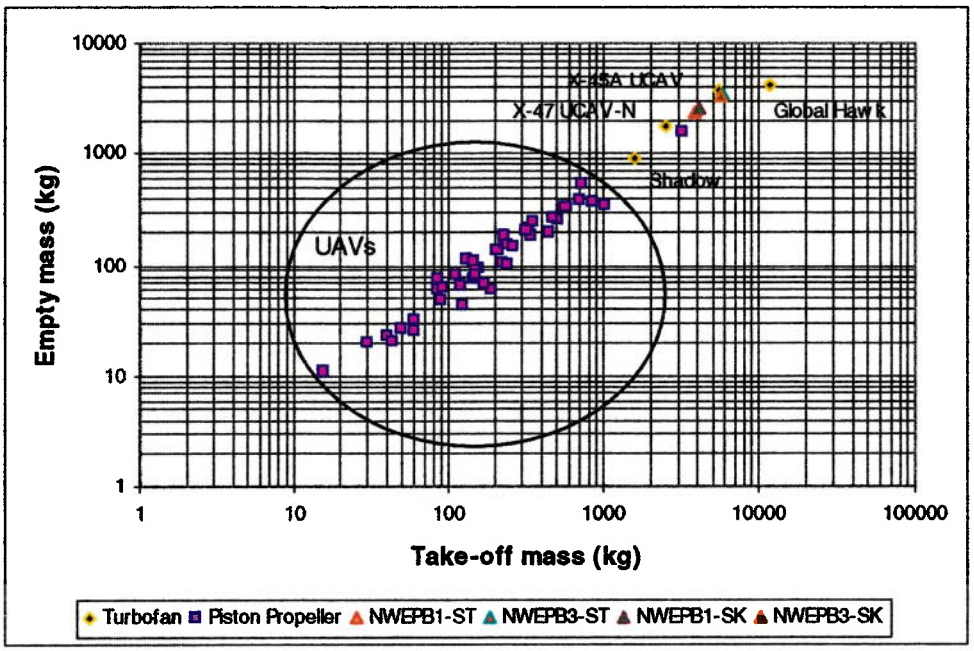

Figure 8-6: Empty Mass Estimation Correlation with Mass Trends for UCAV/UAV

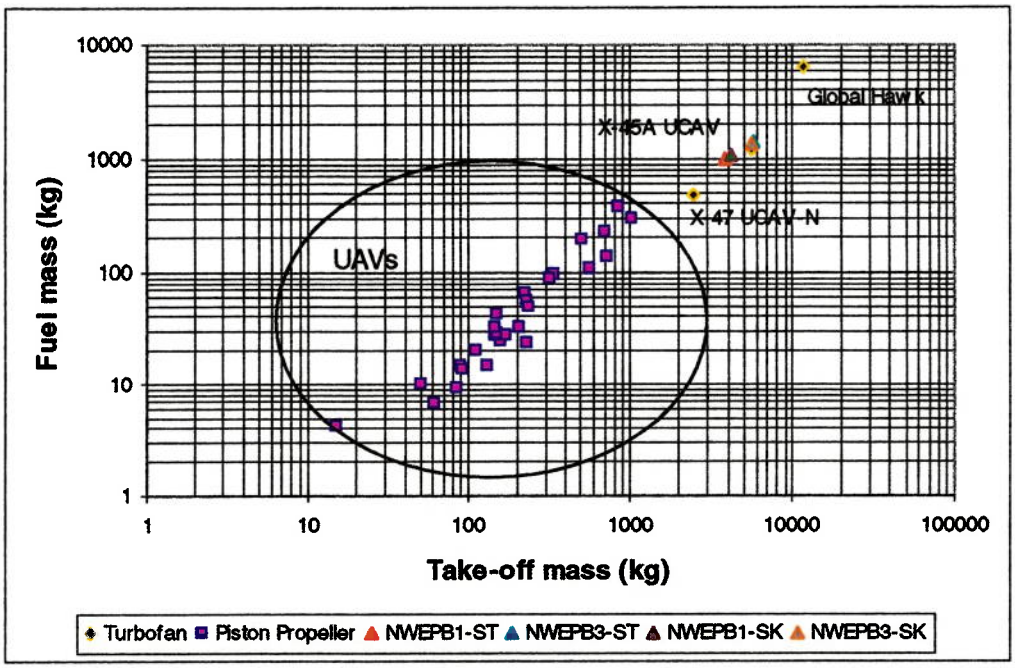

Figure 8-7: Fuel Mass Estimation Correlation with Mass Trends for UCAV/UAV

Figure 8-6 and Figure 8-7 present the mass estimation correlation of these UCAV-optimized configurations with the empty and fuel mass trends for the UCAVs and UAVs, respectively. Both charts are presented using the logarithmic scale due to the big gap between the differences in mass of typical aircraft configurations, mentioned previously. It can be seen that, most of the UAVs and/or UCAVs operated with the piston-propeller engines are precisely small and light. On the other hand, the UCAVs and/or some aspects of the UAVs functioned with the jet engines produce higher masses.

The four UCAV-optimized configurations are found to have the empty mass and the fuel mass correlated with the trends of the X-45A UCAV, and the Pegasus X-47 UCAV-N, which are operated with turbofan engines. Moreover, these aircraft are based on the tailless configuration and are designed for a primary role of SEAD/strike, which are corresponding to the aim of the design synthesis. The close correlation between the aircraft empty mass and the fuel mass are significant, as this demonstrates that the aircraft are of the correct size for internal fuel storage, although the lack of data for the aircraft design missions prevents direct comparison of those results. This correlation shows that the methodologies of the UCAV design and optimization synthesis provide the accurate results and allow the utility of the models to perform the individual studies.

8.2 Packaging and Configuration Options

The UCAV design synthesis methodology described in the previous chapters is capable of modelling two main types of flying wing configuration: the straight-tapered wing and the multi-kinks wing planforms. Before starting with the detailed coding of the aircraft design synthesis process, it is necessary to set up the *packaging specification* to define the above selected configuration and arrange the packaging aspects (see section 4.2.6 of Chapter 4). This represents a variety of particular designs, which is capable of being modelled using this design synthesis process. According to the requirements of the packaging specification for the UCAV design required by the user, in order to prevent the investigations from being too large, only the single option of the type of materials, the type of airfoils and the wing thickness ratio for inboard and outboard airfoils, and the wing twist distribution has been considered.

Assuming that the UCAVs are constructed from the carbon-fibre composite with the thickness ratio at inboard section of 15 percent and that at outboard section of 9 percent. The type of airfoils selected for both sections is based on the symmetrical airfoils. With the option of these wing thickness ratio selections, the airfoil at inboard section is the NACA 67_1-015 and that at the outboard section is the NACA 66-009. The wing is twisted from the half of the semi-wingspan to the wingtip. The study will determine the effect on the objective function, in this case the take-off mass, and also the geometry of the flying wing by varying the values of the design trades such as the cruise range, the centre of gravity, and the aspect ratio. UCAV-optimized configurations generated for a variety of packaging aspects for straight-tapered wing and multi-kinks wing planforms are presented and discussed in the following sub-sections.

8.2.1 Internal Weapon Bay

According to Figure 4-4 of Chapter 4, OPT2 and OPT4 are considered for the optimized configurations generated using the UCAV design synthesis model. OPT2 is the single weapon bay located at the aircraft centreline with two-engine installations outboard of the weapon bay. OPT4 is the complete packaging aspect considered for flying wing UCAV, which consists of one single weapon bay located at aircraft centreline with two-engine installations one on each side, and two outer weapon bays outboard of the engine bays. The 460-kg JDAM is loaded in the inner weapon bay and two 241-kg MK-82 general-purpose bombs are loaded in the two outer bays, one bomb in each bay.

These two packaging aspects are applied for the straight-tapered wing and the single-kink wing configurations performing the studies identified. Assuming that the single-kink wing planform has the fixed wing leading edge sweep and allow the optimizer to size the wing chord and the spanwise position of kink varying the trailing edge sweep between the kink positions to accommodate the packaging. During the optimization process, the size and initial mass of the weapons and weapon bays remains constant. Only the position may be varied by changing the value of two independent coordinates describing the positioning of the bays in the longitudinal and lateral directions. The dimensions of the weapon bays are one of the main sizing drivers for the wing configuration, significantly influencing its geometry, layout and mass.

Figure 8-8 illustrates the UCAV-optimized configurations with internal weapon bay packaging aspects. Only the straight-tapered wing planform with OPT2 packaging aspect, and the single-kink wing planform with OPT4 packaging aspect are presented.

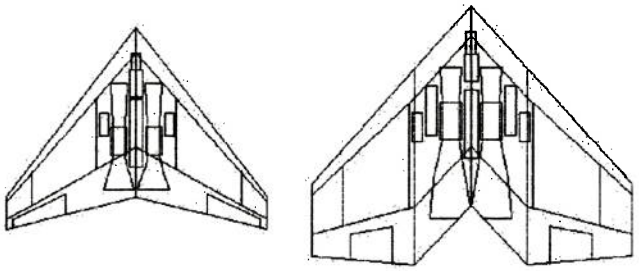

Figure 8-8: UCAV-Optimized Configurations with Internal Weapon Bay Packaging Aspects

Figure 8-9 presents the aircraft wing-structure, fuel, empty, and take-off mass values for the above aircraft configuration solutions. Increasing the number of internal weapon bays for both configurations produces the predictable results. The straight-tapered wing planform is found to have the empty mass and the gross mass increases of 42.75% and 49.60%, respectively (NWEPB3-ST vs. NWEPB1-ST). The single-kink wing planform has the mass increases of 26.01% for the empty mass and 34.72% for the take-off mass (NWEPB3-SK vs. NWEPB1-SK), which are less than those of the straight-tapered wing planform. This is because the former can only allow the wing chord at root and tip, and the wingspan to be sizing by the optimizer to accommodate the entire packaging in order to meet the overall requirements, thus, the size of the aircraft with the additional weapon bays may become much larger. For the kink configuration, the optimizer can also size the wing chord and the spanwise position of kink. This can develop more flexible shape of the aircraft in order to accommodate all the packaging, thus the aircraft mass increases from the number of weapon bays are not considerably high.

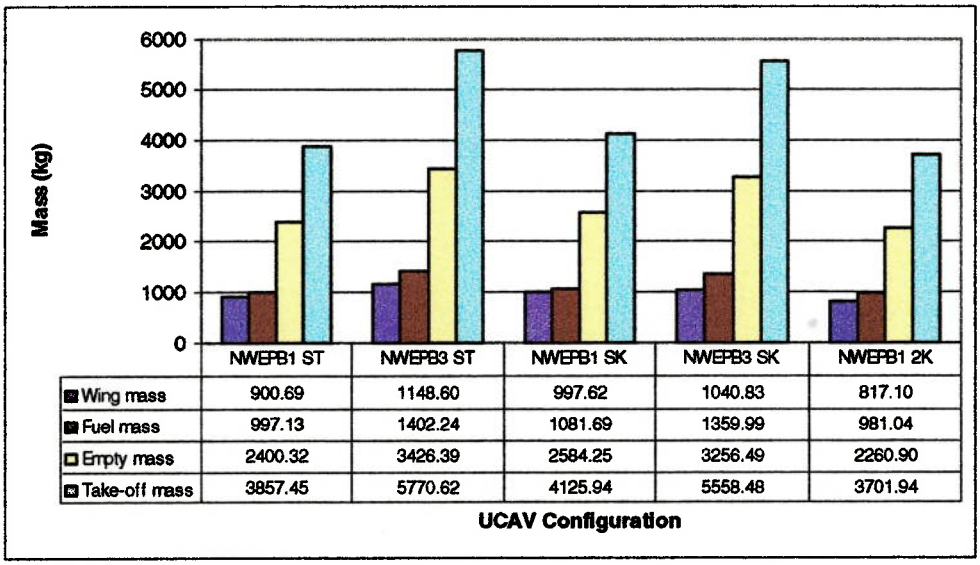

Figure 8-9: UCAV Configuration Masses with Internal Weapon Bay

Alternatively, consider the corresponding number of weapon bays in different aircraft configurations; the overall mass values produce reasonably similar results. The single-kink wing planform with the OPT2 packaging aspect (NWEPB1-SK) has the mass increases of 7.66% and 6.96% for the empty and take-off mass, respectively, over the straight-tapered wing planform (NWEPB1-ST). For the single-kink wing planform with OPT4 packaging aspect (NWEPB3-SK), the empty mass is 4.96% and the take-off mass is 3.68% less than those of the straight-tapered wing planform (NWEPB3-ST). This can be described that, since the dimension of the weapon bay does not change, the optimizer is being able to size the equivalent length of the wing root centreline chord for all the configurations with the same packaging aspects to accommodate the centre weapon bay. With this length of the wing root chord, it must also ensure to provide the sufficient remaining volume in the wing box to be able to accommodate the propulsion system (intake diffusers, engines, and two-dimensional nozzles), the two outer weapon bays (OPT4 packaging aspect), the undercarriage bay, and the integral tanks.

As mentioned previously, the straight-tapered wing configuration can only allow the wing chord at root and tip, and the wingspan to be sizing by the optimizer, thus all the packaging must be constrained within the tapered wing box performing the appropriate values of the aircraft masses. By additionally optimising on the wing chord and the spanwise position of kink(s) for the kink-wing configuration can develop more flexible shape of the aircraft to accommodate all the packaging. The slightly increased or decreased values of the aircraft masses result from the appropriate location of the kink(s) not to interfere with the control devices and applicable to accommodate all the packaging, thus affecting the planform area of the aircraft. In order to prove the more accurate results of the different aircraft configurations with the corresponding number of weapon bays, the two-kinks wing planform with the OPT2 packaging aspect (NWEPB1-2K) was also performed, which obtained the empty mass and take-off mass decreases of 5.81% and 4.03%, respectively, below the straight-tapered wing planform (NWEPB1-ST). Figure 8-10 ascertains the minor change of these aircraft masses between the straight-tapered wing and the two-kinks wing planforms.

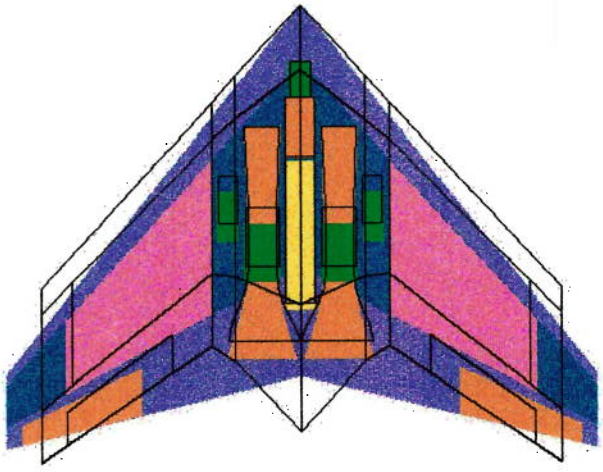

Figure 8-10: UCAV Configurations Comparison with Corresponding Number of Internal Weapon Bays

Figure 8-11 presents the trade study of a cruise range in order to determine the increase in the design take-off gross mass for the above aircraft configurations, on condition that the required range is increased as required by the customer. According to the mission performance requirements described previously, the required total cruise range of 400 nautical miles (740.80 kilometres) was set up for the aircraft to complete the mission. As can be seen by increasing the arbitrarily selected ranges, the take-off mass for the straight-tapered wing configurations increases smoothly as compared to those of the single-kink wing planforms. The latter can be described that in some values of the specified cruise ranges, the sizing of the wing chord and the spanwise position of kink(s) during the optimization process may affect the packaging accommodation and the position of the control devices. In order to meet the constraint requirements to ensure that all wing kinks are in the appropriate positions without interfering the control devices and applicable to accommodate all the packaging, the result may increase the wing structural mass of the aircraft thus increasing the larger empty and take-off masses.

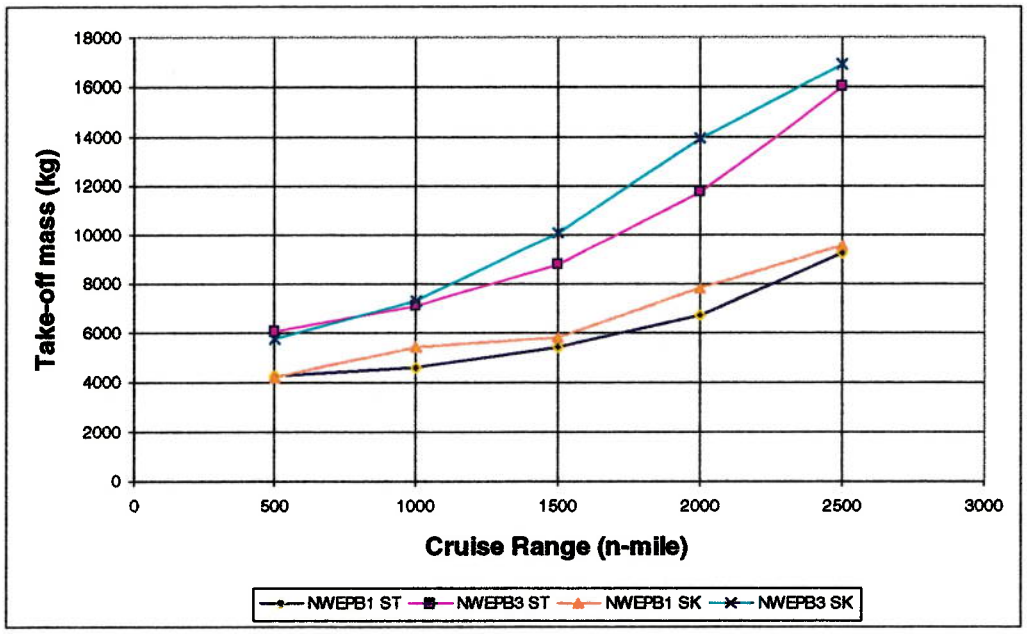

Figure 8-11: Cruise Range Trade of UCAV Configurations with Internal Weapon Bay

As can be seen from the chart that by increasing the cruise range, the take-off mass of the aircraft configurations with the OPT4 packaging aspect seem to increase rapidly as compared to those configurations with the OPT2 packaging aspect. At the beginning this can be described for all the aircraft configurations with both packaging aspects that, when the range increases the aircraft requires additional fuel in order to achieve the entire mission. Due to this reason, the wing area must be increased to provide sufficient volume for the extra fuel, thus increasing the wing structural mass. Moreover, the larger wing area also increases the drag on the aircraft. As a result, the size of the engine(s) expands in order to produce the excess thrust to stabilize the aircraft drag, thus performing heavier aircraft.

With the OPT4 packaging aspect, the aircraft consists of three weapon bays carrying the weapons to perform the mission. According to Table 8-1, during the bombs drop mission segment, the aircraft is assumed to release all the weapons on board. As a result, the CG location of the aircraft at the end of the mission segment moves immediately (see Figure 7-13 section 7.5 of Chapter 7). Additionally, considering the centre of gravity excursion for the cruise mission segment, as the range increases the aircraft CG is greatly varied due to fuel burned throughout the segment. This affects the position of forward and aft CGs in order to constrain the rapid change of the aircraft CG at the end of the cruise and bombs drop mission segments to remain within the acceptable limits. As a result of all these effects, the aircraft configurations with the OPT4 packaging aspect requires an additional extension of the CG range, which directly affects the increase of the geometries of the aircraft thus increasing the larger wing structural mass and hence the take-off mass.

8.2.2 Engine Installation

The same set of configuration options was operated as for the study of the single- and twin-engine installation; i.e. the straight-tapered wing and the single-kink wing planforms. Assuming that the single-kink wing planform has the fixed wing leading edge sweep and allows the optimizer to size the wing chord and the spanwise position of the kink varying the trailing edge sweep between the kink positions to accommodate the packaging. According to Figure 4-4 of Chapter 4, OPT3s present both packaging aspects. The engine(s) is located at the aircraft centreline with two outer weapon bays loaded with the 460-kg JDAM in each bay. The engine size and the number of engines will strongly affect the aircraft packaging, geometry, and mass. Figure 8-12 illustrates the UCAV-optimized configurations with OPT3 packaging aspects. Only the straight-tapered wing planform with twin-engine, and the single-kink wing planform with single-engine installations are presented.

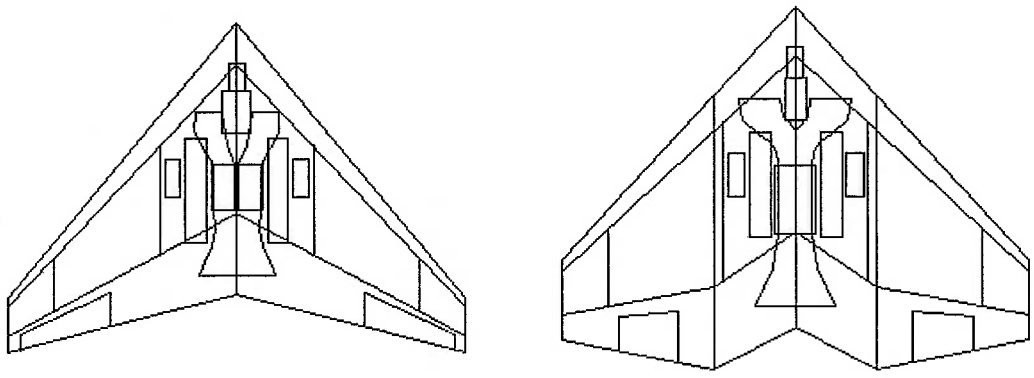

Figure 8-12: UCAV-Optimized Configurations with Engine Installation Packaging Aspects

The results of the mass totals for the UCAV-optimized configurations with packaging aspects of single- and twin-engine installations are presented in Figure 8-13. As can be seen, the UCAV configurations with the twin-engine installation produce the design take-off mass lower than those with the single-engine installation.

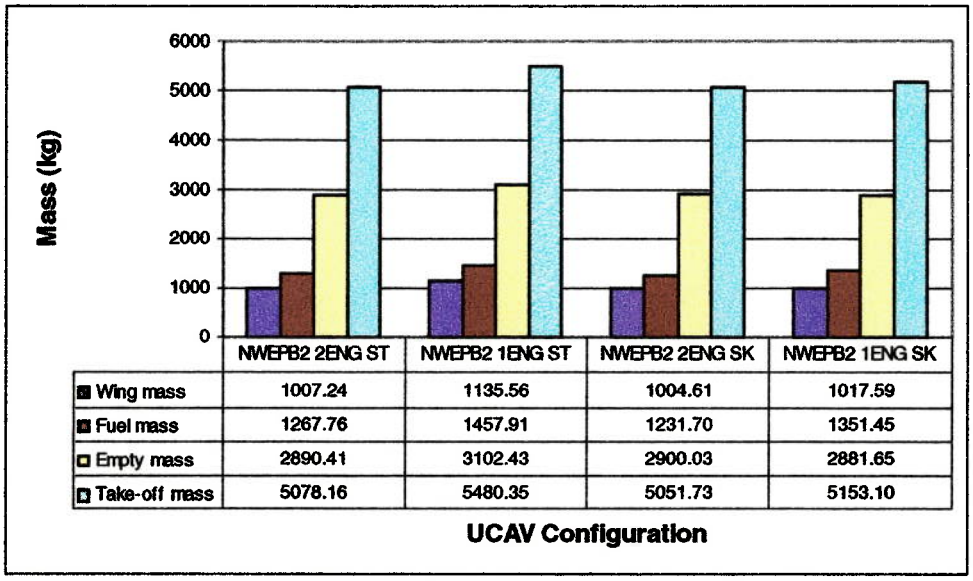

Figure 8-13: UCAV Configuration Masses with Engine Installation

Consider the straight-tapered wing planform, the single-engine design (NWEPB2-1ENG-ST) has the mass increases of 7.34% and 7.92% for the empty mass and the take-off mass, respectively, over the twin-engine configuration (NWEPB2-2ENG-ST). On the contrary, the single-kink wing configuration with single engine (NWEPB2-1ENG-SK) has the mass decrease of 0.63% for the empty mass, slightly below that with the twin engine (NWEPB2-2ENG-SK) due to the reduction of one nozzle. However, the take-off mass of the single engine (NWEPB2-1ENG-SK) is 2.01% higher than the twin-engine configuration (NWEPB2-2ENG-SK).

The increase of the design take-off mass on both straight-tapered wing and single-kink wing configurations can be explained that by reducing the number of engines, the size of the engine must increase in order to produce the required thrust to perform the similar mission. As the engine size increases, it extends the length of the aircraft centreline to expand the airfoil thickness acceptable for fitting the entire propulsion system (intake diffusers, engines, and two-dimensional nozzles) internally. As a result, the geometry of the aircraft becomes larger causing the total mass to be increased.

Similar to the study mentioned in the previous sub-section, the corresponding type of engines with different aircraft configurations can produce precisely similar results of the overall masses. Consider the twin-engine design, the single-kink wing planform (NWEPB2-2ENG-SK) has the mass increase of 0.33% for the empty mass, slightly over the straight-tapered wing planform (NWEPB2-2ENG-ST). By examining the breakdown masses of individual components for these two configurations, it is found that the empty mass increase of the single-kink wing planform (NWEPB2-2ENG-SK) comes from the mass increment of the two-dimensional nozzles. Due to the aspect of the kink configuration, the aircraft CGs locate consistently closed to the forward limit position, applicable to provide an adequate distance from the aft CG to the main undercarriage to meet the requirement for ground clearance (see section 6.2 of

Chapter 6). Thus, the position of the engines may also move slightly forward due to the above reason, constraining the nozzles to extend their length. The empty mass of the single-kink wing planform is, therefore, increased slightly as compared to the straight-tapered wing planform. On the contrary, the single-kink wing planform (NWEPB2-2ENG-SK) results in the mass decrease of 0.52% for the take-off mass, slightly below the straight-tapered wing planform (NWEPB2-2ENG-ST). The decrease of the take-off mass comes from the flexible shape of the aircraft sized by the spanwise position and the chord length of the kink to reduce the redundant area on the aircraft.

The single-kink wing configuration with the single engine (NWEPB2-1ENG-SK) also indicates a similar take-off mass decrease. The single-kink wing configuration results in the mass decrease of 5.97% for the take-off mass, below the straight-tapered wing configuration (NWEPB2-1ENG-ST). Moreover, the empty mass of the single-kink wing (NWEPB2-1ENG-SK) is also 7.12% less than that of the straight-tapered wing planform (NWEPB2-1ENG-ST). This result does not oppose to the above explanation for the increment of the nozzle's length. However, with the single-engine design, an individual engine is located at the aircraft centreline allowing the kink parameters to be more flexible in sizing by the optimizer to accommodate all the remaining components and thus, reducing more wing area and also the empty mass of the aircraft. Figure 8-14 proves the precise results of these aircraft masses by comparing the size of the straight-tapered wing with the single-kink wing planforms based on the single-engine installation.

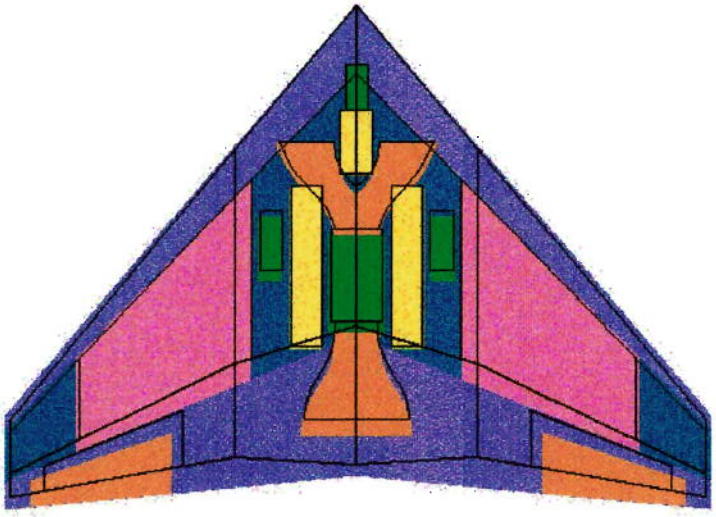

Figure 8-14: UCAV Configurations Comparison with Corresponding Number of Engines Installation

Figure 8-15 presents the trade study of the target CG based on the empty mass of the aircraft in order to determine the development in the design take-off mass for all the above aircraft configurations. It can be seen that, the take-off mass is increased as the CG is moved rearward. This is because the CG location of the main undercarriage must be located behind the aircraft aft CG in order to meet the required angle off the vertical being greater than or equal to the tipback angle or the minimum angle of 15-

degree for ground clearance (see section 6.2 of Chapter 6). The main undercarriage bay must also be fitted inside the wing box of the aircraft. As the aircraft target CG moves rearward, in order to maintain the position of the main undercarriage to meet the requirement and not extrude out of the wing box or the thickness of the airfoil, the aircraft centreline is extended reflecting in an increase in the wing area and hence the aircraft mass.

Moreover, in terms of the longitudinal control, as the aircraft target CG moves rearward, the distance from the trailing edge split elevons to the aircraft CG becomes shorter. To maintain the balance of the aircraft, either the size of the split elevons must be increased or the aircraft centreline be extended as mentioned above, thus resulting in a heavier aircraft. Additionally, the engine must be sized to provide sufficient vertical force at the intake inlet in order to corporate the split elevons to trim and control the aircraft (see section 7.2.2 of Chapter 7). The size of the engine also affects the mass increase on the aircraft.

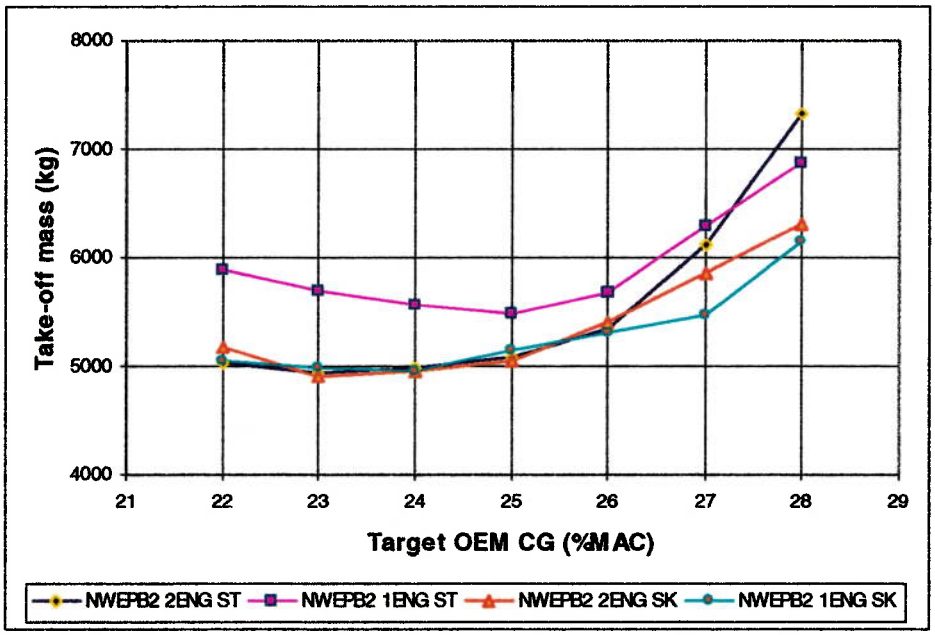

Figure 8-15: Centre of Gravity Trade of UCAV Configurations with Engine Installation: Take-off Mass Consideration

As the target CG moves rearward, the twin-engine design for both configurations seems to increase the mass higher than the single-engine designs. According to the previous explanation, the size of the engine varies to provide the vertical force at the intake inlet for the longitudinal control. This directly affects to the geometry of the intake diffuser and the two-dimensional nozzle. The twin-engine design would require extra volume to accommodate the increased size of these components internally, as compared to the single-engine configuration, thus affecting the mass increase on the aircraft.

Consider closely the single-kink wing configuration on the trade study, it can be seen that the masses of the twin-engine design (NWEPB2-2ENG-SK) vary slightly with those of the single-engine model (NWEPB2-1ENG-SK). This is due to the flexible

shape of the aircraft sized by the kink parameters along the wingspan that are capable of maintaining the precise minimum area for both configurations to fit all the components internally.

Consider the straight-tapered wing configuration, when the target CG moves forward the single-engine design tends to increase the mass further as compared to the twin-engine model. This is also due to the effects on the longitudinal control. As the position of the engine moves forward, the distance from the intake inlet to the aircraft CG becomes shorter, thus reducing the balance of the aircraft obtained from the vertical force at intake inlet. To maintain the balance of the aircraft, the engine is needed to enlarge the size to provide the mass flow rate into inlet adequate for determining the required vertical force. Thus, this affects directly to the mass increase on the aircraft particularly the single-engine design. Moreover, the effect of mass increment from the two-dimensional nozzles also enlarges the additional mass of the single-engine configuration.

The effect on the CG range of the aircraft varied by the target CG of the aircraft empty mass is one of the trade studies that could be considered as shown in Figure 8-16. A case of the single-kink wing configuration with twin-engine installation is presented.

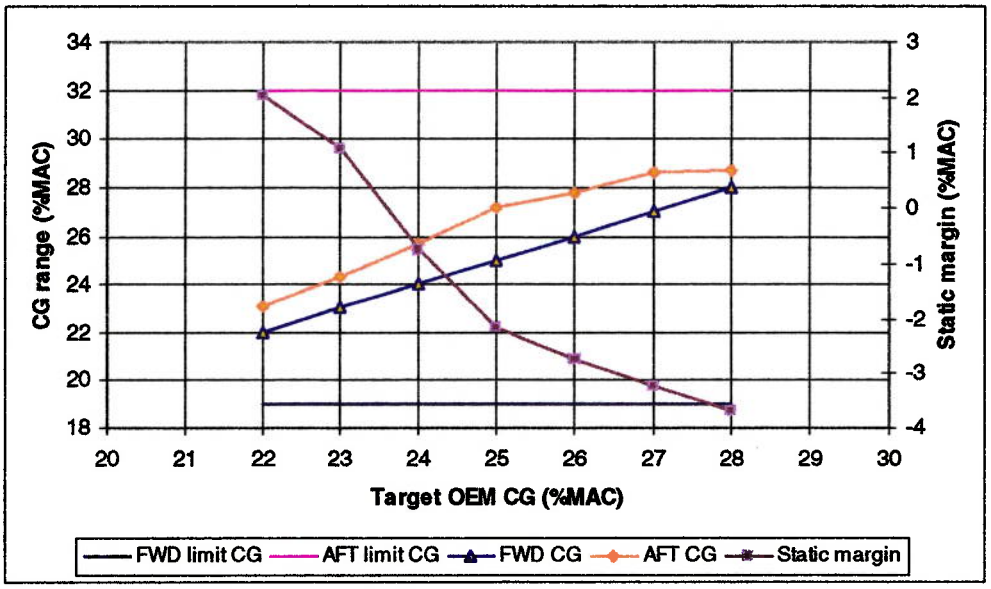

Figure 8-16: Centre of Gravity Trade of UCAV Configurations with Engine Installation: Centre of Gravity's Range Consideration

It can be seen that, the aircraft CG of the empty mass is consistently appropriate to the aircraft forward CG position. As the aircraft aspect is swept backward, this provides the CG of fuel and the weapons to be located behind the CG of the empty mass. Thus, the aircraft aft CG is the maximum value between the aircraft CG of the zero fuel mass and the take-off mass. The range of the aircraft CG is affected by fuel burned and/or payload released during each mission segment. The aircraft CG varies at the end of individual segments after the fuel is burned and/or payload released and must remain within the forward and aft CG position to ensure the balance of the aircraft. At

the end of the mission, only the reserve fuel is available in the fuel tank moving the aircraft CG close to the CG of the empty mass.

At some values of the target CG at the forward and aft positions, the forward and aft CGs of the aircraft move towards the same point. This can be defined that the geometries of the wing is varied up to the limit that they are applicable to accommodate all the components. Due to the limit of the aircraft geometries provides the closet range between the aircraft forward and aft CG, which is able to control the aircraft CG as fuel decreases in each mission segment and the aircraft CG after releasing the weapon(s) to remain within the limit in achieving the mission. Changing the target CG beyond these values would prevent a feasible aircraft from being sized.

8.2.3 Control Devices Position

According to section 5.1.3.6 of Chapter 5, the control surfaces and/or high-lift devices designed for UCAV consist of trailing edge, leading edge and inlaid control surfaces. The last two devices can be set to zero by the user in the packaging specification providing no leading edge and/or inlaid control surfaces have been selected. The study has determined four particular designs of control devices position based on the straight-tapered wing configuration with the OPT2 packaging aspect (see Figure 4-4 of Chapter 4).

A pair of leading edge control surfaces was applied for all cases. The options of NW2SE = 1 and NW2SE = 2 were considered for the trailing edge control surfaces to perform different functions of flaps, elevators, rudders, and ailerons (see section 5.1.3.6 of Chapter 5). The two cases of the above designs were applied the inlaid control surfaces to act as rudders and ailerons and allowed the trailing edge control surfaces to act only in the functions of flaps and elevators. These options have influenced the size and mass of the aircraft. Figure 8-17 presents the UCAV-optimized configuration comprising of a pair of leading edge control surfaces and inlaid control surfaces, and two pairs of trailing edge control surfaces (flaps and split elevons).

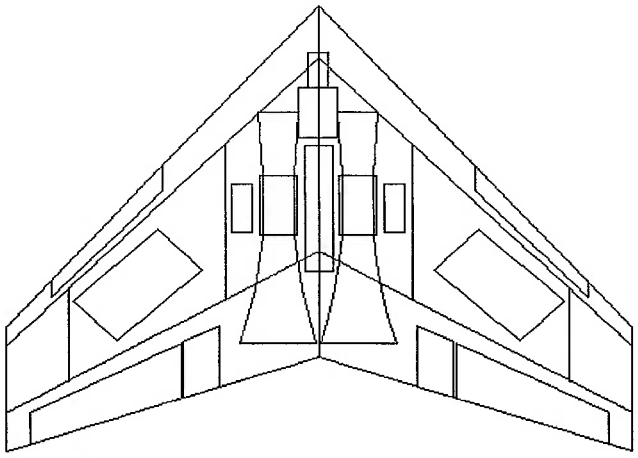

Figure 8-17: UCAV-Optimized Configurations with Control Devices Position

The Pegasus X-47 UCAV-N has provided the concept of applying the inlaid control surfaces on the top and bottom of the wing structure in order to take the place of a split drag rudder at the trailing edge to provide directional stability, as described in the literature search section 2.2.2 of Chapter 2 and section 7.2 of Chapter 7. They are supposed to have a lower radar cross section than a split drag rudder at the wing trailing edge, thus increasing the low-observable characteristics. However, the inlaid control surfaces require close examination of the airflow effect that they have on the trailing edge control surfaces positioned directly behind them[48]. The main research on this sub-section is to determine that the position of the control surfaces at the wing trailing edge and/or the inlaid control surfaces on the top and bottom of the wing structure has influenced the size and mass of the aircraft.

Figure 8-18 presents the aircraft wing structure, fuel, empty, and take-off mass values for the UCAV-optimized OPT2 configurations providing the leading edge control surfaces, trailing edge control surfaces, and/or inlaid control surfaces to control the aircraft. It should be noted that, the results of this study is obtained by applying the typical values of angle deflections for the different type of the control surfaces to size the aircraft with the specified sideslip angle in order to meet the requirement for the zero yaw stability.

The first part determines that an increase in the amount of the trailing edge control surfaces to perform different functions influences the size and mass of the aircraft. Consider the UCAV configurations without the inlaid control surfaces on the wing structure, the configuration with flaps and split elevons at trailing edge (TCS2-LCS1-INLY0) results in the mass decreases of 0.81% for the empty mass and 0.80% for the take-off mass, as compared to the configuration with only one pair of split elevons at the trailing edge (TCS1-LCS1-INLY0). For the aircraft configurations providing the inlaid control surfaces on the wing structure, the configuration with flaps and split elevons at trailing edge (TCS2-LCS1-INLY1) show a mass decrease of 1.04% and 0.88% for the empty and take-off masses, respectively, below the configuration providing only one pair of split elevons (TCS1-LCS1-INLY1).

Although the results shown are not much different, it does ensure that the increase in the amount of the trailing edge control surfaces will result in the lighter aircraft as they reduce all the loads carried by only one pair of the split elevons to trim and control the aircraft. This can be defined when the inboard flaps and the outboard split elevons are applied, the split elevons must be positioned outboard to the wing tip, which gains the largest available distance to the aircraft centre of gravity location, as described in section 7.2.2 of Chapter 7. So a small deflection produces an additional pitching moment to trim and control the aircraft. This moment also varies linearly with the sweep angle, which can be defined that for the wing with large sweep angle, only small deflections of the control devices are required. In accordance with the outboard position, the sizes of the split elevons are reduced corresponding to the wing sweep angle, thus achieving the lighter aircraft.

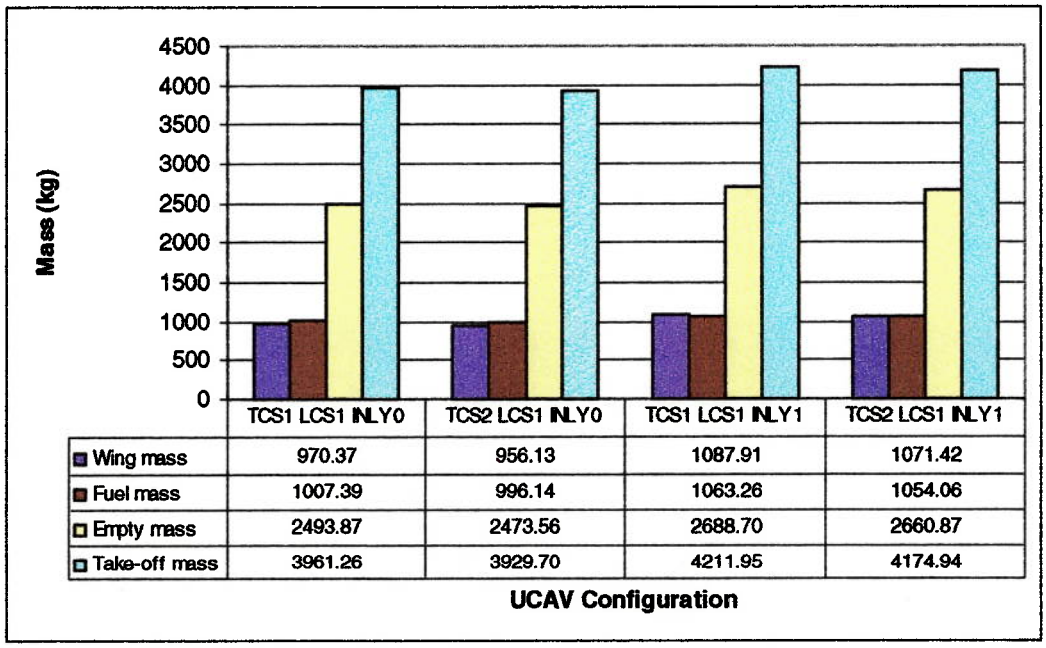

Figure 8-18: UCAV Configuration Masses with Control Devices Position

Alternatively, the second part is aimed at determining that the presence of the inlaid control surfaces on the wing structure to be responsible for the duties of rudders and ailerons has influenced the size and mass of the aircraft. Consider the aircraft configurations providing the split elevons at the wing trailing edge, the inlays configuration (TCS1-LCS1-INLY1) results in the mass increases of 7.81% for the empty mass and 6.33% for the take-off mass, over the configuration not providing the inlays (TCS1-LCS1-INLY0). For the aircraft configurations providing the inboard flaps and outboard split elevons at wing trailing edge, the inlays model (TCS2-LCS1-INLY1) has the mass increases of 7.57% and 6.24% for the empty and take-off mass, respectively, over the configuration not providing the inlays (TCS2-LCS1-INLY0).

At the beginning of this investigation for the new type of control surfaces on the wing structure, it would be expected that the presence of the inlaid control surfaces would reduce the load of control carried by the split elevons at the wing trailing edge, thus producing the lighter aircraft. On the contrary, the presence of the inlays on the wing structure adds up the additional structural mass and the mass of the actuators to the aircraft. Moreover, the tail of the inlays must be constrained not to interfere with the trailing edge devices, thus increasing the area of the wing box to accommodate these devices. The inlaid control surfaces may provide minimum drag in term of aerodynamics and perform good directional control in term of stability and control. However, in terms of packaging and configuration aspects, the presence of the inlaid control surfaces on the wing structure results in the increment of size and mass of the aircraft.

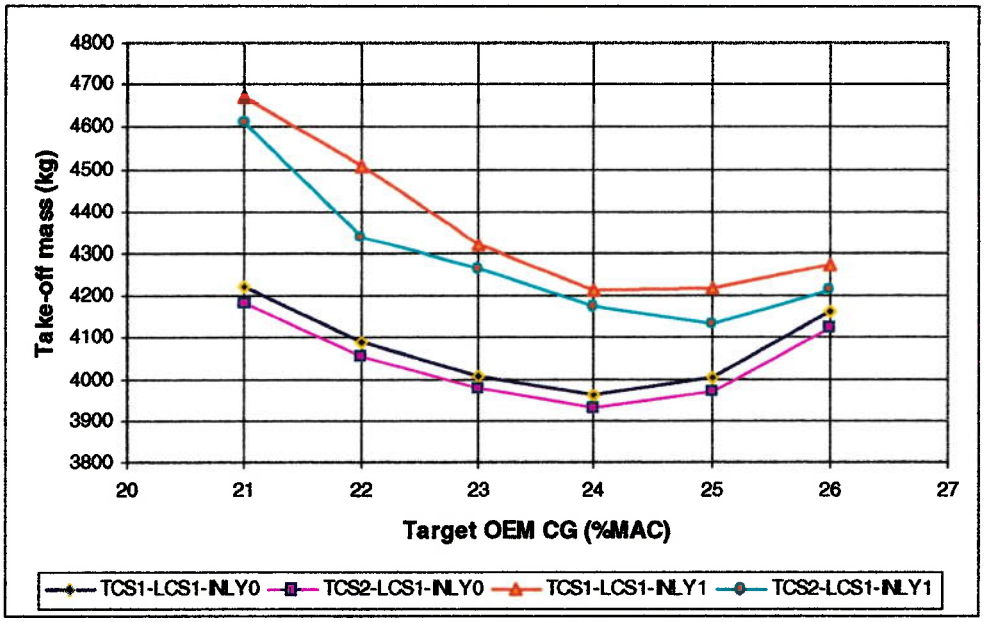

Figure 8-19: Centre of Gravity Trade of UCAV Configurations with Control Devices Position

In order to ensure the effects on the size and mass of the aircraft being influenced by the presence of the inlaid control surfaces, Figure 8-19 presents the trade study of the target CG based on the aircraft empty mass in order to determine the development in the design take-off mass for all the control device configurations. It can be seen that, the presence of inlaid control surfaces produces heavier aircraft as discussed previously. On condition that the target CG is moved forward, the inlay configurations seem to increase the mass further as compared to the configurations without the inlays. This is due to the increase of the wing geometries up to the limit that being able to accommodate all the components and balance the aircraft, which may reduce the trailing edge area to provide the appropriate size of the trailing edge control surfaces to trim and control the aircraft. Moreover, as all the aircraft CGs moves closely to the same point and due to the limit of the wing geometries affecting the trailing edge area mentioned above, the distance of the split elevons to the centre of gravity location becomes shorter as the trailing edge sweep moves slightly forward, thus the size of the split elevons must increase to produce the additional pitching moment to trim and control the aircraft. With the presence of the inlaid control surfaces, the mass increase due to the above reasons also add up the increment mass of the inlays and their actuators, thus performing the heavier aircraft.

8.2.4 Internal Weapons Carriage

To increase the low-observable characteristics and avoid the problems of possessing high drag and providing additional radar and visual reflection points caused by external weapons, the option for weapons carriage is internal. Although this is partly due to the mass penalty imposed by an internal weapon bay and its required doors, but it also due to the prevalent desire to maximize striking performance at the expense of

alternate mission performance. However, only an internal weapon bay can completely eliminate the weapons' contribution to radar cross section.

The weapons selected for performing the study of UCAV design have been obtained from three typical types used with the modern combat aircraft to form the weapon bay; the 241-kg MK-82 general purpose bomb, the 530-kg AGM-84 long-range air-to-surface missile, and the 900-kg GBU-27 laser-guided bomb. Figure 8-20 illustrates the aspect of these selected weapons and the full description of these weapons is presented in the list of weapons in Appendix B.

Figure 8-20: Weapons Selection[71]

The straight-tapered wing configuration with the OPT2 packaging aspect (see Figure 4-4 of Chapter 4) was generated as for the study of the number of store points in the lateral direction. The increase in dimension of the weapon bay with different sizes of weapons and their number of store points will strongly affect the packaging, geometry, and mass of the aircraft.

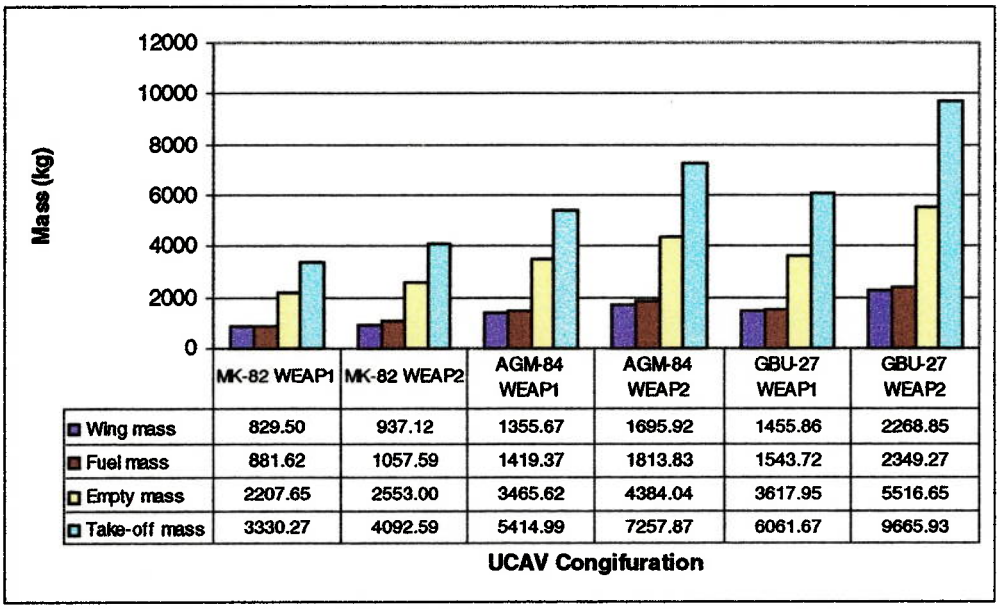

	MK-82 WEAP1	MK-82 WEAP2	AGM-84 WEAP1	AGM-84 WEAP2	GBU-27 WEAP1	GBU-27 WEAP2
Wing mass	829.50	937.12	1355.67	1695.92	1455.86	2268.85
Fuel mass	881.62	1057.59	1419.37	1813.83	1543.72	2349.27
Empty mass	2207.65	2553.00	3465.62	4384.04	3617.95	5516.65
Take-off mass	3330.27	4092.59	5414.99	7257.87	6061.67	9665.93

Figure 8-21: UCAV Configuration Masses with Internal Weapons Carriage

The results presented in Figure 8-21 summarise the mass effects of the internal carriage of the weapons shown above on the straight-tapered wing configuration with OPT2 packaging aspect. Increasing the dimension of the weapon bay with different size of weapons and their number of the store points produces the expected results. The study is applied with an increase of two store points in the lateral direction. Consider the aircraft loaded with the 241-kg MK-82 bomb, the configuration equipped with two stores (MK-82 WEAP2) has the mass increases of 15.64% for the empty mass and 22.89% for the take-off mass, over the same configuration with only one store (MK-82 WEAP1). Similarly, the aircraft armed with two 530-kg AGM-84 missiles (AGM-84 WEAP2) has the mass increases of 26.50% and 34.03% for the empty and take-off mass, respectively, over that with one store (AGM-84 WEAP1). The two 900-kg GBU-27 bombs configuration (GBU-27 WEAP2) is found to have the mass increases of 52.48% for the empty mass and 59.46% for the take-off mass, over the aircraft with one store (GBU-27 WEAP1).

This shows that when the dimension of the weapon bay is changed with the increased number of store points, the wing root centreline chord and the wingspan are expanded to provide sufficient volume in the wing box in order to fit this increased size. Thus the wing area increases performing the larger aircraft mass. Moreover, when the aircraft becomes larger, in order to complete the same mission and meet all the constraint requirements for the point performances, the larger engines are required to produce higher thrust, which directly consume more fuel throughout the mission. To ensure that the increased number of store points in the weapon bay directly affects the size of the aircraft, the aircraft configurations equipped with the one and two MK-82 bombs are presented in Figure 8-22.

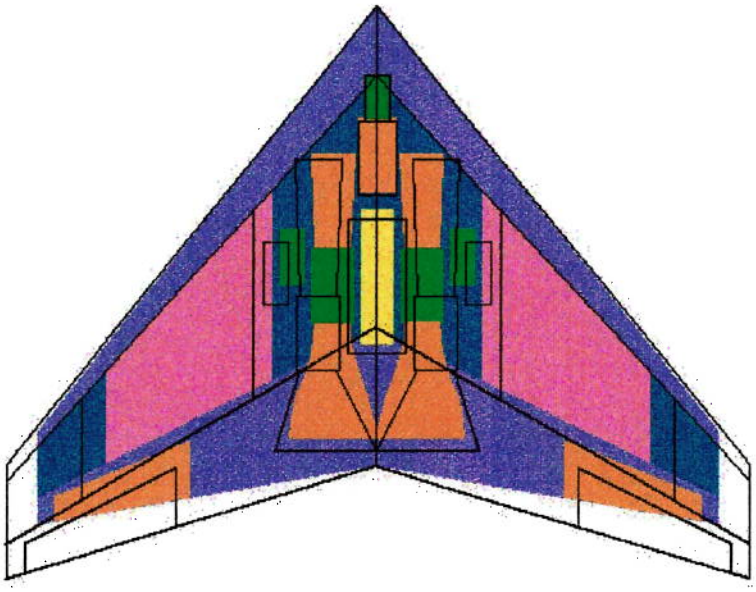

Figure 8-22: UCAV Configurations Comparison with Different Number of Internal Weapons Carriage

Due to the different size and mass of the weapons and their number of the store points to size the dimension of the weapon bay, thus the different percentage of mass increases between the one and two GBU-27 bombs configurations (GBU-27 WEAP2

vs. GBU-27 WEAP1) vary higher than those configurations equipped with the MK-82 bombs (MK-82 WEAP2 vs. MK-82 WEAP1). To support the above explanation with these changes, a trade study of the target CG is presented showing an increase of the wing area of these cases, which is directly influenced to the aircraft mass, as illustrated in Figure 8-23.

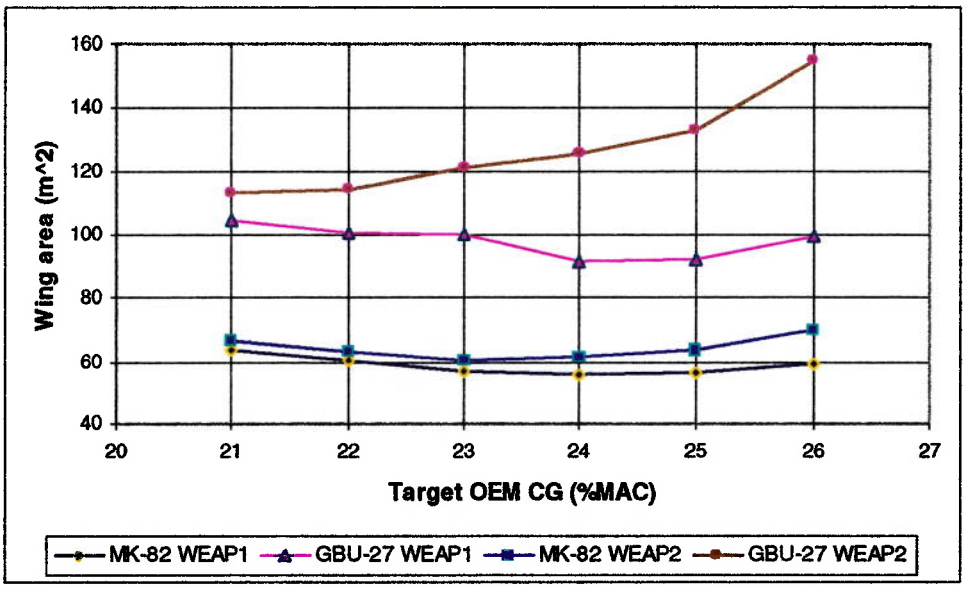

Figure 8-23: Centre of Gravity Trade of UCAV Configurations with Internal Weapons Carriage: Wing Area Consideration

The GBU-27 bomb has the tail span and the length of 0.72 and 4.32 metre, respectively, compared to 0.38-metre tail span and 2.21-metre length of the MK-82 bomb. Therefore, from the above figure, the greater variation of the wing area between the one and two GBU-27 bombs configurations ascertains that the size and mass of the bombs affects precisely to the larger mass increases.

Additionally, the trade study shows that when the target CG is moved rearward, the two bombs-loaded configurations seem to increase the wing area to a greater extent from the single bomb-loaded configurations. At first, this can be described in the similar manner that explained to the engine configurations. The location of the main undercarriage must locate behind the aircraft aft CG in order to meet the constraint requirement to ensure that the trailing edge of the aircraft does not touch the ground during the aircraft nose-up altitude. Moreover, the main undercarriage must be fitted inside the wing box of the aircraft. On condition that the target CG is moved rearward, thus the wing geometries must be sized to accommodate the main undercarriage and meet the ground clearance requirement and maintain the aircraft CG within the forward and aft limitations, which will reflect an increase in the wing area and hence the aircraft mass.

For the two-bombs loaded configurations, the width of the weapon bay expands further thus reducing the angle off the vertical from the main undercarriage position to the aircraft CG. Thus the wing geometries must be sized further in order to fit the main undercarriage inside the wing box and provide sufficient angle to meet the

requirement for ground clearance, thus increasing the larger wing area and hence the aircraft mass. The wing area of the two-bombs loaded configurations increases to a greater extent from the single-bomb loaded configurations without converging to the closed values as compared to the engine configurations. This is because the dimension of the weapon bay remains unchanged providing the size of all the aircraft configurations to increase linearly.

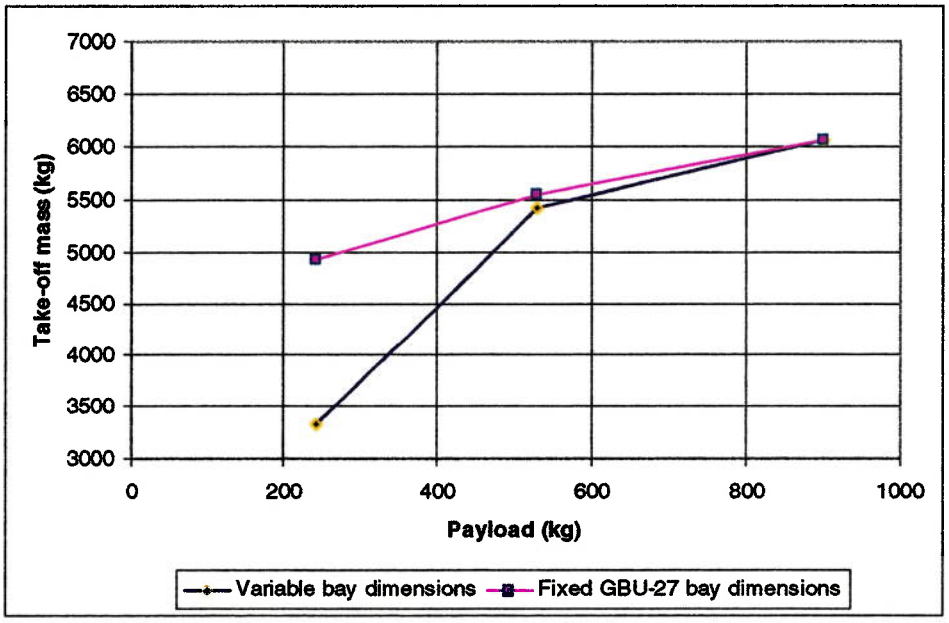

Figure 8-24: Payload Trade of UCAV Configurations with Internal Weapons Carriage

Alternatively, the payload trade study can also be considered for the internal weapons carriage, as shown in Figure 8-24. Only the aircraft configuration equipped with the single store in the weapon bay of the above three different types of weapon is presented. As can be seen, the lower trend line varies rapidly when the 530-kg AGM-84 missile is replaced the 241-kg MK-82 bomb loaded in the weapon bay to perform the mission. The aircraft take-off mass is found to have the mass increase of 62.60%. By loading the 900-kg GBU-27 bomb, an increase of the take-ff mass compared to the mass of the aircraft armed with the AGM-84 missile is 11.94%. This non-linear trend line can be described that the dimension of the weapon bay is varied with the size of all the weapons selected, thus the wing root centreline chord must be sized to accommodate this changeable dimension. Compare the length of 2.21 metre of the MK-82 bomb to 4.32-metre length of the GBU-27 bomb; the weapon bay length expands twice from the original dimension, thus directly constrains the larger size of aircraft.

To achieve the smooth variation of the payload trade, the upper trend line is performed by applying the fixed dimension of the weapon bay based on the geometry of the GBU-27 bomb to equip all the selected weapons. As a result, the more accurate values of the aircraft take-off mass obtained from these different types of weapon are achieved. Undoubtedly, the take-off mass of the aircraft loaded with the MK-82 bomb must increase due to the bigger size of the weapon bay, which expands the geometry

of the aircraft. For the AGM-84 missile-loaded configuration, the take-off mass does slightly increase, as the size of this weapon is not considerably different from that of the GBU-27 bomb. To ascertain that the dimension of the weapon bay directly affects the size of the aircraft, the comparison between the aircraft configurations equipped with the MK-82 bomb and the GBU-27 bomb is presented in Figure 8-25.

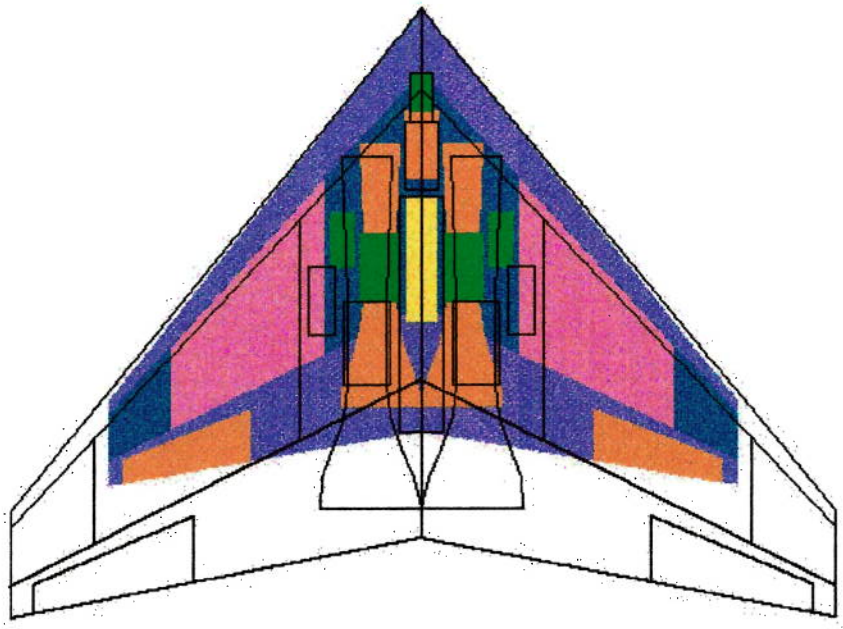

Figure 8-25: UCAV Configurations Comparison with Different Types of Internal Weapons Carriage

8.2.5 Inboard Airfoil Selection

According to section 4.2.7 of Chapter 4, the concept of airfoils selected for UCAV configuration is an attempt to choose all types of either symmetrical or asymmetrical airfoils to fit all the components internally without the use of any fairing on the shape of the aircraft. This would be beneficial for low observability since it would provide a "cleaner" shape. Moreover, this would be helpful if, in future, the new type of airfoils is required to fit these components. The selected airfoils have been obtained from typical NACA series to set the configuration design aspects of the UCAV.

The inboard section of the wing presented a big challenge for the airfoil selection, since it was required to have an airfoil that would allow for all the packaging to be fitted. The study has determined two selected airfoils: the NACA 67_1-015 symmetrical airfoil, and the NACA 65_2-415 asymmetrical airfoil. Both types of airfoil have the thickness to chord ratio of 15 percent (RTW = 15 set by the user in the packaging specification). They were applied for the straight-tapered wing configuration with the OPT2, OPT3 (twin engine configuration), and OPT4 packaging aspects (see Figure 4-4 of Chapter 4). The different type of airfoils has significantly affected the packaging, geometry and mass of the aircraft.

The results of the mass totals for the UCAV-optimized configurations with all the above packaging aspects are presented in Figure 8-26. All the results are based on the aspect ratio of 2.70. It can be seen that, the aircraft configurations with the asymmetrical airfoil produce higher masses than those with the symmetrical airfoil. With OPT2 packaging aspect, the asymmetrical airfoil configuration (NWEPB1-ASYM) is found to have the mass increases of 31.43% for the empty mass and 28.60% for the take-off mass, over the symmetrical airfoil configuration (NWEPB1-SYM). Consider the OP3 packaging aspect with the twin-engine installation; the asymmetrical airfoil configuration (NWEPB2-ASYM) has the mass increases of 40.68% and 33.81% for the empty and take-off mass, respectively, over the symmetrical airfoil configuration (NWEPB2-SYM). The asymmetrical airfoil configuration with the OPT4 packaging aspect (NWEPB3-ASYM) has the mass increases of 26.48% for the empty mass and 22.27% for the take-off mass, over the symmetrical airfoil configuration (NWEPB3-SYM). The aircraft configurations with all three packaging aspects produce the considerably similar results of the mass increases when all the components are packaged within the asymmetrical airfoil, as compared to the symmetrical airfoil.

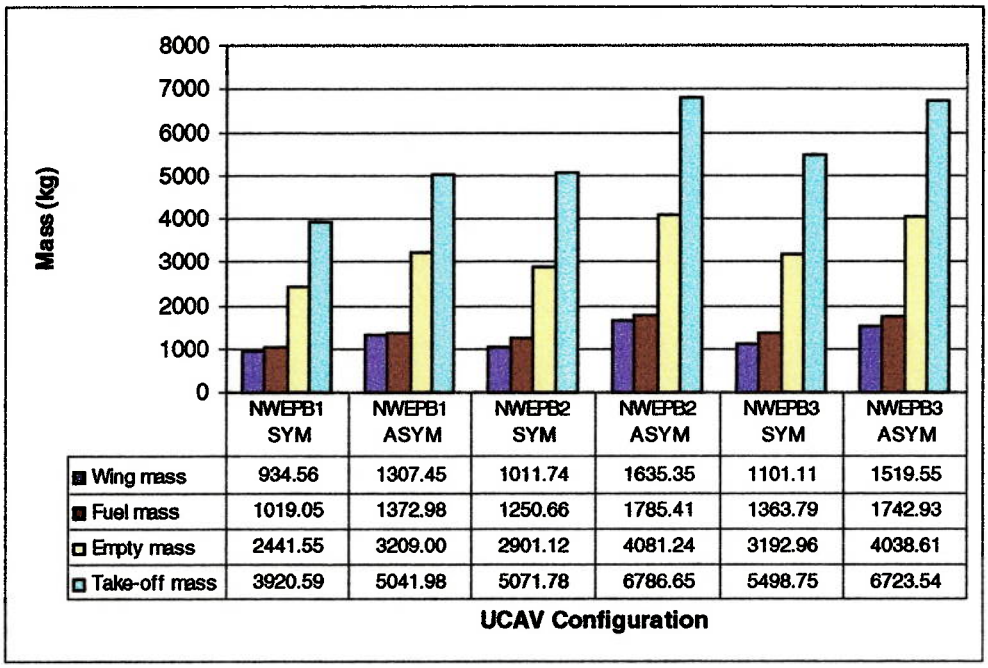

	NWEPB1 SYM	NWEPB1 ASYM	NWEPB2 SYM	NWEPB2 ASYM	NWEPB3 SYM	NWEPB3 ASYM
Wing mass	934.56	1307.45	1011.74	1635.35	1101.11	1519.55
Fuel mass	1019.05	1372.98	1250.66	1785.41	1363.79	1742.93
Empty mass	2441.55	3209.00	2901.12	4081.24	3192.96	4038.61
Take-off mass	3920.59	5041.98	5071.78	6786.65	5498.75	6723.54

Figure 8-26: UCAV Configuration Masses with Inboard Airfoil Selection

Undoubtedly, the asymmetrical airfoil configurations have the wing box volume less than the symmetrical airfoil planforms due to the wing camber of the airfoil. This directly affects the packaging to be fitted inside the wing box of the aircraft. The wing root centreline chord and the wingspan must expand to increase the thickness of the airfoil in order to accommodate all the components, thus increasing the mass of the aircraft. Moreover, increase the thickness of the airfoil causes the additional drag on the aircraft. In order to minimize the aircraft drag, the size of the engine(s) must expand in order to produce the excess thrust to stabilize the aircraft drag, thus performing heavier aircraft. To ensure the mass increases of the asymmetrical airfoil

configurations compared to those of the symmetrical airfoil planforms, Figure 8-27 presents the configuration layout of both airfoils with the OPT2 packaging aspect.

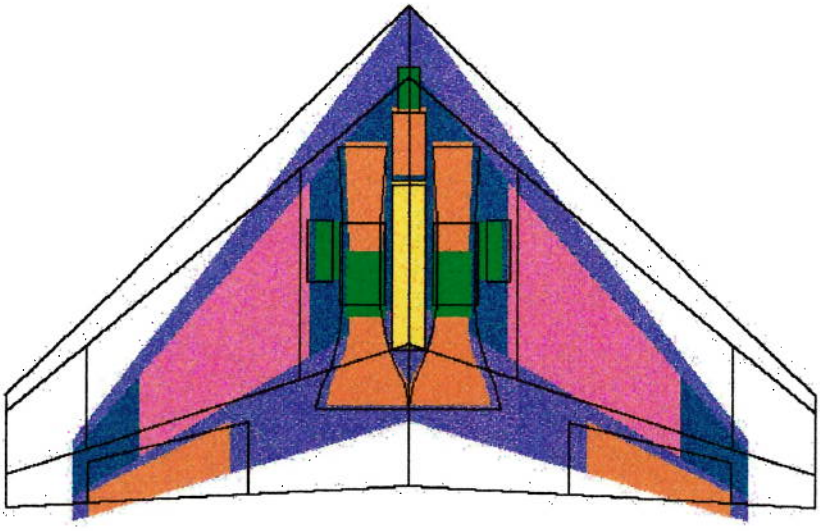

Figure 8-27: UCAV Configurations Comparison with Different Types of Inboard Airfoil Selection

As can be seen from the figure, the planform layout of the asymmetrical airfoil configuration has the wing leading edge sweep less than that of the symmetrical airfoil configuration. This is due to the position of the two-dimensional nozzles to be integrated within the wing trailing edge. As described in section 5.1.3.3 of Chapter 5, the height of the nozzle exit is limit by the relative thickness of airfoil at the trailing edge in area of the engine position. As the asymmetrical airfoil provide the small area at aft region, thus it constrains the nozzles forward until the relative thickness of the airfoil is met. As a result, the weapon bay must also move forward as its rear face is constrained by the position of the nozzles. This may allow the front face of all the bays extruded out of the airfoil. In order to prevent this extrusion, the wing sweep must reduce and also expands the wing root centreline chord and the wingspan to provide sufficient volume to accommodate all the packaging.

As mentioned previously, the above results were obtained at the aspect ratio of 2.70. In order to investigate the effect of asymmetrical airfoil configuration with the packaging, a trade study of the aspect ratio was performed as shown in Figure 8-28. The symmetrical airfoil configuration was also determined to compare with the asymmetrical airfoil planform. Both cases were determined based on the OPT2 packaging aspect.

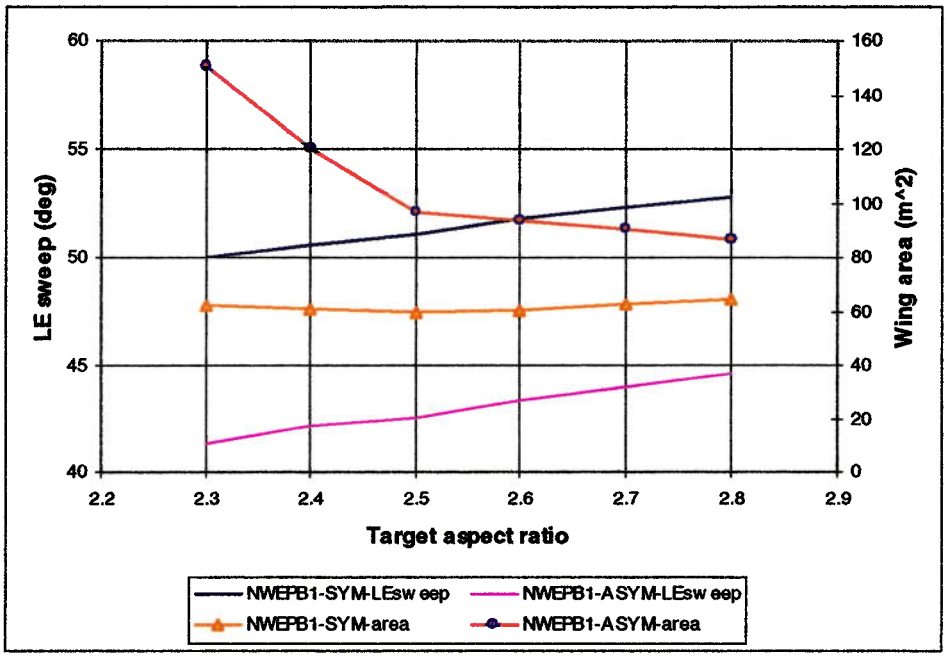

Figure 8-28: Aspect Ratio Trade of UCAV Configurations with Inboard Airfoil Selection: Leading Edge Sweep and Wing Area Consideration

From the chart it can be seen that, the leading edge sweep of the aircraft with both types of airfoil varies slightly when the aspect ratio is changed. Consider the symmetrical airfoil configuration, the change in aspect ratio does not take much effect to the wing area and also the leading edge sweep. In term of the packaging, it can be defined that, when the aspect ratio is changed, the optimizer attempts not to vary the wing area as aircraft provides sufficient volume to accommodate all the packaging and is able to minimise the aircraft mass. By doing this, the wingspan and the wing root centreline chord is slightly changed by the optimizer to perform a considerably similar result of the wing area. Because of the fixed thickness to chord ratio, the wing leading edge must be varied slightly in order to maintain the wing structural mass at as low a value as possible. The variation of the wing leading edge sweep also maintains the distance of the split elevons at the wing trailing edge to the centre of gravity location to balance the aircraft, thus reducing the size of the split elevons and hence the wing structural mass (see section 7.2.2 of Chapter 7).

For the asymmetrical airfoil configuration, changing the wing aspect ratio affects the variation of the wing area corresponding to the wing-leading sweep. When the aspect ratio is constrained, this is influenced to the wingspan and the wing area of the aircraft. As the wingspan is varied to fit all the packaging in the asymmetrical airfoil, the wing area must also vary in order to maintain the target aspect ratio. The wing leading edge is varied to help accommodating all the packaging and maintains aircraft centre of gravity to balance the aircraft. Increasing the aspect ratio also increases the wing-leading sweep similar to the symmetrical airfoil configuration, moving the packaging to the front region of the asymmetrical airfoil, which contain more area available to accommodate the entire packaging better. Thus the wingspan and the wing root centreline chord is able to become shorter after the entire packaging is fitted and thus reducing the wing area of the aircraft.

8.2.6 UCAV and Manned Combat Aircraft Comparison

Modern military aircraft are very large, heavy, complex, and expensive because of the human-related systems they must carry, for example, the environmental systems, the ejection seats, and the instrumentations. By eliminating these requirements, the UCAV can be built much smaller, much lighter, and more aerodynamic than its manned counterpart. Being smaller, the UCAV would be harder to detect by radar. In addition, the absence of a cockpit means that the engine air intake can be buried in the upper surface as illustrated in Figure 8-2, which is the most favourable position for maintaining the low observability.

To study the aircraft mass and geometry penalties caused by the presence of a human pilot, the comparison between the UCAV and the manned combat aircraft configurations was considered. The option set by the user in the packaging specification, TAC, selects the type of aircraft to be synthesized. This option arranged different avionic instruments in the radar bay located at the aircraft nose according to the aircraft configuration. For the selection of manned combat aircraft estimation, the systems that are necessitated by the presence of a human pilot have been added, including the gun and the ammunition. A mass of 90 kg per crewmember was applied for all manned aircraft configurations.

The ultimate load factor is calculated according to the aircraft configuration, by multiplying the 7.33g design load factor by the safety factor of 1.33 for the UCAV and by that of 1.5 for the manned aircraft. To investigate the accuracy of penalties between these two configurations, the safety factor of 1.5 was also applied to the design load factor for the UCAV. The straight-tapered wing planform with OPT2 packaging aspect was selected for performing these case studies. The entire configurations were loaded with the 460-kg JDAM in the weapon bay.

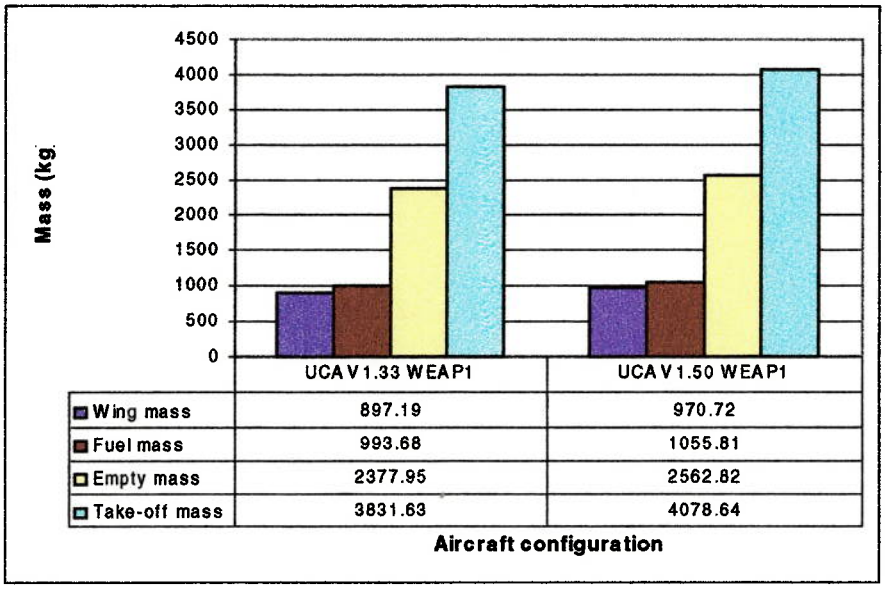

Figure 8-29: UCAV Configuration Masses with Different Values of Safety Factor Consideration

In advance of considering the comparison between the UCAV and the manned combat aircraft configurations, Figure 8-29 presents the accuracy of mass penalties caused by the different values of safety factor applied for performing the ultimate load factor in the calculation of the wing structural mass for the UCAV. It can be seen that, the UCAV configuration with 1.50 safety-factor value (UCAV1.50-WEAP1) results in the mass increases of 8.20% for the wing structural mass, 7.77% for the empty mass and 6.45% for the take-off mass, over the configuration with 1.33 safety-factor value (UCAV1.33-WEAP1). The results from applying the higher value of the safety factor do not cause many penalties on the masses and also the geometry of the UCAV, as presented in the following table:

Aircraft	**UCAV**			
Parameter	**Unit**	**SF 1.33**	**SF 1.50**	**%**
Wingspan	m	12.51	12.67	1.28%
Wing root chord	m	8.02	8.30	3.49%
Wing tip chord	m	1.60	1.83	14.38%
Wing leading edge sweep	deg	51.73	51.23	-0.97%
Wing area	m^2	60.23	64.17	6.54%
Engine maximum thrust	N	21,903.57	23,322.01	6.48%
Wing structural mass	kg	897.19	970.72	8.20%
Fuel mass	kg	993.68	1,055.81	6.25%
Empty mass	kg	2,377.95	2,562.82	7.77%
Take-off mass	kg	3,831.63	4,078.64	6.45%
Wing loading	kg/m^2	63.62	63.56	-0.09%
Thrust loading		0.58	0.58	0.00%

Table 8-5: UCAV Configurations Comparison with Different Values of Safety Factor Consideration

As can be seen from the table, the external geometries and the masses of the UCAV configuration with 1.50 safety-factor value increase slightly as compared to those of the configuration with 1.33 safety-factor value. The wing leading edge sweep reduces to some extent in order to move the aircraft centre of gravity forward for balance. Reducing the sweep creates the additional drag on the aircraft, thus the engine(s) expands to some extent increasing the excess thrust to stabilize the aircraft drag. The fuel mass increase of 6.25% is required by the larger engine(s) in order to achieve the performance requirements. The wing structural mass is directly increased from the specified safety-factor value in order to satisfy either adequate torsional stiffness or bending and shear constraints. Moreover, the mass increment of the wing also obtains from the control surfaces and miscellaneous structures related to the wing. The wing area increases to accommodate the larger engines and additional fuel, thus increasing the aircraft masses. The wing loading and the thrust loading result in a minor change that which they are required to perform the similar mission. Due to a minor change of the geometry and mass of the aircraft obtained from the estimation using the different values of the safety factor, thus the UCAV configuration with 1.33 safety-factor value is selected for the comparison of the aircraft mass and geometry penalties with the manned combat aircraft using 1.50 safety-factor value.

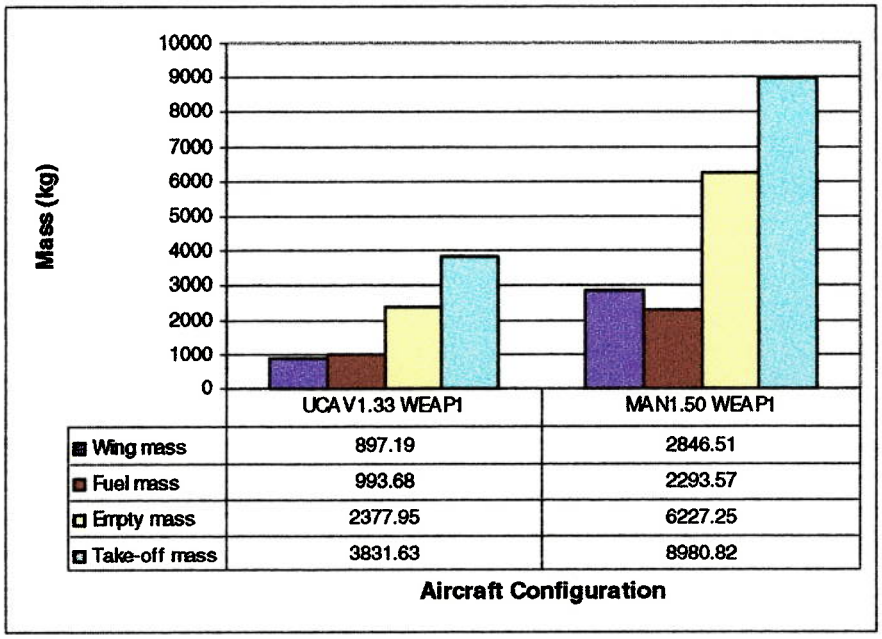

Figure 8-30: UCAV and Manned Combat Aircraft Configuration Masses

Figure 8-30 presents the aircraft wing-structure, fuel, empty, and take-off mass values for the UCAV and manned combat aircraft configuration solutions. As can be seen, the manned combat aircraft (MAN1.50-WEAP1) is found to have the mass increases of 161.87% for the empty mass and 134.39% for the take-off mass, over the UCAV (UCAV1.33-WEAP1). On the other hand, the UCAV (UCAV1.33-WEAP1) has the mass decreases of 38.19% for the empty mass and 42.66% for the take off mass, below the manned combat aircraft (MAN1.50-WEAP1). The penalties caused by the presence of a human pilot provide a big change as compared to the UCAV. To ascertain this trade, Table 8-6 summarises the aircraft components and their mass of the manned combat aircraft compared to those of the UCAV:

Components		Mass (kg)		
		UCAV (SF 1.33)	Man Combat (SF 1.50)	
			Comparable Combat Systems	Complete Combat Systems
Wing		897.19	2,846.51	2,982.17
Nose undercarriage		30.02	61.61	67.13
Main undercarriage		217.40	448.42	488.76
Engine installation		409.05	1,100.18	1,311.90
Two-dimensional nozzles		80.32	146.08	169.46
Avionics	MMS	51.34	51.34	127.84
	FMS	119.04	119.04	119.04
	SMS	8.32	8.32	8.32
	EWS	9.64	9.64	9.64

Components		Mass (kg)		
		UCAV (SF 1.33)	Man Combat (SF 1.50)	
			Comparable Combat Systems	Complete Combat Systems
Systems	Air condition	6.56	82.89	92.78
	De-icing	25.79	46.82	50.05
	Electrical	132.20	269.69	293.70
	Flight control	134.47	285.34	311.69
	Fuel	75.42	174.08	184.08
Internal pylon/launcher		62.50	62.50	62.50
Weapon bay increment		118.69	124.18	125.30
Cockpit		-	300.62	300.62
Gun		-	-	120.00
Empty Mass		**2,377.95**	**6,137.25**	**6,824.99**
Weapon in centre bay (JDAM)		460.00	460.00	460.00
Ammunition		-	-	80.00
Pilot		-	90.00	90.00
Zero Fuel Mass		**2,837.95**	**6,687.25**	**7,454.99**
Fuel		993.68	2,293.57	2,425.32
Take-off Mass		**3,831.63**	**8,980.82**	**9,880.31**

Table 8-6: UCAV and Manned Combat Aircraft Configuration Masses Comparison

As can be seen, the systems necessitated by the presence of a human pilot (including the gun, the ammunition, and the fighter multimode radar on the right column) have been added to the nose area of the aircraft. These components add the additional masses to the aircraft and constrain the aircraft centre of gravity moving forward, thus rotates the aircraft further nose down. This is because of the flying wing configuration; the wing aerodynamic centre position is located behind the aircraft centre of gravity that the lift through the wing aerodynamic centre and the wing moment about the aerodynamic centre consistently produce the negative values of the pitching moment. Moving the aircraft CG forward increase the distance from the wing aerodynamic centre to the aircraft CG, thus providing the aircraft further nose-down attitude. To balance the aircraft, the positive pitching moment produced by the vertical force at the inlet front face and the operation of the control devices is required (see section 7.2.2 of Chapter 7). This vertical force is based on the engine mass flow rate into inlet, thus this further stabilized pitching moment directly expands the size of the engines and the dimensions of the intake diffuser. On condition that the positive pitching moment is not adequate to balance the aircraft, the operation of the control devices is unavoidable to accomplish the additional pitching moment, thus affecting their dimensions. The mass increases by the presence of a human pilot also affect the size and position of the undercarriage. Moreover, the extra air condition is necessary for the presence of the cockpit. With all these changes of the internal components and also the presence of the cockpit directly affect the increase of the aircraft geometry in order to accommodate all these variable components and balance the aircraft, thus

generating the heavier aircraft. In order to ascertain that by eliminating these requirements of the human-related systems and the presence of the human pilot can build much smaller and much lighter UCAV than its manned counterpart, Figure 8-31 shows the comparison between the geometry of the UCAV and the manned combat aircraft with comparable combat systems.

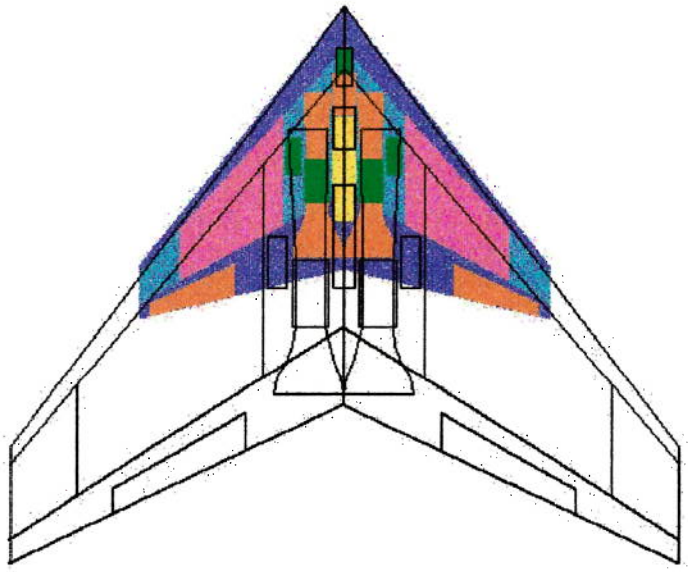

Figure 8-31: UCAV and Manned Combat Aircraft Configurations Comparison

The manned combat aircraft with complete combat systems (including the gun, the ammunition, and the fighter multimode radar, as presented on the right column of Table 8-6) requires additional fuel to carry the ammunition used during the strafe mission segment. This affects the increase of the aircraft geometry in order to accommodate all these variable components and provide sufficient volume for containing the mission fuel required, thus generating the heavier aircraft.

8.3 Summary

This chapter has demonstrated the capabilities of the UCAV design synthesis model and its operation with the optimization tool, given an example of the convergence path achieved for one of the aircraft solutions. The example aircraft specifications, including detailed mission and point performance requirements have been described for performing the studies identified. The validation of the synthesis methodology applied for the Pegasus X-47 UCAV-N was accomplished and also compared some possible masses produced by this code with several configurations of the existing UCAVs and some configuration aspects of the UAVs. Finally, the individual studies for a variety of packaging and configuration design aspects have demonstrated showing the flexibility and capability of the design tool in modelling and optimising many configurations of the UCAV and also the optional manned combat aircraft for direct comparisons of packaging, configuration layout and mass.

CHAPTER 9

9 Discussion and Conclusions

This chapter is aimed to provide a review of the research study, and provide additional discussion of the research objectives. Additionally, the lists of improvements that could be made to some of the models are added, including a suggestion of the areas for further work, and finally outline some overall conclusions of the research study.

9.1 Accomplishment of Project Objectives

Historically, only UAVs have been constructed primarily applied for reconnaissance and observation but not for combat operations. A new type of UAV – an Uninhabited Combat Air Vehicle (UCAV), as its name implies, the UCAV goes beyond the observation and is designed to attack the enemy targets.

The overall aim of the research study is to produce a useable, working model to optimize the design of the UCAV, principally the investigation of the packaging and configuration design aspects. Generally, the UAVs have been designed in a similar way to the existing manned aircraft with the exception of no human operator onboard and carried only the effective avionics instruments for observing the targets. The methodology for UCAV in this research study is aimed to incorporate the advanced technology in the form of design for low observable (stealth) concept based on the "flying wing" design with all the components including the weapon(s) packaged internally to perform the configuration design aspect.

The achievement of these aims required a large composition of work, which included: the formulation of a possible packaging and configuration design aspect estimating methodology for the UCAV flying wing configuration, the design accomplishment for the conceptual design of the UCAV, the use of optimization processes, and the incorporation of all of these models into a comprehensible software tool. This section will review each of the major creations of work that have subscribed to this thesis and discuss the operative use of them to meet their particular aims.

9.1.1 Review of Literature Search

The literature search and the sufficient background were an invaluable principal step in the development of the design aspects of the UCAV concept synthesis. The literature search of the UCAV ascertained an extremely useful activity at the start of the project to achieve all of the objectives comprising of: determining the state of the art in the subject, gathering data and models applicable for the development of the tool, and performing the perfect solution for the optimum design.

Using the information gathered from the literature search, the UCAV packaging and configuration design aspect was defined to contain as many as possible of the general features of the stealth technology. They included an option for flying wing with tailless span-loader; internal weapons carriage; curved engine intakes; and employing the two-dimensional nozzles.

The UCAV concept indicated that the air-to-ground attack: especially the Suppression of Enemy Air Defenses (SEAD), and deep penetration strikes would be the primary missions for the UCAV. Alternative roles for the UCAV might be used for the air-to-air combat or the C4ISR similar to the existing UAVs. Using this information, the mission performance analysis for the UCAV design was considered with four typical mission profiles: the low-level strike mission, the counterair mission, the surveillance and reconnaissance mission, and the ferry mission. The latter mission was determined considering the use of auxiliary fuel tanks carried inside the internal weapon bays for a ferry range. The aim of this calculation for the mission performance analysis was to accumulate the avionics instruments and the weapons required for that particular mission, to size the avionics bays and the weapon bays in order to achieve the investigation of various packaging and configuration design aspects of UCAV.

It is fair to say that the literature review considerably achieved all of its original aims. Since this aircraft breaks away from the conventional concepts, the further analysis and development would be challenged in repeating all documented search for the accomplishment of the perfect design.

9.1.2 Initial Sizing Study

As the UCAV was a fundamental departure from a conventional design, it was possible to work on improving the definition of the design. The first step in the design procedure consisted of obtaining the rough estimate of the general properties of the aircraft. The initial sizing program for the military jet trainer aircraft provided the opportunity to gain some early knowledge on the primary variables and constraints requirements that would apply for the design synthesis methodology of the UCAV, and to understand the use of the optimization technique to find out the solution. It is an initial sizing study that the basic questions of configuration arrangement, size and mass, and performance are answered. Aircraft must normally meet very inflexible range, endurance, and velocity objectives while carrying a given payload. It is important, to be able to predict the minimum aircraft mass and fuel mass needed to accomplish a given mission.

For an initial sizing study, the primary design variables were used to make the first estimate of the required total mass and fuel mass to determine if they really would perform the design mission. Actual mass, aerodynamics, and propulsion characteristics were analysed and subsequently used to do a detailed sizing calculation. Furthermore, the performance capabilities of the design were calculated and compared to the design requirements. Optimization techniques were then used to find the lightest aircraft that would both perform the design mission and meet all performance requirements by allowing the determination of optimum aircraft design variables for a given set of data.

The initial sizing program has been demonstrated to deliver realistic results for a military jet trainer aircraft model as compared its design specification with the existing similar aircraft. This case study provided a sufficient knowledge and information in advance of activating the UCAV design. Moreover, it is worthy to gain all information on the major parameters needed for the conceptual design process for the UCAV.

9.1.3 Concept of Configuration and Design Aspect

A detailed description of the overall structure of the synthesis and optimization process for the UCAV design had been represented diagrammatically with a brief explanation of the major sections of the model. The input data required for the synthesis was described comprising of: the packaging specification, the design variables, the external variables, the airfoil coordinates, the weapon selections and dimensions, and the avionics instruments and dimensions. All these input data were primarily applied for setting the packaging and configuration design aspects of the UCAV to perform the estimations throughout the procedure.

The second section has presented a diagrammatic representation and a detailed description of the packaging and configuration design aspects. Before beginning with the detailed coding of the aircraft design synthesis process, the packaging specification was required to define the conceptual sketch of the UCAV. At this stage, no calculations have been performed concerning the design, apart from those required for initial sizing. The packaging specification represented a variety of particular designs, which was capable of being modelled using this design synthesis process. The packaging aspects have been set up comprising of avionics and sensor bays, internal weapon bays, engine bays, undercarriage bays, intake diffusers, two-dimensional nozzles, and fuel tanks. As the UCAV concept was based on the flying wing configuration, the wing centreline and the wingspan were two of the most critical variables necessary to accommodate all the packaging internally avoiding at all cost the use of any fairing on the shape of the aircraft to perform the configuration design aspect.

A detailed description of the overall operation and structure of the synthesis code and the packaging specification build-up provided a good start for the production of the software tool in order to allow effective planning and efficient coding to take place.

9.1.4 Airframe Estimation

The purpose of this module is to present the visibility of the airframe estimation methodology for the UCAV flying wing design, including the aircraft design variables, the aircraft components and packaging layout, the mass estimation and the internal volume available for fuel storage.

For a conceptual design synthesis, the sizing procedures developed for the UCAV flying wing design have been maintained intentionally simple, acceptable to the number of variables to be kept at minimum, and powerfully develop the code. The requirements for the variables and constraints were built from the outset to be able to allow variation of the packaging arrangements and the geometrical parameters of the aircraft, thus providing some margin to perform an optimization. Therefore, it was

necessary to determine the relationships between the packaging aspects and the various geometrical parameters of the aircraft to certify consistency across the design.

Gathering the avionics equipment desired for the combat aircraft and the UAVs, and estimating the dimension, volume, and mass carried out the avionics bay. Due to rapid advances in the capability of avionics, allowance for the avionics growth was considered in terms of volume. If such an allowance were not made, increasing the capability of the avionics suite would degrade the reliability and the maintainability of the aircraft, and be more expensive.

One of the fundamental decisions to be taken before determining the aircraft-packaging layout was the number of engines. To a large extent, this was a policy decision influenced by the considerations of safety, cost-effectiveness, and availability. The number of engines had a profound influence on the aircraft packaging aspect, dictating the disposition of the intake ducts, the two-dimensional nozzles, the weapon bay(s), the undercarriage bay, and the fuel tanks. As the number of engines was selected, the dimensions of the engines were required to determine the engine bay. They were obtained by scaling from some nominal engine's size by whatever scale factor was required to provide the desired thrust. The length of the engine bay, combining with the lengths of the intake duct and the two-dimensional nozzle, and the distance from aircraft nose to the intake inlet, leaded to alternative values for one of the minimum allowable overall length of the aircraft (the option of engine located at aircraft centreline). The inequalities of this result compared with the aircraft centreline were formed into constraints that were summarised during the optimization process.

The weapons selected for the UCAV were obtained from the typical types used with the modern combat aircraft to form the weapon bay(s). However, the maximum flexibility for the internal weapon bay was considered in order to permit the integration of current and future weapons. This is especially important when setting the dimensions of the weapon bay. The bay dimensions were, therefore, synthesized by the number of store stations lengthwise, in width and in height, with some clearance factors to allow the existing weapons or anticipate successful fielding of a new generation of the small weapons.

The estimation of the mass effected on the weapon bay required additional consideration on the mass of the doors, when protruded out into the airstreams. When the doors are opened, the mass of the doors would be directly proportional to the aircraft's dive speed. Additionally, the mass of the weapon launcher would cause the mass effect of the weapon bay.

The geometry of the intake diffuser is relatively complex and required a minimum length as a factor of the engine's diameter to ensure a satisfactory entry flow at the engine compressor. As the aircraft is based on the flying wing design configuration, care must be taken for the design of the intake inlet, that this may impose a high curvature for the flow to enter the intake, which may cause it to separate. Another factor that weighs against this location is that in high-speed flight, the formation of shock waves may occur close to the intake, thus reducing further its efficiency.

The requirement for the nonaxisymmetric or two-dimensional nozzle is to hide the hottest part of the engine from as many angles as possible in order to reduce the infrared and radar signatures (design for stealth). Moreover, it can be easily fitted to the wing trailing edge area of the flying wing design. The height of the nozzle exit is limited by the relative thickness of airfoil at aircraft trailing edge in area of engine position. Thus the overall length of the aircraft with the propulsion system located at the aircraft centreline mentioned above, compared with the wing root centreline chord would also meet this constraint. The remaining space at the end of the nozzle was kept available for the installation of the thrust vectoring.

The undercarriage bay is one of the most important considerations for the UCAV packaging. The geometry of the main and nose undercarriage were derived from a number of correlations with a reference landing mass. One difficulty was the determination of the ratio of the design landing mass to the take-off mass. For simplicity in the absence of more precise information, the ratio of 0.85 for the military combat aircraft has been obtained to determine the reference landing mass for this design synthesis process[58].

The airfoil shape has much more significant impact upon the aerodynamics. The concept of airfoils selected for the UCAV design was an attempt to choose all types of either symmetrical or asymmetrical airfoils to fit all the components internally without the use of any fairing on the aircraft shape. However, some of the aircraft cross-section definitions, such as the area available for the two-dimensional nozzles mentioned above, need careful analysis in the overall aircraft geometry algorithm to ensure their robustness.

Additionally the wing planform is the most relatively complex, as it is required to pack all the components internally. The concept of the flying wing configurations has been considered with several designs based on two main categories: the straight-tapered wing and the multi-kinks wing planforms. For the straight-tapered wing, only the wing centreline and the wingspan are concerned for the accommodation of all the packaging. On the contrary, the multi-kinks wing configuration, care must be taken for the position of the kinks to be located at the appropriate position along the wingspan with no interfering with the position of the overall control surfaces, and applicable to accommodate all the packaging.

The control surfaces designed for the UCAV mainly consist of the trailing edge control surfaces, and the option of the leading edge and the inlaid control surfaces. The inlays have been considered to help reducing the duties of the trailing edge split elevons, by taking the responsibility for the duties of rudders and ailerons, similar to the Pegasus X-47 UCAV-N design[48]. However, the presence of the inlaid control surfaces on the wing box structure has strongly affected the increase of the wing structural mass as they require the sufficient area for the precise dimension to perform their duties, although they may provide minimum drag in term of aerodynamics and perform good directional control in term of stability and control.

The packaging arrangement for the positions of the major components within the aircraft was considered both spanwise and chordwise directions. The former set up the packaging arrangement by the option of packaging aspects set by the user in the packaging specification. The latter was controlled by the constraints of two

conditions: the constraint sized by the thickness of the airfoil along chordwise station, and the limitation between the front and rear spars.

The method of fuel volume control was explained, and had been found that there were no discrete fuel tank volume limits to introduce discontinuities to any of the constraints, or the objective function.

The mass estimation of the aircraft was a critical part of the conceptual design, since it deeply affected the whole sizing of the vehicle. To perform an accurate estimation of the mass, it was necessary to perform a breakdown of the aircraft into several of its major components and estimate the individual mass of each of them. This is usually performed using the statistical correlation built up from the existing aircraft. As the UCAV consists solely of a wing, the masses of components such as a fuselage or tail surfaces were not considered. The wing structural mass estimation applied in the conceptual design synthesis was the most critical part principally for the multi-kinks wing configuration, although the method presented in Chapter 5 was seen to be more accurate than the other methods. It should be stated however, that the multi-kinks wing configuration were substantially different from the straight-tapered wing, therefore great caution should be taken in analysing the results. Unfortunately, since there were no available data concerning the method of wing structural mass estimation for the multi-kinks flying wing configurations, it was unavoidable to straightforwardly assume that the applied method would be valid achievable to provide the acceptable results.

The airframe estimation methodology for the UCAV flying wing design has been demonstrated to deliver realistic results for a variety of particular designs. The total aircraft mass obtained from the converged value of the first iterative process in this module was saved applying as the starting value for the corresponding calculation at the next entry into the remainder of the aircraft analysis procedure.

9.1.5 Configuration Layout

Once the aircraft was sized and the configuration design aspect has achieved, it was necessary to consider the configuration layout of the UCAV, which included: the aircraft centre of gravity, the undercarriage arrangement, the wing area and volume distribution, and the geometries of intake and two-dimensional nozzle ducts. These arrangements of the configuration layout have a major effect upon the packaging particularly for the flying wing configuration.

Although the final procedure in sizing ensured that sufficient internal volume existed applicable to accommodate all the components, the specific locations of each component were also important. This is because the position of the centre of gravity of the aircraft must be controlled so that, at all times throughout the mission, as fuel is burned and payload offloaded or expended, the aircraft centre of gravity will remain at acceptable values between the range of forward and aft limitations. The aircraft CG of the possible aircraft mass presented in the design synthesis was calculated in three cases: the empty mass, the zero fuel mass, and the design take-off mass. The results were specified the minimum value being the forward CG and the maximum value being the aft CG. The aircraft centre of CG has a major effect upon the packaging particularly the undercarriage arrangement.

The CG position of the main undercarriage was set at aft of the wing quarter-chord point from the aircraft nose. The position of the main undercarriage must also locate behind the aircraft aft CG adequate to perform the angle off the vertical to meet the required angle of the tipback angle or minimum required angle of 15 degrees, so that the trailing edge of the aircraft does not touch the ground during the aircraft nose-up attitude. Thus, it affects directly to the packaging and configuration aspects of the aircraft. At the start of performing the synthesis code, the main undercarriage was assumed to retract backward. This prevented the main undercarriage bay moving rearward, it being constrained by the rear spar position or the thickness of airfoil. Moreover, the distance from the main undercarriage to the aircraft CG could not provide adequate angle off the vertical to meet the requirement for ground clearance. It was therefore, decided to provide the main undercarriage retracting forward achievable to solve all these problems. Furthermore, the forward-retracting undercarriage was desirable since in the event of the deployment actuator, the main leg could be unlocked and the effects of gravity and slipstream would pull the leg to place.

The aim of determining the wing (aircraft) area and volume distribution was to use further for predicting and minimizing the supersonic wave drag and the transonic drag rise, on condition that the UCAV was operated in the supersonic regions.

The geometry of the intake diffuser is slightly different for the single- and twin-engine aircraft. Flexibility needs to be provided for three different-dimensional geometry-arrangements. The need is to curve them around the internal weapon bay providing some degree of "snaking" (S-shaped intake duct) in order to hide the engine face from the intake inlet for the radar detection as much as possible.

The geometry of the transition duct designed for a nonaxisymmetric nozzle or a two-dimensional nozzle required the same constant cross-sectional area distribution and curve wall-shape equation. The maximum slope angle of transition sidewalls and top or bottom walls were limited to 45 degrees or less to prevent the flow separation[19]. For this reason, the maximum wall angle can be decreased with increasing the transition-duct length. Therefore, the length of the transition duct is necessary to provide an adequate distance for a good transition from circular to rectangular cross-section, without causing excessive losses. From this data, the minimum length of the nozzle duct has been developed to meet the requirements that the duct must be as short as possible to minimize the mass of the propulsion system installation and it should be long enough to prevent any flow separation.

The overall methods of the configuration layout for the UCAV were necessary to be considered as they affected directly to the aircraft packaging and configuration design aspect. With further work, the use of the wing area and volume distribution would be performed for the aerodynamic prediction of the UCAV in the supersonic regions.

9.1.6 Characteristic Analyses

The characteristic analyses were divided into five main parts describing the respective modules: aerodynamic, static stability and control, engine performance, mission and point performance, and centre of gravity excursion. The purpose of developing these

modules was to provide the accurate investigation of the packaging and configuration design aspects of the UCAV.

The aerodynamic module consisted of two sections that predict available lift coefficient, and aircraft drag respectively. The lift model was composed of: the wing lift-curve slope, the spanwise lift distribution, the wing maximum lift coefficient, and the wing lift increment due to control surfaces. The lift characteristics were considered for their ability to predict the relevant aerodynamic properties in subsonic regions, and their applicability to low-aspect ratio wing configurations. The drag model is dependent of two major factors: the parasite drag and the induced drag. Significant drag characteristics were required by the performance analyses in its cruise configuration over much of the speed range, and for take-off and landing settings to evaluate the required distance. Realistic results are produced, which have been validated with real data, where possible. However, this aerodynamic module provided an uncomplicated method for the design synthesis process, in order to accomplish the investigation of various packaging and configuration design aspects for UCAV. With further work, the more complex and accurate methods for the prediction of the aerodynamic performance may be required to provide the correct balance of accuracy and efficiency, particularly for the flying wing configuration.

For the UCAV design synthesis process, the simple method used to determine the static stability and control is required in order to find out the sizes and to consider the positions of control devices, as they affect directly to the packaging and configuration design aspects, and the mass of the UCAV. The location of the wing aerodynamic centre is considered to begin with, as it is a critical term for the flying wing configuration to achieve the estimation of this module. The static longitudinal and lateral-directional stabilities and controls are subsequently determined to accomplish the requirements. The accurate results are produced, which have been compared with different particular designs of UCAV, where possible. With further work, the additional and accurate methods would require to provide the correct balance of accuracy and efficiency for the static stability and control of the flying wing tailless aircraft. The presence of the thrust vectoring would provide a good result for the lateral-directional control.

The engine performance module provides the information of certain basic engine characteristics for the design synthesis of UCAV. The most possible representation of variation of thrust and specific fuel consumption with flight conditions are the two primary characteristics, which are necessary for the estimations of the mission performance to determine the available fuel required to complete the aircraft mission. Furthermore, they are needed for the point performance analysis to compare the delivered performance of the designed aircraft with the required performance figures.

The point and mission performance modules form a very important part of the aircraft design synthesis, as it is these two modules that essentially drive the size of the aircraft. These two modules represent the conclusion of all the previous estimations, since it accommodates the data obtained from the component sizing, aerodynamic, engine performance, and the mass estimation. Where it has been to validate point performance data, the results have been shown to be impressive for a conceptual design methodology. There will always be area for improvement, but without

significant increases in the number of data points available, it is difficult to suggest specific modifications.

For simplicity, the method used to determine the fuel mass fraction for all mission segments in this design synthesis is calculated as a discrete change in mass due to payload released and fuel burned. This is done by setting an input parameter in each mission segment to select the options for the weapon status and its relative mass required for that segment as shown in Table 7-7 of Chapter 7. For the UCAV design with an internal weapon bay, the bomb dropped mission segment starts from bay-doors open, release weapon(s), and ends after doors closed. The range credit has been taken and so the fuel penalty is occurred. The fuel mass fraction of this mission segment is thus, based on the duration to perform the weapon-released segment at required altitude and speed set in the mission performance codes. The results of the mission performance estimations are certainly realistic; increasing confidence in the final size of the designs produced using this design synthesis process.

The centre of gravity excursion module is required to examine the range of the aircraft centre of gravity to remain within the acceptable limits throughout the mission. The range of aircraft centre of gravity is affected by fuel burned and/or payload released during each mission segment. With a variety of particular designs of the UCAV flying wing configuration, the results of the CG excursion are realistic, providing all the components being scaled correctly and located at the suitable position inside the aircraft, producing the effective design.

Overall, the methods of the characteristic analyses applied for the UCAV have the advantage of good accuracy, without the need for computationally excessive estimations. However, in order to ensure the robustness of these models primarily the aerodynamics, and the static stability and control modules, the more complex and accurate methods would be required to provide the correct balance of accuracy and efficiency.

9.1.7 Optimization

The optimization tool has formed a significant part in achieving the overall solutions of the work. A basic understanding of the optimization process was felt to be beneficial for the author, who had no expressive experience of the optimization. Although not given a complete explanation, details of some of the major problems affecting the gradient-based searches were featured, and the measures taken to reduce the risk of these occurring had been described.

During the development of the design synthesis methodology for the UCAV, care was taken to provide for the requirements of linking the design synthesis with the numerical optimizer to ensure that the results of the calculations were continuous in the design space. The optimization tool, LSGRG2, has been found to be an efficient and powerful tool for producing optimized conceptual designs for the UCAV. Negligible problems with convergence have been met, although the possibility remains that a local minimum would break off the process before the global minimum can be achieved. However, this is probably more a characteristic of the objective function than failing of the optimization tool, and can be investigated by diminishing the constraints in the first instance or setting new bounds for the design variables. The

presentation of various results is one of the robustness of the UCAV design synthesis code, and will not be possible without the use of the optimizer to accomplish the design iteration routine.

Additionally, various constraints were allowed by the optimizer to increase realism, such as the checks of the packaging being fitted within the wing box of the aircraft. Further analysis will be necessary to develop the additional constraints appropriate for this type of aircraft.

9.1.8 Validation and Comparison with Existing UCAV

Validation of the individual model has been discussed with the presentation of the model methodology. According to the UCAV flying wing configuration, only the Pegasus X-47 UCAV-N could validate with this methodology. With the exception of the aircraft performance, the avionics instruments, and internal weapons carriage, the model has been validated, although the extent to which this has taken place was determined by the data available. Moreover, by allowing the major parameters of the aircraft to be sized by the optimizer also provide the accurate results to ensure the robustness of the model methodology.

Comparison of the UCAV models produced by this design synthesis code with the existing UCAVs and/or UAVs has found to be more difficult. This is because they are designed for the different purposes based on their configurations and sizes in order to perform the typical mission. Moreover, most of the UAVs are operated with the piston-propeller engines, and they are only designed to perform the primary mission of intelligence, reconnaissance, surveillance and target acquisition. As the UCAV is designed for the aim of performing the combat mission with the use of the jet engine, thus the correlated data of the UCAV models will be possible to make the comparison only with those of the existing UCAVs based on the similar designs and missions. The results shown in Chapter 8 has ensured that the UCAV model produced by the UCAV design synthesis methodology are realistic, although the lack of data for the aircraft design missions prevents direct comparison of those results.

9.1.9 Generation of Results

The result of Chapter 8 have shown that the UCAV design synthesis and optimization tool developed is operating, and is capable of generating meaningful results with various particular designs of packaging arrangements with the flying wing configurations. The investigations produced some interesting data especially: the increment of internal weapon bays with various flying wing configurations, the differences between straight-tapered wing and multi-kinks wing configurations with the single and twin engine designs, the effects of control devices position, the impact of internal weapons carriage, the effects of packaging arrangements on different airfoil selections, and the comparison between the UCAV and manned combat aircraft produced by this design synthesis code. In terms of demonstrating the capability and operation of the UCAV conceptual design and optimization synthesis, the aims of the study were achieved. The results generated should provide a basis for discussion, and for more detailed studies to be performed on the desired configurations identified.

The knowledge obtained from the research of the packaging and configuration design aspects of UCAV was felt to be beneficial for the author to understand the problems from the investigation for a variety of particular designs. As the concept of UCAV presented in this thesis was based on the flying wing design, the wing planform itself has provided a big challenge to develop the perfect package to be fitted internally. The appropriate position of individual components must be carefully considered, as it affects the aircraft centre of gravity, the configuration aspect, the geometry, and the aircraft masses. The presence of the kink(s) on the wing planform provided the more flexible shape for the UCAV flying wing to accommodate all the components internally without possessing any redundant area, which would perform the lighter and stealthier aircraft. However, care must be taken to constrain the position of the kink(s) not to interfere with the control surfaces.

The position of the control surfaces also played an important role for the packaging aspect. The investigation for the presence of the inlaid control surfaces has shown that their dimensions has directly influenced the wing box structure to be able to fit these devices with no interfering with the trailing edge control surfaces. Moreover, their position on the top and bottom of the wing structure would reduce the volume of the wing box to contain fuel. The position of the control surfaces at wing trailing edge and leading edge seems to produce a preferable design.

For the UCAV flying wing configuration, it was found that only the fuel tanks located in the wing box area would provide sufficient volume to contain the fuel to accomplish the whole mission. Extra fuel tanks would be obtained, if necessary, by allowing the available volume enclosing the packaging to be filled with fuel.

The development of the software tool for the research of the packaging and configuration design aspects of UCAV was aimed to be more flexible in order to meet the growth of new technologies in many areas, such as: the advanced airfoils, the future weapons, the avionics instruments, and the advanced materials.

9.2 Areas of Further Work

From individual chapters in this thesis, and the discussion above, there were many areas of the work that could be improved. Due to the limited time to perform the research, a large number of areas were identified for further research.

9.2.1 Further Utilization of Methodology

Following from the above statement, there directly was insufficient time to take advantage of the full ability of the methodology to generate detailed results on the packaging and configuration design aspects of UCAV. Several areas have been identified for further study utilizing aspects of the UCAV conceptual design synthesis tool.

9.2.1.1 Advanced Materials Consideration

The option of advanced materials set by the user in the packaging specification allows the UCAV to be constructed with the aluminium alloys or the carbon-fibre composite.

The overall case studies of the UCAV configurations produced in Chapter 8 have used the typical value of the material factors of the carbon-fibre composite for the investigation of the wing structural mass of the aircraft. The metallic UCAV would provide a good study to investigate the size and mass growth of the aircraft compared to the composite UCAV.

Foam matrix is the alternative choice of advanced material selection for the UCAV design, as applied for the structures of the X-45 UCAV mentioned in the literature search. The foam matrix is suited for structures like wings, control surfaces, and similar contour parts. The benefits of the foam matrix UCAV include lightweight, reduced parts count, seamless construction, reproducibility, shorter production-cycle time and lower cost. In addition, use of the foam eliminates hollow cavities in the structure. This improves damage resistance in handling and assembly and reduces the possibility of delamination or allowing water to enter the core. To allow the UCAV design synthesis code producing the foam matrix UCAV, the data of material properties such as the material shear modulus for the foam matrix are required. The foam matrix UCAV would be a good comparison of the size and mass with the metallic and composite models.

9.2.1.2 Advanced Airfoils Selection

The concept of airfoils selected for UCAV configuration is an attempt to choose all types of either symmetrical or asymmetrical airfoils to fit all the components internally without the use of any fairing on the shape of aircraft. The airfoil coordinates are one of the main sizing drivers for all the components, significantly affecting the arrangement of their positions in the vertical, longitudinal and lateral directions. As can be seen from the case study of inboard airfoil selection presented in Chapter 8, the asymmetrical airfoil is proved to be more difficult to accommodate all the components internally due to the limit area at aft region, thus increasing the size and mass of the aircraft. However, the results shown were applied only with one type of airfoil with the thickness ratio of 15 percent. The option set by the user in the packaging specification allows various selections of airfoils corresponding to the relative thickness ratios to be synthesized. Thus, by changing the new airfoil types with similar thickness ratio or setting both new data would provide a significant change for the packaging accommodation and also the configuration design aspect of UCAV.

9.2.1.3 Saw Toothed-Shape Configurations

The option of multi-kinks wing configuration set by the user in the packaging specification allows the synthesis code to produce various configuration design aspects for the UCAV, as shown in Figure 4-6 of Chapter 4. The saw toothed-shape configuration, similar to the B-2 stealth bomber planform, is one of the most critical configuration aspects to be synthesized. By investigating the packaging aspect of the B-2, it was found that all the packaging was accommodated within the inboard kink and allowed the other outboard kinks to size the appropriate sweep for the trailing edge control surfaces to perform their functions. Moreover, the remaining outboard area of the wingspan were contained the fuel tanks, which was more than 50 percent of the half of wingspan. The B-2 requires large area of wing box to carry extra fuel to perform the long-range attack mission. On the contrary, the UCAV may not require

this large wing box area to accommodate fuel tank. The UCAV design synthesis code could size all the kinks to be flexible over the spanwise position of the packaging to produce much smaller and lighter aircraft, and provide appropriate sweep angle for the control surfaces to perform their functions.

Some of these will require significant modifications to the aircraft synthesis: Wing structural mass, aerodynamics, and static stability and control models, but the modular nature of the code should allow these modifications to be made as additions, without the need for a major re-write of large sections of code. It should be noted that these modifications are suggested as improvements, rather than corrections of perceived deficiencies in the overall model.

9.2.2 General Recommendations for Further Study

As mentioned above, there were many areas of the work that could be improved. These following sections include the prioritised list of recommended improvements for the UCAV design synthesis and optimization tool.

9.2.2.1 Development of Wing Structural Mass Modelling

The wing structural mass estimation for the multi-kinks wing configuration is one of the weakest areas in the study, and is generally recognised as an area requiring further investigation. So far, the method developed for calculating the wing structural mass was based on the straight-tapered wing configuration or the single-kink wing configuration with a minor change of the sweep angle between the kink. The mass was determined in the aspect of equivalent wing planform. In order to develop the accurate method to determine the wing structural mass for the multi-kinks wing configuration, the structural mass would be determined with individual panels and calculated the area ratio of those panels related to the total planform area to perform the total wing structural mass. This modification would make valuable contribution to the tool.

9.2.2.2 Upgrade of Avionics Instruments and Weapons

Due to a rapid growth of the UCAV designs, many companies have developed the modern avionics instruments and weapons acceptable for this type of aircraft. At the start of performing the synthesis code, the UCAV was only the demonstrator, thus the avionics instruments were gathered from those applied for the manned combat aircraft or the UAVs to perform the avionics bay. Similarly, the weapons were gathered from the typical types used with the fighter aircraft to size the internal weapon bay. Upgrade of these avionics instruments and weapons would lead the operation of the UCAV to be more efficiency. The UCAV design synthesis code has provided the maximum flexibility for the avionics bay and the internal weapon bay in order to permit the integration of current and future avionics instruments and weapons. These improvements would increase the reliability and maintainability of the UCAV.

9.2.2.3 Improvement of Aerodynamic and Stability Modelling

As mentioned previously, the aerodynamic and the static stability and control modules provide the uncomplicated methods for the design synthesis code in order to

accomplish the investigation of various packaging and configuration design aspects for UCAV. To enhance the accurate and realistic solution of the UCAV design, the models rely directly on the flying wing, and stealthy shape could be obtained. The improvement of these models should increase confidence in the design methodology of the UCAV.

9.2.2.4 Investigation of Cost Modelling

Consideration of costs is of fundamental importance at all phases of the aircraft design process. The ultimate success or failure of a project is significantly dependent upon the costs associated with its initial acquisition and operation. A selling price of an aircraft is largely determines by market forces and to be profitable for the manufacturer it must be possible to produce it for less than the market price. A consideration of the various aspects of aircraft costs is thus essential at the very outset of a project. The development of the cost module would produce beneficial contributions to the UCAV design synthesis model.

9.3 Conclusions

A software tool of the UCAV conceptual design and optimization synthesis was developed capable of generating conceptual design data for various packaging and configuration aspects of UCAV flying wing design, and optimising those designs for functions of minimum mass. The aircraft configuration was defined taken into account the common features of stealthy aircraft such as, the flying-wing tailless design, the internal weapons carriage, curved engine intakes, and employing the two-dimensional nozzles. With several options of packaging specification, the design synthesis allows greater flexibility in the choice of aircraft packaging and configuration design aspects, which could be enhanced by a more precise definition of the dimension and layout of the avionics bay, the internal weapon bay, the engine bay, the undercarriage bay, and the fuel tanks.

A series of results has been generated to present the effects of changing the aircraft packaging and configuration aspects including: the increment of internal weapon bays with various flying wing configurations, the differences between straight-tapered wing and multi-kinks wing configurations with the single and twin engine designs, the effects of control devices position, the impact of internal weapons carriage, the effects of packaging arrangements on different airfoil selections, and the comparison between the UCAV and manned combat aircraft produced by this design synthesis code. Reasonable explanations for the changes resulting from one design to the next have been given, and all the converged designs occur realistic.

The UCAV conceptual design and optimization synthesis model provides the acceptable results for a variety of packaging and configuration aspects of UCAV. The objective function of minimum design take-off mass is satisfactory and proves to be very accurate compared to the existing UCAV. Additionally, the software tool is validated for the existing aircraft with similar design. With development of the future weapons, avionics instruments, and advanced materials designed for UCAV, the aircraft should become lighter and smaller, further increasing the differences in the aircraft designs.

The development of the conceptual design synthesis for the UCAV packaging and configuration design aspects was a complex task due to the large amount of new information necessitating inclusion in the new algorithms. The further work would certainly be necessary to ensure the adaptation of the synthesis. Some of the suggestions in the previous section would improve the ability to investigate the design effects of advanced technologies, allowing conceptual design and balance of investment studies.

In summary, the work undertaken for this research program has produced a detail survey of the initial sizing program for the military jet trainer aircraft, in order to gain some early knowledge on the primary variables and constraints requirements and understand the optimization technique that would apply for the design synthesis methodology for the UCAV. A survey of the available information on stealth has lead to the definition of the packaging and configuration design aspects of the aircraft, producing the design synthesis for the UCAV. The configuration layout and the characteristic analyses would improve the investigation of various particular designs of the UCAV to be more realistic. A set of numerical optimization routines allowed the determination of the optimum aircraft design for a given configuration (i.e. straight-tapered wing or multi-kinks wing planforms with a variety of packaging aspects). Comparisons of these solutions have enabled the best result to be selected. Further work would be necessary to enhance the synthesis allowing conceptual design and balance of investment studies. In term of the overall objectives, the research has been successful. This thesis will optimistically improve the appropriate decision process for future UCAV systems.

References

1. Abbott, I. H., and A. E. V. Doenhoff. *Theory of Wing Sections*. Dover Publication, Inc., USA, 1959.

2. Abzug, M. J., and E. Larrabee. *Airplane Stability and Control; a History of the Technologies That Made Aviation Possible*. Cambridge University Press, United Kingdom, 1997.

3. AF 2025. "Space Operations: Through the Looking Glass (Global Area Strike System)." Web page, August 1996. Available at http://www.au.af.mil/au/2025.

4. "Aircraft Mass Prediction: Powerplants, Systems and Equipment, DAeT 9218." College of Aeronautics, Cranfield University.

5. "Aircraft Mass Prediction: Structural Components, DAeT 9317." College of Aeronautics, Cranfield University.

6. "Aircraft Project Design: Climb and Manoeuvre, Takeoff and Landing Conditions, DAeT 9250." College of Aeronautics, Cranfield University.

7. Anderson, JR. J. D. *Introduction to Flight*. McGraw-Hill Book Company, Singapore, 1989.

8. Ashley, S. "Robotic Bombers: Unmanned Strike Aircraft Begin to Take Off." Web page, June 2001. Available at http://www.sciam.com/techbiz.

9. Asselin, M. *An Introduction to Aircraft Performance*. American Institute of Aeronautics and Astronautics, Inc., USA, 1997.

10. AviationNow Staff and Wire. "UCAV Makes 14-minute Maiden Flight." Web page, May 2002. Available at http://www.aviationnow.com/avnow/news.

11. Baker, D. "Reaching Those Parts That Other Can't." *Air International* (2000): 180.

12. Ball, R. E. *The Fundamental of Aircraft Combat Survivability Analysis and Design*. American Institute of Aeronautics and Astronautics, Inc., USA, 1985.

13. Barrie, D. "Dull, Dirty and Dangerous." *Flight International* (1997): 58.

14. Berrier, B. L., J. L. Palcza, and G. K. Richey. "Nonaxisymmetric Nozzle Technology Program - An Overview." *AIAA Paper 77-1225* (1977).

15. Berrier, B. L., and R. J. Re. "Effect of Several Geometric Parameters on the Static Internal Performance of Three Nonaxisymmetric Nozzle Concepts." *NASA TP-1468* (1979).

16. Blecher, T., E. Simonsen, and J. Walker. "Boeing X-45A Unmanned Combat Air Vehicle Begins Flight Testing." Web page, May 2002. Available at http://www.boeing.com/news/releases/2002/q2/nr_020523m.html.

17. Brandt, S. A., R. J. Stiles, J. J. Bertin, and R. Whitford. *Introduction to Aeronautics: A Design Perspective*. American Institute of Aeronautics and Aeronautics, Inc., Verginia, USA, 1997.

18. Brown, D. A. "The Future of Navy Fighter: UCAV: The Future Fighter." *Aviation Week & Space Technology* (1999): S1.

19. Burley II, J. R., L. S. Bangert, and J. R. Carlson. "Static Investigation of Circular-to-Rectangular Transition Ducts for High-Aspect-Ratio Nonaxisymmetric Nozzles." *NASA TP-2534* (1986).

20. Butcher, I. A. "Future Offensive Air System - A UAV Solution."*Fourteen International Conference, Bristol, United Kingdom*1999.

21. Capone, F. J. "Aeropropulsive Characteristics of Twin Nonaxisymmetric Vectoring Nozzles Installed With Forward-Swept and Aft-Swept Wings." *NASA TP-1778* (1981).

22. Capone, F. J., and D. L. Maiden. "Performance of Twin Two-Dimensional Wedge Nozzles Including Thrust Vectoring and Reversing Effects at Speeds Up to Mach 2.20." *NASA TN D-8449* (1977).

23. Capone, F. J., R. J. Re, and E. A. Bare. "Thrust Reversing Effects on Twin-Engine Aircraft Having Nonaxisymmetric Nozzles." *AIAA Paper 81-2639* (1981).

24. Cherry, M. C. "A Discussion of a Modular Unmanned Demonstration Air Vehicle." *AGARD-CP-600* 1 (1997).

25. Chudoba, B. *A Project Method for Calculating Spanwise Lift Distribution on Swept and Unswept Wings at Subsonic Speeds*. Airbus Industrie, 1992-1993.

26. Clark, R. M. "Uninhabited Combat Aerial Vehicle: Airpower by the People, For the People, But Not Within the People." *CADRE* 8 (2000).

27. Crane Aerospace. "Brake Control Systems for Unmanned (Pilotless) Air Vehicles." Web page, 2001. Available at http://www.hydroaire.com/event/monthly_sept.htm.

28. Cranfield University. "Aerospace Vehicle Design Group Project: U-99 Uninhabited Tactical Aircraft." *Aerogram* 10, no. 1 (2001): 20.

29. Daigle, C. C. "Unmanned Combat Air Vehicle Technology." Web page, Available at http://faculty.erau.edu/pratta/Archive/u/ucav.html.

30. "DARPA and Air Force Select Boeing to Build UCAV Demonstrator System." Web page, March 1999. Available at http://www.defenselink.mil/news.

31. "DARPA and Air Force Select UCAV Contractors." Web page, April 1998. Available at http://www.fas.org/man/dod-101/sys/ac/docs/b04161998_bt178-98.

32. Department of Aeronautical & Astronautical Engineering, University of Illinois. "Storm Shadow: Unmanned Strike Fighter/ Uninhabited Combat Aerial Vehicle Design Project." Web page, 1998. Available at http://www.aerospaceweb.org.

33. Diederich, F. W. "A Simple Approximate Method for Obtaining Spanwise Lift Distributions Over Swept Wings." *NACA Reports RM L7I07* (1948).

34. Dole, C. E., and J. E. Lewis. *Flight Theory and Aerodynamics: A Practical Guide for Operational Safety*. John Wiley & Sons, INC., USA, 2000.

35. Dornheim, M. A. "McDonnell Douglas Rolls Out X-36." *Aviation Week & Space Technology* (1996): 20.

36. Dornheim, M. A. "X-36 to Test Agility of Tailless Design." *Aviation Week & Space Technology* (1996): 20.

37. Edwards Air Force Base. "Flying Wing History." Web page, June 2000. Available at http://www.edwards.af.mil/history/docs_html.

38. "Equation for Calculation of International Standard Atmosphere and Associated Off-Standard Atmosphere." *ESDU 77022* (1977).

39. "F-15 2-D Nozzle System Integration Study." *NASA CR-145295* 1 (1978).

40. Fallon, W. J. "Lethal and Survivable Air Weapons Systems: Essential Today and Tomorrow." *Aircraft Survivability, Joint Technical Coordinating Group on Aircraft Survivability* (1999).

41. Fielding, C., Flight Control Systems Technologist. "The Design of Fly-By-Wire Flight Control Systems." Web page, 2000. Available at http://www.shef.ac.uk/~acse/ukacc/activities/flybywire.pdf.

42. Francis, M. "Advanced Unmanned Vehicle Systems." Web page, 1996. Available at http://www.arpa.mil/ARPATech-96/slides/francis/100/1.gif.

43. Fulghum, D. A. "Boeing Plans Unmanned Fighter." *Aviation Week & Space Technology* (1996): 20.

44. Fulghum, D. A. "Decades Are Needed to Perfect Unmanned War PLanes." *Aviation Week & Space Technology* (1998): 70.

45. Fulghum, D. A. "High-G Flying Wings Seen for Unmanned Combat." *Aviation Week & Space Technology* (1996): 58.

46. Fulghum, D. A. "Next-Generation UCAVs Will Feature New Weapons, Engine, 21st Century Fighters." *Aviation Week & Space Technology* (1998): 71.

47. Fulghum, D. A. "Payload, Not Airframe, Drives UCAV Research." *Aviation Week & Space Technology* (1997): 51.

48. Fulghum, D. A. and R. Wall. "New Demonstrator Spurs Navy UCAV Development." Web page, February 2001. Available at http://www.aviationnow.com/content/publication/awst/20010219/avi_stor.htm.

49. Fulghum, D. A. and R. Wall. "Russia Awakens to Unmanned Aircraft." Web page, October 2001. Available at http://www.aviationnow.com/avnow/news.

50. Gardner, P. "Unmanned Tactical Aircraft: A Radically New Tactical Air Vehicle and Mission Concept." *AGARD-CP-600* 2 (1997).

51. "Geometrical Properties of Cranked and Straight Tapered Wing Planforms." *ESDU 76003* (1976).

52. Goebel, G. "UCAVs." Web page, February 2002. Available at http://www.vectorsite.net/avuavd.html.

53. Gunston, B. *Jane's Aero-Engines*. Jane's Defense Data, United Kingdom, 1997.

54. Haisty, B. S. "Affordable Stealth." *Lockheed Martin's* (2000).

55. Hancock, D. "Joint Doctrine for Theater Counterair Operations." Web page, April 1986. Available at http://www.adtdl.army.mil/cgi-bin/atdl.dll/jt.

56. Hart, C. "Kites: An Historical Survey.", 25. Mount Vernon, USA, 1982.

57. Hoak, D., D. Ellison, and et al. *USAF Stability and Control DATCOM*. Air Force Flight Dynamics Laboratory, Wright-Patterson Air Force Base, Ohio, USA, 1974.

58. Howe, D. *Aircraft Conceptual Design Synthesis*. Professional Engineering Publishing Limited, United Kingdom, 2000.

59. Howe, D. "Estimation of Drag Coefficient for Initial Design Work, AVT-AVD 9603." College of Aeronautics, Cranfield University.

60. Howe, D. "Influence of Stealth Requirements on Aircraft Design, AVD 9810." College of Aeronautics, Cranfield University.

61. Hu, B. K., and J. L. Prof. Stollery. "The Performance of 60 Degree Delta Wings: The Effects of Leading Edge Radius on Vortex Flaps and The Wing." *College of Aeronautics Report No. 9004* (1990).

62. Hughes, D. "Dassault Sees Rafale As UCAV Fight Leader." *Asian Aerospace 2000, Aviation Week & Space Technology* (2000): 38.

63. Hura, M., G. McLeod, R. Meric, P. Sauer, J. Jacobs, D. Norton, and T. Hamilton. "Enhancing Dynamic Command and Control of Air Operations Against Time Critical Targets." Web page, 2002. Available at http://www.rand.org/publications/MR/MR1496/.

64. Jackson, P. *Jane's All the World's Aircraft: 1998-99*. Directory & Database Publishers Association, United Kingdom, 1998.

65. Johnson, C. *Jane's Avionics: 1998-99*. Directory & Database Publishers Association, United Kingdom, 1998.

66. Jone, J. *Stealth Technology: The Art of Black Magic*. Airlife Publishing Ltd., United Kingdom, 1989.

67. Kandebo, S. W. "Boeing Premieres UCAV Demonstrator." Web page, October 2000. Available at http://www.aviationnow.com/content/publication/awst/20001002/aw30b.htm.

68. Kandebo, S. W. "SEAD, Other Ground Attack Capabilities Planned for UCAVs." Web page, October 2000. Available at http://www.aviationnow.com/content/publication/awst/20001002/aw30a.htm.

69. Lasdon, L. S. *LSGRG2 User's Guide*. MSIS Department, The University of Texas at Austin, 1997.

70. Lawson, C. "UCAVs may Find Niche in 21st Century." Web page, June 1998. Available at http://www.fas.org/man/dod-101/sys/ac/docs/980625-ucav.htm.

71. Lennox, D. S., and A. Rees. *Jane's Air-Launched Weapons*. Jane's Defense Data, United Kingdom, 1990.

72. "Lift-Curve Slope and Aerodynamic Centre Position of Wings in Inviscid Subsonic Flow." *ESDU 70011* .

73. Lockheed lmco. "Lockheed Martin Today." Web page, Available at http://www.lmco.com/file3/lmtoday/9711/future.html.

74. Lockheed Raptor. "F-22 Raptor." Web page, 2002. Available at http://www.f22fighter.com.

75. Lockheed Raptor. "Lockheed Martin F-22 Raptor." *Air International* (1998).

76. Lopez, R. "As Northrop Grumman Reveals Stealth Design." *Flight International* (1997): 20.

77. Lopez, R. "USN Considers Future UCAV." *Flight International* (1997): 20.

78. Lovell, D. A. "The Application of Multivariate Optimization to Combat Aircraft Design." *Technical Report TR 88003* (1988).

79. Macci, S. H. "Method for Predicting Wing Structural Mass at Preliminary Design Stage." *Aircraft Structures and Materials*. IMechE Seminar Publication ed., 11. Vol. 10. Mechanical Engineering Publications Limited, London, 1996.

80. Maclean, A. "Unmanned Combat Air Vehicles." Web page, Available at http://www.maclean-nj.com/opinions/stories/4.htm.

81. Mason, M. L., and B. L. Berrier. "Static Investigation of Several Yaw Vectoring Concepts on Nonaxisymmetric Nozzles." *NASA TP-2432* (1985).

82. McCall, G. H. and J. A. Corder. "New World Vistas: Technologies for Arming the Air Force of the 21st Century." Web page, Available at http://www.fas.org/spp/military/docops/usaf/vistas.htm.

83. McDaid, H., and D. Oliver. *Robot Warrior: The Top Secret History of the Pilotless Plane*. Orion Media, United Kingdom, 1997.

84. McDaid, H., and D. Oliver. *Smart Weapons*. Barnes and Noble, USA, 1997.

85. McManners, H. "Missiles Threaten to Down the RAF." *The Sunday Times,* 24 August 1997.

86. "Method for the Rapid Estimation of Spanwise Loading of Wings With Camber and Twist in Subsonic Attached Flow." *ESDU 83040* (1983).

87. Morocco, J. D. "ETAP to harvest Europe's Technological Expertise." Web page, July 2001. Available at http://www.aviationnow.com/avnow/news.

88. Morris, J. "Northrop's Pegasus UCAV-N Prototype Prepares for Rollout, Flight Later this Year." Web page, July 2001. Available at http://www.aviationnow.com/avnow/news/channel_military.

89. Mothersill, R. J. "A Twin-Engine Version of the Combat Aircraft Multivariate Optimization Program." *Technical Memorandum TM Aero 1902* (1981).

90. Munson, K. *Jane's Unmanned Aerial Vehicles and Targets*. Directory & Database Publishers Association, United Kingdom, 1998-2001.

91. Mustin, J., Lt. "Flesh and Blood: The Call for the Pilot in the Cockpit." Web page, July 2001. Available at http://www.airpower.maxwell.af.mil/ airchronicles/cgo/mustin.html.

92. Nicolai, L. M. "Considerations for Affordable Aerospace Systems." *AGARD-CP-600* 1 (1997).

93. Niu, M. C. Y. *Airframe Structural Design*. Conmilit Press Ltd., Hong Kong, 1995.

94. "Northrop's Big Wing - The B-2 (Part 1)." *Air International* (1993): 287.

95. Paterson, J. "Survivability Benefits From the Use of Standoff Weapons by Stealth Aircraft." *AIAA 1999-01-5503* (1999).

96. Raymer, D. P. *Aircraft Design: A Conceptual Approach*. American Institute of Aeronautics and Astronautics, Inc., USA, 1992.

97. Re, R. J., and B. L. Berrier. "Static Internal Performance in Single Expansion-Ramp Nozzles With Thrust Vectoring and Reversing." *NASA TP-1962* (1982).

98. Re, R. J., and L. D. Leavitt. "Static Internal Performance Including Thrust Vectoring and Reversing of Two-Dimensional Convergent-Divergent Nozzles." *NASA TP-2253* (1984).

99. Reeh, D. "Flying Combat in the 21st Century." *Aviation Week & Space Technology* (2000): 57.

100. Roberts, F., Captain. "Unmanned Aerial Vehicle: Should We Leave the White Scarves and Anti-G Suits Behind?" Web page, 2002. Available at http://www.military.com/New.

101. Rosenberg, B. "Foam Material Surfboards Supplies Lift for X-45 UCAV." Web page, March 2002. Available at http://www.aviationnow.com/content/publication/awst/20020318/aw69.htm.

102. Roskam, J. *Airplane Design Part I: Preliminary Sizing of Airplanes*. Roskam Aviation and Engineering Corporation, USA, 1985.

103. Roskam, J. *Airplane Design Part V: Component Weight Estimation*. Roskam Aviation and Engineering Corporation, USA, 1989.

104. Rowell, E. D. "A New Idea Takes Off: Air Warfare Machines Heading Toward Next Generation." Web page, December 2000. Available at http://abcnews.go.com/sections/scitech/CuttingEdge/cuttingedge001215.html.

105. Ruane, M. E. "Air Force: Robotic Pilots." Web page, 1996. Available at http://www.seattletimes.com/extra/browse/html/flyb_020196.htm.

106. Scott, W. B. "X-36 Testing Gives Boeing Jump on UCAV Work." *Aviation Week & Space Technology* (1998): 58.

107. Seddon, J., and E. L. Goldsmith. *Intake Aerodynamics*. BSP Professional Books, USA, 1985.

108. Seigers, F. "Conceptual Design Synthesis and Optimization for New Generations of Combat Aircraft." *COA Report 9606, Cranfield University* (1996).

109. Seigers, F. "Design Synthesis for Swept-Wing Combat Aircraft Incorporating Stealth Technology." *COA Report 9402, Cranfield University* (1994).

110. Shea, D. "Raytheon Selected for UCAV Program." Web page, May 1998. Available at http://www.raytheon.com/press/1998/may/ucav.html.

111. Shradar, W. "Radar Technology Applied to Air Traffic Control." *IEEE Transactions on Communication* Com-21, No. 5 (1973).

112. "Smart Weapons Air-to-Surface Missiles JSOW JASSM Tomahawk." Web page, Available at http://www.danshistory.com/smartm.html.

113. SpaceDaily. "Northrop Grumman gets Contract Boost for Unmanned Combat Plane." Web page, May 2002. Available at http://www.spacedaily.com/news/uav-02j.html.

114. "Stealth Aircraft: Eagles among Sparrows." Web page, Available at http://www.fas.org/spp/aircraft/part06.htm.

115. Sumich, M. and R. O. Bailey. "X-36 Tailless Fighter Agility Research Aircraft." Web page, 1997. Available at http://atrs.arc.nasa.gov/r_t/1997/aero/revol.html.

116. Sutton, S. ""Pegasus" Unmanned Combat Air Vehicle - Navy (UCAV-N)." Web page, November 2001. Available at http://www.capitol.northgrum.com.

117. Sweetman, B. *Aircraft 2000: The Future of Aerospace Technology*. Hamlyn Publishing Group Limited, United Kingdom, 1984.

118. Sweetman, B. "Stealth Aircraft - History, Technology and Outlook." *ASME Paper 90-GT-172* (1990).

119. Sweetman, B. *Stealth Aircraft: Secrets of Future Airpower*. Airlife Publishing Ltd., United Kingdom, 1986.

120. Sweetman, B. *Stealth Bomber: Invisible Warplane, Black Budget*. Airlife Publishing Ltd., United Kingdom, 1989.

121. Sweetman, B. "UCAVs Spread Their Wings." Web page, May 2001. Available at http://www.janes.com/aerospace/military/news/idr/idr010504_1_n.shtml.

122. Tailless web FAS. "X-36." Web page, Available at http://www.fas.org/man/dod-101/sys/ac/x-36.htm.

123. Teixeira da Costa, A. L. "Conceptual Design of an Unmanned Tactical Aircraft." MSc Thesis, Cranfield University, 1998.

124. Thompson, K. E. "F-16 Uninhabited Air Combat Vehicles." Web page, April 1998. Available at http://www.fas.org/man/dod-101/sys/ac/docs/98-282.htm.

125. Torenbeek, E. *Synthesis of Subsonic Airplane Design*. Delft University Press, Holland, 1982.

126. Turnbull, A. "A Preliminary Sizing Method for Unmanned Aircraft Using Multi-Variate Optimization." College of Aeronautics, Cranfield University, 1990.

127. "UAV Evolution." Web page, Available at http://www.sd-auvsi.org/pdfs/uavdod_103101.pdf.

128. "UAV Technologies and Combat Operations Executive Summary." Web page, 1996. Available at http://www.fas.org/man/dod-101/sys/ac/docs/ucav96/afrttech.htm.

129. UCAV web AIAA. "Unmanned Strike Fighter." Web page, Available at http://www.aiaa.org/information/design/rfp-adc.html.

130. UCAV web DARPA. "Unmanned Combat Air Vehicle." Web page, Available at http://www.darpa.mil/tto/programs/ucav.html.

131. UCAV web FAS. "Unmanned Combat Air Vehicle." Web page, Available at http://www.fas.org/man/dod-101/sys/ac/ucav.htm.

132. UCAV web FAS. "Unmanned Combat Vehicle Advanced Technology Demonstration." Web page, March 1998. Available at http://www.fas.org/man/dod-101/sys/ac/docs/ucav-sol.html.

133. USAF Museum. "The Ealry History of Flying Wing was Featured during January 1998." Web page, January 1998. Available at http://www.wpafb.af.mil/museum/fta/fta198.htm.

134. Wagner, W. "Lightning Bugs and Other Reconnaissance Drones." *Armed Force Journal International* (1981).

135. Walker, J. "Boeing X-45A Unmanned Combat Air Vehicle Begins Flight Testing." Web page, May 2002. Available at http://www.boeing.com/news/releases/2002/q2/nr_020523m_facts.html.

136. Wall, R. "Boeing Wins UCAV Contract." *Aviation Week & Space Technology* (1999): 84.

137. Wall, R. "Northrop Grumman's UCAV Program Bid." *Aviation Week & Space Technology* (1998): 59.

138. Webber, R. T. "Aircraft Survivability: A Balanced Susceptibility Reduction Approach." *Aircraft Survivability, Joint Technical Coordinating Group on Aircraft Survivability* (1999).

139. Well, R. C., D. J. Hamlin, and R. B. Smith. "Flight Safety Considerations for UCAV Aircraft."*Fourteen International Conference, Bristol, UK* 1999.

140. Wheeler, M. O. "Start and the ABM Treaty - What are the Implications of their Linkage?" Web page, October 2000. Available at http://website.lineone.net.

141. Whitford, R. *Design for Air Combat*. Jane's Publishing Company Limited, United Kingdom, 1987.

142. Whitford, R. "Designing for Stealth in Fighter Aircraft: Stealth From the Aircraft Designer's Viewpoint." *AIAA-965540* (1996).

143. Whittle, R. G. "The Development of Preliminary Design and Assessment Methodologies for Enhanced Combat Aircraft Supportability." PhD Thesis, Department of Aeronautics, Imperial College of Science, Technology & Medicine, 1997.

144. Williams, J. C. "Balancing Affordability and Performance in Aircraft Engines." *AGARD-CP-600* 1 (1997).

145. Zaloga, S. J., Teal Group Corp. "Conflicts Spur Interest in UAVs." Web page, 2002. Available at http://www.aviationnow.com/content/publication/awst/2002outlook/aw103.htm.

146. Zaloga, S. L. "Growing Plains As UAVs Evolve: Unmanned Combat Aerial Vehicles." *Aviation Week & Space Technology, Aerospace Source Book* (1999): 97.

APPENDIX A

A: Output Data of Initial Sizing Study

This appendix summarizes the output data for the conceptual design of the military jet trainer aircraft. It contains an initial estimation of the value of take-off mass, a summary of group mass statements, fuel fractions and aircraft mass for each phase of mission, point performance analysis, and a comparison of design specification with the existing similar aircraft. This case study provides a sufficient knowledge and information in advance of activating the UCAV design.

A.1 Initial Mass Estimation

An initial estimation of the value of take-off mass is usually obtained by comparing the design requirements of the aircraft model with the mission capabilities of similar aircraft. A military jet trainer model has been estimated to carry 2,000-kg bombs with maximum speed of 200 metres per second and cruise range up to 2,000 km. Table A-1 represents typical data of several military jet trainer aircraft (data obtain from Jane's All the World Aircraft[64] 1998-99).

Military Jet Trainer	Take-off Mass (kg) (stores)	Payload (kg)	Max. Speed (m/s)	Range (km)	Take-off Distance (m)	Landing Distance (m)
Pampa FMA IA 63	5,000	1,230	208	2,111	424	461
Karakorum8 NAMC K-8	4,330	943	224	2,250	410	512
Albatross L-39	5,800	1,500	175	1,690	520	610
Alca L-159	8,000	2,340	260	2,530	440	725
Goshawk Bae T-45	9,387	N/A	280	1,532	N/A	N/A
Aermacchi MB-339c	6,350	1,814	255	2,037	550	480
Bae Hawk 100	9,100	3,000	250	2,519	640	605
Kawasaki T-4	7,500	N/A	288	1,668	555	646
Mapo Mig-AT	5,690	N/A	278	1,200	540	570
Yakovlev Yak-130	6,200	N/A	278	2,220	310	485

Table A-1: Military Jet Trainer Aircraft Data

From these data, an initial guess value for take-off mass (*Mto_es*) is ranged between a bound of 4,000 and 10,000 kg. Following the calculations presented in Chapter 3, the design take-off mass, aerodynamics, engine performance, mission fuel mass, and point performance analysis of the aircraft are accomplished. With an optimization process, the results are obtained showing the final parameters requirements for setting up the aircraft configuration.

A.2 Summary of Design Take-off Mass Build-up

Basically the design take-off mass can be broken into crew mass, payload mass, fuel mass, and empty mass. The total empty mass of the aircraft is the sum of all components arranged in structure, propulsion, and systems and equipment groups. The empty mass plus mass of those items necessary for the aircraft to be operational becomes the operational empty mass. For the military combat and jet trainer aircraft, the only item of interest is the mass of crew provisions. The sum of the payload and the fuel appropriate to a given mission gives the disposable mass. Once the total design take-off mass is performed, it is kept as a sizing variable, after linking to other modules, subjected to variation with the initial take-off mass estimation during the iterative process until the values converge.

According to the methods presented in section 3.2.2 of Chapter 3, a summary of group mass statements for a military jet trainer aircraft model is shown below:

Components		**Mass before Iteration (kg)**	**Mass after Iteration (kg)**
Wing		711	276
Empennage		174	84
Fuselage		623	620
Undercarriages		281	281
Structure Group		**1,790**	**1,261**
Engine Installation		746	746
Propulsion Group		**746**	**746**
Fuel System		210	210
Flying Control System		145	145
Power Supply Systems	Hydraulics	268	268
	Electric	289	289
Environmental Control Systems	Air Conditioning	63	63
	De-Icing	39	39
Instruments		106	106
Furnishings		120	120
Military Armament		455	455
Miscellaneous		9	6
Systems and Equipment Group		**1,704**	**1,701**
Empty Mass		**4,239**	**3,708**
Crew		180	180
Operating Empty Mass		**4,419**	**3,888**
Payload (Bombs)		2,000	2,000
Fuel	Fuel Fraction Estimation	1,400	1,112
	Mission Fuel Calculation	1,503	
Disposable Mass		**3,400** (FF) **3,503** (MF)	**3,112**
Take-off Mass		**7,819** (FF)	**7,000**

Table A-2: Military Jet Trainer Aircraft Model: Group Mass Statements Summary

Figure 3-2 of Chapter 3 is represented again in this appendix to demonstrate a linear relationship between empty mass and total aircraft take-off mass of the existing military jet trainer aircraft.

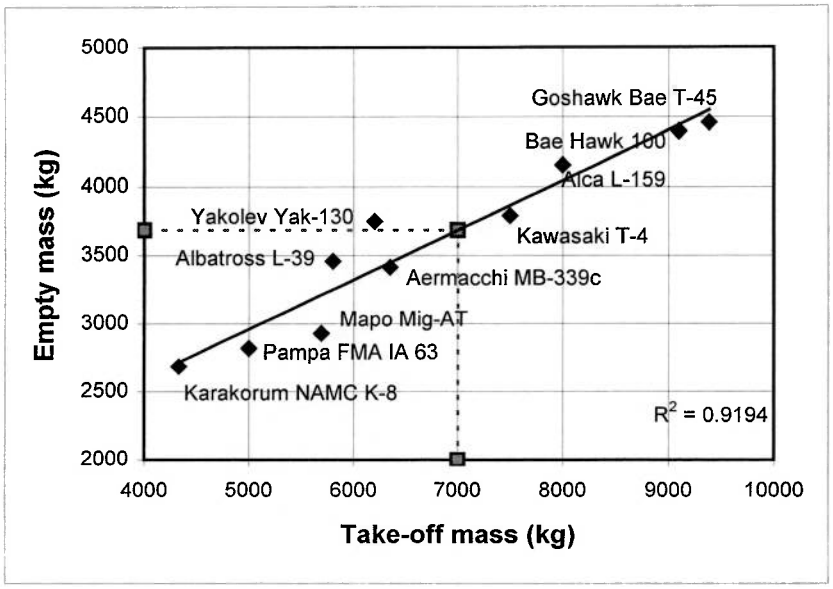

Figure A-1: Mass Estimation Correlation with Mass Trends for Military Jet Trainer Aircraft

The trend line is established to be an adequate representation as the minimum allowable value of empty mass at the current state-of-the-art of aircraft conceptual design. Having considered inserting the 7,000-kg take-off mass of military jet trainer model to the graph, a gradient of trend line results the value of empty mass at 3,683 kg. This value is compared to the calculated empty mass obtained from an initial sizing study as shown in Table A-2 above. The calculated empty mass gives a result of 3,708 kg, which is very closed to the minimum allowable value. Although above methods are simple, this output data shows that accurate results can be achieved.

A.3 Mission Fuel Mass Results

The design take-off mass is used to performed the estimation of mission fuel mass. The deep strike mission, as shown in Figure 3-1 of Chapter 3, is considered as a design mission to determine the mission fuel mass for an initial sizing study. To determine the fuel mass actually use during the mission, the fuel-fraction method is applied that the aircraft mission is broken down into a number of mission phases to calculate fuel mass in each phase. This is an accurate method to determine the value of mission fuel mass. Once the total mission fuel mass is performed, it is subjected to variation with the fuel mass obtained from the method of fuel mass fraction, during the iteration procedure to meet the final result.

Table A-3 gives the final results of the fuel fractions determined by the methods presented in section 3.2.5 of Chapter 3 with the corresponding aircraft mass and fuel mass for each of the mission phases.

Fuel Fractions		Phase	Aircraft Mass (kg)	Fuel Mass (kg)
		Engine start	7,000	
Warm-up, Taxi, Take-off	0.9900			70
		Transition to climb	6,930	
Accelerate & climb	0.9838			112
		Top of climb	6,818	
Cruise-out	0.9600			273
		Over Target Area	6,545	
Loiter	0.9800			131
		Surveillance	6,414	
Descent	0.9900			64
		Close to target	6,350	
Dash-out	0.9946			35
		Reach target	6,315	
Bombs drop	1.0000	Bomb released	4,315	0
Strafe	0.9309	Reconnaissance	4,282	33
		Fire ammo	3,986	
Dash-in	0.9286			32
		Second climb	3,954	
Accelerate & Climb	0.9893			43
		Top of climb	3,911	
Cruise-in	0.9487			200
		Return to base	3,711	
Descent	0.9900			37
		Approach & flare	3,674	
Landing	0.9950			17
		End mission	3,655	
Reserve fuel				65
Mission fuel mass				**1,112**

Table A-3: Military Jet Trainer Aircraft: Summary of Fuel Fraction and Aircraft Mass for Each Phase of Mission

A.4 Point Performance Analysis

The estimations of point performance are the required constraints compared to the data in the design requirements in the form of inequality function during the optimization routine. The size and mass of an aircraft are critically dependent upon the point performance capabilities. Therefore, the point performance calculations must be accurate, if a realistic design is to be produced.

A wide range of the calculations of point performance is available, so that a detailed set of requirements is drawn up in this initial sizing program for any particular study. Following the methods of calculation for point performance analysis presented in

section 3.2.6 of Chapter 3, the results are achieved within the margin set by the design requirements as shown in Table A-4 and A-5.

Point Performance		Design Requirements	Mach Number	Altitude (m)
Take-off distance (m)		≤ 650	≈ 0	0
Landing distance (m)		≤ 650	≈ 0	0
Rate of climb (m/s)	Stores	≥ 15	0.4	1,524
	Clean	≥ 20	0.45	1,524
Time to climb (sec)	Stores	≤ 550	0.4	1,524
	Clean	≤ 450	0.45	1,524
Sustained turn rate (deg/s)	Stores	≥ 9	Cruise-out	6,500
	Clean	≥ 12	Cruise-in	6,500
Radius of turn (m)	Stores	≤ 1,500	Cruise-out	6,500
	Clean	≤ 1,200	Cruise-in	6,500

Table A-4: Military Jet Trainer Aircraft: Point Performance Requirements

Point Performance		Design Requirements	Calculation Performing
Take-off distance (m)		≤ 650	514
Landing distance (m)		≤ 650	614
Rate of climb (m/s)	Stores	≥ 15	17.08
	Clean	≥ 20	22.30
Time to climb (sec)	Stores	≤ 550	380.47
	Clean	≤ 450	252.23
Sustained turn rate (deg/s)	Stores	≥ 9	9
	Clean	≥ 12	12.18
Radius of turn (m)	Stores	≤ 1,500	1,396.30
	Clean	≤ 1,200	1,182.47

Table A-5: Military Jet Trainer Aircraft: Summary of Point Performance Analysis

A.5 Comparison of Design Specifications

To summarise, the design specifications of the military jet trainer model are compared with the specifications of similar aircraft. The BAE Hawk 100 and the Albatross L-39 are the primary selections. The BAE Hawk 100 is the two-seat basic and advance jet trainer with air defence and ground attack capability, manufactured by the British Aerospace Defence in the United Kingdom. The Aero Vodochody manufactures the Albatross L-39 in the Czech Republic, which is a two-seat jet trainer with armed and combat variants. Table A-6 demonstrates the design specifications of these two aircraft and the military jet trainer model.

Design Specifications		Unit	BAE Hawk 100	Albatross L-39	Jet Trainer Model
Mass and Loading					
Max. Take-off mass (stores)		kg	9,100	5,800	7,000
Landing mass		kg	7,650	5,700	6,860
Empty mass		kg	4,400	3,458	3,708
Max. Weapon load		kg	3,000	1,100	2,000
Total fuel capacity		kg	1,304	1,014	1,248
Wing loading		kg/m^2	545.40	308.51	562.63
Thrust loading		kg/kN	350	296.56	378.73
Dimensions					
Wing aspect ratio			4.90	4.76	4.94
Wing thickness ratio			0.109	0.12	0.20
Wing taper ratio			0.34	0.50	0.30
Wing area		m^2	16.69	18.80	12.44
Wing span		m	9.08	9.46	7.84
Quarter-chord sweep		deg	21.30	1.45	21.72
Leading edge sweep		deg	26	6.30	27
Propulsion					
Number of engines			1	1	1
Engine thrust at SSL		N	26,000	16,868	26,000
Engine bypass ratio			0.7	0.7	0.7
Performance					
Number of pilots			2	2	2
Positive limit load factor			8	8	8
Take-off ground run distance		m	640	520	514
Landing ground roll distance		m	605	610	614
Max. Approach speed		m/s	80	70	65
Cruise altitude		m	9,150	5,000	6,500
Cruise range		km	2,519	1,690	2,000
Speed at SSL	Stores	m/s	250	190	190
	Clean		277	210	208
Cruise Mach number	Stores		0.85	0.75	0.70
	Clean		0.88	0.80	0.75
Rate of climb	Stores	m/s	40	12	17.08
	Clean		60	22	22.30
Time to climb	Stores	sec	550	400	380.47
	Clean		450	300	252.23
Sustained turn rate	Stores	deg/s	10	9	9
	Clean		15	12	12.18
Radius of turn	Stores	m	1,800	1,500	1,396.30
	Clean		1,500	1,300	1,182.47

Table A-6: Military Jet Trainer Aircraft: Comparison of Design Specifications

APPENDIX B

B: Lists of Data

This appendix presents the lists of avionics instruments and weapons applied for the design synthesis of UCAV. It must be noted that the items listed are used to estimate the mass of each item to perform avionics and weapon bay, respectively. In practice, further advance systems are applicable for this analysis.

The list of avionics instruments has been primarily gathered from Jane's Avionics[65] and Jane's Unmanned Aerial Vehicles and Targets[90]. Further information has been collected from data sources of Internet[74]. Many instruments are manufactured for Unmanned Aerial Vehicle (UAV) or else designed for fighter aircraft. The list of avionics instruments is presented in section B.1.

The list of weapons has been accumulated from Jane's Air-Launched Weapons[71]. The weapons selected for UCAV have been obtained from typical types used with modern combat aircraft. The list of weapons is shown in section B.2.

Additionally, this appendix presents the list of existing UCAVs and UAVs providing some correlated data in order to make the comparison with the UCAV configurations produced by the design synthesis model. The data have been gathered from Jane's Unmanned Aerial Vehicles and Targets[90]. Additional data have been collected from data sources of Internet[16],[48]. The list of UCAVs and UAVs are shown in section B.3.

B.1 List of Avionics Instruments

Equipment	Model	Company	Length (mm)	Width (mm)	Height (mm)	Mass (kg)	Power	Remark	Note
Mission Management System (MMS)									
SAR	MSAR	Lockheed Martin	394.00	330.00	165.00	19.50	N/A	Radar Unit	**Radar Suite**
			430.00	300.00	100.00	8.00		Processor	
MTI Radar	SLAM-R	Lockheed Martin	715.00	200.00	560.00	36.30	400 W	Receiver/Transmitter	
			580.00	200.00	200.00			Antenna	
FLIR	Ultra 3000	FLIR Systems Inc.	414.00	260.00	260.00	22.20	28 V DC	Dual-sensor (EO/IR)	**Sensor Suite**
Infrared Linescan	SAT Cyclope 2000	SAGEM SA	170.00	170.00	200.00	5.00	70 W	IRLS Sensor	
Flight Management System (FMS)									
IFMU Computer	AN/AYK-14 (V)	Computing Devices International	194.00	257.00	356.00	16.00	50-300 W	32-bit (Typical)	**Flight Control Suite**
SEM-E Backplane	MIL-STD 1553B	Aydin Telemetry							
Air Data System	HG 1140	Honeywell	152.40	111.76	50.80	0.91	6 W	Multirole Air Data Computer	
Fly-by-Wire System	F-16 FBW	Lear Astronics	457.00	254.00	203.00	20.00	150 W	Baseline F-16 C/D	
Data Link	AN/ASW-54(X)	Harris Corporation	128.30	180.60	273.00	6.23	28 V DC	Interoperable Tactical Data Link	**Navigation Suite**
Radar Altimeter	HG 7705	Honeywell	194.00	95.00	72.00	1.55	12 W	Including Antenna	
AHRS Magnetometer	SKH-4210	Kearfott	177.80	177.80	279.40	12.70	N/A	Ring Laser Gyro Technology	
GPS/INS	LN-100G	Litton	177.80	177.80	241.30	8.60	25 W	Combined GPS/INS	
MLS	MLZ-850	Honeywell	354.00	84.00	99.00	2.09	15 W	Receiver	
			139.70	60.40	66.70	0.45		Controller	
Data Recorder	ESPAR	Dassault & SFIM	118.00	120.00	220.00	8.00	<20 W	Flight-data Recorder	
Narrowband LOS UHF/SATCOM	MX 42000	Raytheon Systems	N/A	N/A	N/A	9.98	300 W	UHF SATCOM Data Link	**Communication Suite**
Wideband LOS	ST-800S/L	Aydin Telemetry	50.80	76.20	20.30	0.20	10 W	Microwave Transmitter	
ATC	AT 150	Narco Avionics	159.00	45.00	286.00	1.68	28 V DC	Receiver/Transmitter	
IFF Transponder/Interrogator	TSB 2500 (CIT)	Thomson-CSF	228.60	157.20	193.50	10.00	500 W	CIT	**Identification Suite**
Missile Approach Warner	AN/AAR-44 (V)	Raytheon	101.60	152.40	406.40	9.09	28 V DC	Advance Missile Warning	
Laser Warner	LWR	Daimler-Benz	240.00	129.00	110.00	3.60	51 W	Laser Warning Receiver	
Electronic Warfare System (EWS)									
EW	Monarch	GEC-Marconi	350.00	150.00	180.00	4.00	50 W	Radar Jammer	**Starboard Wing**
Chaff/Flare Dispenser	Vicon 78-500	W Vinten	572.00	122.00	122.00	25.00	28 V DC	12 Infrared Decoy Flares/Chaffs	**Port Wing**
Store Management System (SMS)									
Weapon Control Panel	SMS 2600 WPU	Computing Devices Company	20.00	130.00	300.00	6.00	29 W	Weapon Processing Unit	**Weapon Control Suite**
	SMS 2600 PIU		170.00	57.00	235.00	1.50		Pylon Interface Unit	
Weapon Release	MIL-STD 1760								
Power Supplies									
Power Supply Module **(Each Suite)**		Boeing	162.81	152.15	14.73	0.82	400 W	Baseline F-22	

B.2 List of Weapons

Air-to-Air Missile											
Specification		*Short Range (<10 km)*		*Medium Range (10-100 km)*						*Long Range (>100 km)*	
Designation		**AIM-9M Sidewinder**		**AIM-120C AMRAAM**		**AIM-7 Sparrow**		**530D Super**		**AIM-54C Phoenix**	
Baseline Aircraft		F-15, F-16, F/A-18, F-22		F-15, F-16, F/A-18, F-22		F-4, F-14, F-15, F/A-18		Mirage 2000		F-14	
Type		Infra-Red		Radar-guided		Radar-guided		Radar-guided		Radar-guided	
Mission		CAS, OCA		CAS, OCA		CAS, OCA		CAS, OCA		CAS, OCA	
Powerplant		Solid propellant		Solid propellant		Solid propellant		Solid propellant		Solid propellant	
Warhead		9.5 kg High explosive blast fragmentation		22 kg High explosive directed fragmentation		39 kg High explosive blast fragmentation		30 kg High explosive fragmentation		60 kg High explosive continuous rod	
Fuze	Guidance	Laser	Infra-red	Radar	Inertial & active radar	Radar	Semi-active radar	Active radar	Semi-active radar	Active radar	Active radar
Length (mm)	W-span (mm)	2,870	640	3,650	530	3,660	1,020	3,800	620	3,960	920
Diameter (mm)	Range (km)	127	8	178	50	203	45	263	40	380	150
Volume (m^3)	Mass (kg)	1.176	87	1.025	157	3.808	230	1.461	270	3.352	463
Company		Raytheon company and Loral Autoneutronics		Huges Missile Systems and Raytheon Company		Huges Missile Systems and Raytheon Company		Matra SA		Huges Missile Systems and Raytheon Company	

Air-to-Surface Missile											
Specification		*Short Range (<10 km)*		*Medium Range (10-100 km)*						*Long Range (>100 km)*	
Designation		**AGM-122 Sidearm**		**AGM-88 Harm**		**ALARM**		**AGM-65H Maverick**		**AGM-84 Harpoon**	
Baseline Aircraft		F/A-18		F-4, F-15, F-16, F/A-18		Tornado GR1		F-4, F-15, F-16, F/A-18		F/A-18	
Type		Anti-radar		High-speed anti-radar		Air-launched Anti-radar		Laser-guided		Radar-guided	
Mission		CAS, Interdiction, DS		DS		CAS, Interdiction, DS		CAS, Interdiction, DS		Maritime Ship Attack	
Powerplant		Solid propellant		Solid propellant		Solid propellant		Solid propellant		Turbofan	
Warhead		10.2 kg High explosive blast fragmentation		66 kg High explosive fragmentation		High explosive fragmentation		136 kg Blast penetrator		220 kg High explosive blast penetration	
Fuze	Guidance	Active laser & impact	Passive radar	Active laser	Passive radar	Active laser	Passive radar	Impact	Active radar	Impact	Active radar
Length (mm)	W-span (mm)	3,000	640	4,170	1130	4,300	720	2,600	720	3,900	910
Diameter (mm)	Range (km)	127	8	254	25	224	45	305	25	343	120
Volume (m^3)	Mass (kg)	1.229	91	5.325	361	2.229	268	1.348	305	3.230	530
Company		Motolora Inc.		Texas Instruments		British Aerospace and GEC-Marconi		Huges Missile Systems and Raytheon Company		McDonnell Douglas and Texas Instruments	

Bomb									
Specification		*JDAM*		*Cluster Bombs and Sub-munitions*					
Designation		**GBU-32**		**CBU-87/B**		**CBU-89/B**		**CBU-97/B**	
Baseline Aircraft		F-15, F/A-18, F-22		F-15, F-16, F/A-18, B-2		F-15, F-16, F/A-18, B-2		A-10, F-15, F-16, B-2	
Type		Tail guidance kits Near precision-guided 'smart' munition		Multipurpose (Combined Effects Munition CEM)		Anti-tank and area denial (Gator Mind System)		Anti-tank (Sensor Fuzed Weapon SFW)	
Mission		CAS, OCA, Interdiction, DS		CAS, Interdiction, DS		CAS, Interdiction, DS		CAS, Interdiction, DS	
Warhead		Fit on MK 83 1,000-pound-class conventional bomb		202 BLU-97/B bomblets		72 BLU-91/B anti-tank and 22 BLU-92/B anti-personnel		10 BLU-108/B bomblets	
Length (mm)	Tail span (mm)	3,040	480	2,330	520	2,340	520	2,340	520
Diameter (mm)	Lug Spacing (mm)	357	N/A	396	356	406	356	406	356
Volume (m^3)	Mass (kg)	0.700	460	0.630	430	0.633	322	0.633	450
Company		McDonnell Douglas Aerospace		Alliant Techsystems		Aerojet General and Honeywell		Textron Defense Systems	

Bomb											
Specification		*General Purpose Bombs*				*Laser-Guided Bombs and Systems*					
Designation		**MK 82**		**MK 84**		**GBU-12**		**GBU-24A**		**GBU-27**	
Baseline Aircraft		F-14, F-16, F/A-18, B-2		F-14, F-16, F-117A, B-2		F-15, F-16, F/A-18, F-117A		F-14, F/A-18		F-117A, B-2	
Type		Low drag		Low drag		Paveway		Paveway		Penetrating	
Mission		CAS, Interdiction, DS		CAS, Interdiction, DS		Interdiction		CAS, Interdiction, OCA		CAS, Interdiction, OCA	
Warhead		89 kg Tritonal, Minol, H-6 or PBXN-109		428 kg Tritonal or H-6		89 kg Tritonal		240 kg Tritonal		428 kg Tritonal or H-6	
Length (mm)	T-span (mm)	2,210	380	3,840	640	3,330	430	4,260	940	4,320	720
Diameter (mm)	L-space (mm)	273	356 or 762	460	762	273	356 or 762	370	762	460	762
Volume (m^3)	Mass (kg)	0.319	241	1.573	894	0.616	225	3.764	900	2.239	900
Company		Nad Crane		Nad Crane		Texas Instruments		Texas Instruments		Lockheed Missiles	

Gun (Optional Manned Aircraft)									
Specification		*20-mm Gun*				*25-mm Gun*			
Designation		**M61 A2 Cannon**		**M61 A1 Cannon**		**GAU-12/U Equaliser**		**ADEN 25 Cannon**	
Baseline Aircraft		F-22		F-14, F-15, F-16, F/A-18		AV-8A		Harrier GR Mk7	
Type	Number of Barrels	Hydraulically gatling	6	Hydraulically gatling	6	Automatic gatling	5	Cannon	1
Fire Rate (rds/min)	Muzzle Vel(m/s)	6,000	1,036	6,600	1,036	4,200	1,097	1,650-1,850	1,050
Length (mm)	Mass (kg)	1,880	120	1,880	120	2,130	127	2,470	92
Company		General Electric		General Electric		General Electric		British Aerospace	

B.3 List of UCAVs and UAVs

Company	UCAV & UAV	Country	Fuel Mass (kg)	Empty Mass (kg)	Take-off Mass (kg)	Remark
Aerosonde	Aerosonde Mk 1	Australia	5.00	8.20	13.40	Long range/endurance UAV
C.Craft	Eyrie Mk 7		65.00	105.00	225.00	Multirole UAV
Thales	Epervire	Belgium	26.00	101.00	147.00	Battlefield reconnaissance UAV
Bombardier	CL-89	Canada	N/A	78.20	156.00	Surveillance drone
Alcore	Chacal 2	France	N/A	30.00	75.00	Multipurpose UAV
Altec	MART Mk II		20.00	81.00	110.00	Battlefield reconnaissance UAV
	S-Mart		N/A	75.00	144.00	Battlefield RSTA UAV
CAC Systemes	Fox AT 1		N/A	60.00	85.00	RS UAV
	Fox TX		N/A	65.00	120.00	Electronic warfare UAV
Dassault	AVE		N/A	35.00	60.00	UCAV demonstrator
SAGEM	Sperwer & Ugglan		N/A	212.00	330.00	STA UAV
EMT	Luna 2000	Germany	N/A	20.00	30.00	Battlefield RSTA UAV
STN ATLAS-3 Sigma	Nearchos	Greece	N/A	60.00	190.00	Multirole UAV
ADE	Nishant	India	N/A	252.00	350.00	RSTA UAV
AAI/IAI	RQ-2 Pioneer	International	32.70	138.00	205.00	Short/medium range SI-gathering UAV
INTA/Ceselsa/EADS Dornier	SIVA		55.00	160.00	230.00	Surveillance UAV
TRW/IAI	RQ-5A Hunter		136.00	540.00	726.00	Short range RSTA UAV
EMIT	Sting & Blue Horizon	Israel	42.00	80.00	150.00	Long endurance surveillance UAV
IAI	Scout		25.00	96.00	159.00	Multipurpose tactical UAV
Silver Arrow	Hermes 450		N/A	200.00	450.00	Long endurance UAV
	Micro-V		10.00	27.20	50.00	Battlefield surveillance UAV
Meteor	Mirach 26	Italy	24.00	186.00	230.00	Close-range tactical UAV
	Mirach 150		86.00	254.00	380.00	Medium-range tactical UAV
Daewoo	Doyosae	Korea	15.00	113.00	130.00	Research prototype UAV
AWC	AWC Mk II	Pakistan	N/A	26.00	60.00	Low-cost STA UAV
Kentron	Seeker	South Africa	49.00	151.00	240.00	RTA & artillery fire correction UAV
TAT	Nasnas Mk I	Tunisia	N/A	43.00	125.00	Reconnaissance & multipurpose UAV
AES	Nibbio	UAE	N/A	102.00	240.00	Multirole tactical UAV
Flight Refuelling	Raven	UK	9.30	75.00	84.00	Close-range surveillance UAV
Meggitt	ASR-4 Spectre		27.20	111.60	144.70	Multirole UAV
	Phantom		N/A	23.00	40.00	Battlefield close-range RS UAV

Company	UCAV & UAV	Country	Fuel Mass (kg)	Empty Mass (kg)	Take-off Mass (kg)	Remark
AAI	RQ-7A Shadow 200	USA	28.60	91.00	149.00	STA UAV
	Shadow 600		N/A	148.40	265.00	Multirole UAV
AeroViroment	Hiline		96.60	185.00	341.00	HALE UAV
Aurora	Aurora UCAV		N/A	57.60	64.60	UCAV demonstrator
BAE Systems	R4E Skyeye		109.00	334.00	567.00	Multipurpose UAV
BAI	Javelin		N/A	3.95	7.71	Reconnaissance & communications relay UAV
	Tern		N/A	20.40	43.10	Multipurpose UAV
Boeing	X-45 A		1,220.16	3,629.00	5,530.00	UCAV for SEAD and other strike missions
Daedalus	Truck/Dakota		6.80	32.20	60.30	RS UAV
General Atomics	Gnat 750		193.00	254.00	511.00	All-altitude multi-mission long-endurance UAV
	I-Gnat/Rotax 912		227.00	385.00	703.00	
	Predator B 003 Altair		N/A	1,588.00	3,175.00	Scientific research UAV
	Prowler I		90.70	204.00	317.00	Close-range tactical UAV
	RQ-1 Predator		295.00	350.00	1,020.00	Medium-altitude tactical endurance UAV
GSE	Vindicator		N/A	268.00	476.00	Short-range tactical UAV
Insitu	Seascan		4.30	11.00	15.40	Small reconnaissance UAV
IAT	Flash MK-105		15.00	48.00	90.00	Short-range multirole UAV
Meggitt	Sentry HP		32.70	81.60	147.40	Short-range RSTA and relay UAV
Mi-Tex	Vixen		13.60	63.50	90.70	Close-range multirole tactical UAV
NASA	RAPTOR		381.00	367.00	853.00	HALE UAV demonstrator
Northrop Grumman	RQ-4A Global Hawk		6,577.00	4,173.00	11,612.00	HAE surveillance UAV
	Scarab		N/A	496.00	1,077.00	Tactical reconnaissance UAV
	Starbird		27.20	68.00	172.00	Lightweight tactical UAV
	Pegasus X-47		471.74	1,739.53	2,490.76	Naval UCAV

APPENDIX C

C: Methodology Implementation

This appendix presents a brief description of the entire input data files and subroutines associated with the design synthesis and optimization process of UCAV. The main program used by the design synthesis is called '*ucavopt.for*', which was developed during the design of the UCAV, as described fully in the main text. The design synthesis is controlled by means of a number of input data files specifying various design parameters, as described in Chapter 4 and Chapter 5, including the additional details presented in this appendix. The subroutines are developed in the various isolated modules and are linked with the main programs to accomplish the analysis.

Data File (xxx.dat)	Description	Note
DATINPUT	Packaging specification and design variables including optimizer control values	Chapter 4 and Chapter 5
DATUCAV	Mandatory data required for implementing the overall calculations throughout the entire process	
DATAVI	Avionics instruments and their dimensions to size for the avionics bays	
DATWEAP	Weapons loaded on the aircraft internally and/or externally (optional) and their dimensions to size for the internal weapon bays	
DATAF	Airfoil coordinates for inboard and outboard sections of wing	
DATAFTWS	Asymmetric airfoil coordinates for twist distribution	Chapter 7
DATMISS	General data associated with the various missions for UCAV	
DATMISS1	Design parameters of mission and point performance requirements for low-level strike mission	These input data files are controlled by the type of missions (TMISS) and are only called to the correlative mission module.
DATMISS2	Design parameters of mission and point performance requirements for counterair mission	
DATMISS3	Design parameters of mission and point performance requirements for ISR mission	
DATMISS4	Design parameters of mission and point performance requirements for ferry mission	
DATXCOOR	X-coordinates applied for geometries of intake diffuser and two-dimensional nozzle ducts and aircraft cross-sectional area	

Module (xxx.for)	Subroutine	Description
SUBBAYPO	WINGAF	Airfoil coordinates at relative spanwise station
	XBAY	Maximum depths of wing airfoil and their distances from aircraft nose at the relative span position of bays required for the calculation of packaging layout
	XODR	Chordwise position of bays at relative span position
SUBFUEL	OWFUEL	Cross-sectional area of fuel tanks
	RLWFUEL	CG of centre of fuel volume
SUBMATM	ATTOLD	Atmospheric data at sea-level condition for relative mission segment
	ATXM	Atmospheric data at variable flight conditions for relative mission segment
SUBMCG	MSMASS	Aircraft mass at the end of each mission segment due to fuel burn and/or weapon release
	MISSCG	CG locations of aircraft at the end of each mission segment due to fuel burn and/or weapon release
	MSMASSCG	Absolute fuel mass fraction at the end of each mission segment due to duration, range, and variation of thrust and fuel consumption
SUBMDRAG	DRAGSSL	Aircraft drag at sea-level condition for relative mission segment
	DRAGFLT	Aircraft drag at variable flight conditions for relative mission segment
SUBMDRGI	DLWTOLD	Drag due to lift based on wing computed at sea-level condition for relative mission segment
	DLCSTOLD	Drag due to lift based on trailing edge control devices computed at sea-level condition for relative mission segment
	DLXM	Drag due to lift based on wing computed at variable flight conditions for relative mission segment
SUBMDRGZ	DCWTOLD	Zero-lift drag based on wing computed at sea-level condition for relative mission segment (component drag)
	DCCTOLD	Zero-lift drag based on cockpit (optional manned aircraft) computed at sea-level condition for relative mission segment (component drag)
	DCSTOLD	Zero-lift drag based on external stores (optional weapon selections) computed at sea-level condition for relative mission segment (component drag)
	DMPTOLD	Zero-lift drag based on external pylons (optional weapon selections) computed at sea-level condition for relative mission segment (miscellaneous drag)
	DMUTOLD	Zero-lift drag based on undercarriages computed at sea-level condition for relative mission segment (miscellaneous drag)
	DMTTOLD	Zero-lift drag based on trailing edge control devices computed at sea-level condition for relative mission segment (miscellaneous drag)

Module (xxx.for)	Subroutine	Description
SUBMDRGZ (Continued)	DCWXM	Zero-lift drag based on wing computed at variable flight conditions for relative mission segment (component drag)
	DCCXM	Zero-lift drag based on cockpit (optional manned aircraft) computed at variable flight conditions for relative mission segment (component drag)
	DCSXM	Zero-lift drag based on external stores (optional weapon selections) computed at variable flight conditions for relative mission segment (component drag)
	DCBXM	Zero-lift drag based on weapon bay doors computed at variable flight conditions for relative mission segment (component drag)
	DMXM	Zero-lift drag based on external pylons computed at variable flight conditions for relative mission segment (miscellaneous drag)
SUBMISS	MSFXWSTW	Wing loading and thrust loading at individual mission segment
SUBMISS1	MISSION1	Low-level strike mission (primary mission) selected for UCAV. This module is controlled by the type of missions (TMISS=1) and by the correlative input data from file 'DATMISS1.DAT'.
SUBMISS2	MISSION2	Counterair mission (alternative role) selected for UCAV. This module is controlled by the type of missions (TMISS=2) and by the correlative input data from file 'DATMISS2.DAT'.
SUBMISS3	MISSION3	ISR mission (alternative role) selected for UCAV. This module is controlled by the type of missions (TMISS=3) and by the correlative input data from file 'DATMISS3.DAT'.
SUBMISS4	MISSION4	Ferry mission (secondary mission) selected for UCAV. This module is controlled by the type of missions (TMISS=4) and by the correlative input data from file 'DATMISS4.DAT'.
SUBMLIFT	LIFTTO	Lift of the aircraft at take-off condition
	LIFTLD	Lift of the aircraft at landing condition
SUBMPFM	SGTOLD	Ground roll distance for take-off and landing conditions
	STFTOLD	Transition distance for take-off condition and flare distance for landing condition
	SCATOLD	Horizontal distance travelled during the climb to clear the obstacle height for take-off condition and approach distance for landing condition
	STOLD	Total take-off and landing distance
SUBMPROP	TTOLD	Engine thrust at sea-level condition
	FCTOLD	Specific fuel consumption at sea-level condition

Module (xxx.for)	Subroutine	Description	
SUBMPROP (Continued)	TXM	Engine thrust at variable flight conditions	
	FCXM	Specific fuel consumption at variable flight conditions	
SUBMSACC	SEGACC	Accelerate segment	Performance analysis
SUBMSCBT	SEGDRB	Weapon release or drop bomb segment	
	SEGSTF	Strafe segment	
	SEGCBT	Combat segment	
SUBMSCL	SEGACCL	Accelerate to climb segment	
	SEGCL	Climb segment	
SUBMSCRU	SEGCRU	Cruise segment	
SUBMSDC	SEGDC	Descent segment	
SUBMSDSH	SEGDSH	Dash segment	
SUBMSLD	SEGLD	Landing segment	
SUBMSLTR	SEGLTR	Loiter segment	
SUBMSTO	SEGSTRT	Engine start and warm-up segment	
	SEGTAXI	Taxi segment	
	SEGTO	Take-off segment	
SUBMSTRN	SEGTRN	Turn segment	
SUBSCPCH	CMWING	Wing pitching moment	
	CMWTSE	Wing pitching moment increment with trailing edge control devices	
	CMWLSL	Wing pitching moment increment with leading edge control devices	
	CMTPGI	Engine contributions upon pitching moment	
	CMCLGEF	Ground effects upon pitching moment	
	CMUME	Main undercarriage effects upon pitching moment	
SUBSCROL	CLBWING	Wing rolling moment	
	CLBWTSE	Wing rolling moment due to trailing edge control devices	
SUBSCTRM	TRMTSE	Wing lift and pitching moment with trailing edge devices for trim analysis	
SUBSCYAW	CNBWING	Wing yawing moment	
	CNBWTSE	Wing yawing moment due to trailing edge control devices	
	CNBTPGI	Engine contributions upon yawing moment	
SUBWCHRD	XCWST	Wing chord at relative spanwise station for straight tapered wing planform	
	XCWK	Wing chord at relative spanwise station for multi-kinks wing planform	
	XCWC	Wing chord at relative spanwise station for equivalent wing planform	
SUBWDRAG	CDZEROL	Zero-lift drag for trim analysis	
	CDINDCE	Drag due to lift for trim analysis	
SUBWEAPB	WIB	Detail sizing of the internal weapon bays	
	WOB	Detail sizing of the external stores	
	MTWIB	Mass increment due to internal weapon bays	

Module (xxx.for)	Subroutine	Description	
SUBWLE	XWST	Distance of wing leading edge from nose at relative spanwise station for straight tapered wing planform	
	XWK	Distance of wing leading edge from nose at relative spanwise station for multi-kinks wing planform	
	WINGLER	Wing leading edge radius at relative spanwise station	
SUBWLIFT	CLSCAPH	Airfoil section lift-curve slope in incompressible flow	Spanwise lift distribution
	CLALPHA	Ratio for section lift-curve slope correction	
	FALIFTD	Additional lift distribution component due to sweep	
	FCALFTD	Coefficients for additional lift distribution	
	FCUCLMX	Taper ratio correction factors	Wing maximum lift
	CLWCMX	Maximum lift coefficient	
	CLSCBSE	Section lift increment with trailing edge control devices	Lift increment with control devices
	CLSCBSL	Section lift increment with leading edge control devices	
	CLWICS	Wing lift increment with control devices	
	CLMXBSE	Wing maximum lift increment with trailing edge control devices	
	CLMXBSL	Wing maximum lift increment with leading edge control devices	
SUBWMASS	MWWC	Wing structural mass	
SUBWMAT	FULTMTE	Ultimate load factor for structural design	
	FMATMASS	Mass factor for structural design	
	FMATPROP	Material factor for structural design	
	FSKINR	Skin roughness value for component drag estimation	
SUBWPTCH (DATCOM)	CMCP1	Subsonic centre of pressure location at maximum lift based on effects on leading edge shape	Wing pitching moment
	FCUCMCP	Taper ratio correction factor for pitching moment	
	CMCP2	Subsonic centre of pressure increment at maximum lift based on planform effect	
	CMSTBI	Stability index for pitching moment	
	CMCP3	Subsonic wing centre of pressure increment based on high angle of attack (stability index)	
	CMARI	Aspect ratio index for pitching moment	
	CMCP4	Subsonic wing centre of pressure increment based on high angle of attack (aspect ratio index)	

Module (xxx.for)	Subroutine	Description	
SUBWPTCH (Continued)	CMCLISE	Ratio of pitching moment increment to lift increment due to trailing edge control devices	Wing pitching moment increment with control devices
	CMFCIT1	Factor for partial-span trailing edge control devices	
	CMFCIT2	Factor for partial-span trailing edge control devices on swept wing	
	CMEFL	Pitching moment effectiveness due to leading edge control devices	
	CMLGEC	Variation in circulation with lift and height above ground (ground effects upon pitching moment)	
SUBWROLL (DATCOM)	CLBQW2	Wing sweep contribution to wing rolling moment	Wing rolling moment
	CLBFKMQ	Compressibility factor for wing sweep contribution to wing rolling moment	
	CLBAW	Wing aspect ratio contribution to wing rolling moment	
	CLBDIHE	Effect of uniform geometric dihedral on wing rolling moment	
	CLBFKMD	Compressibility factor for dihedral effect to wing rolling moment	
	CLBTWST	Effect of wing twist on wing rolling moment	
	CLBFSE	Aileron rolling moment parameter (wing rolling moment due to trailing edge control devices)	
SUBWTC	WINGTC	Wing thickness to chord ratio at relative spanwise station	
SUBWTWST	ALPHAC	Incremental local twist angle for cambered wing section	
SUBWVOL	WINGVOL	Volume distribution of the aircraft	
SUBWYAW (DATCOM)	CNBFSE	Factor for yawing moment due to aileron deflection (wing yawing moment due to trailing edge control devices)	

APPENDIX D

D: UCAV Output Data

This appendix presents the output data of some cases of the UCAV-optimized configuration developed by the UCAV design synthesis and optimization model, described in Chapter 8. Only the packaging and configuration design aspects of individual case are presented. The results shown in this appendix consist of: the example UCAV configuration, the validation with the existing aircraft – the Pegasus X-47 UCAV-N, and the packaging and configuration options.

D.1 Example UCAV Configuration

The configuration is based on the straight-tapered wing planform with the single weapon bay located at centreline of the aircraft, as shown in Figure 8-2 of Chapter 8.

```
------------------------------
--- UCAV PACKAGING SUMMARY ---
------------------------------

* UCAV PACKAGING CONFIGURATION

 1) Type of stores          = 1 :Internal store
 2) Number of weapon bays   = 1 :Single weapon bay on centreline
 3) Type of missions        = 1 :SEAD/strike
 4) Number of engines       = 1 :Single-engine installation
 5) Type of aircraft        = 0 :Unmanned aircraft
 6) Type of materials       = 2 :Carbon-fibre composite construction
 7) Number of kinks in wing = 0 :Straight taper wing
 8) Number of split elevons on half span = 2
 9) Number of slats on half span         = 0
10) Number of split rudders on half span = 0
11) Type of airfoils at wing inboard section  = 1 :Symmetrical airfoil
12) Type of airfoils at wing outboard section = 1 :Symmetrical airfoil
13) Thickness ratio at wing inboard section  = 15%
14) Thickness ratio at wing outboard section =  9%
15) Twist distribution      = 1 :Twist wing

-------------------------
*UCAV PACKAGING OPTIMIZER*

                                    INITIAL   FINAL    LOWER    UPPER
  1 Wing span (m)           [BW]    13.0000  12.4711   6.0000  40.0000
  2 Wing root chord (m)     [CWCC]   9.0000   8.0220   6.0000  20.0000
  3 Wing tip chord (m)      [CWCT]   2.0000   1.6044   0.0100   4.0000
  4 Front spar fraction     [FCWD]   0.1500   0.1500   0.0600   0.1500
  5 Rear spar fraction      [FCWR]   0.7000   0.7301   0.7000   0.8000
  6 Wing leading edge sweep[QWLR]   50.0000  51.8117   0.0100  60.0000
  7 Elevon mean chord (m)   [CWSE]   1.0000   0.8079   0.5000   3.0000
  8 Elevon inner span       [FYSEI]  0.2500   0.3823   0.1000   0.9500
  9 Elevon inner span       [FYSEI]  0.6500   0.5121   0.1000   0.9500
 10 Elevon outer span       [FYSEO]  0.4500   0.5040   0.1000   0.9500
 11 Elevon outer span       [FYSEO]  0.7500   0.9500   0.1000   0.9500
 12 Wing tank span factor   [FY2WFO] 0.5000   0.0613   0.0100   1.0000
 13 Wing tank front factor  [FCWFD]  0.0000   0.0000   0.0000   0.0000
 14 Wing tank rear factor   [FCWFR]  1.0000   1.0000   1.0000   1.0000
 15 Weap bayl axial factor  [FXLIB1] 0.5000   0.4171   0.0000   1.0000
```

```
 16 Engine axial factor     [FXLPG]       0.5000   0.2645   0.0000   1.0000
 17 Engine scale factor     [RTP]         1.5000   0.5508   0.5000   2.5000

 ------------------------------
 *UCAV FIXED MASS CONTRIBUTION*

 ------------------------------
 * AVIONICS BAY

MISSION MANAGEMENT SYSTEM
Mass & volume of radar suite              =    28.32 kg   0.1404 m^3
Mass & volume of sensor suite             =    23.02 kg   0.0605 m^3

FLIGHT MANAGEMENT SYSTEM
Mass & volume of flight control suite     =    45.03 kg   0.1634 m^3
Mass & volume of navigation suite         =    40.44 kg   0.1925 m^3
Mass & volume of communication suite      =    12.68 kg   0.0949 m^3
Mass & volume of identification suite     =    20.89 kg   0.1556 m^3

STORE MANAGEMENT SYSTEM
Mass & volume of weapon control suite     =     8.32 kg   0.0620 m^3

ELECTRONIC WARFARE SYSTEM
Mass & volume of electronic warfare suite =     4.82 kg   0.0322 m^3
Mass & volume of countermeasures suite    =     4.82 kg   0.0322 m^3

Total avionics mass                       =   188.34 kg

Length of radar avionics suite            =  0.8022 m
Length of flight management avionics suite =  1.2861 m
Length of weapon control avionics suite   =  0.5697 m

Radome length                             =  1.2033 m

 ------------------------------
 * WEAPON BAY

WEAPON BAY 1
Total number of weapon bay 1                  = 1
Total number of weapons in each weapon bay 1  = 1
Total mass of weapons in weapon bay 1         =   460.00 kg
Total mass of internal pylons in weapon bay 1 =    62.50 kg

WEAPON BAY 2
Total number of weapon bay 2                  = 0
Total number of weapons in each weapon bay 2  = 0
Total mass of weapons in weapon bay 2         =     0.00 kg
Total mass of internal pylons in weapon bay 2 =     0.00 kg

INTERNAL WEAPON BAY
Total mass of weapons in internal weapon bays =   460.00 kg

WEAPON BAY DIMENSION
              L(m)     W(m)     H(m)    V(m^3)
Weapon bay 1  3.1900   0.6300   0.6300  1.2661
Weapon bay 2  0.0000   0.0000   0.0000  0.0000

EXTERNAL STORES
Total number of weapons at port store         = 0
Total mass of weapons at port store           =     0.00 kg
Total number of weapons at starboard store    = 0
Total mass of weapons at starboard store      =     0.00 kg
External store wetted area                    =  0.0000 m^2
Total mass of external pylons                 =     0.00 kg

Total mass of weapons at external stores      =     0.00 kg


TOTAL WEAPONS
Total mass of weapons on aircraft             =   460.00 kg

 ---------------------------------
 *UCAV VARIABLE MASS CONTRIBUTION*

 ------------------------------
 * ENGINE BAY
```

```
 TWO SINGLE-ENGINE INSTALLATIONS

ENGINE & ENGINE BAY DIMENSION
Overall length of engine  =  1.2817 m
Diameter of engine        =  0.6034 m

Total nozzle exit area    =    0.29 m^2

Maximum engine bay height =  0.7241 m
Maximum engine bay width  =  0.7241 m

ENGINE BAY VOLUME
Volume of engine bay           =  0.5278 m^3

PROPULSION SYSTEM MASS
Total mass of engines          =   360.14 kg
Engine installation mass       =    46.82 kg

Total mass of propulsion system =   406.96 kg

ENGINE STATIC THRUST
Total maximum sea-level static thrust of engines =  21801.59 N
Bypass ratio of total engines   =    8.00

 ------------------------------
 * UNDERCARRIAGE BAY

NOSE UNDERCARRIAGE
Length of nose undercarriage leg         =  0.5806 m
Nose undercarriage wheel & tyre diameter =  0.3809 m
Nose undercarriage wheel & tyre width    =  0.1520 m

MAIN UNDERCARRIAGE
Length of each main undercarriage leg    =  0.7846 m
Main undercarriage wheel & tyre diameter =  0.5246 m
Main undercarriage wheel & tyre width    =  0.1417 m

UNDERCARRIAGE MASS
Structural mass of nose undercarriage            =    26.55 kg
Structural mass of total main undercarriage      =   192.25 kg
Mass of hydraulics associated with undercarriage =    25.83 kg

UNDERCARRIAGE GROSS MASS
Total mass of nose undercarriage with hydraulics =    29.68 kg
Total mass of main undercarriage with hydraulics =   214.94 kg

UNDERCARRIAGE BAY DIMENSION
              L(m)     H(m)     W(m)    V(m^3)
Nose UC bay  0.7711   0.4190   0.2280   0.0737
Main UC bay  1.0469   0.5771   0.2125   0.1284

 ------------------------------
 * FLYING WING

 STRAIGHT TAPERED WING

FLYING WING SPECIFICATION
Wing centreline section & chord  0.0000 m  8.0220 m
Wing tip section & chord         6.2355 m  1.6044 m
Wing gross span               = 12.4711 m
Gross wing aspect ratio       =  2.5910
Gross wing area               =   60.03 m^2
Wing wetted area              =  122.13 m^2
Mean thickness ratio          =  0.1110
Average wing chord            =  4.8132 m

Wing geometric mean chord     =  4.8132 m
Wing aerodynamic mean chord   =  5.5263 m
Distance of wing mean 1/4 chord point from nose =  4.4644 m

Equivalent wing root chord         =  8.0220 m
Equivalent wing taper ratio        =  0.2000
Equivalent wing leading edge sweep = 51.8117 degree
Equivalent wing quarter chord sweep= 45.3985 degree
Equivalent wing mid-chord sweep    = 37.1151 degree

Maximum depth at wing centreline chord =  1.2033 m
```

```
Maximum depth at wing tip chord        =  0.1444 m

Wing maximum cross-sectional area      =   11.27 m^2
Flying wing total volume               =   29.40 m^3

Centre of wing volume (true wing)      =  0.1013
Centre of wing volume (equivalent wing)=  0.0000

Wing aerodynamic centre (%MAC)         =  0.0300


WING BOX
Wing front spar from nose at root      =  1.2033 m
Wing rear spar from nose at root       =  5.8569 m

Wing front spar from nose at tip       =  0.2407 m
Wing rear spar from nose at tip        =  1.1714 m

Wing box root chord                    =  4.6536 m
Wing box tip chord                     =  0.9307 m
Wing box gross span                    = 12.4711 m
Gross wing box planform area           =   34.82 m^2
Gross wing box aspect ratio            =  4.4665

Equivalent wing box root chord         =  4.6536 m
Equivalent wing box taper ratio        =  0.2000
Equivalent wing box leading edge sweep = 48.1615 degree
Equivalent wing box centreline sweep   = 44.2097 degree


WING SPANWISE LIFT DISTRUBITION
Mach number for design diving speed =  1.1755
Effective Mach number               =  0.5103
Effective angle of sweepback        = 55.8846 degree
Average angle of attack             =  5.5601 degree

 ------------------------------
 * BAY POSITION

ENGINE BAY POSITION
Spanwise station to engine bay section             =  0.4650  0.8270  1.1891 m
Wing chord at engine bay section                   =  7.5434  7.1708  6.7982 m
Wing leading edge at engine bay section from nose  =  0.5912  1.0514  1.5117 m

Minimum distance of engine inlet from nose         =  3.2605 m
Maximum distance of engine exit from nose          =  6.9502 m
Axial space available for length of engine         =  3.6897 m

Axial distance from nose to engine front face      =  4.5726 m
Axial distance from nose to transition duct entrance=  5.8544 m


WEAPON BAY 1 POSITION
Spanwise station to weapon bay 1 section           =  0.0000  0.0000  0.3150 m
Wing chord at weapon bay 1 section                 =  8.0220  8.0220  7.6978 m
Wing leading edge at weapon bay 1 section from nose =  0.0000  0.0000  0.4005 m

Minimum distance of weapon bay1 front face from nose=  3.2605 m
Maximum distance of weapon bay1 rear face from nose =  6.7422 m
Axial space available for length of weapon bay 1    =  3.2982 m

Axial distance from nose to weapon bay 1 front face =  3.3461 m


WEAPON BAY 2 POSITION
Spanwise station to weapon bay 2 section           =  0.0000  0.0000  0.0000 m
Wing chord at weapon bay 2 section                 =  0.0000  0.0000  0.0000 m
Wing leading edge at weapon bay 2 section from nose =  0.0000  0.0000  0.0000 m

Minimum distance of weapon bay2 front face from nose=  0.0000 m
Maximum distance of weapon bay2 rear face from nose =  0.0000 m
Axial space available for length of weapon bay 2    =  0.0000 m

Axial distance from nose to weapon bay 2 front face =  0.0000 m


MAIN UNDERCARRIAGE BAY POSITION
```

```
Spanwise station to main uc bay section            =  1.3391  1.4453  1.5516 m
Wing chord at main uc bay section                  =  6.6438  6.5345  6.4251 m
Wing leading edge at main uc bay section from nose =  1.7024  1.8374  1.9725 m

Minimum distance of main uc bay front face from nose=  2.9363 m
Maximum distance of main uc bay rear face from nose =  6.5531 m
Axial space available for length of main uc bay     =  3.6168 m

Axial distance from nose to main uc bay front face  =  4.0201 m

 ------------------------------
 * INTAKE DIFFUSER

Cross sectional area of intake inlet  =  0.2859 m^2
Cross sectional area of intake exit   =  0.2859 m^2
Equivalent diameter of intake inlet   =  0.6034 m
Diameter of intake exit               =  0.6034 m

Width of intake inlet                 =  0.7562 m
Height of intake inlet                =  0.3781 m
Width of intake inlet projected into horizontal =  0.7562 m
Height of intake inlet projected into vertical  =  0.3781 m

Distance of intake inlet from nose    =  2.6174 m
Length of intake diffuser             =  1.9552 m

Spanwise station to intake inlet      =  0.8270 m
Spanwise station to intake exit       =  0.8270 m
Vertical distance of intake inlet     =  0.3065 m
Vertical distance of intake exit      =  0.0000 m
Wing leading edge at intake from nose =  1.0514 m

Volume of each intake diffuser        =  0.5591 m^3

 ------------------------------
 * 2-DIMENSIONAL NOZZLE

Aspect ratio of nozzle transition duct exit=  8.4139

SINGLE ENGINE INSTALLATION
Half-height of nozzle transition duct exit =  0.0922 m
Half-width of nozzle transition duct exit  =  0.7241 m

Length of nozzle transition duct      =  1.7757 m

Volume of nozzle transition duct      =  1.3388 m^3
Total mass of nozzle transition duct =    84.17 kg

 ------------------------------
 * TRAILING EDGE SPLIT ELEVON

Total number of all split elevons = 4

ELEVON 1
Elevon inner span,chrd &wchrd =  2.3840  1.0574  5.5684 m
Elevon outer span,chrd &wchrd =  3.1429  0.9091  4.7873 m
Elevon mean chord             =  0.9833 m
Total span of elevon          =  1.5179 m
Aspect ratio of each elevon   =  0.7719
Elevon hinge line sweep       = 21.2406 deg
Total planform area of elevon =    1.49 m^2
Total wing area over elevon   =    7.86 m^2
ELEVONS LIFT & MOMENT             TO      LD
Elevon deflection             =   30.00   60.00 deg
Section lift increment        =  0.8633  1.2537
Wing lift increment           =  0.0526  0.0764
Wing pitch increment          = -0.0027 -0.0039
Sect max lift increment       =  0.6547  0.8850
Wing max lift increment       =  0.0799  0.1080

ELEVON 2
Elevon inner span,chrd &wchrd =  3.1929  0.8993  4.7359 m
Elevon outer span,chrd &wchrd =  5.9238  0.3656  1.9253 m
Elevon mean chord             =  0.6325 m
Total span of elevon          =  5.4617 m
Aspect ratio of each elevon   =  4.3178
Elevon hinge line sweep       = 21.2406 deg
```

```
Total planform area of elevon =    3.45 m^2
Total wing area over elevon   =   18.19 m^2
ELEVONS LIFT & MOMENT              TO      LD
Elevon deflection             =   30.00   60.00 deg
Section lift increment        =  0.0000  0.0000
Wing lift increment           =  0.0000  0.0000
Wing pitch increment          =  0.0000  0.0000
Sect max lift increment       =  0.0000  0.0000
Wing max lift increment       =  0.0000  0.0000


All split elevons gross span          =   6.9796 m
Split elevon mean chord               =   0.8079 m
All split elevons planform area       =     4.95 m^2
Total wing planform area over split elevons   =   26.05 m^2

WING TRAILING EDGE
Gross area of wing trailing edge aft of rear spar    =   11.78 m^2
Planform area of fixed section of wing TE aft of r/s =    6.83 m^2

 ------------------------------
 * LEADING EDGE SLAT

Total number of all slats = 0


All slats gross span          =   0.0000 m
Slat mean chord               =   0.0000 m
All slats planform area       =     0.00 m^2
Total wing planform area over slats   =    0.00 m^2

WING LEADING EDGE
Total planform area of wing leading edge             =    6.55 m^2
Planform area of fixed section of wing LE fwd of f/s =    2.18 m^2

 ------------------------------
 * TRAILING EDGE SPLIT RUDDER

Total number of all split rudders = 2

SPLIT RUDDER 2
Rudder inner span & wchrd     =  3.1929  4.7359 m
Rudder outer span & wchrd     =  5.9238  1.9253 m
Aspect ratio of each rudder   =  4.3178
Rudder hinge line sweep       = 21.2406 deg
SPLIT RUDDERS LIFT & MOMENT      Aileron Rudder
Split rudder deflection       =   20.00   25.00 deg
Section lift increment        =  0.7176  0.8127
Wing lift increment           =  0.1033  0.1169
Wing yaw effectiveness        = -0.0049  0.0056
Wing roll effectiveness       =  0.0590 -0.0668

 ------------------------------
 * FUEL

- CENTRE FUEL TANK -
Total span of centre fuel tank =  0.6300 m

CENTRE FUEL TANK 1 (FRONT)
Centre fuel tank 1 front face from nose =  3.2605 m
Centre fuel tank 1 rear face from nose  =  3.3461 m
Total fuel volume of centre tank 1    =  0.0509 m^3
Fuel mass used in centre fuel tank 1  =     0.00 kg
M-arm of centre fuel tank 1 from nose =  3.3033 m

CENTRE FUEL TANK 2 (REAR)
Centre fuel tank 2 front face from nose =  6.5361 m
Centre fuel tank 2 rear face from nose  =  6.7422 m
Total fuel volume of centre tank 2    =  0.0509 m^3
Fuel mass used in centre fuel tank 2  =     0.00 kg
M-arm of centre fuel tank 2 from nose =  6.6369 m

CENTRE FUEL TANK 3 (TOP)
Centre fuel tank 3 front face from nose =  3.3461 m
Centre fuel tank 3 rear face from nose  =  4.9411 m
Total fuel volume of centre tank 3    =  0.1132 m^3
Fuel mass used in centre fuel tank 3  =     0.00 kg
```

```
M-arm of centre fuel tank 3 from nose =  4.1145 m

TOTAL CENTRE FUEL TANK CAPACITY
Total area of centre fuel tank        =  1.1886 m^2
Total fuel volume of centre tank      =  0.2150 m^3
Total fuel mass used in centre tank   =     0.00 kg


- INBOARD FUEL TANK -
Total span of inboard fuel tank =  0.0000 m

INBOARD FUEL TANK 1 (FRONT)
Inboard fuel tank 1 front face from nose =  0.0000 m
Inboard fuel tank 1 rear face from nose  =  0.0000 m
Total fuel volume of inbrd tank 1     =  0.0000 m^3
Fuel mass used in inbrd fuel tank 1   =     0.00 kg
M-arm of inbrd fuel tank 1 from nose  =  0.0000 m

INBOARD FUEL TANK 2 (REAR)
Inboard fuel tank 2 front face from nose =  0.0000 m
Inboard fuel tank 2 rear face from nose  =  0.0000 m
Total fuel volume of inbrd tank 2     =  0.0000 m^3
Fuel mass used in inbrd fuel tank 2   =     0.00 kg
M-arm of inbrd fuel tank 2 from nose  =  0.0000 m

INBOARD FUEL TANK 3 (TOP)
Inboard fuel tank 3 front face from nose =  0.0000 m
Inboard fuel tank 3 rear face from nose  =  0.0000 m
Total fuel volume of inbrd tank 3     =  0.0000 m^3
Fuel mass used in inbrd fuel tank 3   =     0.00 kg
M-arm of inbrd fuel tank 3 from nose  =  0.0000 m

TOTAL INBOARD FUEL TANK CAPACITY
Total area of inboard fuel tank       =  0.0000 m^2
Total fuel volume of inbrd tank       =  0.0000 m^3
Total fuel mass used in inbrd tank    =     0.00 kg


- OUTBOARD FUEL TANK -
Total span of outboard fuel tank =  0.4250 m

OUTBOARD FUEL TANK 1 (FRONT)
Outboard fuel tank 1 front face from nose =  2.9363 m
Outboard fuel tank 1 rear face from nose  =  4.0201 m
Total fuel volume of outbrd tank 1    =  0.3298 m^3
Fuel mass used in outbrd fuel tank 1  =     0.00 kg
M-arm of outbrd fuel tank 1 from nose =  3.4885 m

OUTBOARD FUEL TANK 2 (REAR)
Outboard fuel tank 2 front face from nose =  5.0670 m
Outboard fuel tank 2 rear face from nose  =  6.5531 m
Total fuel volume of outbrd tank 2    =  0.3685 m^3
Fuel mass used in outbrd fuel tank 2  =     0.00 kg
M-arm of outbrd fuel tank 2 from nose =  5.7611 m

TOTAL OUTBOARD FUEL TANK CAPACITY
Total area of outboard fuel tank      =  1.0922 m^2
Total fuel volume of outbrd tank      =  0.6983 m^3
Total fuel mass used in outbrd tank   =     0.00 kg


- WING FUEL TANK -
Wing fuel tank spanwise station 0 =  1.7016 m
Wing fuel tank spanwise station 1 =  2.0439 m
Total span available for wing fuel tank          =  0.6846 m
Total wing box area available for wing fuel tank =  2.4203 m^2

WING FUEL TANK CAPACITY
Total fuel volume of wing tank        =  1.2584 m^3
Total fuel mass used in wing tank     =   977.17 kg


- OPTIONAL WEAPON BAY FUEL TANK -
Total fuel volume of weapon bay tank1=  0.0000 m^3
Fuel mass used in weapon bay tank 1  =     0.00 kg

Total fuel volume of weapon bay tank2=  0.0000 m^3
```

```
Fuel mass used in weapon bay tank 2  =     0.00 kg

TOTAL WEAPON BAY FUEL TANK CAPACITY
Total fuel volume of weapon bay tank      =  0.0000 m^3
Total fuel mass used in weapon bay tank   =     0.00 kg


- UCAV TOTAL FUEL CAPACITY -
Total area containing fuel tank      =  4.7012 m^2
Total internal fuel volume           =  2.1718 m^3
Total mass of available internal fuel=  1686.42 kg

Total fuel mass used on aircraft     =   977.17 kg

 ------------------------------
 * UCAV MASS & CG

- UCAV MASS -

WING BOX
Ultimate load factor           =    9.75
Wing inertia relief load       =   939.56 kg

Wing box mass (Torsion)        =   111.32 kg
Wing box mass (Bending)        =   159.33 kg
Total wing box mass            =   159.33 kg

CONTROL SURFACES
Wing leading edge mass         =    35.52 kg
Wing fixed trailing edge mass  =    55.76 kg

TEcs mass (flap)               =     6.25 kg
TEcs mass (aileron)            =    50.83 kg
Total TE control surfaces mass =    57.07 kg

Inlaids mass (rudder)          =     0.00 kg
Inlaids mass (spoiler)         =     0.00 kg
Total inlaids CS mass          =     0.00 kg

AUXILIARY
Miscellaneous attachments      =    25.37 kg
External paint                 =    20.47 kg
Low Observable treatments      =   226.80 kg
Basic ribs in strutural box    =   285.36     0.00 kg

FLYING WING
Total wing structural mass     =   865.69 kg

MASS INCREMENT DUE TO INTERNAL WEAPON BAYS
Mass increment due to weap bay1=   117.77 kg
Mass increment due to weap bay2=     0.00 kg

AIRCRAFT SYSTEM
Mass of air systems            =     6.41 kg
Mass of de-icing system        =    25.53 kg
Mass of electrical systems     =   130.74 kg
Mass of flight control systems =   132.86 kg
Mass of fuel system            =    74.17 kg

COMPLETE AIRCRAFT
Total aircraft payload         =   460.00 kg
Mass of fixed-role equipment   =   250.84 kg
Total mass of fuel on aircraft =   977.17 kg

Empty mass             =   2339.77 kg
Operational empty mass =   2339.77 kg
Zero fuel mass         =   2799.77 kg

Total take-off mass    =   3776.94 kg
Landing mass           =   3210.40 kg

Wing loading           =   62.9219 kg/m^2
Thrust loading         =    0.5886


WING STRUCTURAL MASS COMPARISON
Howe method 1 (COA)    =    865.69 kg (theoretical)
```

```
Howe method 2 (COA)     =   1310.97 kg (empirical)
Lovell method (RAE)     =   1796.53 kg
Roskam method (USAF)    =    605.36 kg
Roskam method (USN)     =    898.52 kg
Raymer method           =    684.86 kg
Whitford method         =    830.25 kg


- CENTRE OF GRAVITY -

OPERATIONAL EMPTY MASS
Total aircraft pitching moment about nose=  10340.73 kg.m
Distance of aircraft CG from nose        =  4.4195 m
CG relative to aerodynamic mean chord    =  24.19%

ZERO FUEL MASS
Total aircraft pitching moment about nose=  12613.64 kg.m
Distance of aircraft CG from nose        =  4.5052 m
CG relative to aerodynamic mean chord    =  25.74%

TOTAL TAKE-OFF MASS
Total aircraft pitching moment about nose=  17459.99 kg.m
Distance of aircraft CG from nose        =  4.6228 m
CG relative to aerodynamic mean chord    =  27.87%
Static margin                            =  -2.87%

Distance of aircraft fwd CG from nose  =  4.1328 m
Fwd CG relative to AMC                 =  19.00%
Distance of aircraft aft CG from nose  =  4.8512 m
Aft CG relative to AMC                 =  32.00%

Reference spanwise distance of aircraft CG             =  0.0000 m
Reference vertical distance of aircraft CG from ground =  1.2934 m


- UNDERCARRIAGE ARRANGEMENTS -

UNDERCARRIAGE ARRANGEMENTS
Axial distance from nose wheel to main wheel =  3.4282 m
Axial angle from nose wheel to main wheel    = 22.8603 degree

Axial distance from nose UC to aircraft aft CG position     =  3.0339 m
Axial distance from aircraft forward CG position to main UC =  0.5975 m
Axial distance from aircraft aft CG position to main UC     =  0.3942 m

AIRCRAFT OVERTURN ANGLE
Aircraft static ground line    =  1.3318 m
Aircraft overturn angle        = 44.1623 degree

AIRCRAFT TIPBACK & STATIC TAILDOWN ANGLE
Axial distance from main uc to tail =  4.5147 m
Height due to tipback angle         =  1.3761 m

Aircraft tipback angle         = 16.9517 degree
Aircraft static taildown angle = 14.8997 degree

AIRCRAFT ANGLE OFF VERTICAL
Angle off vertical             = 16.9517 degree

UNDERCARRIAGE STATIC LOADS
Maximum static load       =   3342.59 kg
Maximum nose static load  =    658.27 kg
Minimum nose static load  =    434.35 kg
Nose dynamic braking load =    435.93 kg

Maximum static load as a fraction of total load      =   88.50%
Maximum nose static load as a fraction of total load =   17.43%
Minimum nose static load as a fraction of total load =   11.50%

MAIN UNDERCARRIAGE SHOCK ABSORBER STROKE
Main undercarriage rolling radius        =  0.1749 m
Main undercarriage tyre stroke           =  0.0874 m
Main undercarriage shock absorber stroke =  0.4900 m

UNDERCARRIAGES FRONTAL AREA
Oleo load of each main undercarriage =   1671.30 kg
Oleo load of nose undercarriage      =   1094.19 kg
```

```
Oleo diameter of main undercarriage  =  0.0170 m
Oleo diameter of nose undercarriage  =  0.0138 m

Frontal area of each main undercarriage leg          =  0.0134 m^2
Frontal area of each main undercarriage wheel & tyre =  0.0619 m^2

Frontal area of nose undercarriage leg          =  0.0080 m^2
Frontal area of nose undercarriage wheel & tyre =  0.0483 m^2

 ------------------------
 *UCAV COMPONENT SUMMARY*

 --- MASS & BALANCE ---
 Aircraft component  Mass   Range   X-Marm    XMoment   Y-Marm    YMoment
                     (kg)   (%)     (m)       (kg.m)    (m)       (kg.m)
Wing (port)          432.84   11.46  5.0245   2174.81 -2.7436  -1187.57
Wing (starboard)     432.84   11.46  5.0245   2174.81  2.7436   1187.57
Nose UC               29.68    0.79  1.5888     47.16  0.0000      0.00
Main UC (port)       107.47    2.85  5.0170    539.19 -1.4453   -155.33
Main UC (stbd)       107.47    2.85  5.0170    539.19  1.4453    155.33
Engine (port)        203.48    5.39  5.2135   1060.84 -0.8270   -168.28
Engine (stbd)        203.48    5.39  5.2135   1060.84  0.8270    168.28
Nozzle (port)         42.08    1.11  6.7422    283.73 -0.8270    -34.80
Nozzle (stbd)         42.08    1.11  6.7422    283.73  0.8270     34.80
Avionics(MMS)         51.34    1.36  0.8022     41.18  0.0000      0.00
Avionics(FMS)        119.04    3.15  2.6174    311.58  0.0000      0.00
Avionics(SMS)         8.32    0.22  2.2959     19.10  0.0000      0.00
Avionics(EWS-port)    4.82    0.13  6.7382     32.48 -5.3002    -25.55
Avionics(EWS-stbd)    4.82    0.13  6.7382     32.48  5.3002     25.55
Air system            6.41    0.17  2.2959     14.72  0.0000      0.00
De-icing system      25.53    0.68  2.2959     58.62  0.0000      0.00
Electrical system   130.74    3.46  2.2959    300.18  0.0000      0.00
FCS                 132.86    3.52  2.2959    305.05  0.0000      0.00
Fuel system          74.17    1.96  2.2959    170.28  0.0000      0.00
W bay1 pylon         62.50    1.65  4.9411    308.82  0.0000      0.00
W bay1 increment    117.77    3.12  4.9411    581.94  0.0000      0.00
Residual fuel         0.00    0.00  2.2959      0.00  0.0000      0.00
     OEM           2339.77   61.95  4.4195  10340.73                0.00

Weap in bay1        460.00   12.18  4.9411   2272.91  0.0000      0.00
     ZFM           2799.77   74.13  4.5052  12613.64                0.00

Wing tank (port)    488.58   12.94  4.9596   2423.17 -1.8522   -904.95
Wing tank (stbd)    488.58   12.94  4.9596   2423.17  1.8522    904.95
Centre tank1          0.00    0.00  3.3033      0.00  0.0000      0.00
Centre tank2          0.00    0.00  6.6369      0.00  0.0000      0.00
Centre tank3          0.00    0.00  4.1145      0.00  0.0000      0.00
Outbrd tank1(port)    0.00    0.00  3.4885      0.00 -1.4453      0.00
Outbrd tank1(stbd)    0.00    0.00  3.4885      0.00  1.4453      0.00
Outbrd tank2(port)    0.00    0.00  5.7611      0.00 -1.4453      0.00
Outbrd tank2(stbd)    0.00    0.00  5.7611      0.00  1.4453      0.00
     AUM           3776.94  100.00  4.6228  17459.99                0.00


 --- MASS & BALANCE (continued) ---
 Aircraft component  Mass   Z-Marm    ZMoment   Z-Marm    ZMoment
                     (kg)   dwn(m)    (kg.m)    up (m)    (kg.m)
Wing (port)          432.84  1.2934    559.85  0.0000       0.00
Wing (starboard)     432.84  1.2934    559.85  0.0000       0.00
Nose UC               29.68  0.9595     28.48 -0.3339      -9.91
Main UC (port)       107.47  0.9595    103.12 -0.3339     -35.88
Main UC (stbd)       107.47  0.9595    103.12 -0.3339     -35.88
Engine (port)        203.48  1.2934    263.18  0.0000       0.00
Engine (stbd)        203.48  1.2934    263.18  0.0000       0.00
Nozzle (port)         42.08  1.2934     54.43  0.0000       0.00
Nozzle (stbd)         42.08  1.2934     54.43  0.0000       0.00
Avionics(MMS)         51.34  1.2934     66.40  0.0000       0.00
Avionics(FMS)        119.04  1.2934    153.97  0.0000       0.00
Avionics(SMS)         8.32  1.2934     10.76  0.0000       0.00
Avionics(EWS-port)    4.82  1.2934      6.23  0.0000       0.00
Avionics(EWS-stbd)    4.82  1.2934      6.23  0.0000       0.00
Air system            6.41  1.5029      9.64  0.2095       1.34
De-icing system      25.53  1.5029     38.37  0.2095       5.35
Electrical system   130.74  1.6554    216.44  0.3620      47.33
FCS                 132.86  1.6554    219.95  0.3620      48.10
Fuel system          74.17  1.6554    122.78  0.3620      26.85
```

```
W bay1 pylon          62.50  1.6084    100.53  0.3150      19.69
W bay1 increment     117.77  1.2934    152.33  0.0000       0.00
Residual fuel          0.00  1.2331      0.00 -0.0603       0.00
     OEM            2339.77            3093.27              66.99

Weap in bay1         460.00  1.2934    594.97  0.0000       0.00
     ZFM            2799.77            3688.24              66.99

Wing tank (port)     488.58  1.2934    631.94  0.0000       0.00
Wing tank (stbd)     488.58  1.2934    631.94  0.0000       0.00
Centre tank1           0.00  1.2934      0.00  0.0000       0.00
Centre tank2           0.00  1.2934      0.00  0.0000       0.00
Centre tank3           0.00  1.6084      0.00  0.3150       0.00
Outbrd tank1(port)     0.00  1.2934      0.00  0.0000       0.00
Outbrd tank1(stbd)     0.00  1.2934      0.00  0.0000       0.00
Outbrd tank2(port)     0.00  1.2934      0.00  0.0000       0.00
Outbrd tank2(stbd)     0.00  1.2934      0.00  0.0000       0.00
     AUM            3776.94            4952.12              66.99
```

D.2 Validation with Existing Aircraft

The configuration is based on the *baseline* geometry of the Pegasus X-47 UCAV-N example planform, providing all major parameters being optimized, as shown in Table 8-4 of Chapter 8.

```
------------------------------
--- UCAV PACKAGING SUMMARY ---
------------------------------

* UCAV PACKAGING CONFIGURATION

 1) Type of stores          = 1 :Internal store
 2) Number of weapon bays   = 2 :Two weapon bays outboard of engines
 3) Type of missions        = 1 :SEAD/strike
 4) Number of engines       = 1 :Single-engine installation
 5) Type of aircraft        = 0 :Unmanned aircraft
 6) Type of materials       = 2 :Carbon-fibre composite construction
 7) Number of kinks in wing = 0 :Straight taper wing
 8) Number of split elevons on half span = 1
 9) Number of slats on half span         = 0
10) Number of split rudders on half span = 0
11) Type of airfoils at wing inboard section  = 1 :Symmetrical airfoil
12) Type of airfoils at wing outboard section = 1 :Symmetrical airfoil
13) Thickness ratio at wing inboard section  = 18%
14) Thickness ratio at wing outboard section =  9%
15) Twist distribution      = 0 :Untwist wing

--------------------------
*UCAV PACKAGING OPTIMIZER*

                                      INITIAL    FINAL     LOWER     UPPER
  1 Wing span (m)           [BW]       8.5000    8.7627    6.0000    9.0000
  2 Wing root chord (m)     [CWCC]     8.5000    8.0102    6.0000    9.0000
  3 Wing tip chord (m)      [CWCT]     0.0100    0.0100    0.0100    0.0100
  4 Front spar fraction     [FCWD]     0.1500    0.1500    0.0600    0.1500
  5 Rear spar fraction      [FCWR]     0.7000    0.6600    0.6600    0.8000
  6 Wing leading edge sweep[QWLR]     55.0000   55.9635   54.0000   56.0000
  7 Elevon mean chord (m)   [CWSE]     1.0000    0.5000    0.5000    3.0000
  8 Elevon inner span       [FYSEI]    0.4000    0.6606    0.1000    0.9500
  9 Elevon outer span       [FYSEO]    0.7000    0.8606    0.1000    0.9500
 10 Wing tank span factor   [FY2WFO]   0.5000    0.5195    0.0100    1.0000
 11 Wing tank front factor  [FCWFD]    0.0000    0.0000    0.0000    0.0000
 12 Wing tank rear factor   [FCWFR]    0.5000    0.5430    0.0100    1.0000
 13 Weap bay1 axial factor  [FXLIB1]   0.5000    0.2215    0.0000    1.0000
 14 Engine axial factor     [FXLPG]    0.5000    0.0000    0.0000    1.0000
 15 Engine scale factor     [RTP]      1.5000    0.6641    0.5000    2.5000

------------------------------
*UCAV FIXED MASS CONTRIBUTION*

------------------------------
```

```
 * AVIONICS BAY

MISSION MANAGEMENT SYSTEM
Mass & volume of radar suite              =    28.32 kg   0.1404 m^3
Mass & volume of sensor suite             =    23.02 kg   0.0605 m^3

FLIGHT MANAGEMENT SYSTEM
Mass & volume of flight control suite     =    45.03 kg   0.1634 m^3
Mass & volume of navigation suite         =    40.44 kg   0.1925 m^3
Mass & volume of communication suite      =    12.68 kg   0.0949 m^3
Mass & volume of identification suite     =    20.89 kg   0.1556 m^3

STORE MANAGEMENT SYSTEM
Mass & volume of weapon control suite     =     8.32 kg   0.0620 m^3

ELECTRONIC WARFARE SYSTEM
Mass & volume of electronic warfare suite =     4.82 kg   0.0322 m^3
Mass & volume of countermeasures suite    =     4.82 kg   0.0322 m^3

Total avionics mass                       =   188.34 kg

Length of radar avionics suite            =  0.8022 m
Length of flight management avionics suite =  1.2861 m
Length of weapon control avionics suite   =  0.5697 m

Radome length                             =  1.2033 m

 ------------------------------
 * WEAPON BAY.

WEAPON BAY 1
Total number of weapon bay 1                  = 1
Total number of weapons in each weapon bay 1  = 1
Total mass of weapons in weapon bay 1         =   113.40 kg
Total mass of internal pylons in weapon bay 1 =    62.50 kg

WEAPON BAY 2
Total number of weapon bay 2                  = 1
Total number of weapons in each weapon bay 2  = 1
Total mass of weapons in weapon bay 2         =   113.40 kg
Total mass of internal pylons in weapon bay 2 =    62.50 kg

INTERNAL WEAPON BAY
Total mass of weapons in internal weapon bays =   226.80 kg

WEAPON BAY DIMENSION
              L(m)     W(m)     H(m)    V(m^3)
Weapon bay 1  2.3600   0.5300   0.5300  0.6629
Weapon bay 2  2.3600   0.5300   0.5300  0.6629

EXTERNAL STORES
Total number of weapons at port store         = 0
Total mass of weapons at port store           =     0.00 kg
Total number of weapons at starboard store    = 0
Total mass of weapons at starboard store      =     0.00 kg
External store wetted area                    =  0.0000 m^2
Total mass of external pylons                 =     0.00 kg

Total mass of weapons at external stores      =     0.00 kg


TOTAL WEAPONS
Total mass of weapons on aircraft             =   226.80 kg

 ---------------------------------
 *UCAV VARIABLE MASS CONTRIBUTION*

 ------------------------------
 * ENGINE BAY

 ONE SINGLE-ENGINE INSTALLATION

ENGINE & ENGINE BAY DIMENSION
Overall length of engine  =  1.4074 m
Diameter of engine        =  0.6625 m

Total nozzle exit area    =    0.34 m^2
```

```
Maximum engine bay height =  0.7950 m
Maximum engine bay width  =  0.7950 m

ENGINE BAY VOLUME
Volume of engine bay           =  0.6987 m^3

PROPULSION SYSTEM MASS
Total mass of engines          =   221.20 kg
Engine installation mass       =    28.76 kg

Total mass of propulsion system =   249.96 kg

ENGINE STATIC THRUST
Total maximum sea-level static thrust of engines =  13142.61 N
Bypass ratio of total engines   =    4.00
 ------------------------------
 * UNDERCARRIAGE BAY

NOSE UNDERCARRIAGE
Length of nose undercarriage leg         =  0.4604 m
Nose undercarriage wheel & tyre diameter =  0.3586 m
Nose undercarriage wheel & tyre width    =  0.1520 m

MAIN UNDERCARRIAGE
Length of each main undercarriage leg    =  0.6222 m
Main undercarriage wheel & tyre diameter =  0.4871 m
Main undercarriage wheel & tyre width    =  0.1294 m

UNDERCARRIAGE MASS
Structural mass of nose undercarriage            =    19.26 kg
Structural mass of total main undercarriage      =   138.93 kg
Mass of hydraulics associated with undercarriage =    18.08 kg

UNDERCARRIAGE GROSS MASS
Total mass of nose undercarriage with hydraulics =    21.46 kg
Total mass of main undercarriage with hydraulics =   154.81 kg

UNDERCARRIAGE BAY DIMENSION
             .L(m).   ,H(m)     W(m)    V(m^3)
Nose UC bay  0.6397   0.3945   0.2280   0.0575
Main UC bay  0.8658   0.5359   0.1941   0.0900

 ------------------------------
 * FLYING WING

 STRAIGHT TAPERED WING

FLYING WING SPECIFICATION
Wing centreline section & chord  0.0000 m  8.0000 m
Wing tip section & chord         4.3814 m  0.0100 m
Wing gross span                =  8.7627 m
Gross wing aspect ratio        =  2.1879
Gross wing area                =   35.09 m^2
Wing wetted area               =   71.52 m^2
Mean thickness ratio           =  0.1171
Average wing chord             =  4.0050 m

Wing geometric mean chord      =  4.0050 m
Wing aerodynamic mean chord    =  5.3333 m
Distance of wing mean 1/4 chord point from nose =  3.4983 m

Equivalent wing root chord          =  8.0000 m
Equivalent wing taper ratio         =  0.0013
Equivalent wing leading edge sweep = 55.9635 degree
Equivalent wing quarter chord sweep= 45.6966 degree
Equivalent wing mid-chord sweep    = 29.6272 degree

Maximum depth at wing centreline chord =  1.4400 m
Maximum depth at wing tip chord        =  0.0009 m

Wing maximum cross-sectional area      =    4.90 m^2
Flying wing total volume               =   19.15 m^3

Centre of wing volume (true wing)      =  0.1307
Centre of wing volume (equivalent wing)=  0.0000
```

```
Wing aerodynamic centre (%MAC)          =  0.0300


WING BOX
Wing front spar from nose at root       =  1.2000 m
Wing rear spar from nose at root        =  5.2800 m

Wing front spar from nose at tip        =  0.0015 m
Wing rear spar from nose at tip         =  0.0066 m

Wing box root chord                     =  4.0800 m
Wing box tip chord                      =  0.0051 m
Wing box gross span                     =  8.7627 m
Gross wing box planform area            =   17.90 m^2
Gross wing box aspect ratio             =  4.2901

Equivalent wing box root chord          =  4.0800 m
Equivalent wing box taper ratio         =  0.0013
Equivalent wing box leading edge sweep = 50.3577 degree
Equivalent wing box centreline sweep   = 45.4405 degree


WING SPANWISE LIFT DISTRUBITION
Mach number for design diving speed =  1.1755
Effective Mach number               =  0.4595
Effective angle of sweepback        = 53.6845 degree
Average angle of attack             =  3.9706 degree

 ------------------------------
 * BAY POSITION

ENGINE BAY POSITION
Spanwise station to engine bay section              =  0.0000  0.0000  0.3975 m
Wing chord at engine bay section                    =  8.0000  8.0000  7.2751 m
Wing leading edge at engine bay section from nose   =  0.0000  0.0000  0.5885 m

Minimum distance of engine inlet from nose          =  3.1291 m
Maximum distance of engine exit from nose           =  6.4086 m
Axial space available for length of engine          =  3.2795 m

Axial distance from nose to engine front face       =  3.1291 m
Axial distance from nose to transition duct entrance=  4.5365 m


WEAPON BAY 1 POSITION
Spanwise station to weapon bay 1 section            =  0.5475  0.8125  1.0775 m
Wing chord at weapon bay 1 section                  =  7.0015  6.5183  6.0350 m
Wing leading edge at weapon bay 1 section from nose =  0.8106  1.2030  1.5953 m

Minimum distance of weapon bay1 front face from nose=  2.6468 m
Maximum distance of weapon bay1 rear face from nose =  5.8363 m
Axial space available for length of weapon bay 1    =  3.1895 m

Axial distance from nose to weapon bay 1 front face =  2.6468 m


WEAPON BAY 2 POSITION
Spanwise station to weapon bay 2 section            =  0.5475  0.8125  1.0775 m
Wing chord at weapon bay 2 section                  =  7.0015  6.5183  6.0350 m
Wing leading edge at weapon bay 2 section from nose =  0.8106  1.2030  1.5953 m

Minimum distance of weapon bay2 front face from nose=  2.6468 m
Maximum distance of weapon bay2 rear face from nose =  5.8363 m
Axial space available for length of weapon bay 2    =  3.1895 m

Axial distance from nose to weapon bay 2 front face =  2.6468 m


MAIN UNDERCARRIAGE BAY POSITION
Spanwise station to main uc bay section             =  1.2275  1.3245  1.4216 m
Wing chord at main uc bay section                   =  5.7615  5.5845  5.4076 m
Wing leading edge at main uc bay section from nose  =  1.8174  1.9610  2.1047 m

Minimum distance of main uc bay front face from nose=  2.9158 m
Maximum distance of main uc bay rear face from nose =  5.6199 m
Axial space available for length of main uc bay     =  2.4334 m
```

```
Axial distance from nose to main uc bay front face  =  3.9816 m

 ------------------------------
 * INTAKE DIFFUSER

Cross sectional area of intake inlet  =  0.2463 m^2
Cross sectional area of intake exit   =  0.3448 m^2
Equivalent diameter of intake inlet   =  0.5599 m
Diameter of intake exit               =  0.6625 m

Width of intake inlet                 =  0.7018 m
Height of intake inlet                =  0.3509 m
Width of intake inlet projected into horizontal =  0.7018 m
Height of intake inlet projected into vertical  =  0.3509 m

Distance of intake inlet from nose    =  2.4861 m
Length of intake diffuser             =  0.6431 m

Spanwise station to intake inlet      =  0.8125 m
Spanwise station to intake exit       =  0.0000 m
Vertical distance of intake inlet     =  0.2909 m
Vertical distance of intake exit      =  0.0000 m
Wing leading edge at intake from nose =  1.2030 m

Volume of each intake diffuser        =  0.1900 m^3

 ------------------------------
 * 2-DIMENSIONAL NOZZLE

Aspect ratio of nozzle transition duct exit=  7.3339

SINGLE ENGINE INSTALLATION
Half-height of nozzle transition duct exit =  0.1084 m
Half-width of nozzle transition duct exit  =  0.7950 m

Length of nozzle transition duct     =  2.5996 m

Volume of nozzle transition duct     =  2.3631 m^3
Total mass of nozzle transition duct =    64.42 kg

 ------------------------------
 * TRAILING EDGE SPLIT ELEVON

Total number of all split elevons = 2

ELEVON 1
Elevon inner span,chrd &wchrd =  2.8942  0.7077  2.7221 m
Elevon outer span,chrd &wchrd =  3.7705  0.2923  1.1241 m
Elevon mean chord             =  0.5000 m
Total span of elevon          =  1.7525 m
Aspect ratio of each elevon   =  1.7525
Elevon hinge line sweep       =  0.7161 deg
Total planform area of elevon =    0.88 m^2
Total wing area over elevon   =    3.37 m^2
ELEVONS LIFT & MOMENT             TO      LD
Elevon deflection             =   30.00   60.00 deg
Section lift increment        =  0.9519  1.4714
Wing lift increment           =  0.0513  0.0792
Wing pitch increment          = -0.0024 -0.0037
Sect max lift increment       =  0.6628  0.8961
Wing max lift increment       =  0.0637  0.0860


All split elevons gross span      =  1.7525 m
Split elevon mean chord           =  0.5000 m
All split elevons planform area   =    0.88 m^2
Total wing planform area over split elevons   =    3.37 m^2

WING TRAILING EDGE
Gross area of wing trailing edge aft of rear spar    =    7.65 m^2
Planform area of fixed section of wing TE aft of r/s =    6.78 m^2

 ------------------------------
 * LEADING EDGE SLAT

Total number of all slats = 0
```

```
All slats gross span          =   0.0000 m
Slat mean chord               =   0.0000 m
All slats planform area       =     0.00 m^2
Total wing planform area over slats   =    0.00 m^2

WING LEADING EDGE
Total planform area of wing leading edge            =    3.38 m^2
Planform area of fixed section of wing LE fwd of f/s =    1.13 m^2

 ------------------------------
 * TRAILING EDGE SPLIT RUDDER

Total number of all split rudders = 2

SPLIT RUDDER 1
Rudder inner span & wchrd     =  2.8942  2.7221 m
Rudder outer span & wchrd     =  3.7705  1.1241 m
Aspect ratio of each rudder   =  1.7525
Rudder hinge line sweep       =  0.7161 deg
SPLIT RUDDERS LIFT & MOMENT     Aileron Rudder
Split rudder deflection       =   20.00   25.00 deg
Section lift increment        =  0.8544  0.9387
Wing lift increment           =  0.0460  0.0505
Wing yaw effectiveness        = -0.0016  0.0017
Wing roll effectiveness       =  0.0291 -0.0319

 ------------------------------
 * FUEL

- CENTRE FUEL TANK -
Total span of centre fuel tank =  0.0000 m

CENTRE FUEL TANK 1 (FRONT)
Centre fuel tank 1 front face from nose =  0.0000 m
Centre fuel tank 1 rear face from nose  =  0.0000 m
Total fuel volume of centre tank 1    =  0.0000 m^3
Fuel mass used in centre fuel tank 1  =     0.00 kg
M-arm of centre fuel tank 1 from nose =  0.0000 m

CENTRE FUEL TANK 2 (REAR)
Centre fuel tank 2 front face from nose =  0.0000 m
Centre fuel tank 2 rear face from nose  =  0.0000 m
Total fuel volume of centre tank 2    =  0.0000 m^3
Fuel mass used in centre fuel tank 2  =     0.00 kg
M-arm of centre fuel tank 2 from nose =  0.0000 m

CENTRE FUEL TANK 3 (TOP)
Centre fuel tank 3 front face from nose =  0.0000 m
Centre fuel tank 3 rear face from nose  =  0.0000 m
Total fuel volume of centre tank 3    =  0.0000 m^3
Fuel mass used in centre fuel tank 3  =     0.00 kg
M-arm of centre fuel tank 3 from nose =  0.0000 m

TOTAL CENTRE FUEL TANK CAPACITY
Total area of centre fuel tank        =  0.0000 m^2
Total fuel volume of centre tank      =  0.0000 m^3
Total fuel mass used in centre tank   =     0.00 kg


- INBOARD FUEL TANK -
Total span of inboard fuel tank =  1.0600 m

INBOARD FUEL TANK 1 (FRONT)
Inboard fuel tank 1 front face from nose =  2.6468 m
Inboard fuel tank 1 rear face from nose  =  2.6468 m
Total fuel volume of inbrd tank 1     =  0.0000 m^3
Fuel mass used in inbrd fuel tank 1   =     0.00 kg
M-arm of inbrd fuel tank 1 from nose  =  2.6468 m

INBOARD FUEL TANK 2 (REAR)
Inboard fuel tank 2 front face from nose =  5.0068 m
Inboard fuel tank 2 rear face from nose  =  5.8363 m
Total fuel volume of inbrd tank 2     =  0.5363 m^3
Fuel mass used in inbrd fuel tank 2   =     0.00 kg
M-arm of inbrd fuel tank 2 from nose  =  5.4034 m
```

```
INBOARD FUEL TANK 3 (TOP)
Inboard fuel tank 3 front face from nose =  2.6468 m
Inboard fuel tank 3 rear face from nose  =  3.8268 m
Total fuel volume of inbrd tank 3      =  0.2298 m^3
Fuel mass used in inbrd fuel tank 3    =     0.00 kg
M-arm of inbrd fuel tank 3 from nose   =  3.2399 m

TOTAL INBOARD FUEL TANK CAPACITY
Total area of inboard fuel tank        =  2.1300 m^2
Total fuel volume of inbrd tank        =  0.7661 m^3
Total fuel mass used in inbrd tank     =     0.00 kg


- OUTBOARD FUEL TANK -
Total span of outboard fuel tank =  0.3881 m

OUTBOARD FUEL TANK 1 (FRONT)
Outboard fuel tank 1 front face from nose =  2.9158 m
Outboard fuel tank 1 rear face from nose  =  3.9816 m
Total fuel volume of outbrd tank 1     =  0.2394 m^3
Fuel mass used in outbrd fuel tank 1   =     0.00 kg
M-arm of outbrd fuel tank 1 from nose =  3.4581 m

OUTBOARD FUEL TANK 2 (REAR)
Outboard fuel tank 2 front face from nose =  4.8474 m
Outboard fuel tank 2 rear face from nose  =  5.6199 m
Total fuel volume of outbrd tank 2     =  0.1466 m^3
Fuel mass used in outbrd fuel tank 2   =     0.00 kg
M-arm of outbrd fuel tank 2 from nose =  5.2197 m

TOTAL OUTBOARD FUEL TANK CAPACITY
Total area of outboard fuel tank       =  0.7135 m^2
Total fuel volume of outbrd tank       =  0.3861 m^3
Total fuel mass used in outbrd tank    =     0.00 kg


- WING FUEL TANK -
Wing fuel tank spanwise station 0 =  1.5716 m
Wing fuel tank spanwise station 1 =  2.6481 m
Total span available for wing fuel tank          =  2.1530 m
Total wing box area available for wing fuel tank =  2.4757 m^2

WING FUEL TANK CAPACITY
Total fuel volume of wing tank         =  0.5898 m^3
Total fuel mass used in wing tank      =   457.96 kg


- OPTIONAL WEAPON BAY FUEL TANK -
Total fuel volume of weapon bay tank1=  0.0000 m^3
Fuel mass used in weapon bay tank 1  =     0.00 kg

Total fuel volume of weapon bay tank2=  0.0000 m^3
Fuel mass used in weapon bay tank 2  =     0.00 kg

TOTAL WEAPON BAY FUEL TANK CAPACITY
Total fuel volume of weapon bay tank      =  0.0000 m^3
Total fuel mass used in weapon bay tank   =     0.00 kg


- UCAV TOTAL FUEL CAPACITY -
Total area containing fuel tank      =  5.3192 m^2
Total internal fuel volume           =  1.7419 m^3
Total mass of available internal fuel=  1352.60 kg

Total fuel mass used on aircraft     =   457.96 kg

 ------------------------------
 * UCAV MASS & CG

- UCAV MASS -

WING BOX
Ultimate load factor           =    3.99
Wing inertia relief load       =  821.41 kg

Wing box mass (Torsion)        =   51.34 kg
```

```
Wing box mass (Bending)          =    45.33 kg
Total wing box mass              =    51.34 kg

CONTROL SURFACES
Wing leading edge mass           =    14.43 kg
Wing fixed trailing edge mass    =    43.04 kg

TEcs mass (flap)                 =     2.79 kg
TEcs mass (aileron)              =    14.68 kg
Total TE control surfaces mass   =    14.68 kg

Inlaids mass (rudder)            =     0.00 kg
Inlaids mass (spoiler)           =     0.00 kg
Total inlaids CS mass            =     0.00 kg

AUXILIARY
Miscellaneous attachments        =    21.04 kg
External paint                   =    11.97 kg
Low Observable treatments        =   226.80 kg
Basic ribs in strutural box      =   172.05      0.00 kg

FLYING WING
Total wing structural mass       =   555.34 kg

MASS INCREMENT DUE TO INTERNAL WEAPON BAYS
Mass increment due to weap bay1=     73.88 kg
Mass increment due to weap bay2=     73.88 kg

AIRCRAFT SYSTEM
Mass of air systems              =     2.73 kg
Mass of de-icing system          =    18.79 kg
Mass of electrical systems       =    94.96 kg
Mass of flight control systems   =    93.59 kg
Mass of fuel system              =    34.76 kg

COMPLETE AIRCRAFT
Total aircraft payload           =   226.80 kg
Mass of fixed-role equipment     =   313.34 kg
Total mass of fuel on aircraft   =   457.96 kg

Empty mass               =   1751.92 kg
Operational empty mass   =   1751.92 kg
Zero fuel mass           =   1978.72 kg

Total take-off mass      =   2436.68 kg
Landing mass             =   2071.18 kg

Wing loading             =   69.4315 kg/m^2
Thrust loading           =    0.5500


WING STRUCTURAL MASS COMPARISON
Howe method 1 (COA)      =    555.34 kg (theoretical)
Howe method 2 (COA)      =    549.62 kg (empirical)
Lovell method (RAE)      =   1127.84 kg
Roskam method (USAF)     =    303.57 kg
Roskam method (USN)      =    409.47 kg
Raymer method            =    360.64 kg
Whitford method          =    425.50 kg


- CENTRE OF GRAVITY -

OPERATIONAL EMPTY MASS
Total aircraft pitching moment about nose=   6302.59 kg.m
Distance of aircraft CG from nose        =   3.5975 m
CG relative to aerodynamic mean chord    =   26.86%

ZERO FUEL MASS
Total aircraft pitching moment about nose=   7170.52 kg.m
Distance of aircraft CG from nose        =   3.6238 m
CG relative to aerodynamic mean chord    =   27.35%

TOTAL TAKE-OFF MASS
Total aircraft pitching moment about nose=   9118.18 kg.m
Distance of aircraft CG from nose        =   3.7421 m
CG relative to aerodynamic mean chord    =   29.57%
```

```
Static margin                                  =  -4.57%

Distance of aircraft fwd CG from nose  =  3.1783 m
Fwd CG relative to AMC                 =  19.00%
Distance of aircraft aft CG from nose  =  3.8716 m
Aft CG relative to AMC                 =  32.00%

Reference spanwise distance of aircraft CG             =  0.0000 m
Reference vertical distance of aircraft CG from ground =  1.0453 m


- UNDERCARRIAGE ARRANGEMENTS -

UNDERCARRIAGE ARRANGEMENTS
Axial distance from nose wheel to main wheel =  2.5084 m
Axial angle from nose wheel to main wheel    = 27.8356 degree

Axial distance from nose UC to aircraft aft CG position     =  2.2189 m
Axial distance from aircraft forward CG position to main UC =  0.4341 m
Axial distance from aircraft aft CG position to main UC     =  0.2896 m

AIRCRAFT OVERTURN ANGLE
Aircraft static ground line    =  1.1713 m
Aircraft overturn angle        = 41.7468 degree

AIRCRAFT TIPBACK & STATIC TAILDOWN ANGLE
Axial distance from main uc to tail =  3.9684 m
Height due to tipback angle         =  1.0993 m

Aircraft tipback angle         = 15.4830 degree
Aircraft static taildown angle = 13.2836 degree

AIRCRAFT ANGLE OFF VERTICAL
Angle off vertical             = 15.4830 degree

UNDERCARRIAGE STATIC LOADS
Maximum static load       =   2155.41 kg
Maximum nose static load  =    421.64 kg
Minimum nose static load  =    281.27 kg
Nose dynamic braking load =    310.62 kg

Maximum static load as a fraction of total load      =   88.46%
Maximum nose static load as a fraction of total load =   17.30%
Minimum nose static load as a fraction of total load =   11.54%

MAIN UNDERCARRIAGE SHOCK ABSORBER STROKE
Main undercarriage rolling radius        =  0.1624 m
Main undercarriage tyre stroke           =  0.0812 m
Main undercarriage shock absorber stroke =  0.4946 m

UNDERCARRIAGES FRONTAL AREA
Oleo load of each main undercarriage =   1077.71 kg
Oleo load of nose undercarriage      =    732.26 kg

Oleo diameter of main undercarriage  =  0.0137 m
Oleo diameter of nose undercarriage  =  0.0113 m

Frontal area of each main undercarriage leg          =  0.0085 m^2
Frontal area of each main undercarriage wheel & tyre =  0.0525 m^2

Frontal area of nose undercarriage leg          =  0.0052 m^2
Frontal area of nose undercarriage wheel & tyre =  0.0454 m^2

 ------------------------
 *UCAV COMPONENT SUMMARY*

 --- MASS & BALANCE ---
 Aircraft component  Mass   Range   X-Marm   XMoment  Y-Marm   YMoment
                     (kg)    (%)      (m)     (kg.m)     (m)     (kg.m)
Wing (port)         277.67   11.40  4.1951   1164.86 -1.9278   -535.29
Wing (starboard)    277.67   11.40  4.1951   1164.86  1.9278    535.29
Nose UC              21.46    0.88  1.5232     32.68  0.0000      0.00
Main UC (port)       77.41    3.18  4.0316    312.07 -1.3245   -102.53
Main UC (stbd)       77.41    3.18  4.0316    312.07  1.3245    102.53
Engine              249.96   10.26  3.8328    958.04  0.0000      0.00
Nozzle               64.42    2.64  5.8363    375.95  0.0000      0.00
Avionics(MMS)        51.34    2.11  0.8022     41.18  0.0000      0.00
```

Avionics(FMS)	119.04	4.89	2.4861	295.94	0.0000	0.00
Avionics(SMS)	8.32	0.34	2.1645	18.01	0.0000	0.00
Avionics(EWS-port)	4.82	0.20	5.5137	26.58	-3.7242	-17.95
Avionics(EWS-stbd)	4.82	0.20	5.5137	26.58	3.7242	17.95
Air system	2.73	0.11	2.1645	5.90	0.0000	0.00
De-icing system	18.79	0.77	2.1645	40.66	0.0000	0.00
Electrical system	94.96	3.90	2.1645	205.54	0.0000	0.00
FCS	93.59	3.84	2.1645	202.59	0.0000	0.00
Fuel system	34.76	1.43	2.1645	75.24	0.0000	0.00
W bay1 pylon	62.50	2.56	3.8268	239.18	-0.8125	-50.78
W bay2 pylon	62.50	2.56	3.8268	239.18	0.8125	50.78
W bay1 increment	73.88	3.03	3.8268	282.74	-0.8125	-60.03
W bay2 increment	73.88	3.03	3.8268	282.74	0.8125	60.03
Residual fuel	0.00	0.00	2.1645	0.00	0.0000	0.00
OEM	1751.92	71.90	3.5975	6302.59		0.00
Weap in bay1	113.40	4.65	3.8268	433.96	-0.8125	-92.14
Weap in bay2	113.40	4.65	3.8268	433.96	0.8125	92.14
ZFM	1978.72	81.21	3.6238	7170.52		0.00
Wing tank (port)	228.98	9.40	4.2529	973.83	-2.0452	-468.32
Wing tank (stbd)	228.98	9.40	4.2529	973.83	2.0452	468.32
Inbrd tank1(port)	0.00	0.00	2.6468	0.00	-0.8125	0.00
Inbrd tank1(stbd)	0.00	0.00	2.6468	0.00	0.8125	0.00
Inbrd tank2(port)	0.00	0.00	5.4034	0.00	-0.8125	0.00
Inbrd tank2(stbd)	0.00	0.00	5.4034	0.00	0.8125	0.00
Inbrd tank3(port)	0.00	0.00	3.2399	0.00	-0.8125	0.00
Inbrd tank3(stbd)	0.00	0.00	3.2399	0.00	0.8125	0.00
Outbrd tank1(port)	0.00	0.00	3.4581	0.00	-1.3245	0.00
Outbrd tank1(stbd)	0.00	0.00	3.4581	0.00	1.3245	0.00
Outbrd tank2(port)	0.00	0.00	5.2197	0.00	-1.3245	0.00
Outbrd tank2(stbd)	0.00	0.00	5.2197	0.00	1.3245	0.00
AUM	2436.68	100.00	3.7421	9118.18		0.00

--- MASS & BALANCE (continued) ---

Aircraft component	Mass (kg)	Z-Marm dwn(m)	ZMoment (kg.m)	Z-Marm up (m)	ZMoment (kg.m)
Wing (port)	277.67	1.0453	290.25	0.0000	0.00
Wing (starboard)	277.67	1.0453	290.25	0.0000	0.00
Nose UC	21.46	0.7846	16.83	-0.2607	-5.59
Main UC (port)	77.41	0.7846	60.73	-0.2607	-20.18
Main UC (stbd)	77.41	0.7846	60.73	-0.2607	-20.18
Engine	249.96	1.0453	261.28	0.0000	0.00
Nozzle	64.42	1.0453	67.33	0.0000	0.00
Avionics(MMS)	51.34	1.0453	53.67	0.0000	0.00
Avionics(FMS)	119.04	1.0453	124.43	0.0000	0.00
Avionics(SMS)	8.32	1.0453	8.70	0.0000	0.00
Avionics(EWS-port)	4.82	1.0453	5.04	0.0000	0.00
Avionics(EWS-stbd)	4.82	1.0453	5.04	0.0000	0.00
Air system	2.73	1.2425	3.39	0.1972	0.54
De-icing system	18.79	1.2425	23.34	0.1972	3.71
Electrical system	94.96	1.4428	137.01	0.3975	37.75
FCS	93.59	1.4428	135.04	0.3975	37.21
Fuel system	34.76	1.4428	50.15	0.3975	13.82
W bay1 pylon	62.50	1.3103	81.89	0.2650	16.56
W bay2 pylon	62.50	1.3103	81.89	0.2650	16.56
W bay1 increment	73.88	1.0453	77.23	0.0000	0.00
W bay2 increment	73.88	1.0453	77.23	0.0000	0.00
Residual fuel	0.00	0.9790	0.00	-0.0663	0.00
OEM	1751.92		1911.45		80.18
Weap in bay1	113.40	1.0453	118.54	0.0000	0.00
Weap in bay2	113.40	1.0453	118.54	0.0000	0.00
ZFM	1978.72		2148.52		80.18
Wing tank (port)	228.98	1.0453	239.35	0.0000	0.00
Wing tank (stbd)	228.98	1.0453	239.35	0.0000	0.00
Inbrd tank1(port)	0.00	1.0453	0.00	0.0000	0.00
Inbrd tank1(stbd)	0.00	1.0453	0.00	0.0000	0.00
Inbrd tank2(port)	0.00	1.0453	0.00	0.0000	0.00
Inbrd tank2(stbd)	0.00	1.0453	0.00	0.0000	0.00
Inbrd tank3(port)	0.00	1.3103	0.00	0.2650	0.00
Inbrd tank3(stbd)	0.00	1.3103	0.00	0.2650	0.00
Outbrd tank1(port)	0.00	1.0453	0.00	0.0000	0.00
Outbrd tank1(stbd)	0.00	1.0453	0.00	0.0000	0.00
Outbrd tank2(port)	0.00	1.0453	0.00	0.0000	0.00

```
Outbrd tank2(stbd)     0.00  1.0453       0.00  0.0000       0.00
     AUM            2436.68             2627.23              80.18
```

D.3 Packaging and Configuration Options

Internal Weapon Bay: The configuration is based on the straight-tapered wing planform with the single weapon bay located at the aircraft centreline and two-engine installations outboard of the weapon bay (NWEPB1-ST), as illustrated in Figure 8-8 of Chapter 8.

```
 ------------------------------
 --- UCAV PACKAGING SUMMARY --- .
 ------------------------------

 * UCAV PACKAGING CONFIGURATION

 1) Type of stores          = 1 :Internal store
 2) Number of weapon bays   = 1 :Single weapon bay on centreline
 3) Type of missions        = 1 :SEAD/strike
 4) Number of engines       = 1 :Single-engine installation
 5) Type of aircraft        = 0 :Unmanned aircraft
 6) Type of materials       = 2 :Carbon-fibre composite construction
 7) Number of kinks in wing = 0 :Straight taper wing
 8) Number of split elevons on half span = 1
 9) Number of slats on half span         = 0
10) Number of split rudders on half span = 0
11) Type of airfoils at wing inboard section  = 1 :Symmetrical airfoil
12) Type of airfoils at wing outboard section = 1 :Symmetrical airfoil
13) Thickness ratio at wing inboard section  = 15%
14) Thickness ratio at wing outboard section =  9%
15) Twist distribution      = 1 :Twist wing

 --------------------------
 *UCAV PACKAGING OPTIMIZER*

                                          INITIAL   FINAL    LOWER    UPPER
   1 Wing span (m)           [BW]        25.0000  12.5686   6.0000  40.0000
   2 Wing root chord (m)     [CWCC]      15.0000   8.0220   6.0000  20.0000
   3 Wing tip chord (m)      [CWCT]       2.0000   1.6044   0.0100   4.0000
   4 Front spar fraction     [FCWD]       0.1500   0.1500   0.1500   0.1500
   5 Rear spar fraction      [FCWR]       0.7000   0.7000   0.7000   0.7000
   6 Wing leading edge sweep[QWLR]       50.0000  51.7481   0.0100  60.0000
   7 Elevon mean chord (m)   [CWSE]       1.0000   0.7111   0.5000   3.0000
   8 Elevon inner span       [FYSEI]      0.4000   0.5427   0.1000   0.9500
   9 Elevon outer span       [FYSEO]      0.7000   0.9500   0.1000   0.9500
  10 Wing tank span factor   [FY2WFO]     0.5000   0.0686   0.0100   1.0000
  11 Wing tank front factor  [FCWFD]      0.0000   0.0000   0.0000   0.0000
  12 Wing tank rear factor   [FCWFR]      1.0000   1.0000   1.0000   1.0000
  13 Weap bay1 axial factor  [FXLIB1]     0.5000   0.4201   0.0000   1.0000
  14 Engine axial factor     [FXLPG]      0.5000   0.2844   0.0000   1.0000
  15 Engine scale factor     [RTP]        1.5000   0.5735   0.5000   2.5000

 ------------------------------
 *UCAV FIXED MASS CONTRIBUTION*

 ------------------------------
 * AVIONICS BAY

MISSION MANAGEMENT SYSTEM
Mass & volume of radar suite          =    28.32 kg   0.1404 m^3
Mass & volume of sensor suite         =    23.02 kg   0.0605 m^3

FLIGHT MANAGEMENT SYSTEM
Mass & volume of flight control suite =    45.03 kg   0.1634 m^3
Mass & volume of navigation suite     =    40.44 kg   0.1925 m^3
Mass & volume of communication suite  =    12.68 kg   0.0949 m^3
Mass & volume of identification suite =    20.89 kg   0.1556 m^3

STORE MANAGEMENT SYSTEM
Mass & volume of weapon control suite =     8.32 kg   0.0620 m^3
```

```
ELECTRONIC WARFARE SYSTEM
Mass & volume of electronic warfare suite  =     4.82 kg   0.0322 m^3
Mass & volume of countermeasures suite     =     4.82 kg   0.0322 m^3

Total avionics mass                        =   188.34 kg

Length of radar avionics suite             =  0.8022 m
Length of flight management avionics suite =  1.2861 m
Length of weapon control avionics suite    =  0.5697 m

Radome length                              =  1.2033 m

 ------------------------------
 * WEAPON BAY

WEAPON BAY 1
Total number of weapon bay 1                  = 1
Total number of weapons in each weapon bay 1  = 1
Total mass of weapons in weapon bay 1         =   460.00 kg
Total mass of internal pylons in weapon bay 1 =    62.50 kg

WEAPON BAY 2
Total number of weapon bay 2                  = 0
Total number of weapons in each weapon bay 2  = 0
Total mass of weapons in weapon bay 2         =     0.00 kg
Total mass of internal pylons in weapon bay 2 =     0.00 kg

INTERNAL WEAPON BAY
Total mass of weapons in internal weapon bays =   460.00 kg

WEAPON BAY DIMENSION
               L(m)    W(m)    H(m)    V(m^3)
Weapon bay 1  3.1900  0.6300  0.6300  1.2661
Weapon bay 2  0.0000  0.0000  0.0000  0.0000

EXTERNAL STORES
Total number of weapons at port store         = 0
Total mass of weapons at port store           =     0.00 kg
Total number of weapons at starboard store    = 0
Total mass of weapons at starboard store      =     0.00 kg
External store wetted area                    =  0.0000 m^2
Total mass of external pylons                 =     0.00 kg

Total mass of weapons at external stores      =     0.00 kg


TOTAL WEAPONS
Total mass of weapons on aircraft             =   460.00 kg

 ---------------------------------
 *UCAV VARIABLE MASS CONTRIBUTION*

 ------------------------------
 * ENGINE BAY

 TWO SINGLE-ENGINE INSTALLATIONS

ENGINE & ENGINE BAY DIMENSION
Overall length of engine  =  1.3078 m
Diameter of engine        =  0.6157 m

Total nozzle exit area    =    0.30 m^2

Maximum engine bay height =  0.7388 m
Maximum engine bay width  =  0.7388 m

ENGINE BAY VOLUME
Volume of engine bay           =  0.5606 m^3

PROPULSION SYSTEM MASS
Total mass of engines          =   376.45 kg
Engine installation mass       =    48.94 kg

Total mass of propulsion system =   425.39 kg

ENGINE STATIC THRUST
```

```
Total maximum sea-level static thrust of engines =  22697.17 N
Bypass ratio of total engines   =    8.00

 ------------------------------
 * UNDERCARRIAGE BAY

NOSE UNDERCARRIAGE
Length of nose undercarriage leg         =  0.5872 m
Nose undercarriage wheel & tyre diameter =  0.3823 m
Nose undercarriage wheel & tyre width    =  0.1520 m

MAIN UNDERCARRIAGE
Length of each main undercarriage leg    =  0.7934 m
Main undercarriage wheel & tyre diameter =  0.5269 m
Main undercarriage wheel & tyre width    =  0.1424 m

UNDERCARRIAGE MASS
Structural mass of nose undercarriage            =    26.98 kg
Structural mass of total main undercarriage      =   195.45 kg
Mass of hydraulics associated with undercarriage =    26.30 kg

UNDERCARRIAGE GROSS MASS
Total mass of nose undercarriage with hydraulics =    30.17 kg
Total mass of main undercarriage with hydraulics =   218.56 kg

UNDERCARRIAGE BAY DIMENSION
              L(m)     H(m)     W(m)    V(m^3)
Nose UC bay  0.7783  0.4205  0.2280  0.0746
Main UC bay  1.0569  0.5796  0.2136  0.1308

 ------------------------------
 * FLYING WING

 STRAIGHT TAPERED WING

FLYING WING SPECIFICATION
Wing centreline section & chord  0.0000 m  8.0220 m
Wing tip section & chord         6.2843 m  1.6044 m
Wing gross span               = 12.5686 m
Gross wing aspect ratio       =  2.6113
Gross wing area               =   60.50 m^2
Wing wetted area              =  123.09 m^2
Mean thickness ratio          =  0.1110
Average wing chord            =  4.8132 m

Wing geometric mean chord     =  4.8132 m
Wing aerodynamic mean chord   =  5.5263 m
Distance of wing mean 1/4 chord point from nose =  4.4814 m

Equivalent wing root chord         =  8.0220 m
Equivalent wing taper ratio        =  0.2000
Equivalent wing leading edge sweep = 51.7481 degree
Equivalent wing quarter chord sweep= 45.3730 degree
Equivalent wing mid-chord sweep    = 37.1549 degree

Maximum depth at wing centreline chord =  1.2033 m
Maximum depth at wing tip chord        =  0.1444 m

Wing maximum cross-sectional area      =   11.42 m^2
Flying wing total volume               =   29.64 m^3

Centre of wing volume (true wing)      =  0.1007
Centre of wing volume (equivalent wing)=  0.0000

Wing aerodynamic centre (%MAC)         =  0.0300


WING BOX
Wing front spar from nose at root      =  1.2033 m
Wing rear spar from nose at root       =  5.6154 m

Wing front spar from nose at tip       =  0.2407 m
Wing rear spar from nose at tip        =  1.1231 m

Wing box root chord                    =  4.4121 m
Wing box tip chord                     =  0.8824 m
Wing box gross span                    = 12.5686 m
```

```
Gross wing box planform area          =   33.27 m^2
Gross wing box aspect ratio           =  4.7478

Equivalent wing box root chord        =  4.4121 m
Equivalent wing box taper ratio       =  0.2000
Equivalent wing box leading edge sweep = 48.1181 degree
Equivalent wing box centreline sweep   = 44.6418 degree


WING SPANWISE LIFT DISTRUBITION
Mach number for design diving speed =  1.1755
Effective Mach number               =  0.5112
Effective angle of sweepback        = 55.9030 degree
Average angle of attack             =  5.5604 degree

 ------------------------------
 * BAY POSITION

ENGINE BAY POSITION
Spanwise station to engine bay section              =  0.4650  0.8344  1.2038 m
Wing chord at engine bay section                    =  7.5471  7.1699  6.7927 m
Wing leading edge at engine bay section from nose   =  0.5898  1.0584  1.5269 m

Minimum distance of engine inlet from nose          =  3.2677 m
Maximum distance of engine exit from nose           =  6.9610 m
Axial space available for length of engine          =  3.6934 m

Axial distance from nose to engine front face       =  4.6784 m
Axial distance from nose to transition duct entrance=  5.9862 m


WEAPON BAY 1 POSITION
Spanwise station to weapon bay 1 section            =  0.0000  0.0000  0.3150 m
Wing chord at weapon bay 1 section                  =  8.0220  8.0220  7.7003 m
Wing leading edge at weapon bay 1 section from nose =  0.0000  0.0000  0.3995 m

Minimum distance of weapon bay1 front face from nose=  3.2677 m
Maximum distance of weapon bay1 rear face from nose =  6.8132 m
Axial space available for length of weapon bay 1    =  3.2921 m

Axial distance from nose to weapon bay 1 front face =  3.3698 m


WEAPON BAY 2 POSITION
Spanwise station to weapon bay 2 section            =  0.0000  0.0000  0.0000 m
Wing chord at weapon bay 2 section                  =  0.0000  0.0000  0.0000 m
Wing leading edge at weapon bay 2 section from nose =  0.0000  0.0000  0.0000 m

Minimum distance of weapon bay2 front face from nose=  0.0000 m
Maximum distance of weapon bay2 rear face from nose =  0.0000 m
Axial space available for length of weapon bay 2    =  0.0000 m

Axial distance from nose to weapon bay 2 front face =  0.0000 m


MAIN UNDERCARRIAGE BAY POSITION
Spanwise station to main uc bay section             =  1.3538  1.4606  1.5674 m
Wing chord at main uc bay section                   =  6.6395  6.5304  6.4213 m
Wing leading edge at main uc bay section from nose  =  1.7172  1.8526  1.9881 m

Minimum distance of main uc bay front face from nose=  2.9513 m
Maximum distance of main uc bay rear face from nose =  6.3648 m
Axial space available for length of main uc bay     =  3.4135 m

Axial distance from nose to main uc bay front face  =  4.0272 m

 ------------------------------
 * INTAKE DIFFUSER

Cross sectional area of intake inlet  =  0.2977 m^2
Cross sectional area of intake exit   =  0.2977 m^2
Equivalent diameter of intake inlet   =  0.6157 m
Diameter of intake exit               =  0.6157 m

Width of intake inlet                 =  0.7716 m
Height of intake inlet                =  0.3858 m
Width of intake inlet projected into horizontal =  0.7716 m
```

```
Height of intake inlet projected into vertical  =  0.3858 m

Distance of intake inlet from nose    =  2.6246 m
Length of intake diffuser             =  2.0538 m

Spanwise station to intake inlet      =  0.8344 m
Spanwise station to intake exit       =  0.8344 m
Vertical distance of intake inlet     =  0.3104 m
Vertical distance of intake exit      =  0.0000 m
Wing leading edge at intake from nose =  1.0584 m

Volume of each intake diffuser        =  0.6114 m^3

 ------------------------------
 * 2-DIMENSIONAL NOZZLE

Aspect ratio of nozzle transition duct exit=  8.3136

SINGLE ENGINE INSTALLATION
Half-height of nozzle transition duct exit =  0.0946 m
Half-width of nozzle transition duct exit  =  0.7388 m

Length of nozzle transition duct     =  1.6541 m

Volume of nozzle transition duct     =  1.2984 m^3
Total mass of nozzle transition duct =    79.65 kg

 ------------------------------
 * TRAILING EDGE SPLIT ELEVON

Total number of all split elevons = 2

ELEVON 1
Elevon inner span,chrd &wchrd =  3.4106  0.9986  4.5391 m
Elevon outer span,chrd &wchrd =  5.9701  0.4236  1.9253 m
Elevon mean chord             =  0.7111 m
Total span of elevon          =  5.1190 m
Aspect ratio of each elevon   =  3.5995
Elevon hinge line sweep       = 22.5725 deg
Total planform area of elevon =    3.64 m^2
Total wing area over elevon   =   16.55 m^2
ELEVONS LIFT & MOMENT             TO      LD
Elevon deflection             =   30.00   60.00 deg
Section lift increment        =  0.8928  1.3198
Wing lift increment           =  0.1162  0.1717
Wing pitch increment          = -0.0157 -0.0232
Sect max lift increment       =  0.6690  0.9045
Wing max lift increment       =  0.1690  0.2284


All split elevons gross span          =   5.1190 m
Split elevon mean chord               =   0.7111 m
All split elevons planform area       =     3.64 m^2
Total wing planform area over split elevons   =   16.55 m^2

WING TRAILING EDGE
Gross area of wing trailing edge aft of rear spar    =   13.17 m^2
Planform area of fixed section of wing TE aft of r/s =    9.53 m^2

 ------------------------------
 * LEADING EDGE SLAT

Total number of all slats = 0


All slats gross span          =   0.0000 m
Slat mean chord               =   0.0000 m
All slats planform area       =     0.00 m^2
Total wing planform area over slats   =    0.00 m^2

WING LEADING EDGE
Total planform area of wing leading edge             =    6.59 m^2
Planform area of fixed section of wing LE fwd of f/s =    2.20 m^2

 ------------------------------
 * TRAILING EDGE SPLIT RUDDER
```

```
Total number of all split rudders = 2

SPLIT RUDDER 1
Rudder inner span & wchrd      =  3.4106  4.5391 m
Rudder outer span & wchrd      =  5.9701  1.9253 m
Aspect ratio of each rudder    =  3.5995
Rudder hinge line sweep        = 22.5725 deg
SPLIT RUDDERS LIFT & MOMENT      Aileron Rudder
Split rudder deflection        =   20.00   25.00 deg
Section lift increment         =  0.7712  0.8624
Wing lift increment            =  0.1004  0.1122
Wing yaw effectiveness         = -0.0050  0.0055
Wing roll effectiveness        =  0.0588 -0.0657

 ------------------------------
 * FUEL

- CENTRE FUEL TANK -
Total span of centre fuel tank =  0.6300 m

CENTRE FUEL TANK 1 (FRONT)
Centre fuel tank 1 front face from nose =  3.2677 m
Centre fuel tank 1 rear face from nose  =  3.3698 m
Total fuel volume of centre tank 1     =  0.0607 m^3
Fuel mass used in centre fuel tank 1   =     0.00 kg
M-arm of centre fuel tank 1 from nose =  3.3187 m

CENTRE FUEL TANK 2 (REAR)
Centre fuel tank 2 front face from nose =  6.5598 m
Centre fuel tank 2 rear face from nose  =  6.8132 m
Total fuel volume of centre tank 2     =  0.0607 m^3
Fuel mass used in centre fuel tank 2   =     0.00 kg
M-arm of centre fuel tank 2 from nose =  6.6829 m

CENTRE FUEL TANK 3 (TOP)
Centre fuel tank 3 front face from nose =  3.3698 m
Centre fuel tank 3 rear face from nose  =  4.9648 m
Total fuel volume of centre tank 3     =  0.1113 m^3
Fuel mass used in centre fuel tank 3   =     0.00 kg
M-arm of centre fuel tank 3 from nose =  4.1377 m

TOTAL CENTRE FUEL TANK CAPACITY
Total area of centre fuel tank         =  1.2289 m^2
Total fuel volume of centre tank       =  0.2326 m^3
Total fuel mass used in centre tank    =     0.00 kg


- INBOARD FUEL TANK -
Total span of inboard fuel tank =  0.0000 m

INBOARD FUEL TANK 1 (FRONT)
Inboard fuel tank 1 front face from nose =  0.0000 m
Inboard fuel tank 1 rear face from nose  =  0.0000 m
Total fuel volume of inbrd tank 1      =  0.0000 m^3
Fuel mass used in inbrd fuel tank 1    =     0.00 kg
M-arm of inbrd fuel tank 1 from nose   =  0.0000 m

INBOARD FUEL TANK 2 (REAR)
Inboard fuel tank 2 front face from nose =  0.0000 m
Inboard fuel tank 2 rear face from nose  =  0.0000 m
Total fuel volume of inbrd tank 2      =  0.0000 m^3
Fuel mass used in inbrd fuel tank 2    =     0.00 kg
M-arm of inbrd fuel tank 2 from nose   =  0.0000 m

INBOARD FUEL TANK 3 (TOP)
Inboard fuel tank 3 front face from nose =  0.0000 m
Inboard fuel tank 3 rear face from nose  =  0.0000 m
Total fuel volume of inbrd tank 3      =  0.0000 m^3
Fuel mass used in inbrd fuel tank 3    =     0.00 kg
M-arm of inbrd fuel tank 3 from nose   =  0.0000 m

TOTAL INBOARD FUEL TANK CAPACITY
Total area of inboard fuel tank         =  0.0000 m^2
Total fuel volume of inbrd tank         =  0.0000 m^3
Total fuel mass used in inbrd tank      =     0.00 kg
```

```
- OUTBOARD FUEL TANK -
Total span of outboard fuel tank =  0.4272 m

OUTBOARD FUEL TANK 1 (FRONT)
Outboard fuel tank 1 front face from nose =  2.9513 m
Outboard fuel tank 1 rear face from nose  =  4.0272 m
Total fuel volume of outbrd tank 1    =  0.3289 m^3
Fuel mass used in outbrd fuel tank 1  =     0.00 kg
M-arm of outbrd fuel tank 1 from nose =  3.4995 m

OUTBOARD FUEL TANK 2 (REAR)
Outboard fuel tank 2 front face from nose =  5.0840 m
Outboard fuel tank 2 rear face from nose  =  6.3648 m
Total fuel volume of outbrd tank 2    =  0.3281 m^3
Fuel mass used in outbrd fuel tank 2  =     0.00 kg
M-arm of outbrd fuel tank 2 from nose =  5.6905 m

TOTAL OUTBOARD FUEL TANK CAPACITY
Total area of outboard fuel tank       =  1.0068 m^2
Total fuel volume of outbrd tank       =  0.6571 m^3
Total fuel mass used in outbrd tank    =     0.00 kg


- WING FUEL TANK -
Wing fuel tank spanwise station 0 =  1.7174 m
Wing fuel tank spanwise station 1 =  2.0842 m
Total span available for wing fuel tank          =  0.7336 m
Total wing box area available for wing fuel tank =  2.4534 m^2

WING FUEL TANK CAPACITY
Total fuel volume of wing tank         =  1.2841 m^3
Total fuel mass used in wing tank      =   997.13 kg


- OPTIONAL WEAPON BAY FUEL TANK -
Total fuel volume of weapon bay tank1=  0.0000 m^3
Fuel mass used in weapon bay tank 1  =     0.00 kg

Total fuel volume of weapon bay tank2=  0.0000 m^3
Fuel mass used in weapon bay tank 2  =     0.00 kg

TOTAL WEAPON BAY FUEL TANK CAPACITY
Total fuel volume of weapon bay tank      =  0.0000 m^3
Total fuel mass used in weapon bay tank   =     0.00 kg


- UCAV TOTAL FUEL CAPACITY -
Total area containing fuel tank      =  4.6891 m^2
Total internal fuel volume           =  2.1738 m^3
Total mass of available internal fuel=  1687.95 kg

Total fuel mass used on aircraft     =   997.13 kg

 ------------------------------
 * UCAV MASS & CG

- UCAV MASS -

WING BOX
Ultimate load factor           =    9.75
Wing inertia relief load       =  963.99 kg

Wing box mass (Torsion)        =  123.11 kg
Wing box mass (Bending)        =  178.01 kg
Total wing box mass            =  178.01 kg

CONTROL SURFACES
Wing leading edge mass         =   35.84 kg
Wing fixed trailing edge mass  =   84.21 kg

TEcs mass (flap)               =   21.71 kg
TEcs mass (aileron)            =   56.07 kg
Total TE control surfaces mass =   56.07 kg

Inlaids mass (rudder)          =    0.00 kg
Inlaids mass (spoiler)         =    0.00 kg
Total inlaids CS mass          =    0.00 kg
```

```
AUXILIARY
Miscellaneous attachments      =    26.46 kg
External paint                 =    20.63 kg
Low Observable treatments      =   226.80 kg
Basic ribs in strutural box    =   272.67     0.00 kg

FLYING WING
Total wing structural mass     =   900.69 kg

MASS INCREMENT DUE TO INTERNAL WEAPON BAYS
Mass increment due to weap bay1=   118.68 kg
Mass increment due to weap bay2=     0.00 kg

AIRCRAFT SYSTEM
Mass of air systems            =     6.63 kg
Mass of de-icing system        =    25.91 kg
Mass of electrical systems     =   132.89 kg
Mass of flight control systems =   135.22 kg
Mass of fuel system            =    75.68 kg

COMPLETE AIRCRAFT
Total aircraft payload         =   460.00 kg
Mass of fixed-role equipment   =   250.84 kg
Total mass of fuel on aircraft =   997.13 kg

Empty mass             =   2400.32 kg
Operational empty mass =   2400.32 kg
Zero fuel mass         =   2860.32 kg

Total take-off mass    =   3857.45 kg
Landing mass           =   3278.83 kg

Wing loading           =   63.7645 kg/m^2
Thrust loading         =    0.6000


WING STRUCTURAL MASS COMPARISON
Howe method 1 (COA)    =    900.69 kg (theoretical)
Howe method 2 (COA)    =   1329.59 kg (empirical)
Lovell method (RAE)    =   1800.46 kg
Roskam method (USAF)   =    614.89 kg
Roskam method (USN)    =    912.00 kg
Raymer method          =    688.88 kg
Whitford method        =    842.42 kg


- CENTRE OF GRAVITY -

OPERATIONAL EMPTY MASS
Total aircraft pitching moment about nose=  10701.17 kg.m
Distance of aircraft CG from nose        =  4.4582 m
CG relative to aerodynamic mean chord    =  24.58%

ZERO FUEL MASS
Total aircraft pitching moment about nose=  12984.98 kg.m
Distance of aircraft CG from nose        =  4.5397 m
CG relative to aerodynamic mean chord    =  26.05%

TOTAL TAKE-OFF MASS
Total aircraft pitching moment about nose=  17887.20 kg.m
Distance of aircraft CG from nose        =  4.6371 m
CG relative to aerodynamic mean chord    =  27.82%
Static margin                            =  -2.82%

Distance of aircraft fwd CG from nose  =  4.1498 m
Fwd CG relative to AMC                 =  19.00%
Distance of aircraft aft CG from nose  =  4.8683 m
Aft CG relative to AMC                 =  32.00%

Reference spanwise distance of aircraft CG             =  0.0000 m
Reference vertical distance of aircraft CG from ground =  1.3028 m


- UNDERCARRIAGE ARRANGEMENTS -

UNDERCARRIAGE ARRANGEMENTS
```

```
Axial distance from nose wheel to main wheel =  3.4416 m
Axial angle from nose wheel to main wheel    = 22.9961 degree

Axial distance from nose UC to aircraft aft CG position     =  3.0446 m
Axial distance from aircraft forward CG position to main UC =  0.5758 m
Axial distance from aircraft aft CG position to main UC     =  0.3970 m

AIRCRAFT OVERTURN ANGLE
Aircraft static ground line    =  1.3445 m
Aircraft overturn angle        = 44.0976 degree

AIRCRAFT TIPBACK & STATIC TAILDOWN ANGLE
Axial distance from main uc to tail =  4.5414 m
Height due to tipback angle         =  1.3838 m

Aircraft tipback angle         = 16.9468 degree
Aircraft static taildown angle = 14.8981 degree

AIRCRAFT ANGLE OFF VERTICAL
Angle off vertical             = 16.9468 degree

UNDERCARRIAGE STATIC LOADS
Maximum static load       =   3412.49 kg
Maximum nose static load  =    645.39 kg
Minimum nose static load  =    444.96 kg
Nose dynamic braking load =    446.71 kg

Maximum static load as a fraction of total load      =   88.46%
Maximum nose static load as a fraction of total load =   16.73%
Minimum nose static load as a fraction of total load =   11.54%

MAIN UNDERCARRIAGE SHOCK ABSORBER STROKE
Main undercarriage rolling radius        =  0.1756 m
Main undercarriage tyre stroke           =  0.0878 m
Main undercarriage shock absorber stroke =  0.4898 m

UNDERCARRIAGES FRONTAL AREA
Oleo load of each main undercarriage =   1706.24 kg
Oleo load of nose undercarriage      =   1092.10 kg

Oleo diameter of main undercarriage  =  0.0172 m
Oleo diameter of nose undercarriage  =  0.0138 m

Frontal area of each main undercarriage leg          =  0.0136 m^2
Frontal area of each main undercarriage wheel & tyre =  0.0625 m^2

Frontal area of nose undercarriage leg          =  0.0081 m^2
Frontal area of nose undercarriage wheel & tyre =  0.0484 m^2

------------------------
*UCAV COMPONENT SUMMARY*

--- MASS & BALANCE ---
```

Aircraft component	Mass (kg)	Range (%)	X-Marm (m)	XMoment (kg.m)	Y-Marm (m)	YMoment (kg.m)
Wing (port)	450.34	11.67	5.0379	2268.78	-2.7651	-1245.24
Wing (starboard)	450.34	11.67	5.0379	2268.78	2.7651	1245.24
Nose UC	30.17	0.78	1.5924	48.05	0.0000	0.00
Main UC (port)	109.28	2.83	5.0340	550.11	-1.4606	-159.61
Main UC (stbd)	109.28	2.83	5.0340	550.11	1.4606	159.61
Engine (port)	212.69	5.51	5.3323	1134.14	-0.8344	-177.47
Engine (stbd)	212.69	5.51	5.3323	1134.14	0.8344	177.47
Nozzle (port)	39.83	1.03	6.8132	271.35	-0.8344	-33.23
Nozzle (stbd)	39.83	1.03	6.8132	271.35	0.8344	33.23
Avionics(MMS)	51.34	1.33	0.8022	41.18	0.0000	0.00
Avionics(FMS)	119.04	3.09	2.6246	312.44	0.0000	0.00
Avionics(SMS)	8.32	0.22	2.3031	19.16	0.0000	0.00
Avionics(EWS-port)	4.82	0.12	6.7754	32.66	-5.3417	-25.75
Avionics(EWS-stbd)	4.82	0.12	6.7754	32.66	5.3417	25.75
Air system	6.63	0.17	2.3031	15.28	0.0000	0.00
De-icing system	25.91	0.67	2.3031	59.68	0.0000	0.00
Electrical system	132.89	3.45	2.3031	306.07	0.0000	0.00
FCS	135.22	3.51	2.3031	311.43	0.0000	0.00
Fuel system	75.68	1.96	2.3031	174.30	0.0000	0.00
W bay1 pylon	62.50	1.62	4.9648	310.30	0.0000	0.00
W bay1 increment	118.68	3.08	4.9648	589.22	0.0000	0.00
Residual fuel	0.00	0.00	2.3031	0.00	0.0000	0.00

OEM	2400.32	62.23	4.4582	10701.17		0.00
Weap in bay1	460.00	11.92	4.9648	2283.81	0.0000	0.00
ZFM	2860.32	74.15	4.5397	12984.98		0.00
Wing tank (port)	498.56	12.92	4.9163	2451.11	-1.8788	-936.70
Wing tank (stbd)	498.56	12.92	4.9163	2451.11	1.8788	936.70
Centre tank1	0.00	0.00	3.3187	0.00	0.0000	0.00
Centre tank2	0.00	0.00	6.6829	0.00	0.0000	0.00
Centre tank3	0.00	0.00	4.1377	0.00	0.0000	0.00
Outbrd tank1(port)	0.00	0.00	3.4995	0.00	-1.4606	0.00
Outbrd tank1(stbd)	0.00	0.00	3.4995	0.00	1.4606	0.00
Outbrd tank2(port)	0.00	0.00	5.6905	0.00	-1.4606	0.00
Outbrd tank2(stbd)	0.00	0.00	5.6905	0.00	1.4606	0.00
AUM	3857.45	100.00	4.6371	17887.20		0.00

--- MASS & BALANCE (continued) ---

Aircraft component	Mass (kg)	Z-Marm dwn(m)	ZMoment (kg.m)	Z-Marm up (m)	ZMoment (kg.m)
Wing (port)	450.34	1.3028	586.72	0.0000	0.00
Wing (starboard)	450.34	1.3028	586.72	0.0000	0.00
Nose UC	30.17	0.9691	29.24	-0.3338	-10.07
Main UC (port)	109.28	0.9691	105.90	-0.3338	-36.47
Main UC (stbd)	109.28	0.9691	105.90	-0.3338	-36.47
Engine (port)	212.69	1.3028	277.10	0.0000	0.00
Engine (stbd)	212.69	1.3028	277.10	0.0000	0.00
Nozzle (port)	39.83	1.3028	51.89	0.0000	0.00
Nozzle (stbd)	39.83	1.3028	51.89	0.0000	0.00
Avionics(MMS)	51.34	1.3028	66.89	0.0000	0.00
Avionics(FMS)	119.04	1.3028	155.09	0.0000	0.00
Avionics(SMS)	8.32	1.3028	10.84	0.0000	0.00
Avionics(EWS-port)	4.82	1.3028	6.28	0.0000	0.00
Avionics(EWS-stbd)	4.82	1.3028	6.28	0.0000	0.00
Air system	6.63	1.5131	10.04	0.2102	1.39
De-icing system	25.91	1.5131	39.21	0.2102	5.45
Electrical system	132.89	1.6722	222.23	0.3694	49.09
FCS	135.22	1.6722	226.12	0.3694	49.95
Fuel system	75.68	1.6722	126.56	0.3694	27.96
W bay1 pylon	62.50	1.6178	101.11	0.3150	19.69
W bay1 increment	118.68	1.3028	154.62	0.0000	0.00
Residual fuel	0.00	1.2413	0.00	-0.0616	0.00
OEM	2400.32		3197.71		70.51
Weap in bay1	460.00	1.3028	599.30	0.0000	0.00
ZFM	2860.32		3797.01		70.51
Wing tank (port)	498.56	1.3028	649.54	0.0000	0.00
Wing tank (stbd)	498.56	1.3028	649.54	0.0000	0.00
Centre tank1	0.00	1.3028	0.00	0.0000	0.00
Centre tank2	0.00	1.3028	0.00	0.0000	0.00
Centre tank3	0.00	1.6178	0.00	0.3150	0.00
Outbrd tank1(port)	0.00	1.3028	0.00	0.0000	0.00
Outbrd tank1(stbd)	0.00	1.3028	0.00	0.0000	0.00
Outbrd tank2(port)	0.00	1.3028	0.00	0.0000	0.00
Outbrd tank2(stbd)	0.00	1.3028	0.00	0.0000	0.00
AUM	3857.45		5096.09		70.51

Engine Installation: The configuration is based on the single-kink wing planform with the single engine installation located at the aircraft centreline and two outer weapon bays (NWEPB2-1ENG -SK), as illustrated in Figure 8-12 of Chapter 8.

```
------------------------------
--- UCAV PACKAGING SUMMARY ---
------------------------------

* UCAV PACKAGING CONFIGURATION

1) Type of stores          = 1 :Internal store
2) Number of weapon bays   = 2 :Two weapon bays outboard of engines
3) Type of missions        = 1 :SEAD/strike
4) Number of engines       = 1 :Single-engine installation
5) Type of aircraft        = 0 :Unmanned aircraft
6) Type of materials       = 2 :Carbon-fibre composite construction
```

```
 7) Number of kinks in wing = 1 :Multi-kink wing
 8) Number of split elevons on half span = 1
 9) Number of slats on half span         = 0
10) Number of split rudders on half span = 0
11) Type of airfoils at wing inboard section  = 1 :Symmetrical airfoil
12) Type of airfoils at wing outboard section = 1 :Symmetrical airfoil
13) Thickness ratio at wing inboard section  = 15%
14) Thickness ratio at wing outboard section =  9%
15) Twist distribution      = 1 :Twist wing

 --------------------------
 *UCAV PACKAGING OPTIMIZER*

                                      INITIAL    FINAL     LOWER     UPPER
  1 Wing span (m)           [BW]      12.0000   13.6148    6.0000   18.0000
  2 Wing root chord (m)     [CWCC]     9.0000    9.1353    6.0000   12.0000
  3 Wing tip chord (m)      [CWCT]     2.0000    1.5622    0.0100    4.0000
  4 Front spar fraction     [FCWD]     0.1500    0.1500    0.1500    0.1500
  5 Rear spar fraction      [FCWR]     0.7000    0.7000    0.7000    0.7000
  6 Wing leading edge sweep[QWLR]     50.0000   50.4081    0.0100   60.0000
  7 Wing leading edge sweep[QWLR]     50.0000   50.4081    0.0100   60.0000
  8 Wing chord at kink (m) [CWK]      6.0000    6.1003    3.0000   12.0000
  9 Kink span factor        [FBW2K]    0.5000    0.3500    0.3500    0.5000
 10 Elevon mean chord (m)   [CWSE]     1.0000    0.9581    0.5000    3.0000
 11 Elevon inner span       [FYSEI]    0.5000    0.5000    0.5000    0.5000
 12 Elevon outer span       [FYSEO]    0.7000    0.7000    0.5500    0.9500
 13 Wing tank span factor   [FY2WFO]   0.5000    0.6502    0.0100    1.0000
 14 Wing tank front factor  [FCWFD]    0.0000    0.0000    0.0000    0.0000
 15 Wing tank rear factor   [FCWFR]    0.5000    0.3147    0.0100    1.0000
 16 Weap bay1 axial factor  [FXLIB1]   0.5000    0.3056    0.0000    1.0000
 17 Engine axial factor     [FXLPG]    0.5000    0.1894    0.0000    1.0000
 18 Engine scale factor     [RTP]      1.5000    1.1374    0.5000    2.5000

 ------------------------------
 *UCAV FIXED MASS CONTRIBUTION*

 ------------------------------
 * AVIONICS BAY

MISSION MANAGEMENT SYSTEM
Mass & volume of radar suite               =    28.32 kg   0.1404 m^3
Mass & volume of sensor suite              =    23.02 kg   0.0605 m^3

FLIGHT MANAGEMENT SYSTEM
Mass & volume of flight control suite      =    45.03 kg   0.1634 m^3
Mass & volume of navigation suite          =    40.44 kg   0.1925 m^3
Mass & volume of communication suite       =    12.68 kg   0.0949 m^3
Mass & volume of identification suite      =    20.89 kg   0.1556 m^3

STORE MANAGEMENT SYSTEM
Mass & volume of weapon control suite      =     8.32 kg   0.0620 m^3

ELECTRONIC WARFARE SYSTEM
Mass & volume of electronic warfare suite  =     4.82 kg   0.0322 m^3
Mass & volume of countermeasures suite     =     4.82 kg   0.0322 m^3

Total avionics mass                        =   188.34 kg

Length of radar avionics suite             =  0.8022 m
Length of flight management avionics suite =  1.2861 m
Length of weapon control avionics suite    =  0.5697 m

Radome length                              =  1.2033 m

 ------------------------------
 * WEAPON BAY

WEAPON BAY 1
Total number of weapon bay 1                 = 1
Total number of weapons in each weapon bay 1 = 1
Total mass of weapons in weapon bay 1        =   460.00 kg
Total mass of internal pylons in weapon bay 1 =    62.50 kg

WEAPON BAY 2
Total number of weapon bay 2                 = 1
Total number of weapons in each weapon bay 2 = 1
Total mass of weapons in weapon bay 2        =   460.00 kg
```

```
Total mass of internal pylons in weapon bay 2 =    62.50 kg

INTERNAL WEAPON BAY
Total mass of weapons in internal weapon bays =   920.00 kg

WEAPON BAY DIMENSION
               L(m)     W(m)     H(m)    V(m^3)
Weapon bay 1  3.1900   0.6300   0.6300   1.2661
Weapon bay 2  3.1900   0.6300   0.6300   1.2661

EXTERNAL STORES
Total number of weapons at port store          = 0
Total mass of weapons at port store            =     0.00 kg
Total number of weapons at starboard store     = 0
Total mass of weapons at starboard store       =     0.00 kg
External store wetted area                     =  0.0000 m^2
Total mass of external pylons                  =     0.00 kg

Total mass of weapons at external stores       =     0.00 kg


TOTAL WEAPONS
Total mass of weapons on aircraft              =   920.00 kg

 ---------------------------------
 *UCAV VARIABLE MASS CONTRIBUTION*

 ------------------------------
 * ENGINE BAY

 ONE SINGLE-ENGINE INSTALLATION

ENGINE & ENGINE BAY DIMENSION
Overall length of engine  =  1.8418 m
Diameter of engine        =  0.8670 m

Total nozzle exit area    =    0.59 m^2

Maximum engine bay height =  1.0405 m
Maximum engine bay width  =  1.0405 m

ENGINE BAY VOLUME
Volume of engine bay            =  1.5659 m^3

PROPULSION SYSTEM MASS
Total mass of engines           =   399.78 kg
Engine installation mass        =    51.97 kg

Total mass of propulsion system =   451.75 kg

ENGINE STATIC THRUST
Total maximum sea-level static thrust of engines =  22508.41 N
Bypass ratio of total engines   =    4.00

 ------------------------------
 * UNDERCARRIAGE BAY

NOSE UNDERCARRIAGE
Length of nose undercarriage leg         =  0.6844 m
Nose undercarriage wheel & tyre diameter =  0.4039 m
Nose undercarriage wheel & tyre width    =  0.1520 m

MAIN UNDERCARRIAGE
Length of each main undercarriage leg    =  0.9249 m
Main undercarriage wheel & tyre diameter =  0.5631 m
Main undercarriage wheel & tyre width    =  0.1543 m

UNDERCARRIAGE MASS
Structural mass of nose undercarriage            =    34.03 kg
Structural mass of total main undercarriage      =   246.99 kg
Mass of hydraulics associated with undercarriage =    33.78 kg

UNDERCARRIAGE GROSS MASS
Total mass of nose undercarriage with hydraulics =    38.12 kg
Total mass of main undercarriage with hydraulics =   276.68 kg

UNDERCARRIAGE BAY DIMENSION
```

```
              L(m)     H(m)     W(m)    V(m^3)
Nose UC bay   0.8863   0.4442   0.2280   0.0898
Main UC bay   1.2064   0.6194   0.2315   0.1730

 ------------------------------
 * FLYING WING

 MULTI-KINK WING

FLYING WING SPECIFICATION
Wing centreline section & chord  0.0000 m  9.1353 m
Wing tip section & chord         6.8074 m  1.5622 m
Wing gross span               = 13.6148 m
Gross wing aspect ratio       =  2.6403
Gross wing area               =   70.21 m^2
Wing wetted area              =  142.73 m^2
Mean thickness ratio          =  0.1077
Average wing chord            =  5.1866 m

Wing geometric mean chord     =  5.1566 m
Wing aerodynamic mean chord   =  6.0576 m
Distance of wing mean 1/4 chord point from nose =  4.6379 m

Equivalent wing root chord         =  8.7509 m
Equivalent wing taper ratio        =  0.1785
Equivalent wing leading edge sweep = 50.4081 degree
Equivalent wing quarter chord sweep= 43.3843 degree
Equivalent wing mid-chord sweep    = 34.2599 degree

Maximum depth at wing centreline chord =  1.3126 m
Maximum depth at wing tip chord        =  0.1406 m

Wing maximum cross-sectional area      =   10.88 m^2
Flying wing total volume               =   36.61 m^3

Centre of wing volume (true wing)      =  0.1200
Centre of wing volume (equivalent wing)=  0.1066

Wing aerodynamic centre (%MAC)         =  0.0948

Spanwise station to wing kink  0 =   0.0000 m
Wing chord at kink             0 =   9.1353 m
Thickness ratio at kink        0 =   0.1500
Taper ratio at kink            0 =   0.0000
Leading edge sweep at kink     0 =   0.0000 degree
Trailing edge sweep at kink    0 =   0.0000 degree
Length to TE from nose at kink 0 =   9.1353 m

Spanwise station to wing kink  1 =   2.3826 m
Wing chord at kink             1 =   6.1003 m
Thickness ratio at kink        1 =   0.1112
Taper ratio at kink            1 =   0.6678
Leading edge sweep at kink     1 =  50.4081 degree
Trailing edge sweep at kink    1 =  -3.7005 degree
Length to TE from nose at kink 1 =   8.9812 m

Spanwise station to wing kink  2 =   6.8074 m
Wing chord at kink             2 =   1.5622 m
Thickness ratio at kink        2 =   0.0900
Taper ratio at kink            2 =   0.2561
Leading edge sweep at kink     2 =  50.4081 degree
Trailing edge sweep at kink    2 =  10.3994 degree
Length to TE from nose at kink 2 =   9.7933 m


WING BOX
Wing front spar from nose at root      =  1.3703 m
Wing rear spar from nose at root       =  6.3947 m

Wing front spar from nose at tip       =  0.2343 m
Wing rear spar from nose at tip        =  1.0935 m

Wing box root chord                    =  5.0244 m
Wing box tip chord                     =  0.8592 m
Wing box gross span                    = 13.6148 m
Gross wing box planform area           =   38.61 m^2
Gross wing box aspect ratio            =  4.8005
```

```
Equivalent wing box root chord         =  4.8130 m
Equivalent wing box taper ratio        =  0.1785
Equivalent wing box leading edge sweep = 46.4172 degree
Equivalent wing box centreline sweep   = 42.5747 degree


WING SPANWISE LIFT DISTRUBITION
Mach number for design diving speed =  1.1755
Effective Mach number               =  0.5444
Effective angle of sweepback        = 54.9745 degree
Average angle of attack             =  5.5424 degree

 ------------------------------
 * BAY POSITION

ENGINE BAY POSITION
Spanwise station to engine bay section              =  0.0000  0.0000  0.5202 m
Wing chord at engine bay section                    =  9.1353  9.1353  8.4726 m
Wing leading edge at engine bay section from nose   =  0.0000  0.0000  0.6290 m

Minimum distance of engine inlet from nose          =  3.3757 m
Maximum distance of engine exit from nose           =  6.9835 m
Axial space available for length of engine          =  3.6078 m

Axial distance from nose to engine front face       =  4.4668 m
Axial distance from nose to transition duct entrance=  6.3086 m


WEAPON BAY 1 POSITION
Spanwise station to weapon bay 1 section            =  0.6702  0.9852  1.3002 m
Wing chord at weapon bay 1 section                  =  8.2816  7.8803  7.4791 m
Wing leading edge at weapon bay 1 section from nose =  0.8104  1.1913  1.5722 m

Minimum distance of weapon bay1 front face from nose=  3.5997 m
Maximum distance of weapon bay1 rear face from nose =  7.2815 m
Axial space available for length of weapon bay 1    =  3.5817 m

Axial distance from nose to weapon bay 1 front face =  3.5997 m


WEAPON BAY 2 POSITION
Spanwise station to weapon bay 2 section            =  0.6702  0.9852  1.3002 m
Wing chord at weapon bay 2 section                  =  8.2816  7.8803  7.4791 m
Wing leading edge at weapon bay 2 section from nose =  0.8104  1.1913  1.5722 m

Minimum distance of weapon bay2 front face from nose=  3.5997 m
Maximum distance of weapon bay2 rear face from nose =  7.2815 m
Axial space available for length of weapon bay 2    =  3.5817 m

Axial distance from nose to weapon bay 2 front face =  3.5997 m


MAIN UNDERCARRIAGE BAY POSITION
Spanwise station to main uc bay section             =  1.4502  1.5660  1.6817 m
Wing chord at main uc bay section                   =  7.2880  7.1406  6.9932 m
Wing leading edge at main uc bay section from nose  =  1.7535  1.8935  2.0334 m

Minimum distance of main uc bay front face from nose=  3.0824 m
Maximum distance of main uc bay rear face from nose =  6.8551 m
Axial space available for length of main uc bay     =  3.4231 m

Axial distance from nose to main uc bay front face  =  4.0872 m

 ------------------------------
 * INTAKE DIFFUSER

Cross sectional area of intake inlet  =  0.5904 m^2
Cross sectional area of intake exit   =  0.5904 m^2
Equivalent diameter of intake inlet   =  0.8670 m
Diameter of intake exit               =  0.8670 m

Width of intake inlet                 =  1.0867 m
Height of intake inlet                =  0.5433 m
Width of intake inlet projected into horizontal =  1.0867 m
Height of intake inlet projected into vertical  =  0.5433 m
```

```
Distance of intake inlet from nose    =  2.7327 m
Length of intake diffuser             =  1.7341 m

Spanwise station to intake inlet      =  0.9852 m
Spanwise station to intake exit       =  0.0000 m
Vertical distance of intake inlet     =  0.3873 m
Vertical distance of intake exit      =  0.0000 m
Wing leading edge at intake from nose =  1.1913 m

Volume of each intake diffuser        =  1.0239 m^3

 ------------------------------
 * 2-DIMENSIONAL NOZZLE

Aspect ratio of nozzle transition duct exit=  7.3339

SINGLE ENGINE INSTALLATION
Half-height of nozzle transition duct exit =  0.1419 m
Half-width of nozzle transition duct exit  =  1.0405 m

Length of nozzle transition duct      =  1.9458 m

Volume of nozzle transition duct      =  3.0293 m^3
Total mass of nozzle transition duct =    63.10 kg

 ------------------------------
 * TRAILING EDGE SPLIT ELEVON

Total number of all split elevons = 2

ELEVON 1
Elevon inner span,chrd &wchrd =  3.4037  1.1117  5.0531 m
Elevon outer span,chrd &wchrd =  4.7652  0.8045  3.6567 m
Elevon mean chord             =  0.9581 m
Total span of elevon          =  2.7230 m
Aspect ratio of each elevon   =  1.4210
Elevon hinge line sweep       = 18.1265 deg
Total planform area of elevon =    2.61 m^2
Total wing area over elevon   =   11.86 m^2
ELEVONS LIFT & MOMENT             TO      LD
Elevon deflection             =   30.00   60.00 deg
Section lift increment        =  0.9064  1.3400
Wing lift increment           =  0.0794  0.1174
Wing pitch increment          = -0.0060 -0.0089
Sect max lift increment       =  0.6690  0.9045
Wing max lift increment       =  0.1074  0.1452


All split elevons gross span          =   2.7230 m
Split elevon mean chord               =   0.9581 m
All split elevons planform area       =     2.61 m^2
Total wing planform area over split elevons   =   11.86 m^2

WING TRAILING EDGE
Gross area of wing trailing edge aft of rear spar    =   15.39 m^2
Planform area of fixed section of wing TE aft of r/s =   12.79 m^2

 ------------------------------
 * LEADING EDGE SLAT

Total number of all slats = 0


All slats gross span          =   0.0000 m
Slat mean chord               =   0.0000 m
All slats planform area       =     0.00 m^2
Total wing planform area over slats   =    0.00 m^2

WING LEADING EDGE
Total planform area of wing leading edge            =    7.70 m^2
Planform area of fixed section of wing LE fwd of f/s =    2.57 m^2

 ------------------------------
 * TRAILING EDGE SPLIT RUDDER

Total number of all split rudders = 2
```

```
SPLIT RUDDER 1
Rudder inner span & wchrd      =  3.4037  5.0531 m
Rudder outer span & wchrd      =  4.7652  3.6567 m
Aspect ratio of each rudder    =  1.4210
Rudder hinge line sweep        = 18.1265 deg
SPLIT RUDDERS LIFT & MOMENT      Aileron Rudder
Split rudder deflection        =   20.00   25.00 deg
Section lift increment         =  0.7830  0.8755
Wing lift increment            =  0.0686  0.0767
Wing yaw effectiveness         = -0.0028  0.0031
Wing roll effectiveness        =  0.0332 -0.0371

 ------------------------------
 * FUEL

- CENTRE FUEL TANK -
Total span of centre fuel tank =  0.0000 m

CENTRE FUEL TANK 1 (FRONT)
Centre fuel tank 1 front face from nose =  0.0000 m
Centre fuel tank 1 rear face from nose  =  0.0000 m
Total fuel volume of centre tank 1     =  0.0000 m^3
Fuel mass used in centre fuel tank 1   =     0.00 kg
M-arm of centre fuel tank 1 from nose  =  0.0000 m

CENTRE FUEL TANK 2 (REAR)
Centre fuel tank 2 front face from nose =  0.0000 m
Centre fuel tank 2 rear face from nose  =  0.0000 m
Total fuel volume of centre tank 2     =  0.0000 m^3
Fuel mass used in centre fuel tank 2   =     0.00 kg
M-arm of centre fuel tank 2 from nose  =  0.0000 m

CENTRE FUEL TANK 3 (TOP)
Centre fuel tank 3 front face from nose =  0.0000 m
Centre fuel tank 3 rear face from nose  =  0.0000 m
Total fuel volume of centre tank 3     =  0.0000 m^3
Fuel mass used in centre fuel tank 3   =     0.00 kg
M-arm of centre fuel tank 3 from nose  =  0.0000 m

TOTAL CENTRE FUEL TANK CAPACITY
Total area of centre fuel tank         =  0.0000 m^2
Total fuel volume of centre tank       =  0.0000 m^3
Total fuel mass used in centre tank    =     0.00 kg


- INBOARD FUEL TANK -
Total span of inboard fuel tank =  1.2600 m

INBOARD FUEL TANK 1 (FRONT)
Inboard fuel tank 1 front face from nose =  3.5997 m
Inboard fuel tank 1 rear face from nose  =  3.5997 m
Total fuel volume of inbrd tank 1      =  0.0000 m^3
Fuel mass used in inbrd fuel tank 1    =     0.00 kg
M-arm of inbrd fuel tank 1 from nose   =  3.5997 m

INBOARD FUEL TANK 2 (REAR)
Inboard fuel tank 2 front face from nose =  6.7897 m
Inboard fuel tank 2 rear face from nose  =  7.2815 m
Total fuel volume of inbrd tank 2      =  0.3097 m^3
Fuel mass used in inbrd fuel tank 2    =     0.00 kg
M-arm of inbrd fuel tank 2 from nose   =  7.0274 m

INBOARD FUEL TANK 3 (TOP)
Inboard fuel tank 3 front face from nose =  3.5997 m
Inboard fuel tank 3 rear face from nose  =  5.1947 m
Total fuel volume of inbrd tank 3      =  0.2586 m^3
Fuel mass used in inbrd fuel tank 3    =     0.00 kg
M-arm of inbrd fuel tank 3 from nose   =  4.3852 m

TOTAL INBOARD FUEL TANK CAPACITY
Total area of inboard fuel tank         =  2.6293 m^2
Total fuel volume of inbrd tank         =  0.5684 m^3
Total fuel mass used in inbrd tank      =     0.00 kg


- OUTBOARD FUEL TANK -
Total span of outboard fuel tank =  0.4629 m
```

```
OUTBOARD FUEL TANK 1 (FRONT)
Outboard fuel tank 1 front face from nose =  3.0824 m
Outboard fuel tank 1 rear face from nose  =  4.0872 m
Total fuel volume of outbrd tank 1    =  0.3241 m^3
Fuel mass used in outbrd fuel tank 1  =     0.00 kg
M-arm of outbrd fuel tank 1 from nose =  3.5946 m

OUTBOARD FUEL TANK 2 (REAR)
Outboard fuel tank 2 front face from nose =  5.2937 m
Outboard fuel tank 2 rear face from nose  =  6.8551 m
Total fuel volume of outbrd tank 2    =  0.4295 m^3
Fuel mass used in outbrd fuel tank 2  =     0.00 kg
M-arm of outbrd fuel tank 2 from nose =  6.0299 m

TOTAL OUTBOARD FUEL TANK CAPACITY
Total area of outboard fuel tank       =  1.1880 m^2
Total fuel volume of outbrd tank       =  0.7536 m^3
Total fuel mass used in outbrd tank    =     0.00 kg


- WING FUEL TANK -
Wing fuel tank spanwise station 0 =  1.8317 m
Wing fuel tank spanwise station 1 =  2.3826 m
Wing fuel tank spanwise station 2 =  4.2343 m
Total span available for wing fuel tank          =  4.8051 m
Total wing box area available for wing fuel tank =  4.5323 m^2

WING FUEL TANK CAPACITY
Total fuel volume of wing tank         =  1.7404 m^3
Total fuel mass used in wing tank      =  1351.45 kg


- OPTIONAL WEAPON BAY FUEL TANK -
Total fuel volume of weapon bay tank1=  0.0000 m^3
Fuel mass used in weapon bay tank 1  =     0.00 kg

Total fuel volume of weapon bay tank2=  0.0000 m^3
Fuel mass used in weapon bay tank 2  =     0.00 kg

TOTAL WEAPON BAY FUEL TANK CAPACITY
Total fuel volume of weapon bay tank      =  0.0000 m^3
Total fuel mass used in weapon bay tank   =     0.00 kg


- UCAV TOTAL FUEL CAPACITY -
Total area containing fuel tank      =  8.3496 m^2
Total internal fuel volume           =  3.0624 m^3
Total mass of available internal fuel=  2377.94 kg

Total fuel mass used on aircraft     =  1351.45 kg

 ------------------------------
 * UCAV MASS & CG

- UCAV MASS -

WING BOX
Ultimate load factor           =    9.75
Wing inertia relief load       =  1888.03 kg

Wing box mass (Torsion)        =   152.99 kg
Wing box mass (Bending)        =   206.10 kg
Total wing box mass            =   206.10 kg

CONTROL SURFACES
Wing leading edge mass         =    42.70 kg
Wing fixed trailing edge mass  =   106.50 kg

TEcs mass (flap)               =    13.96 kg
TEcs mass (aileron)            =    46.26 kg
Total TE control surfaces mass =    46.26 kg

Inlaids mass (rudder)          =     0.00 kg
Inlaids mass (spoiler)         =     0.00 kg
Total inlaids CS mass          =     0.00 kg
```

```
AUXILIARY
Miscellaneous attachments      =    27.58 kg
External paint                 =    23.94 kg
Low Observable treatments      =   226.80 kg
Basic ribs in strutural box    =   337.72   361.85 kg

FLYING WING
Total wing structural mass     =  1017.59 kg

MASS INCREMENT DUE TO INTERNAL WEAPON BAYS
Mass increment due to weap bay1=   117.94 kg
Mass increment due to weap bay2=   117.94 kg

AIRCRAFT SYSTEM
Mass of air systems            =    10.20 kg
Mass of de-icing system        =    31.73 kg
Mass of electrical systems     =   167.49 kg
Mass of flight control systems =   173.19 kg
Mass of fuel system            =   102.58 kg

COMPLETE AIRCRAFT
Total aircraft payload         =   920.00 kg
Mass of fixed-role equipment   =   313.34 kg
Total mass of fuel on aircraft =  1351.45 kg

Empty mass             =   2881.65 kg
Operational empty mass =   2881.65 kg
Zero fuel mass         =   3801.65 kg

Total take-off mass    =   5153.10 kg
Landing mass           =   4380.14 kg

Wing loading           =   73.4002 kg/m^2
Thrust loading         =    0.4454


WING STRUCTURAL MASS COMPARISON
Howe method 1 (COA)    =   1017.59 kg (theoretical)
Howe method 2 (COA)    =   1574.56 kg (empirical)
Lovell method (RAE)    =   2059.10 kg
Roskam method (USAF)   =    714.48 kg
Roskam method (USN)    =   1048.04 kg
Raymer method          =    788.78 kg
Whitford method        =    928.84 kg


- CENTRE OF GRAVITY -

OPERATIONAL EMPTY MASS
Total aircraft pitching moment about nose=  13364.80 kg.m
Distance of aircraft CG from nose        =  4.6379 m
CG relative to aerodynamic mean chord    =  25.00%

ZERO FUEL MASS
Total aircraft pitching moment about nose=  18143.95 kg.m
Distance of aircraft CG from nose        =  4.7727 m
CG relative to aerodynamic mean chord    =  27.22%

TOTAL TAKE-OFF MASS
Total aircraft pitching moment about nose=  24594.06 kg.m
Distance of aircraft CG from nose        =  4.7727 m
CG relative to aerodynamic mean chord    =  27.22%
Static margin                            =  -2.22%

Distance of aircraft fwd CG from nose  =  4.2744 m
Fwd CG relative to AMC                 =  19.00%
Distance of aircraft aft CG from nose  =  5.0619 m
Aft CG relative to AMC                 =  32.00%

Reference spanwise distance of aircraft CG             =  0.0000 m
Reference vertical distance of aircraft CG from ground =  1.4411 m


- UNDERCARRIAGE ARRANGEMENTS -

UNDERCARRIAGE ARRANGEMENTS
Axial distance from nose wheel to main wheel =  3.5972 m
```

```
Axial angle from nose wheel to main wheel    = 23.5248 degree

Axial distance from nose UC to aircraft aft CG position     =  3.1262 m
Axial distance from aircraft forward CG position to main UC =  0.6058 m
Axial distance from aircraft aft CG position to main UC     =  0.4710 m

AIRCRAFT OVERTURN ANGLE
Aircraft static ground line    =  1.4358 m
Aircraft overturn angle        = 45.1054 degree

AIRCRAFT TIPBACK & STATIC TAILDOWN ANGLE
Axial distance from main uc to tail =  4.5496 m
Height due to tipback angle         =  1.4869 m

Aircraft tipback angle         = 18.0987 degree
Aircraft static taildown angle = 15.9377 degree

AIRCRAFT ANGLE OFF VERTICAL
Angle off vertical             = 18.0987 degree

UNDERCARRIAGE STATIC LOADS
Maximum static load       =   4478.40 kg
Maximum nose static load  =    867.77 kg
Minimum nose static load  =    674.70 kg
Nose dynamic braking load =    631.54 kg

Maximum static load as a fraction of total load      =   86.91%
Maximum nose static load as a fraction of total load =   16.84%
Minimum nose static load as a fraction of total load =   13.09%

MAIN UNDERCARRIAGE SHOCK ABSORBER STROKE
Main undercarriage rolling radius        =  0.1877 m
Main undercarriage tyre stroke           =  0.0939 m
Main undercarriage shock absorber stroke =  0.4854 m

UNDERCARRIAGES FRONTAL AREA
Oleo load of each main undercarriage =   2239.20 kg
Oleo load of nose undercarriage      =   1499.31 kg

Oleo diameter of main undercarriage  =  0.0197 m
Oleo diameter of nose undercarriage  =  0.0161 m

Frontal area of each main undercarriage leg          =  0.0182 m^2
Frontal area of each main undercarriage wheel & tyre =  0.0724 m^2

Frontal area of nose undercarriage leg          =  0.0110 m^2
Frontal area of nose undercarriage wheel & tyre =  0.0512 m^2

 -------------------------
 *UCAV COMPONENT SUMMARY*

 --- MASS & BALANCE ---
 Aircraft component  Mass   Range   X-Marm    XMoment   Y-Marm    YMoment
                     (kg)    (%)      (m)     (kg.m)      (m)      (kg.m)
Wing (port)          508.80    9.87  5.3650   2729.68 -2.9952  -1523.97
Wing (starboard)     508.80    9.87  5.3650   2729.68  2.9952   1523.97
Nose UC               38.12    0.74  1.6465     62.77  0.0000      0.00
Main UC (port)       138.34    2.68  5.2437    725.42 -1.5660   -216.64
Main UC (stbd)       138.34    2.68  5.2437    725.42  1.5660    216.64
Engine               451.75    8.77  5.3877   2433.87  0.0000      0.00
Nozzle                63.10    1.22  7.2815    459.45  0.0000      0.00
Avionics(MMS)         51.34    1.00  0.8022     41.18  0.0000      0.00
Avionics(FMS)        119.04    2.31  2.7327    325.30  0.0000      0.00
Avionics(SMS)          8.32    0.16  2.4112     20.06  0.0000      0.00
Avionics(EWS-port)     4.82    0.09  6.9964     33.72 -5.7863    -27.89
Avionics(EWS-stbd)     4.82    0.09  6.9964     33.72  5.7863     27.89
Air system            10.20    0.20  2.4112     24.58  0.0000      0.00
De-icing system       31.73    0.62  2.4112     76.52  0.0000      0.00
Electrical system    167.49    3.25  2.4112    403.84  0.0000      0.00
FCS                  173.19    3.36  2.4112    417.58  0.0000      0.00
Fuel system          102.58    1.99  2.4112    247.33  0.0000      0.00
W bay1 pylon          62.50    1.21  5.1947    324.67 -0.9852    -61.58
W bay2 pylon          62.50    1.21  5.1947    324.67  0.9852     61.58
W bay1 increment     117.94    2.29  5.1947    612.66 -0.9852   -116.20
W bay2 increment     117.94    2.29  5.1947    612.66  0.9852    116.20
Residual fuel          0.00    0.00  2.4112      0.00  0.0000      0.00
     OEM            2881.65   55.92  4.6379  13364.80               0.00
```

Weap in bay1	460.00	8.93	5.1947	2389.58	-0.9852	-453.20
Weap in bay2	460.00	8.93	5.1947	2389.58	0.9852	453.20
ZFM	3801.65	73.77	4.7727	18143.95		0.00
Wing tank (port)	675.73	13.11	4.7727	3225.06	-2.8888	-1952.05
Wing tank (stbd)	675.73	13.11	4.7727	3225.06	2.8888	1952.05
Inbrd tank1(port)	0.00	0.00	3.5997	0.00	-0.9852	0.00
Inbrd tank1(stbd)	0.00	0.00	3.5997	0.00	0.9852	0.00
Inbrd tank2(port)	0.00	0.00	7.0274	0.00	-0.9852	0.00
Inbrd tank2(stbd)	0.00	0.00	7.0274	0.00	0.9852	0.00
Inbrd tank3(port)	0.00	0.00	4.3852	0.00	-0.9852	0.00
Inbrd tank3(stbd)	0.00	0.00	4.3852	0.00	0.9852	0.00
Outbrd tank1(port)	0.00	0.00	3.5946	0.00	-1.5660	0.00
Outbrd tank1(stbd)	0.00	0.00	3.5946	0.00	1.5660	0.00
Outbrd tank2(port)	0.00	0.00	6.0299	0.00	-1.5660	0.00
Outbrd tank2(stbd)	0.00	0.00	6.0299	0.00	1.5660	0.00
AUM	5153.10	100.00	4.7727	24594.06		0.00

--- MASS & BALANCE (continued) ---

Aircraft component	Mass (kg)	Z-Marm dwn(m)	ZMoment (kg.m)	Z-Marm up (m)	ZMoment (kg.m)
Wing (port)	508.80	1.4411	733.23	0.0000	0.00
Wing (starboard)	508.80	1.4411	733.23	0.0000	0.00
Nose UC	38.12	1.1126	42.42	-0.3285	-12.52
Main UC (port)	138.34	1.1126	153.92	-0.3285	-45.45
Main UC (stbd)	138.34	1.1126	153.92	-0.3285	-45.45
Engine	451.75	1.4411	651.01	0.0000	0.00
Nozzle	63.10	1.4411	90.93	0.0000	0.00
Avionics(MMS)	51.34	1.4411	73.99	0.0000	0.00
Avionics(FMS)	119.04	1.4411	171.55	0.0000	0.00
Avionics(SMS)	8.32	1.4411	11.99	0.0000	0.00
Avionics(EWS-port)	4.82	1.4411	6.95	0.0000	0.00
Avionics(EWS-stbd)	4.82	1.4411	6.95	0.0000	0.00
Air system	10.20	1.6632	16.96	0.2221	2.26
De-icing system	31.73	1.6632	52.78	0.2221	7.05
Electrical system	167.49	1.9613	328.50	0.5202	87.13
FCS	173.19	1.9613	339.67	0.5202	90.10
Fuel system	102.58	1.9613	201.18	0.5202	53.36
W bay1 pylon	62.50	1.7561	109.76	0.3150	19.69
W bay2 pylon	62.50	1.7561	109.76	0.3150	19.69
W bay1 increment	117.94	1.4411	169.96	0.0000	0.00
W bay2 increment	117.94	1.4411	169.96	0.0000	0.00
Residual fuel	0.00	1.3544	0.00	-0.0867	0.00
OEM	2881.65		4328.59		175.86
Weap in bay1	460.00	1.4411	662.90	0.0000	0.00
Weap in bay2	460.00	1.4411	662.90	0.0000	0.00
ZFM	3801.65		5654.40		175.86
Wing tank (port)	675.73	1.4411	973.79	0.0000	0.00
Wing tank (stbd)	675.73	1.4411	973.79	0.0000	0.00
Inbrd tank1(port)	0.00	1.4411	0.00	0.0000	0.00
Inbrd tank1(stbd)	0.00	1.4411	0.00	0.0000	0.00
Inbrd tank2(port)	0.00	1.4411	0.00	0.0000	0.00
Inbrd tank2(stbd)	0.00	1.4411	0.00	0.0000	0.00
Inbrd tank3(port)	0.00	1.7561	0.00	0.3150	0.00
Inbrd tank3(stbd)	0.00	1.7561	0.00	0.3150	0.00
Outbrd tank1(port)	0.00	1.4411	0.00	0.0000	0.00
Outbrd tank1(stbd)	0.00	1.4411	0.00	0.0000	0.00
Outbrd tank2(port)	0.00	1.4411	0.00	0.0000	0.00
Outbrd tank2(stbd)	0.00	1.4411	0.00	0.0000	0.00
AUM	5153.10		7601.98		175.86

Internal Weapons Carriage: The configuration is based on the straight-tapered wing planform with the single weapon bay located at the aircraft centreline, equipped with two MK-82 bombs laterally (MK-82 WEAP2), as illustrated in Figure 8-22 of Chapter 8.

```
------------------------------
--- UCAV PACKAGING SUMMARY ---
------------------------------
```

```
 * UCAV PACKAGING CONFIGURATION

 1) Type of stores          = 1 :Internal store
 2) Number of weapon bays   = 1 :Single weapon bay on centreline
 3) Type of missions        = 1 :SEAD/strike
 4) Number of engines       = 1 :Single-engine installation
 5) Type of aircraft        = 0 :Unmanned aircraft
 6) Type of materials       = 2 :Carbon-fibre composite construction
 7) Number of kinks in wing = 0 :Straight taper wing
 8) Number of split elevons on half span = 1
 9) Number of slats on half span         = 0
10) Number of split rudders on half span = 0
11) Type of airfoils at wing inboard section  = 1 :Symmetrical airfoil
12) Type of airfoils at wing outboard section = 1 :Symmetrical airfoil
13) Thickness ratio at wing inboard section  = 15%
14) Thickness ratio at wing outboard section =  9%
15) Twist distribution      = 1 :Twist wing

 -------------------------
 *UCAV PACKAGING OPTIMIZER*

                                      INITIAL    FINAL     LOWER     UPPER
   1 Wing span (m)           [BW]     13.0000   12.7929    6.0000   40.0000
   2 Wing root chord (m)     [CWCC]    9.0000    8.0220    6.0000   20.0000
   3 Wing tip chord (m)      [CWCT]    2.0000    1.9839    0.0100    4.0000
   4 Front spar fraction     [FCWD]    0.1500    0.1500    0.1500    0.1500
   5 Rear spar fraction      [FCWR]    0.7000    0.7000    0.7000    0.7000
   6 Wing leading edge sweep[QWLR]    50.0000   51.3417    0.0100   60.0000
   7 Elevon mean chord (m)   [CWSE]    1.0000    0.7722    0.5000    3.0000
   8 Elevon inner span       [FYSEI]   0.4000    0.5445    0.1000    0.9500
   9 Elevon outer span       [FYSEO]   0.7000    0.9500    0.1000    0.9500
  10 Wing tank span factor   [FY2WFO]  0.5000    0.0841    0.0100    1.0000
  11 Wing tank front factor  [FCWFD]   0.0000    0.0000    0.0000    0.0000
  12 Wing tank rear factor   [FCWFR]   1.0000    1.0000    1.0000    1.0000
  13 Weap bay1 axial factor  [FXLIB1]  0.5000    0.4640    0.0000    1.0000
  14 Engine axial factor     [FXLPG]   0.5000    0.3503    0.0000    1.0000
  15 Engine scale factor     [RTP]     1.5000    0.5869    0.5000    2.5000

 -------------------------------
 *UCAV FIXED MASS CONTRIBUTION*

 -------------------------------
 * AVIONICS BAY

MISSION MANAGEMENT SYSTEM
Mass & volume of radar suite              =    28.32 kg   0.1404 m^3
Mass & volume of sensor suite             =    23.02 kg   0.0605 m^3

FLIGHT MANAGEMENT SYSTEM
Mass & volume of flight control suite     =    45.03 kg   0.1634 m^3
Mass & volume of navigation suite         =    40.44 kg   0.1925 m^3
Mass & volume of communication suite      =    12.68 kg   0.0949 m^3
Mass & volume of identification suite     =    20.89 kg   0.1556 m^3

STORE MANAGEMENT SYSTEM
Mass & volume of weapon control suite     =     8.32 kg   0.0620 m^3

ELECTRONIC WARFARE SYSTEM
Mass & volume of electronic warfare suite =     4.82 kg   0.0322 m^3
Mass & volume of countermeasures suite    =     4.82 kg   0.0322 m^3

Total avionics mass                       =   188.34 kg

Length of radar avionics suite            =  0.8022 m
Length of flight management avionics suite =  1.2861 m
Length of weapon control avionics suite   =  0.5697 m

Radome length                             =  1.2033 m

 -------------------------------
 * WEAPON BAY

WEAPON BAY 1
Total number of weapon bay 1                 = 2
Total number of weapons in each weapon bay 1 = 2
Total mass of weapons in weapon bay 1        =   482.00 kg
```

```
Total mass of internal pylons in weapon bay 1 =   125.00 kg

WEAPON BAY 2
Total number of weapon bay 2                  = 0
Total number of weapons in each weapon bay 2  = 0
Total mass of weapons in weapon bay 2         =     0.00 kg
Total mass of internal pylons in weapon bay 2 =     0.00 kg

INTERNAL WEAPON BAY
Total mass of weapons in internal weapon bays =   482.00 kg

WEAPON BAY DIMENSION
               L(m)     W(m)     H(m)    V(m^3)
Weapon bay 1  2.3600   0.9850   0.5300   1.2320
Weapon bay 2  0.0000   0.0000   0.0000   0.0000

EXTERNAL STORES
Total number of weapons at port store         = 0
Total mass of weapons at port store           =     0.00 kg
Total number of weapons at starboard store    = 0
Total mass of weapons at starboard store      =     0.00 kg
External store wetted area                    =  0.0000 m^2
Total mass of external pylons                 =     0.00 kg

Total mass of weapons at external stores      =     0.00 kg


TOTAL WEAPONS
Total mass of weapons on aircraft             =   482.00 kg

 ---------------------------------
 *UCAV VARIABLE MASS CONTRIBUTION*

 ------------------------------
 * ENGINE BAY

 TWO SINGLE-ENGINE INSTALLATIONS

ENGINE & ENGINE BAY DIMENSION
Overall length of engine  =  1.3231 m
Diameter of engine        =  0.6228 m

Total nozzle exit area    =    0.30 m^2

Maximum engine bay height =  0.7474 m
Maximum engine bay width  =  0.7474 m

ENGINE BAY VOLUME
Volume of engine bay            =  0.5805 m^3

PROPULSION SYSTEM MASS
Total mass of engines           =   386.18 kg
Engine installation mass        =    50.20 kg

Total mass of propulsion system =   436.38 kg

ENGINE STATIC THRUST
Total maximum sea-level static thrust of engines =  23229.73 N
Bypass ratio of total engines   =    8.00

 ------------------------------
 * UNDERCARRIAGE BAY

NOSE UNDERCARRIAGE
Length of nose undercarriage leg         =  0.6058 m
Nose undercarriage wheel & tyre diameter =  0.3862 m
Nose undercarriage wheel & tyre width    =  0.1520 m

MAIN UNDERCARRIAGE
Length of each main undercarriage leg    =  0.8187 m
Main undercarriage wheel & tyre diameter =  0.5334 m
Main undercarriage wheel & tyre width    =  0.1446 m

UNDERCARRIAGE MASS
Structural mass of nose undercarriage            =    28.26 kg
Structural mass of total main undercarriage      =   204.80 kg
Mass of hydraulics associated with undercarriage =    27.66 kg
```

```
UNDERCARRIAGE GROSS MASS
Total mass of nose undercarriage with hydraulics =    31.62 kg
Total mass of main undercarriage with hydraulics =   229.10 kg

UNDERCARRIAGE BAY DIMENSION
              L(m)     H(m)     W(m)    V(m^3)
Nose UC bay  0.7989   0.4248   0.2280   0.0774
Main UC bay  1.0854   0.5868   0.2169   0.1381

 ------------------------------
 * FLYING WING

 STRAIGHT TAPERED WING

FLYING WING SPECIFICATION
Wing centreline section & chord  0.0000 m  8.0220 m
Wing tip section & chord         6.3965 m  1.9839 m
Wing gross span               = 12.7929 m
Gross wing aspect ratio       =  2.5571
Gross wing area               =   64.00 m^2
Wing wetted area              =  130.25 m^2
Mean thickness ratio          =  0.1117
Average wing chord            =  5.0030 m

Wing geometric mean chord     =  5.0030 m
Wing aerodynamic mean chord   =  5.6102 m
Distance of wing mean 1/4 chord point from nose =  4.5964 m

Equivalent wing root chord         =  8.0220 m
Equivalent wing taper ratio        =  0.2473
Equivalent wing leading edge sweep = 51.3417 degree
Equivalent wing quarter chord sweep= 45.4004 degree
Equivalent wing mid-chord sweep    = 37.8859 degree

Maximum depth at wing centreline chord =  1.2033 m
Maximum depth at wing tip chord        =  0.1786 m

Wing maximum cross-sectional area      =   13.18 m^2
Flying wing total volume               =   31.77 m^3

Centre of wing volume (true wing)      =  0.1026
Centre of wing volume (equivalent wing)=  0.0000

Wing aerodynamic centre (%MAC)         =  0.0300


WING BOX
Wing front spar from nose at root      =  1.2033 m
Wing rear spar from nose at root       =  5.6154 m

Wing front spar from nose at tip       =  0.2976 m
Wing rear spar from nose at tip        =  1.3888 m

Wing box root chord                    =  4.4121 m
Wing box tip chord                     =  1.0912 m
Wing box gross span                    = 12.7929 m
Gross wing box planform area           =   35.20 m^2
Gross wing box aspect ratio            =  4.6492

Equivalent wing box root chord         =  4.4121 m
Equivalent wing box taper ratio        =  0.2473
Equivalent wing box leading edge sweep = 47.9450 degree
Equivalent wing box centreline sweep   = 44.7259 degree


WING SPANWISE LIFT DISTRUBITION
Mach number for design diving speed =  1.1755
Effective Mach number               =  0.5156
Effective angle of sweepback        = 56.2005 degree
Average angle of attack             =  5.5758 degree

 ------------------------------
 * BAY POSITION

ENGINE BAY POSITION
Spanwise station to engine bay section          =  0.6425  1.0162  1.3899 m
```

```
Wing chord at engine bay section                    =  7.4155  7.0627  6.7100 m
Wing leading edge at engine bay section from nose   =  0.8032  1.2703  1.7375 m

Minimum distance of engine inlet from nose          =  3.2883 m
Maximum distance of engine exit from nose           =  7.1055 m
Axial space available for length of engine          =  3.8171 m

Axial distance from nose to engine front face       =  5.0556 m
Axial distance from nose to transition duct entrance=  6.3787 m


WEAPON BAY 1 POSITION
Spanwise station to weapon bay 1 section            =  0.0000  0.0000  0.4925 m
Wing chord at weapon bay 1 section                  =  8.0220  8.0220  7.5571 m
Wing leading edge at weapon bay 1 section from nose =  0.0000  0.0000  0.6157 m

Minimum distance of weapon bay1 front face from nose=  3.2883 m
Maximum distance of weapon bay1 rear face from nose =  7.0776 m
Axial space available for length of weapon bay 1    =  3.3730 m

Axial distance from nose to weapon bay 1 front face =  3.7221 m


WEAPON BAY 2 POSITION
Spanwise station to weapon bay 2 section            =  0.0000  0.0000  0.0000 m
Wing chord at weapon bay 2 section                  =  0.0000  0.0000  0.0000 m
Wing leading edge at weapon bay 2 section from nose =  0.0000  0.0000  0.0000 m

Minimum distance of weapon bay2 front face from nose=  0.0000 m
Maximum distance of weapon bay2 rear face from nose =  0.0000 m
Axial space available for length of weapon bay 2    =  0.0000 m

Axial distance from nose to weapon bay 2 front face =  0.0000 m


MAIN UNDERCARRIAGE BAY POSITION
Spanwise station to main uc bay section             =  1.5399  1.6483  1.7568 m
Wing chord at main uc bay section                   =  6.5684  6.4660  6.3637 m
Wing leading edge at main uc bay section from nose  =  1.9250  2.0605  2.1961 m

Minimum distance of main uc bay front face from nose=  3.1506 m
Maximum distance of main uc bay rear face from nose =  6.5229 m
Axial space available for length of main uc bay     =  3.3722 m

Axial distance from nose to main uc bay front face  =  4.1220 m

 ------------------------------
 * INTAKE DIFFUSER

Cross sectional area of intake inlet  =  0.3047 m^2
Cross sectional area of intake exit   =  0.3047 m^2
Equivalent diameter of intake inlet   =  0.6228 m
Diameter of intake exit               =  0.6228 m

Width of intake inlet                 =  0.7806 m
Height of intake inlet                =  0.3903 m
Width of intake inlet projected into horizontal =  0.7806 m
Height of intake inlet projected into vertical  =  0.3903 m

Distance of intake inlet from nose    =  2.6453 m
Length of intake diffuser             =  2.4103 m

Spanwise station to intake inlet      =  1.0162 m
Spanwise station to intake exit       =  1.0162 m
Vertical distance of intake inlet     =  0.2983 m
Vertical distance of intake exit      =  0.0000 m
Wing leading edge at intake from nose =  1.2703 m

Volume of each intake diffuser        =  0.7344 m^3

 ------------------------------
 * 2-DIMENSIONAL NOZZLE

Aspect ratio of nozzle transition duct exit= 10.2086

SINGLE ENGINE INSTALLATION
Half-height of nozzle transition duct exit =  0.0864 m
```

```
Half-width of nozzle transition duct exit  =  0.7474 m

Length of nozzle transition duct     =  1.3978 m

Volume of nozzle transition duct     =  1.1229 m^3
Total mass of nozzle transition duct =    73.39 kg

 ------------------------------
 * TRAILING EDGE SPLIT ELEVON

Total number of all split elevons = 2

ELEVON 1
Elevon inner span,chrd &wchrd =  3.4826  1.0416  4.7345 m
Elevon outer span,chrd &wchrd =  6.0766  0.5029  2.2858 m
Elevon mean chord             =  0.7722 m
Total span of elevon          =  5.1880 m
Aspect ratio of each elevon   =  3.3591
Elevon hinge line sweep       = 24.7900 deg
Total planform area of elevon =    4.01 m^2
Total wing area over elevon   =   18.21 m^2
ELEVONS LIFT & MOMENT             TO      LD
Elevon deflection             =   30.00   60.00 deg
Section lift increment        =  0.8896  1.3152
Wing lift increment           =  0.1151  0.1701
Wing pitch increment          = -0.0158 -0.0233
Sect max lift increment       =  0.6690  0.9045
Wing max lift increment       =  0.1728  0.2336


All split elevons gross span          =   5.1880 m
Split elevon mean chord               =   0.7722 m
All split elevons planform area       =     4.01 m^2
Total wing planform area over split elevons   =   18.21 m^2

WING TRAILING EDGE
Gross area of wing trailing edge aft of rear spar    =   13.46 m^2
Planform area of fixed section of wing TE aft of r/s =    9.45 m^2

 ------------------------------
 * LEADING EDGE SLAT

Total number of all slats = 0


All slats gross span          =   0.0000 m
Slat mean chord               =   0.0000 m
All slats planform area       =     0.00 m^2
Total wing planform area over slats   =    0.00 m^2

WING LEADING EDGE
Total planform area of wing leading edge             =    6.73 m^2
Planform area of fixed section of wing LE fwd of f/s =    2.24 m^2

 ------------------------------
 * TRAILING EDGE SPLIT RUDDER

Total number of all split rudders = 2

SPLIT RUDDER 1
Rudder inner span & wchrd     =  3.4826  4.7345 m
Rudder outer span & wchrd     =  6.0766  2.2858 m
Aspect ratio of each rudder   =  3.3591
Rudder hinge line sweep       = 24.7900 deg
SPLIT RUDDERS LIFT & MOMENT     Aileron Rudder
Split rudder deflection       =   20.00   25.00 deg
Section lift increment        =  0.7685  0.8593
Wing lift increment           =  0.0994  0.1111
Wing yaw effectiveness        = -0.0049  0.0055
Wing roll effectiveness       =  0.0583 -0.0652

 ------------------------------
 * FUEL

- CENTRE FUEL TANK -
Total span of centre fuel tank =  0.9850 m
```

```
CENTRE FUEL TANK 1 (FRONT)
Centre fuel tank 1 front face from nose =  3.2883 m
Centre fuel tank 1 rear face from nose  =  3.7221 m
Total fuel volume of centre tank 1     =  0.3975 m^3
Fuel mass used in centre fuel tank 1   =     0.00 kg
M-arm of centre fuel tank 1 from nose =  3.5040 m

CENTRE FUEL TANK 2 (REAR)
Centre fuel tank 2 front face from nose =  6.0821 m
Centre fuel tank 2 rear face from nose  =  7.0776 m
Total fuel volume of centre tank 2     =  0.3975 m^3
Fuel mass used in centre fuel tank 2   =     0.00 kg
M-arm of centre fuel tank 2 from nose =  6.5286 m

CENTRE FUEL TANK 3 (TOP)
Centre fuel tank 3 front face from nose =  3.7221 m
Centre fuel tank 3 rear face from nose  =  4.9021 m
Total fuel volume of centre tank 3     =  0.1877 m^3
Fuel mass used in centre fuel tank 3   =     0.00 kg
M-arm of centre fuel tank 3 from nose =  4.2942 m

TOTAL CENTRE FUEL TANK CAPACITY
Total area of centre fuel tank         =  2.5701 m^2
Total fuel volume of centre tank       =  0.9826 m^3
Total fuel mass used in centre tank    =     0.00 kg


- INBOARD FUEL TANK -
Total span of inboard fuel tank =  0.0000 m

INBOARD FUEL TANK 1 (FRONT)
Inboard fuel tank 1 front face from nose =  0.0000 m
Inboard fuel tank 1 rear face from nose  =  0.0000 m
Total fuel volume of inbrd tank 1      =  0.0000 m^3
Fuel mass used in inbrd fuel tank 1    =     0.00 kg
M-arm of inbrd fuel tank 1 from nose   =  0.0000 m

INBOARD FUEL TANK 2 (REAR)
Inboard fuel tank 2 front face from nose =  0.0000 m
Inboard fuel tank 2 rear face from nose  =  0.0000 m
Total fuel volume of inbrd tank 2      =  0.0000 m^3
Fuel mass used in inbrd fuel tank 2    =     0.00 kg
M-arm of inbrd fuel tank 2 from nose   =  0.0000 m

INBOARD FUEL TANK 3 (TOP)
Inboard fuel tank 3 front face from nose =  0.0000 m
Inboard fuel tank 3 rear face from nose  =  0.0000 m
Total fuel volume of inbrd tank 3      =  0.0000 m^3
Fuel mass used in inbrd fuel tank 3    =     0.00 kg
M-arm of inbrd fuel tank 3 from nose   =  0.0000 m

TOTAL INBOARD FUEL TANK CAPACITY
Total area of inboard fuel tank         =  0.0000 m^2
Total fuel volume of inbrd tank         =  0.0000 m^3
Total fuel mass used in inbrd tank      =     0.00 kg


- OUTBOARD FUEL TANK -
Total span of outboard fuel tank =  0.4337 m

OUTBOARD FUEL TANK 1 (FRONT)
Outboard fuel tank 1 front face from nose =  3.1506 m
Outboard fuel tank 1 rear face from nose  =  4.1220 m
Total fuel volume of outbrd tank 1     =  0.2962 m^3
Fuel mass used in outbrd fuel tank 1   =     0.00 kg
M-arm of outbrd fuel tank 1 from nose =  3.6456 m

OUTBOARD FUEL TANK 2 (REAR)
Outboard fuel tank 2 front face from nose =  5.2074 m
Outboard fuel tank 2 rear face from nose  =  6.5229 m
Total fuel volume of outbrd tank 2     =  0.3395 m^3
Fuel mass used in outbrd fuel tank 2   =     0.00 kg
M-arm of outbrd fuel tank 2 from nose =  5.8298 m

TOTAL OUTBOARD FUEL TANK CAPACITY
Total area of outboard fuel tank        =  0.9918 m^2
Total fuel volume of outbrd tank        =  0.6357 m^3
```

```
Total fuel mass used in outbrd tank    =     0.00 kg


- WING FUEL TANK -
Wing fuel tank spanwise station 0 =  1.9068 m
Wing fuel tank spanwise station 1 =  2.3141 m
Total span available for wing fuel tank          =  0.8148 m
Total wing box area available for wing fuel tank =  2.7021 m^2

WING FUEL TANK CAPACITY
Total fuel volume of wing tank         =  1.3620 m^3
Total fuel mass used in wing tank      =  1057.59 kg


- OPTIONAL WEAPON BAY FUEL TANK -
Total fuel volume of weapon bay tank1=  0.0000 m^3
Fuel mass used in weapon bay tank 1  =     0.00 kg

Total fuel volume of weapon bay tank2=  0.0000 m^3
Fuel mass used in weapon bay tank 2  =     0.00 kg

TOTAL WEAPON BAY FUEL TANK CAPACITY
Total fuel volume of weapon bay tank      =  0.0000 m^3
Total fuel mass used in weapon bay tank   =     0.00 kg


- UCAV TOTAL FUEL CAPACITY -
Total area containing fuel tank      =  6.2640 m^2
Total internal fuel volume           =  2.9803 m^3
Total mass of available internal fuel=  2314.19 kg

Total fuel mass used on aircraft     =  1057.59 kg

 ------------------------------
 * UCAV MASS & CG

- UCAV MASS -

WING BOX
Ultimate load factor           =    9.75
Wing inertia relief load       =  1120.73 kg

Wing box mass (Torsion)        =   130.25 kg
Wing box mass (Bending)        =   184.99 kg
Total wing box mass            =   184.99 kg

CONTROL SURFACES
Wing leading edge mass         =    36.49 kg
Wing fixed trailing edge mass  =    84.29 kg

TEcs mass (flap)               =    24.89 kg
TEcs mass (aileron)            =    62.23 kg
Total TE control surfaces mass =    62.23 kg

Inlaids mass (rudder)          =     0.00 kg
Inlaids mass (spoiler)         =     0.00 kg
Total inlaids CS mass          =     0.00 kg

AUXILIARY
Miscellaneous attachments      =    26.79 kg
External paint                 =    21.82 kg
Low Observable treatments      =   226.80 kg
Basic ribs in strutural box    =   293.71     0.00 kg

FLYING WING
Total wing structural mass     =   937.12 kg

MASS INCREMENT DUE TO INTERNAL WEAPON BAYS
Mass increment due to weap bay1=   136.21 kg
Mass increment due to weap bay2=     0.00 kg

AIRCRAFT SYSTEM
Mass of air systems            =     7.28 kg
Mass of de-icing system        =    27.01 kg
Mass of electrical systems     =   139.17 kg
Mass of flight control systems =   142.11 kg
Mass of fuel system            =    80.27 kg
```

```
COMPLETE AIRCRAFT
Total aircraft payload         =   482.00 kg
Mass of fixed-role equipment   =   313.34 kg
Total mass of fuel on aircraft =  1057.59 kg

Empty mass             =   2553.00 kg
Operational empty mass =   2553.00 kg
Zero fuel mass         =   3035.00 kg

Total take-off mass    =   4092.59 kg
Landing mass           =   3478.70 kg

Wing loading           =   63.9440 kg/m^2
Thrust loading         =    0.5788


WING STRUCTURAL MASS COMPARISON
Howe method 1 (COA)    =    937.12 kg (theoretical)
Howe method 2 (COA)    =   1434.95 kg (empirical)
Lovell method (RAE)    =   1905.46 kg
Roskam method (USAF)   =    656.45 kg
Roskam method (USN)    =    969.71 kg
Raymer method          =    714.77 kg
Whitford method        =    861.13 kg


- CENTRE OF GRAVITY -

OPERATIONAL EMPTY MASS
Total aircraft pitching moment about nose=  11734.52 kg.m
Distance of aircraft CG from nose        =  4.5964 m
CG relative to aerodynamic mean chord    =  25.00%

ZERO FUEL MASS
Total aircraft pitching moment about nose=  14097.33 kg.m
Distance of aircraft CG from nose        =  4.6449 m
CG relative to aerodynamic mean chord    =  25.87%

TOTAL TAKE-OFF MASS
Total aircraft pitching moment about nose=  19514.25 kg.m
Distance of aircraft CG from nose        =  4.7682 m
CG relative to aerodynamic mean chord    =  28.06%
Static margin                            =  -3.06%

Distance of aircraft fwd CG from nose  =  4.2598 m
Fwd CG relative to AMC                 =  19.00%
Distance of aircraft aft CG from nose  =  4.9891 m
Aft CG relative to AMC                 =  32.00%

Reference spanwise distance of aircraft CG             =  0.0000 m
Reference vertical distance of aircraft CG from ground =  1.3251 m


- UNDERCARRIAGE ARRANGEMENTS -

UNDERCARRIAGE ARRANGEMENTS
Axial distance from nose wheel to main wheel =  3.5546 m
Axial angle from nose wheel to main wheel    = 24.8778 degree

Axial distance from nose UC to aircraft aft CG position     =  3.1654 m
Axial distance from aircraft forward CG position to main UC =  0.5610 m
Axial distance from aircraft aft CG position to main UC     =  0.3892 m

AIRCRAFT OVERTURN ANGLE
Aircraft static ground line    =  1.4954 m
Aircraft overturn angle        = 41.5442 degree

AIRCRAFT TIPBACK & STATIC TAILDOWN ANGLE
Axial distance from main uc to tail =  4.8226 m
Height due to tipback angle         =  1.4165 m

Aircraft tipback angle         = 16.3687 degree
Aircraft static taildown angle = 14.4051 degree

AIRCRAFT ANGLE OFF VERTICAL
Angle off vertical             = 16.3687 degree
```

```
UNDERCARRIAGE STATIC LOADS
Maximum static load       =   3644.48 kg
Maximum nose static load  =    645.93 kg
Minimum nose static load  =    448.10 kg
Nose dynamic braking load =    466.70 kg

Maximum static load as a fraction of total load      =   89.05%
Maximum nose static load as a fraction of total load =   15.78%
Minimum nose static load as a fraction of total load =   10.95%

MAIN UNDERCARRIAGE SHOCK ABSORBER STROKE
Main undercarriage rolling radius        =  0.1778 m
Main undercarriage tyre stroke           =  0.0889 m
Main undercarriage shock absorber stroke =  0.4890 m

UNDERCARRIAGES FRONTAL AREA
Oleo load of each main undercarriage =   1822.24 kg
Oleo load of nose undercarriage      =   1112.63 kg

Oleo diameter of main undercarriage  =  0.0178 m
Oleo diameter of nose undercarriage  =  0.0139 m

Frontal area of each main undercarriage leg          =  0.0145 m^2
Frontal area of each main undercarriage wheel & tyre =  0.0643 m^2

Frontal area of nose undercarriage leg          =  0.0084 m^2
Frontal area of nose undercarriage wheel & tyre =  0.0489 m^2

 -------------------------
 *UCAV COMPONENT SUMMARY*

 --- MASS & BALANCE ---
 Aircraft component  Mass  Range   X-Marm   XMoment  Y-Marm   YMoment
                     (kg)   (%)     (m)     (kg.m)     (m)     (kg.m)
Wing (port)          468.56  11.45  5.1720   2423.40 -2.8144  -1318.73
Wing (starboard)     468.56  11.45  5.1720   2423.40  2.8144   1318.73
Nose UC               31.62   0.77  1.6028     50.68  0.0000      0.00
Main UC (port)       114.55   2.80  5.1574    590.79 -1.6483   -188.82
Main UC (stbd)       114.55   2.80  5.1574    590.79  1.6483    188.82
Engine (port)        218.19   5.33  5.7171   1247.42 -1.0162   -221.72
Engine (stbd)        218.19   5.33  5.7171   1247.42  1.0162    221.72
Nozzle (port)         36.69   0.90  7.0776    259.70 -1.0162    -37.29
Nozzle (stbd)         36.69   0.90  7.0776    259.70  1.0162     37.29
Avionics(MMS)         51.34   1.25  0.8022     41.18  0.0000      0.00
Avionics(FMS)        119.04   2.91  2.6453    314.89  0.0000      0.00
Avionics(SMS)          8.32   0.20  2.3237     19.33  0.0000      0.00
Avionics(EWS-port)     4.82   0.12  6.7966     32.76 -5.4370    -26.21
Avionics(EWS-stbd)     4.82   0.12  6.7966     32.76  5.4370     26.21
Air system             7.28   0.18  2.3237     16.92  0.0000      0.00
De-icing system       27.01   0.66  2.3237     62.76  0.0000      0.00
Electrical system    139.17   3.40  2.3237    323.40  0.0000      0.00
FCS                  142.11   3.47  2.3237    330.23  0.0000      0.00
Fuel system           80.27   1.96  2.3237    186.53  0.0000      0.00
W bay1 pylon         125.00   3.05  4.9021    612.76  0.0000      0.00
W bay1 increment     136.21   3.33  4.9021    667.70  0.0000      0.00
Residual fuel          0.00   0.00  2.3237      0.00  0.0000      0.00
     OEM            2553.00  62.38  4.5964  11734.52               0.00

Weap in bay1         482.00  11.78  4.9021   2362.81  0.0000      0.00
     ZFM            3035.00  74.16  4.6449  14097.33               0.00

Wing tank (port)     528.80  12.92  5.1220   2708.46 -2.0860  -1103.07
Wing tank (stbd)     528.80  12.92  5.1220   2708.46  2.0860   1103.07
Centre tank1           0.00   0.00  3.5040      0.00  0.0000      0.00
Centre tank2           0.00   0.00  6.5286      0.00  0.0000      0.00
Centre tank3           0.00   0.00  4.2942      0.00  0.0000      0.00
Outbrd tank1(port)     0.00   0.00  3.6456      0.00 -1.6483      0.00
Outbrd tank1(stbd)     0.00   0.00  3.6456      0.00  1.6483      0.00
Outbrd tank2(port)     0.00   0.00  5.8298      0.00 -1.6483      0.00
Outbrd tank2(stbd)     0.00   0.00  5.8298      0.00  1.6483      0.00
     AUM            4092.59 100.00  4.7682  19514.25               0.00


 --- MASS & BALANCE (continued) ---
 Aircraft component  Mass  Z-Marm   ZMoment  Z-Marm   ZMoment
                     (kg)  dwn(m)   (kg.m)   up (m)   (kg.m)
```

Wing (port)	468.56	1.3251	620.87	0.0000	0.00
Wing (starboard)	468.56	1.3251	620.87	0.0000	0.00
Nose UC	31.62	0.9965	31.51	-0.3286	-10.39
Main UC (port)	114.55	0.9965	114.15	-0.3286	-37.64
Main UC (stbd)	114.55	0.9965	114.15	-0.3286	-37.64
Engine (port)	218.19	1.3251	289.11	0.0000	0.00
Engine (stbd)	218.19	1.3251	289.11	0.0000	0.00
Nozzle (port)	36.69	1.3251	48.62	0.0000	0.00
Nozzle (stbd)	36.69	1.3251	48.62	0.0000	0.00
Avionics(MMS)	51.34	1.3251	68.03	0.0000	0.00
Avionics(FMS)	119.04	1.3251	157.74	0.0000	0.00
Avionics(SMS)	8.32	1.3251	11.02	0.0000	0.00
Avionics(EWS-port)	4.82	1.3251	6.39	0.0000	0.00
Avionics(EWS-stbd)	4.82	1.3251	6.39	0.0000	0.00
Air system	7.28	1.5375	11.19	0.2124	1.55
De-icing system	27.01	1.5375	41.52	0.2124	5.74
Electrical system	139.17	1.6988	236.42	0.3737	52.01
FCS	142.11	1.6988	241.42	0.3737	53.11
Fuel system	80.27	1.6988	136.36	0.3737	30.00
W bay1 pylon	125.00	1.5901	198.76	0.2650	33.12
W bay1 increment	136.21	1.3251	180.48	0.0000	0.00
Residual fuel	0.00	1.2628	0.00	-0.0623	0.00
OEM	2553.00		3472.73		89.86
Weap in bay1	482.00	1.3251	638.68	0.0000	0.00
ZFM	3035.00		4111.41		89.86
Wing tank (port)	528.80	1.3251	700.69	0.0000	0.00
Wing tank (stbd)	528.80	1.3251	700.69	0.0000	0.00
Centre tank1	0.00	1.3251	0.00	0.0000	0.00
Centre tank2	0.00	1.3251	0.00	0.0000	0.00
Centre tank3	0.00	1.5901	0.00	0.2650	0.00
Outbrd tank1(port)	0.00	1.3251	0.00	0.0000	0.00
Outbrd tank1(stbd)	0.00	1.3251	0.00	0.0000	0.00
Outbrd tank2(port)	0.00	1.3251	0.00	0.0000	0.00
Outbrd tank2(stbd)	0.00	1.3251	0.00	0.0000	0.00
AUM	4092.59		5512.78		89.86

Inboard Airfoil Selection: The configuration is based on the straight-tapered wing planform with the single weapon bay located at the aircraft centreline, accommodated in the NACA 65_2-415 asymmetrical airfoil (NWEPB1-ASYM), as illustrated in Figure 8-27 of Chapter 8.

```
------------------------------
--- UCAV PACKAGING SUMMARY ---
------------------------------

* UCAV PACKAGING CONFIGURATION

 1) Type of stores          = 1 :Internal store
 2) Number of weapon bays   = 1 :Single weapon bay on centreline
 3) Type of missions        = 1 :SEAD/strike
 4) Number of engines       = 1 :Single-engine installation
 5) Type of aircraft        = 0 :Unmanned aircraft
 6) Type of materials       = 2 :Carbon-fibre composite construction
 7) Number of kinks in wing = 0 :Straight taper wing
 8) Number of split elevons on half span = 1
 9) Number of slats on half span         = 0
10) Number of split rudders on half span = 0
11) Type of airfoils at wing inboard section  = 2 :Asymmetrical airfoil
12) Type of airfoils at wing outboard section = 1 :Symmetrical airfoil
13) Thickness ratio at wing inboard section  = 15%
14) Thickness ratio at wing outboard section =  9%
15) Twist distribution      = 1 :Twist wing

--------------------------
*UCAV PACKAGING OPTIMIZER*

                                    INITIAL    FINAL     LOWER     UPPER
  1 Wing span (m)          [BW]     15.0000   15.5977    6.0000   40.0000
  2 Wing root chord (m)    [CWCC]    9.0000    9.3225    6.0000   20.0000
  3 Wing tip chord (m)     [CWCT]    2.0000    2.2313    0.0100    4.0000
  4 Front spar fraction    [FCWD]    0.1500    0.1500    0.1500    0.1500
```

```
   5 Rear spar fraction      [FCWR]        0.7000   0.7000   0.7000   0.7000
   6 Wing leading edge sweep[QWLR]        50.0000  43.9915   0.0100  60.0000
   7 Elevon mean chord (m)   [CWSE]        1.0000   1.2776   0.5000   3.0000
   8 Elevon inner span       [FYSEI]       0.4000   0.3957   0.1000   0.9500
   9 Elevon outer span       [FYSEO]       0.7000   0.5957   0.1000   0.9500
  10 Wing tank span factor   [FY2WFO]      0.5000   0.0384   0.0100   1.0000
  11 Wing tank front factor  [FCWFD]       0.0000   0.0000   0.0000   0.0000
  12 Wing tank rear factor   [FCWFR]       1.0000   1.0000   1.0000   1.0000
  13 Weap bay1 axial factor  [FXLIB1]      0.5000   0.3701   0.0000   1.0000
  14 Engine axial factor     [FXLPG]       0.5000   0.1382   0.0000   1.0000
  15 Engine scale factor     [RTP]         1.5000   0.8208   0.5000   2.5000

 ------------------------------
 *UCAV FIXED MASS CONTRIBUTION*

 ------------------------------
 * AVIONICS BAY

MISSION MANAGEMENT SYSTEM
Mass & volume of radar suite              =    28.32 kg   0.1404 m^3
Mass & volume of sensor suite             =    23.02 kg   0.0605 m^3

FLIGHT MANAGEMENT SYSTEM
Mass & volume of flight control suite     =    45.03 kg   0.1634 m^3
Mass & volume of navigation suite         =    40.44 kg   0.1925 m^3
Mass & volume of communication suite      =    12.68 kg   0.0949 m^3
Mass & volume of identification suite     =    20.89 kg   0.1556 m^3

STORE MANAGEMENT SYSTEM
Mass & volume of weapon control suite     =     8.32 kg   0.0620 m^3

ELECTRONIC WARFARE SYSTEM
Mass & volume of electronic warfare suite =     4.82 kg   0.0322 m^3
Mass & volume of countermeasures suite    =     4.82 kg   0.0322 m^3

Total avionics mass                       =   188.34 kg

Length of radar avionics suite            =  0.8022 m
Length of flight management avionics suite =  1.2861 m
Length of weapon control avionics suite   =  0.5697 m

Radome length                             =  1.2033 m

 ------------------------------
 * WEAPON BAY

WEAPON BAY 1
Total number of weapon bay 1                  = 1
Total number of weapons in each weapon bay 1  = 1
Total mass of weapons in weapon bay 1         =   460.00 kg
Total mass of internal pylons in weapon bay 1 =    62.50 kg

WEAPON BAY 2
Total number of weapon bay 2                  = 0
Total number of weapons in each weapon bay 2  = 0
Total mass of weapons in weapon bay 2         =     0.00 kg
Total mass of internal pylons in weapon bay 2 =     0.00 kg

INTERNAL WEAPON BAY
Total mass of weapons in internal weapon bays =   460.00 kg

WEAPON BAY DIMENSION
              L(m)     W(m)     H(m)    V(m^3)
Weapon bay 1  3.1900   0.6300   0.6300  1.2661
Weapon bay 2  0.0000   0.0000   0.0000  0.0000

EXTERNAL STORES
Total number of weapons at port store         = 0
Total mass of weapons at port store           =     0.00 kg
Total number of weapons at starboard store    = 0
Total mass of weapons at starboard store      =     0.00 kg
External store wetted area                    =  0.0000 m^2
Total mass of external pylons                 =     0.00 kg

Total mass of weapons at external stores      =     0.00 kg
```

```
TOTAL WEAPONS
Total mass of weapons on aircraft              =   460.00 kg

 --------------------------------
 *UCAV VARIABLE MASS CONTRIBUTION*

 ------------------------------
 * ENGINE BAY

 TWO SINGLE-ENGINE INSTALLATIONS

ENGINE & ENGINE BAY DIMENSION
Overall length of engine  =  1.5646 m
Diameter of engine        =  0.7366 m

Total nozzle exit area    =    0.43 m^2

Maximum engine bay height =  0.8839 m
Maximum engine bay width  =  0.8839 m

ENGINE BAY VOLUME
Volume of engine bay            =  0.9600 m^3

PROPULSION SYSTEM MASS
Total mass of engines           =   558.48 kg
Engine installation mass        =    72.60 kg

Total mass of propulsion system =   631.08 kg

ENGINE STATIC THRUST
Total maximum sea-level static thrust of engines =  32486.25 N
Bypass ratio of total engines   =    8.00

 ------------------------------
 * UNDERCARRIAGE BAY

NOSE UNDERCARRIAGE
Length of nose undercarriage leg         =  0.6766 m
Nose undercarriage wheel & tyre diameter =  0.4020 m
Nose undercarriage wheel & tyre width    =  0.1520 m

MAIN UNDERCARRIAGE
Length of each main undercarriage leg    =  0.9143 m
Main undercarriage wheel & tyre diameter =  0.5600 m
Main undercarriage wheel & tyre width    =  0.1533 m

UNDERCARRIAGE MASS
Structural mass of nose undercarriage            =    33.43 kg
Structural mass of total main undercarriage      =   242.57 kg
Mass of hydraulics associated with undercarriage =    33.14 kg

UNDERCARRIAGE GROSS MASS
Total mass of nose undercarriage with hydraulics =    37.44 kg
Total mass of main undercarriage with hydraulics =   271.70 kg

UNDERCARRIAGE BAY DIMENSION
              L(m)    H(m)    W(m)   V(m^3)
Nose UC bay  0.8776  0.4422  0.2280  0.0885
Main UC bay  1.1943  0.6160  0.2299  0.1692

 ------------------------------
 * FLYING WING

 STRAIGHT TAPERED WING

FLYING WING SPECIFICATION
Wing centreline section & chord  0.0000 m  9.3225 m
Wing tip section & chord         7.7988 m  2.2313 m
Wing gross span               = 15.5977 m
Gross wing aspect ratio       =  2.7000
Gross wing area               =   90.11 m^2
Wing wetted area              =  183.32 m^2
Mean thickness ratio          =  0.1104
Average wing chord            =  5.7769 m

Wing geometric mean chord     =  5.7769 m
Wing aerodynamic mean chord   =  6.5023 m
```

```
Distance of wing mean 1/4 chord point from nose =  4.6199 m

Equivalent wing root chord          =  9.3225 m
Equivalent wing taper ratio         =  0.2393
Equivalent wing leading edge sweep = 43.9915 degree
Equivalent wing quarter chord sweep= 36.4305 degree
Equivalent wing mid-chord sweep     = 27.0566 degree

Maximum depth at wing centreline chord =  1.3984 m
Maximum depth at wing tip chord        =  0.2008 m

Wing maximum cross-sectional area      =   15.11 m^2
Flying wing total volume               =   51.20 m^3

Centre of wing volume (true wing)      =  0.1237
Centre of wing volume (equivalent wing)=  0.0000

Wing aerodynamic centre (%MAC)         =  0.0300


WING BOX
Wing front spar from nose at root      =  1.3984 m
Wing rear spar from nose at root       =  6.5258 m

Wing front spar from nose at tip       =  0.3347 m
Wing rear spar from nose at tip        =  1.5619 m

Wing box root chord                    =  5.1274 m
Wing box tip chord                     =  1.2272 m
Wing box gross span                    = 15.5977 m
Gross wing box planform area           =   49.56 m^2
Gross wing box aspect ratio            =  4.9091

Equivalent wing box root chord         =  5.1274 m
Equivalent wing box taper ratio        =  0.2393
Equivalent wing box leading edge sweep = 39.6592 degree
Equivalent wing box centreline sweep   = 35.5782 degree


WING SPANWISE LIFT DISTRUBITION
Mach number for design diving speed =  1.1755
Effective Mach number               =  0.6804
Effective angle of sweepback        = 54.1297 degree
Average angle of attack             =  3.7149 degree

 ------------------------------
 * BAY POSITION

ENGINE BAY POSITION
Spanwise station to engine bay section             =  0.4650  0.9069  1.3489 m
Wing chord at engine bay section                   =  8.8997  8.4979  8.0961 m
Wing leading edge at engine bay section from nose  =  0.4489  0.8756  1.3022 m

Minimum distance of engine inlet from nose         =  3.3670 m
Maximum distance of engine exit from nose          =  6.9795 m
Axial space available for length of engine         =  3.6125 m

Axial distance from nose to engine front face      =  4.1970 m
Axial distance from nose to transition duct entrance=  5.7616 m


WEAPON BAY 1 POSITION
Spanwise station to weapon bay 1 section           =  0.0000  0.0000  0.3150 m
Wing chord at weapon bay 1 section                 =  9.3225  9.3225  9.0361 m
Wing leading edge at weapon bay 1 section from nose =  0.0000  0.0000  0.3041 m

Minimum distance of weapon bay1 front face from nose=  3.3670 m
Maximum distance of weapon bay1 rear face from nose =  6.7754 m
Axial space available for length of weapon bay 1    =  3.2736 m

Axial distance from nose to weapon bay 1 front face =  3.4506 m


WEAPON BAY 2 POSITION
Spanwise station to weapon bay 2 section           =  0.0000  0.0000  0.0000 m
Wing chord at weapon bay 2 section                 =  0.0000  0.0000  0.0000 m
Wing leading edge at weapon bay 2 section from nose =  0.0000  0.0000  0.0000 m
```

```
Minimum distance of weapon bay2 front face from nose=  0.0000 m
Maximum distance of weapon bay2 rear face from nose =  0.0000 m
Axial space available for length of weapon bay 2    =  0.0000 m

Axial distance from nose to weapon bay 2 front face =  0.0000 m


MAIN UNDERCARRIAGE BAY POSITION
Spanwise station to main uc bay section             =  1.4989  1.6138  1.7288 m
Wing chord at main uc bay section                   =  7.9597  7.8551  7.7506 m
Wing leading edge at main uc bay section from nose  =  1.4470  1.5580  1.6690 m

Minimum distance of main uc bay front face from nose=  2.8316 m
Maximum distance of main uc bay rear face from nose =  6.7754 m
Axial space available for length of main uc bay     =  3.9439 m

Axial distance from nose to main uc bay front face  =  4.1259 m

 ------------------------------
 * INTAKE DIFFUSER

Cross sectional area of intake inlet  =  0.4261 m^2
Cross sectional area of intake exit   =  0.4261 m^2
Equivalent diameter of intake inlet   =  0.7366 m
Diameter of intake exit               =  0.7366 m

Width of intake inlet                 =  0.9231 m
Height of intake inlet                =  0.4616 m
Width of intake inlet projected into horizontal =  0.9231 m
Height of intake inlet projected into vertical  =  0.4616 m

Distance of intake inlet from nose    =  2.7239 m
Length of intake diffuser             =  1.4731 m

Spanwise station to intake inlet      =  0.9069 m
Spanwise station to intake exit       =  0.9069 m
Vertical distance of intake inlet     =  0.3694 m
Vertical distance of intake exit      =  0.1734 m
Wing leading edge at intake from nose =  0.8756 m

Volume of each intake diffuser        =  0.6277 m^3

 ------------------------------
 * 2-DIMENSIONAL NOZZLE

Aspect ratio of nozzle transition duct exit=  7.5265

SINGLE ENGINE INSTALLATION
Half-height of nozzle transition duct exit =  0.1190 m
Half-width of nozzle transition duct exit  =  0.8839 m

Length of nozzle transition duct     =  2.0276 m

Volume of nozzle transition duct     =  2.2780 m^3
Total mass of nozzle transition duct =   112.74 kg

 ------------------------------
 * TRAILING EDGE SPLIT ELEVON

Total number of all split elevons = 2

ELEVON 1
Elevon inner span,chrd &wchrd =  3.0862  1.4336  6.5164 m
Elevon outer span,chrd &wchrd =  4.6459  1.1216  5.0981 m
Elevon mean chord             =  1.2776 m
Total span of elevon          =  3.1195 m
Aspect ratio of each elevon   =  1.2209
Elevon hinge line sweep       = 11.6493 deg
Total planform area of elevon =    3.99 m^2
Total wing area over elevon   =   18.12 m^2
ELEVONS LIFT & MOMENT            TO      LD
Elevon deflection             =   30.00   60.00 deg
Section lift increment        =  0.9687  1.4321
Wing lift increment           =  0.0927  0.1371
Wing pitch increment          = -0.0069 -0.0102
Sect max lift increment       =  0.6690  0.9044
```

```
Wing max lift increment       =  0.1317  0.1781


All split elevons gross span          =   3.1195 m
Split elevon mean chord               =   1.2776 m
All split elevons planform area       =     3.99 m^2
Total wing planform area over split elevons   =   18.12 m^2

WING TRAILING EDGE
Gross area of wing trailing edge aft of rear spar    =   20.30 m^2
Planform area of fixed section of wing TE aft of r/s =   16.32 m^2

 ------------------------------
 * LEADING EDGE SLAT

Total number of all slats = 0


All slats gross span          =   0.0000 m
Slat mean chord               =   0.0000 m
All slats planform area       =     0.00 m^2
Total wing planform area over slats   =    0.00 m^2

WING LEADING EDGE
Total planform area of wing leading edge             =   10.15 m^2
Planform area of fixed section of wing LE fwd of f/s =    3.38 m^2

 ------------------------------
 * TRAILING EDGE SPLIT RUDDER

Total number of all split rudders = 2

SPLIT RUDDER 1
Rudder inner span & wchrd     =  3.0862  6.5164 m
Rudder outer span & wchrd     =  4.6459  5.0981 m
Aspect ratio of each rudder   =  1.2209
Rudder hinge line sweep       = 11.6493 deg
SPLIT RUDDERS LIFT & MOMENT     Aileron Rudder
Split rudder deflection       =   20.00   25.00 deg
Section lift increment        =  0.8368  0.9358
Wing lift increment           =  0.0801  0.0896
Wing yaw effectiveness        = -0.0020  0.0022
Wing roll effectiveness       =  0.0302 -0.0338

 ------------------------------
 * FUEL

- CENTRE FUEL TANK -
Total span of centre fuel tank =  0.6300 m

CENTRE FUEL TANK 1 (FRONT)
Centre fuel tank 1 front face from nose =  3.3670 m
Centre fuel tank 1 rear face from nose  =  3.4506 m
Total fuel volume of centre tank 1    =  0.0587 m^3
Fuel mass used in centre fuel tank 1  =     0.00 kg
M-arm of centre fuel tank 1 from nose =  3.4088 m

CENTRE FUEL TANK 2 (REAR)
Centre fuel tank 2 front face from nose =  6.6406 m
Centre fuel tank 2 rear face from nose  =  6.7754 m
Total fuel volume of centre tank 2    =  0.0587 m^3
Fuel mass used in centre fuel tank 2  =     0.00 kg
M-arm of centre fuel tank 2 from nose =  6.7075 m

CENTRE FUEL TANK 3 (TOP)
Centre fuel tank 3 front face from nose =  3.4506 m
Centre fuel tank 3 rear face from nose  =  5.0456 m
Total fuel volume of centre tank 3    =  0.2278 m^3
Fuel mass used in centre fuel tank 3  =     0.00 kg
M-arm of centre fuel tank 3 from nose =  4.2313 m

TOTAL CENTRE FUEL TANK CAPACITY
Total area of centre fuel tank        =  1.1425 m^2
Total fuel volume of centre tank      =  0.3453 m^3
Total fuel mass used in centre tank   =     0.00 kg
```

```
- INBOARD FUEL TANK -
Total span of inboard fuel tank =  0.0000 m

INBOARD FUEL TANK 1 (FRONT)
Inboard fuel tank 1 front face from nose =  0.0000 m
Inboard fuel tank 1 rear face from nose  =  0.0000 m
Total fuel volume of inbrd tank 1     =  0.0000 m^3
Fuel mass used in inbrd fuel tank 1   =     0.00 kg
M-arm of inbrd fuel tank 1 from nose  =  0.0000 m

INBOARD FUEL TANK 2 (REAR)
Inboard fuel tank 2 front face from nose =  0.0000 m
Inboard fuel tank 2 rear face from nose  =  0.0000 m
Total fuel volume of inbrd tank 2     =  0.0000 m^3
Fuel mass used in inbrd fuel tank 2   =     0.00 kg
M-arm of inbrd fuel tank 2 from nose  =  0.0000 m

INBOARD FUEL TANK 3 (TOP)
Inboard fuel tank 3 front face from nose =  0.0000 m
Inboard fuel tank 3 rear face from nose  =  0.0000 m
Total fuel volume of inbrd tank 3     =  0.0000 m^3
Fuel mass used in inbrd fuel tank 3   =     0.00 kg
M-arm of inbrd fuel tank 3 from nose  =  0.0000 m

TOTAL INBOARD FUEL TANK CAPACITY
Total area of inboard fuel tank       =  0.0000 m^2
Total fuel volume of inbrd tank       =  0.0000 m^3
Total fuel mass used in inbrd tank    =     0.00 kg


- OUTBOARD FUEL TANK -
Total span of outboard fuel tank =  0.4599 m

OUTBOARD FUEL TANK 1 (FRONT)
Outboard fuel tank 1 front face from nose =  2.8316 m
Outboard fuel tank 1 rear face from nose  =  4.1259 m
Total fuel volume of outbrd tank 1    =  0.5162 m^3
Fuel mass used in outbrd fuel tank 1  =     0.00 kg
M-arm of outbrd fuel tank 1 from nose =  3.4922 m

OUTBOARD FUEL TANK 2 (REAR)
Outboard fuel tank 2 front face from nose =  5.3202 m
Outboard fuel tank 2 rear face from nose  =  6.7754 m
Total fuel volume of outbrd tank 2    =  0.5052 m^3
Fuel mass used in outbrd fuel tank 2  =     0.00 kg
M-arm of outbrd fuel tank 2 from nose =  6.0149 m

TOTAL OUTBOARD FUEL TANK CAPACITY
Total area of outboard fuel tank      =  1.2644 m^2
Total fuel volume of outbrd tank      =  1.0214 m^3
Total fuel mass used in outbrd tank   =     0.00 kg


- WING FUEL TANK -
Wing fuel tank spanwise station 0 =  1.8788 m
Wing fuel tank spanwise station 1 =  2.1905 m
Total span available for wing fuel tank          =  0.6235 m
Total wing box area available for wing fuel tank =  2.5625 m^2

WING FUEL TANK CAPACITY
Total fuel volume of wing tank        =  1.7682 m^3
Total fuel mass used in wing tank     =  1372.98 kg


- OPTIONAL WEAPON BAY FUEL TANK -
Total fuel volume of weapon bay tank1=  0.0000 m^3
Fuel mass used in weapon bay tank 1  =     0.00 kg

Total fuel volume of weapon bay tank2=  0.0000 m^3
Fuel mass used in weapon bay tank 2  =     0.00 kg

TOTAL WEAPON BAY FUEL TANK CAPACITY
Total fuel volume of weapon bay tank     =  0.0000 m^3
Total fuel mass used in weapon bay tank  =     0.00 kg


- UCAV TOTAL FUEL CAPACITY -
```

```
Total area containing fuel tank      =  4.9694 m^2
Total internal fuel volume           =  3.1348 m^3
Total mass of available internal fuel=  2434.20 kg

Total fuel mass used on aircraft     =  1372.98 kg

 ------------------------------
 * UCAV MASS & CG

- UCAV MASS -

WING BOX
Ultimate load factor           =    9.75
Wing inertia relief load       =  1149.60 kg

Wing box mass (Torsion)        =   225.42 kg
Wing box mass (Bending)        =   259.65 kg
Total wing box mass            =   259.65 kg

CONTROL SURFACES
Wing leading edge mass         =    61.96 kg
Wing fixed trailing edge mass  =   135.95 kg

TEcs mass (flap)               =    25.09 kg
TEcs mass (aileron)            =    76.14 kg
Total TE control surfaces mass =    76.14 kg

Inlaids mass (rudder)          =     0.00 kg
Inlaids mass (spoiler)         =     0.00 kg
Total inlaids CS mass          =     0.00 kg

AUXILIARY
Miscellaneous attachments      =    30.68 kg
External paint                 =    30.73 kg
Low Observable treatments      =   226.80 kg
Basic ribs in strutural box    =   485.54     0.00 kg

FLYING WING
Total wing structural mass     =  1307.45 kg

MASS INCREMENT DUE TO INTERNAL WEAPON BAYS
Mass increment due to weap bay1=   117.95 kg
Mass increment due to weap bay2=     0.00 kg

AIRCRAFT SYSTEM
Mass of air systems            =     9.89 kg
Mass of de-icing system        =    31.25 kg
Mass of electrical systems     =   164.52 kg
Mass of flight control systems =   169.93 kg
Mass of fuel system            =   104.21 kg

COMPLETE AIRCRAFT
Total aircraft payload         =   460.00 kg
Mass of fixed-role equipment   =   250.84 kg
Total mass of fuel on aircraft =  1372.98 kg

Empty mass             =   3209.00 kg
Operational empty mass =   3209.00 kg
Zero fuel mass         =   3669.00 kg

Total take-off mass    =   5041.98 kg
Landing mass           =   4285.69 kg

Wing loading           =   55.9557 kg/m^2
Thrust loading         =    0.6570


WING STRUCTURAL MASS COMPARISON
Howe method 1 (COA)    =   1307.45 kg (theoretical)
Howe method 2 (COA)    =   1897.47 kg (empirical)
Lovell method (RAE)    =   2491.72 kg
Roskam method (USAF)   =    795.33 kg
Roskam method (USN)    =   1153.10 kg
Raymer method          =    840.17 kg
Whitford method        =   1080.62 kg
```

```
- CENTRE OF GRAVITY -

OPERATIONAL EMPTY MASS
Total aircraft pitching moment about nose=  15001.77 kg.m
Distance of aircraft CG from nose        =  4.6749 m
CG relative to aerodynamic mean chord    =  25.85%

ZERO FUEL MASS
Total aircraft pitching moment about nose=  17322.74 kg.m
Distance of aircraft CG from nose        =  4.7214 m
CG relative to aerodynamic mean chord    =  26.56%

TOTAL TAKE-OFF MASS
Total aircraft pitching moment about nose=  24250.42 kg.m
Distance of aircraft CG from nose        =  4.8097 m
CG relative to aerodynamic mean chord    =  27.92%
Static margin                            =  -2.92%

Distance of aircraft fwd CG from nose  =  4.2298 m
Fwd CG relative to AMC                 =  19.00%
Distance of aircraft aft CG from nose  =  5.0751 m
Aft CG relative to AMC                 =  32.00%

Reference spanwise distance of aircraft CG             =  0.0000 m
Reference vertical distance of aircraft CG from ground =  1.4044 m


- UNDERCARRIAGE ARRANGEMENTS -

UNDERCARRIAGE ARRANGEMENTS
Axial distance from nose wheel to main wheel =  3.6281 m
Axial angle from nose wheel to main wheel    = 23.9802 degree

Axial distance from nose UC to aircraft aft CG position     =  3.1676 m
Axial distance from aircraft forward CG position to main UC =  0.5953 m
Axial distance from aircraft aft CG position to main UC     =  0.4605 m

AIRCRAFT OVERTURN ANGLE
Aircraft static ground line    =  1.4745 m
Aircraft overturn angle        = 43.6056 degree

AIRCRAFT TIPBACK & STATIC TAILDOWN ANGLE
Axial distance from main uc to tail =  4.4902 m
Height due to tipback angle         =  1.4721 m

Aircraft tipback angle         = 18.1522 degree
Aircraft static taildown angle = 15.9757 degree

AIRCRAFT ANGLE OFF VERTICAL
Angle off vertical             = 18.1522 degree

UNDERCARRIAGE STATIC LOADS
Maximum static load       =  4402.07 kg
Maximum nose static load  =   827.24 kg
Minimum nose static load  =   639.91 kg
Nose dynamic braking load =   597.08 kg

Maximum static load as a fraction of total load      =  87.31%
Maximum nose static load as a fraction of total load =  16.41%
Minimum nose static load as a fraction of total load =  12.69%

MAIN UNDERCARRIAGE SHOCK ABSORBER STROKE
Main undercarriage rolling radius        =  0.1867 m
Main undercarriage tyre stroke           =  0.0933 m
Main undercarriage shock absorber stroke =  0.4858 m

UNDERCARRIAGES FRONTAL AREA
Oleo load of each main undercarriage =  2201.04 kg
Oleo load of nose undercarriage      =  1424.32 kg

Oleo diameter of main undercarriage  =  0.0195 m
Oleo diameter of nose undercarriage  =  0.0157 m

Frontal area of each main undercarriage leg          =  0.0179 m^2
Frontal area of each main undercarriage wheel & tyre =  0.0715 m^2

Frontal area of nose undercarriage leg          =  0.0106 m^2
```

```
Frontal area of nose undercarriage wheel & tyre =  0.0509 m^2

 ------------------------
 *UCAV COMPONENT SUMMARY*

 --- MASS & BALANCE --- .
 Aircraft component  Mass   Range   X-Marm   XMoment  Y-Marm   YMoment
                     (kg)   (%)     (m)      (kg.m)   (m)      (kg.m)
Wing (port)          653.72  12.97  5.4242   3545.96 -3.4315  -2243.25
Wing (starboard)     653.72  12.97  5.4242   3545.96  3.4315   2243.25
Nose UC               37.44   0.74  1.6421     61.48  0.0000      0.00
Main UC (port)       135.85   2.69  5.2702    715.95 -1.6138   -219.24
Main UC (stbd)       135.85   2.69  5.2702    715.95  1.6138    219.24
Engine (port)        315.54   6.26  4.9793   1571.17 -0.9069   -286.17
Engine (stbd)        315.54   6.26  4.9793   1571.17  0.9069    286.17
Nozzle (port)         56.37   1.12  6.7754    381.93 -0.9069    -51.12
Nozzle (stbd)         56.37   1.12  6.7754    381.93  0.9069     51.12
Avionics(MMS)         51.34   1.02  0.8022     41.18  0.0000      0.00
Avionics(FMS)        119.04   2.36  2.7239    324.25  0.0000      0.00
Avionics(SMS)          8.32   0.17  2.4024     19.99  0.0000      0.00
Avionics(EWS-port)     4.82   0.10  6.3997     30.85 -6.6290    -31.95
Avionics(EWS-stbd)     4.82   0.10  6.3997     30.85  6.6290     31.95
Air system             9.89   0.20  2.4024     23.76  0.0000      0.00
De-icing system       31.25   0.62  2.4024     75.09  0.0000      0.00
Electrical system    164.52   3.26  2.4024    395.24  0.0000      0.00
FCS                  169.93   3.37  2.4024    408.24  0.0000      0.00
Fuel system          104.21   2.07  2.4024    250.35  0.0000      0.00
W bay1 pylon          62.50   1.24  5.0456    315.35  0.0000      0.00
W bay1 increment     117.95   2.34  5.0456    595.12  0.0000      0.00
Residual fuel         0.00    0.00  2.4024      0.00  0.0000      0.00
     OEM            3209.00   63.65  4.6749  15001.77                0.00

Weap in bay1         460.00    9.12  5.0456   2320.97  0.0000      0.00
     ZFM            3669.00   72.77  4.7214  17322.74                0.00

Wing tank (port)     686.49   13.62  5.0457   3463.84 -2.0160  -1383.93
Wing tank (stbd)     686.49   13.62  5.0457   3463.84  2.0160   1383.93
Centre tank1           0.00    0.00  3.4088      0.00  0.0000      0.00
Centre tank2           0.00    0.00  6.7075      0.00  0.0000      0.00
Centre tank3           0.00    0.00  4.2313      0.00  0.0000      0.00
Outbrd tank1(port)     0.00    0.00  3.4922      0.00 -1.6138      0.00
Outbrd tank1(stbd)     0.00    0.00  3.4922      0.00  1.6138      0.00
Outbrd tank2(port)     0.00    0.00  6.0149      0.00 -1.6138      0.00
Outbrd tank2(stbd)     0.00    0.00  6.0149      0.00  1.6138      0.00
     AUM            5041.98  100.00  4.8097  24250.42                0.00
```

UCAV and Manned Combat Aircraft Comparison: The manned combat aircraft configuration is presented, based on the straight-tapered wing planform with the single weapon bay located at the aircraft centreline, and the safety factor of 1.50 (MAN1.50-WEAP1), as illustrated in Figure 8-31 of Chapter 8.

```
 ------------------------------
 --- UCAV PACKAGING SUMMARY ---
 ------------------------------

 * UCAV PACKAGING CONFIGURATION

 1) Type of stores          = 1 :Internal store
 2) Number of weapon bays   = 1 :Single weapon bay on centreline
 3) Type of missions        = 1 :SEAD/strike
 4) Number of engines       = 1 :Single-engine installation
 5) Type of aircraft        = 1 :Manned aircraft
 6) Type of materials       = 2 :Carbon-fibre composite construction
 7) Number of kinks in wing = 0 :Straight taper wing
 8) Number of split elevons on half span = 1
 9) Number of slats on half span         = 0
10) Number of split rudders on half span = 0
11) Type of airfoils at wing inboard section  = 1 :Symmetrical airfoil
12) Type of airfoils at wing outboard section = 1 :Symmetrical airfoil
13) Thickness ratio at wing inboard section  = 15%
14) Thickness ratio at wing outboard section =  9%
15) Twist distribution      = 1 :Twist wing
```

```
--------------------------
*UCAV PACKAGING OPTIMIZER*

                                      INITIAL    FINAL     LOWER     UPPER
  1 Wing span (m)           [BW]      20.0000   20.4341    6.0000   40.0000
  2 Wing root chord (m)     [CWCC]    15.0000   12.2181    6.0000   20.0000
  3 Wing tip chord (m)      [CWCT]     2.0000    3.5005    0.0100    4.0000
  4 Front spar fraction     [FCWD]     0.1500    0.1500    0.0600    0.1500
  5 Rear spar fraction      [FCWR]     0.7000    0.8000    0.7000    0.8000
  6 Wing leading edge sweep[QWLR]     50.0000   52.9296    0.0100   60.0000
  7 Elevon mean chord (m)   [CWSE]     1.0000    1.0546    0.5000    3.0000
  8 Elevon inner span       [FYSEI]    0.4000    0.2934    0.1000    0.9500
  9 Elevon outer span       [FYSEO]    0.7000    0.4934    0.1000    0.9500
 10 Wing tank span factor   [FY2WFO]   0.5000    0.0147    0.0100    1.0000
 11 Wing tank front factor  [FCWFD]    0.0000    0.0000    0.0000    0.0000
 12 Wing tank rear factor   [FCWFR]    1.0000    1.0000    1.0000    1.0000
 13 Weap bay1 axial factor  [FXLIB1]   0.5000    0.4429    0.0000    1.0000
 14 Engine axial factor     [FXLPG]    0.5000    0.4064    0.0000    1.0000
 15 Engine scale factor     [RTP]      1.5000    1.3604    0.5000    2.5000

------------------------------
*UCAV FIXED MASS CONTRIBUTION*

------------------------------
* COCKPIT

Cockpit canopy wetted area  =  0.7896 m^2

Mass of cockpit windscreen  =    67.25 kg
Mass of cockpit canopy      =    53.37 kg
Mass of pilot               =    90.00 kg
Mass of cockpit instruments =   180.00 kg

------------------------------
* AVIONICS BAY

MISSION MANAGEMENT SYSTEM
Mass & volume of radar suite                =    28.32 kg   0.1404 m^3
Mass & volume of sensor suite               =    23.02 kg   0.0605 m^3

FLIGHT MANAGEMENT SYSTEM
Mass & volume of flight control suite       =    45.03 kg   0.1634 m^3
Mass & volume of navigation suite           =    40.44 kg   0.1925 m^3
Mass & volume of communication suite        =    12.68 kg   0.0949 m^3
Mass & volume of identification suite       =    20.89 kg   0.1556 m^3

STORE MANAGEMENT SYSTEM
Mass & volume of weapon control suite       =     8.32 kg   0.0620 m^3

ELECTRONIC WARFARE SYSTEM
Mass & volume of electronic warfare suite   =     4.82 kg   0.0322 m^3
Mass & volume of countermeasures suite      =     4.82 kg   0.0322 m^3

Total avionics mass                         =   188.34 kg

Length of radar avionics suite              =  0.8022 m
Length of flight management avionics suite  =  1.2861 m
Length of weapon control avionics suite     =  0.5697 m

Radome length                               =  1.2033 m

------------------------------
* WEAPON BAY

WEAPON BAY 1
Total number of weapon bay 1                = 1
Total number of weapons in each weapon bay 1  = 1
Total mass of weapons in weapon bay 1       =   460.00 kg
Total mass of internal pylons in weapon bay 1 =    62.50 kg

WEAPON BAY 2
Total number of weapon bay 2                = 0
Total number of weapons in each weapon bay 2  = 0
Total mass of weapons in weapon bay 2       =     0.00 kg
Total mass of internal pylons in weapon bay 2 =     0.00 kg

INTERNAL WEAPON BAY
```

```
Total mass of weapons in internal weapon bays =   460.00 kg

WEAPON BAY DIMENSION
              L(m)     W(m)     H(m)    V(m^3)
Weapon bay 1  3.1900   0.6300   0.6300  1.2661
Weapon bay 2  0.0000   0.0000   0.0000  0.0000

EXTERNAL STORES
Total number of weapons at port store          = 0
Total mass of weapons at port store            =     0.00 kg
Total number of weapons at starboard store     = 0
Total mass of weapons at starboard store       =     0.00 kg
External store wetted area                     =   0.0000 m^2
Total mass of external pylons.                 =     0.00 kg

Total mass of weapons at external stores       =     0.00 kg


TOTAL WEAPONS
Total mass of weapons on aircraft              =   460.00 kg

 ---------------------------------
 *UCAV VARIABLE MASS CONTRIBUTION*

 -------------------------------
 * ENGINE BAY

 TWO SINGLE-ENGINE INSTALLATIONS

ENGINE & ENGINE BAY DIMENSION
Overall length of engine  =  2.0143 m
Diameter of engine        =  0.9482 m

Total nozzle exit area    =    0.71 m^2

Maximum engine bay height =  1.1379 m
Maximum engine bay width  =  1.1379 m

ENGINE BAY VOLUME
Volume of engine bay            =  2.0484 m^3

PROPULSION SYSTEM MASS
Total mass of engines           =   973.62 kg
Engine installation mass        =   126.57 kg

Total mass of propulsion system =  1100.19 kg

ENGINE STATIC THRUST
Total maximum sea-level static thrust of engines =  53844.09 N
Bypass ratio of total engines   =    8.00

 -------------------------------
 * UNDERCARRIAGE BAY

NOSE UNDERCARRIAGE
Length of nose undercarriage leg         =  0.9184 m
Nose undercarriage wheel & tyre diameter =  0.4676 m
Nose undercarriage wheel & tyre width    =  0.1520 m

MAIN UNDERCARRIAGE
Length of each main undercarriage leg    =  1.2410 m
Main undercarriage wheel & tyre diameter =  0.6701 m
Main undercarriage wheel & tyre width    =  0.1894 m

UNDERCARRIAGE MASS
Structural mass of nose undercarriage            =    54.86 kg
Structural mass of total main undercarriage      =   399.26 kg
Mass of hydraulics associated with undercarriage =    55.91 kg

UNDERCARRIAGE GROSS MASS
Total mass of nose undercarriage with hydraulics =    61.61 kg
Total mass of main undercarriage with hydraulics =   448.41 kg

UNDERCARRIAGE BAY DIMENSION
              L(m)     H(m)     W(m)    V(m^3)
Nose UC bay   1.1522   0.5144   0.2280  0.1351
Main UC bay   1.5761   0.7372   0.2842  0.3302
```

```
------------------------------
* FLYING WING

STRAIGHT TAPERED WING

FLYING WING SPECIFICATION
Wing centreline section & chord  0.0000 m 12.2181 m
Wing tip section & chord        10.2171 m  3.5005 m
Wing gross span               = 20.4341 m
Gross wing aspect ratio       =  2.6000
Gross wing area               =  160.60 m^2
Wing wetted area              =  326.69 m^2
Mean thickness ratio          =  0.1100
Average wing chord            =  7.8593 m

Wing geometric mean chord     =  7.8593 m
Wing aerodynamic mean chord   =  8.6651 m
Distance of wing mean 1/4 chord point from nose =  7.6782 m

Equivalent wing root chord         = 12.2181 m
Equivalent wing taper ratio        =  0.2865
Equivalent wing leading edge sweep = 52.9296 degree
Equivalent wing quarter chord sweep= 47.9933 degree
Equivalent wing mid-chord sweep    = 41.8935 degree

Maximum depth at wing centreline chord =  1.8327 m
Maximum depth at wing tip chord        =  0.3150 m

Wing maximum cross-sectional area      =   38.84 m^2
Flying wing total volume               =  119.75 m^3

Centre of wing volume (true wing)      =  0.0936
Centre of wing volume (equivalent wing)=  0.0000

Wing aerodynamic centre (%MAC)         =  0.0300


WING BOX
Wing front spar from nose at root      =  1.8327 m
Wing rear spar from nose at root       =  9.7745 m

Wing front spar from nose at tip       =  0.5251 m
Wing rear spar from nose at tip        =  2.8004 m

Wing box root chord                    =  7.9417 m
Wing box tip chord                     =  2.2753 m
Wing box gross span                    = 20.4341 m
Gross wing box planform area           =  104.39 m^2
Gross wing box aspect ratio            =  4.0000

Equivalent wing box root chord         =  7.9417 m
Equivalent wing box taper ratio        =  0.2865
Equivalent wing box leading edge sweep = 50.0926 degree
Equivalent wing box centreline sweep   = 46.2978 degree


WING SPANWISE LIFT DISTRUBITION
Mach number for design diving speed =  1.1755
Effective Mach number               =  0.4742
Effective angle of sweepback        = 57.5632 degree
Average angle of attack             =  5.5984 degree

------------------------------
* BAY POSITION

ENGINE BAY POSITION
Spanwise station to engine bay section             =  0.4650  1.0339  1.6029 m
Wing chord at engine bay section                   = 11.8213 11.3359 10.8504 m
Wing leading edge at engine bay section from nose  =  0.6155  1.3686  2.1217 m

Minimum distance of engine inlet from nose         =  4.3495 m
Maximum distance of engine exit from nose          = 10.8020 m
Axial space available for length of engine         =  6.4526 m

Axial distance from nose to engine front face      =  7.7447 m
Axial distance from nose to transition duct entrance=  9.7590 m
```

```
WEAPON BAY 1 POSITION
Spanwise station to weapon bay 1 section           =  0.0000  0.0000  0.3150 m
Wing chord at weapon bay 1 section                 = 12.2181 12.2181 11.9493 m
Wing leading edge at weapon bay 1 section from nose =  0.0000  0.0000  0.4170 m

Minimum distance of weapon bay1 front face from nose=  4.3495 m
Maximum distance of weapon bay1 rear face from nose = 10.8230 m
Axial space available for length of weapon bay 1    =  6.2244 m

Axial distance from nose to weapon bay 1 front face =  5.4118 m


WEAPON BAY 2 POSITION
Spanwise station to weapon bay 2 section           =  0.0000  0.0000  0.0000 m
Wing chord at weapon bay 2 section                 =  0.0000  0.0000  0.0000 m
Wing leading edge at weapon bay 2 section from nose =  0.0000  0.0000  0.0000 m

Minimum distance of weapon bay2 front face from nose=  0.0000 m
Maximum distance of weapon bay2 rear face from nose =  0.0000 m
Axial space available for length of weapon bay 2    =  0.0000 m

Axial distance from nose to weapon bay 2 front face =  0.0000 m


MAIN UNDERCARRIAGE BAY POSITION
Spanwise station to main uc bay section            =  1.7529  1.8950  2.0371 m
Wing chord at main uc bay section                  = 10.7224 10.6012 10.4800 m
Wing leading edge at main uc bay section from nose =  2.3202  2.5083  2.6964 m

Minimum distance of main uc bay front face from nose=  4.2684 m
Maximum distance of main uc bay rear face from nose = 10.8230 m
Axial space available for length of main uc bay     =  6.5547 m

Axial distance from nose to main uc bay front face  =  7.0186 m

 ------------------------------
 * INTAKE DIFFUSER

Cross sectional area of intake inlet  =  0.7062 m^2
Cross sectional area of intake exit   =  0.7062 m^2
Equivalent diameter of intake inlet   =  0.9482 m
Diameter of intake exit               =  0.9482 m

Width of intake inlet                 =  1.1885 m
Height of intake inlet                =  0.5942 m
Width of intake inlet projected into horizontal =  1.1885 m
Height of intake inlet projected into vertical  =  0.5942 m

Distance of intake inlet from nose    =  3.7064 m
Length of intake diffuser             =  4.0383 m

Spanwise station to intake inlet.     =  1.1189 m
Spanwise station to intake exit       =  1.0339 m
Vertical distance of intake inlet     =  0.4640 m
Vertical distance of intake exit      =  0.0000 m
Wing leading edge at intake from nose =  1.4811 m

Volume of each intake diffuser        =  2.8519 m^3

 ------------------------------
 * 2-DIMENSIONAL NOZZLE

Aspect ratio of nozzle transition duct exit=  6.6792

SINGLE ENGINE INSTALLATION
Half-height of nozzle transition duct exit =  0.1626 m
Half-width of nozzle transition duct exit  =  1.1379 m

Length of nozzle transition duct      =  2.1281 m

Volume of nozzle transition duct      =  3.9627 m^3
Total mass of nozzle transition duct =   146.08 kg

 ------------------------------
 * TRAILING EDGE SPLIT ELEVON
```

```
Total number of all split elevons = 2

ELEVON 1
Elevon inner span,chrd &wchrd =  2.9978  1.1592  9.6602 m
Elevon outer span,chrd &wchrd =  5.0413  0.9500  7.9167 m
Elevon mean chord             =  1.0546 m
Total span of elevon          =  4.0868 m
Aspect ratio of each elevon   =  1.9376
Elevon hinge line sweep       = 28.6882 deg
Total planform area of elevon =    4.31 m^2
Total wing area over elevon   =   35.92 m^2
ELEVONS LIFT & MOMENT            TO      LD
Elevon deflection             =   30.00   60.00 deg
Section lift increment        =  0.6320  1.0341
Wing lift increment           =  0.0639  0.1046
Wing pitch increment          = -0.0057 -0.0093
Sect max lift increment       =  0.5570  0.7530
Wing max lift increment       =  0.1093  0.1477


All split elevons gross span          =   4.0868 m
Split elevon mean chord               =   1.0546 m
All split elevons planform area       =     4.31 m^2
Total wing planform area over split elevons   =   35.92 m^2

WING TRAILING EDGE
Gross area of wing trailing edge aft of rear spar    =   24.82 m^2
Planform area of fixed section of wing TE aft of r/s =   20.51 m^2

 ------------------------------
 * LEADING EDGE SLAT

Total number of all slats = 0


All slats gross span          =   0.0000 m
Slat mean chord               =   0.0000 m
All slats planform area       =     0.00 m^2
Total wing planform area over slats   =    0.00 m^2

WING LEADING EDGE
Total planform area of wing leading edge             =   18.62 m^2
Planform area of fixed section of wing LE fwd of f/s =    6.21 m^2

 ------------------------------
 * TRAILING EDGE SPLIT RUDDER

Total number of all split rudders = 2

SPLIT RUDDER 1
Rudder inner span & wchrd     =  2.9978  9.6602 m
Rudder outer span & wchrd     =  5.0413  7.9167 m
Aspect ratio of each rudder   =  1.9376
Rudder hinge line sweep       = 28.6882 deg
SPLIT RUDDERS LIFT & MOMENT     Aileron Rudder
Split rudder deflection       =   20.00   25.00 deg
Section lift increment        =  0.5390  0.6071
Wing lift increment           =  0.0545  0.0614
Wing yaw effectiveness        = -0.0014  0.0016
Wing roll effectiveness       =  0.0181 -0.0203

 ------------------------------
 * FUEL

- CENTRE FUEL TANK -
Total span of centre fuel tank =  0.6300 m

CENTRE FUEL TANK 1 (FRONT)
Centre fuel tank 1 front face from nose =  4.3495 m
Centre fuel tank 1 rear face from nose  =  5.4118 m
Total fuel volume of centre tank 1    =  0.9659 m^3
Fuel mass used in centre fuel tank 1  =     0.00 kg
M-arm of centre fuel tank 1 from nose =  4.8775 m

CENTRE FUEL TANK 2 (REAR)
Centre fuel tank 2 front face from nose =  8.6018 m
```

```
Centre fuel tank 2 rear face from nose  = 10.8230 m
Total fuel volume of centre tank 2     =  0.9659 m^3
Fuel mass used in centre fuel tank 2   =     0.00 kg
M-arm of centre fuel tank 2 from nose  =  9.5684 m

CENTRE FUEL TANK 3 (TOP)
Centre fuel tank 3 front face from nose =  5.4118 m
Centre fuel tank 3 rear face from nose  =  7.0068 m
Total fuel volume of centre tank 3     =  0.3564 m^3
Fuel mass used in centre fuel tank 3   =     0.00 kg
M-arm of centre fuel tank 3 from nose  =  6.1911 m

TOTAL CENTRE FUEL TANK CAPACITY
Total area of centre fuel tank         =  3.0735 m^2
Total fuel volume of centre tank       =  2.2882 m^3
Total fuel mass used in centre tank    =     0.00 kg


- INBOARD FUEL TANK -
Total span of inboard fuel tank =  0.0000 m

INBOARD FUEL TANK 1 (FRONT)
Inboard fuel tank 1 front face from nose =  0.0000 m
Inboard fuel tank 1 rear face from nose  =  0.0000 m
Total fuel volume of inbrd tank 1      =  0.0000 m^3
Fuel mass used in inbrd fuel tank 1    =     0.00 kg
M-arm of inbrd fuel tank 1 from nose   =  0.0000 m

INBOARD FUEL TANK 2 (REAR)
Inboard fuel tank 2 front face from nose =  0.0000 m
Inboard fuel tank 2 rear face from nose  =  0.0000 m
Total fuel volume of inbrd tank 2      =  0.0000 m^3
Fuel mass used in inbrd fuel tank 2    =     0.00 kg
M-arm of inbrd fuel tank 2 from nose   =  0.0000 m

INBOARD FUEL TANK 3 (TOP)
Inboard fuel tank 3 front face from nose =  0.0000 m
Inboard fuel tank 3 rear face from nose  =  0.0000 m
Total fuel volume of inbrd tank 3      =  0.0000 m^3
Fuel mass used in inbrd fuel tank 3    =     0.00 kg
M-arm of inbrd fuel tank 3 from nose   =  0.0000 m

TOTAL INBOARD FUEL TANK CAPACITY
Total area of inboard fuel tank        =  0.0000 m^2
Total fuel volume of inbrd tank        =  0.0000 m^3
Total fuel mass used in inbrd tank     =     0.00 kg


- OUTBOARD FUEL TANK -
Total span of outboard fuel tank =  0.5683 m

OUTBOARD FUEL TANK 1 (FRONT)
Outboard fuel tank 1 front face from nose =  4.2684 m
Outboard fuel tank 1 rear face from nose  =  7.0186 m
Total fuel volume of outbrd tank 1     =  1.8705 m^3
Fuel mass used in outbrd fuel tank 1   =     0.00 kg
M-arm of outbrd fuel tank 1 from nose  =  5.6628 m

OUTBOARD FUEL TANK 2 (REAR)
Outboard fuel tank 2 front face from nose =  8.5947 m
Outboard fuel tank 2 rear face from nose  = 10.8230 m
Total fuel volume of outbrd tank 2     =  1.0596 m^3
Fuel mass used in outbrd fuel tank 2   =     0.00 kg
M-arm of outbrd fuel tank 2 from nose  =  9.6153 m

TOTAL OUTBOARD FUEL TANK CAPACITY
Total area of outboard fuel tank       =  2.8295 m^2
Total fuel volume of outbrd tank       =  2.9301 m^3
Total fuel mass used in outbrd tank    =     0.00 kg


- WING FUEL TANK -
Wing fuel tank spanwise station 0 =  2.1871 m
Wing fuel tank spanwise station 1 =  2.4230 m
Total span available for wing fuel tank          =  0.4719 m
Total wing box area available for wing fuel tank =  3.1447 m^2
```

```
WING FUEL TANK CAPACITY
Total fuel volume of wing tank          =  2.9537 m^3
Total fuel mass used in wing tank       =  2293.57 kg


- OPTIONAL WEAPON BAY FUEL TANK -
Total fuel volume of weapon bay tank1=  0.0000 m^3
Fuel mass used in weapon bay tank 1  =     0.00 kg

Total fuel volume of weapon bay tank2=  0.0000 m^3
Fuel mass used in weapon bay tank 2  =     0.00 kg

TOTAL WEAPON BAY FUEL TANK CAPACITY
Total fuel volume of weapon bay tank       =  0.0000 m^3
Total fuel mass used in weapon bay tank    =     0.00 kg

- UCAV TOTAL FUEL CAPACITY -
Total area containing fuel tank       =  9.0477 m^2
Total internal fuel volume            =  8.1720 m^3
Total mass of available internal fuel=  6345.56 kg

Total fuel mass used on aircraft      =  2293.57 kg

 ------------------------------
 * UCAV MASS & CG

- UCAV MASS -

WING BOX
Ultimate load factor            =   11.00
Wing inertia relief load        =  1663.07 kg

Wing box mass (Torsion)         =   438.46 kg
Wing box mass (Bending)         =   712.95 kg
Total wing box mass             =   712.95 kg

CONTROL SURFACES
Wing leading edge mass          =   144.57 kg
Wing fixed trailing edge mass   =   174.71 kg

TEcs mass (flap)                =    25.74 kg
TEcs mass (aileron)             =    67.04 kg
Total TE control surfaces mass  =    67.04 kg

Inlaids mass (rudder)           =     0.00 kg
Inlaids mass (spoiler)          =     0.00 kg
Total inlaids CS mass           =     0.00 kg

AUXILIARY
Miscellaneous attachments       =    43.97 kg
External paint                  =    54.76 kg
Low Observable treatments       =   226.80 kg
Basic ribs in strutural box     =  1421.71      0.00 kg

FLYING WING
Total wing structural mass      =  2846.51 kg

MASS INCREMENT DUE TO INTERNAL WEAPON BAYS
Mass increment due to weap bay1=   124.18 kg
Mass increment due to weap bay2=     0.00 kg

AIRCRAFT SYSTEM
Mass of air systems             =    82.89 kg
Mass of de-icing system         =    46.82 kg
Mass of electrical systems      =   269.69 kg
Mass of flight control systems  =   285.34 kg
Mass of fuel system             =   174.08 kg

COMPLETE AIRCRAFT
Total aircraft payload          =   550.00 kg
Mass of fixed-role equipment    =   430.84 kg
Total mass of fuel on aircraft  =  2293.57 kg

Empty mass              =   6137.25 kg
Operational empty mass  =   6227.25 kg
Zero fuel mass          =   6687.25 kg
```

```
Total take-off mass     =   8980.82 kg
Landing mass            =   7633.70 kg

Wing loading            =   55.9212 kg/m^2
Thrust loading          =    0.6114


WING STRUCTURAL MASS COMPARISON
Howe method 1 (COA)     =   2846.51 kg (theoretical)
Howe method 2 (COA)     =   4665.71 kg (empirical)
Lovell method (RAE)     =   6992.65 kg
Roskam method (USAF)    =   1824.85 kg
Roskam method (USN)     =   2325.09 kg
Raymer method           =   1669.27 kg
Whitford method         =   1988.89 kg


- CENTRE OF GRAVITY -

OPERATIONAL EMPTY MASS
Total aircraft pitching moment about nose=  44703.67 kg.m
Distance of aircraft CG from nose        =  7.2840 m
CG relative to aerodynamic mean chord    =  20.45%

ZERO FUEL MASS
Total aircraft pitching moment about nose=  48092.14 kg.m
Distance of aircraft CG from nose        =  7.1916 m
CG relative to aerodynamic mean chord    =  19.38%

TOTAL TAKE-OFF MASS
Total aircraft pitching moment about nose=  65586.51 kg.m
Distance of aircraft CG from nose        =  7.3030 m
CG relative to aerodynamic mean chord    =  20.67%
Static margin                            =   4.33%

Distance of aircraft fwd CG from nose  =  7.1583 m
Fwd CG relative to AMC                 =  19.00%
Distance of aircraft aft CG from nose  =  8.2847 m
Aft CG relative to AMC                 =  32.00%

Reference spanwise distance of aircraft CG             =  0.0000 m
Reference vertical distance of aircraft CG from ground =  2.0243 m


- UNDERCARRIAGE ARRANGEMENTS -

UNDERCARRIAGE ARRANGEMENTS
Axial distance from nose wheel to main wheel =  6.7653 m
Axial angle from nose wheel to main wheel    = 15.6477 degree

Axial distance from nose UC to aircraft aft CG position     =  5.5236 m
Axial distance from aircraft forward CG position to main UC =  1.3531 m
Axial distance from aircraft aft CG position to main UC     =  1.2417 m

AIRCRAFT OVERTURN ANGLE
Aircraft static ground line    =  1.8247 m
Aircraft overturn angle        = 47.9671 degree

AIRCRAFT TIPBACK & STATIC TAILDOWN ANGLE
Axial distance from main uc to tail =  8.4798 m
Height due to tipback angle         =  2.0851 m

Aircraft tipback angle         = 13.8141 degree
Aircraft static taildown angle = 12.3824 degree

AIRCRAFT ANGLE OFF VERTICAL
Angle off vertical             = 31.5260 degree

UNDERCARRIAGE STATIC LOADS
Maximum static load       =   7332.45 kg
Maximum nose static load  =   1796.16 kg
Minimum nose static load  =   1648.37 kg
Nose dynamic braking load =    822.04 kg

Maximum static load as a fraction of total load      =   81.65%
Maximum nose static load as a fraction of total load =   20.00%
```

Minimum nose static load as a fraction of total load = 18.35%

MAIN UNDERCARRIAGE SHOCK ABSORBER STROKE
Main undercarriage rolling radius = 0.2234 m
Main undercarriage tyre stroke = 0.1117 m
Main undercarriage shock absorber stroke = 0.4725 m

UNDERCARRIAGES FRONTAL AREA
Oleo load of each main undercarriage = 3666.23 kg
Oleo load of nose undercarriage = 2618.21 kg

Oleo diameter of main undercarriage = 0.0252 m
Oleo diameter of nose undercarriage = 0.0213 m

Frontal area of each main undercarriage leg = 0.0313 m^2
Frontal area of each main undercarriage wheel & tyre = 0.1058 m^2

Frontal area of nose undercarriage leg = 0.0196 m^2
Frontal area of nose undercarriage wheel & tyre = 0.0592 m^2

UCAV COMPONENT SUMMARY

--- MASS & BALANCE ---

Aircraft component	Mass (kg)	Range (%)	X-Marm (m)	XMoment (kg.m)	Y-Marm (m)	YMoment (kg.m)
Wing (port)	1423.25	15.85	8.4890	12082.08	-4.4955	-6398.26
Wing (starboard)	1423.25	15.85	8.4890	12082.08	4.4955	6398.26
Nose UC	61.61	0.69	1.7794	109.63	0.0000	0.00
Main UC (port)	224.21	2.50	8.5447	1915.77	-1.8950	-424.87
Main UC (stbd)	224.21	2.50	8.5447	1915.77	1.8950	424.87
Engine (port)	550.09	6.13	8.7518	4814.33	-1.0339	-568.77
Engine (stbd)	550.09	6.13	8.7518	4814.33	1.0339	568.77
Nozzle (port)	73.04	0.81	10.8230	790.49	-1.0339	-75.52
Nozzle (stbd)	73.04	0.81	10.8230	790.49	1.0339	75.52
Avionics(MMS)	51.34	0.57	0.8022	41.18	0.0000	0.00
Avionics(FMS)	119.04	1.33	3.7064	441.21	0.0000	0.00
Avionics(SMS)	8.32	0.09	3.3849	28.16	0.0000	0.00
Avionics(EWS-port)	4.82	0.05	11.4953	55.41	-8.6845	-41.86
Avionics(EWS-stbd)	4.82	0.05	11.4953	55.41	8.6845	41.86
Air system	82.89	0.92	3.3849	280.57	0.0000	0.00
De-icing system	46.82	0.52	3.3849	158.47	0.0000	0.00
Electrical system	269.69	3.00	3.3849	912.86	0.0000	0.00
FCS	285.34	3.18	3.3849	965.84	0.0000	0.00
Fuel system	174.08	1.94	3.3849	589.25	0.0000	0.00
Gun	0.00	0.00	2.2033	0.00	0.5500	0.00
W bay1 pylon	62.50	0.70	7.0068	437.92	0.0000	0.00
W bay1 increment	124.18	1.38	7.0068	870.12	0.0000	0.00
Cockpit	300.62	3.35	1.8373	552.31	0.0000	0.00
Residual fuel	0.00	0.00	3.3849	0.00	0.0000	0.00
OEM	6137.25	68.34	7.2840	44703.67		0.00
Ammunition	0.00	0.00	3.3849	0.00	0.5500	0.00
Weap in bay1	460.00	5.12	7.0068	3223.12	0.0000	0.00
Pilot	90.00	1.00	1.8373	165.35	0.0000	0.00
ZFM	6687.25	74.46	7.1916	48092.14		0.00
Wing tank (port)	1146.79	12.77	7.6276	8747.19	-2.2909	-2627.16
Wing tank (stbd)	1146.79	12.77	7.6276	8747.19	2.2909	2627.16
Centre tank1	0.00	0.00	4.8775	0.00	0.0000	0.00
Centre tank2	0.00	0.00	9.5684	0.00	0.0000	0.00
Centre tank3	0.00	0.00	6.1911	0.00	0.0000	0.00
Outbrd tank1(port)	0.00	0.00	5.6628	0.00	-1.8950	0.00
Outbrd tank1(stbd)	0.00	0.00	5.6628	0.00	1.8950	0.00
Outbrd tank2(port)	0.00	0.00	9.6153	0.00	-1.8950	0.00
Outbrd tank2(stbd)	0.00	0.00	9.6153	0.00	1.8950	0.00
AUM	8980.82	100.00	7.3030	65586.51		0.00

--- MASS & BALANCE (continued) ---

Aircraft component	Mass (kg)	Z-Marm dwn(m)	ZMoment (kg.m)	Z-Marm up (m)	ZMoment (kg.m)
Wing (port)	1423.25	2.0243	2881.02	0.0000	0.00
Wing (starboard)	1423.25	2.0243	2881.02	0.0000	0.00
Nose UC	61.61	1.4644	90.22	-0.5598	-34.49
Main UC (port)	224.21	1.4644	328.33	-0.5598	-125.52
Main UC (stbd)	224.21	1.4644	328.33	-0.5598	-125.52

Engine (port)	550.09	2.0243	1113.53	0.0000	0.00
Engine (stbd)	550.09	2.0243	1113.53	0.0000	0.00
Nozzle (port)	73.04	2.0243	147.85	0.0000	0.00
Nozzle (stbd)	73.04	2.0243	147.85	0.0000	0.00
Avionics(MMS)	51.34	2.0243	103.93	0.0000	0.00
Avionics(FMS)	119.04	2.0243	240.97	0.0000	0.00
Avionics(SMS)	8.32	2.0243	16.84	0.0000	0.00
Avionics(EWS-port)	4.82	2.0243	9.76	0.0000	0.00
Avionics(EWS-stbd)	4.82	2.0243	9.76	0.0000	0.00
Air system	82.89	2.2814	189.11	0.2572	21.32
De-icing system	46.82	2.2814	106.81	0.2572	12.04
Electrical system	269.69	2.5932	699.35	0.5689	153.44
FCS	285.34	2.5932	739.94	0.5689	162.34
Fuel system	174.08	2.5932	451.43	0.5689	99.04
Gun	0.00	2.0243	0.00	0.0000	0.00
W bay1 pylon	62.50	2.3393	146.20	0.3150	19.69
W bay1 increment	124.18	2.0243	251.38	0.0000	0.00
Cockpit	300.62	2.2814	685.84	0.2572	77.32
Residual fuel	0.00	1.9294	0.00	-0.0948	0.00
OEM	6137.25		12682.98		259.65
Ammunition	0.00	2.0243	0.00	0.0000	0.00
Weap in bay1	460.00	2.0243	931.16	0.0000	0.00
Pilot	90.00	2.2814	205.33	0.2572	23.15
ZFM	6687.25		13819.47		282.80
Wing tank (port)	1146.79	2.0243	2321.38	0.0000	0.00
Wing tank (stbd)	1146.79	2.0243	2321.38	0.0000	0.00
Centre tank1	0.00	2.0243	0.00	0.0000	0.00
Centre tank2	0.00	2.0243	0.00	0.0000	0.00
Centre tank3	0.00	2.3393	0.00	0.3150	0.00
Outbrd tank1(port)	0.00	2.0243	0.00	0.0000	0.00
Outbrd tank1(stbd)	0.00	2.0243	0.00	0.0000	0.00
Outbrd tank2(port)	0.00	2.0243	0.00	0.0000	0.00
Outbrd tank2(stbd)	0.00	2.0243	0.00	0.0000	0.00
AUM	8980.82		18462.24		282.80